Author:
Hyett, David John

Title:
Phosphonites and diphosphites derived from biphenanthrol for use in asymmetric catalysis.

PHOSPHONITES AND DIPHOSPHITES DERIVED FROM BIPHENANTHROL FOR USE IN ASYMMETRIC CATALYSIS

by

David John Hyett

A Thesis submitted to the University of Bristol in accordance with the requirements for the Degree of Doctor of Philosophy in the School of Chemistry, Faculty of Science.

July 1999

ABSTRACT

Chapter 1 contains a review of phosphonites in asymmetric catalysis and recent developments in asymmetric hydrogenation and asymmetric hydroformylation catalysis.

Chapter 2 is concerned with new phosphonite ligands for asymmetric catalysis. A new three-step synthesis of 9,9'-biphenanthryl-10,10'-diol ('biphenanthrol') in 36% yield from phenanthrene is reported. The ligands $PhP(OR)_2$, $PhP(OR')_2$, $(RO)_2PCH_2CH_2P(OR)_2$ and $Ph_2PCH_2CH_2P(OR)_2$ derived from 'biphenanthrol' $(HOR)_2$ and dimethyl-1,1'-binaphthyl-2,2'-dihydroxy-3,3'-dicarboxylate $(HOR')_2$ have been synthesised and their Pt(0, II) and Rh(I) chemistry is discussed. The crystal structures of two complexes of the type $[PtCl_2(phosphonite)_2]$ have been determined. The monophosphonite, diphosphonite and phosphinophosphonite complexes $[Rh(cod)P_2]BF_4$ derived from (*S*)-'biphenanthrol' are described.

In Chapter 3, the chemistry of some new diphosphites is described. The diastereomeric mixture of $(RO)_2P(ORRO)P(OR)_2$ ('biphenanthrite') is formed by reacting (±)-'biphenanthrol' with PCl_3. Optically pure (*R,R,R*)-'biphenanthrite' is similarly prepared from (*R*)-'biphenanthrol'. The side-products and intermediates in this reaction are identified by their independent syntheses: $ClP(OR)_2$, $H(O)P(OR)_2$, $(RO)_2POP(OR)_2$ and $(HORRO)P(OR)_2$. Dehydration of 'biphenanthrol' also occurs to give a furan, which was characterised by X-ray crystallography. Two equivalents of (*R*)-$ClP(OR)_2$ react with (*R*)- or (*S*)-'binaphthol' $(HOR'')_2$ to give (*R,R,R*)- and (*R,S,R*)-$(RO)_2P(OR''R''O)P(OR)_2$ ('pnp'). The disodium salt of (±)-'biphenanthrol' reacts with two equivalents of (±)-$ClP(OR)_2$ to yield the single {(*R,S,R*) / (*S,R,S*)}-diastereomer of 'biphenanthrite'. The Pt(II), Pd(II) and Rh(I) coordination chemistry of these new diphosphites is reported. The complexes $[MCl_2(diphosphite)]$ are fluxional due to the conformational flexibility of the nine-membered chelate ring and the crystal structures of (*R,R,R*)- and (*S,R,S*)-$[PtCl_2$('biphenanthrite')] show very different ring conformations. The hydroformylation of styrenes catalysed by rhodium(I) complexes of (*R,R,R*)-'biphenanthrite', (*R,S,R*)-'pnp' and (*R,R,R*)-'pnp' is reported. The 'biphenanthrite' complex gives 50% branched aldehyde and no asymmetric induction. The complex of (*R,S,R*)-'pnp' gives 91-96% branched aldehyde and up to 72% ee. The differences in the catalytic properties of the diastereomers is discussed.

In Chapter 4, the asymmetric hydrogenation of α-enamides with rhodium(I) complexes of the new phosphonites and diphosphites as catalysts is discussed. The diphosphonite complex shows low activity and a modest ee (up to 41%) but the analogous phosphinophosphonite complex is highly active and gives high ee's (up to 88%). This is the first phosphinophosphonite to be used in asymmetric hydrogenation. The monophosphonite complex is very active and the ee's of up to 92% are the highest obtained with a monodentate ligand in asymmetric α-enamide hydrogenation.

Chapter 5 gives the experimental details for the chemistry reported in this thesis.

This thesis is dedicated to my mum and dad for all of their love and support throughout my education.

ACKNOWLEDGEMENTS

After a five year endeavour such as this there are clearly a large number of people to say thank you to, so surely no one will mind if I change the habit of a lifetime and bang on for a while.

First and foremost I must say a very big thank you to my supervisors, Paul and Jo. Paul has been inspirational throughout my PhD - his constant enthusiasm (and optimism!) have kept me going through some very tough times (including an infamous all-nighter), his shockers (which rival even mine!) have kept me endlessly amused (remember the fat bloke from the DTI) and his three hour stints have given me something to aspire to but most of all I am grateful for his friendship. Jo, on the other hand, has his own unique way of inspiring students and I am grateful for the sound organic teaching that he has (literally) ground into me. The toughening-up process he believes in is infamous, but one I am sure has benefited me greatly. I'm also indebted to Jo, and Beadie, for introducing me to one of life's finer culinary delights - the curry!

I must also thank my industrial supervisors Drs Malcolm Hill and Dave Tapolczay (whose name I have never been able to spell) from GlaxoWellcome and especially Dr John Clough of Zeneca Agrochemicals for arranging a most enjoyable three months at Jealott's Hill. That leads me on to thanking the people there (Russell, Tish and especially Peter) for putting up with my endless questions and for the weekly humiliation of my fantasy football team - "You chose Vinnie Jones in midfield?"

Thanks must also go to Professor Neil Connelly for his help in arranging innumerable extensions and for nagging me during the final week before my deadline.

Other people too have helped in the production of this thesis. Thanks to Charles (for trans-global IT advice), my proof-readers (Emma, Giles {and what a fine job this pair did!}, Emily and Slegs) and to my crystallographers (Di and Amy). Special thanks to Amy; not only for putting up with crystals of the lowest quality that lost solvent as soon as they were removed from the NMR tubes I had the audacity to submit them in but also for her help in printing the structures out - not the easiest of tasks as we found out! Thanks to Professor Guy Orpen as well for his crystallographic banter and those yearly pep talks without which I'm sure I'd never have had the motivation to work as hard as I did!?

A few other people are worthy of special mention: Milena, for literally teaching me everything I know about phosphites, not to mention her passion for debate (me, a sexist?), and the Salsa queens Elena and Aina, for all their help with the catalysis work done throughout this project and for a fantastic time in Spain (for which I must also thank Emily 'I'm not drunk, it's the size of the Bacardis they have here' Horwood).

The technical staff at both Reading and Bristol have also been fantastic during my PhD. Thanks to Tony, Darryl and Adrian (Bristol) for helping me even though I'm not a member of the Ward / McCleverty group and especially John Warrington

(Reading) for sharing my cynical view of aspects of Reading life and continually informing me of new ways you can die or be maimed whilst doing chemistry. Thanks also to the NMR and mass spectrometry services at Bristol for their invaluable help.

And now to the people who have made my time as a PhD student so enjoyable. The members of the Pringle group past and present have been fantastic, namely: Milena 'You English don't know how to drink' Costa, 'Gentleman' Jim Fleming, Jason 'I'll be in the hazards lab' Green, Chris 'I'm never late - it's the missus' Cobley, Dave 'The short, miserable git' Brewin, Katie 'I can't walk uphill' Mason, Vicky 'I can touch my elbows behind my back' Gee, Chuck 'Maurice' Carraz, Gayle 'I started the ridiculous shoes thing' Harrison, Rob 'Catchphrase' Pugh, Emily 'Optimism' Horwood, Giles 'Essex Boy' Brown (who was a fantastic project student and the only bloke I know to pull in a kebab shop), Ian 'Nice bloke' Norton, Emma 'Hotspot' Lloyd-Jones, Aina 'Chunder Queen' Mozzarella, Mike 'Linda, tell Paul...' Eberhard, Soni 'Karate' Basra, Julie 'What nationality am I?' Scott, Greg 'Presentation - great, free booze' Sellers, Vick 'Paul's not my boyfriend' Rylott and last, but certainly not least, Rich 'Mr Excitable' Jones.

The Reading crowd, you'll be relieved to know, is somewhat smaller. Thanks to all of the Sweeney group, namely Ian 'Curry' Beadham, Big Jenny Knight, Alex 'The human distillery' Richecoeur, Pete 'Patch' Laughton, Alex Cantrill (for bringing a bit of culture to a group without much), Chee 'Don't mess with me' Hau, Smasher 'Jarvis', Chrisseh 'Slippers and Pipe' Shaw (Love you Janet!!), Rachel (for being a girl in the Sweeney group), Ali 'Honesty is the best policy' Tavassoli, Ross 'After Dark' Mabon, Andy 'Street fighter' Mclaren and Wee E Stock. I'd particularly like to thank Ross, Andy and Vicky for making the journey to Bristol for my viva.

Thanks to everyone I've ever played footie with and also 'The Fruitbat' team in Reading for being a great bunch of lads. On a more sombre note, I'd like to remember Danny, a great bloke who was tragically killed in a car accident earlier this year.

There are many other friends who are too numerous too mention, but I'd like to thank a few special ones. Thanks to Carl 'Shocker' Otter for the odd night out, to Al and the Treble T (the Oxford boys), to Dave, Jonny, Rich and Jak (the Merton gang) but perhaps most of all to Ash who has been there right the way from start to finish and who has kept me going throughout.

On a somewhat more cynical note I'd like to thank Reading University for suing me for a bill I'd already paid (noone's happy about that!) but I'd genuinely like to thank the staff at the BRI for patching me up whenever needed, a frequent occurrence.

And finally I'd like to thank the people who matter most of all, my family. The thesis is dedicated to mum and dad for everything (but I just wish I could have finished before you retired dad!) but I'd like to thank the rest of my family as well (Rob, Gran, Linda and now Dave) and remember Phyllis and Mac who would have been so proud.

MEMORANDUM

The work described in this Thesis was carried out in the School of Chemistry at the University of Bristol between October 1994 and July 1999. Unless otherwise acknowledged within the text, it is the original work of the author and has not been submitted previously for a degree. In addition, any views expressed in this Thesis are those of the author, and not of the University.

D. J. Hyett

David John Hyett
University of Bristol
July 1999

Contents

Page No.

Title i
Abstract ii
Dedication iii
Acknowledgements iv
Memorandum vi
Contents vii
Abbreviations xi

Table of contents

Chapter 1: Introduction 1

Chapter 2: Phosphonites: Synthesis and Coordination Chemistry 37

Chapter 3: Cyclic Aryl Diphosphites: Synthesis, Coordination Chemistry and Application in Asymmetric Hydroformylation..... 78

Chapter 4: Asymmetric Hydrogenation of α-Enamides: Mechanism and Catalytic Results..... 127

Chapter 5: Experimental 168

References:..... 193

Chapter 1: Introduction

1.1 Introduction 2
1.2 The importance of the asymmetric hydrogenation reaction of α-enamides ... 4
1.3 Chiral phosphonites as ligands in asymmetric catalysis..... 6
1.3.1 Monophosphonites 6
1.3.1.1 Monodentate phosphorus(III) ligands in asymmetric catalysis..... 9
1.3.2 Diphosphonites 11
1.3.3 Phosphinophosphonites 14
1.4 Chiral diphosphites as ligands for asymmetric hydrogenation 16
1.5 The asymmetric hydroformylation of styrene derivatives..... 18
1.5.1 The importance of the asymmetric hydroformylation reaction of styrene derivatives..... 18
1.5.2 General features of asymmetric hydroformylation..... 19
1.5.3 Recent developments in the asymmetric hydroformylation of styrene derivatives..... 21
1.5.4 Mechanistic features of the asymmetric hydroformylation of styrene derivatives..... 26
1.6 Project aims and thesis outline 35

Chapter 2: Phosphonites: Synthesis and Coordination Chemistry

2.1 Syntheses of 9,9'-biphenanthryl-10,10'-diol (**2.2**) and dimethyl-1,1'-binaphthyl-2,2'-dihydroxy-3,3'-dicarboxylate (**2.1**)..... 38
2.2 Synthesis of phosphonites derived from 9,9'-biphenanthryl-10,10'-diol (**2.2**) and dimethyl-1,1'-binaphthyl-2,2'-dihydroxy-3,3'-dicarboxylate (**2.1**) 43
2.2.1 Mono- and diphosphonite syntheses from $RPCl_2$ species..... 43
2.2.2 Phosphinophosphonite synthesis from $RP(NMe_2)_2$ species 49
2.3 Coordination chemistry of phosphonites derived from 9,9'-biphenanthryl-10,10'-diol (**2.2**) and dimethyl-1,1'-binaphthyl-2,2'-dihydroxy-3,3'-dicarboxylate (**2.1**)..... 51
2.3.1 Dichloroplatinum(II) complexes 51
2.3.1.1 Monophosphonites (**2.11**) and (**2.12**) 51
2.3.1.2 Diphosphonite (**2.16**) and phosphinophosphonite (**2.21**) 57
2.3.2 Rhodium(I) complexes..... 60

2.3.2.1 Monophosphonites (**2.11**) and (**2.12**) 60
2.3.2.2 Diphosphonite (*S*,*S*)-(**2.16**)..... 63
2.3.2.3 Phosphinophosphonite (**2.21**) 63
2.3.3 Platinum(0) complexes - NMR studies 67
2.3.3.1 Monophosphonite (**2.12**)..... 67
2.3.3.2 Phosphinophosphonite (**2.21**) 72
2.4 Discussion of ^{31}P and ^{195}Pt NMR chemical shifts and coupling constants . . 74

Chapter 3: Cyclic Aryl Diphosphites: Synthesis, Coordination Chemistry and Application in Asymmetric Hydroformylation

3.1 Introduction 79
3.2 Synthesis of cyclic aryl phosphites derived from 9,9'-biphenanthryl-10,10'-diol (**3.2**)..... 80
3.2.1 Synthesis of the diphosphite 'biphenanthrite' (**3.4**) from biphenanthrol..... 81
3.2.1.1 Synthesis of chlorophosphite (**3.10**) from biphenanthrol (**3.2**)..... 88
3.2.1.2 Synthesis of 'POP'pyrophosphite (*S*,*S*)-(**3.12**) from optically pure biphenanthrol (*S*)-(**3.2**) 91
3.2.1.3 Synthesis of 'dangler' monophosphite (*S*,*S*)-(**3.9**) from optically pure biphenanthrol (*S*)-(**3.2**) 92
3.2.1.4 Synthesis of the (*R*,*S*,*R*)- / (*S*,*R*,*S*)-diastereomer of 'biphenanthrite' (**3.4**) 97
3.2.1.5 Synthesis of the diastereomeric mixture of 'biphenanthrite' (**3.4**)..... 100
3.2.1.6 Synthesis of optically pure (*R*,*R*,*R*)-'biphenanthrite' (**3.4**) from (*R*)-biphenanthrol (**3.2**)..... 101
3.2.2 Synthesis of mixed diphosphites derived from biphenanthrol (**3.2**) and binaphthol 102
3.2.2.1 Synthesis of the mixed diphosphite 'pnp' (**3.5**) 102
3.2.2.2 Attempted synthesis of mixed diphosphite 'npn' (**3.22**)... 105
3.3 Synthesis of cyclic aryl phosphites derived from dimethyl-1,1'-binaphthyl-2,2'-dihydroxy-3,3'-dicarboxylate (**3.3**)..... 107
3.4 Discussion of ^{31}P NMR chemical shifts..... 110
3.5 Coordination chemistry of cyclic aryl diphosphites 112
3.5.1 Complexes of tris(9,9'-biphenanthryl-10,10'-diyl)diphosphite 'biphenanthrite' (**3.4**)..... 112

3.5.1.1 Dichloroplatinum(II) complexes..... 112
3.5.1.2 Platinum(0) complex of the (*R,S,R*) / (*S,R,S*)-diastereomer..... 118
3.5.2 Complexes of bis(9,9'-biphenanthryl-10,10'-diyl)-μ-(1,1'-binaphthyl-2,2'-diyl)diphosphite 'pnp' (**3.5**) 119
3.5.2.1 Dichloroplatinum(II) complexes..... 119
3.5.2.2 Dichloropalladium(II) complexes..... 121
3.5.2.3 Rhodium(I) complexes 122
3.6 Asymmetric hydroformylation of styrene derivatives catalysed by rhodium(I) complexes of cyclic aryl diphosphites..... 123

Chapter 4: Asymmetric Hydrogenation of α-Enamides: Mechanism and Catalytic Results

4.1 Introduction to the transition metal-catalysed hydrogenation of olefins..... 128
4.1.1 General mode of action of cationic rhodium(I) complexes [Rh(diene)L_2]X in the hydrogenation of simple olefins 128
4.1.2 The mechanism of asymmetric induction in hydrogenation reactions catalysed by cationic rhodium(I) complexes [Rh(diene)L_2]X..... 133
4.1.3 State-of-the-art asymmetric hydrogenation systems..... 147
4.2 Cationic rhodium(I)-phosphonite complexes as catalysts for asymmetric hydrogenation..... 151
4.2.1 Monophosphonites 154
4.2.2 Bidentate phosphonites 158
4.3 Cationic rhodium(I)-diphosphite complexes as catalysts for asymmetric hydrogenation..... 165

Chapter 5: Experimental

E.1 General experimental details..... 169
E.2 Chapter 2: Phosphonites: Synthesis and Coordination Chemistry..... 170
E.3 Chapter 3: Cyclic Aryl Diphosphites: Synthesis, Coordination Chemistry and Application in Asymmetric Hydroformylation 183
E.4 Chapter 4: Rhodium(I) Complexes of Phosphonites and Phosphites as Catalysts for the Asymmetric Hydrogenation of α-Enamides..... 192

References.....194

ABBREVIATIONS

General

Ac	acetyl
acac	acetylacetonate
aq	aqueous
Ar	aryl
Bn	benzyl
Boc	*tert*-butoxycarbonyl
b.p.	boiling point at ^{o}C at 760 mmHg pressure, unless otherwise noted
^{n}Bu	*normal*-butyl
^{t}Bu	*tert*-butyl
Bz	benzoyl
cod	*cis,cis*-1,5-cyclooctadiene
d	day(s)
dmso	dimethyl sulphoxide
dpm	dipivaloylmethane
ee	enantiomeric excess
eq	equivalent(s)
Et	ethyl
GC	Gas Chromatography
h	hour(s)
L	ligand
M	metal
Me	methyl
min	minute(s)
mol equiv	mole equivalent(s)
m.p.	melting point in ^{o}C
nb	norbornene
Ph	phenyl
^{i}Pr	*iso*-propyl
R	alkyl or aryl
RT	room temperature
S	solvent
Tf	trifluoromethanesulphonyl
THF	tetrahydrofuran
Ts	*para*-toluenesulphonyl
xs	excess

NMR data

NMR	Nuclear Magnetic Resonance
p.p.m.	parts per million
s	singlet
br s	broad singlet
d	doublet
dd	doublet of doublets
ddd	doublet of doublets of doublets
t	triplet
dt	doublet of triplets
td	triplet of doublets
m	multiplet
{^{1}H}	proton decoupled
quin	quintet
δ	chemical shift (in p.p.m.)
J	coupling constant

Mass spectrometry data

CI	Chemical Ionisation
EI	Electron Impact
FAB	Fast Atom Bombardment
m/z	mass/charge

Infra-red spectrometry data

IR	Infra-red
cm^{-1}	wavenumbers
υ	stretching frequency

Chapter 1

Introduction

1.1 Introduction

This thesis is concerned with the development of new catalysts for the asymmetric hydrogenation of α-enamides and the asymmetric hydroformylation of styrene derivatives. The ligands reported herein contain the phosphacycle moieties (**1.1**) and (**1.2**) derived from the corresponding biphenols.

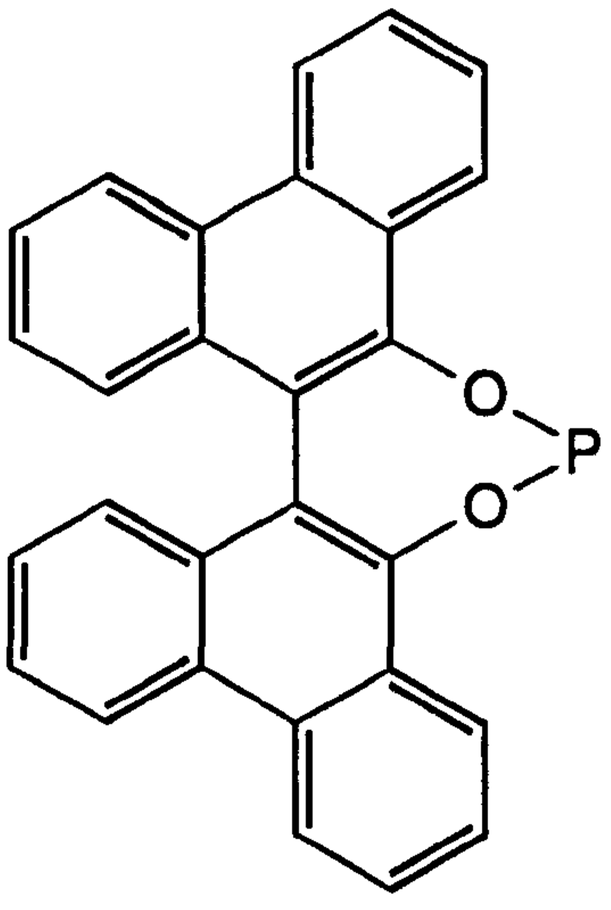

(1.1)

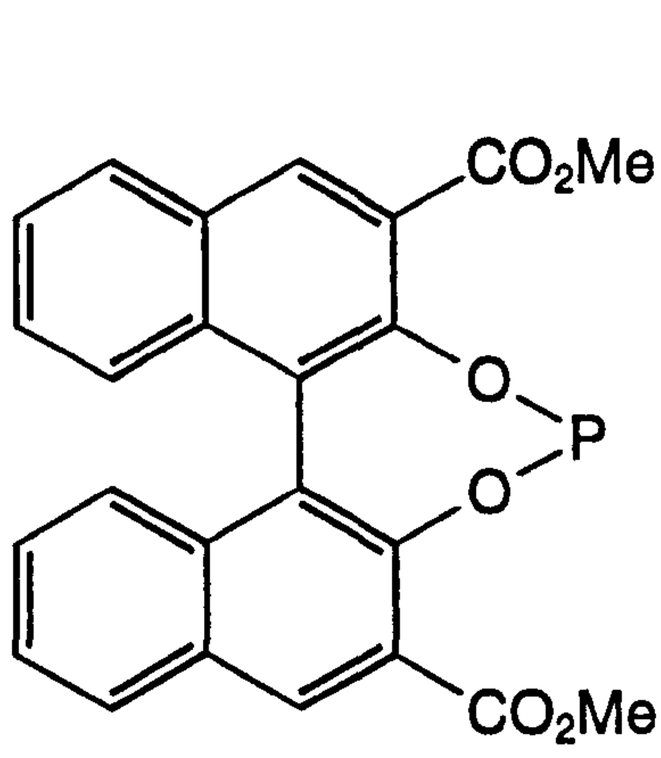

(1.2)

There is a marked twist about the central biaryl C-C bond and rotation about this bond is prevented by steric interactions between the *peri* protons. Thus, these diols are chiral. Chirality in biphenols such as 9,9'-biphenanthryl-10,10'-diol (**1.3**) (referred to hereafter as biphenanthrol) is assigned by viewing the biphenol group along the central biaryl C-C bond, aligning the oxygen on the aromatic ring in the foreground so that it is pointing downwards and following the atom priorities down from top to bottom, see Figure 1.1.

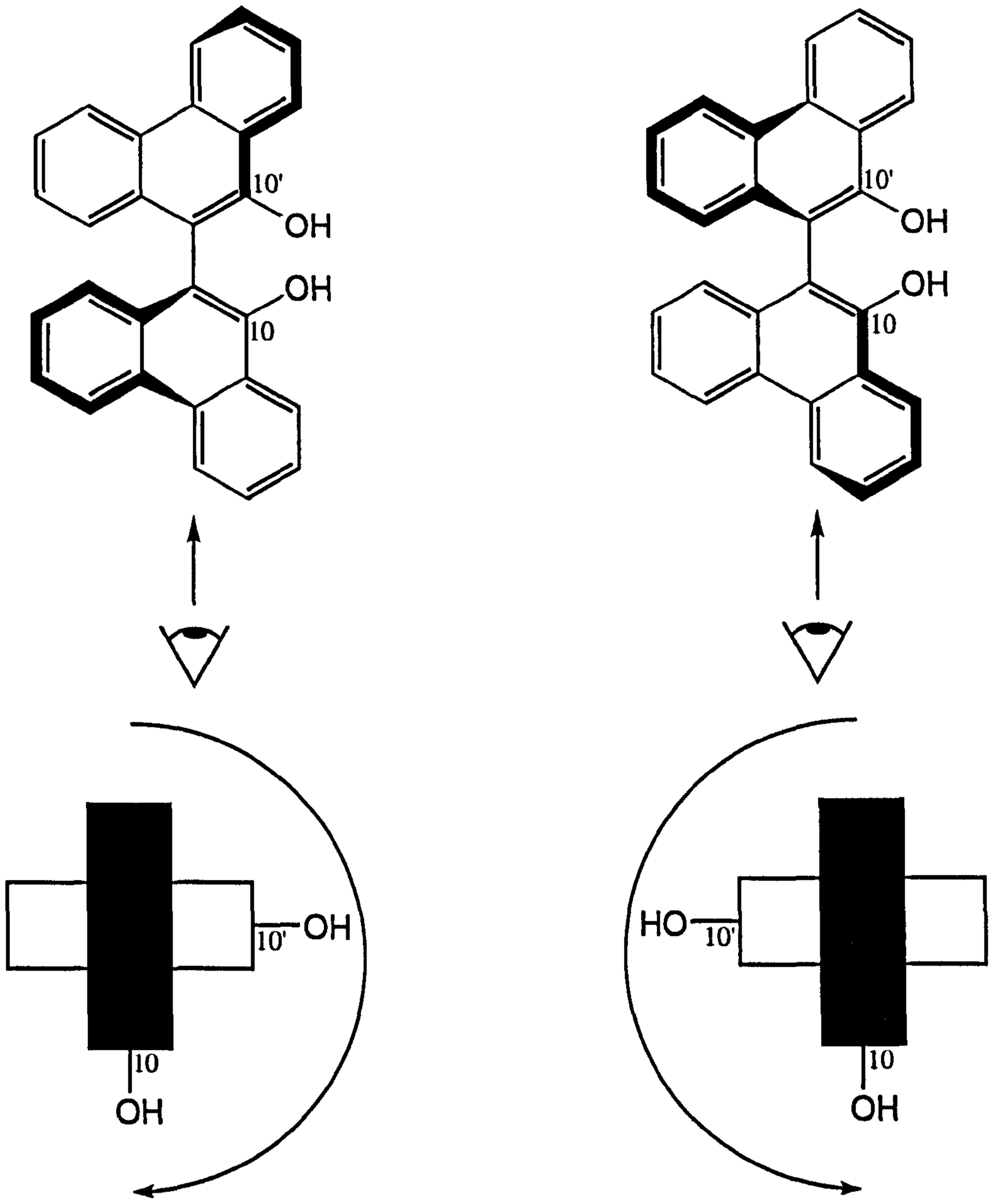

(*R*)-biphenanthrol (**1.3**) (*S*)-biphenanthrol (**1.3**)

Figure 1.1: Assignment of chirality in biphenols such as biphenanthrol (**1.3**)

In the first part of this Chapter the importance of the asymmetric hydrogenation of α-enamides is discussed but the mechanism of this reaction and the state-of-the-art ligand systems are treated in depth in Chapter 4. A summary of the use of chiral phosphonites in asymmetric catalysis will be presented, including a review of the few monodentate phosphorus(III) ligands that are successful in this area. This will be followed by an examination of the use of phosphites in asymmetric hydrogenation.

In the second part of this Chapter the asymmetric hydroformylation reaction of styrene derivatives is discussed in terms of the importance of this process and recent developments in this area with special attention given to cyclic diphosphites.

This Chapter concludes with a summary of the aims of this project.

1.2 The importance of the asymmetric hydrogenation reaction of α-enamides

Enantiomerically pure compounds are increasingly important in the pharmaceutical, agrochemical and cosmetics industry because for several applications only one of the enantiomers exhibits the desired biological activity, whilst the optical antipode is inactive or may even cause the reverse or an alternative, detrimental effect.[1,2,3] In general, for commercial purposes catalysts inducing a selectivity exceeding 90% are required.[4]

Unnatural α-amino acids (i.e. those that are not one of the twenty genetically-encoded L-amino acids) are playing an increasingly prominent role in pharmaceutical research since they surmount many of the limitations associated with proteinogenic amino acids. Peptide properties such as potency, transport, resistance to proteolytic breakdown and absolute bioavailability may be vastly improved through incorporation of unnatural α-amino acids.[5,6] Thus, unnatural α-amino acids are employed in the design of novel biologically active peptides and peptidomimetic therapeutics.[7,8] In addition, they are also valuable synthetic intermediates[9,10] and auxiliaries[11] in their own right for the production of other chiral compounds and have recently been employed in the generation of diverse combinatorial libraries.[12] With such practical application, the need for more convenient synthetic access to these compounds continues to escalate. Indeed it was the desire to obtain enantiomerically pure α-amino acids that provided the initial impetus for the research into asymmetric catalytic hydrogenations over thirty years ago.[13,14] The goal is clear: to develop a catalyst that will allow the enantioselective addition of hydrogen to the C=C double bond of an α-enamide substrate, see Equation 1.1.

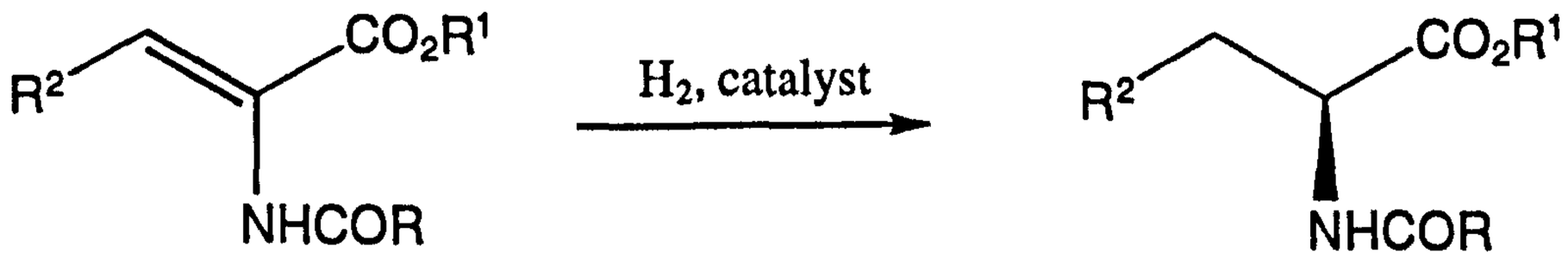

Equation 1.1

Despite the significant challenges presented by this goal, continuous refinement of catalysts and ligands has led to the emergence of asymmetric hydrogenation as one of the most practicable and cost-effective routes to unnatural α-amino acids in essentially enantiomerically pure form. Cationic rhodium(I) complexes of the type [Rh(diene)(diphosphine)]X (diene = *cis,cis*-1,5-cyclooctadiene or *cis,cis*-2,5-norbornadiene, diphosphine = chiral diphosphine, X = non-coordinating anion such as BF_4^-, SbF_6^-, OTf^- *etc.*) are the most efficient and enantioselective catalysts for this

process, see Chapter 4. Indeed, asymmetric hydrogenation has now advanced to the level where it has been exploited by industry; examples include Monsanto's commercial production of L-Dopa (**1.4**) for the treatment of Parkinson's disease[15] and the multi-ton synthesis of (*S*)-phenylalanine for use in the sweetener Aspartame (**1.5**).[16]

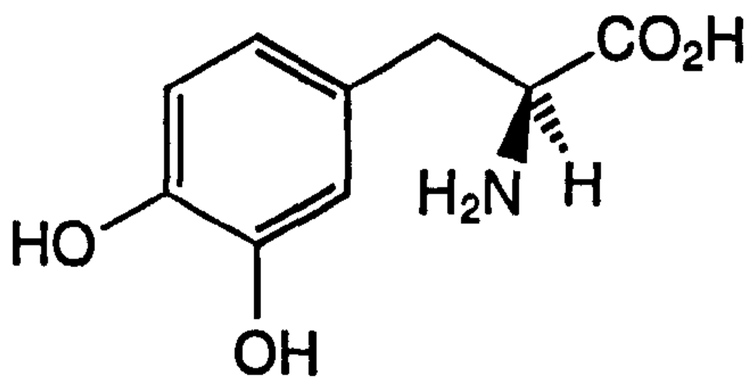

L-Dopa (**1.4**)

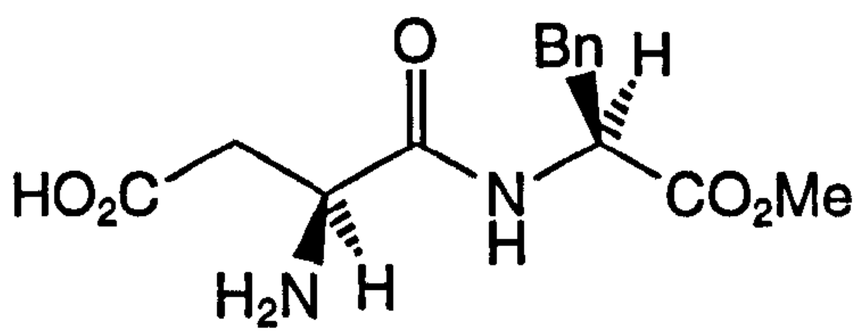

Aspartame (**1.5**)

Despite these successes, cumbersome optical resolutions still operate to a large extent in industry for the production of fine chemicals. This is at least partly due to the fact that the chiral diphosphine ligands are generally synthesised *via* challenging, multistep sequences with the result that few are commercially available or, for those that are, tend to be expensive. With this in mind, there is a continual search for new ligands for this process that can be easily synthesised in high yields from cheap, readily available starting materials.

Recently, readily synthesised chiral phosphonites[17,18] and phosphites[19,20] for asymmetric hydrogenation have been reported. In principle the many commercially available chiral diols allow the synthesis of a wide range of these ligands (Scheme 1.1).

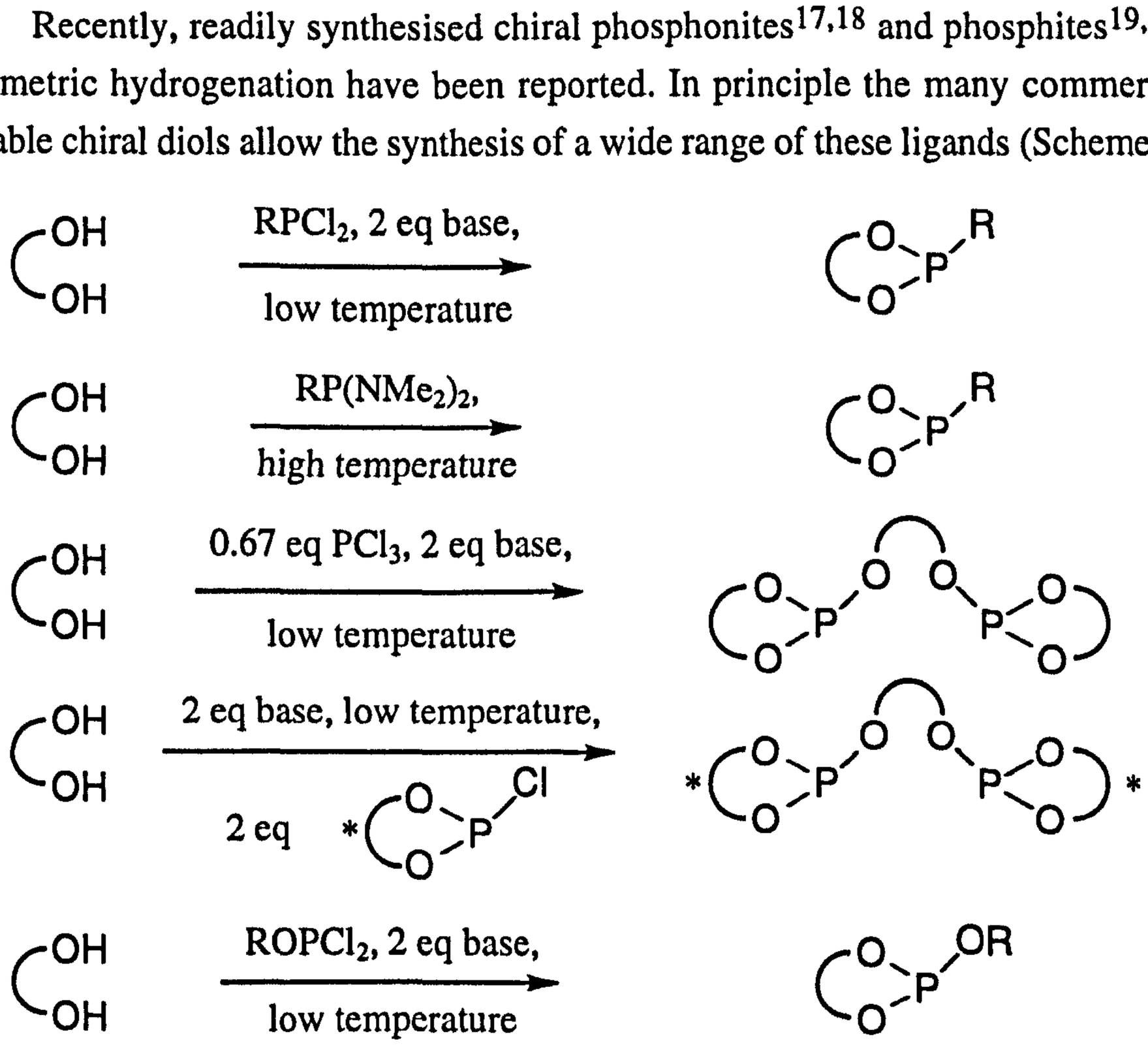

Scheme 1.1: General methods for the synthesis of phosphonites and phosphites

The application of chiral phosphonites as ligands for asymmetric catalysis and the use of chiral phosphites for the asymmetric hydrogenation of α-enamides are still relatively unexplored areas. The examples that have appeared in the literature to date will now be discussed in detail.

1.3 Chiral phosphonites as ligands in asymmetric catalysis

1.3.1 Monophosphonites

In 1981, Richter reported the syntheses of the first chiral phosphonites (**1.6**) and (**1.7**) by reaction of $PhPCl_2$ with diethyl tartrate or 2-(*R*)-3,3-dimethyl-1,2-butanediol respectively in the presence of pyridine.[21]

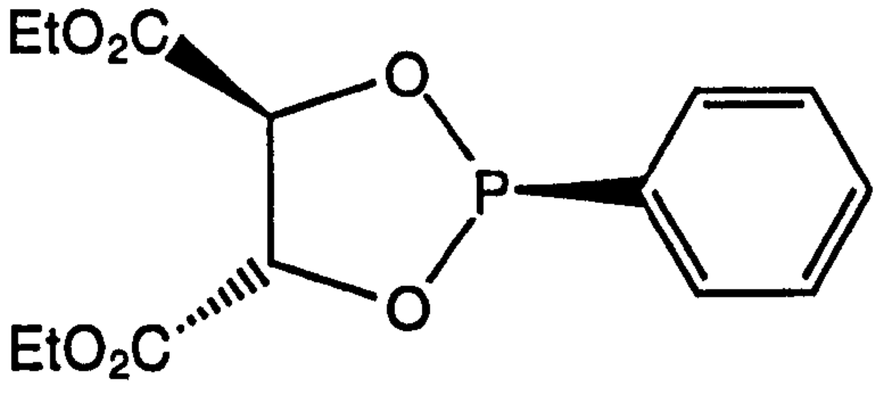

(1.6)

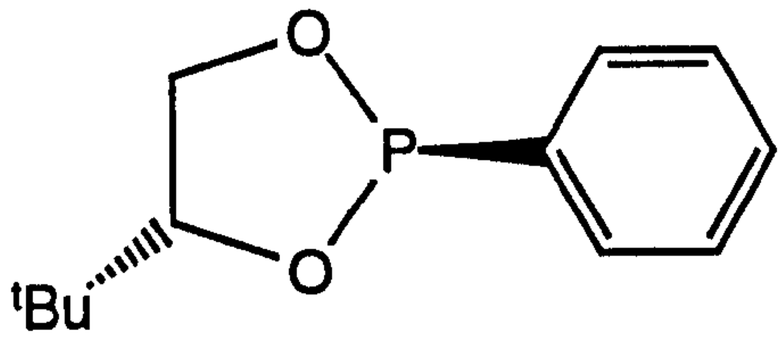

(1.7)

Later, in 1993, the Taddol-derived phosphonites (**1.8**) were synthesised by Seebach and reported to give useful catalysts.[22]

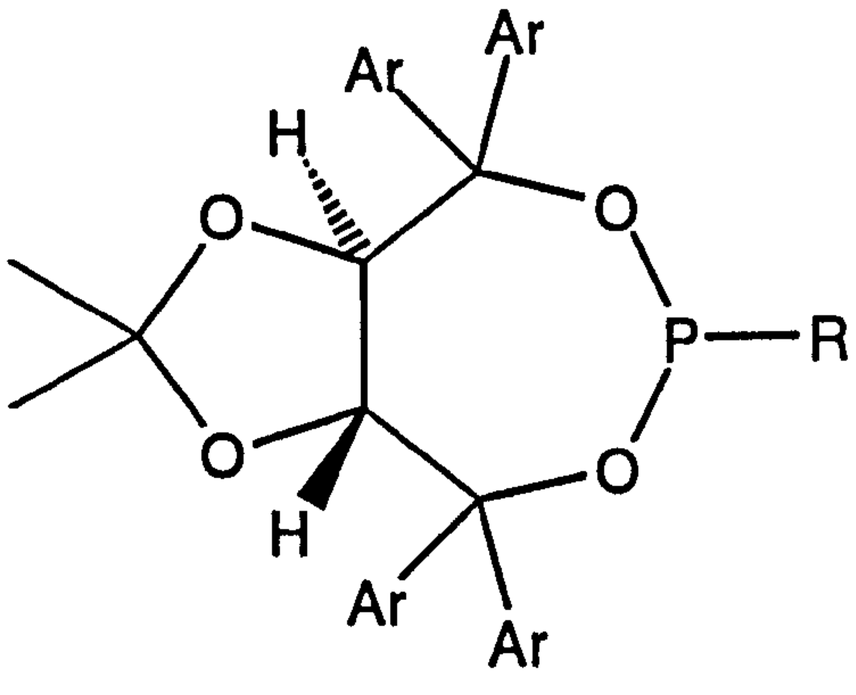

Ar = phenyl; 2-naphthyl

R = Me; Ph; C_6H_4Me-4; $C_6H_2Me_3$-2,4,6; 2-naphthyl

Taddol-derived phosphonites (**1.8**)

Rhodium complexes of these phosphonites were tested for the asymmetric hydroformylation and hydroboration of styrene and the asymmetric hydroformylation of 2-butene, whilst palladium complexes were tested for the asymmetric hydrosilylation of styrene.[23] The catalysts were very regioselective (no product resulting from 1-butene was observed and for all cases with styrene the product resulting from Markovnikov addition was greatly favoured) but the enantioselectivities were poor. However, the

rhodium complexes gave excellent ee's (87%) for the asymmetric hydrosilylation of aromatic ketones, see Scheme 1.2.

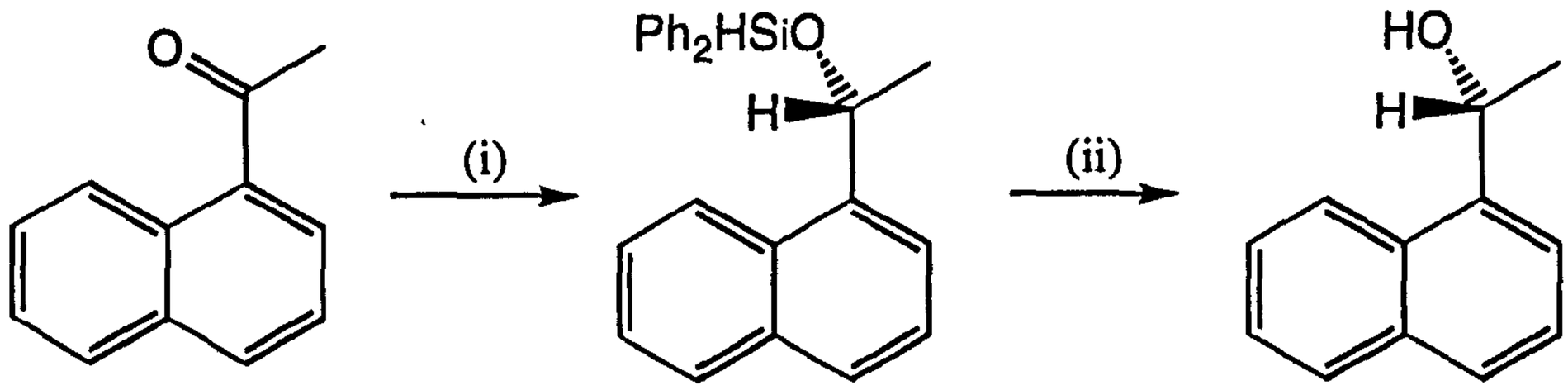

Reaction conditions: 87% ee, 92%
(i) 0.01 eq [{Rh(cod)Cl}$_2$], 0.1 eq (**1.8**) (R = Ar = 2-naphthyl), Ph_2SiH_2 (1.2 eq), benzene, 0-20 °C, 10-15 h
(ii) TsOH in MeOH

Scheme 1.2: Asymmetric hydrosilylation of aromatic ketones catalysed by rhodium(I) complexes of Taddol-derived monophosphonites (**1.8**)

More recently, Scharf *et al.* have published the synthesis of a series of chiral cyclic monophosphonites (**1.9**), (**1.10**) and (**1.11**).[24]

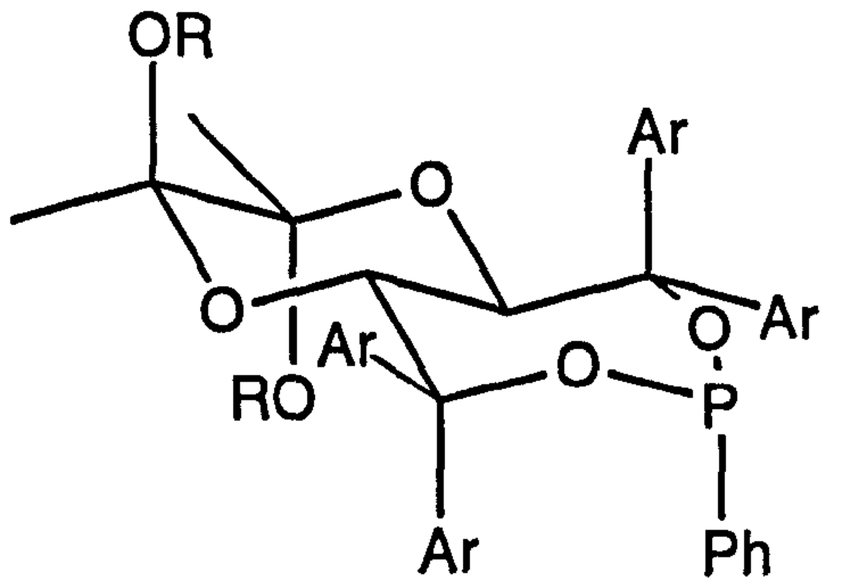

(1.9)

R = Me, Et; Ar = Ph, 2-naphthyl

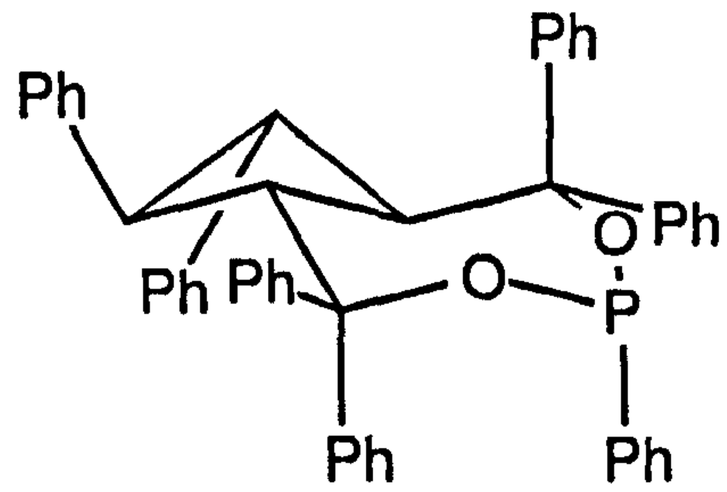

(1.10)

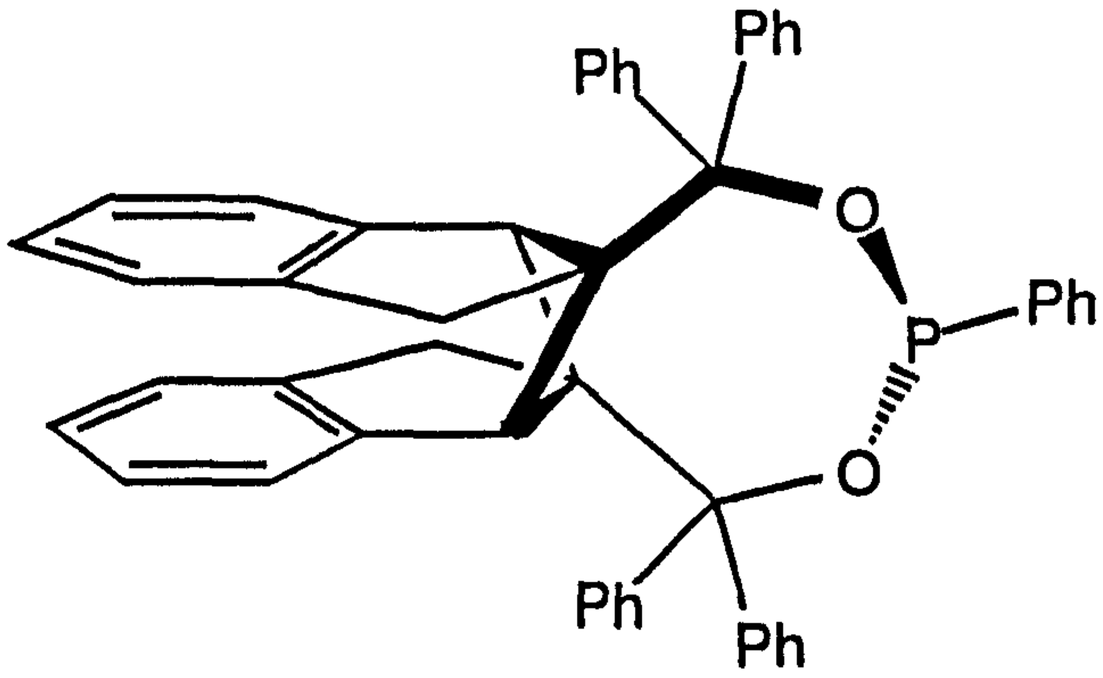

(1.11)

Rhodium(I) complexes of these ligands have been evaluated in the asymmetric hydrosilylation of ketones, with the attainment of enantioselectivities up to 82% for acetophenone (**1.12**) and 86% for pivalophenone (**1.13**).[24]

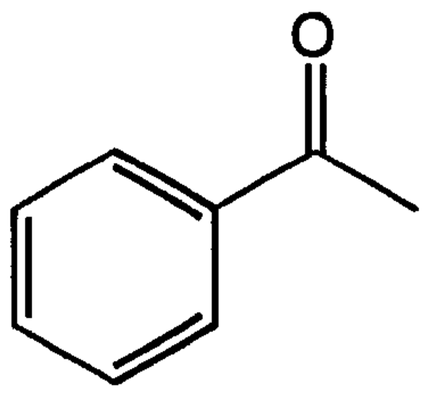

(1.12)

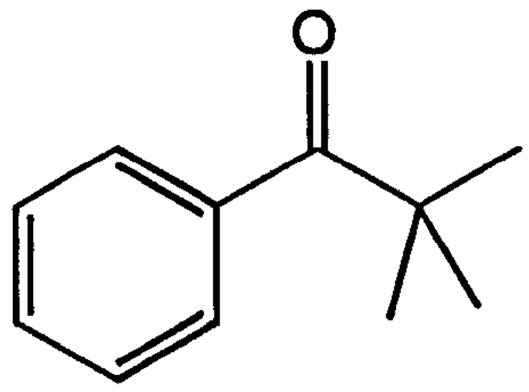

(1.13)

It therefore seems that there is great potential for the use of monophosphonites in the asymmetric hydrosilylation reaction of alkyl aryl ketones. However, it should be noted that asymmetric hydrosilylation appears to be an exception to the rule that enantioselective catalysis is generally much more effective with bidentate, preferably C_2-symmetric ligands since high enantioselectivities have been observed using monodentate phosphorus(III) ligands for several hydrosilylation reactions.[25-31] Further, it has been shown that the use of bidentate phosphorus ligands normally does not lead to better enantioselectivities for this process.[32-35] However, to the best of our knowledge monophosphonites had not been previously employed in the asymmetric hydrogenation of α-enamides until recent work in our group[36] showed that a rhodium(I) complex of the cyclic aryl monophosphonite (**1.14**), derived from binaphthol and $PhPCl_2$,[37] was an efficient catalyst for the asymmetric hydrogenation of methyl-2-acetamidoacrylate (**1.15**), see Equation 1.2.

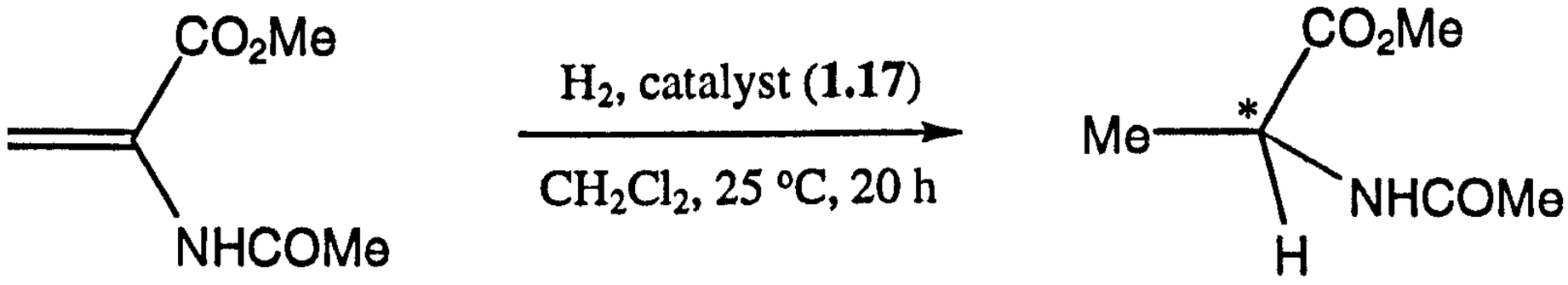

(1.15)

(1.16)

100% conversion, 73% ee

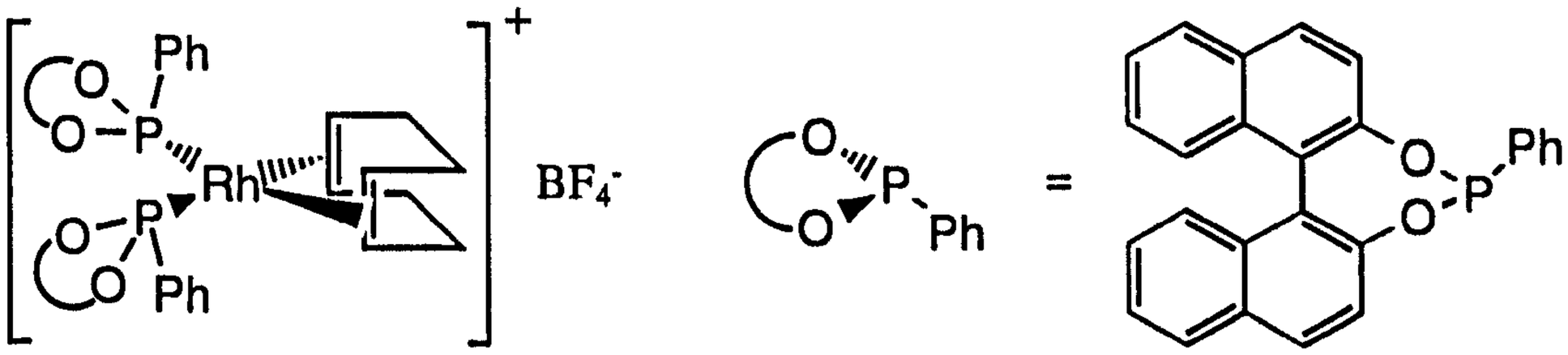

Catalyst: (**1.17**)

(1.14)

Equation 1.2

This was the highest enantioselectivity for the asymmetric hydrogenation of methyl-2-acetamidoacrylate (**1.15**) obtained using a monodentate phosphorus(III) ligand. This exciting result is discussed in more detail in Section 4.2.1. However, it is appropriate now to mention briefly the few other monodentate phosphorus(III) ligands that have been successfully employed in asymmetric catalysis.

1.3.1.1 Monodentate phosphorus(III) ligands in asymmetric catalysis

Perhaps the most successful monodentate phosphorus(III) ligand to date is Hayashi's monophosphine MOP (**1.18**).[38,39] A palladium complex of this ligand catalyses the asymmetric hydrosilylation of alkyl-substituted terminal olefins with excellent regio- (favouring Markovnikov addition) and enantioselectivities (>94% ee),[39] see Scheme 1.3.

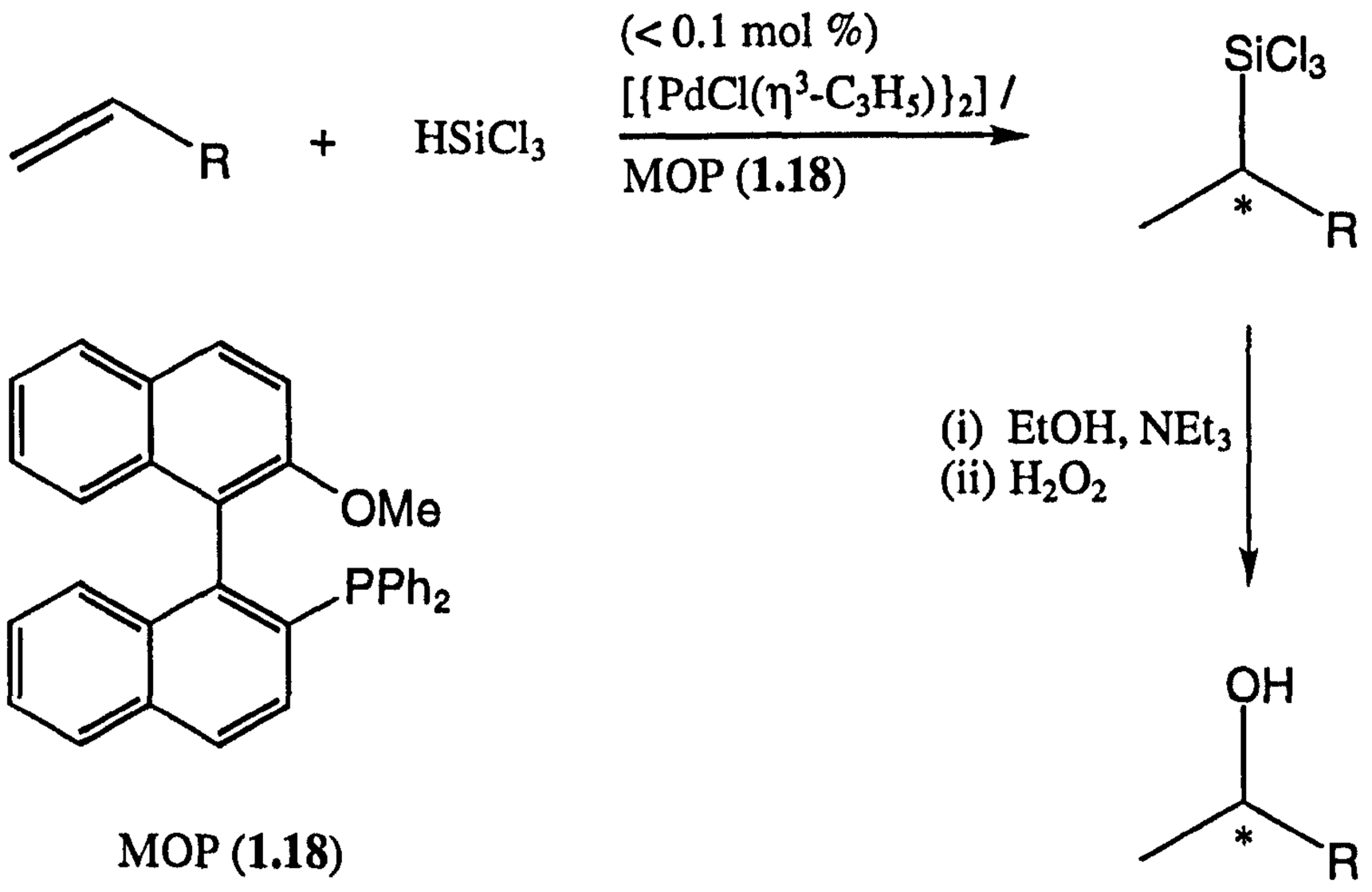

MOP (**1.18**)

Scheme 1.3: The asymmetric hydrosilylation of alkyl-substituted terminal olefins catalysed by a palladium complex of MOP (**1.18**)

Wills has recently reported the synthesis of a range of diazaphospholidines (**1.19**) which are P-N analogues of the P-O phosphonites.[40]

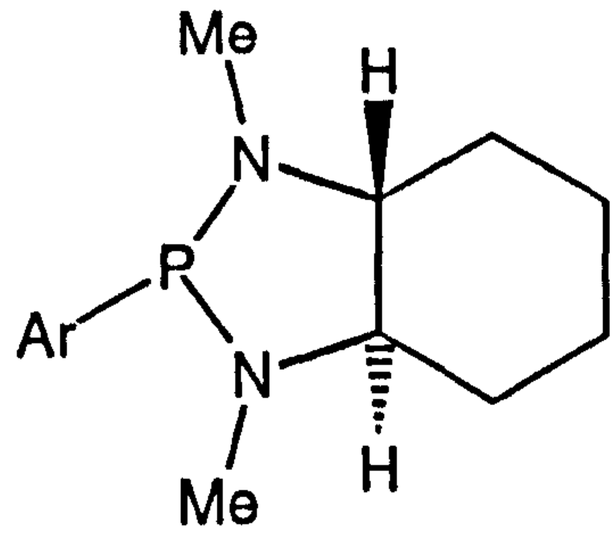

(1.19)

These ligands have been employed in asymmetric allylic substitution reactions, see Equations 1.3 and 1.4, resulting in high yields and enantioselectivities.[40]

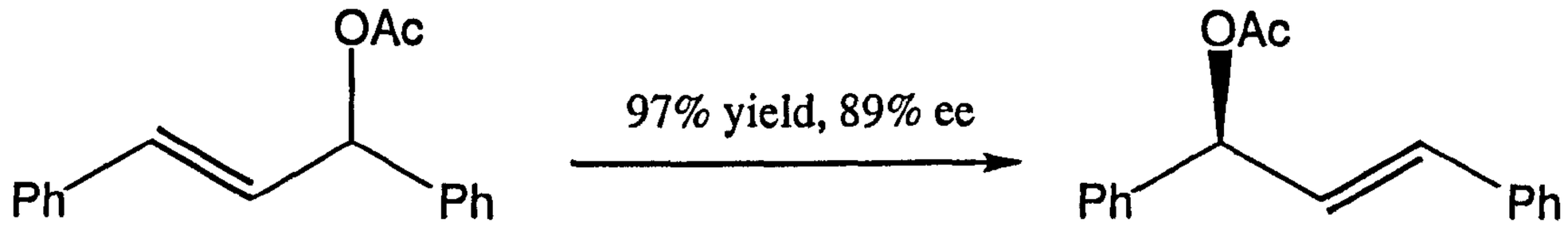

Reaction conditions:
$[\{Pd(\eta^3\text{-}C_3H_5)Cl\}_2]$, dimethyl malonate, $(Me_3Si)N{=}CMe(OSiMe_3)$, NaOAc, CH_2Cl_2, (**1.19**) (Ar = C_6H_4OMe-2)

Equation 1.3

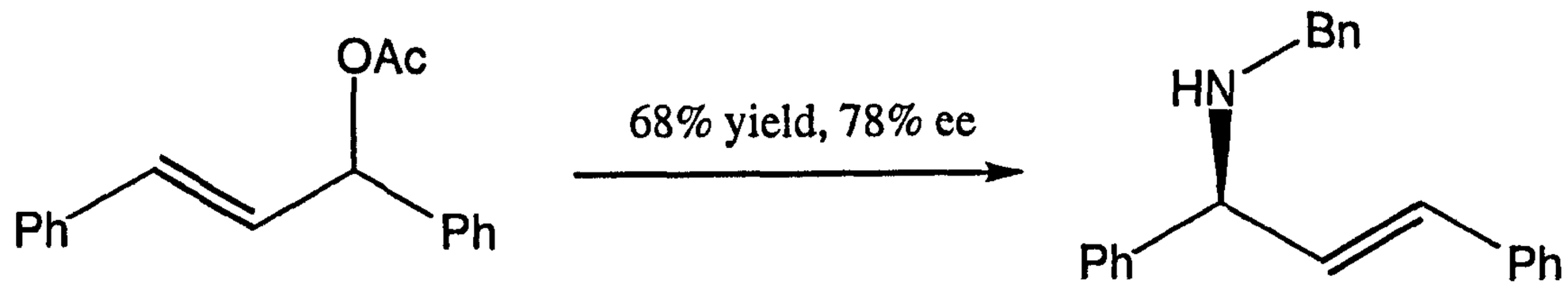

Reaction conditions:
$[\{Pd(\eta^3\text{-}C_3H_5)Cl\}_2]$, $BnNH_2$, NaOAc, CH_2Cl_2, (**1.19**) (Ar = C_6H_4OMe-2)

Equation 1.4

The monophosphonites of Seebach[22,23] and Scharf[24] and their application in asymmetric hydrosilylation have already been mentioned. However, the only two monodentate phosphorus(III) ligands in the literature to have been successfully employed in asymmetric hydrogenation are the monodentate phosphine Camp (**1.20**) and the monophosphinite (**1.21**).

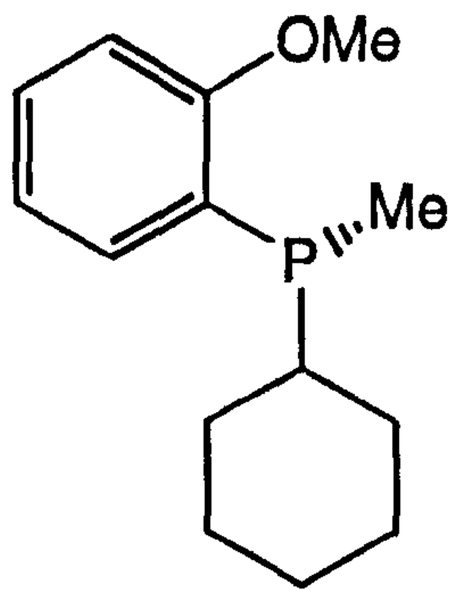

(1.20), Camp

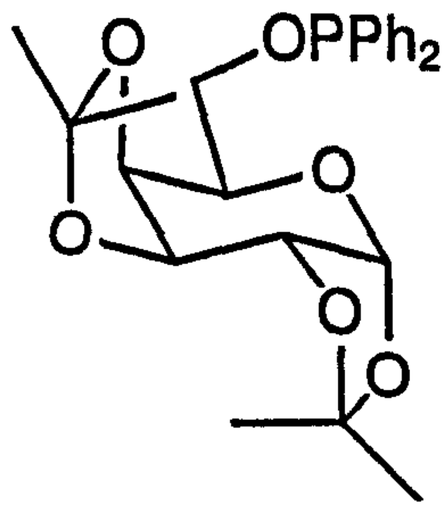

(1.21)

Enantioselectivities of 86% and 67% respectively were obtained in the asymmetric hydrogenation of (*Z*)-2-acetamidocinnamic acid (**1.22**).

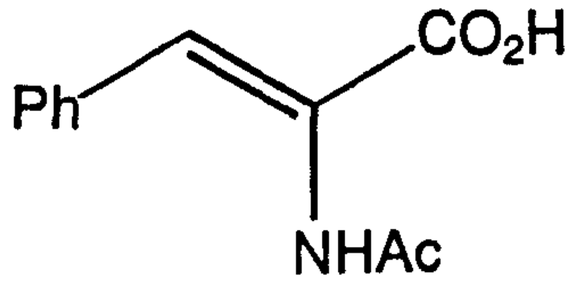

(1.22)

These results are considered in more depth in Section 4.1.3.

It is apparent that there are only a few successful applications of monodentate phosphorus(III) ligands in asymmetric catalysis. This makes the discovery of the monophosphonite (**1.14**) as a ligand for effecting the hydrogenation of α-enamides with high enantioselectivity all the more exciting and this result is the basis for the monophosphonite work that will be described in Sections 2.3.1 and 4.2.1.

1.3.2 Diphosphonites

Very little has been reported concerning chiral diphosphonites as ligands in transition metal-catalysed asymmetric reactions. Until recently, the enantioselectivities obtained were poor (0-32%).[41] However, in 1998 Dahlenburg *et al.* reported the synthesis of a range of chiral diphosphonites (**1.23**)-(**1.26**) from optically pure *trans*-1,2-bis(dichlorophosphino)cyclopentane (**1.27**),[17] see Equation 1.5.

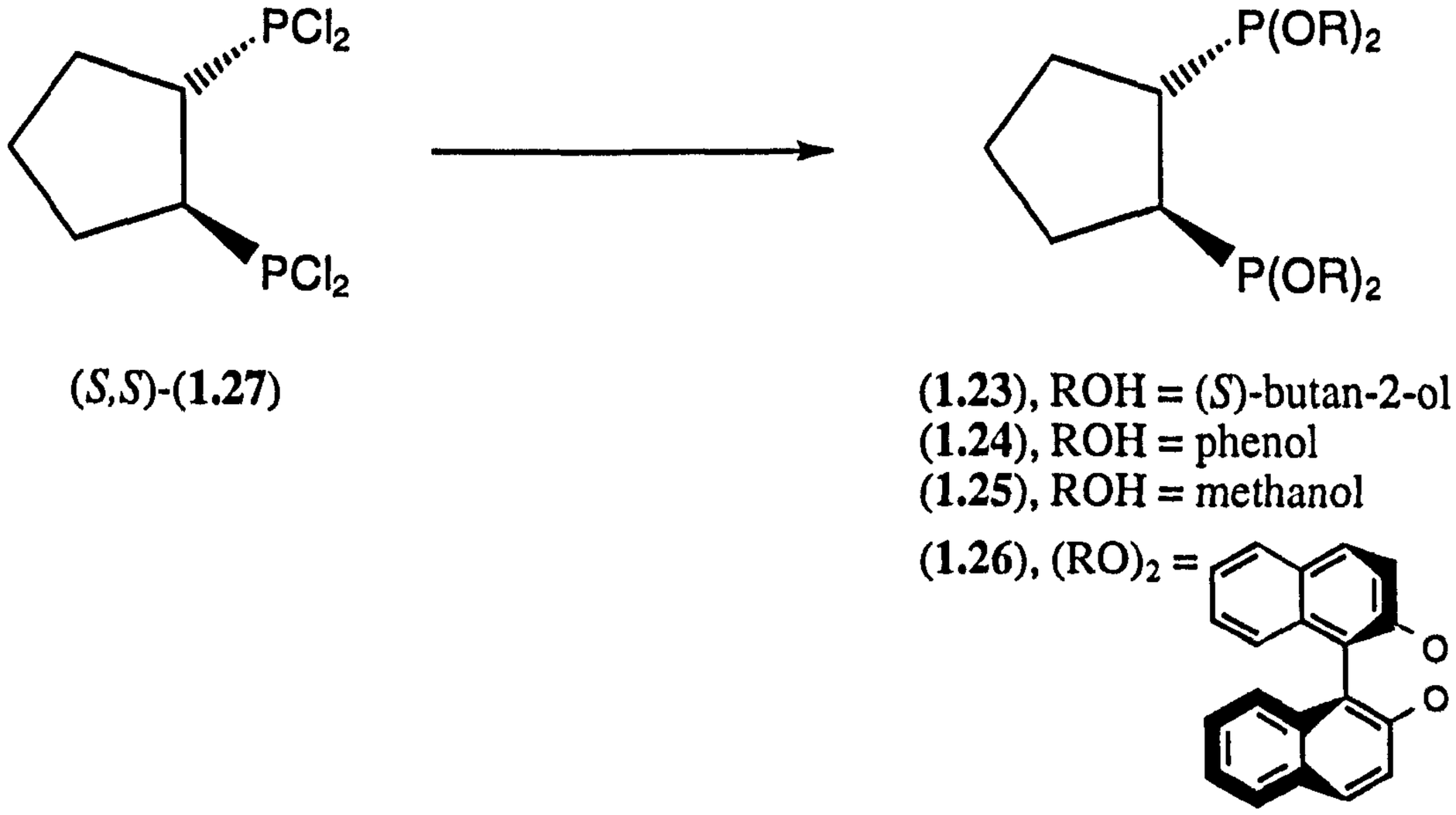

(*S,S*)-(**1.27**)

(**1.23**), ROH = (*S*)-butan-2-ol
(**1.24**), ROH = phenol
(**1.25**), ROH = methanol
(**1.26**), $(RO)_2$ =

Equation 1.5

Cationic rhodium(I) complexes of these ligands were tested as catalysts for the asymmetric hydrogenation of (*Z*)-2-acetamidocinnamic acid (**1.22**) with enantioselectivities up to 78% being reported.[17]

Reetz has also recently reported the syntheses of two optically pure diphosphonites (*R,R*)-(**1.28**) and (*R,R*)-(**1.29**).[18]

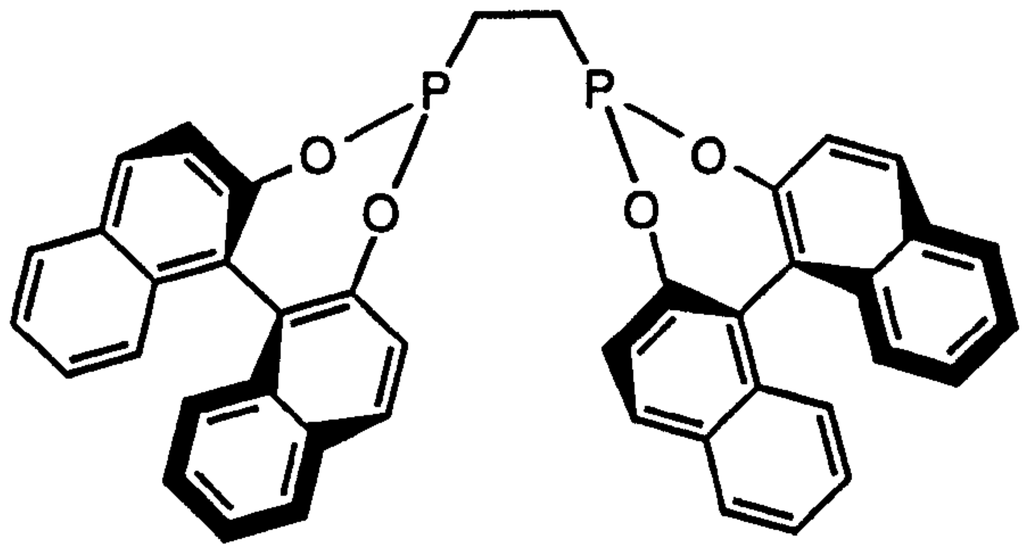

(*R,R*)-(**1.28**)

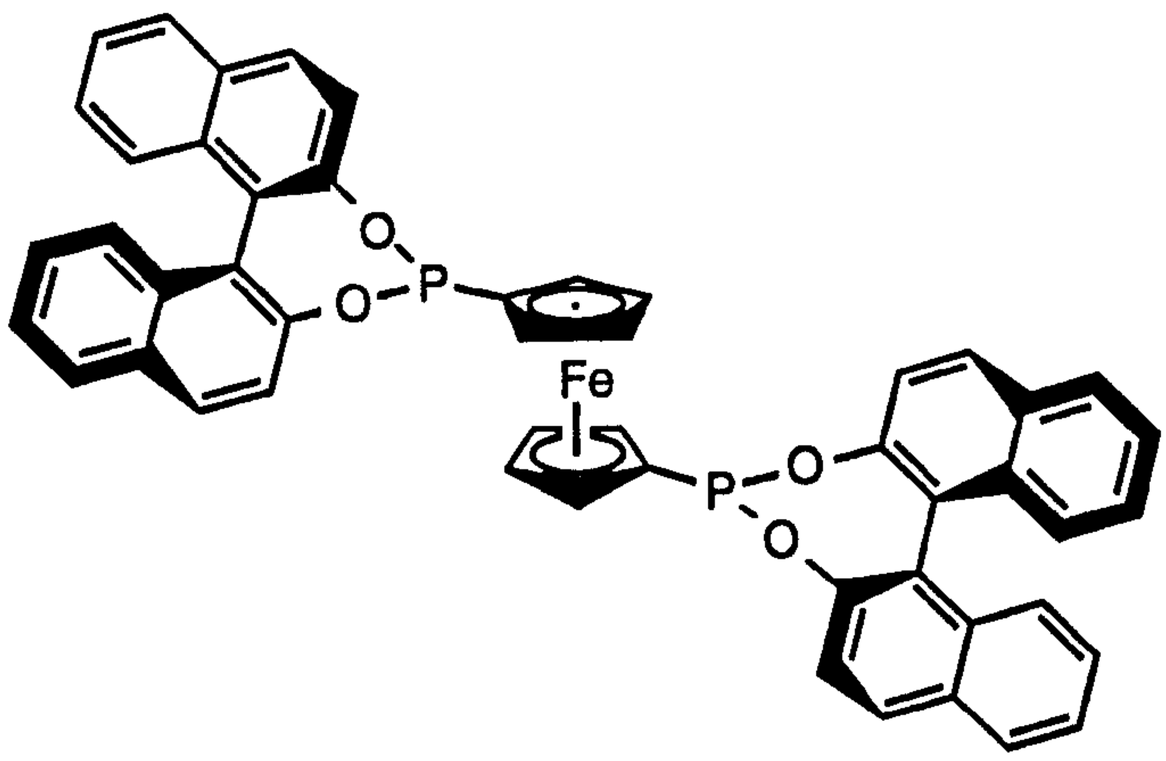

(*R,R*)-(**1.29**)

The rhodium(I) complexes of these chiral diphosphonites are excellent catalysts for the hydrogenation of the prochiral olefins (**1.30**) and (**1.15**), see Scheme 1.4, with complete conversion of substrate to product occurring with enantioselectivities in the range 90-99.5%.[18]

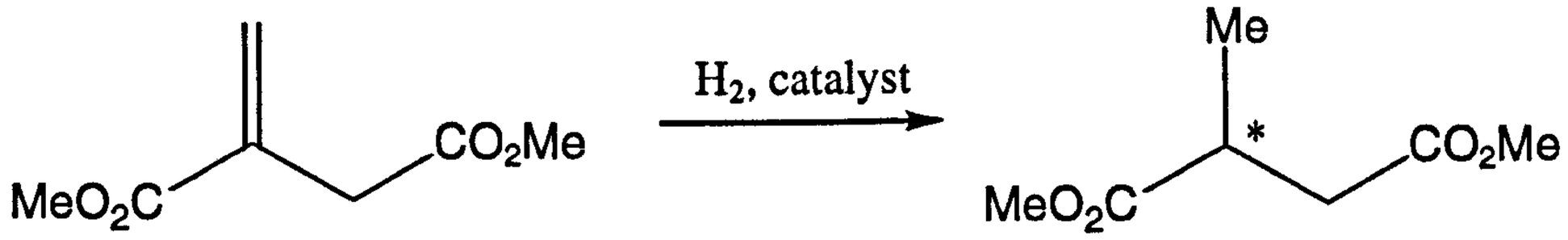

(1.30)

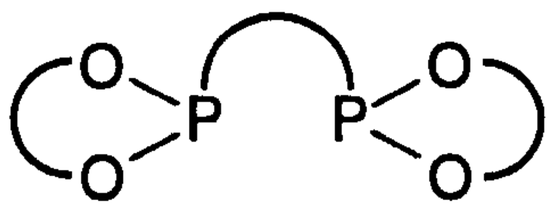

= (**1.28**); 100% yield, 97-99% ee
= (**1.29**); 100% yield, >99.5% ee

Catalyst:

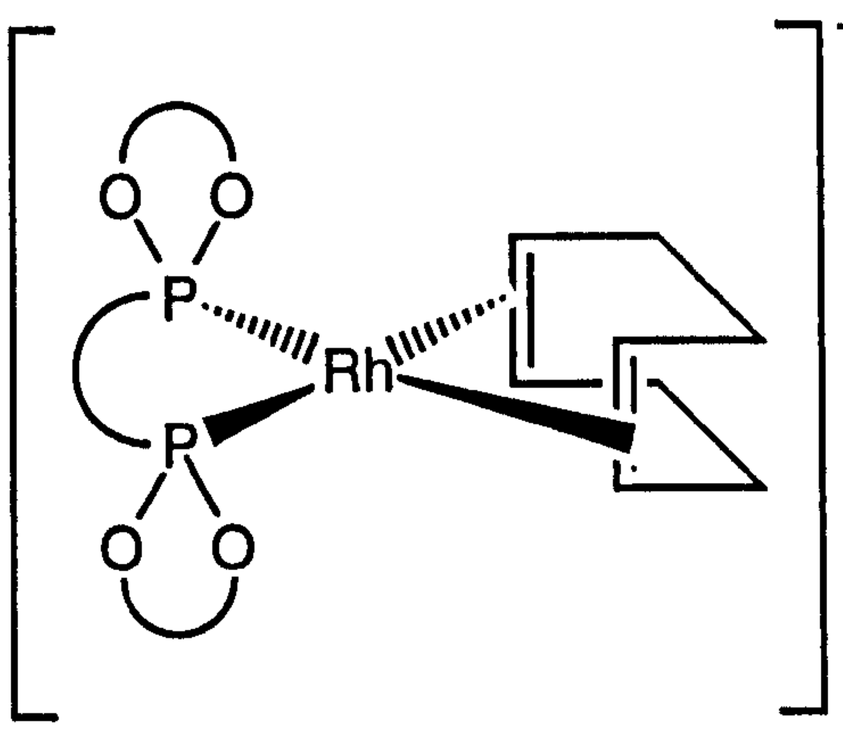

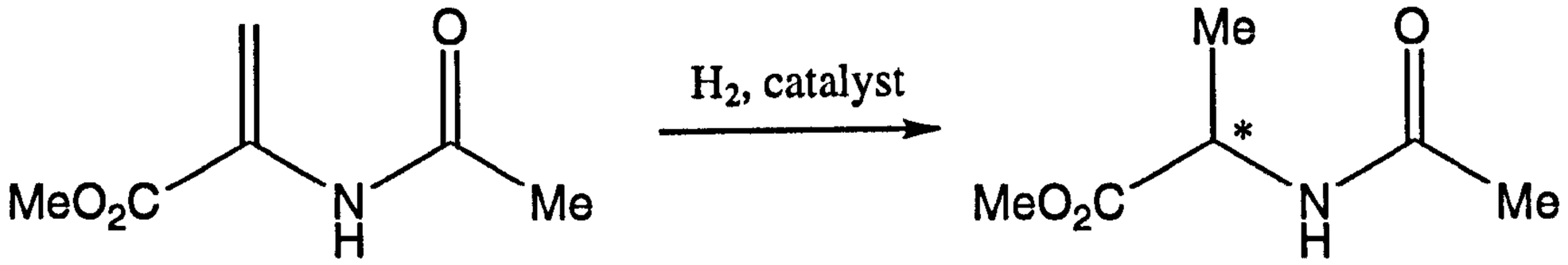

(1.15)

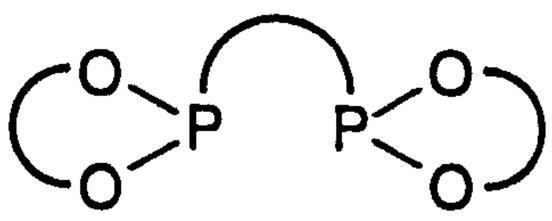

= (**1.28**); 100% yield, 90% ee
= (**1.29**); 100% yield, 99.5% ee

Scheme 1.4: Hydrogenation reactions catalysed by rhodium(I) complexes of Reetz's diphosphonite ligands (**1.28**) and (**1.29**)

Pastor has recently reported upon an extension of this work involving the synthesis of a range of sterically congested ferrocenyl diphosphonite ligands for use in transition metal-catalysed reactions.[42] However, the results obtained with the rhodium(I) catalyst derived from ligand (**1.28**) have prompted our research into diphosphonite chemistry, which is described in Sections 2.3.1 and 4.2.2.

1.3.3 Phosphinophosphonites

Non C_2-symmetric bidentate phosphorus ligands have become the focus of attention in recent years for application in transition metal-catalysed asymmetric synthesis.[43] Notable examples include the phosphinophosphite ligands (*R,S*)-Binaphos (**1.31**)[44,45] and (*S,R*)-Biphemphos (**1.32**).[46] The rhodium(I) complexes of these ligands are efficient catalysts for the hydroformylation of a variety of olefins[44-47] providing enantioselectivities up to 97%. These will be considered in more detail in Section 1.5.

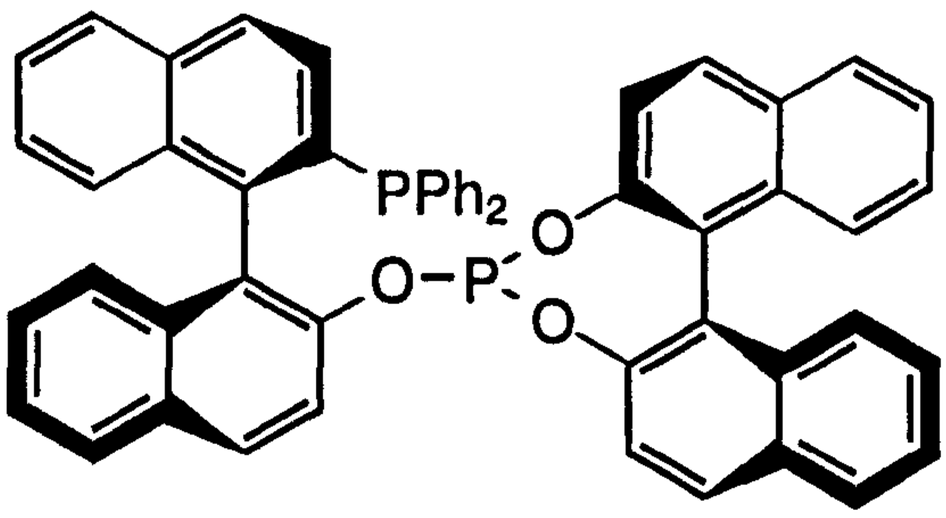

(*R,S*)-Binaphos (**1.31**)

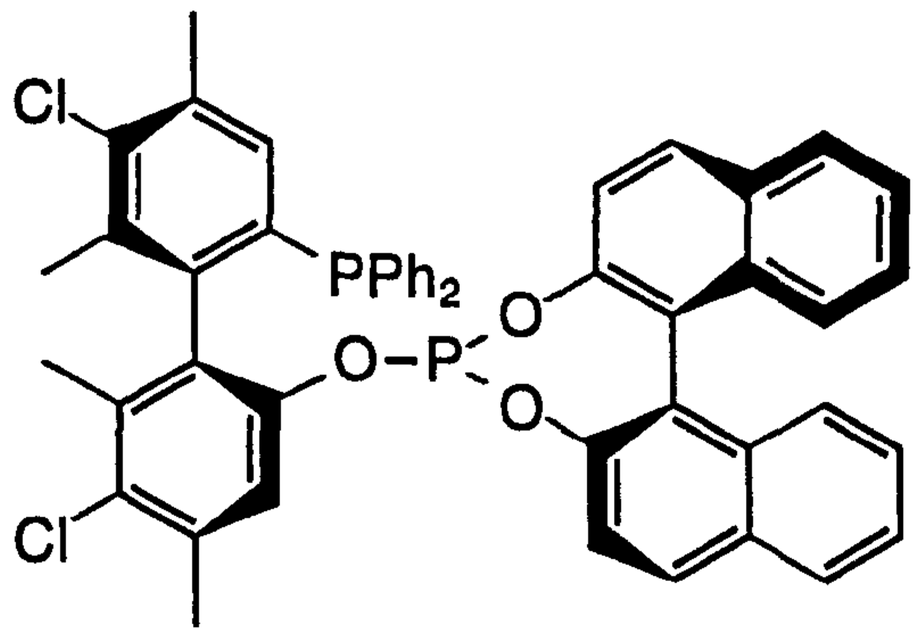

(*S,R*)-Biphemphos (**1.32**)

A range of aminophosphinephosphinite ligands such as (*R,S*)-Ephos (**1.33**)[48] and (*S*)-Valnop (**1.34**)[48,49] derived from naturally occurring amino alcohols has been tested for the asymmetric hydroformylation of styrene. These ligands give high conversions (82-86%), good regioselectivity for the branched isomer (>90%) and moderate enantioselectivity (30%).[48]

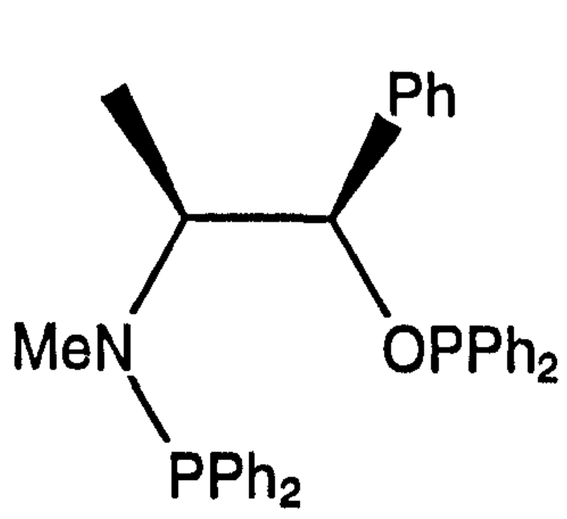

(*R,S*)-Ephos (**1.33**)

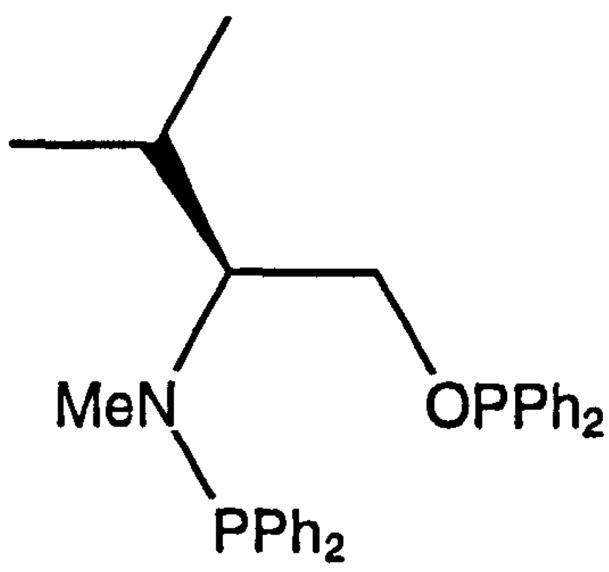

(*S*)-Valnop (**1.34**)

However, there were no examples of chiral mixed phosphinophosphonite ligands until 1998, when Harrison and Pringle synthesised the ligands (**1.35**) and (**1.36**).[50] Due to the extreme moisture-sensitivity of these ligands no applications in asymmetric catalysis have been achieved to date.

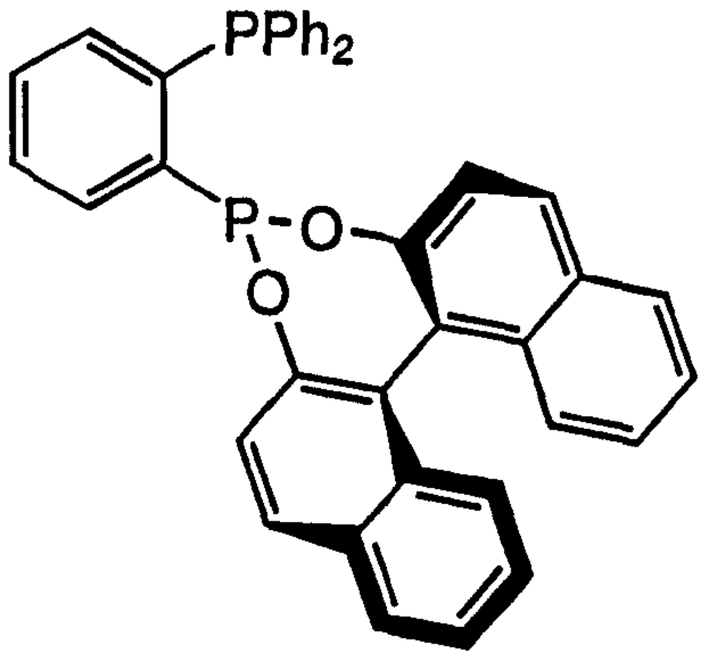

(*S*)-(**1.35**)

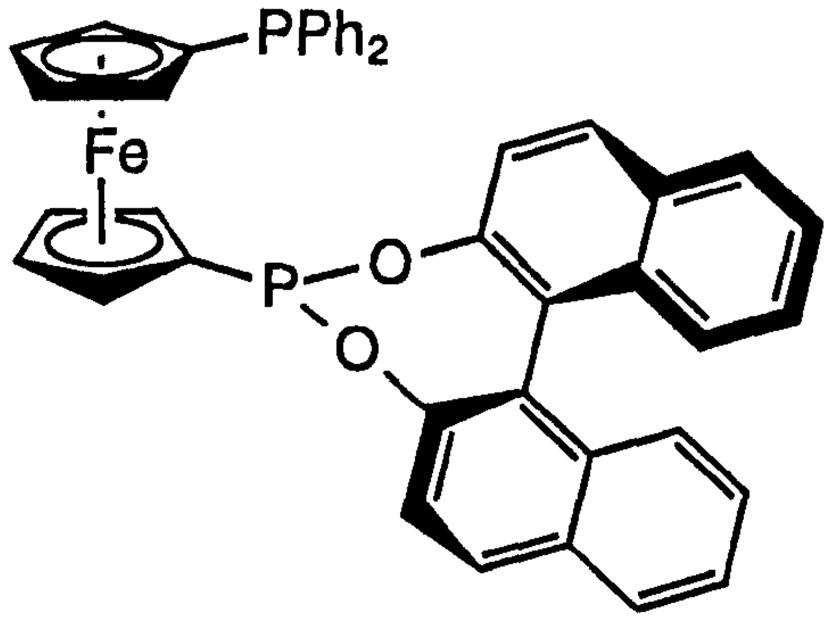

(*R*)-(**1.36**)

In 1998, Carraz and Pringle synthesised the mixed phosphinophosphonite ligand (**1.37**).[51] This ligand has not yet been tested for asymmetric catalysis but the ease with which it can be synthesised has led to the phosphinophosphonite work that we have undertaken, which is reported in Sections 2.3.2 and 4.2.2.

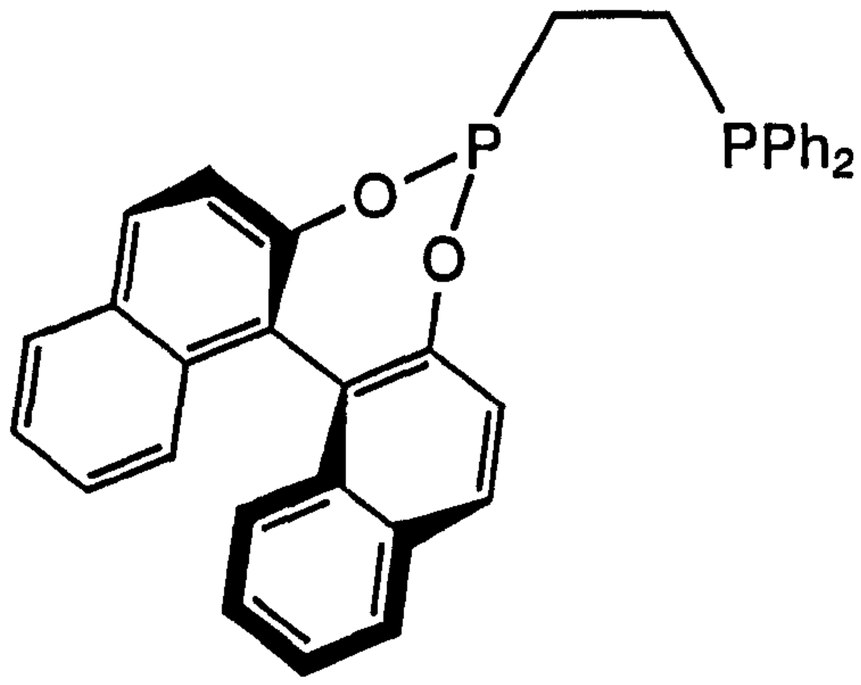

(*R*)-(**1.37**)

Very recently Knight independently reported the synthesis of the chiral phosphinophosphonite ligands (**1.35**) and (**1.38**).[52] Again no applications in asymmetric catalysis have been reported to date.

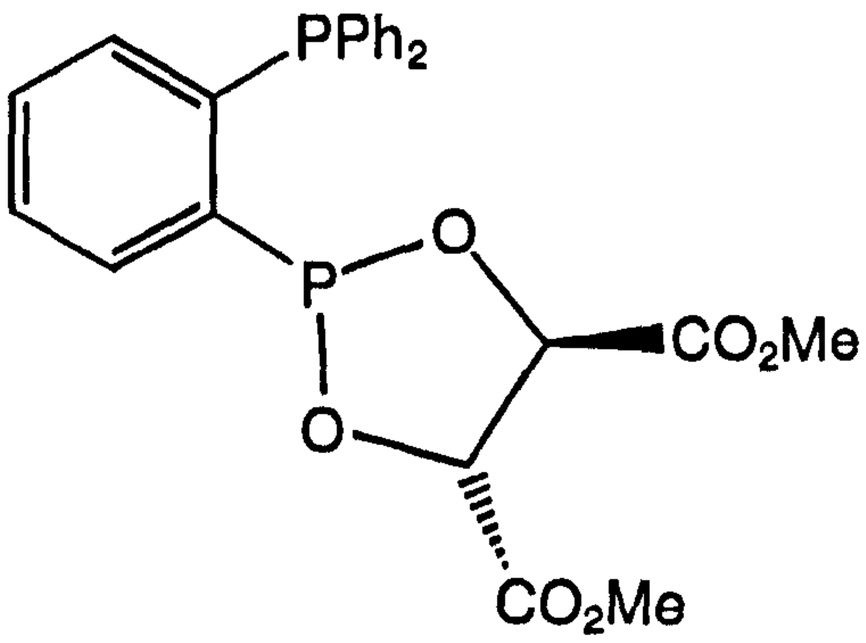

(2*R*,3*R*)-(**1.38**)

1.4 Chiral diphosphites as ligands for asymmetric hydrogenation

Although chiral diphosphites have been extensively used in hydroformylation and hydrocyanation catalysis, there have been very few reports of their application to the asymmetric hydrogenation of α-enamides. In 1990, Wink reported the syntheses of several chiral diphosphites (**1.39**) and their application in the asymmetric hydrogenation of enamides.[19] However, whilst conversions were excellent (>90% after a few hours in acetone at atmospheric pressure and ambient temperature with a substrate:catalyst ratio of 200:1), the enantioselectivities obtained were poor (2-10%).

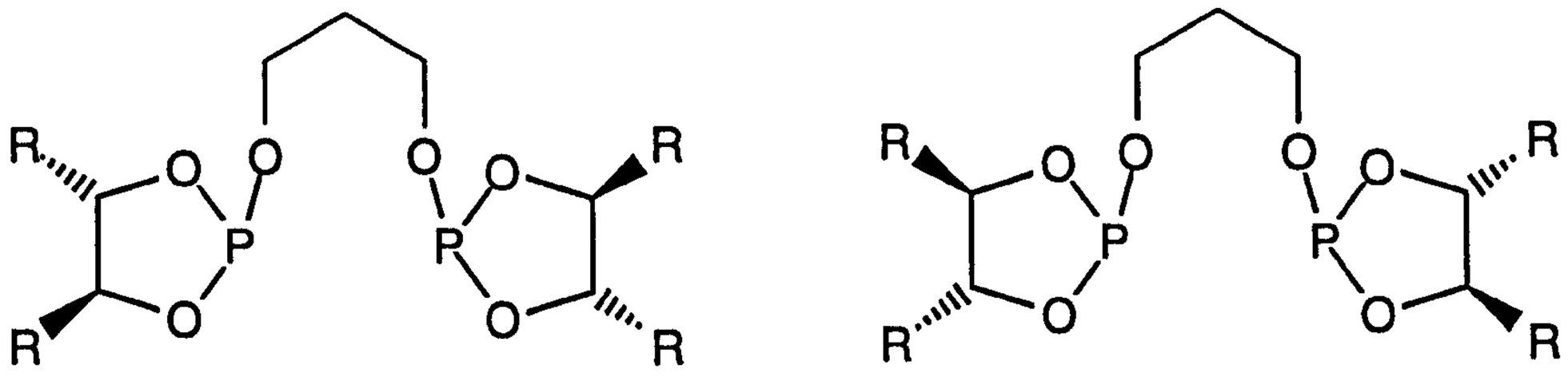

(1.39)

a,b; R = CO_2Et, $CO_2{}^iPr$ **c**; R = Ph

In a recent paper[20] Reetz has reported the synthesis of a range of chiral diphosphites (**1.40**) with the C_2-symmetric diol 1,4:3,6-dianhydro-D-mannite (**1.41**)[53] as a backbone, see Equation 1.6.

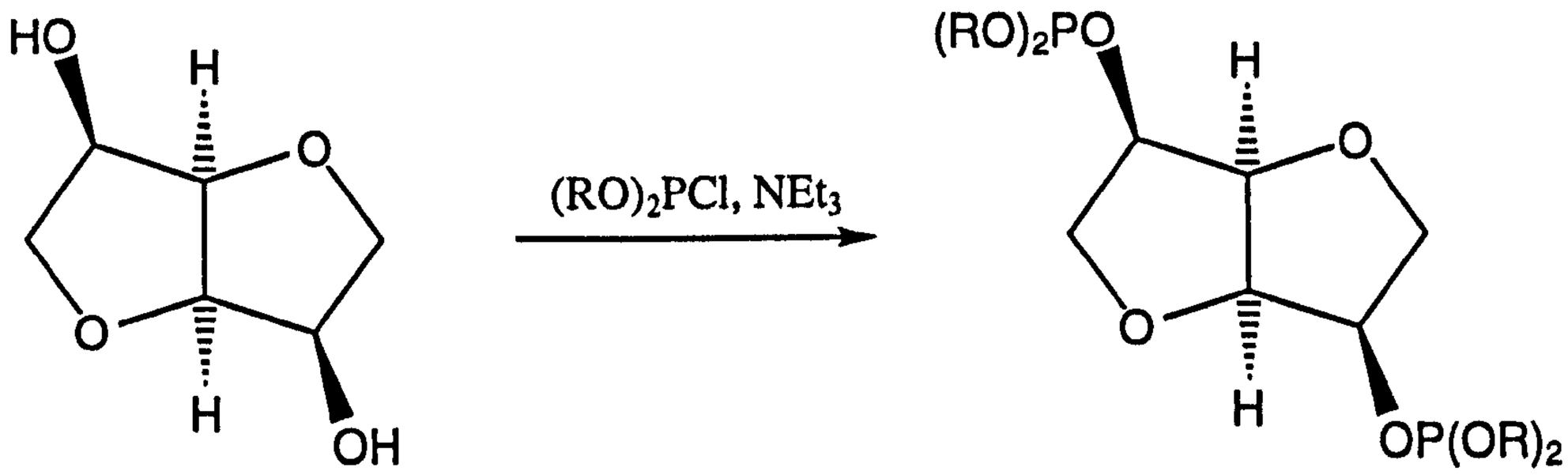

(1.41) **(1.40)**

Equation 1.6

These chiral diphosphites were tested in the asymmetric hydrogenation of dimethyl itaconate (**1.30**). When RO is the achiral 2-naphthoxy (**1.42**) the enantioselectivity was poor (21%) indicating that the transfer of chirality from the backbone to the terminal positions is inefficient. When the optically pure chlorophosphite derived from optically pure binaphthol was reacted with (**1.41**), the resulting diphosphites, (*R*,*R*)-(**1.43**) and (*S*,*S*)-(**1.43**) where the (*R*) and (*S*) labels refer to the absolute configurations of the binaphthyl moieties, gave excellent enantioselectivities of 95% (*R*)

and 88% (*S*) respectively in the hydrogenation reaction but, interestingly, opposite enantiomers of the product were obtained and it appears that the (*R*)-selective catalyst is the 'matched' case. Clearly the chirality of the product is determined by the chirality of the terminal rather than the bridging diol. The significance of this observation will be discussed later in Section 4.3. In fact enantioselectivities up to 98% were obtained when using diphosphite (**1.44**), formed by reaction of (**1.41**) with the racemic chlorophosphite derived from 1,1'-biphenyl-3,3'-dimethyl-2,2'-diol.

(1.42), RO =

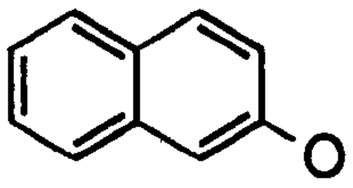

(1.43), $(RO)_2$ =

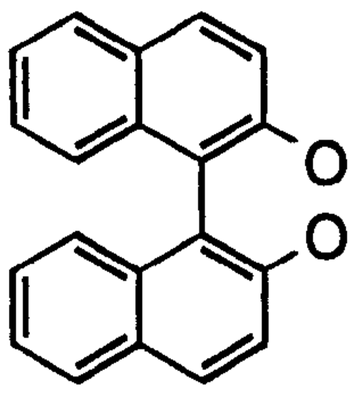

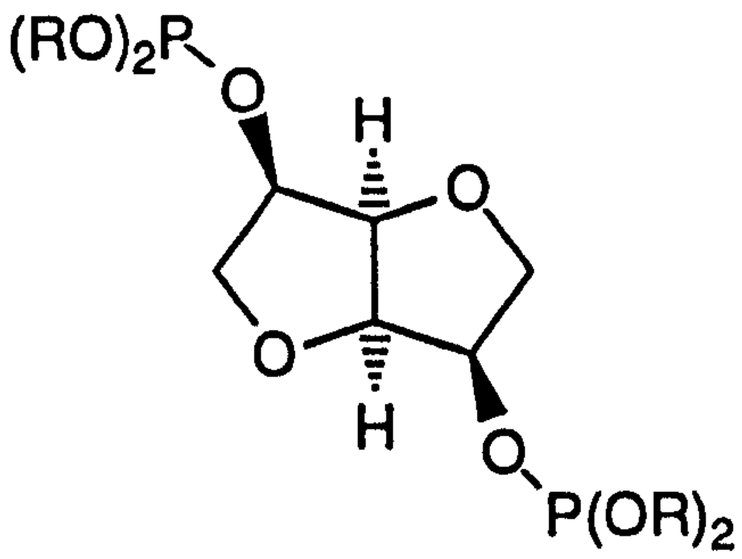

(1.44), $(RO)_2$ =

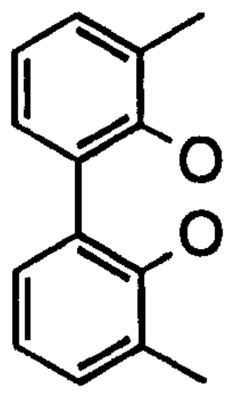

The diphosphites (*R,R*)-(**1.43**) and (**1.44**) were also tested in the asymmetric hydrogenation of methyl-2-acetamidoacrylate (**1.15**) resulting in complete conversion of substrate and excellent enantioselectivities (89% and 81% ee respectively in favour of the product with the (*R*)-configuration). Reetz postulated that in the case of (**1.44**) one of the three diastereomeric metal complexes (corresponding to (*R,R*), (*S,S*) and (*R,S*) in the biphenyl moieties), which are in equilibrium *via* rapid rotation about the biphenyl axis,[54] is a much more active catalyst than the other two and that it is this diastereomer that is responsible for the high enantioselectivities observed. However, (*S,S*)-(**1.43**) afforded a lower conversion (77%) and a much lower enantioselectivity (23% ee in favour of the (*S*)-product), again indicating that the (*R*)-selective catalyst derived from (*R,R*)-(**1.43**) is the 'matched' case.

These results obtained by Reetz have certainly shown the potential of chiral diphosphites for application in the asymmetric hydrogenation of α-enamides, an area which has been almost completely unexplored to date. With this in mind, the chiral diphosphites that we have synthesised primarily for use in asymmetric hydroformylation (see Chapter 3) have been tested for asymmetric hydrogenation and the results are described in Section 4.3.

1.5 The asymmetric hydroformylation of styrene derivatives

1.5.1 The importance of the asymmetric hydroformylation reaction of styrene derivatives

The hydroformylation of alkenes is one of the most important reactions in industrial organic chemistry[55-62] and several reviews have been published dealing with this process.[59,63-67] The asymmetric modification of this reaction has been widely studied since the first report in 1972[68] and this area has also been extensively reviewed.[43,69-74] This Section will concentrate on the asymmetric hydroformylation of styrene derivatives since this process gives (after oxidation of the optically pure aldehyde products) a range of 2-arylpropionic acids, which are an important class of anti-inflammatory agents,[71,75-78] see Scheme 1.5. Indeed, (*S*)-(+)-Ibuprofen (**1.45**) is believed to have a sales potential of one billion US dollars per year as an over-the-counter drug.

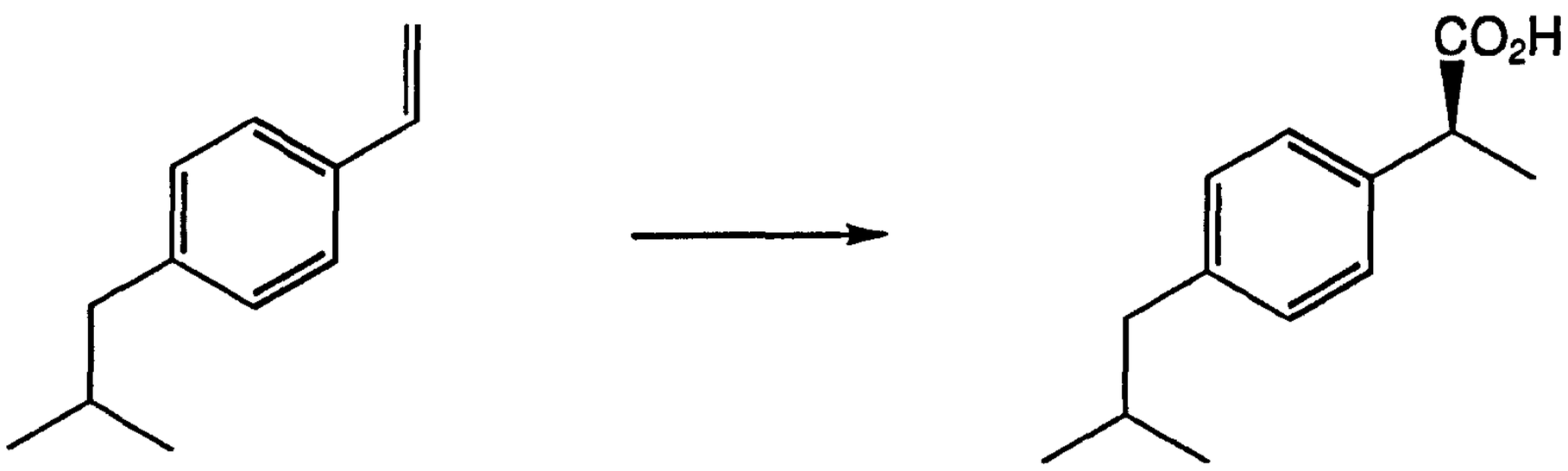

Ibuprofen (**1.45**)

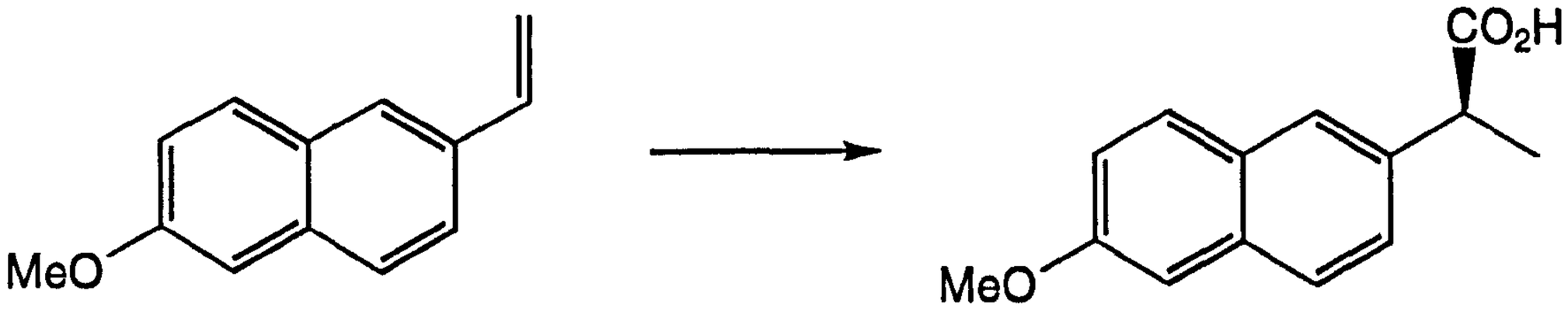

Naproxen (**1.46**)

Reaction conditions:
(i) CO, H_2, catalyst
(ii) oxidation

Scheme 1.5: Asymmetric synthesis of anti-inflammatory drugs *via* asymmetric hydroformylation followed by oxidation

Only one enantiomer of these species is responsible for the biological activity. The enantioselective syntheses of these compounds is therefore desirable. Indeed this goal is part of a growing trend within the pharmaceutical[71] and the agrochemical[79] industries; for example only 11% of chiral pharmaceuticals were produced in the single stereoisomeric form before 1983. This fraction increased to 26% in the period 1983-1987 and it is believed that by the end of the century the figure will have leapt to 80%.

1.5.2 General features of asymmetric hydroformylation

Among the many enantioselective reactions catalysed by transition metals, asymmetric hydroformylation is one of the most challenging. This is because there are several possible selectivity problems, see Equation 1.7.

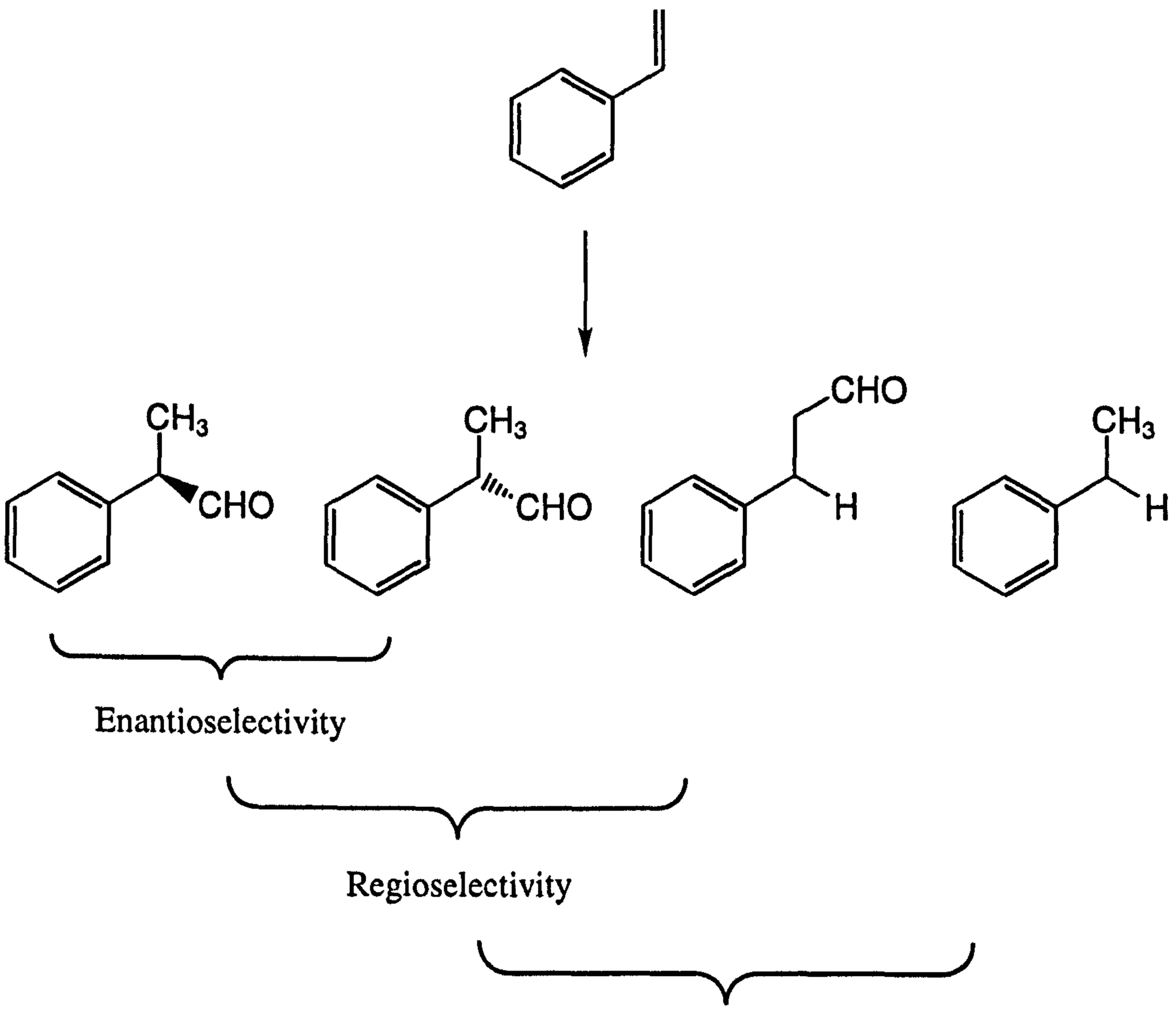

Equation 1.7

Although almost all transition metals have been examined for catalytic activity in hydroformylation, as far as the asymmetric process is concerned only rhodium and platinum-tin catalysts are useful. Rhodium catalysts are usually active even at atmospheric pressure, whilst platinum-tin catalysts are normally only active at fairly

high pressures (greater than 80 bar). Further, chemoselectivity is more of a problem when platinum-tin catalysts are used than when rhodium catalysts are employed.

The use of styrene derivatives as substrates eliminates double bond migration, which is another process catalysed by these complexes and is a serious side-reaction with substrates such as 2-hexene.

Regioselectivity is critical for asymmetric hydroformylation since the branched aldehyde is required. As far as the hydroformylation of vinylarenes is concerned, the linear achiral aldehyde is usually the major product with platinum-tin catalysts, whilst rhodium catalysts favour production of the branched isomer. A further problem of platinum-tin systems is that they also racemise the aldehyde products.

Thus, for activity and selectivity rhodium complexes of phosphorus ligands are the most efficient catalysts. However, up to the end of 1992 the highest enantioselectivity obtained with this metal was 31% using (*R,S*)-Ephos (**1.33**),[48] whereas a 96% ee had been claimed with platinum-tin complexes of BPPM (**1.47**) and BPPM-DBP (**1.48**).[80,81]

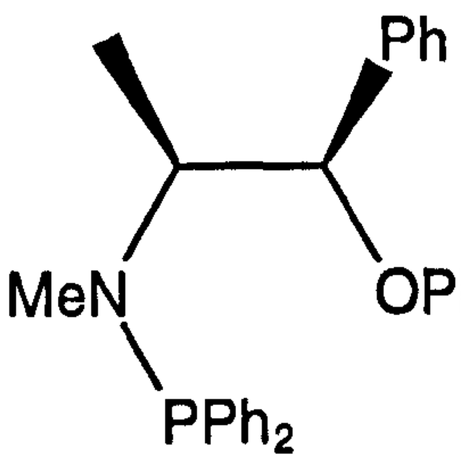

(*R,S*)-Ephos (**1.33**)

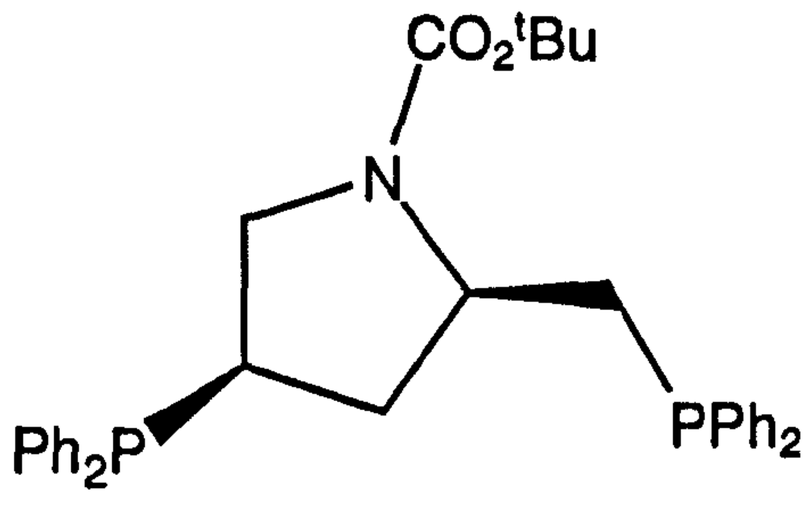

BPPM (**1.47**)

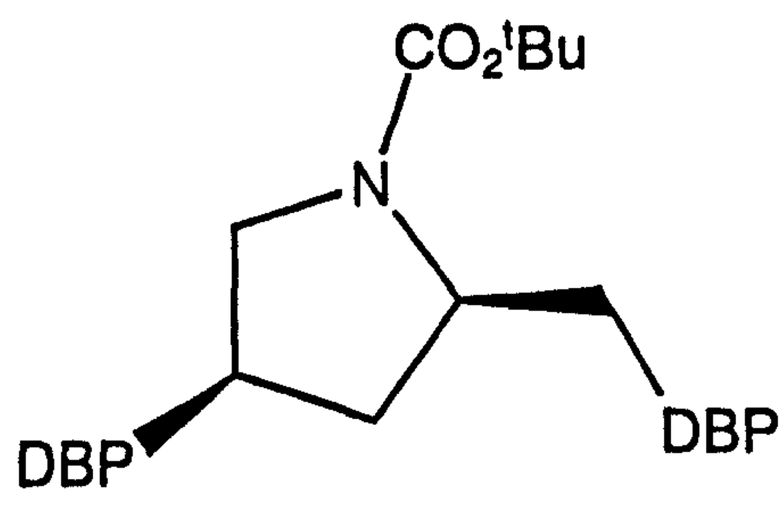

BPPM-DBP (**1.48**)

DBP =

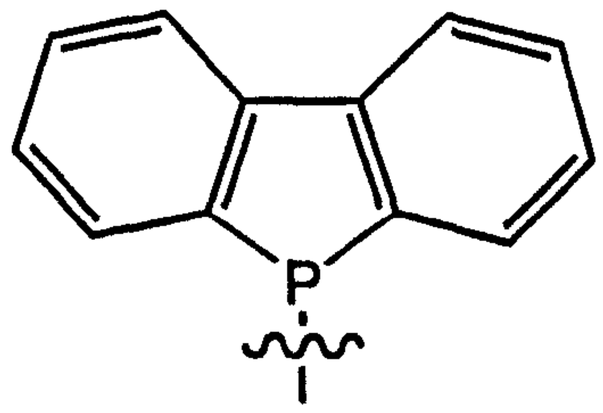

Consequently, at the end of 1992 it was only possible to attain high enantioselectivities at the expense of the chemical yield of the branched aldehyde or *vice versa*. The most significant advances in this area have appeared in the last six years, particularly with respect to the use of chiral chelating phosphites and phosphinophosphites. These will now be dealt with in more detail.

1.5.3 Recent developments in the asymmetric hydroformylation of styrene derivatives

The beneficial effect of phosphites on the catalytic activity and/or regioselectivity of rhodium-catalysed hydroformylation is well documented in the patent literature[82,83] but the use of phosphite ligands in catalysis was not widespread on account of their susceptibility to hydrolysis. However, in 1986 Union Carbide patented the rhodium-phosphite catalysed hydroformylation of butene based on a catalyst system containing monophosphite ligand (**1.49**).[84,85] This was replaced in 1988[82,86] by a wide range of diphosphites closely related to (**1.50**) in order to obtain better regioselectivities but these ligands all have a P(OCCCCO) ring in common. Union Carbide claim that these phosphites are very stable to hydrolysis and this has been attributed to a stabilising effect of this seven-membered ring.

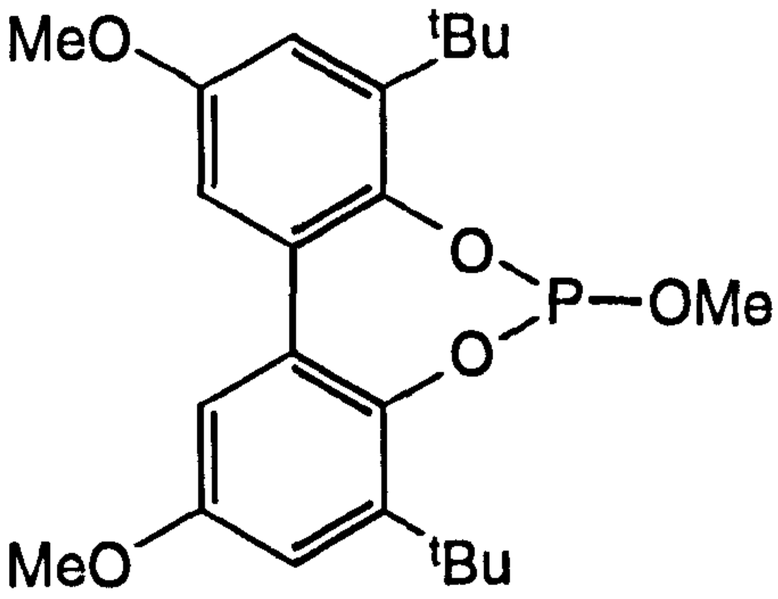

(1.49)

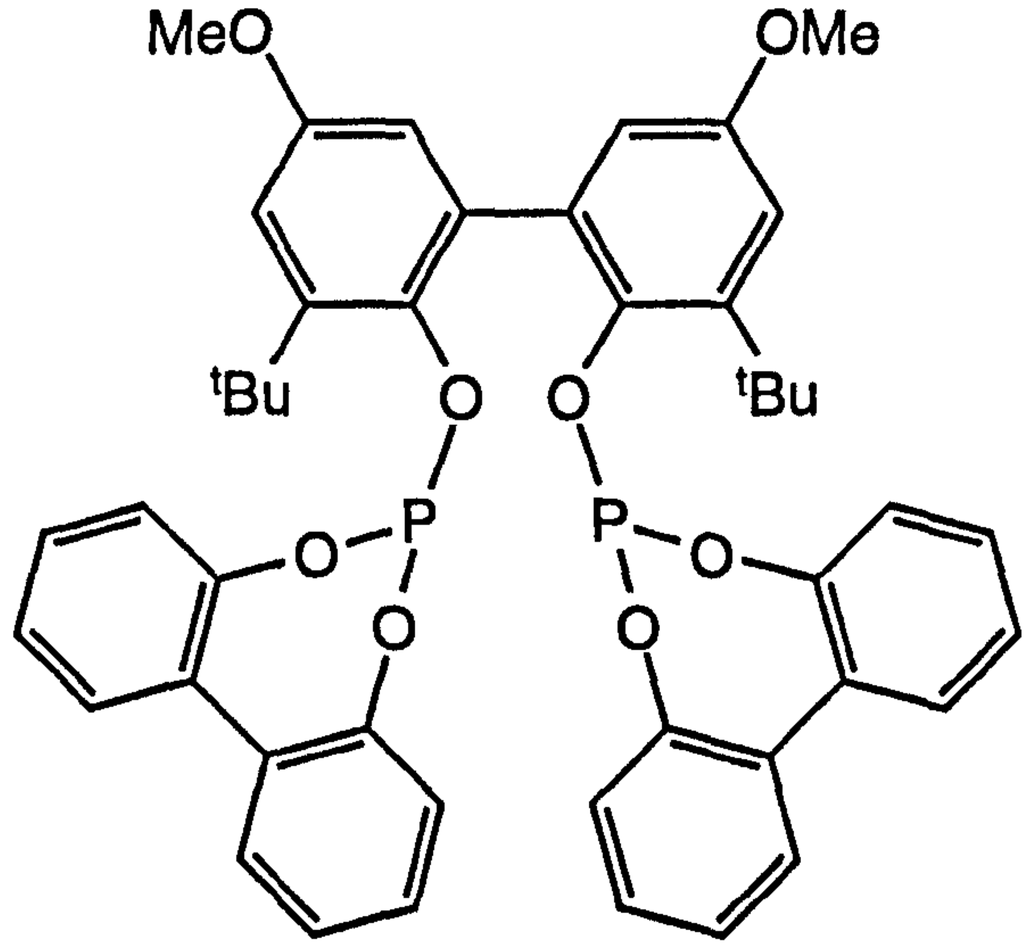

(1.50)

There is little doubt that this is not the only factor in determining the stability of these phosphites to hydrolysis. Van Leeuwen has employed the bulky, acyclic phosphites (**1.51**) and (**1.52**) in the rhodium-catalysed hydroformylation of long-chained olefins and found high activities; these ligands are significantly more stable to hydrolysis than triphenylphosphite despite the lack of a seven-membered P(OCCCCO)

ring.[87-91] It is likely that the ^{t}Bu groups provide steric protection and a hydrophobic environment which confers stability to hydrolysis.

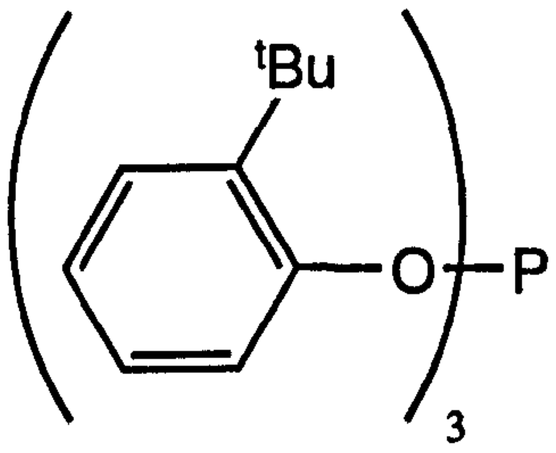

(1.51)

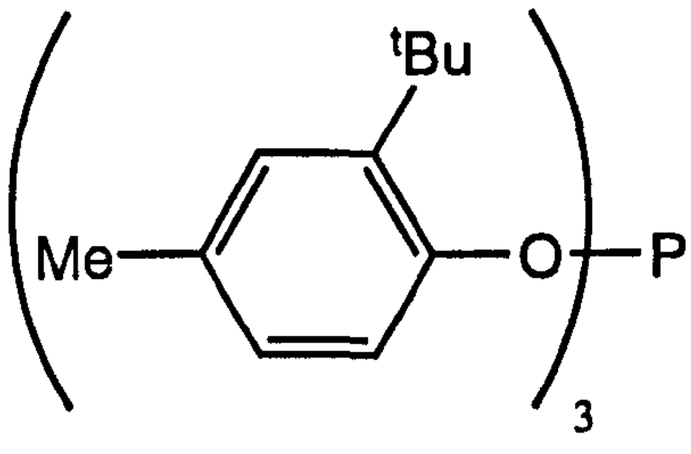

(1.52)

The discovery of kinetically stable phosphites led to a surge of interest in their potential applications in catalysis and thus many publications have appeared since 1988 from several groups.

At the outset, the asymmetric hydroformylation of styrene with chiral diphosphites was far from encouraging since the first attempt by Wink produced a stereorandom reaction with the diphosphite (**1.39**) **c**.[19]

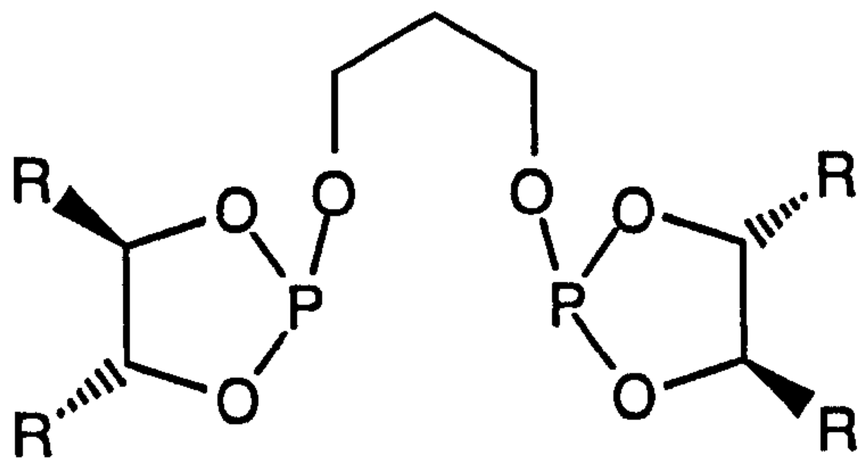

(1.39) c, R = Ph

However, in 1991 Pringle *et al.* reported the synthesis of (*R*,*R*,*R*)-'binaphthite' (**1.53**)[92] and a rhodium(I) complex of this ligand was tested in the asymmetric hydroformylation of styrene and *p*-methoxystyrene. High activities (86% and 70% conversions respectively under mild conditions) and regioselectivities (81% and 69% respectively in favour of the branched aldehyde) were observed but the enantioselectivities were modest (23% and 46% respectively).[93,94] Similarly, high branched regioselectivities were obtained by van Leeuwen *et al.* using the chiral 1,2- and 1,4-diphosphites (**1.54**) and (**1.55**) but the enantioselectivities with styrene were again low (up to 20%).[95]

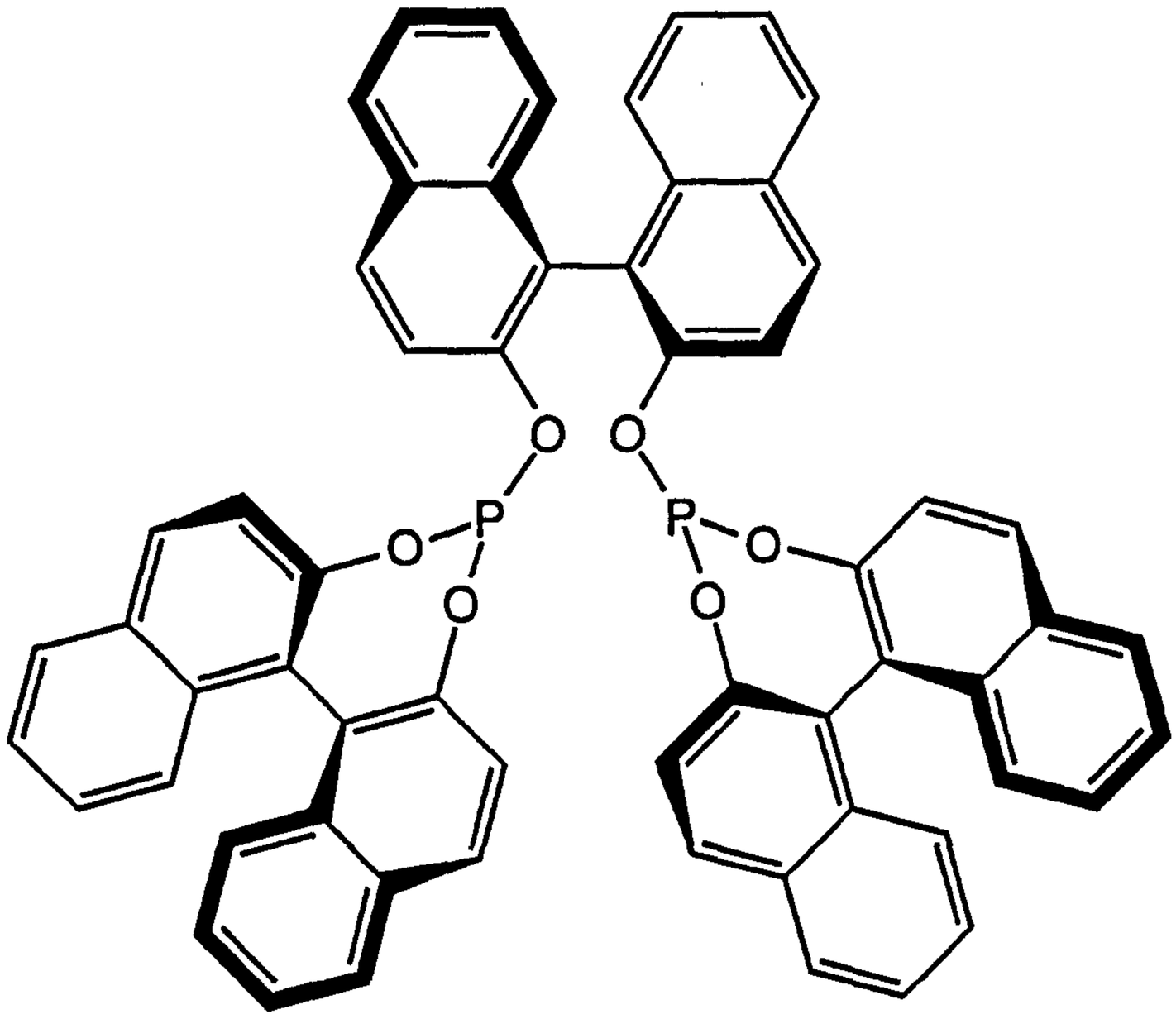

(*R,R,R*)-'binaphthite' (**1.53**)

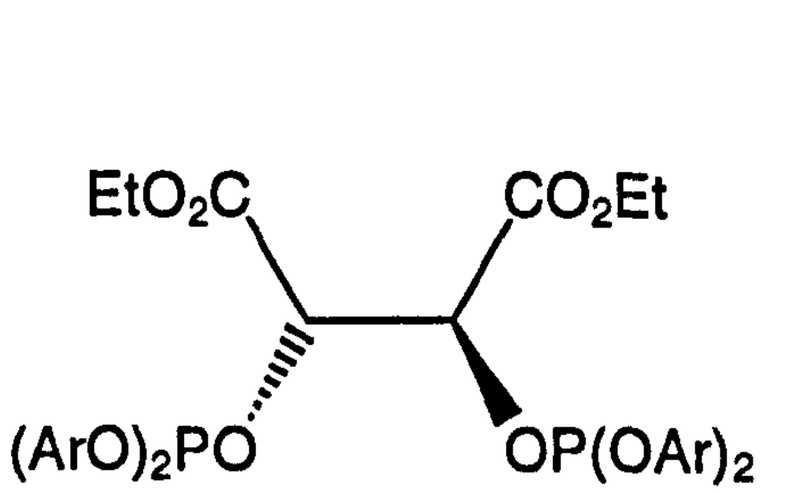

(**1.54**), R = H or R = ^{t}Bu

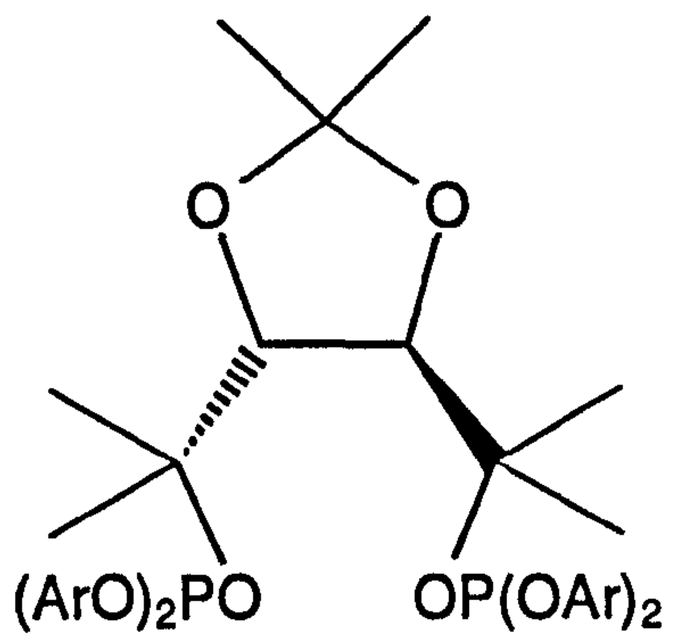

(**1.55**), R = H

$(ArO)_2$ =

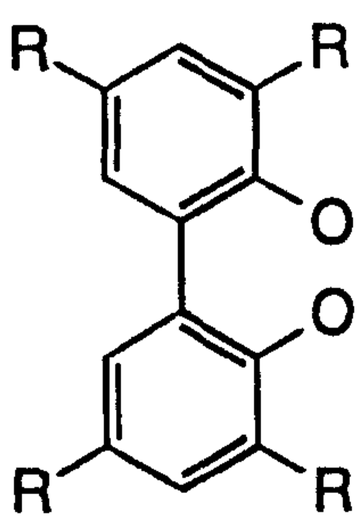

In 1992, Takaya *et al.* published the syntheses of the aryl diphosphites (**1.56**)-(**1.59**) and reported on the application of their complexes with $[Rh(CO)_2(acac)]$ to the asymmetric hydroformylation of vinyl acetate. Regioselectivities up to 94% (in favour of the branched aldehyde) and enantioselectivities up to 49% were achieved.[96] Further, the activity shown by these complexes was much higher than that exhibited by the corresponding rhodium(I) complex of Binap (**1.60**), which gave similar enantioselectivities.

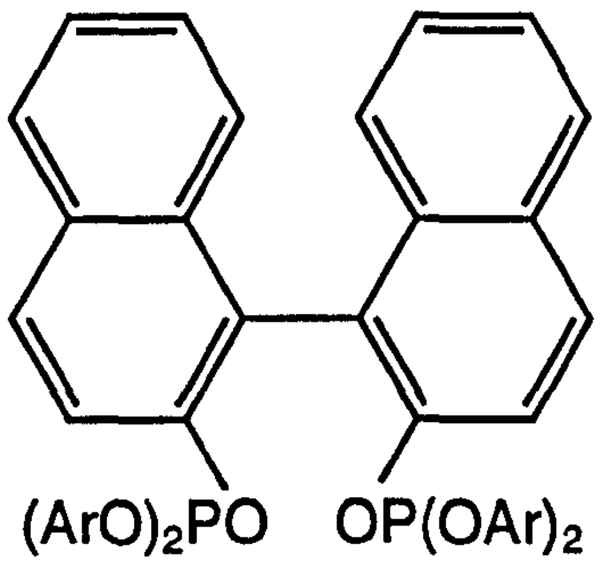

(1.56), Ar = Ph
(1.57), Ar = *p*-tolyl
(1.58), Ar = 3,5-xylyl

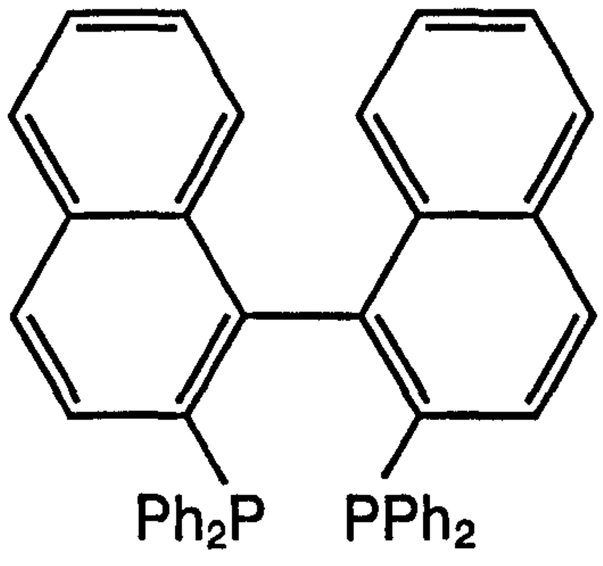

(1.60)

(1.59), $(ArO)_2$ =

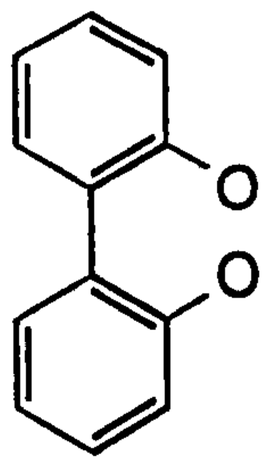

An important breakthrough was reported in 1992 by Union Carbide in a patent on the preparation of the set of bulky diphosphites **(1.61)**, **(1.62)** and **(1.63)**.[97] The rhodium(I) complexes of these ligands catalyse the hydroformylation of styrene at room temperature and moderate pressure in up to 90% ee with more than 98% regioselectivity in favour of the branched aldehyde.[97] The diphosphites **(1.62)** with a 2,4-pentanediol chiral backbone were the most efficient.

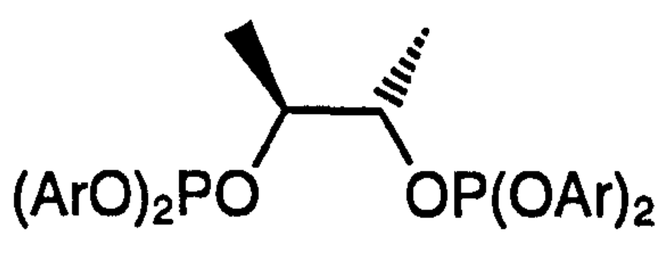

(1.61)

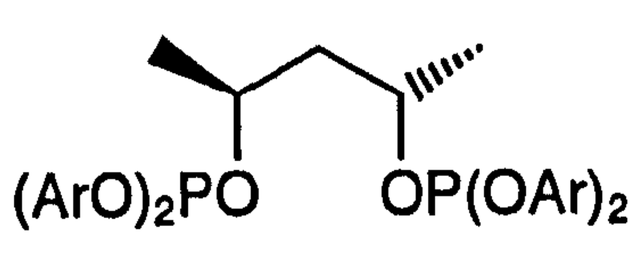

(1.62)

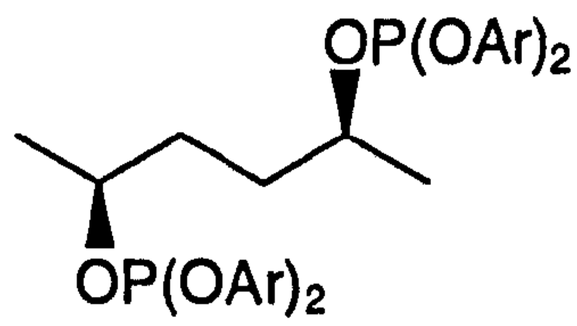

(1.63)

$(ArO)_2$ =

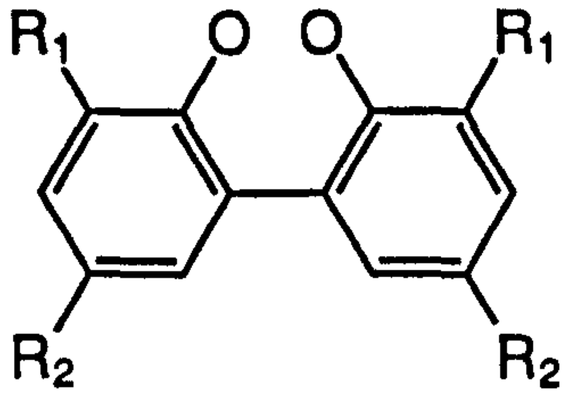

(a) $R_1 = R_2 = H$, or
(b) $R_1 = R_2 = {}^tBu$, or
(c) $R_1 = {}^tBu$; $R_2 = OMe$

Since this patent appeared, numerous other chiral diphosphites have been described in the literature[98-100] but none have improved upon the enantioselectivities obtained by Union Carbide for the hydroformylation of styrene.

RajanBabu has synthesised a series of vicinal carbohydrate phosphinites (**1.64**)-(**1.67**).[101] For the hydroformylation of 6-methoxy-2-vinylnaphthalene, the enantioselectivity was significantly improved when electron-withdrawing substituents were present on the aryl groups, *e.g.* two trifluoromethyl groups (**1.65**) or two fluorine atoms (**1.66**). This clearly illustrates how significant electronic effects can be in determining the asymmetric bias of a catalyst.[102] Whilst high enantioselectivities and regioselectivities were obtained with 6-methoxy-2-vinylnaphthalene as substrate, see Equation 1.8, it was found that these ligands are sensitive to the olefin structure and give unusually large differences of ee with similar substrates; for example the enantioselectivities did not exceed 39% with either 2-vinylnaphthalene, 4-methylstyrene or styrene.

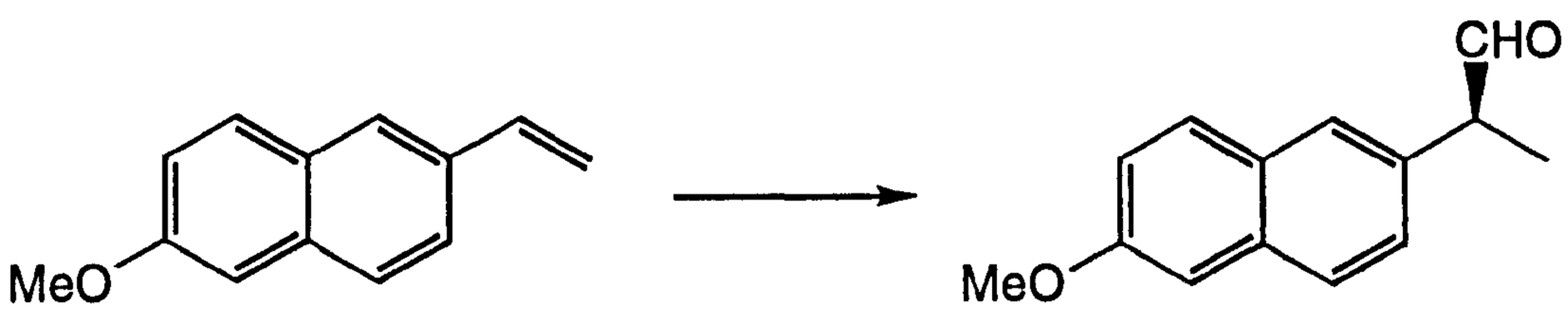

Reaction conditions:
$[Rh(cod)_2]BF_4$ / **(1.65)** (1:1, 0.15%),
Et_3SiH, CO / H_2 (1:1, 110 bar), 25 °C

Regioselectivity 95%, ee 72% (*S*),
20% conversion (18 h)

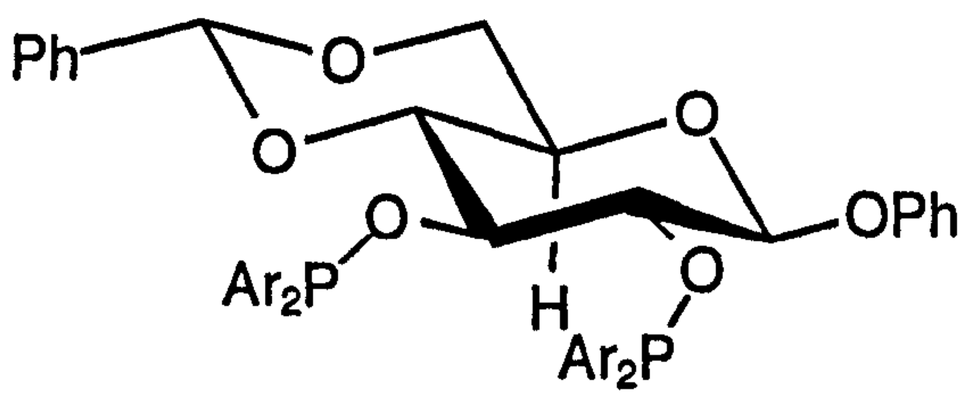

(1.64) Ar = Ph
(1.65) Ar = $C_6H_3(CF_3)_2$-3,5
(1.66) Ar = $C_6H_3F_2$-3,5
(1.67) Ar = $C_6H_3Me_2$-3,5

Equation 1.8

No discussion on asymmetric hydroformylation would be complete without mentioning the phosphinophosphite ligands Binaphos (**1.31**) and Biphemphos (**1.32**) synthesised by Takaya *et al.*[44,46] These ligands are the best that are currently available for the asymmetric hydroformylation of styrene derivatives, with enantioselectivities up to 95% and regioselectivities of 86-90% being routinely obtained.[44,46,47,103,104]

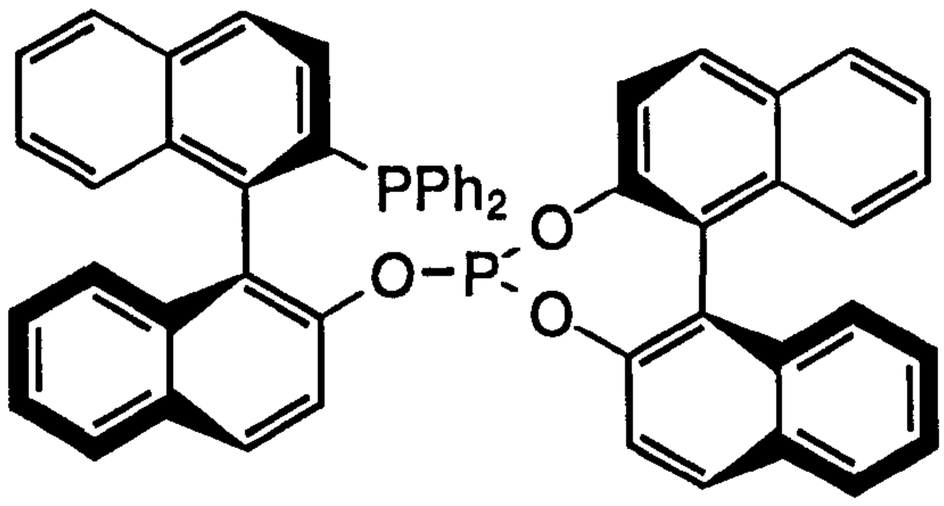

(*R,S*)-Binaphos (**1.31**)

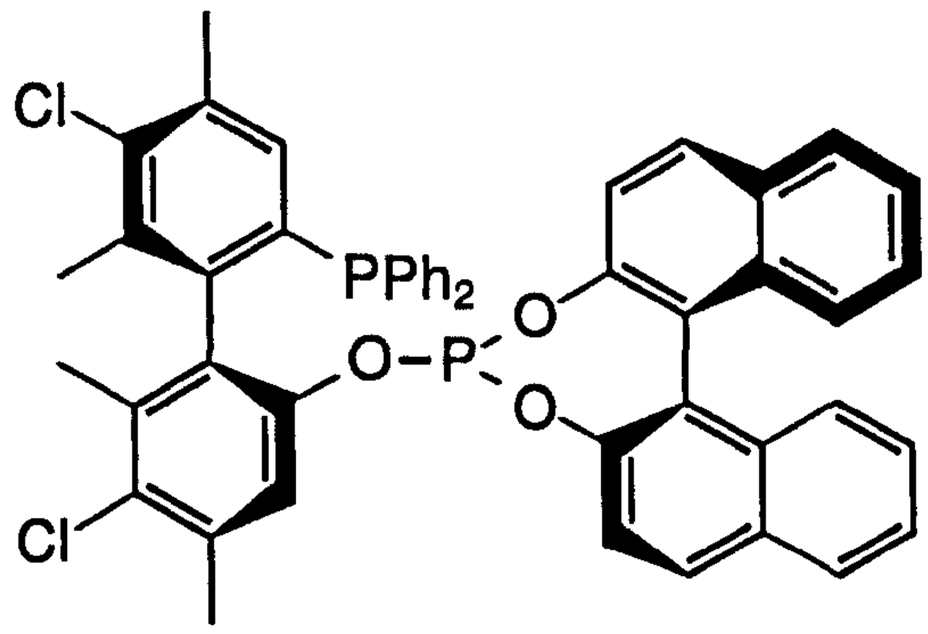

(*S,R*)-Biphemphos (**1.32**)

1.5.4 Mechanistic features of the asymmetric hydroformylation of styrene derivatives

The catalytic cycle for the asymmetric hydroformylation of a styrene derivative catalysed by a rhodium-diphosphite complex is shown in Scheme 1.6. It should be noted that only the reaction pathway leading to formation of the branched aldehyde is illustrated and only one of the two possible diastereomers of (**1.71**), (**1.72**) and (**1.73**) (corresponding in each case to *si*-face coordination of the styrene derivative which leads to formation of the (*S*)-enantiomer of the aldehyde product) is shown. Moreover, only the main equilibria occurring in solution are considered. Despite these simplifications, Scheme 1.6 provides a meaningful picture of the mechanism.

The catalytic species (**1.68**) is generated from the precursor [RhP_2^*(acac)] under standard hydroformylation conditions and is in equilibrium with the trigonal bipyramidal hydridorhodium-diphosphite complexes (**1.69**) and (**1.70**), step (i). Van Leeuwen *et al.* have performed detailed analyses on the solution stuctures of these complexes containing diphosphite ligands.[95,98-100,105,106] They have concluded that either structure (**1.69**) or structure (**1.70**) is stabilised depending on the length and the flexibility of the bridge between the two phosphorus atoms.[105] Brown and Kent have illustrated for the analogous trigonal bipyramidal hydridorhodium-diphosphine complexes that structure (**1.69**) is the least sterically hindered since the two phosphine moieties are both in equatorial positions and the P-Rh-P bond angle is therefore close to 120° whilst in (**1.70**) the axial-equatorial geometry of the two phosphine species brings them closer together with the requirement for a P-Rh-P bond angle of 90°.[107] Van Leeuwen concluded[99,105] that short-bridged diphosphites such as (**1.61**) forming seven-membered chelate rings coordinate in an equatorial-axial manner {structure (**1.70**)}, presumably because they have bite angles closer to 90°. In contrast, longer-bridged diphosphites such as (**1.62**) and (**1.63**) which form eight- and nine-membered chelate rings respectively have larger bite angles and are therefore able to adopt the preferred, less sterically congested bisequatorial configuration (**1.69**).

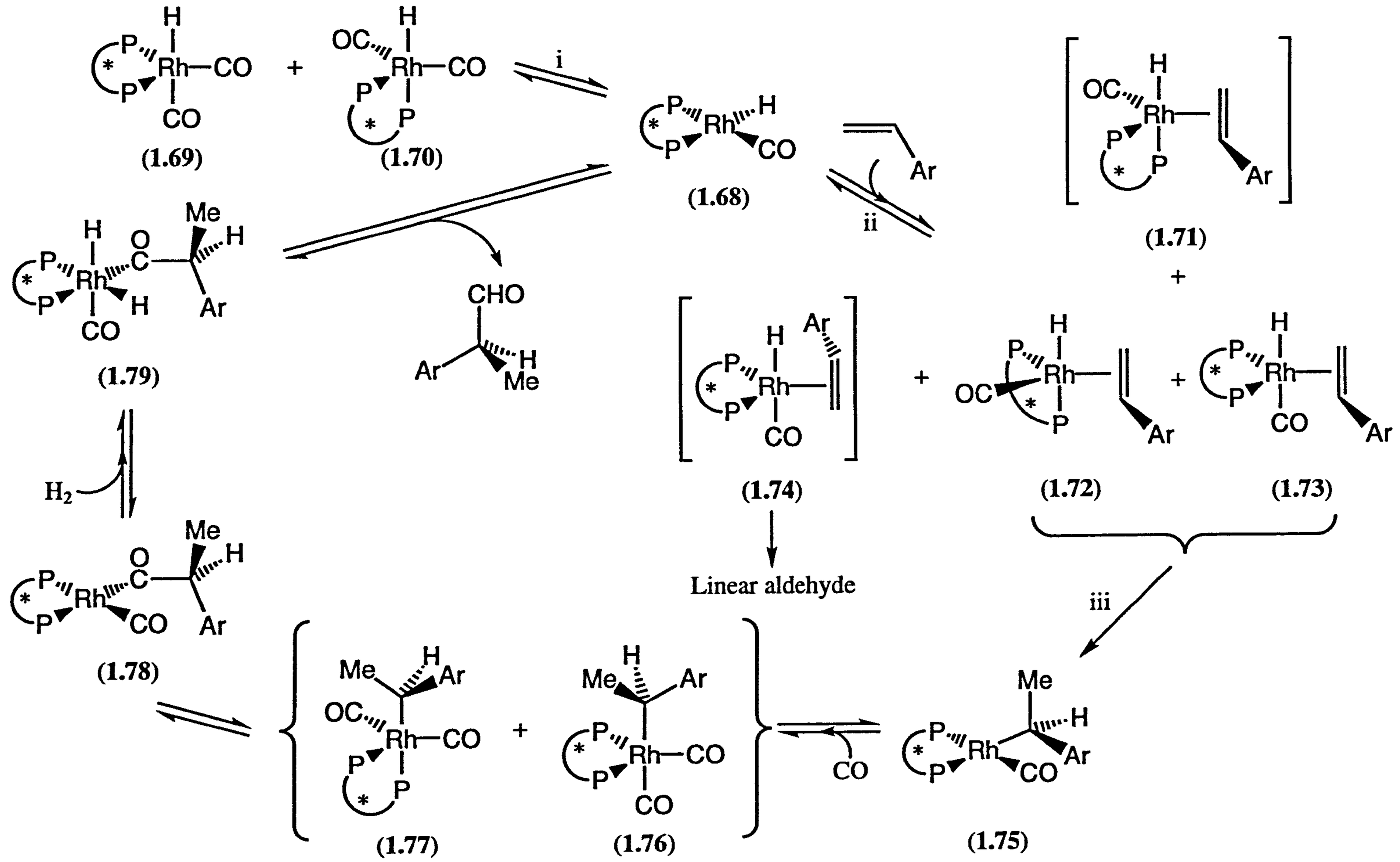

Scheme 1.6: Mechanism of the asymmetric hydroformylation of a styrene derivative catalysed by a rhodium-diphosphite complex

(1.61)

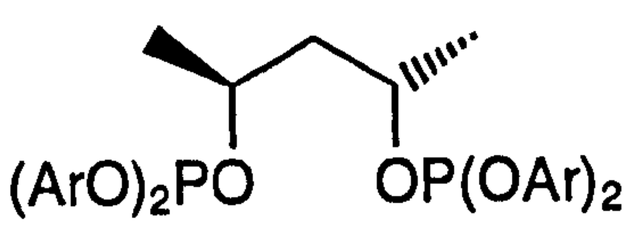

(1.62)

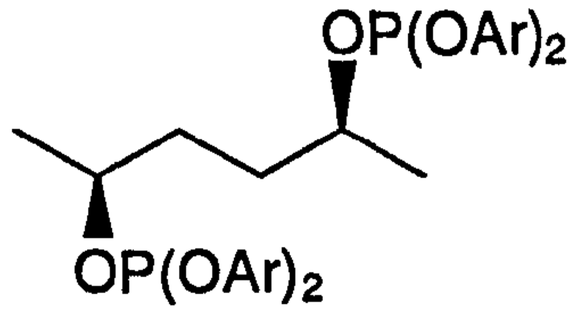

(1.63)

$(ArO)_2$ =

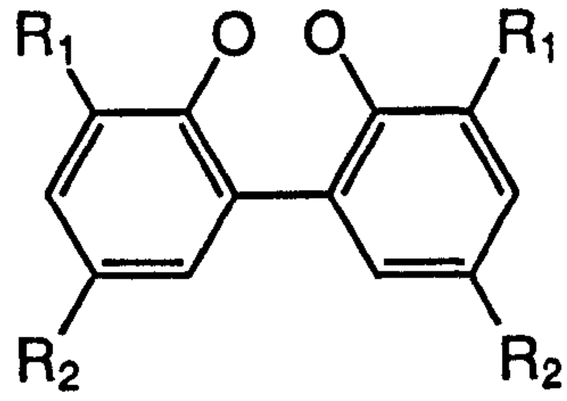

(a) $R_1 = R_2 = H$, or
(b) $R_1 = R_2 = {}^tBu$, or
(c) $R_1 = {}^tBu$; $R_2 = OMe$

Binaphos (**1.31**) and Biphemphos (**1.32**) form trigonal bipyramidal hydridorhodium complexes (**1.80**) with the phosphine equatorial and the phosphite axial.[44] This has been attributed to geometry restrictions imposed by the small natural bite angle (β_n)[108] of these ligands {*e.g.* $\beta_n = 90.4^o$ for (*R,S*)-Binaphos (**1.31**)} and the electronic requirement that the weaker σ-donor (the phosphite) is *trans*- to the strongly σ-donating hydride.[44] This electronic constraint effectively eliminates the extra diastereomeric transition states that are possible on account of the C_1-symmetry of these ligands.

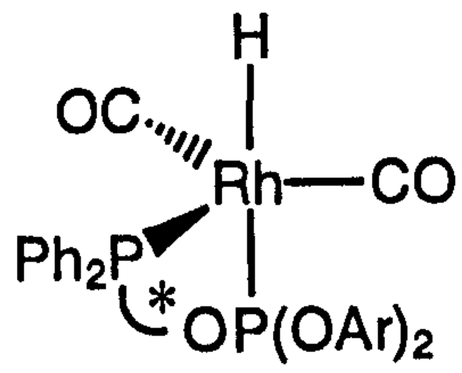

(1.80)

Step (ii) in Scheme 1.6 is coordination of the substrate to (**1.68**) to give two diastereomers (corresponding to *si*- and *re*-face coordination of the olefin) of species (**1.73**) and similarly two diastereomers of each of the species (**1.71**) and (**1.72**). This is followed by β-hydride migration, step (iii), to form the diastereomeric mixture of alkylrhodium species (**1.75**). The regioselectivity of the asymmetric hydroformylation reaction is determined by this β-hydride migration, which is irreversible under standard hydroformylation conditions.[62,103,109-111] Only the pathway leading to the branched aldehyde is shown which, in the case of styrene and its derivatives, is appropriate because the branched alkylrhodium species (**1.75**) is favoured due to coordination of the benzyl group in a η^3-fashion, see Figure 1.2.

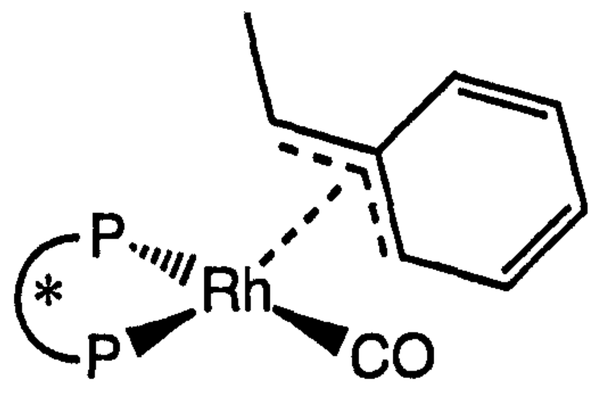

Figure 1.2: η^3-coordination of the benzyl group in the branched alkylrhodium species (**1.75**) of styrene-derived substrates

The enantioselectivity of this process is also determined by the β-hydride migration, step (iii).[62,103,109-111] In trying to rationalise the enantioselectivities obtained, we therefore need to consider the various diastereomeric transition states that lead to formation of the branched alkylrhodium species (**1.75**). The possible species are illustrated in Figure 1.3.

It has been postulated that the formation of a single pair of diastereomeric catalytic intermediates is conducive to higher enantioselectivity.[112,113] For example, if a mixture of species (**1.73**), (**1.71**) and (**1.72**) is formed then there is no guarantee that all three transition states A, B and C will be preferred over A', B' and C' respectively. This may therefore result in opposing enantioselectivities for the different reaction pathways and a resultant low overall enantioselectivity.

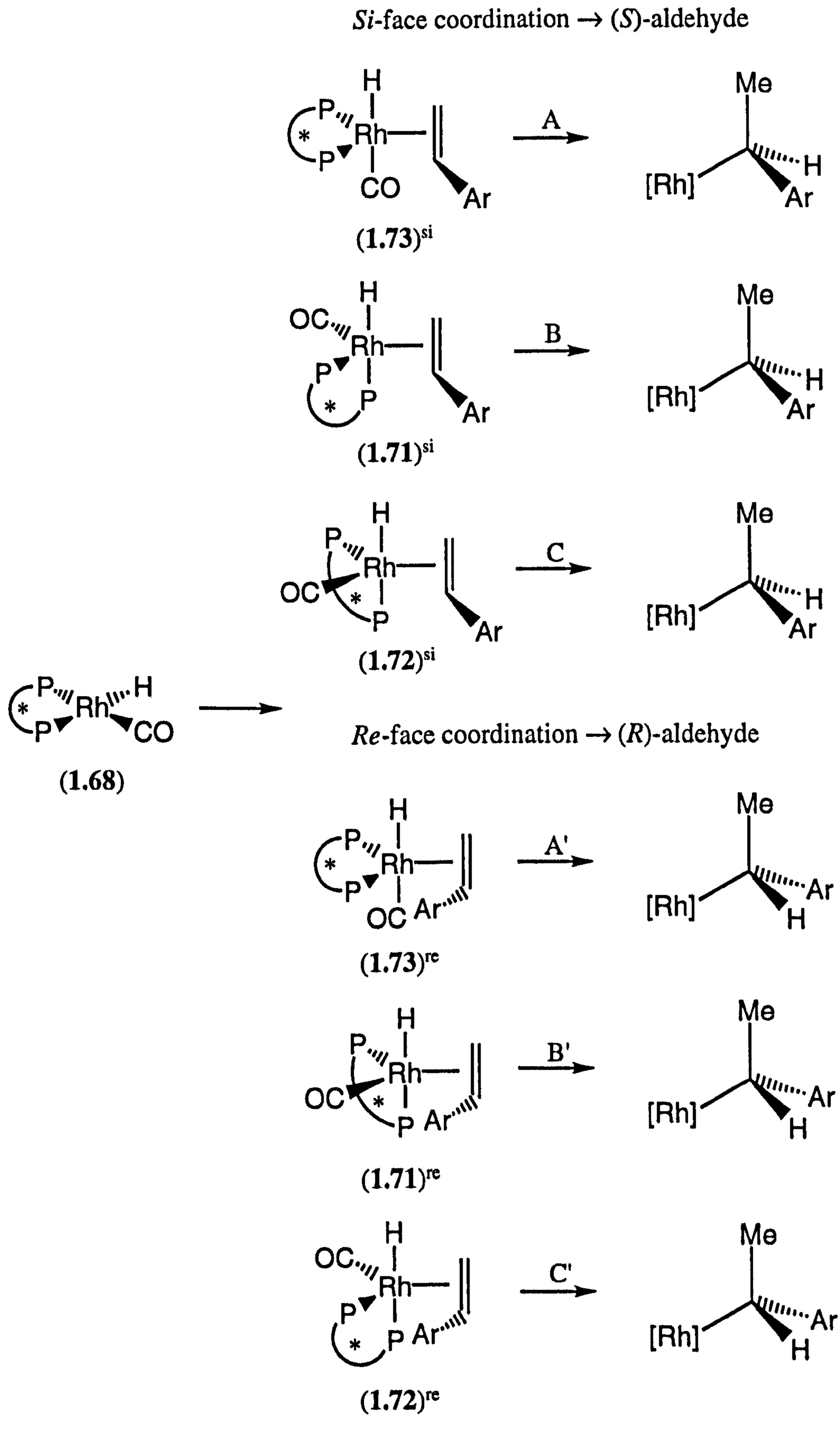

Figure 1.3: The possible transition states leading to formation of the branched alkylrhodium species (**1.75**)

The model of Pino and Consiglio,[114] see Figure 1.4, is useful to consider these transition states in more detail assuming the formation of a single hydridorhodium-dicarbonyl species (**1.69**) or (**1.70**) (or (**1.80**) for phosphinophosphite ligands) is representative of the formation of a single configuration (*i.e.* bisequatorial or axial-equatorial) in the rhodium-substrate complexes (**1.73**) or (**1.71**) / (**1.72**) respectively.

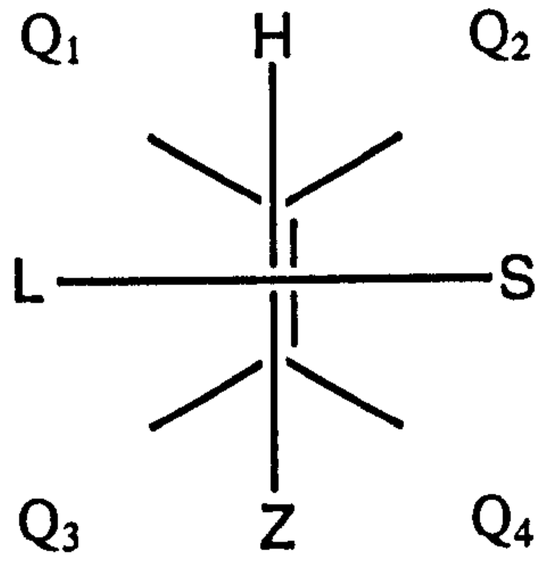

Figure 1.4: The model of Pino and Consiglio for rationalisation of the enantioselectivities obtained in the asymmetric hydroformylation of olefins

In order to form the branched aldehyde the aryl group must be in either Q_3 or Q_4. For bisequatorial species (**1.73**), Z is a carbonyl ligand and L and S are the two phosphite groups. L refers to the phosphite group that presents the more, and S the less, sterically demanding environment. Thus in the case of styrene, the aryl group of the substrate will prefer to be in the least crowded of the lower two quadrants, Q_4.

The situation is more complicated for ligands which adopt the axial-equatorial configuration, where L and Z refer to the phosphorus moieties and S the carbonyl ligand. The C_1-symmetry of (**1.70**) gives rise to two diastereotopic sites for the substrate to bind, see Figure 1.5.

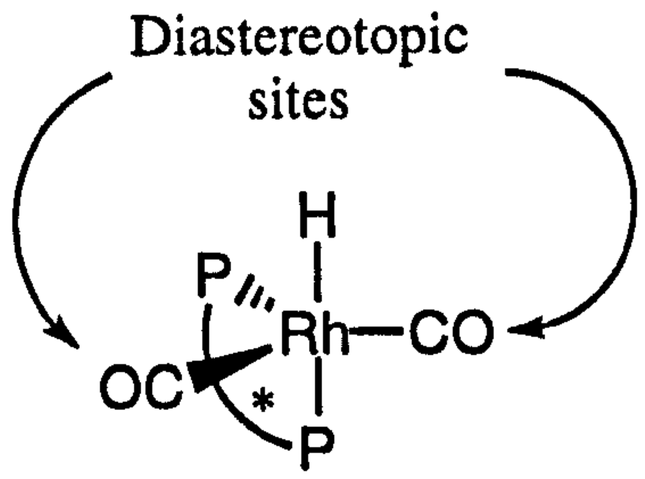

(1.70)

Figure 1.5: Diastereotopic equatorial sites in the hydridorhodium-dicarbonyl complex (**1.70**)

Consequently, there are potentially two diastereomers present, (**1.71**) and (**1.72**), for each mode of substrate coordination which correspond to B, B' and C, C' respectively

in Figure 1.3. The model of Pino and Consiglio predicts that only one diastereomer is feasible for each mode of coordination of the substrate (C, C' in Figure 1.3) where the aryl group occupies Q_4 where it is furthest from the equatorial phosphorus moiety.

It is significant to note that for all the most successful diphosphite ligands {the C_2-symmetric Union Carbide diphosphites (**1.61**), (**1.62**) and (**1.63**)} and Takaya's phosphinophosphites {Binaphos (**1.31**) and Biphemphos (**1.32**)} a single catalytically active species, namely one diastereomer for each of *si*- and *re*-face coordination, is formed. This corresponds to (**1.73**) (A and A' in Figure 1.3) for bisequatorial ligands and (**1.72**) (C and C' in Figure 1.3) for axial-equatorial ligands. It is also significant that the best diphosphite ligands {(**1.62**) forming eight-membered chelate rings} occupy bisequatorial configurations whilst Takaya's ligands form axial-equatorial chelates. Thus, it seems more important to form a single configuration than to form any particular one.

NMR and IR spectroscopic data for the trigonal bipyramidal hydridorhodium complexes of ligands (**1.61**) (**b**) and (**c**), (**1.62**) (**b**) and (**c**) and (**1.63**) (**b**) and (**c**) show that a fluxional process operates that exchanges the two phosphorus atoms.[99] Van Leeuwen has proposed[106] that this is occurring *via* the low-energy rearrangement mechanism postulated by Meakin[115,116] for phosphorus exchange in $[MHL_{4-x}(CO)_x]$ complexes (M = Rh or Ir, x = 1-4, L = monophosphite). This could easily occur without changing the P-Rh-P bite angles appreciably and is illustrated for diphosphite complexes in Figure 1.6.

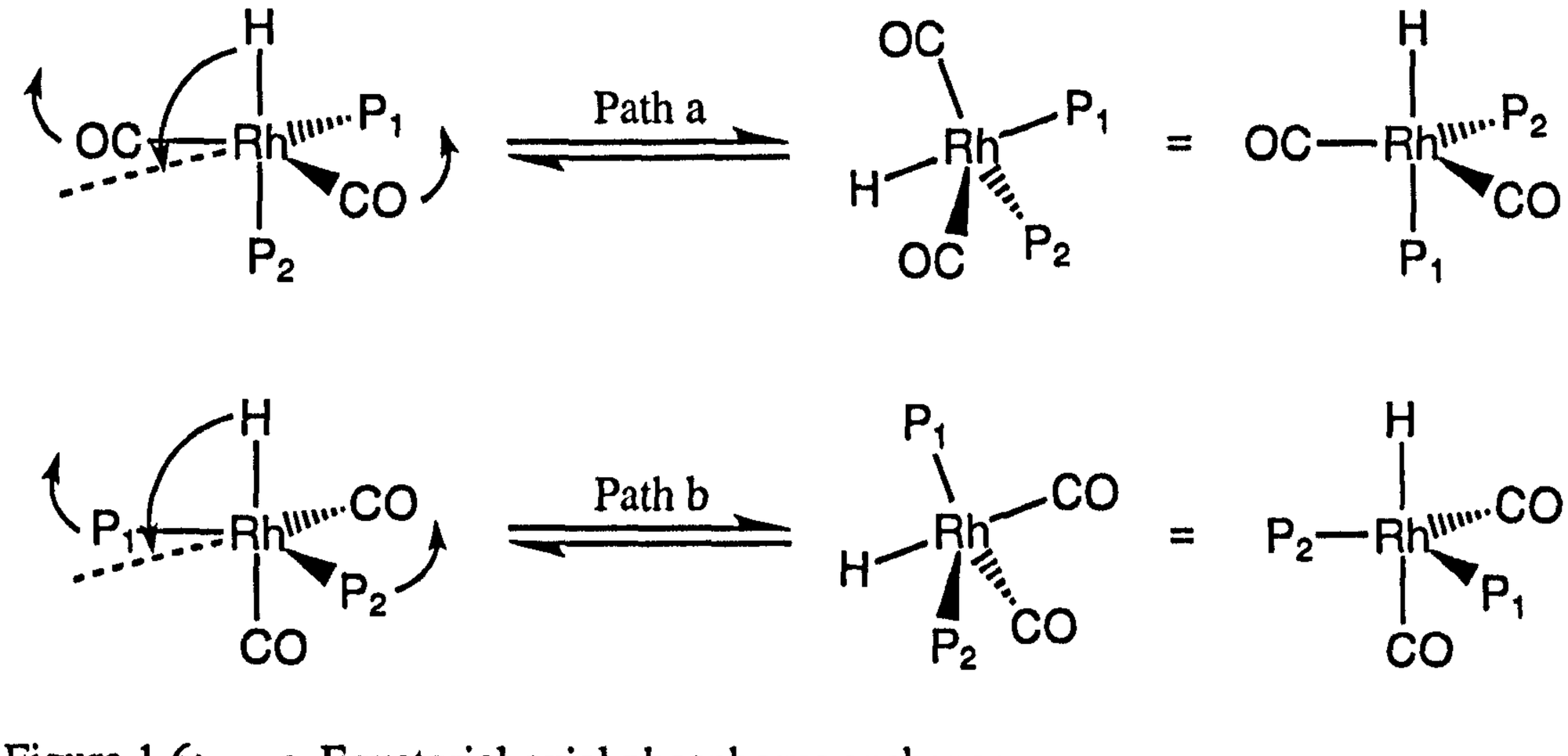

Figure 1.6: a. Equatorial-axial phosphorus exchange
b. Equatorial-equatorial phosphorus exchange

The energy barriers for these processes have been calculated.[106] The lowest energy barriers correspond to equatorial-axial phosphorus exchange in the complexes of ligands (**1.61**) (**a**) and (**b**), which contain seven-membered chelate rings. This seems logical since this process involves movement of two carbonyl ligands, which would be

expected to be easier than the movement of the two phosphite moieties that is required for equatorial-equatorial exchange. Further, on going from eight- {ligands (**1.62**) (**a**) and (**b**)} to nine- {ligands (**1.63**) (**a**) and (**b**)} membered chelate rings, lower energy barriers for phosphorus-phosphorus exchange were observed. This has been attributed to reduced steric congestion in the nine-membered bis equatorial chelate rings. Finally, it was found that increasing the steric bulk of the *ortho*- substituents increased the energy barriers for this exchange process.

The lower the energy barrier for phosphorus-phosphorus exchange, the more flexible the complex will be. There appears to be an inverse correlation between flexibility and efficiency at asymmetric induction since the most flexible complexes {those derived from ligands (**1.61**) (**a**) and (**b**) and ligands (**1.63**) (**a**) and (**b**)} induce low enantioselectivities in the asymmetric hydroformylation of styrene (19%, 25%, 1% and 7% respectively at 40 °C) whilst the more rigid complexes {those derived from ligands (**1.62**) (**a**) and (**b**)} induce higher enantioselectivities (50% and 67% respectively at 40 °C). Significantly, it has been shown that the trigonal bipyramidal complex (**1.80**) derived from (*R*,*S*)-Binaphos (**1.31**) does not exhibit such fluxionality, presumably by virtue of the electronic requirement that the weaker σ-donor (the phosphite moiety) is *trans*- to the strongly σ-donating hydride, and thus forms a very rigid environment around the rhodium.[44] This ligand has the best enantioselectivity known for the asymmetric hydroformylation of styrene (94% at 60 °C).

Another important factor in determining the efficiency of a ligand at asymmetric induction is the principle of chiral cooperativity explored by van Leeuwen *et al.*[100] They found that the three possible diastereomers of diphosphite (**1.81**) exhibited greatly different catalytic properties.

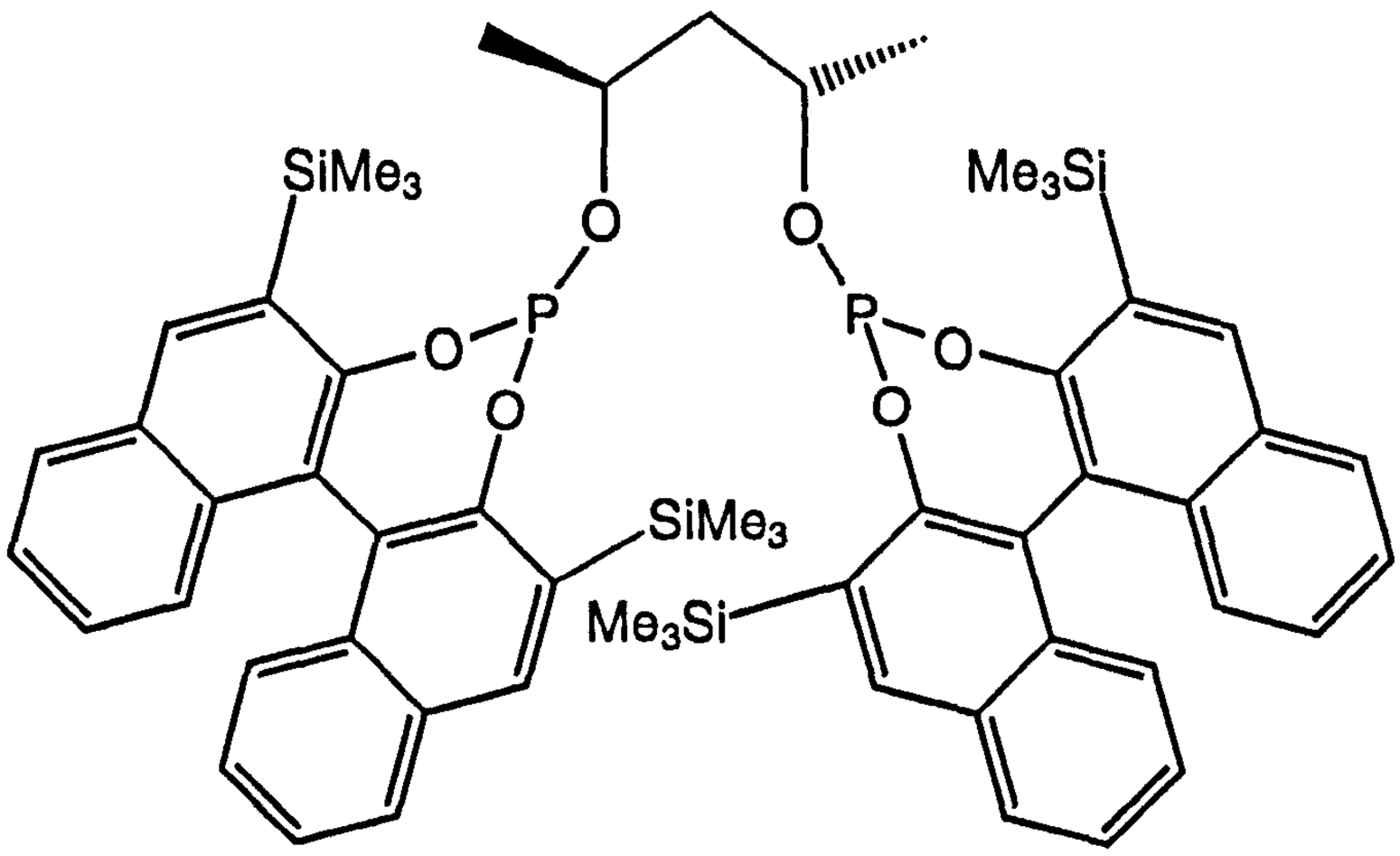

(1.81)

For example, in the asymmetric hydroformylation of styrene catalysed by rhodium(I) complexes of these ligands, the (S_{ax},2*R*,4*R*,S_{ax})-diastereomer (where the *ax* subscript refers to the axial chirality of the binaphthol units) effects a conversion of 38%, a regioselectivity of 88% and an enantioselectivity of 69% (*S*) after 24 h at 25 °C. The (R_{ax},2*R*,4*R*,R_{ax})-diastereomer gives a more active catalyst (18% conversion after 5 h at 25 °C) which effects a higher regioselectivity (95%) but a much lower enantioselectivity, 38% (*S*). Finally, the (R_{ax},2*R*,4*R*,S_{ax})-diastereomer has extremely low activity (2% conversion after 5 h at 25 °C) and exhibits high regioselectivity (91%) but poor asymmetric induction, 23% (*S*).

Consequently, it appears that for diphosphite (**1.81**) the optimal, 'matched' configuration for asymmetric induction and catalytic activity has the terminal units with the same absolute configuration but opposite to the chiral backbone.

The Binaphos ligand (**1.31**) also shows chiral cooperativity.[104] Whilst rhodium(I) complexes of both (*S*,*R*)- and (*R*,*R*)-(**1.31**) have been found to exhibit high catalytic activity and regioselectivity for the branched aldehyde in the asymmetric hydroformylation of styrene, the enantioselectivities obtained are very different. The catalyst derived from (*S*,*R*)-(**1.31**), the 'matched' diastereomer, effects the highest reported enantioselectivity for this reaction, 94% (*S*), but the catalyst derived from the (*R*,*R*)-diastereomer, the 'mismatched' case, gives a much lower enantioselectivity of 25% (*R*). From these results it can be concluded that the sense of enantioface selection is predominantly controlled by the phosphine moiety in Binaphos (**1.31**).

It is interesting to note that there appears to be a correlation between the stability of the hydridorhodium-dicarbonyl complexes derived from the diphosphite ligands {(**1.61**), (**1.62**), (**1.63**) (see Page 28) and (**1.81**)} and from the phosphinophosphite ligand Binaphos (**1.31**) and the enantioselectivities obtained in the asymmetric hydroformylation of styrene. For example, the (S_{ax},2*R*,4*R*,S_{ax})-diastereomer of (**1.81**) forms the most stable hydridorhodium-dicarbonyl complex (**1.69**) with the diphosphite in a bisequatorial configuration.[100] The corresponding complex with the (R_{ax},2*R*,4*R*,S_{ax})-diastereomer is significantly less stable,[100] whilst that of the (R_{ax},2*R*,4*R*,R_{ax})-diastereomer does not even form[100] because in this case a complex mixture of rhodium-diphosphite species is formed including an hydridorhodium-tricarbonyl species in which the diphosphite is acting as a monodentate ligand;[91] the low enantioselectivity and relatively high reaction rates observed for this diastereomer have been attributed to this species.[100]

Similarly, stable hydridorhodium-dicarbonyl complexes are formed by ligands (**1.62**) (**a**) and (**b**), containing an eight-membered chelate ring, and as mentioned earlier these gave the best enantioselectivities. The corresponding complexes formed by ligands (**1.61**) (**a**) and (**b**) and (**1.63**) (**a**) and (**b**), containing seven- and nine-

membered chelate rings respectively, undergo significant decomposition under hydroformylation conditions.[99]

Finally, the hydridorhodium-dicarbonyl complex of the 'mismatched' (*R,R*)-diastereomer of Binaphos (**1.31**) is believed to show significant distortion from the ideal trigonal bipyramidal structure[104] and it is possible that this distortion is at least partly responsible for the lower enantioselectivity obtained with this diastereomer.

In summary, the following features should be incorporated into the ligand in attempts to design a new catalyst for the asymmetric hydroformylation of styrene derivatives:

1. The ligand should form a stable hydridorhodium-dicarbonyl complex under hydroformylation conditions. From previous results with diphosphites, it appears that eight-membered chelate rings are preferred.[99]
2. The ligand should adopt a single configuration in the hydridorhodium-dicarbonyl complex, *i.e.* bisequatorial or axial-equatorial. It appears that the formation of just one configuration is the key factor, rather than which particular one is formed. This goal can be achieved by variation of the natural bite angle of the ligand to suit the required configuration; 90° for axial-equatorial and 120° for bisequatorial.
3. The ligand should possess a rigid backbone so that a rigid dissymmetric environment is created for effective enantioface discrimination. This has been achieved for axial-equatorial coordinating ligands such as Binaphos (**1.31**) by having two phosphorus functionalities with different electronic properties.[104] Alternatively, for diphosphite ligands it has been shown that bulky *ortho*-substituents lead to reduced flexibility in the chelate ring.[106]
4. The 'matched' diastereomer of the ligand must be obtained in order that chiral cooperativity is exhibited.

1.6 Project aims and thesis outline

The overall aim of this project was the design and synthesis of a range of bulky phosphonites and diphosphites derived from the chiral biphenols 9,9'-biphenanthryl-10,10'-diol (**1.3**) and dimethyl-1,1'-binaphthyl-2,2'-dihydroxy-3,3'-dicarboxylate (**1.82**) for application in the asymmetric hydrogenation of α-enamides and, for the diphosphites, the asymmetric hydroformylation of styrene derivatives.

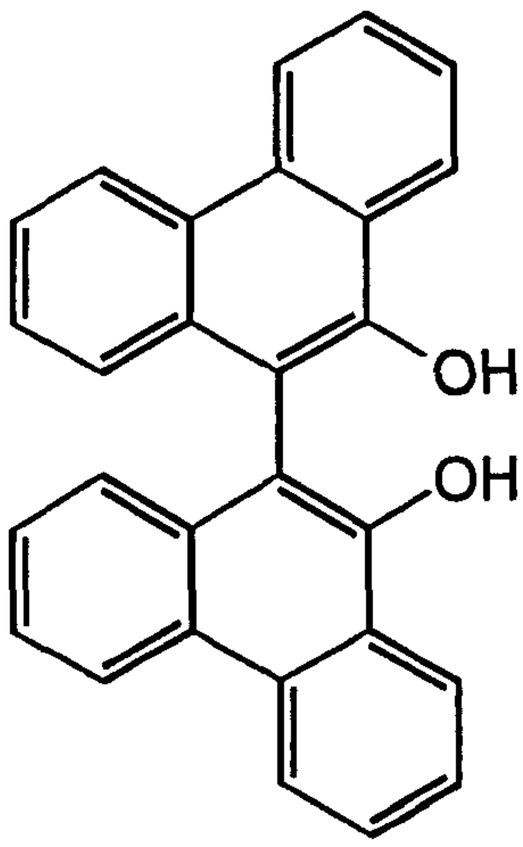

(1.3)

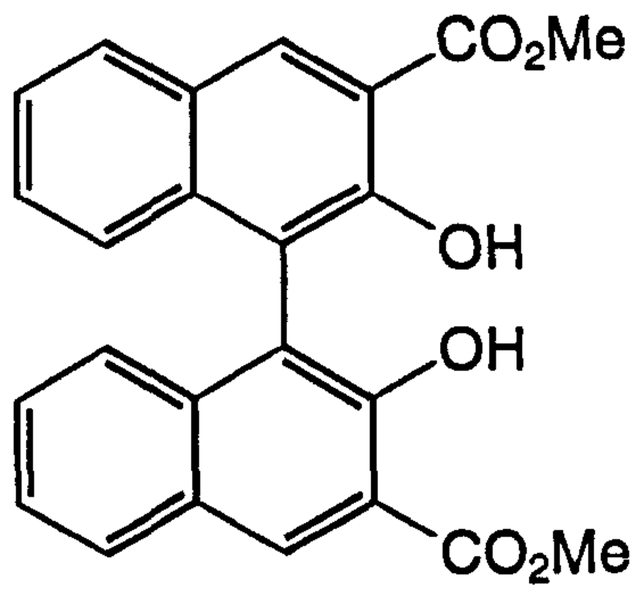

(1.82)

The format of the thesis is outlined below:

Chapter 2 starts with a description of the literature[117] synthesis of (**1.82**) and a new synthesis and a modification of the literature[118] resolution of (**1.3**). The syntheses, characterisation and properties of racemic and optically pure phosphonites derived from these diols is followed by a detailed discussion of the coordination chemistry of these new ligands with platinum(II), platinum(0) and rhodium(I). Throughout the Chapter, the properties of these phosphonites and their complexes are compared to the analogous compounds derived from 1,1'-binaphthyl-2,2'-diol since it was hoped that the increase in steric bulk of the organic backbone of these ligands would be reflected in a difference in the properties of these species.

Chapter 3 describes the syntheses, characterisation and properties of several cyclic aryl phosphites derived from (**1.3**) and (**1.82**). The coordination chemistry of these phosphites with platinum(II), platinum(0), palladium(II) and rhodium(I) is discussed. The diphosphites described herein are analogues of 'binaphthite' (**1.53**) and have been specifically designed for the asymmetric hydroformylation of styrene derivatives, with the intention of improving the selectivities in this reaction by the creation of a larger chiral cavity. Consequently, the results obtained in the asymmetric hydroformylation of styrene and *p*-methoxystyrene using the rhodium(I) complexes of these ligands are presented and compared with those obtained using 'binaphthite'.

Chapter 4 starts with an introduction to the asymmetric hydrogenation reaction of α-enamides. A description of the results that have been obtained in the asymmetric hydrogenation of methyl-2-acetamidoacrylate (**1.15**) and methyl-(Z)-2-acetamidocinnamate using rhodium(I) complexes of the phosphonites described in Chapter 2 and the diphosphites described in Chapter 3 is then presented.

Chapter 5 reports the experimental procedures that have been used throughout the project.

Chapter 2

Phosphonites: Synthesis and Coordination Chemistry

This Chapter starts with a description of the literature[117] synthesis of dimethyl-1,1'-binaphthyl-2,2'-dihydroxy-3,3'-dicarboxylate (**2.1**) and a new synthesis and modified literature[118] resolution of 9,9'-biphenanthryl-10,10'-diol (**2.2**). This is followed by the syntheses, characterisation and properties of racemic and optically pure phosphonites derived from these diols and a detailed discussion of the coordination chemistry of these new ligands with platinum(II), platinum(0) and rhodium(I). Throughout the Chapter comparisons are drawn with the analogous compounds derived from 1,1'-binaphthyl-2,2'-diol which have already been described in Section 1.3. This enables the effect of the steric bulk of the organic backbones upon the properties exhibited by the ligands and their complexes to be assessed.

2.1 Syntheses of 9,9'-biphenanthryl-10,10'-diol (2.2) and dimethyl-1,1'-binaphthyl-2,2'-dihydroxy-3,3'-dicarboxylate (2.1)

The synthesis of (-)-(*S*)-biphenanthrol (**2.2**) *via* a stereoselective oxidative coupling of 9-phenanthrol (**2.3**) has been reported by Yamamoto,[119] see Equation 2.1.

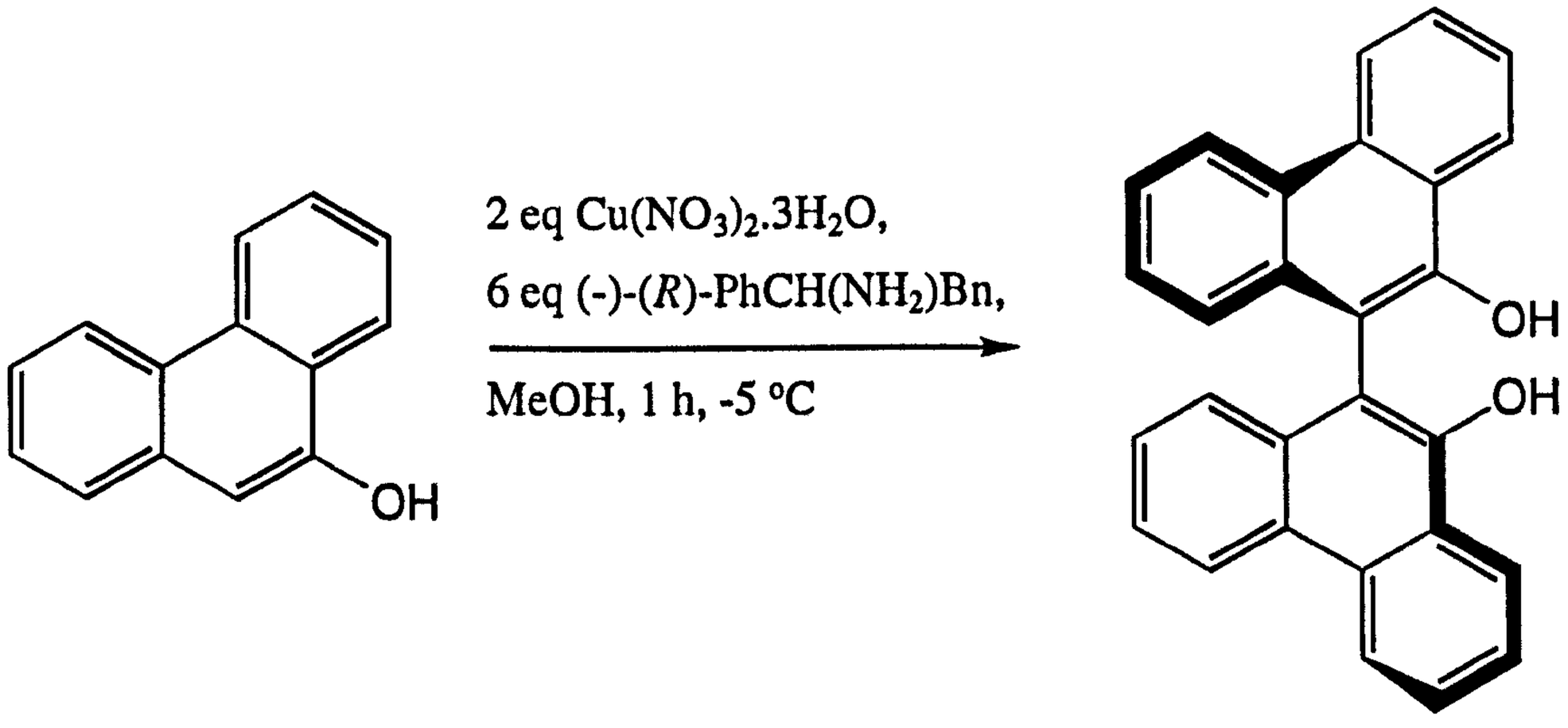

(2.3) **(-)-(*S*)-(2.2)**

Equation 2.1

We initially hoped to utilise this methodology and therefore embarked upon the synthesis of 9-phenanthrol by the route previously reported by Bacon[120] in three stages from phenanthrene (**2.4**) employing electrophilic bromination,[121] copper(I) iodide-catalysed nucleophilic substitution of the bromide (**2.5**) with methoxide[122] and, finally, acid-catalysed hydrolysis of the resultant aryl methyl ether (**2.6**), see Scheme 2.1.

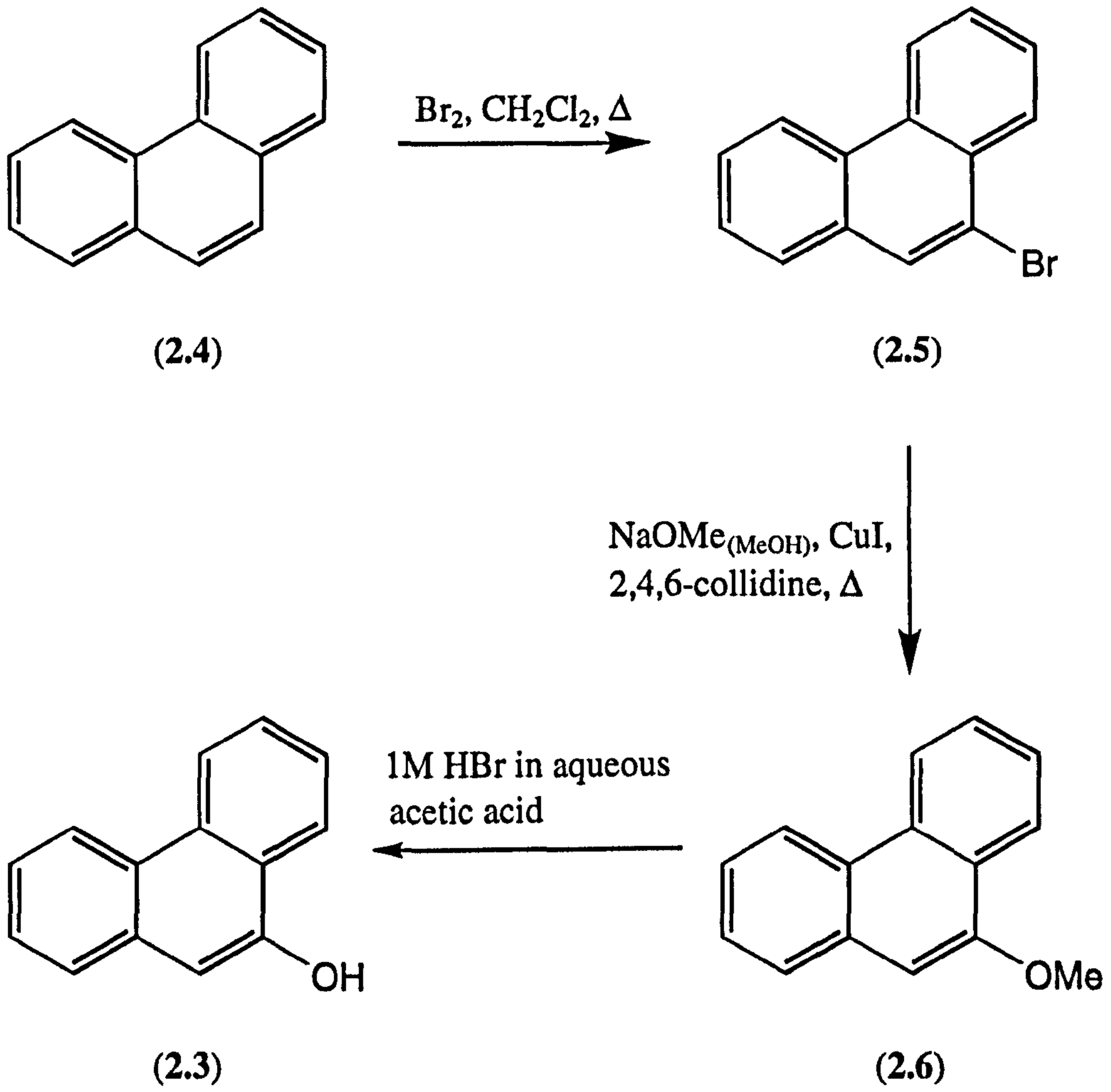

(2.4) **(2.5)** **(2.6)** **(2.3)**

Scheme 2.1: Bacon's synthesis of 9-phenanthrol (**2.3**) from phenanthrene (**2.4**)

Bromination of phenanthrene in the 9-position was carried out using the procedure of Coleman.[121] The product was obtained in 78% yield after distillation, but impurities were still present and recrystallisation from ethanol was essential which lowered the yield to 38%. The 9-bromophenanthrene (**2.5**) underwent a slow photochemical decomposition and hence was stored in the dark.

All attempts to replicate the substitution of bromide by methoxide[122] failed in our hands. Consequently, an alternative method for the transformation of an aryl halide to a phenol was required. One such method reported in the literature involves the formation of the corresponding Grignard reagent, reaction with trimethyl borate and subsequent oxidation.[123] Using this route 9-bromophenanthrene (**2.5**) was converted to 9-phenanthrol (**2.3**) in 94% yield, see Scheme 2.2.

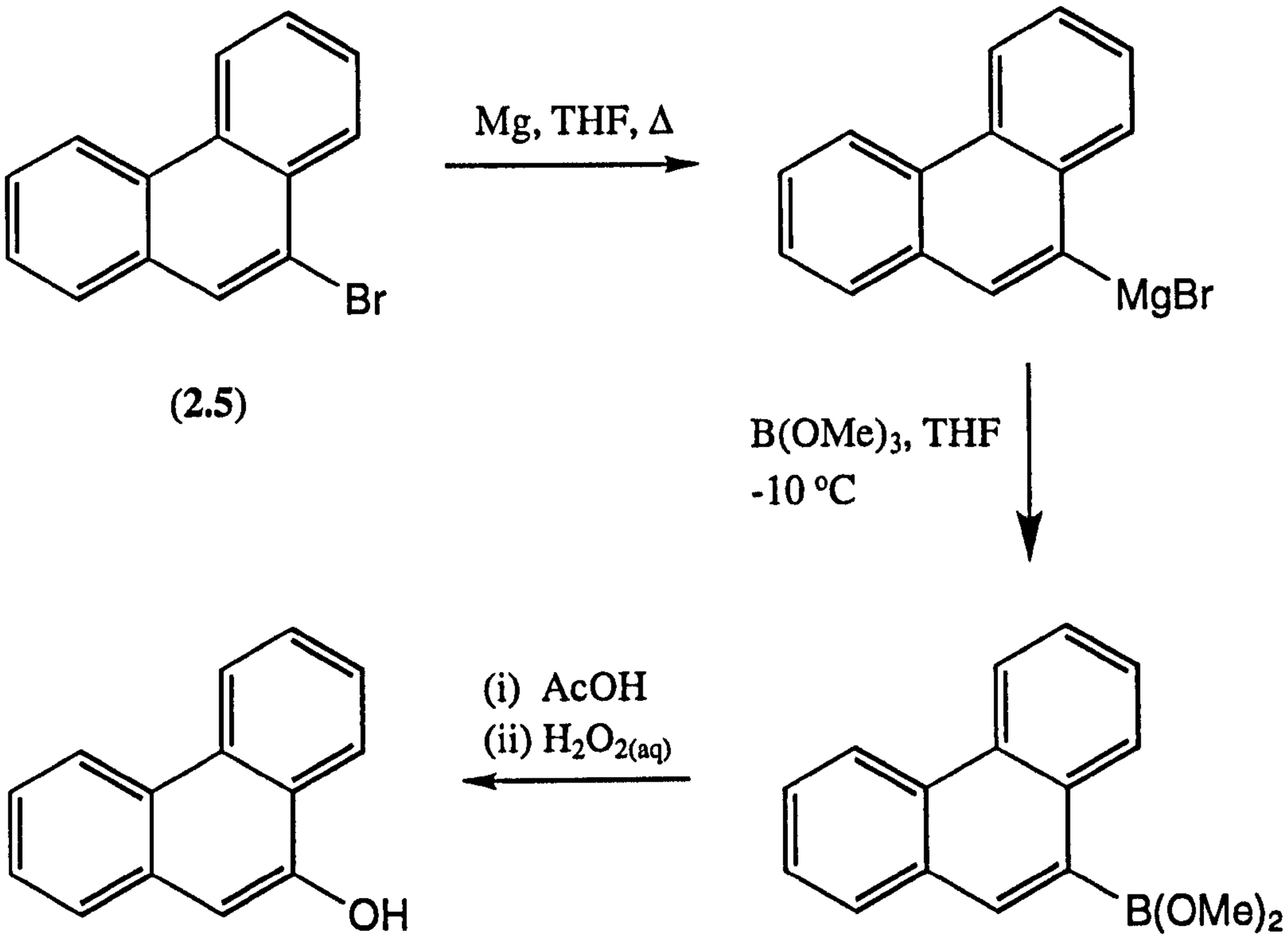

(2.5) **(2.3)**

Scheme 2.2: Synthesis of 9-phenanthrol (**2.3**) from 9-bromophenanthrene (**2.5**)

It is important to note that in all the literature examples glacial acetic acid had to be added after reaction of the Grignard reagent with trimethyl borate, but before peroxide oxidation, to prevent conversion to ArH.

Having achieved the successful synthesis of 9-phenanthrol, the next step was the oxidative coupling,[119] see Equation 2.1. This employs two equivalents of copper(II) nitrate trihydrate as a one-electron donor and six equivalents of (-)-(*R*)-1,2-diphenylethylamine to induce enantioselectivity. Thus the racemic ligand was resolved by fractional crystallisation of its tartrate salt according to the procedure of Söderquist.[124]

The coupling reaction (see Equation 2.1) is reported[119] to proceed in 86% yield after one hour at -5 °C but in our hands no coupling was observed after 24 h at room temperature and, therefore, alternative coupling methods were sought. We discovered that 9-phenanthrol was coupled in quantitative yield upon treatment with two equivalents of copper(II) nitrate trihydrate and six equivalents of benzylamine. Care must be taken to ensure complete dissolution of the copper(II) nitrate trihydrate for reaction to proceed smoothly. It also proved essential to wash the solution of the extracted product with 2M ammonium hydroxide solution to remove any remaining copper salts before purification by silica column chromatography since otherwise

decomposition appeared to occur. Further, the column was eluted with toluene since the biphenanthrol formed 1:1 solvates with ether and chloroform.

The biphenanthrol was resolved by a slightly modified version of the method of Toda.[118] This involved the diastereoselective formation and crystallisation of a 1:2 inclusion complex of (*S*)-(-)-biphenanthrol with (*R,R*)-(+)-*N,N,N',N'*-tetramethyl-2,2-dimethyl-1,3-dioxolane-*trans*-4,5-dicarboxamide (**2.7**),[118] an optically active amide host derived from (*R,R*)-(+)-diethyl tartrate (**2.8**).[118,125] In our hands more ethanol was required to dissolve the biphenanthrol than was reported by Toda (see Experimental) and consequently less of the 1:2 inclusion complex crystallised. We did not isolate the other enantiomer optically pure, which is reported to crystallise from the mother liquor as a 1:1 inclusion complex. However, (*R*)-(+)-biphenanthrol (**2.2**) was obtained optically pure by replication of this procedure using (*S,S*)-(**2.7**), which was readily prepared from (*S,S*)-(-)-diethyl tartrate,[118,125] see Scheme 2.3.

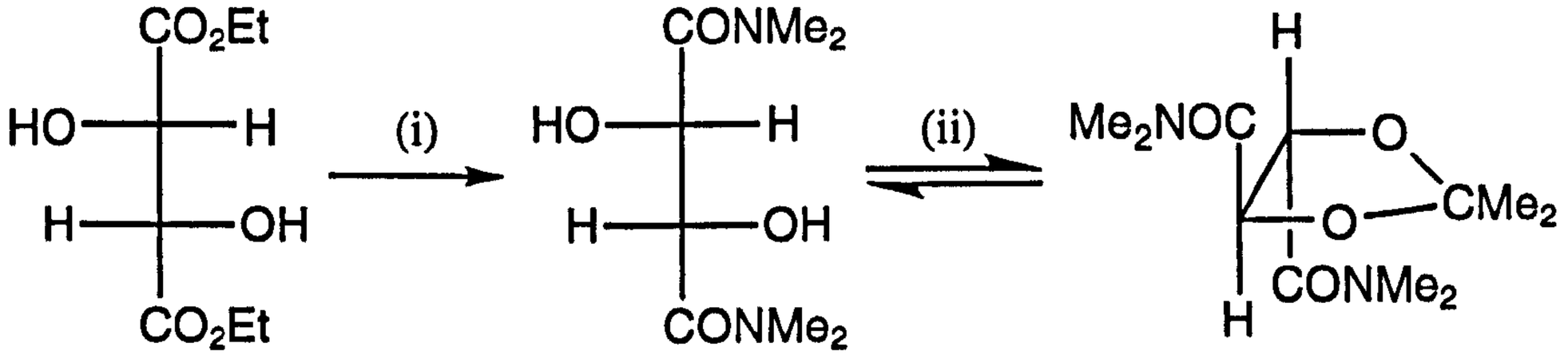

(2.8) **(2.9)** **(2.7)**

Reaction conditions:
(i) Me_2NH, MeOH
(ii) 2 eq 2,2-dimethoxypropane, 0.05 eq *p*-TsOH.H_2O, toluene, Δ

Scheme 2.3: Synthesis of (*S,S*)-(-)-*N,N,N',N'*-tetramethyl-2,2-dimethyl-1,3-dioxolane-*trans*-4,5-dicarboxamide (**2.7**)

The 2,2-dimethoxypropane needs to be freshly distilled before the final step in this sequence in order for the reaction to proceed to completion since it appears that water drives the equilibrium to the left, favouring the diol (**2.9**).

In summary, a synthesis of racemic biphenanthrol (**2.2**) has been achieved in three steps from phenanthrene (**2.4**) in 36% overall yield and the biphenanthrol (**2.2**) has been resolved by a modified version of Toda's procedure[118] in 25% yield (maximum theoretical yield = 50%), see Scheme 2.4.

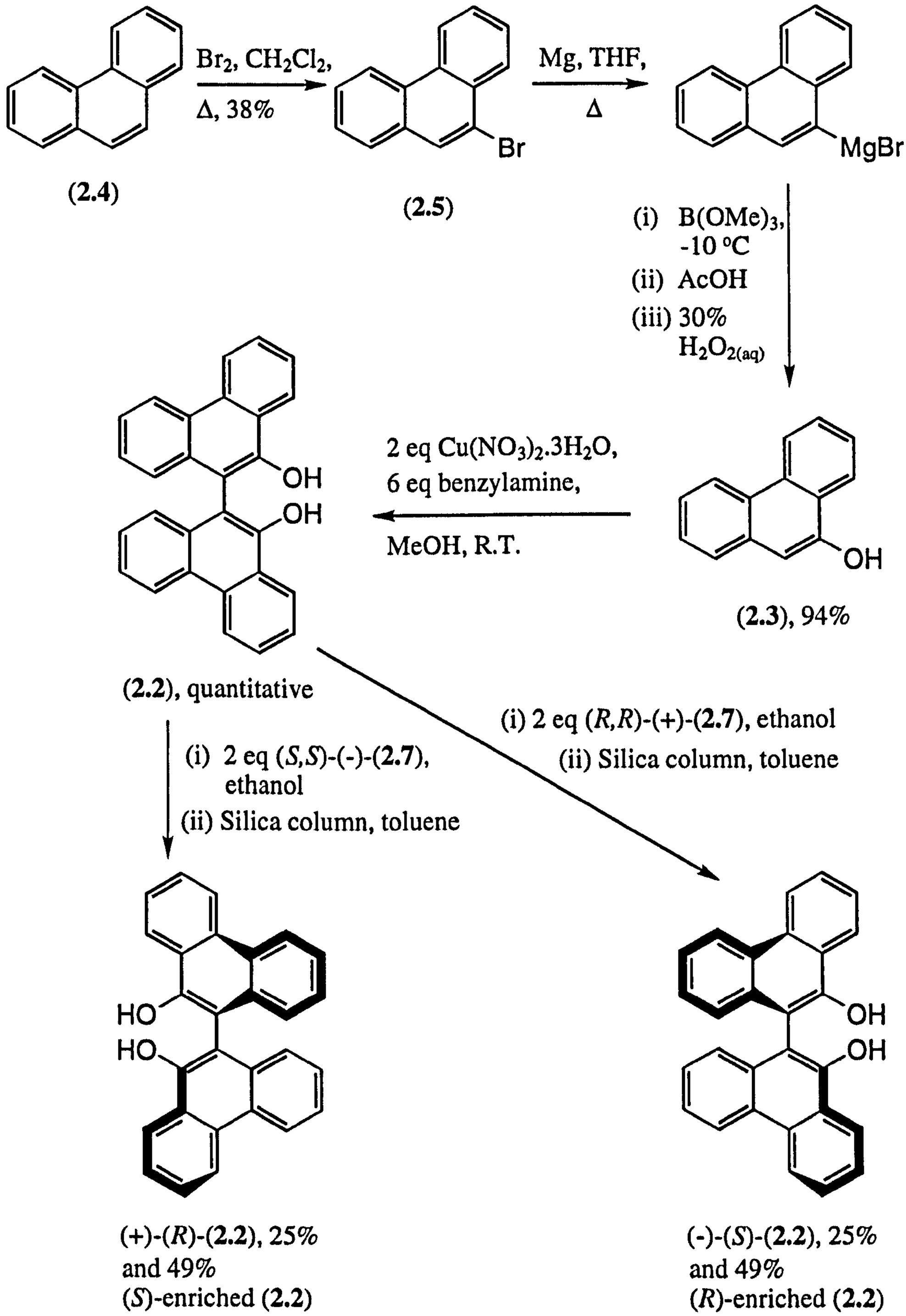

Scheme 2.4: Synthesis of optically pure biphenanthrol (**2.2**) from phenanthrene (**2.4**)

Dimethyl-1,1'-binaphthyl-2,2'-dihydroxy-3,3'-dicarboxylate (**2.1**) was synthesised as a racemic mixture in 73% overall yield from 3-hydroxy-2-naphthoic acid by acid-catalysed esterification followed by oxidative coupling, according to a modification[117] of literature procedures,[126] see Scheme 2.5.

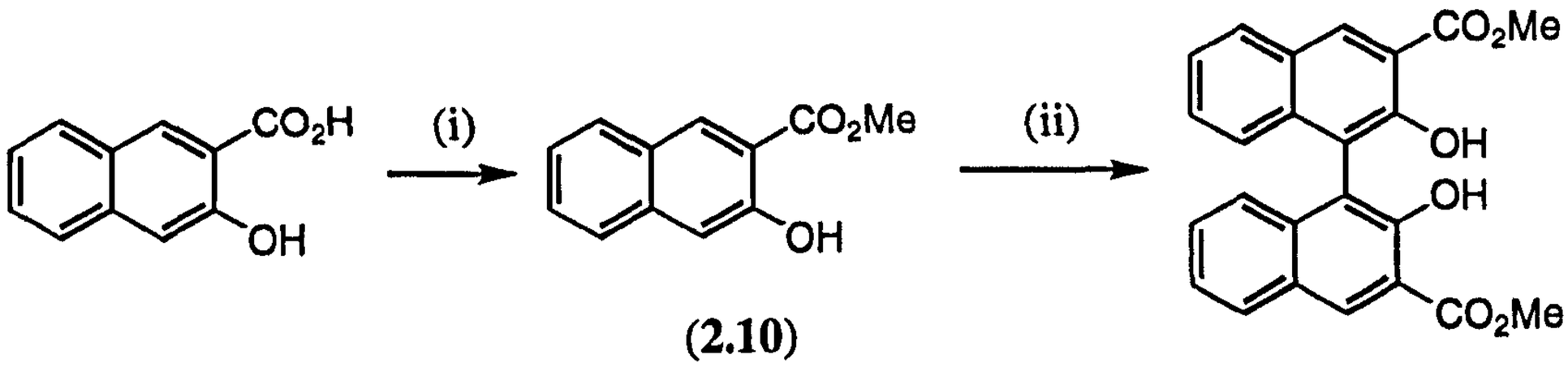

(2.10) **(2.1)**

Reaction conditions:
(i) MeOH, H_2SO_4, Δ
(ii) 2 eq $CuCl_2$, 4 eq $^tBuNH_2$, MeOH, 50 °C

Scheme 2.5: Synthesis of dimethyl-1,1'-binaphthyl-2,2'-dihydroxy-3,3'-dicarboxylate (**2.1**) from 3-hydroxy-2-naphthoic acid

2.2 Synthesis of phosphonites derived from 9,9'-biphenanthryl-10,10'-diol (2.2) and dimethyl-1,1'-binaphthyl-2,2'-dihydroxy-3,3'-dicarboxylate (2.1)

In this Section the preparation, characterisation and properties of a monophosphonite, a diphosphonite and a phosphinophosphonite derived from (**2.2**) and a monophosphonite derived from (**2.1**) are described.

2.2.1 Mono- and diphosphonite syntheses from $RPCl_2$ species

Phosphonites have the general formula $RP(OR')_2$, where both R and R' can be alkyl or aryl. An efficient, established procedure for the synthesis of phosphonites is the condensation of $RPCl_2$ reagents with an alcohol in the presence of a base, such as triethylamine, to remove the HCl produced.[21] Under these conditions the reactions are very exothermic and so are controlled by cooling. Thus, (±)-(**2.11**), (±)-(**2.12**) and (*S*)-(**2.12**) were prepared by reaction of $PhPCl_2$ with (±)-(**2.1**), (±)-(**2.2**) and (*S*)-(**2.2**) respectively in the presence of triethylamine at -10 °C. These reactions are depicted in Equations 2.2 and 2.3. The change of solvent from THF to CH_2Cl_2 for the synthesis of (**2.11**) was because the diester (**2.1**) is insoluble in THF.

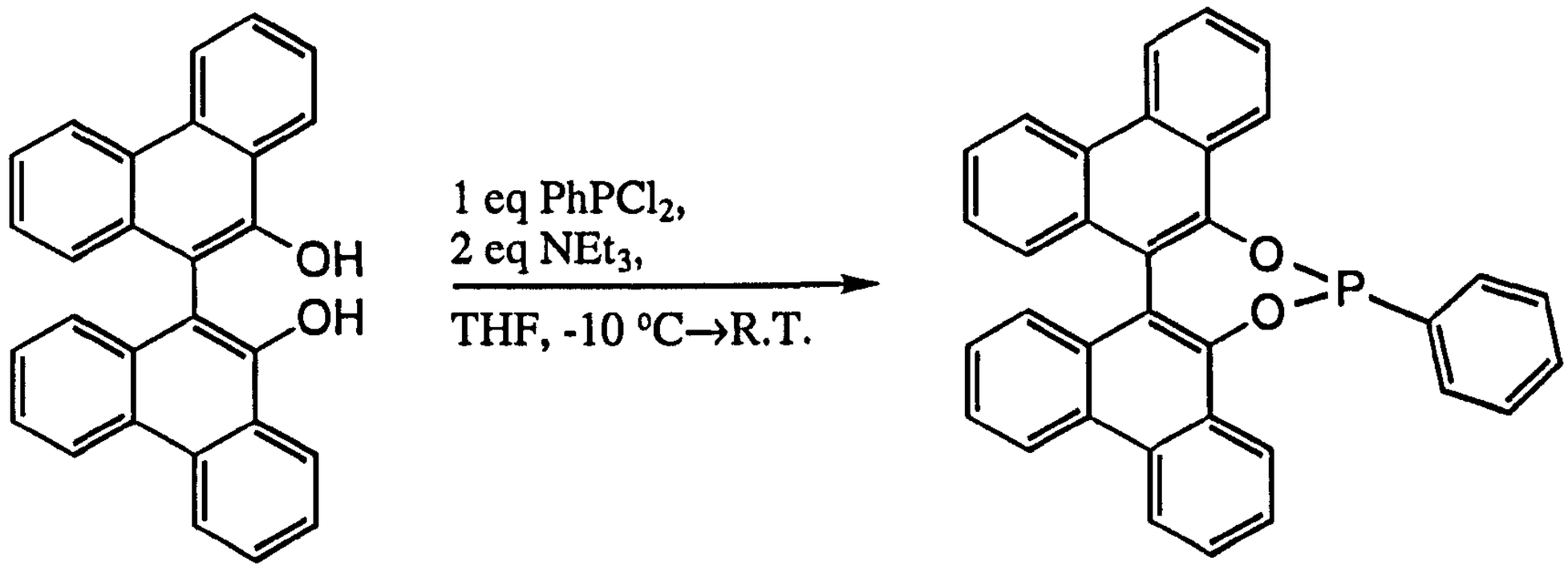

(2.2) **(2.12)**, 81% + 2 $[HNEt_3]Cl$

Equation 2.2

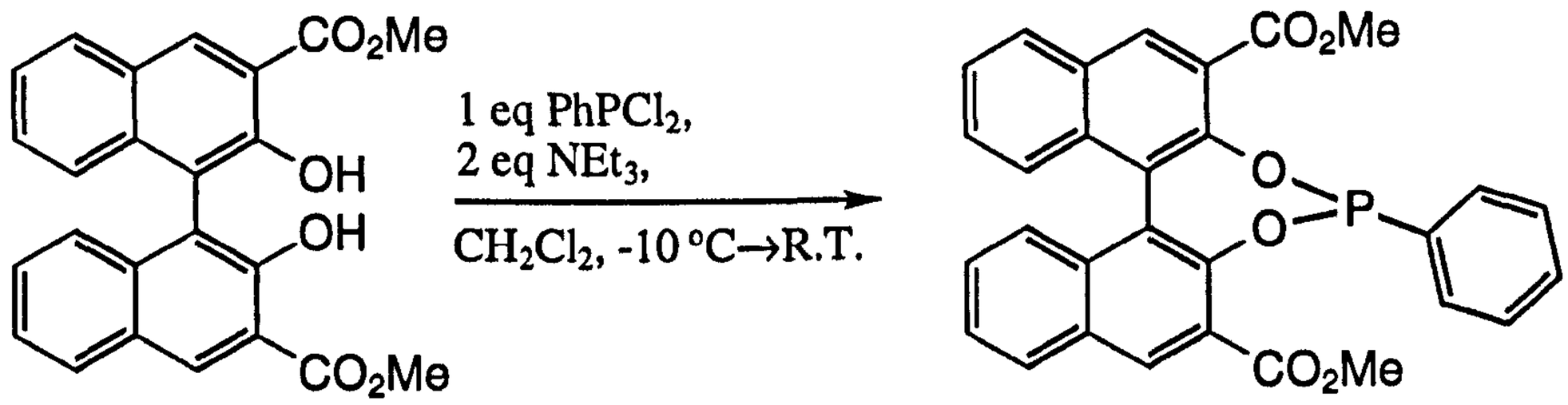

(2.1) **(2.11)**, 33% + 2 $[HNEt_3]Cl$

Equation 2.3

In both reactions (Equations 2.2 and 2.3), upon addition of the triethylamine to a solution of the $PhPCl_2$ a copious precipitate formed. At first it was thought that this may be due to the formation of triethylammonium chloride by reaction of the triethylamine with any HCl produced by reaction of the $PhPCl_2$ with traces of water in the solvent and / or the triethylamine. However, neither PhP(O)(OH)H (**2.13**) (from hydrolysis of the $PhPCl_2$) nor $PhP(O)(OH)_2$ (**2.14**) were observed in the $^{31}P\{^1H\}$ NMR spectrum of the product. We now propose that the precipitate is due to reaction of the triethylamine with the $PhPCl_2$ to form the salt (**2.15**). This salt would be a much more reactive electrophile than $PhPCl_2$ and would react with the phenol to give the monophosphonite, *i.e.* a form of nucleophilic catalysis.

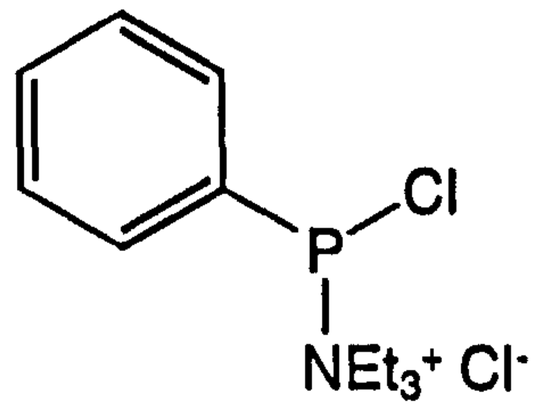

(2.15)

The reactions (Equations 2.2 and 2.3) need to be monitored closely and the monophosphonites (**2.11**) and (**2.12**) should be separated from the $[HNEt_3]Cl$ by filtration as soon as the reactions are complete in order to prevent decomposition catalysed by the acidic byproduct. Phosphonites (**2.11**) and (**2.12**) have been isolated in pure form and have been fully characterised by $^{31}P\{^1H\}$, $^{13}C\{^1H\}$ and ^1H NMR spectroscopy as well as mass spectrometry, see Table 2.1 and Experimental.

Table 2.1: $^{31}P\{^1H\}$ and ^1H NMR data for monophosphonites (**2.11**) and (**2.12**)

Compound	δ_P ($CDCl_3$)[a]	δ_H ($CDCl_3$)[b]
(2.11)	184.4	3.58 (3H, s, MeO)
		3.95 (3H, s, MeO')
		7.24 (1H, d, ^3J(HH) 7.6)
		7.27 (1H, d, ^3J(HH) 7.0)
		7.31-7.41 (5H, m)
		7.45 (1H, d, ^3J(HH) 8.2)
		7.47 (1H, d, ^3J(HH) 8.8)
		7.49 (1H, d, ^3J(HH) 7.9)
		7.51 (1H, d, ^3J(HH) 8.2)
(2.12)	186.5	7.94 (1H, d, ^3J(HH) 7.6)
		8.03 (1H, d, ^3J(HH) 8.6)
		8.32 (1H, s, H4)
		8.69 (1H, s, H4')
		7.07-7.13 (2H, m)
		7.22-7.30 (2H, m)
		7.31-7.37 (2H, m)
		7.40 (1H, d, ^3J(HH) 8.2)
		7.47 (1H, d, ^3J(HH) 8.2)
		7.50-7.63 (6H, m)
		7.69-7.75 (1H, m)
		7.77-7.83 (1H, m)
		8.42 (1H, d, ^3J(HH) 8.2)
		8.63 (1H, d, ^3J(HH) 8.2)
		8.73 (1H, d, ^3J(HH) 8.5)
		8.80 (1H, d, ^3J(HH) 8.2)
		8.84 (1H, d, ^3J(HH) 8.5)

a Spectra recorded at 162 MHz at 28 °C. Chemical shifts (δ) in p.p.m. (±0.1) to high frequency of 85% H_3PO_4.

b Spectra recorded at 400 MHz at 28 °C. Chemical shifts (δ) in p.p.m. (±0.01) to high frequency of tetramethylsilane. Coupling constants (*J*) in Hz (±0.1).

It is interesting to note at this point that both monophosphonites, in contrast to the C_2-symmetry of the starting diols, belong to the C_1 point group (see Figure 2.1) and that, consequently, the hydrogen and carbon atoms are inequivalent, as is borne out by NMR spectroscopy. For example, the two methoxy groups of monophosphonite (**2.11**) are assigned resonances at 3.58 p.p.m. and 3.95 p.p.m. in the ^1H NMR spectrum, see Table 2.1, and are also readily distinguishable in the $^{13}C\{^1H\}$ NMR spectrum, see Experimental.

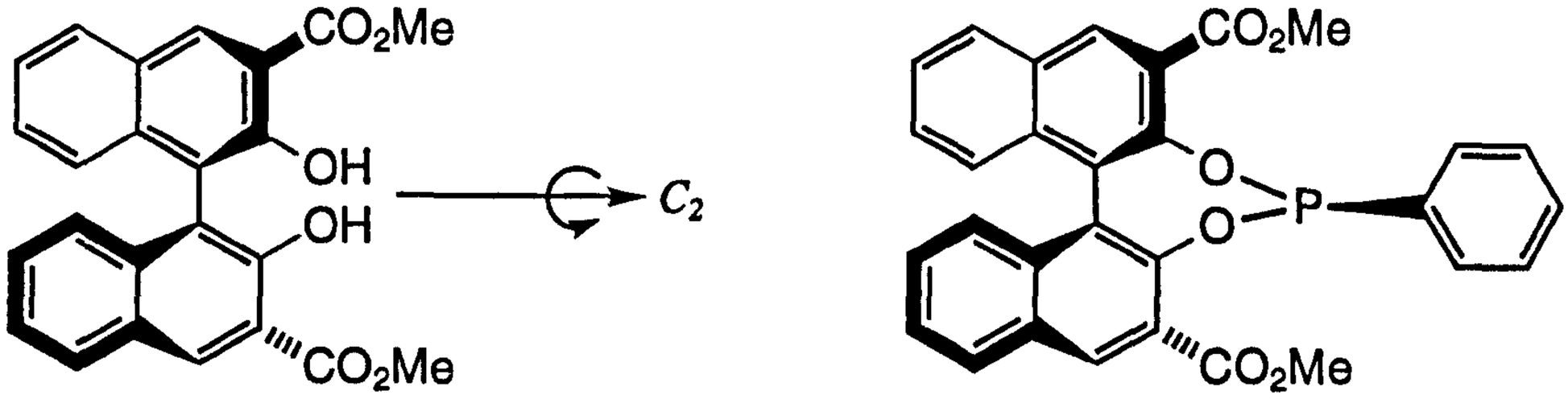

(2.1) **(2.11)**, C_1-symmetry

Figure 2.1: The different symmetry properties of **(2.1)** and **(2.11)**

These monophosphonites are exceptionally moisture-sensitive and, even in the solid state, they undergo significant hydrolysis upon exposure to air for just a few minutes, forming phenylphosphinic acid (**2.13**). We have thus not obtained satisfactory elemental analyses for (**2.11**) and (**2.12**).

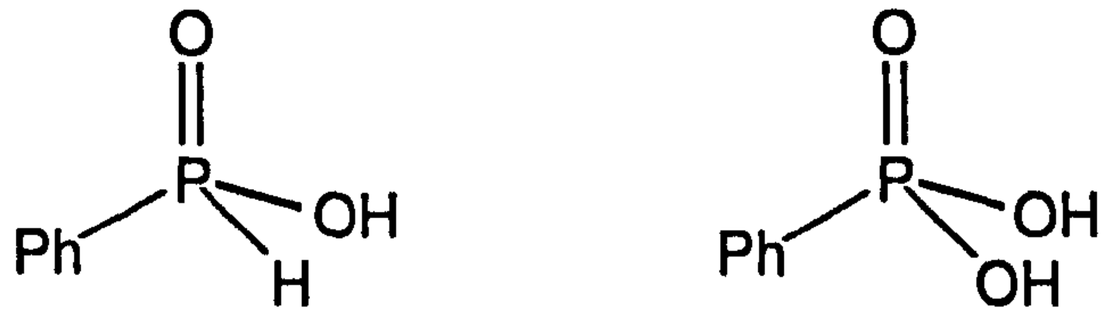

(2.13) **(2.14)**

The diphosphonite (**2.16**) was obtained by reaction of $Cl_2PCH_2CH_2PCl_2$ (**2.17**) with biphenanthrol (**2.2**) in the presence of triethylamine at -10 °C, Equation 2.4.

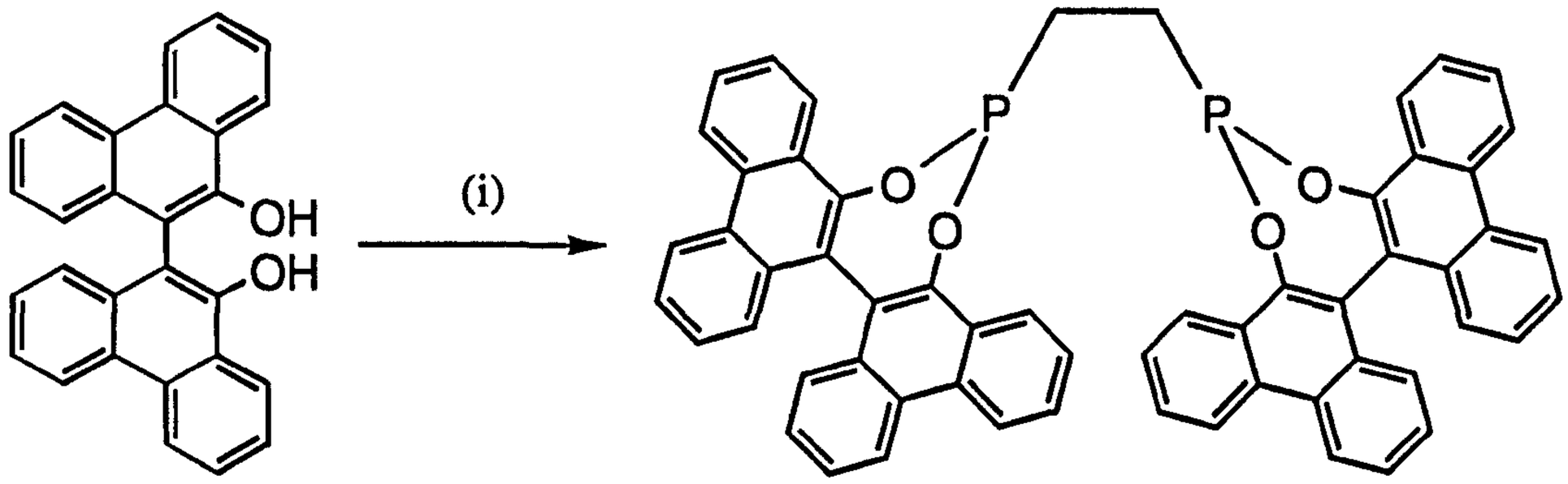

(2.2) **(2.16)**, quantitative

(i) 0.5 eq $Cl_2PCH_2CH_2PCl_2$,
2 eq NEt_3, THF, -10 °C

Equation 2.4

Provided moisture was rigorously excluded and the $[HNEt_3]Cl$ was removed by filtration as soon as the reaction was completed, the diphosphonite (**2.16**) could be obtained in quantitative yield. Once again, a precipitate was observed after the addition of the triethylamine to the solution of (**2.17**). It is postulated that this is due to reaction of the triethylamine with (**2.17**) to form an electrophilic salt analogous to (**2.15**).

Addition of racemic (**2.2**) to $Cl_2PCH_2CH_2PCl_2$ at -10 °C led to a surprising degree of diastereoselectivity. Statistically, a 1:1 mixture of the (*R,R*) / (*S,S*)- and the (*R,S*)-diastereomers would be expected but instead a *ca.* 3:1 mixture in favour of the (*R,S*)-diastereomer was obtained. This diastereomeric mixture has been characterised by $^{31}P\{^1H\}$ NMR spectroscopy, see Table 2.2 and Experimental.

Addition of optically pure (*S*)-(**2.2**) to $Cl_2PCH_2CH_2PCl_2$ gave (*S,S*)-(**2.16**) and this has been fully characterised by $^{31}P\{^1H\}$, ^1H and $^{13}C\{^1H\}$ NMR spectroscopy, see Table 2.2 and Experimental. Once again, the extreme moisture-sensitivity of this compound has precluded the attainment of satisfactory elemental analysis.

Overall (*S,S*)-(**2.16**) is C_2-symmetric and therefore the carbon atoms in one biphenanthryl moiety are equivalent to those in the other biphenanthryl moiety and the two carbons of the ethane bridge are equivalent which is consistent with the $^{13}C\{^1H\}$ NMR spectrum (see Experimental). However, within each biphenanthryl group the carbon atoms are inequivalent as in the monophosphonites (**2.11**) and (**2.12**) and hence twenty-two signals are observed in the aromatic region of the $^{13}C\{^1H\}$ NMR spectrum of (*S,S*)-(**2.16**).

Table 2.2: $^{31}P\{^{1}H\}$ and ^{1}H NMR data for diphosphonite (**2.16**) and intermediate (**2.18**)

Compound	δ_P ($CDCl_3$)[a]	δ_H ($CDCl_3$)[b]
(*S,S*)-(**2.16**)	211.7	1.94-2.08 (2H, m) 2.93-3.06 (2H, m) 7.24-7.36 (8H, m) 7.53-7.76 (12H, m) 8.17 (4H, d, ^{3}J(HH) 8.2) 8.69-8.77 (8H, m)
(*R,S*)-(**2.16**)[c]	212.6	------
(**2.17**)	192.5	------
(**2.18**)[d]	191.7 (d, ^{3}J (PP) 9, P_B) 209.9 (d, ^{3}J (PP) 9, P_A)	------

a Spectra recorded at 162 MHz at 28 °C. Chemical shifts (δ) in p.p.m. (±0.1) to high frequency of 85% H_3PO_4. Coupling constants (*J*) in Hz (±3).

b Spectra recorded at 400 MHz at 28 °C. Chemical shifts (δ) in p.p.m. (±0.01) to high frequency of tetramethylsilane. Coupling constants (*J*) in Hz (±0.1).

c Spectra recorded in $CDCl_3$ / THF (1:4).

d Spectra recorded in $CDCl_3$ / THF (2:3).

The formation of diphosphonite (**2.16**) was followed by $^{31}P\{^{1}H\}$ NMR and an intermediate was detected with inequivalent ^{31}P signals at δ_P 209.9 and 191.7 and ^{3}J(PP) 9 Hz. This can be unambiguously assigned to (**2.18**) by comparison of the chemical shifts with those of $RPCl_2$ and $RP(OR)_2$ species.

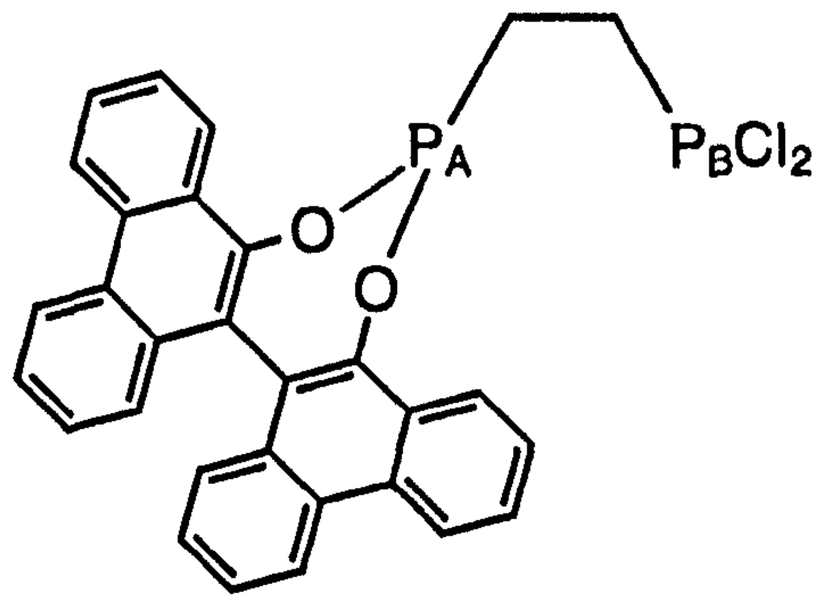

(2.18)

The synthesis of (**2.18**) is a desirable goal, since this compound should be readily converted to a series of C_1-symmetric diphosphonites upon reaction with one of a wide range of cheap, readily available optically active diols, see Equation 2.5.

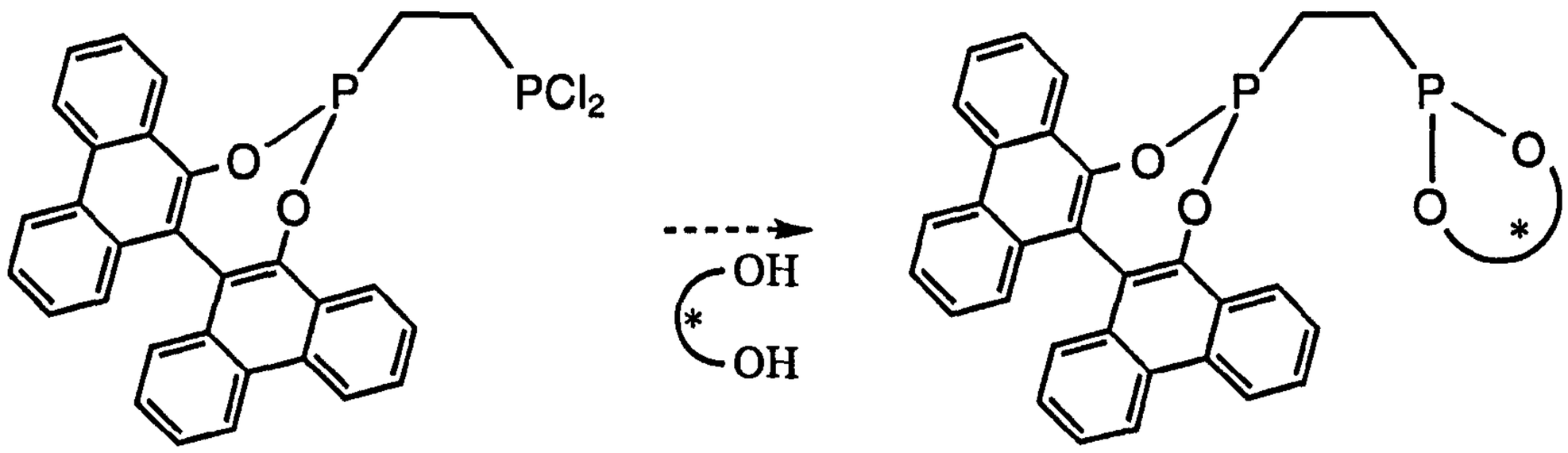

(2.18)

Equation 2.5

2.2.2 Phosphinophosphonite synthesis from $RP(NMe_2)_2$ species

Another convenient method for the synthesis of P-O bonds is by the reaction of alcohols with $R_{(3-x)}P(NMe_2)_x$.[51,127] One advantage of this route is that no base is required and the by-product of the reaction is the volatile dimethylamine. However, the P-N bonds are less reactive than the P-Cl bonds and, consequently, the reactions often require elevated temperatures. Other researchers in this laboratory showed that the mixed phosphinophosphonite (**2.19**) could be synthesised by reaction of binaphthol with $Ph_2PCH_2CH_2P(NMe_2)_2$ (**2.20**),[51] which was synthesised according to the method of King,[128] Scheme 2.6.

(2.20)

(2.19)

Scheme 2.6: Synthesis of the phosphinophosphonite ligand (**2.19**)

Thus, by a similar procedure the mixed phosphinophosphonite derivative of biphenanthrol (**2.21**) was synthesised in 97% yield.

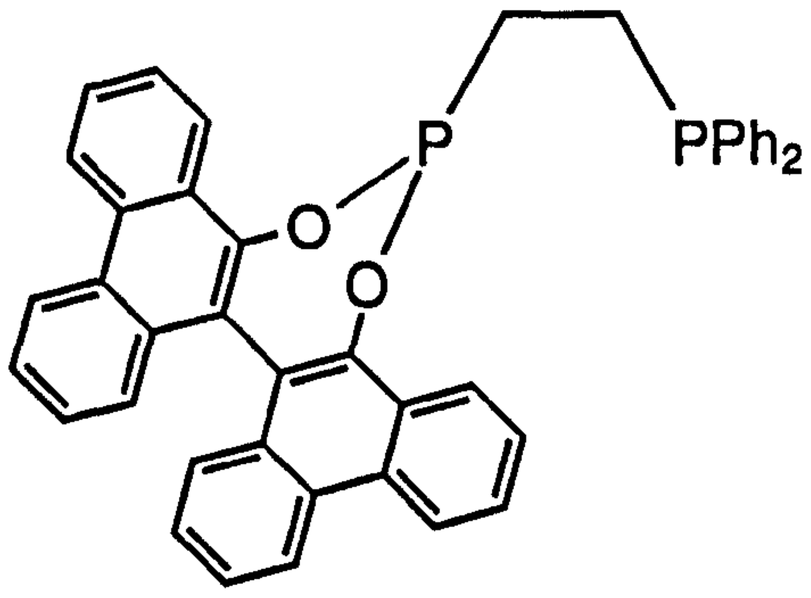

(2.21)

This compound is much more stable to hydrolysis than the monophosphonites (**2.11**) and (**2.12**) and the diphosphonite (**2.16**) and can be briefly handled in air. It has been fully characterised by $^{31}P\{^{1}H\}$, ^{1}H and $^{13}C\{^{1}H\}$ NMR spectroscopy, see Table 2.3 and Experimental.

Table 2.3: $^{31}P\{^{1}H\}$ and ^{1}H NMR data for the phosphinophosphonites (**2.21**) and (**2.19**)

Compound	δ_P ($CDCl_3$)[a]	δ_H ($CDCl_3$)[b]
(**2.21**)	-12.8 (d, ^{3}J(PP) 28, P_B)	1.67-1.79 (2H, m)
	215.5 (d, ^{3}J(PP) 31, P_A)	2.06-2.18 (1H, m)
		2.30-2.40 (1H, m)
		7.14-7.39 (14H, m)
		7.53-7.62 (2H, m)
		7.66 (1H, td, ^{3}J(HH) 7.6, ^{4}J(HH) 1.0)
		7.73 (1H, td, ^{3}J(HH) 7.4, ^{4}J(HH) 1.0)
		7.75-7.81 (2H, m)
		8.19 (1H, dd, ^{3}J(HH) 8.1, ^{4}J(HH) 1.1)
		8.35 (1H, dd, ^{3}J(HH) 7.8, ^{4}J(HH) 1.4)
		8.76 (2H, dd, ^{3}J(HH) 8.2, ^{4}J(HH) 2.5)
		8.79 (2H, d, ^{3}J(HH) 8.2)
(**2.19**)[c,d]	-12.7 (d, ^{3}J(PP) 24, $\underline{P}Ph_2$)	------
	210.3 (d, ^{3}J(PP) 24, $\underline{P}(OR)_2$)	

a Spectra recorded at 162 MHz at 28 °C. Chemical shifts (δ) in p.p.m. (±0.1) to high frequency of 85% H_3PO_4. Coupling constants (*J*) in Hz (±3).

b Spectra recorded at 400 MHz at 28 °C. Chemical shifts (δ) in p.p.m. (±0.01) to high frequency of tetramethylsilane. Coupling constants (*J*) in Hz (±0.1).

c Ref. 51

d Spectra recorded at 162 MHz in THF / C_6D_6 (5:1) at 25 °C. Chemical shifts (δ) in p.p.m. (±0.1) to high frequency of 85% H_3PO_4. Coupling constants (*J*) in Hz (±3).

The assignment of P_A to the phosphonite phosphorus and P_B to the phosphine phosphorus is from the chemical shifts. The $^{13}C\{^1H\}$ NMR spectrum of (**2.21**) (see Experimental) shows thirty-five resonances in the aromatic region due to the carbon atoms of the biphenanthryl moiety being inequivalent {as we have seen already for the diphosphonite (**2.16**)} and also because the two phenyl rings of the diphenylphosphino group are diastereotopic.

2.3 Coordination chemistry of phosphonites derived from 9,9'-biphenanthryl-10,10'-diol (2.2) and dimethyl-1,1'-binaphthyl-2,2'-dihydroxy-3,3'-dicarboxylate (2.1)

In this Section the complexation of the phosphonites (**2.11**), (**2.12**), (**2.16**) and (**2.21**) to platinum(II), platinum(0) and rhodium(I) is discussed.

2.3.1 Dichloroplatinum(II) complexes

The preparation of dichloroplatinum(II) complexes serves as a simple first method for probing the coordination chemistry of these new phosphonite ligands since these complexes are generally stable to hydrolysis and oxidation.

2.3.1.1 Monophosphonites (2.11) and (2.12)

Addition of two equivalents of racemic monophosphonites (**2.11**) and (**2.12**) to $[PtCl_2(cod)]$ in THF gave complexes (**2.22**) and (**2.23**) respectively.

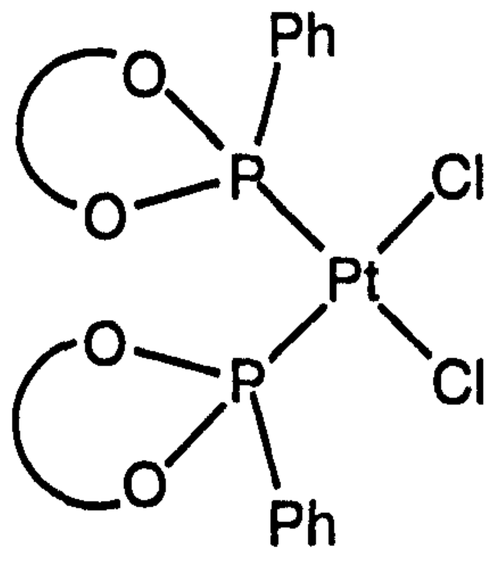

(**2.22**), when = (**2.11**)

(**2.23**), when = (**2.12**)

Use of racemic monophosphonite (**2.12**) might be expected to give a 1:1 mixture of the (*R,S*)- and (*S,S*) / (*R,R*)-diastereomers of (**2.23**). However, we were surprised to discover that a high degree of stereoselectivity is exhibited in the complexation reaction since a 10:1 mixture is obtained. This diastereomeric mixture has been characterised by $^{31}P\{^1H\}$ NMR spectroscopy, see Table 2.4 and Figure 2.2.

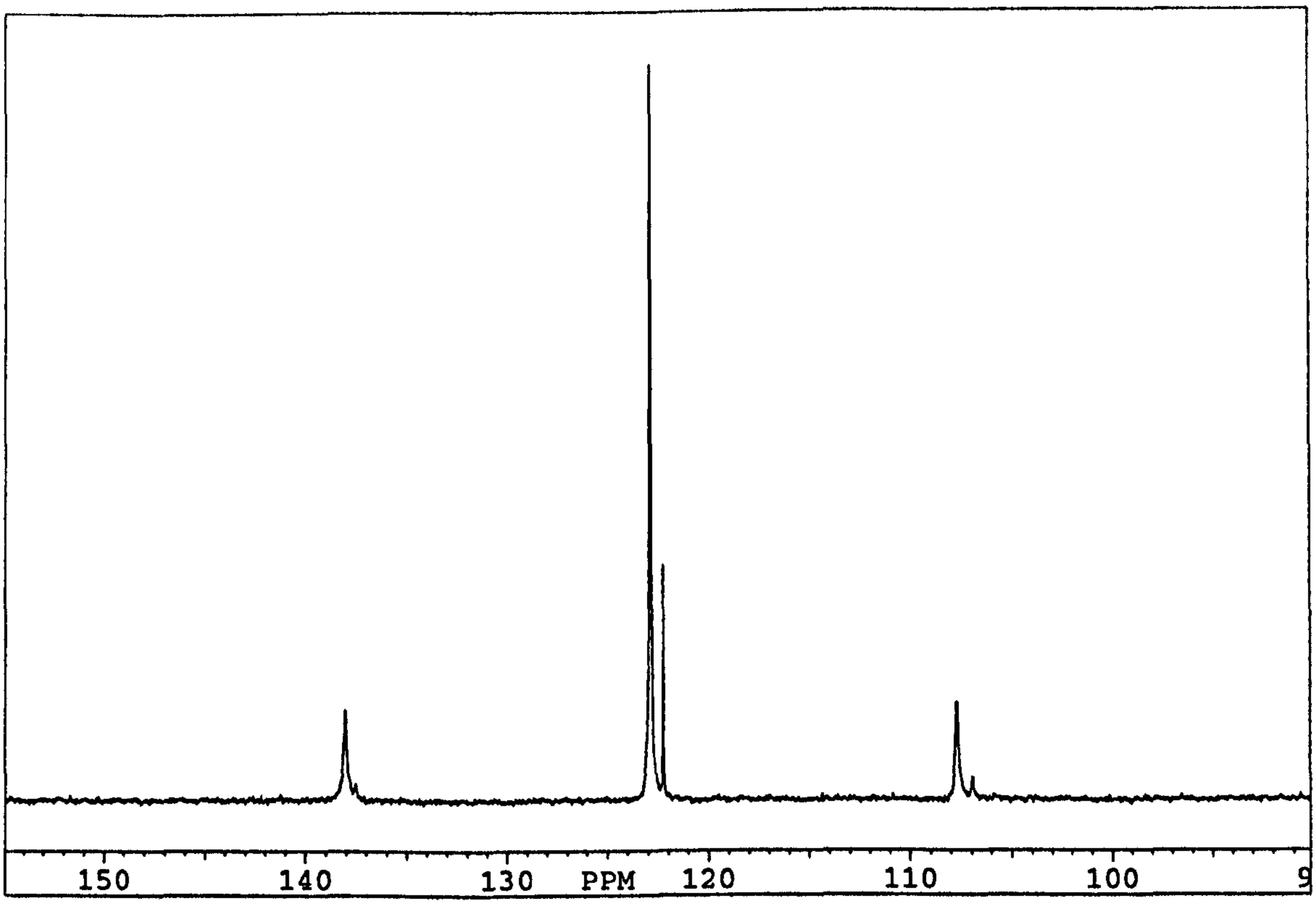

Figure 2.2: $^{31}P\{^{1}H\}$ NMR spectrum of the diastereomeric mixture of dichloroplatinum(II) complexes (*S*,*S*) / (*R*,*R*)- and (*R*,*S*)-(**2.23**)

It appears that even greater selectivity is exhibited in the formation of (**2.22**), since only one diastereomer is observed in the $^{31}P\{^{1}H\}$ and $^{195}Pt\{^{1}H\}$ NMR spectra, see Table 2.4 and Experimental. This complex has been further characterised by $^{13}C\{^{1}H\}$ and ^{1}H NMR spectroscopy and mass spectrometry, see Experimental.

Table 2.4: $^{31}P\{^{1}H\}$ and $^{195}Pt\{^{1}H\}$ NMR data for dichloroplatinum(II) complexes (**2.22**) and (**2.23**)

Complex	Ligand	δ_P[a]	$^{1}J(PPt)$[b]	δ_{Pt}[c]
(*R*,*R*) / (*S*,*S*)-(**2.22**)[d]	(±)-(**2.11**)	123.1 (s)	4979	162.7 (t)
(**2.23**)[e,f]	(±)-(**2.12**)	122.3 (s)	4943	------
(**2.23**)[f,g]	(±)-(**2.12**)	122.9 (s)	4908	------

a Spectra recorded at 162 MHz at 28 °C. Chemical shifts (δ) in p.p.m. (±0.1) to high frequency of 85% H_3PO_4.
b Coupling constants (*J*) measured in Hz (±3).
c Spectra recorded at 85.6 MHz at 28 °C. Chemical shifts (δ) in p.p.m. (±0.1) to high frequency of Ξ (^{195}Pt) 21.4 MHz.
d Single product formed, which was identified as the (*R*,*R*) / (*S*,*S*)-diastereomer by X-ray crystallography. Spectra recorded in CD_2Cl_2.
e Minor isomer.
f Spectra recorded in $CDCl_3$.
g Major isomer.

Single crystals of (**2.22**) have been grown from CD_2Cl_2 and the structure determined by X-ray crystallography carried out by Miss A. Gillon in this department (see Figures 2.3 and 2.4).

The structure was solved in the space group *P*-1 with two independent formula units, four molecules of chloroform and one molecule of THF per unit cell. Elemental analysis has been obtained for these crystals which is consistent with the formula $C_{60}H_{42}O_{12}P_2PtCl_2.0.5(CHCl_3).0.5(C_4H_8O)$, see Experimental. It can be seen from Figure 2.3 that the stereochemistry of both binaphthyl moieties is (*R*) and we can therefore conclude that it is the (*R*,*R*) / (*S*,*S*)-diastereomer of (**2.22**) that is predominantly formed. It is possible that the (*R*,*R*) / (*S*,*S*)-diastereomer of (**2.23**) is also the one that is preferentially formed but this is pure speculation at this stage. Figure 2.3 also clearly illustrates that the coordination geometry at platinum is square planar with the two monophosphonite ligands in a *cis*-arrangement, which is consistent with the high ^1J(PPt) value obtained (see Section 2.4). The Pt-Cl and Pt-P bond lengths (shown in Table 2.5) are similar to those in *cis*-$[PtCl_2\{P(OC_6H_4OMe\text{-}2)_3\}_2]$ (2.343 Å and 2.346 Å for the Pt-Cl bonds; 2.207 Å and 2.199 Å for the Pt-P bonds),[129] which is consistent with this phosphonite (with an aryl group bound to the phosphorus) exerting a similar *trans* influence to a phosphite.

Table 2.5: Selected bond lengths and interatomic distances for the dichloroplatinum(II) complex (*R*,*R*) / (*S*,*S*)-(**2.22**)

Bond	Length (Å)
Pt(11)-Cl(11)	2.3349 (18)
Pt(11)-Cl(12)	2.3339 (18)
Pt(11)-P(12)	2.1969 (18)
Pt(11)-P(11)	2.2007 (19)
Pt(11), H(102)[a]	3.065
Pt(11), H(108)[a]	3.054

a Interatomic distances.

Selected bond angles for the complex (**2.22**) are shown in Table 2.6 and show that there is some deviation from the ideal values of 90° and 180°. This can be attributed to steric congestion between the two bulky *cis*-monophosphonite ligands which, as can be seen from Figure 2.3, also results in P(2) being displaced from the coordination plane.

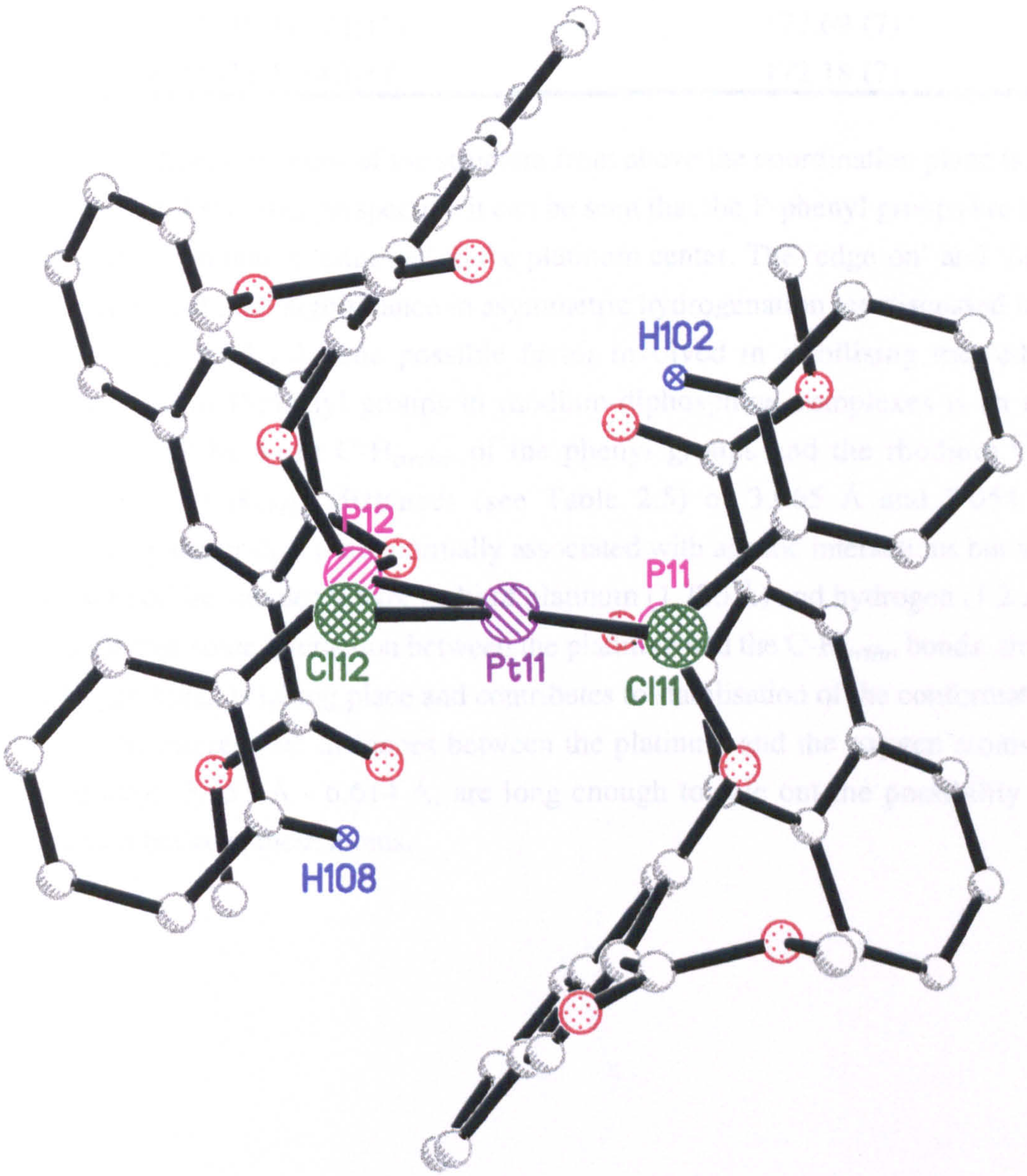

Figure 2.3: Molecular structure of dichloroplatinum(II) complex (*R,R*)-(**2.22**). All except for the *ortho*-hydrogen atoms are omitted for clarity

Table 2.6: Selected bond angles in the dichloroplatinum(II) complex (*R*,*R*) / (*S*,*S*)-**(2.22)**

Bonds	Angle (°)
P(12)-Pt(11)-P(11)	101.25 (7)
P(12)-Pt(11)-Cl(12)	85.05 (7)
P(11)-Pt(11)-Cl(11)	84.74 (7)
Cl(12)-Pt(11)-Cl(11)	89.34 (7)
P(12)-Pt(11)-Cl(11)	172.69 (7)
P(11)-Pt(11)-Cl(12)	172.18 (7)

An alternative view of the structure from above the coordination plane is shown in Figure 2.4. From this perspective it can be seen that the P-phenyl groups are aligned in an orientation that is 'edge-on' to the platinum center. The 'edge-on' and 'face-on' orientations and their significance in asymmetric hydrogenation are discussed in more detail in Section 4.1.2. One possible factor involved in stabilising the 'edge-on' conformation of P-phenyl groups in rhodium-diphosphine complexes is an agostic interaction[130] between C-H_{ortho} of the phenyl groups and the rhodium.[131] The interatomic Pt-H_{ortho} distances (see Table 2.5) of 3.065 Å and 3.054 Å are considerably larger than those normally associated with agostic interactions but are near to the sum of the van der Waals' radii of platinum (1.720 Å) and hydrogen (1.2 Å) so it is feasible that some interaction between the platinum and the C-H_{ortho} bonds, similar to a hydrogen bond, is taking place and contributes to stabilisation of the conformation.

The interatomic distances between the platinum and the oxygen atoms of the ester groups, 3.953 Å - 6.614 Å, are long enough to rule out the possibility of any interaction between these atoms.

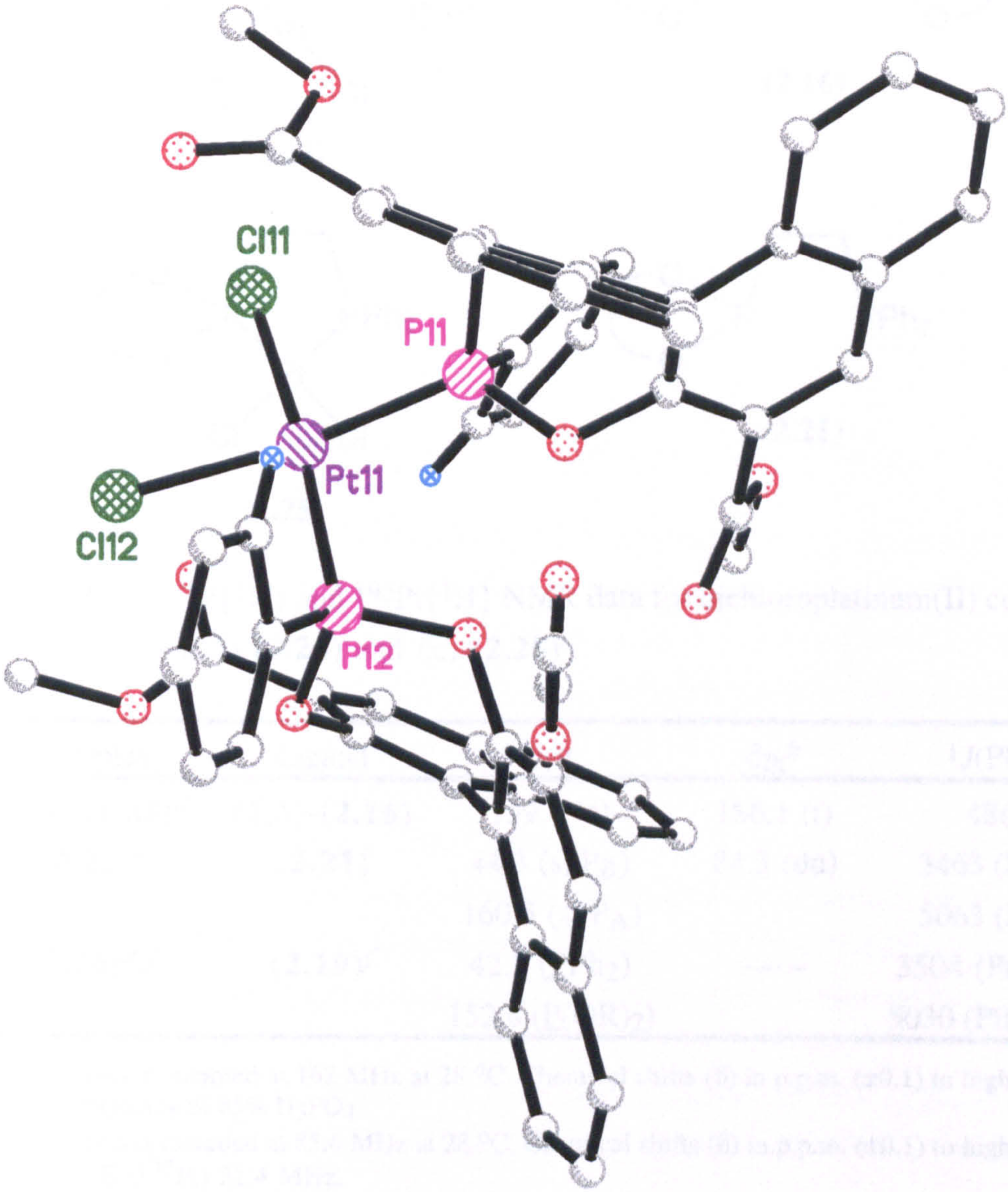

Figure 2.4: Molecular structure of dichloroplatinum(II) complex (*R*,*R*)-(**2.22**) showing the 'edge-on' alignment of the P-phenyl groups with respect to the platinum. All except for the *ortho*-hydrogen atoms are omitted for clarity

2.3.1.2 Diphosphonite (2.16) and phosphinophosphonite (2.21)

The addition of one equivalent of optically pure diphosphonite (*S,S*)-(**2.16**) or racemic phosphinophosphonite (**2.21**) to [$PtCl_2$(cod)] gave dichloroplatinum(II) complexes (*S,S*)-(**2.24**) and (±)-(**2.25**) respectively. These complexes have been fully characterised by $^{31}P\{^1H\}$, $^{13}C\{^1H\}$, $^{195}Pt\{^1H\}$ and ^1H NMR spectroscopy, see Table 2.7 and Experimental.

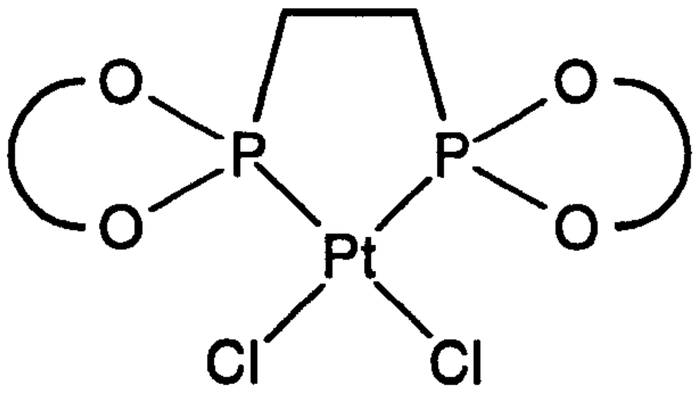

(2.24)

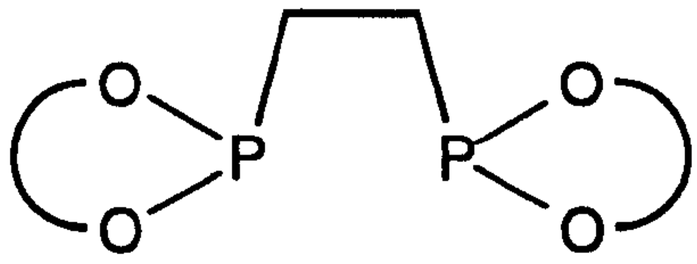

(2.16)

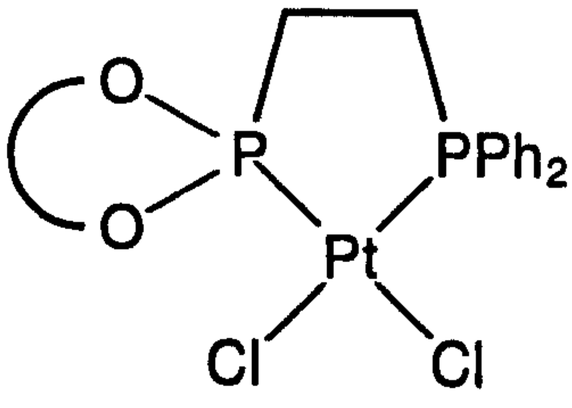

(2.25)

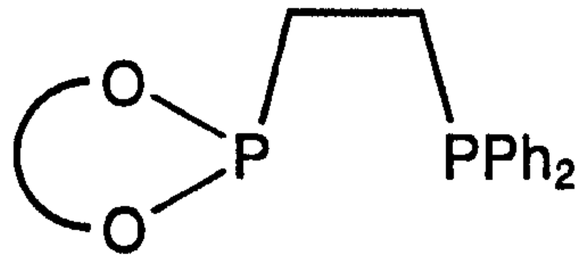

(2.21)

Table 2.7: $^{31}P\{^1H\}$ and $^{195}Pt\{^1H\}$ NMR data for dichloroplatinum(II) complexes (*S,S*)-(**2.24**) and (±)-(**2.25**)

Complex	Ligand	δ_P[a]	δ_{Pt}[b]	^1J(PPt)[c]
(*S,S*)-(**2.24**)[d]	(*S,S*)-(**2.16**)	159.4 (s)	186.1 (t)	4868
(**2.25**)[e]	(**2.21**)	44.3 (s, P_B)	84.3 (dd)	3463 (PtP_B)
		160.5 (s, P_A)		5063 (PtP_A)
(**2.26**)[d,f]	(**2.19**)[f]	42.5 ($\underline{P}Ph_2$)	------	3504 ($PtPPh_2$),
		152.8 ($\underline{P}(OR)_2$)		5030 ($PtP(OR)_2$)

a Spectra recorded at 162 MHz at 28 °C. Chemical shifts (δ) in p.p.m. (±0.1) to high frequency of 85% H_3PO_4.
b Spectra recorded at 85.6 MHz at 28 °C. Chemical shifts (δ) in p.p.m. (±0.1) to high frequency of Ξ (^{195}Pt) 21.4 MHz.
c Coupling constants (*J*) measured in Hz (±3).
d Spectra recorded in CD_2Cl_2.
e Spectra recorded in d_6-dmso.
f Ref. 51

The $^{31}P\{^1H\}$ NMR spectrum of (**2.25**) is shown in Figure 2.5.

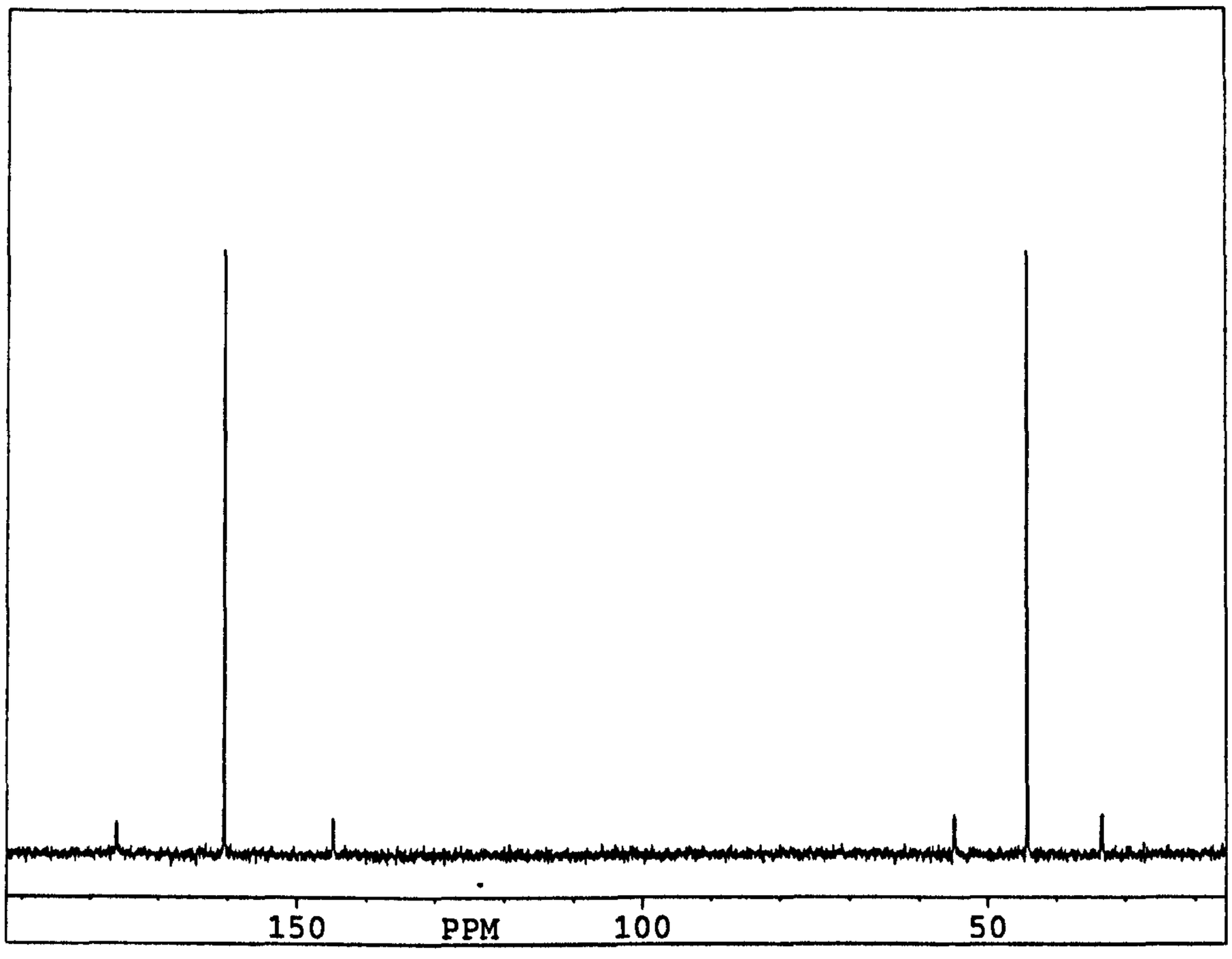

Figure 2.5: $^{31}P\{^{1}H\}$ NMR spectrum of dichloroplatinum(II) complex (**2.25**)

The height of the platinum satellites is much lower than expected due to chemical shift anisotropy. No coupling was observed between the two inequivalent phosphorus atoms. The lower frequency chemical shift and smaller ^{1}J(PtP) allows us to assign P_B to the phosphine phosphorus and thus P_A to the phosphonite phosphorus; the values of these NMR parameters are in close agreement with those obtained for the binaphthol-derived analogue (**2.26**),[51] see Table 2.7.

Complex (**2.25**) has been characterised by mass spectrometry (see Experimental). However, this complex is insoluble in most organic solvents and only sparingly soluble in hot dmso. Consequently attempts to recrystallise this compound for elemental analysis and to grow crystals for X-ray crystallographic studies have been fruitless.

Single crystals of (*S*,*S*)-(**2.24**) have been grown from THF / $CDCl_3$ (3:2) and the structure determined by X-ray crystallography carried out by Miss A. Gillon in this department (see Figure 2.6).

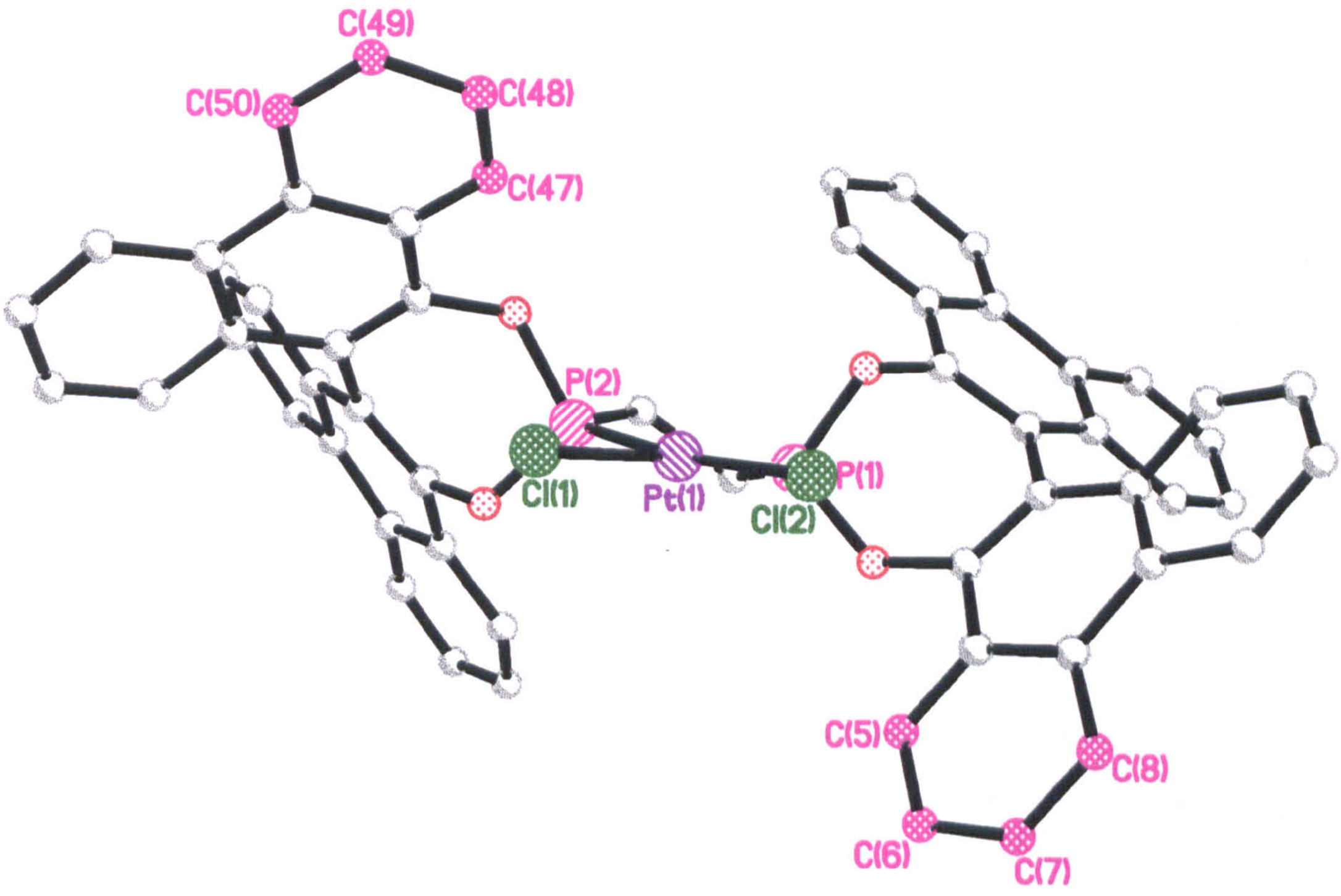

Figure 2.6: Molecular structure of dichloroplatinum(II) complex (*S,S*)-(**2.24**). All hydrogens are omitted for clarity

The structure was solved in the space group $P2_12_12_1$ with a single formula unit, three molecules of THF and two molecules of chloroform present in the unit cell. Elemental analysis has been obtained for these crystals which is consistent with the formula $C_{58}H_{36}O_4P_2PtCl_2.2.5(C_4H_8O).1.5(CHCl_3)$, see Experimental. Figure 2.6 shows that the coordination geometry at platinum is square planar, with the ethane backbone of the five-membered chelate ring in a λ conformation, see Page 141. The selected bond angles in Table 2.8 show small deviations from those of the ideal geometry of 90° and 180°. Presumably this deviation and the displacement of P(2) from the coordination plane, see Figure 2.6, minimises steric interactions.

Table 2.8: Selected bond angles for the dichloroplatinum(II) complex (*S*,*S*)-(**2.24**)

Bonds	Angle (°)
P(2)-Pt(1)-P(1)	85.93 (9)
P(2)-Pt(1)-Cl(1)	91.87 (10)
P(1)-Pt(1)-Cl(2)	91.36 (10)
Cl(2)-Pt(1)-Cl(1)	91.16 (10)
P(2)-Pt(1)-Cl(2)	173.31 (11)
P(1)-Pt(1)-Cl(1)	176.22 (11)

The Pt-Cl and Pt-P bond lengths, see Table 2.9, are similar to those in *cis*-$[PtCl_2\{P(OC_6H_4OMe\text{-}2)_3\}_2]$[129] and monophosphonite (*R*,*R*)-(**2.22**), which is consistent with this phosphonite (with an alkyl group bound to the phosphorus) exerting a similar *trans* influence to a phosphite.

Table 2.9: Selected bond lengths in the dichloroplatinum(II) complex (*S*,*S*)-(**2.24**)

Bond	Length (Å)
Pt(1)-Cl(1)	2.351 (2)
Pt(1)-Cl(2)	2.337 (3)
Pt(1)-P(2)	2.183 (3)
Pt(1)-P(1)	2.189 (2)

2.3.2 Rhodium(I) complexes

2.3.2.1 Monophosphonites (2.11) and (2.12)

Treatment of two equivalents of monophosphonite (*S*)-(**2.12**) with $[Rh(cod)_2]BF_4$ in CH_2Cl_2 gave the rhodium(I) complex (*S*,*S*)-(**2.27**), which is of particular interest as it is a potential catalyst for asymmetric hydrogenation. It has been characterised by $^{31}P\{^1H\}$ NMR spectroscopy, see Table 2.10 and Experimental.

Whilst this complex appears to be stable to hydrolysis and can be briefly handled as a solid in the air, its solutions should be handled under nitrogen to prevent formation of an adduct, (*S,S*)-(**2.28**), with oxygen. This adduct has been observed in the $^{31}P\{^{1}H\}$ NMR spectrum of a sample of (*S,S*)-(**2.27**) left in solution for several days.

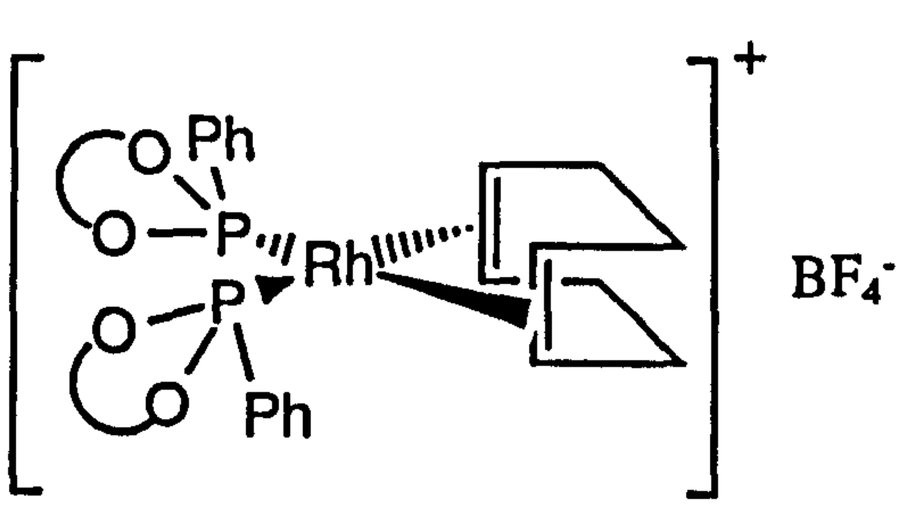

BF_4^-

(2.27)

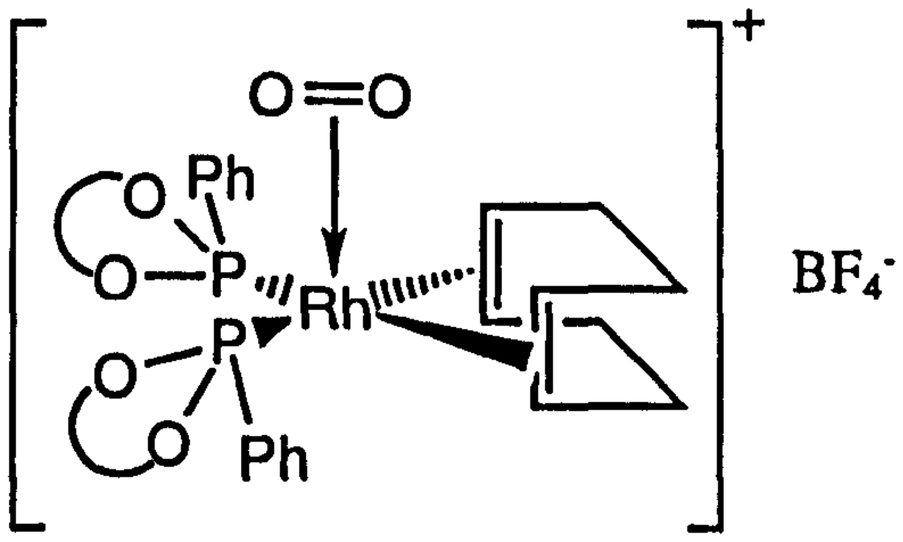

BF_4^-

(2.28)

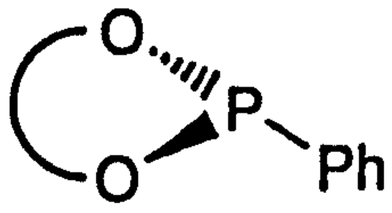

= **(2.12)**

The $^{31}P\{^{1}H\}$ NMR spectrum of a THF / C_6D_6 (3:2) solution of (*S,S*)-(**2.27**) is shown in Figure 2.7. A broad doublet (^{1}J(PRh) 214 Hz) can be observed indicating that the complex is fluxional.

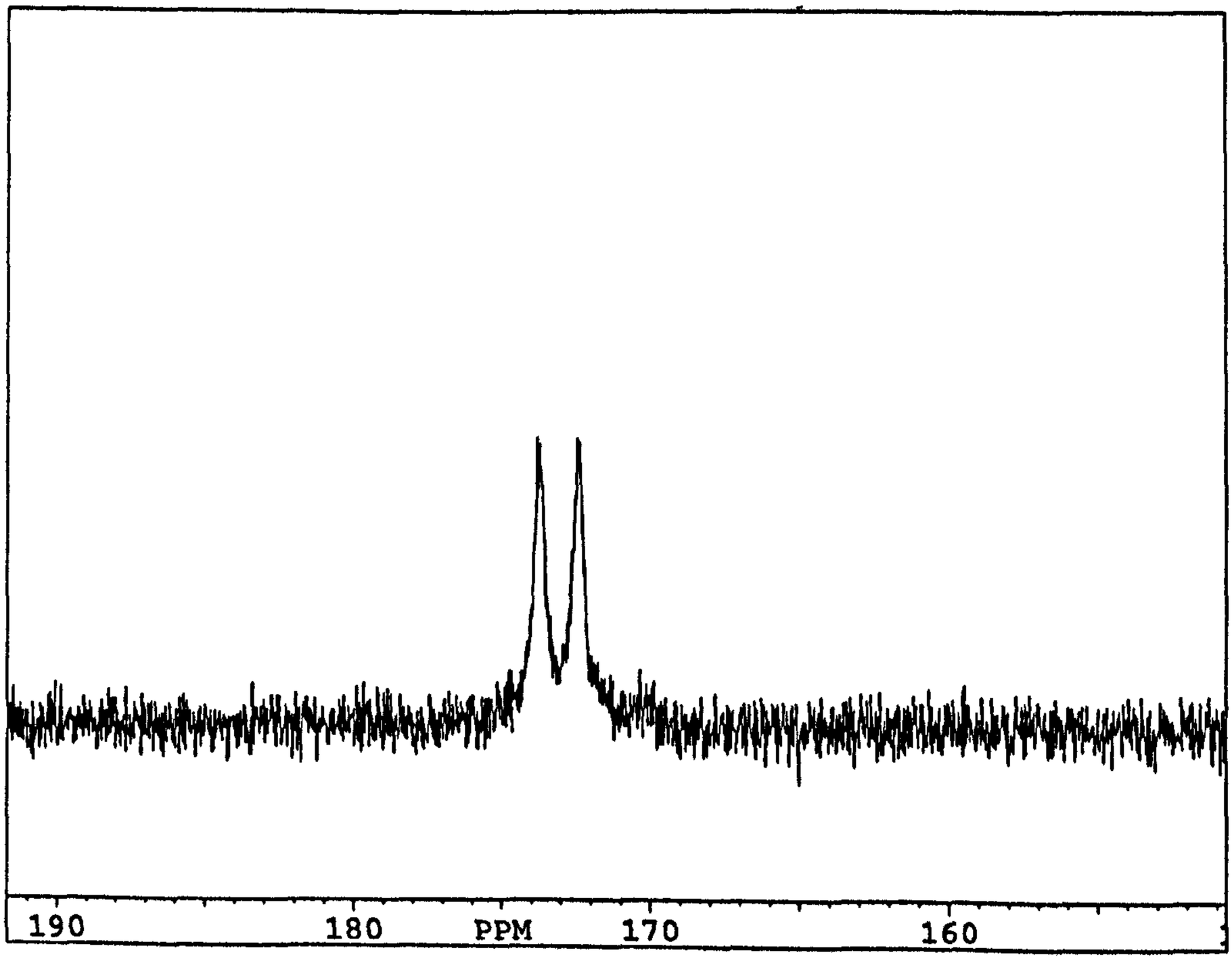

Figure 2.7: $^{31}P\{^{1}H\}$ NMR spectrum of rhodium(I) complex (*S,S*)-(**2.27**)

Two possible sources of the fluxionality are:

i. Steric hindrance impeding rotation about the rhodium-phosphorus bonds.

ii. Rapid association and dissociation of chloride ions present in solution to the metal centre; chloride impurity may be present in the $[Rh(cod)_2]BF_4$ starting material as a result of the route by which it is synthesised, see Scheme 4.1.

However further work, including variable temperature $^{31}P\{^1H\}$ NMR spectroscopy, needs to be carried out to provide insight into this fluxionality.

Treatment of two equivalents of (±)-(**2.11**) or (±)-(**2.12**) with $[Rh(CO)_2(dpm)]$ (where dpm is dipivaloylmethane) in THF did not yield diastereomeric mixtures of the expected bis(monophosphonite) species (**2.29**) and (**2.30**); rather it was found that only one equivalent of monophosphonite was bound to the metal to form the complexes (**2.31**) and (**2.32**) which have been characterised by $^{31}P\{^1H\}$ and ^1H NMR spectroscopy, mass spectrometry and IR spectroscopy, see Table 2.10 and Experimental. This conclusion is based on the following evidence:

i. ^1H NMR spectroscopy shows aromatic : *tert*-butyl integration ratios of 15:18 and 21:18 for compounds (**2.31**) and (**2.32**) respectively. In each case, two singlets are observed at low chemical shifts indicating that the *tert*-butyl groups are inequivalent, see Experimental.

ii. Mass spectrometry shows the presence of the parent ions {$M+Na^+$ for (**2.31**) and $M+H^+$ for (**2.32**)} and, in each case, a fragment ($M-211^+$) consistent with loss of the dpm group, see Experimental.

iii. IR spectroscopy shows the presence of metal carbonyl stretches at 2007.5 cm^{-1} and 2005.0 cm^{-1} for (**2.31**) and (**2.32**) respectively.

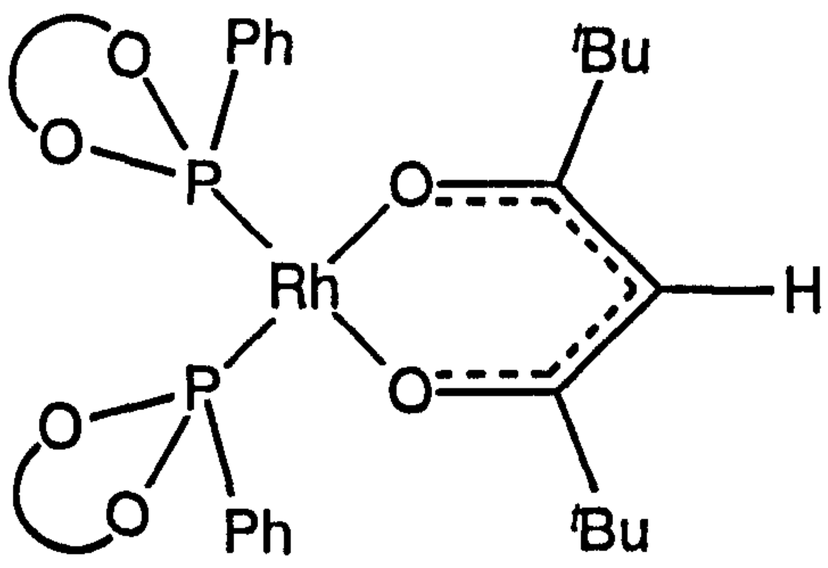

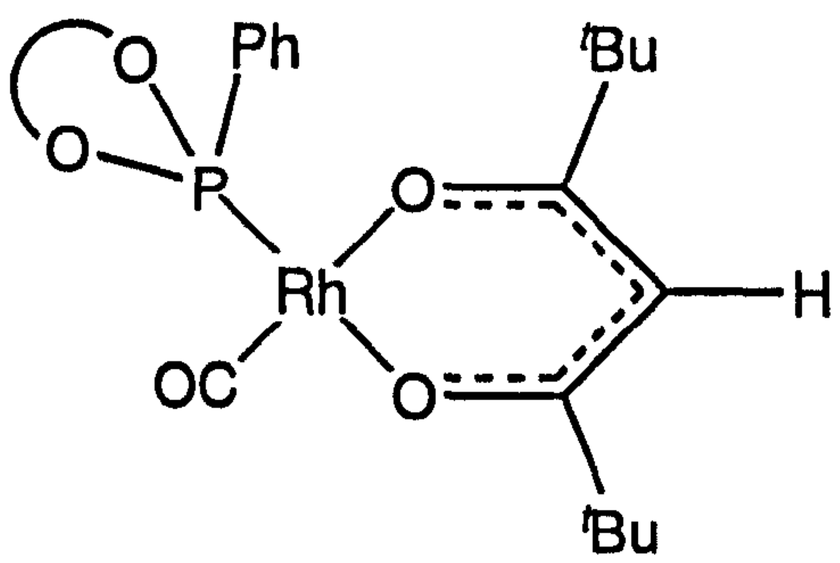

(**2.29**) = (**2.11**) (**2.31**)

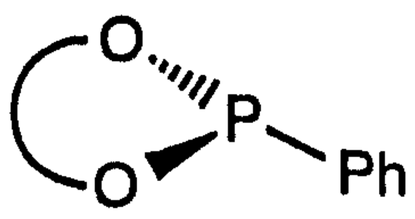

(**2.30**) = (**2.12**) (**2.32**)

These complexes are stable to hydrolysis and they can be handled in air, even in solution, without formation of adducts with oxygen. Consequently they can be separated from any hydrolysed monophosphonite (**2.13**) that might be present by

digestion with methanol and filtration. The hydrolysis product (**2.13**) is soluble in methanol whereas the rhodium complexes are insoluble.

The formation of these monocomplexes may reflect the very bulky nature of the organic backbones of these monophosphonites. Similar behaviour has been observed in the coordination chemistry of bulky calix[4]arene monophosphites.[127]

2.3.2.2 Diphosphonite (S,S)-(2.16)

Treatment of one equivalent of diphosphonite (*S,S*)-(**2.16**) with $[Rh(cod)_2]BF_4$ led to the formation of complex (*S,S*)-(**2.33**), which is of particular interest because of its potential as a catalyst for asymmetric hydrogenation. This complex has been characterised by $^{31}P\{^1H\}$ and ^1H NMR spectroscopy, see Table 2.10 and Experimental. In the presence of an excess of ligand, further reaction occurs to form the bis(chelate) (*S,S*),(*S,S*)-(**2.34**) which has been characterised by $^{31}P\{^1H\}$ NMR spectroscopy, see Table 2.10. Whilst it is prudent to store and handle complex (**2.33**) under nitrogen to prevent any possibility of the formation of a dioxygen adduct, it appears that it is stable to hydrolysis and, even in solution, to oxygen.

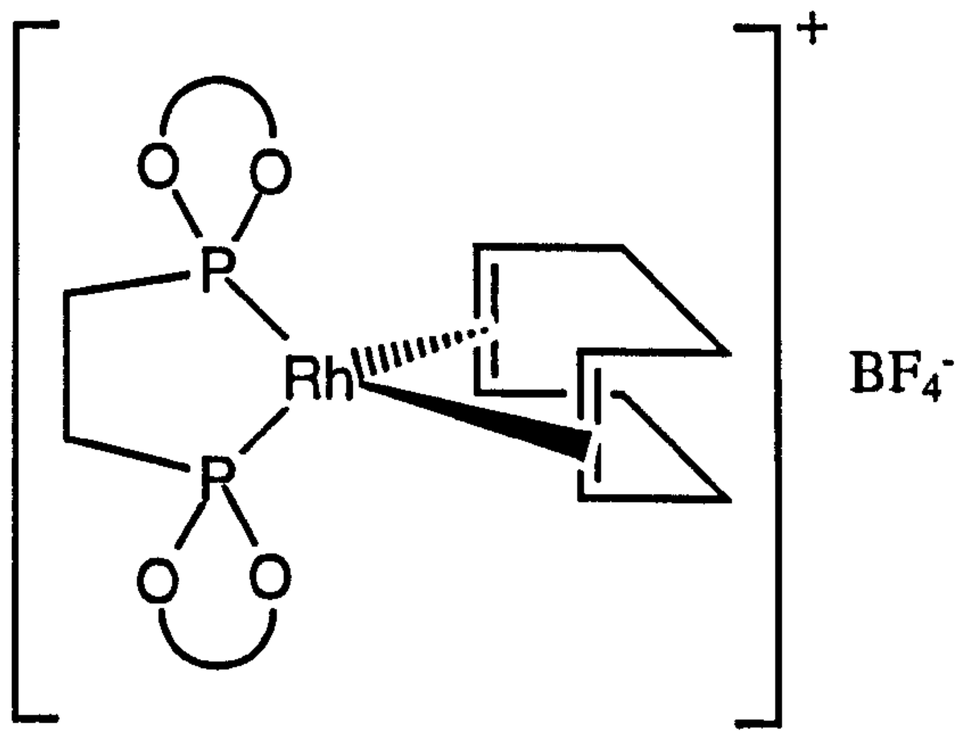

(2.33)

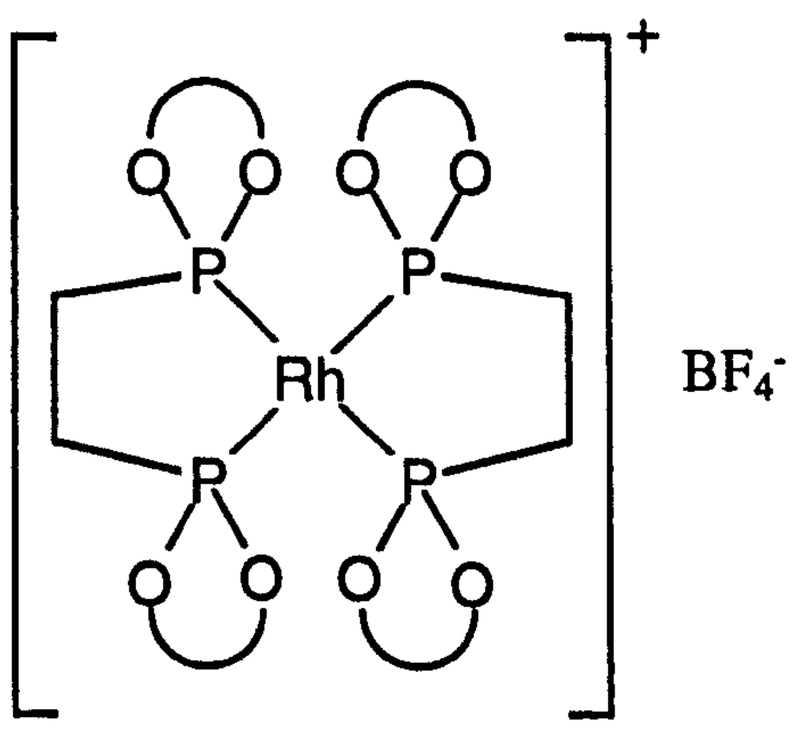

(2.34)

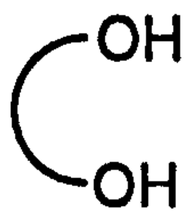

= (2.2)

2.3.2.3 Phosphinophosphonite (2.21)

Treatment of one equivalent of phosphinophosphonite (*S*)-(**2.21**) with $[Rh(cod)_2]BF_4$ gave complex (*S*)-(**2.35**), which is of special interest because of its potential use in asymmetric hydrogenation. The complex was found to be stable to hydrolysis and could be handled in air, although it was stored in an inert atmosphere to prevent any possibility of reaction with oxygen. It has been characterised by $^{31}P\{^1H\}$ NMR spectroscopy, see Table 2.10 and Experimental. The assignment of P_A to the

phosphonite phosphorus and P_B to the phosphine phosphorus is from the chemical shifts.

Complex (*S*)-(**2.35**) can potentially react with an excess of phosphinophosphonite (*S*)-(**2.21**) to form a mixture of the two bis(chelates) (*S,S*)-(**2.36**) and (*S,S*)-(**2.37**). In practice only one of these two species has been observed and has been assigned as (*S,S*)-(**2.36**) from analysis of the $^{31}P\{^{1}H\}$ NMR spectrum, see Table 2.10. The large ^{2}J(PP) value (305 Hz) is indicative of a *trans* relationship between the phosphine and the phosphonite moieties, which have been assigned as P_B and P_A respectively from their chemical shifts. The exclusive formation of bis(chelate) (**2.36**) is in accordance with the antisymbiotic principle which predicts a preference for a strong σ-donor to be *trans* to a weak σ-donor.[132]

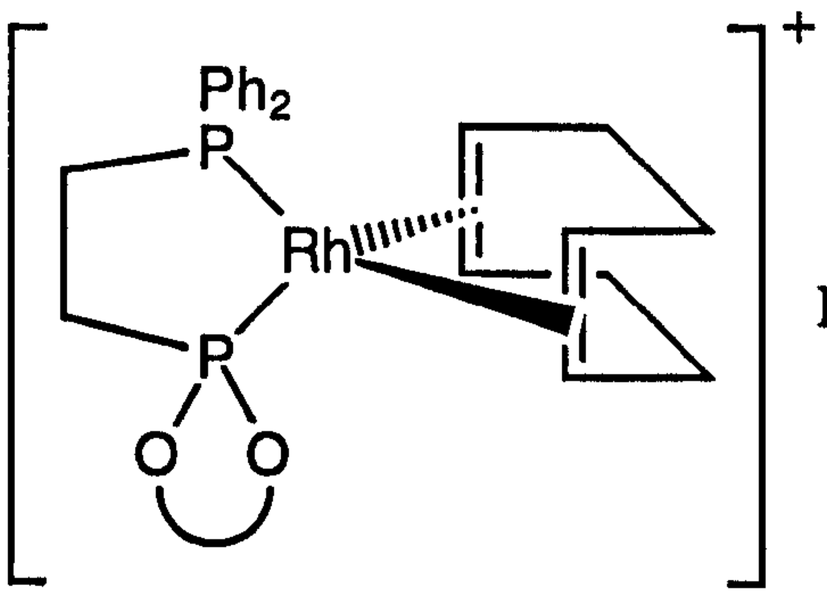

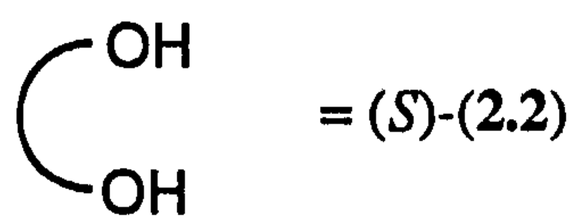

= (*S*)-(**2.2**)

(*S*)-(**2.35**)

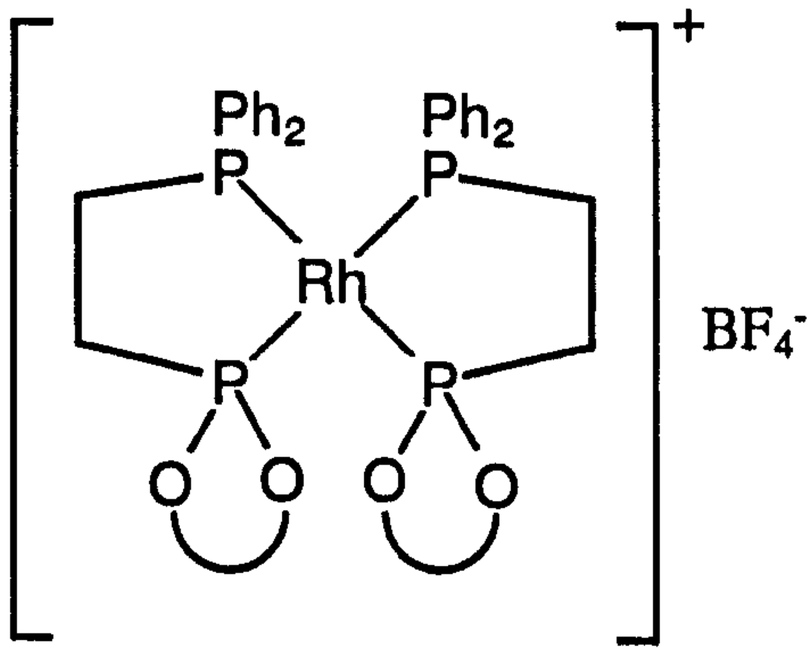

(*S,S*)-(**2.36**)

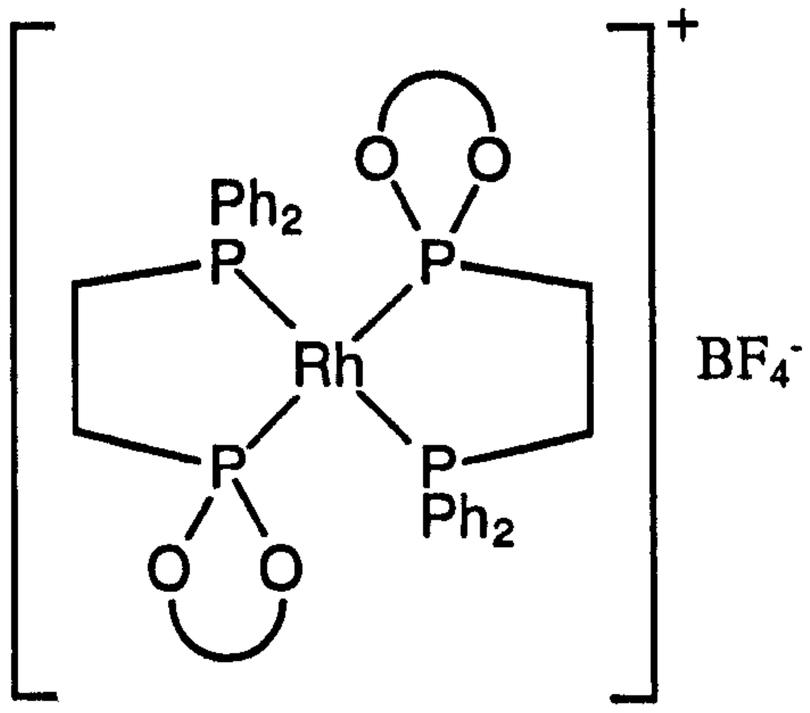

(*S,S*)-(**2.37**)

Reaction of two equivalents of phosphinophosphonite (±)-(**2.21**) with $[\{RhCl(CO)_2\}_2]$ resulted in the formation of a mixture of species which have been characterised by $^{31}P\{^{1}H\}$ NMR spectroscopy, see Table 2.10 and Figure 2.8.

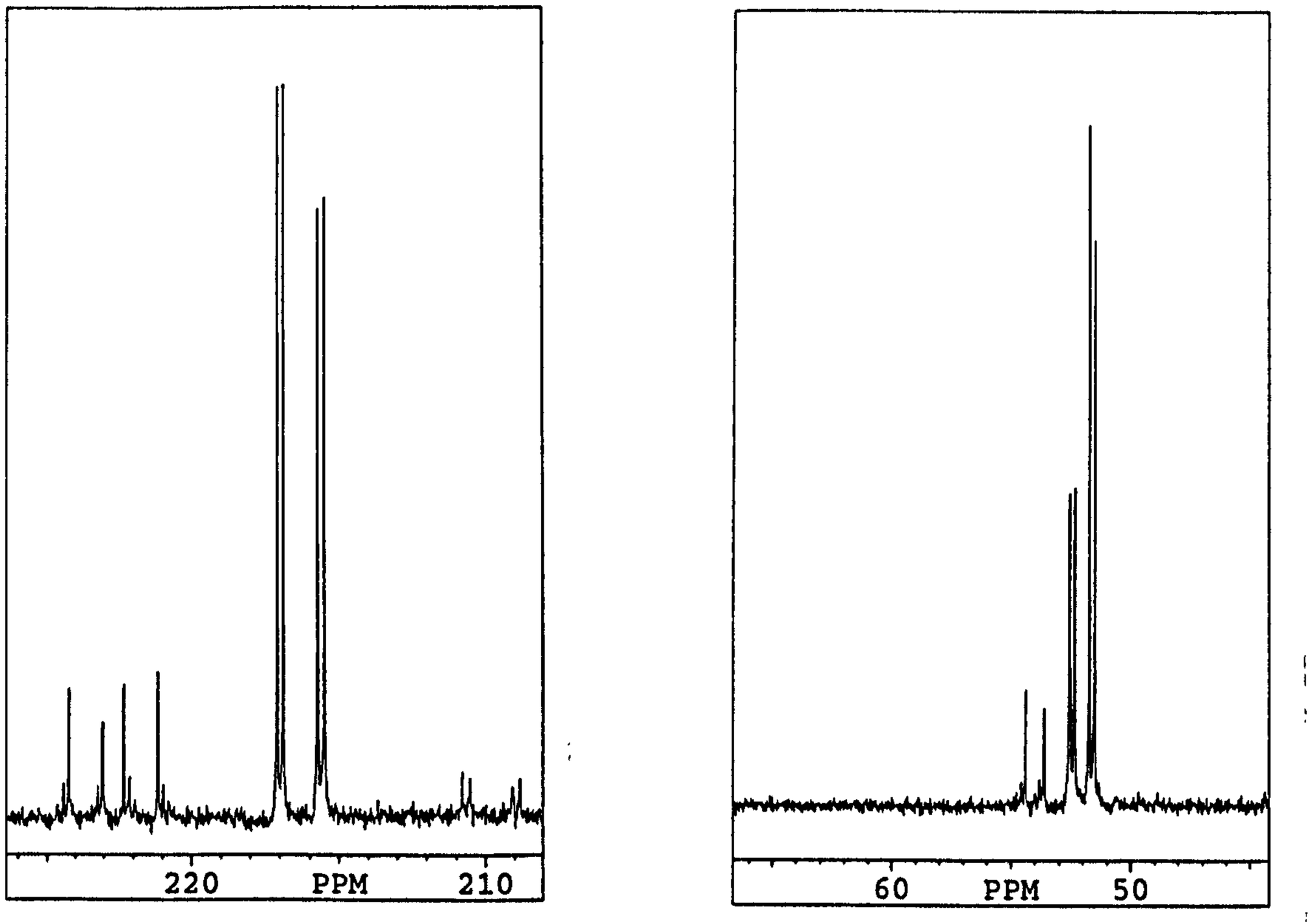

Figure 2.8: $^{31}P\{^{1}H\}$ NMR spectrum of the product mixture obtained by reaction of phosphinophosphonite (±)-(**2.21**) with $[\{RhCl(CO)_2\}_2]$

Whilst the unidentified compound (**2.38**) may correspond to a small proportion of regioisomer (**2.39**) present in the product mixture, the major product has been identified as (**2.40**) by comparison of the spectroscopic data obtained with those of the binaphthol-derived analogue (**2.41**),[51] see Table 2.10. The selectivity for regioisomer (**2.40**) can be rationalised in terms of both steric and electronic arguments. Electronically, one would expect that the thermodynamically favoured isomer would contain the phosphorus moiety with the higher *trans* influence (presumably the phosphine) in the position *trans* to the carbonyl, whilst steric considerations predict the same selectivity since Tolman's cone angles[133] for chloro and carbonyl ligands are 102° and 95° respectively and thus one might expect formation of the regioisomer with the large phosphonite group *trans* to the chloro ligand.

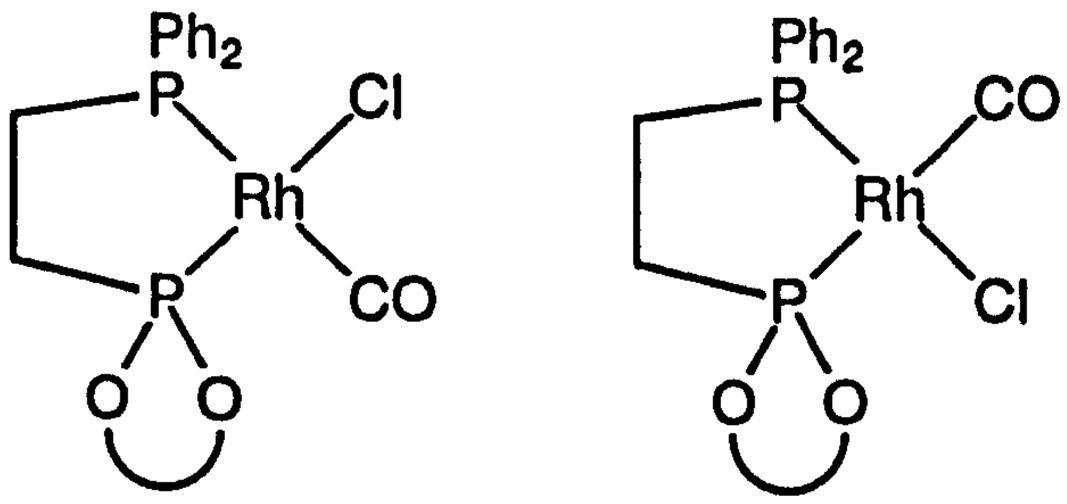

(2.40)

(2.39)

(2.41) when  = (**2.2**) = binaphthol

The other products of the reaction are the two diastereomers {(*R*,*R*) / (*S*,*S*) and (*R*,*S*) *ca.* 2.5:1} of the cationic bis(chelate) complex (**2.36**), except here chloride is the counter-ion.

Table 2.10: $^{31}P\{^{1}H\}$ NMR data for the rhodium(I) complexes of monophosphonites (**2.11**) and (**2.12**), diphosphonite (*S*,*S*)-(**2.16**) and phosphinophosphonite (*S*)-(**2.21**)

Complex	Ligand	δ_P[a]	^{1}J(PRh)[b]	^{2}J(PP)[b]
(*S*,*S*)-(**2.27**)[c]	(*S*)-(**2.12**)	173.1 (br d)	214	------
(**2.31**)[d]	(**2.11**)	187.0 (d)	250	------
(**2.32**)[d]	(**2.12**)	189.2 (d)	248	------
(*S*,*S*)-(**2.33**)[e]	(*S*,*S*)-(**2.16**)	205.7 (d)	229	------
(*S*,*S*),(*S*,*S*)-(**2.34**)[e]	(*S*,*S*)-(**2.16**)	227.0 (d)	183	------
(*S*)-(**2.35**)[c]	(*S*)-(**2.21**)	56.1 (dd, P_B)[f]	153	28
		207.3 (dd, P_A)[g]	220	30
(*S*,*S*)-(**2.36**)[c]	(*S*)-(**2.21**)	52.7 (dd, P_B)[f]	125	305
		222.3 (dd, P_A)[g]	190	305
(*R*,*S*)-(**2.36**)[d]	(**2.21**)	53.1 (dd, P_B)[f]	130	370
		222.7 (dd, P_A)[g]	192	368
(**2.38**)[d,h]	(**2.21**)	77.6 (dd)	201	42
		209.8 (dd)	276	45
(**2.40**)[d]	(**2.21**)	52.0 (dd, P_B)[f]	133	34
		216.3 (dd, P_A)[g]	222	36
(**2.41**)[i,j]	(**2.19**)	49.4 (dd, P_B)[f]	135	36
		214.0 (dd, P_A)[g]	218	36

a Spectra recorded at 162 MHz at 28 °C. Chemical shifts (δ) in p.p.m. (±0.1) to high frequency of 85% H_3PO_4.
b Coupling constants (*J*) measured in Hz (±3).
c Spectra recorded in CH_2Cl_2 / C_6D_6 (3:2).
d Spectra recorded in CD_2Cl_2.
e Spectra recorded in $CDCl_3$.
f P_B assigned as PPh_2.
g P_A assigned as $P(OAr)_2$.
h Unidentified species.
i Ref. 51
j Spectrum recorded in THF.

2.3.3 Platinum(0) complexes - NMR studies

2.3.3.1 Monophosphonite (2.12)

NMR studies have been carried out to investigate the reaction between racemic monophosphonite (**2.12**) and $[Pt(nb)_3]$ (nb = norbornene). Reaction of one equivalent of racemic (**2.12**) with $[Pt(nb)_3]$ resulted in the formation of a diastereomeric mixture of $[Pt(nb)L_2]$ species (**2.42**) (where L represents the monophosphonite ligand) as shown by the $^{195}Pt\{^1H\}$ NMR spectrum (Figure 2.9) which contained two triplets and a doublet of doublets. Surprisingly, none of the complex (**2.43**) with just one phosphonite bound to the metal was formed. Initially it was feared that this was due to an error in the stoicheiometry but the $^{195}Pt\{^1H\}$ NMR spectrum also revealed the presence of unreacted $[Pt(nb)_3]$, thereby eliminating this possibility.

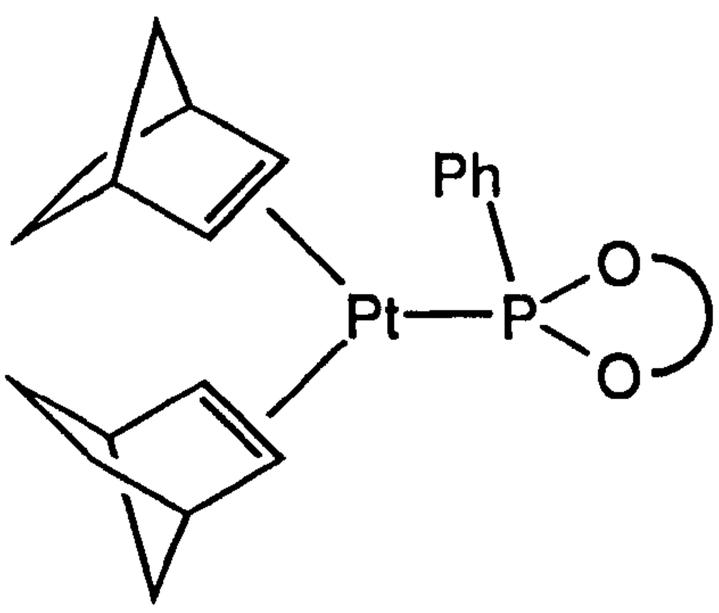

(2.43)

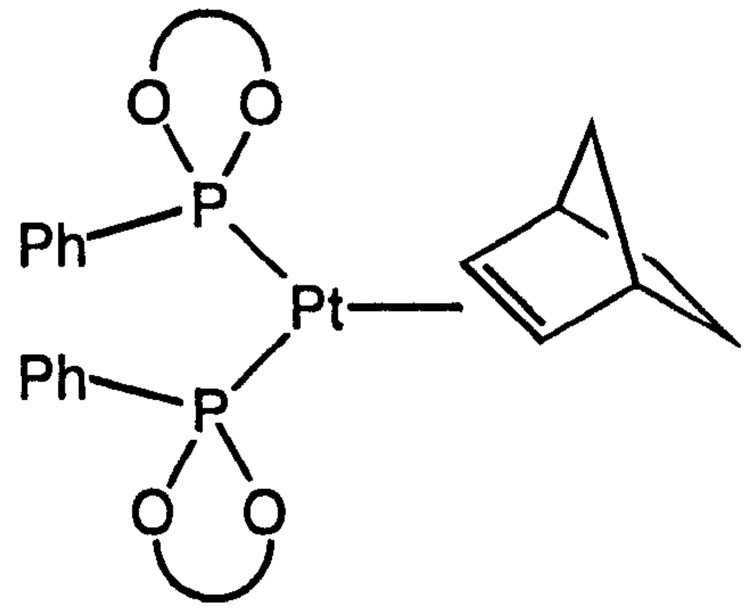

(2.42)

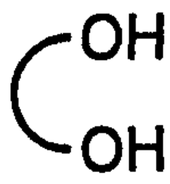

= (2.2)

It can be seen from the $^{31}P\{^1H\}$ NMR spectrum of this diastereomeric mixture, see Figure 2.9, that there are two singlets (each with platinum satellites) and a pair of doublets (again each with platinum satellites). This implies that there are two diastereomers where the phosphorus atoms are equivalent and one diastereomer where the phosphorus atoms are inequivalent.

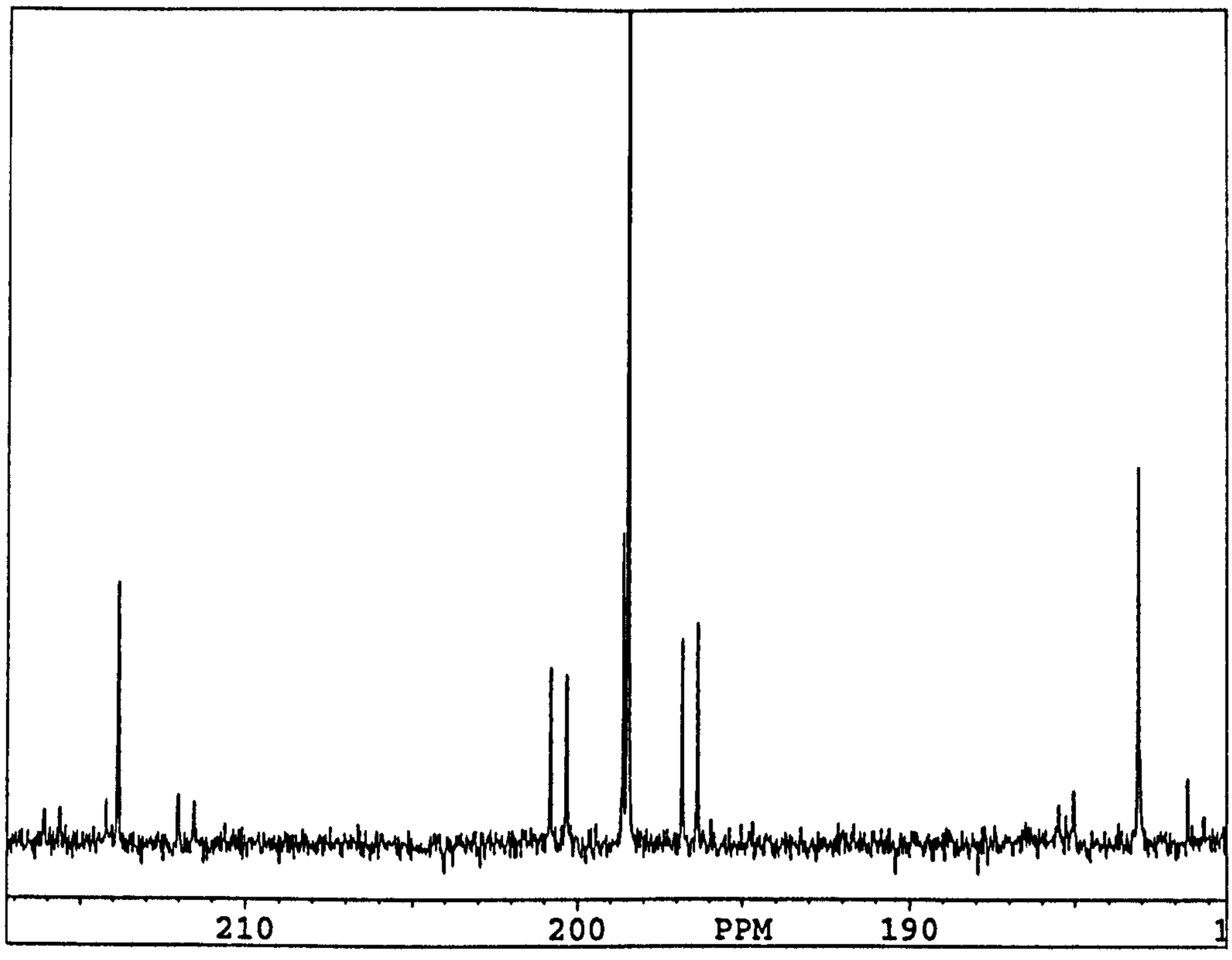

Figure 2.9: $^{31}P\{^{1}H\}$ and $^{195}Pt\{^{1}H\}$ NMR spectra of the diastereomeric mixture of $[Pt(nb)L_2]$ species (**2.42**)

It is important in understanding this phenomenon to take note of the effect of the remaining norbornene ligand upon the symmetry of the molecule. If we consider first of all the square planar platinum(II) complex (**2.23**), it can be seen that in both the (*R*,*S*)- and the (*S*,*S*)-diastereomers the two phosphorus atoms are equivalent, see Figure 2.10. In the former diastereomer they are equivalent by virtue of the mirror plane which is perpendicular to the coordination plane and in the latter diastereomer they are related by the C_2-axis.

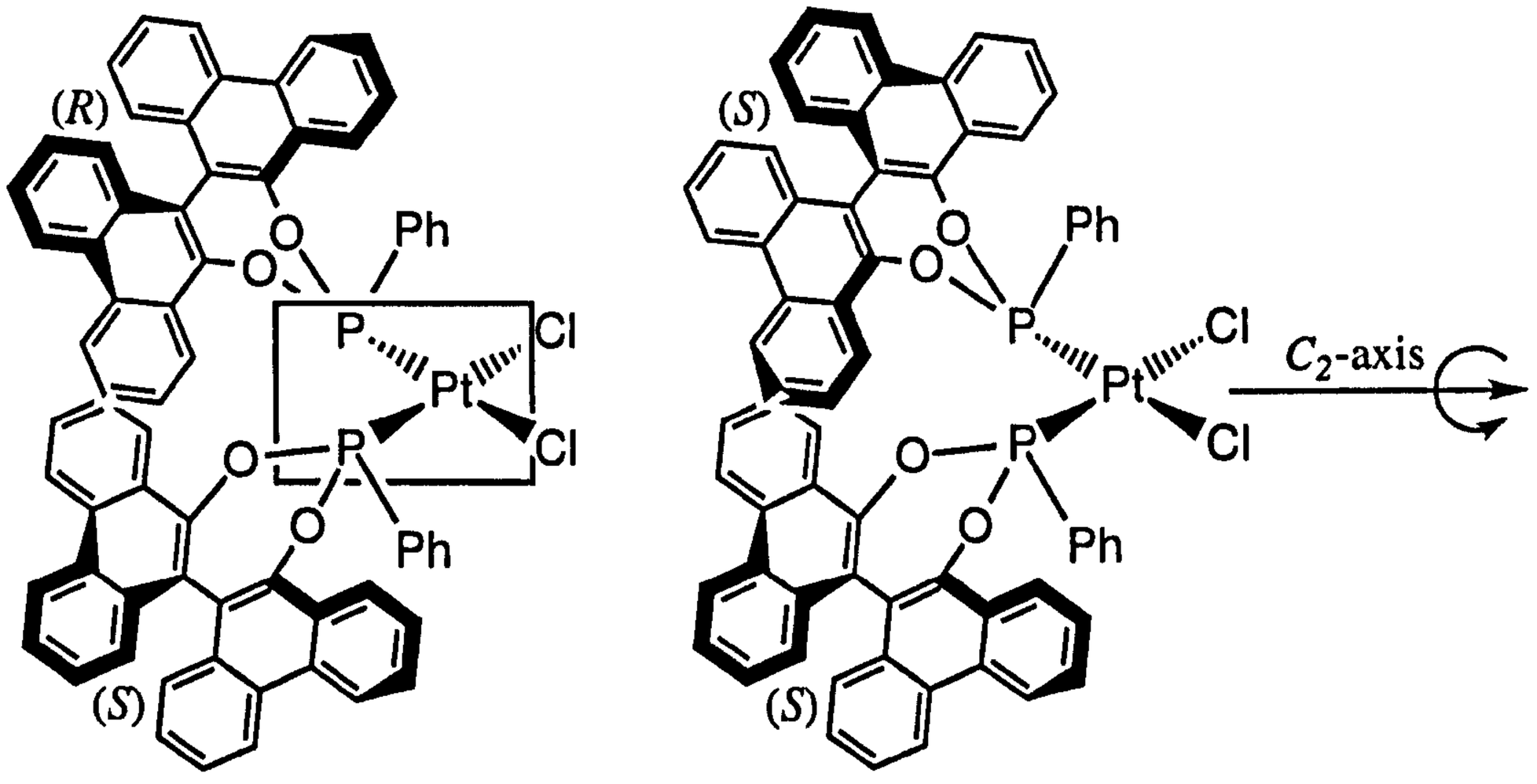

(*R*,*S*)-(**2.23**) (*S*,*S*)-(**2.23**)

Figure 2.10: Symmetry properties of the (*R*,*S*)- and (*S*,*S*)-diastereomers of the square planar dichloroplatinum(II) complex (**2.23**)

When we consider the bis(monophosphonite)platinum(0) complexes (**2.42**) (see Figure 2.11), whilst the mirror plane still exists in the (*R*,*S*)-isomer there is no C_2-axis in the (*S*,*S*)-isomer due to the presence of the remaining norbornene. Consequently, the (*S*,*S*)-diastereomer no longer has equivalent phosphorus atoms and hence this diastereomer would account for the two doublets. Rotation about the Pt-nb bond would equilibrate the two phosphorus atoms, so we can conclude that there is no rotation on the NMR timescale at 28 °C.

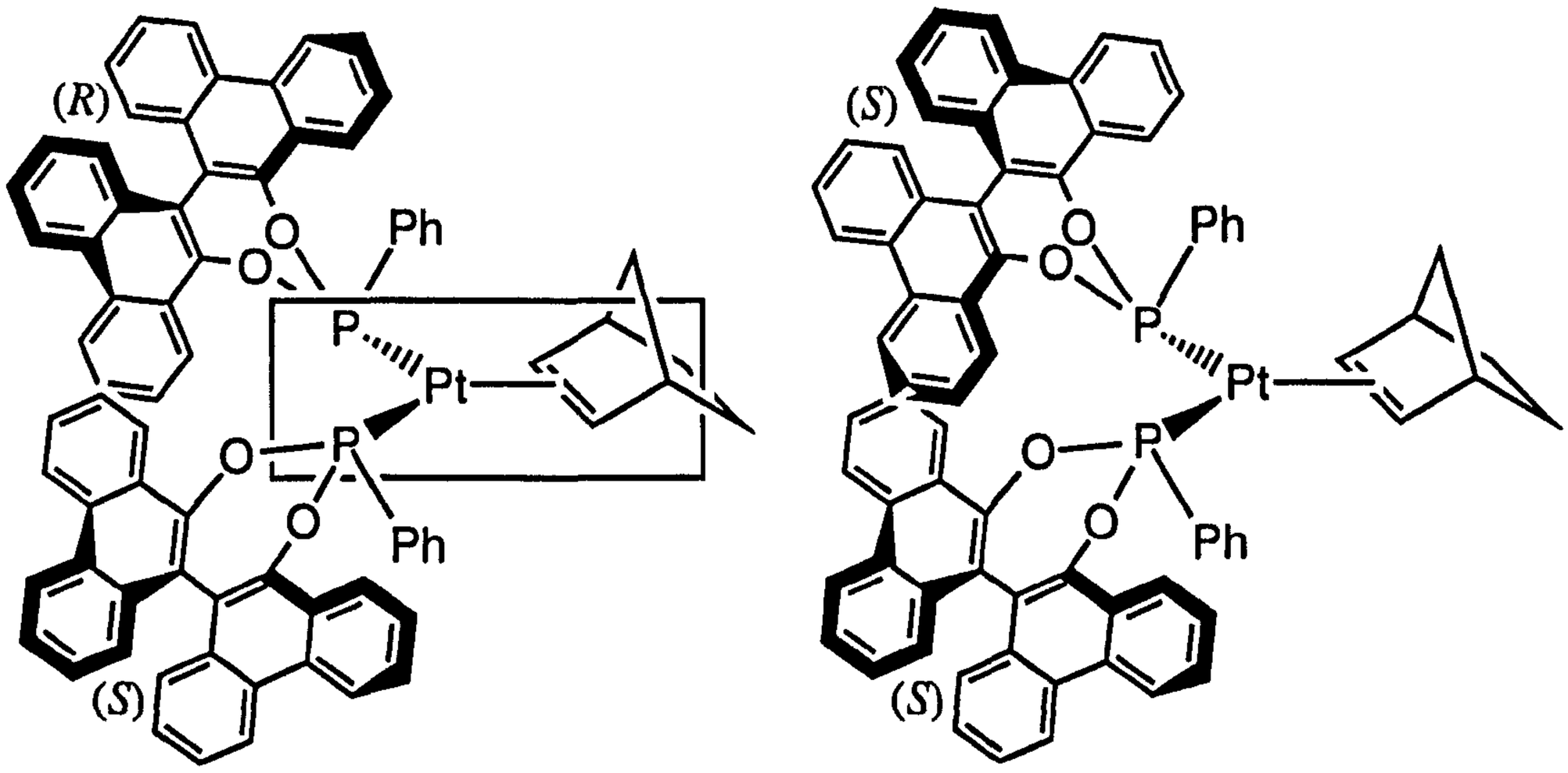

(*R*,*S*)-(**2.42**) (*S*,*S*)-(**2.42**)

Figure 2.11: The effect of the norbornene upon the symmetry properties of the (*R*,*S*)- and (*S*,*S*)-diastereomers of the trigonal planar bis(monophosphonite)platinum(0) complex (**2.42**)

The existence of the mirror plane explains why the two phosphorus atoms of the (*R*,*S*)-diastereomer are equivalent and hence why a singlet is observed. However, it does not explain the presence of the second singlet. This is in fact due to the presence of the (*S*,*R*)-diastereomer, which one might initially believe to be simply the enantiomer of the (*R*,*S*)-compound. However, as is shown in Figure 2.12 the mirror image of the (*R*,*S*)-diastereomer is in fact the (*R*,*S*)-species itself which is clearly not superimposable upon the (*S*,*R*)-species. As non-superimposable, non-mirror images they are diastereomers and hence two singlets are observed. Again, the two diastereomers would be interconverted by rotation about the Pt-nb bond and so the presence of the two singlets indicates that such rotation is hindered on the NMR timescale at 28 °C.

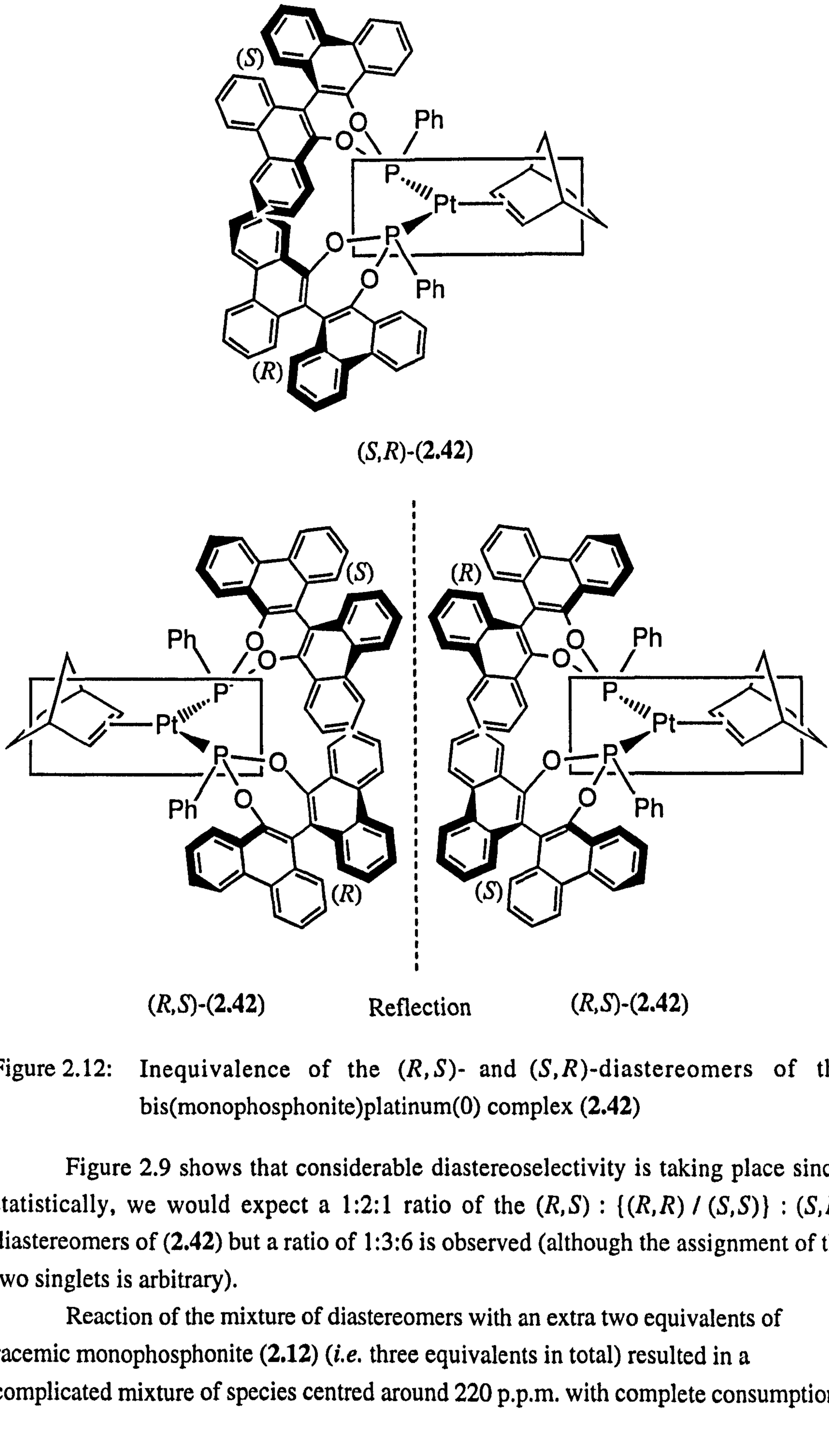

Figure 2.12: Inequivalence of the (*R*,*S*)- and (*S*,*R*)-diastereomers of the bis(monophosphonite)platinum(0) complex (**2.42**)

Figure 2.9 shows that considerable diastereoselectivity is taking place since, statistically, we would expect a 1:2:1 ratio of the (*R*,*S*) : {(*R*,*R*) / (*S*,*S*)} : (*S*,*R*) diastereomers of (**2.42**) but a ratio of 1:3:6 is observed (although the assignment of the two singlets is arbitrary).

Reaction of the mixture of diastereomers with an extra two equivalents of racemic monophosphonite (**2.12**) (*i.e.* three equivalents in total) resulted in a complicated mixture of species centred around 220 p.p.m. with complete consumption

of the diastereomers of (**2.42**). These new species have platinum satellites and may correspond to the diastereomers of the trigonal planar complex with all three norbornene ligands substituted by phosphonite ligands. However, further investigation should be carried out in the future.

These complexes are all oxygen-sensitive. Further, these NMR studies were undertaken in $CDCl_3$ and it was observed that, after long periods, peaks corresponding to the dichloroplatinum(II) complex (**2.23**) started to appear and it can be surmised that this is due to oxidative addition of traces of HCl in the $CDCl_3$ to (**2.42**).

Table 2.11: $^{31}P\{^1H\}$ and $^{195}Pt\{^1H\}$ NMR data for the three diastereomers of the bis(monophosphonite)platinum(0) complex (**2.42**)

Compound	δ_P ($CDCl_3$)[a]	^2J(PP)[b]	δ_{Pt} ($CDCl_3$)[c]	^1J(PPt)[b]
(*S,S*)-(**2.42**)	196.6 (d)	76	-556.1 (dd)	4920
	200.6 (d)	76		4950
(*R,S*)-(**2.42**)[d,e]	198.6 (s)	------	-503.1 (t)	5045
(*S,R*)-(**2.42**)[d,f]	198.5 (s)	------	-538.5 (t)	4976

a Spectra recorded at 162 MHz at 28 °C. Chemical shifts (δ) in p.p.m. (±0.1) to high frequency of 85% H_3PO_4.
b Coupling constants measured in Hz (±3).
c Spectra recorded at 85.6 MHz at 28 °C. Chemical shifts (δ) in p.p.m. (±0.1) to high frequency of Ξ (^{195}Pt) 21.4 MHz.
d The relative assignment of these two diastereomers is arbitrary.
e Minor diastereomer
f Major diastereomer

2.3.3.2 Phosphinophosphonite (2.21)

NMR studies have been carried out on the reaction between racemic phosphinophosphonite (**2.21**) and $[Pt(nb)_3]$. Reaction of one equivalent of racemic (**2.21**) with $[Pt(nb)_3]$ resulted in the formation of a complicated mixture of species as shown by $^{31}P\{^1H\}$ NMR spectroscopy; the phosphonite region of this spectrum is shown in Figure 2.13. It is postulated here that the signal around 183 p.p.m. consists of two overlapping doublets corresponding to the two possible diastereomers {(**2.44**) and (**2.45**) in Figure 2.14} of the mono(chelate) complex. Since these two diastereomers would be interchanged by rotation about the Pt-nb bond, the presence of these two doublets indicates that such rotation is impeded on the NMR timescale.

It is also believed that the complicated signals observed around 198-204 p.p.m. correspond to the two possible diastereomers {(*R,S*)- and (*R,R*) / (*S,S*)-} of the bis(chelate) complex (**2.46**) (see Figure 2.14), each of which would exhibit an AA'XX' spin system. Reaction of the optically pure phosphinophosphonite (**2.19**) derived from binaphthol with $[Pt(nb)_3]$ has been shown to form only the bis(chelate)

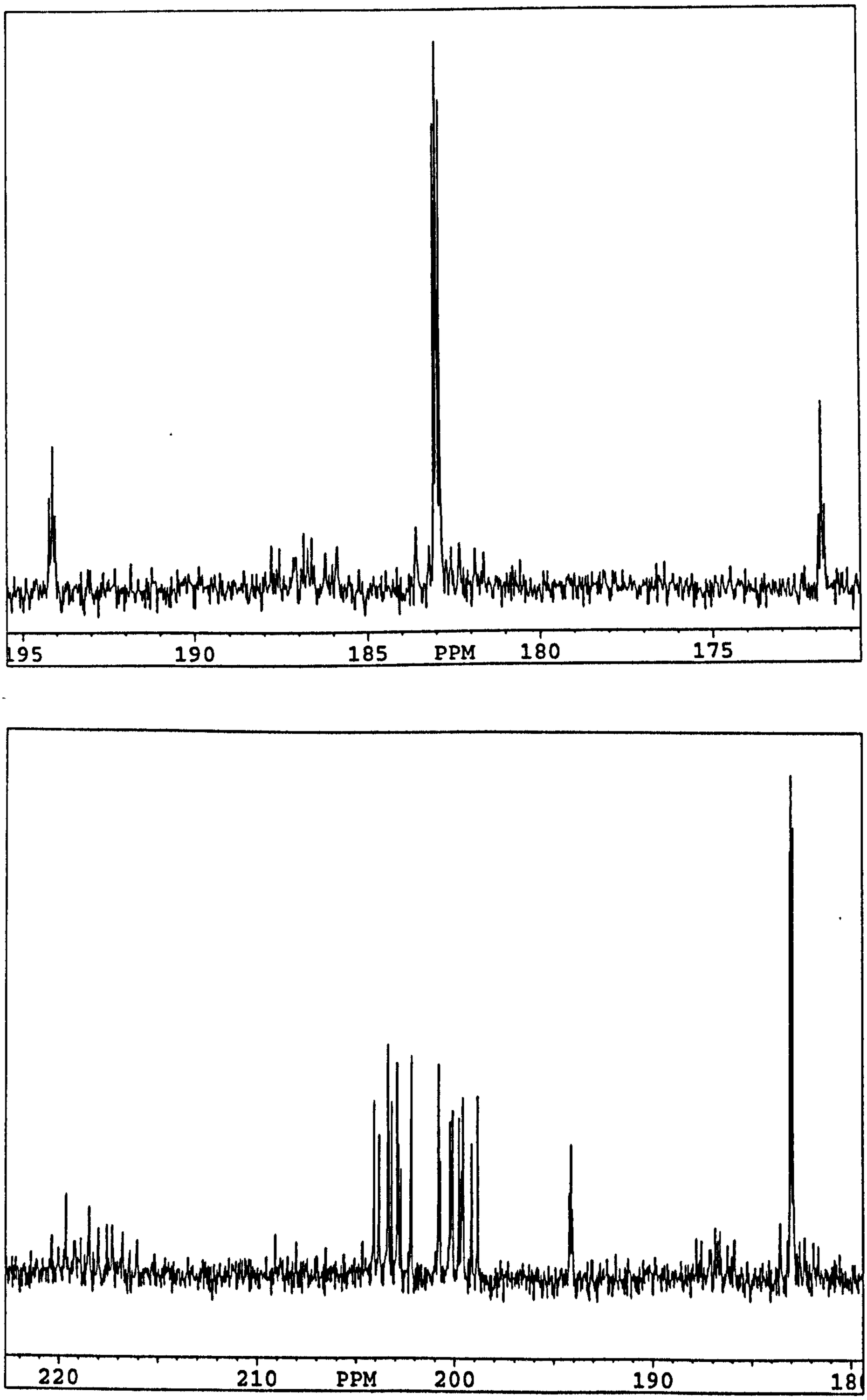

Figure 2.13: The phosphonite region of the $^{31}P\{^{1}H\}$ NMR spectrum of the product mixture obtained upon reaction of 1 equiv of (±)-phosphinophosphonite **(2.21)** with $[Pt(nb)_3]$

which exhibits a multiplet in this region (200-205 p.p.m.).[51] The presence of some mono(chelate) with ligand (**2.21**) would be consistent with the increased steric bulk of this ligand. However, this system has not been further analysed since it should be readily understood when optically pure ligand is used instead of racemate.

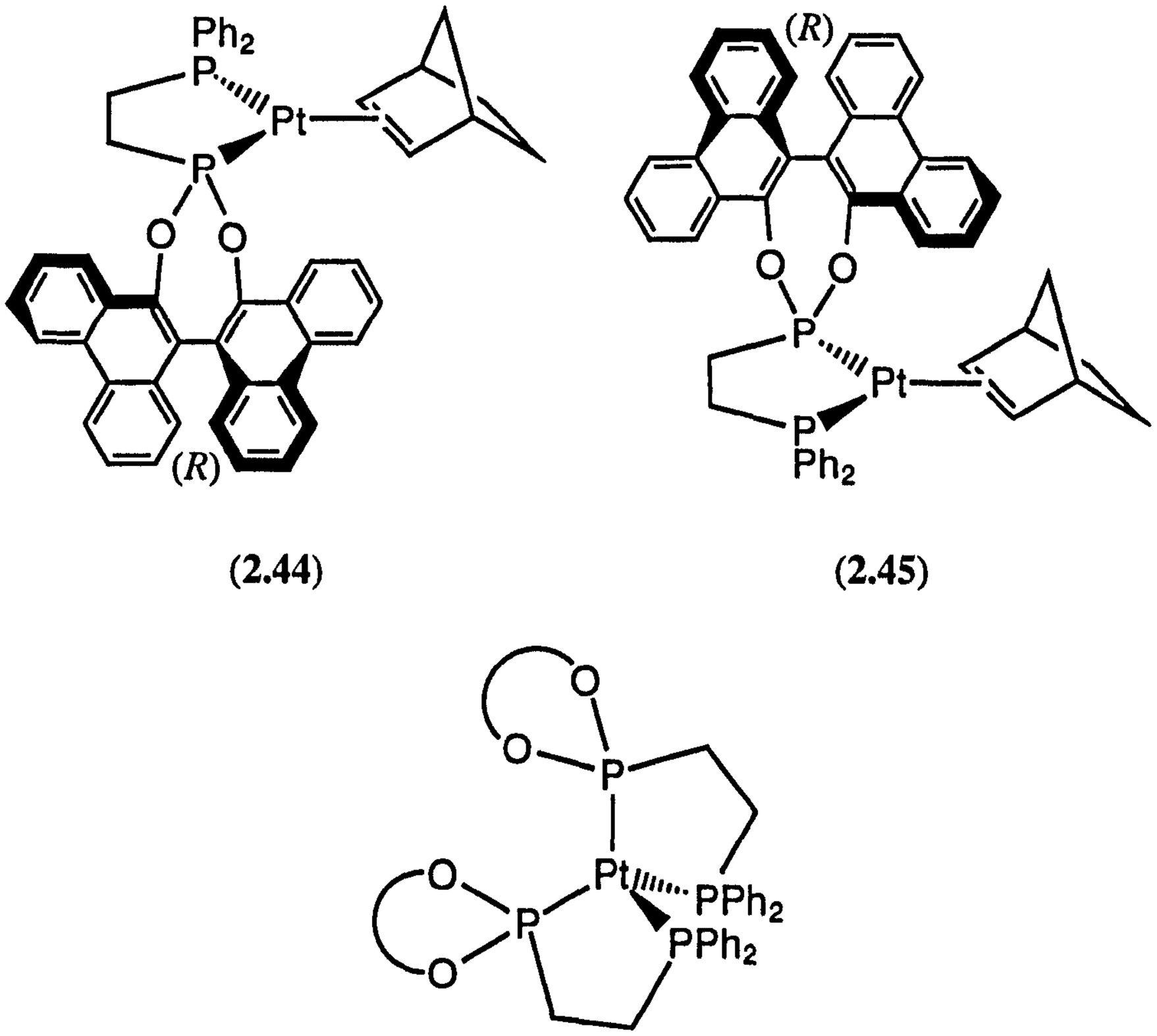

(2.44) **(2.45)**

(2.46)

Figure 2.14: The proposed products of the reaction between phosphinophosphonite (**2.21**) and $[Pt(nb)_3]$; only one enantiomer is shown for (**2.44**) and (**2.45**)

2.4 Discussion of ^{31}P and ^{195}Pt NMR chemical shifts and coupling constants

A trend is apparent for the chemical shift values of these cyclic bis(aryloxy)phosphonites. Where the phosphorus is bound to an alkyl group {as in (**2.16**), (**2.18**) and (**2.21**)}, the chemical shift lies between 210 and 220 p.p.m. but when it is bound to an aryl group {as in (**2.11**) and (**2.12**)}, the phosphorus nucleus is shielded and the chemical shift falls around 185 p.p.m., see Table 2.12. The chemical shifts (δ_P) of (**2.47**),[36,37] (**2.48**)[18,36] and (**2.19**)[51] (the binaphthol

analogues of the monophosphonites, diphosphonite and phosphinophosphonite respectively) are included in Table 2.12 for comparison and lie in similar regions.

Table 2.12: Chemical shift values (δ_P) values for aryl- and alkyl-bis(aryloxy)phosphonites

Compound	δ_P ($CDCl_3$)[a]
(2.11)	184.4
(2.12)	186.5
(2.47)[b]	183.5
(*S,S*)-**(2.16)**	211.7
(*S,R*)-**(2.16)**[c]	212.6
(*R,R*)-**(2.48)**[d]	207.5
(2.18)[e]	191.7 (PCl_2) 209.9 ($P(OAr)_2$)
(2.19)[f]	-12.7 (PPh_2) 210.3 ($P(OAr)_2$)
(2.21)	-12.8 (PPh_2) 215.5 ($P(OAr)_2$)

a Spectra recorded at 162 MHz at 28 °C. Chemical shifts (δ) in p.p.m. (±0.1) to high frequency of 85% H_3PO_4.
b **(2.47)** is the binaphthol analogue of **(2.11)** and **(2.12)**.[36,37]
c Spectrum recorded in $CDCl_3$ / THF (1:4).
d **(2.48)** is the binaphthol analogue of **(2.16)**.[18,36]
e Spectrum recorded in $CDCl_3$ / THF (2:3).
f Spectrum recorded in THF / C_6D_6 (5:1).[51] **(2.19)** is the binaphthol analogue of **(2.21)**.

The $^{31}P\{^1H\}$ and $^{195}Pt\{^1H\}$ NMR data for the dichloroplatinum(II) complexes that have been synthesised are shown in Table 2.13. Again it can be seen that there are two chemical shift (δ_P) ranges depending upon the substituent bound to phosphorus. Complexes of aryl phosphonites possess chemical shifts around 123 p.p.m. whilst the chemical shifts of the complexes derived from alkyl phosphonites are close to 160 p.p.m. However, the coordination chemical shifts ($\Delta\delta$)[133] are similar for both sets of ligands (between -52 and -64 p.p.m.). The high ^1J(PPt) values are consistent with the *cis* conformation that complexes **(2.22)** and **(2.24)** have been shown to adopt (by X-ray crystallography), *i.e.* the phosphonite ligands are *trans* to the chloride ligands which have a low *trans* influence. These values fall in the range 4850-5100 Hz, between those of *cis*-dichloroplatinum(II) phosphite complexes (*cf.* ^1J(PPt) 5793 Hz for *cis*-$[PtCl_2(P(OPh)_3)_2]$)[134] and those of *cis*-dichloroplatinum(II) phosphine complexes (*cf.* ^1J(PPt) 3618 Hz for $[PtCl_2(dppe)]$. This observation reflects the trend

in values of ^1J(PtP) which increase from M-PR_3<M-$P(OR)R_2$<M-$P(OR)_2R$<M-$P(OR)_3$ due to differences in the s-electron density at the phosphorus nucleus.[135]

Table 2.13: $^{31}P\{^1H\}$ and $^{195}Pt\{^1H\}$ NMR data for dichloroplatinum(II) complexes

Complex	Ligand	δ_P[a]	$\Delta\delta$	^1J(PPt)[b]	δ_{Pt}[c]
(*R*,*R*) / (*S*,*S*)-(**2.22**)[d]	(±)-(**2.11**)	123.1	-61.3	4979	162.7
(**2.23**)[e,f]	(±)-(**2.12**)	122.3	-64.2	4943	------
(**2.23**)[f,g]	(±)-(**2.12**)	122.9	-63.6	4908	------
(*S*,*S*)-(**2.24**)[d]	(*S*,*S*)-(**2.16**)	159.4	-52.3	4868	186.1
(**2.25**)[h]	(**2.21**)	44.3 (PPh_2)	+57.1	3463	84.3
		160.5 ($P(OAr)_2$)	-55.0	5063	

a Spectra recorded at 162 MHz at 28 °C. Chemical shifts (δ) in p.p.m. (±0.1) to high frequency of 85% H_3PO_4.
b Coupling constants (*J*) measured in Hz (±3).
c Spectra recorded at 85.6 MHz at 28 °C. Chemical shifts (δ) in p.p.m. (±0.1) to high frequency of Ξ (^{195}Pt) 21.4 MHz.
d Spectra recorded in CD_2Cl_2.
e Minor isomer.
f Spectra recorded in $CDCl_3$.
g Major isomer.
h Spectra recorded in d_6-dmso.

The $^{31}P\{^1H\}$ NMR data for the rhodium(I) complexes that have been synthesised are shown in Table 2.14. It can be seen that the chemical shift values (δ_P) are strongly dependent on the group bound to the phosphorus and the nature of the ancillary ligand. The values of ^1J(PRh) for the phosphonite groups are between those of rhodium(I) phosphite and rhodium(I) phosphine complexes. The higher values of ^1J(PRh) for complexes (**2.31**) and (**2.32**) (*ca.* 250 Hz) compared to that of complex (**2.27**) (214 Hz) reflect the lower *trans* influence of the dpm ligand compared to that of the cod ligand. Similarly, the lower values of ^1J(PRh) for the phosphonite groups in the bis(chelates) (**2.34**) and (**2.36**) (180-195 Hz) compared to those in the mono(chelates) (**2.33**) and (**2.35**) (220-230 Hz) reflect the higher *trans* influences of the phosphonite and phosphine groups respectively compared to that of the cod ligand.

Table 2.14: $^{31}P\{^{1}H\}$ NMR data for the rhodium(I) complexes of monophosphonites (**2.11**) and (**2.12**), diphosphonite (*S,S*)-(**2.16**) and phosphinophosphonite (*S*)-(**2.21**)

Complex	Ligand	δ_P[a]	^{1}J(PRh)[b]	^{2}J(PP)[b]
(*S,S*)-(**2.27**)[c]	(*S*)-(**2.12**)	173.1 (br d)	214	------
(**2.31**)[d]	(**2.11**)	187.0 (d)	250	------
(**2.32**)[d]	(**2.12**)	189.2 (d)	248	------
(*S,S*)-(**2.33**)[e]	(*S,S*)-(**2.16**)	205.7 (d)	229	------
(*S,S*),(*S,S*)-(**2.34**)[e]	(*S,S*)-(**2.16**)	227.0 (d)	183	------
(*S*)-(**2.35**)[c]	(*S*)-(**2.21**)	56.1 (dd, P_B)[f]	153	28
		207.3 (dd, P_A)[g]	220	30
(*S,S*)-(**2.36**)[c]	(*S*)-(**2.21**)	52.7 (dd, P_B)[f]	125	305
		222.3 (dd, P_A)[g]	190	305
(*R,S*)-(**2.36**)[d]	(**2.21**)	53.1 (dd, P_B)[f]	130	370
		222.7 (dd, P_A)[g]	192	368
(**2.40**)[d]	(**2.21**)	52.0 (dd, P_B)[f]	133	34
		216.3 (dd, P_A)[g]	222	36

a Spectra recorded at 162 MHz at 28 °C. Chemical shifts (δ) in p.p.m. (±0.1) to high frequency of 85% H_3PO_4.
b Coupling constants (*J*) measured in Hz (±3).
c Spectra recorded in CH_2Cl_2 / C_6D_6 (3:2).
d Spectra recorded in CD_2Cl_2.
e Spectra recorded in $CDCl_3$.
f P_B assigned as PPh_2.
g P_A assigned as $P(OAr)_2$.

Chapter 3

Cyclic Aryl Diphosphites: Synthesis, Coordination Chemistry and Application in Asymmetric Hydroformylation

3.1 Introduction

The importance of asymmetric hydroformylation and hydrogenation and the role of chiral diphosphites in these processes has already been discussed (see Chapter 1). Further, the importance of the seven-membered P(OCCCCO) rings and the bulky, hydrophobic aromatic groups in conferring kinetic stability to hydrolysis upon cyclic aryl diphosphites such as 'binaphthite' (**3.1**)[92] has also been considered.

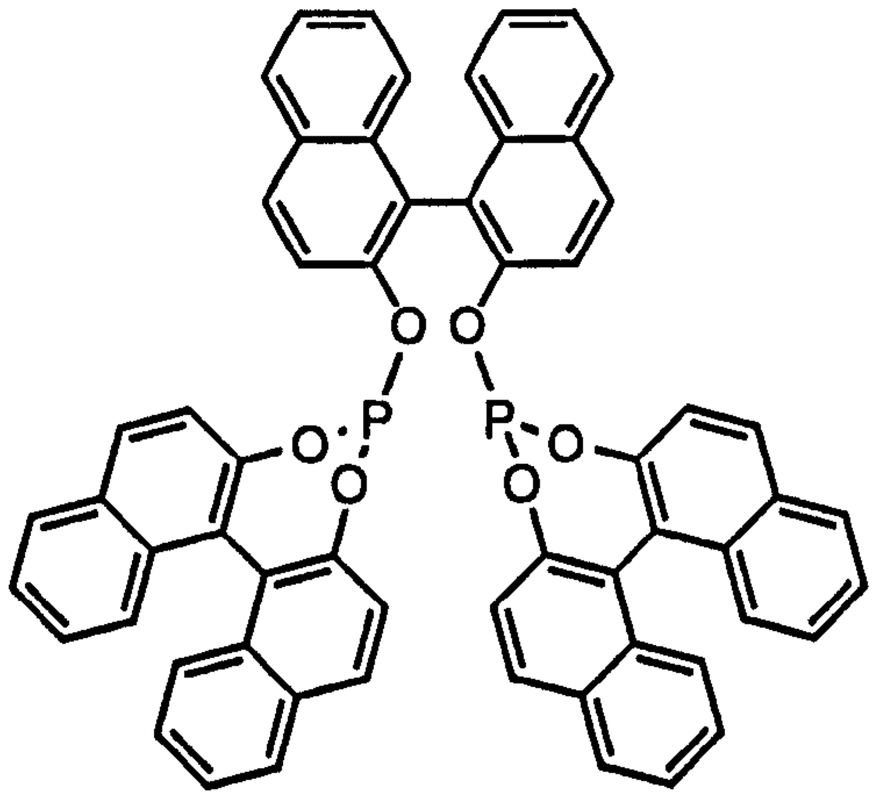

(3.1)

A rhodium(I) complex derived from (*S,S,S*)-(**3.1**) was tested in the asymmetric hydroformylation of styrene and *p*-methoxystyrene. High activities (86% and 70% conversions respectively under mild conditions) and regioselectivities (81% and 69% respectively in favour of the branched aldehyde) were observed but the enantioselectivities after optimisation of the reaction conditions were modest (23% and 46% respectively).[93,94]

We therefore set about the synthesis of a range of cyclic aryl diphosphites containing bulkier organic backbones in the hope that this would create a more sterically discriminating environment and thereby improve the regio- and enantioselectivities obtained, whilst maintaining the high catalytic activities. It was also hoped that the kinetic stability to hydrolysis would be improved by increasing the hydrophobicity of the environment around the potentially labile P-O bonds.

This Chapter describes the preparation, characterisation and properties of cyclic aryl phosphites derived from binaphthol, 9,9'-biphenanthryl-10,10'-diol (**3.2**) (biphenanthrol) and dimethyl-1,1'-binaphthyl-2,2'-dihydroxy-3,3'-dicarboxylate (**3.3**). These phosphites have been prepared as diastereomeric mixtures, as racemates and optically pure. The coordination chemistry of the two diphosphites that have been successfully synthesised with platinum(II), platinum(0), palladium(II) and rhodium(I) is then discussed. Finally, the rhodium(I) complexes of these diphosphites have been tested for the asymmetric hydroformylation of styrene and *p*-methoxystyrene and the results are reported herein.

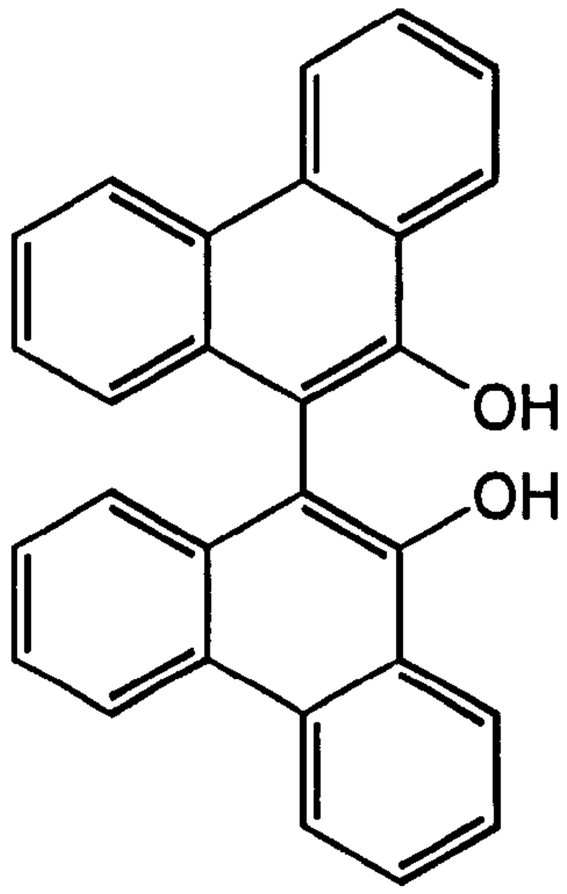

(3.2)

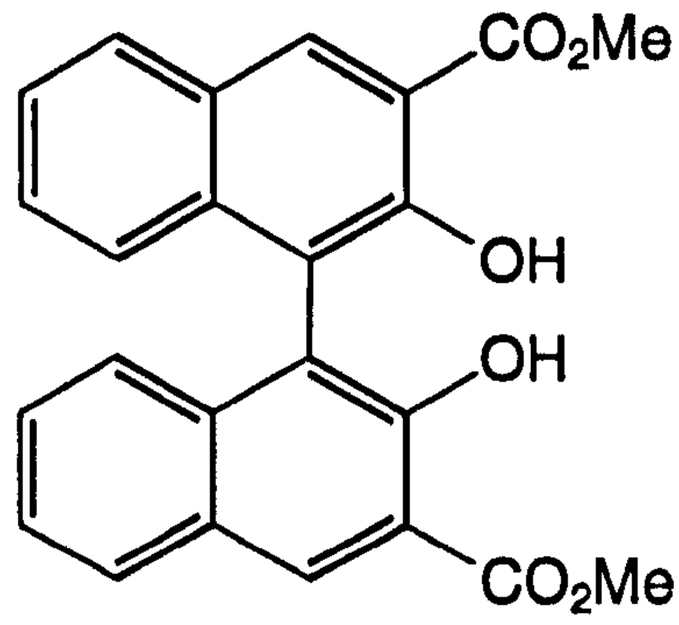

(3.3)

3.2 Synthesis of cyclic aryl phosphites derived from 9,9'-biphenanthryl-10,10'-diol (3.2)

In this Section the attempted syntheses of a range of diphosphites derived from biphenanthrol (**3.2**) are discussed. The dissymmetry of the biphenanthrol means that three diastereomers of 'biphenanthrite' (**3.4**) are possible. The successful syntheses of (i) the mixture of diastereomers, (ii) the single (*R,S,R*) / (*S,R,S*)-diastereomer and (iii) the optically pure (*R,R,R*)-diastereomer are described.

The diphosphite (**3.5**) (referred to hereafter as 'pnp') derived from biphenanthrol (**3.2**) and binaphthol has been successfully synthesised (i) as a mixture of diastereomers, (ii) as the optically pure (*R,S,R*)-diastereomer and (iii) as the optically pure (*R,R,R*)-diastereomer and these syntheses are reported here.

The characterisation and properties of these diphosphites are reported in detail.

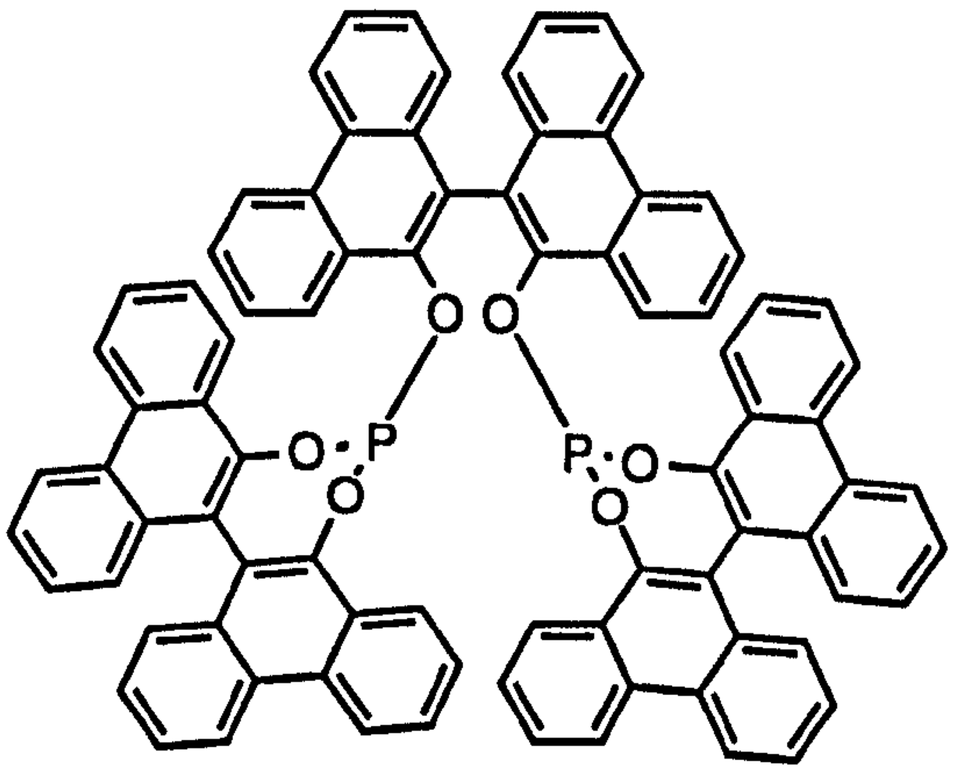

(3.4)

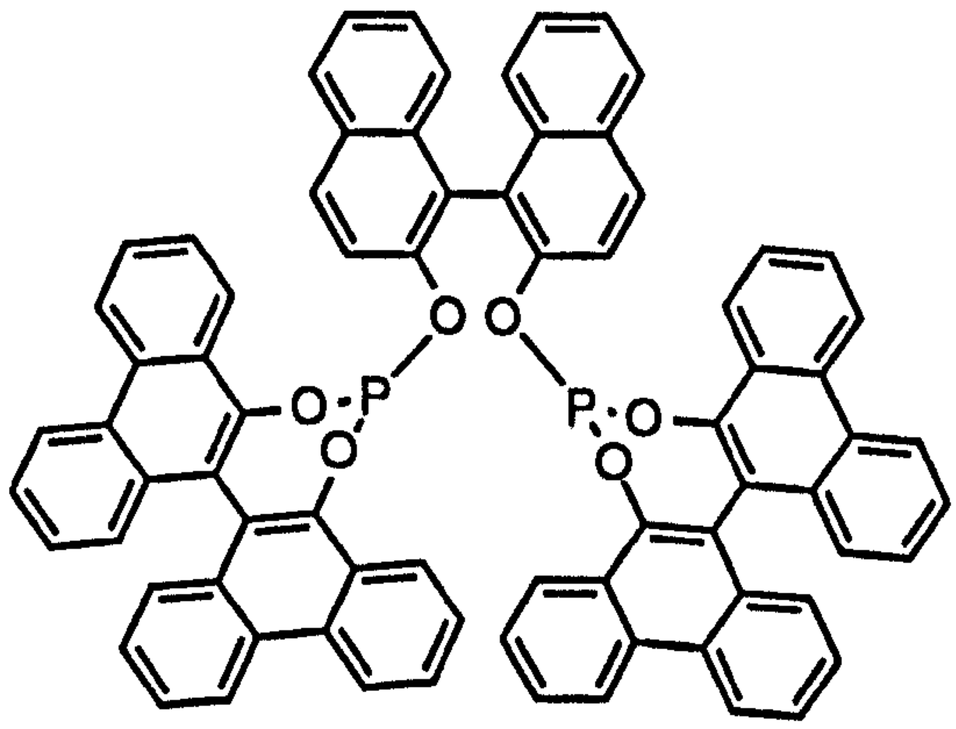

(3.5)

3.2.1 Synthesis of the diphosphite 'biphenanthrite' (3.4) from biphenanthrol

It was initially hoped that 'biphenanthrite' (**3.4**) could be synthesised by a similar procedure to that for 'binaphthite' (**3.1**), see Equation 3.1.

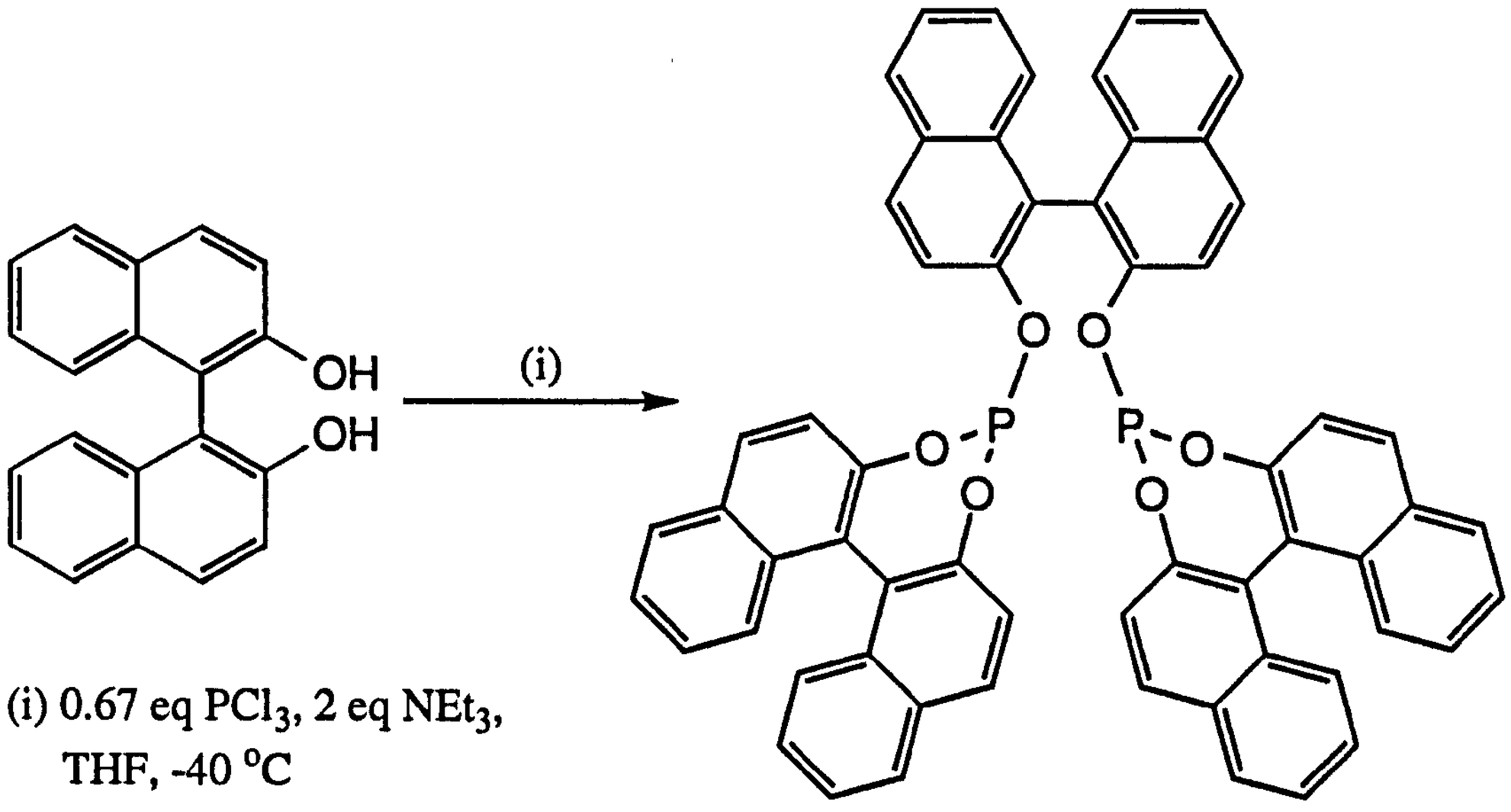

(i) 0.67 eq PCl_3, 2 eq NEt_3,
THF, -40 °C

(3.1)

Equation 3.1

Disappointingly, application of the reaction conditions of Equation 3.1 to the synthesis of the diastereomeric mixture of 'biphenanthrite' (**3.4**) starting with racemic biphenanthrol (**3.2**) led to a complicated mixture of products. A typical $^{31}P\{^1H\}$ NMR spectrum of the crude reaction mixture is shown in Figure 3.1. Changes in solvent affected the absolute values of the chemical shifts of the species present by up to 0.5 p.p.m. and thus in subsequent discussion and interpretation of spectra of crude reaction mixtures it is the relative chemical shifts of the species that are used.

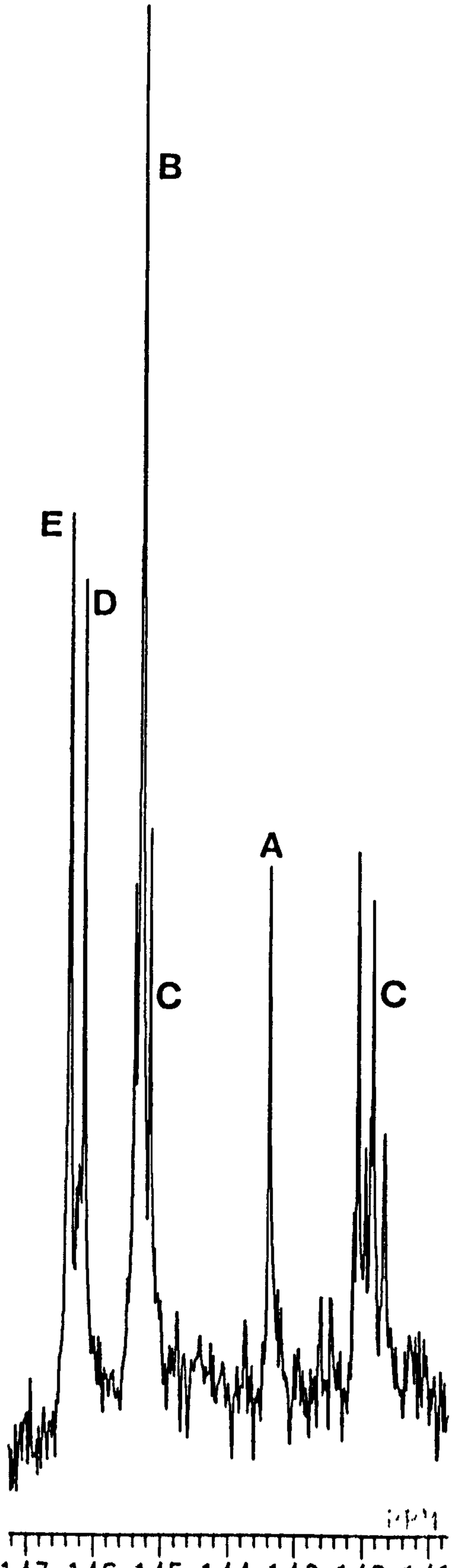

Figure 3.1 A typical $^{31}P\{^{1}H\}$ NMR spectrum of the crude reaction mixture obtained upon reaction of racemic biphenanthrol (**3.2**) with PCl_3 and NEt_3 in THF at -40 °C

As Figure 3.2 illustrates, four signals would be expected in the $^{31}P\{^{1}H\}$ NMR spectrum of the diastereomeric mixture of 'biphenanthrite' (**3.4**), corresponding to the four different types of phosphorus atom in the three possible diastereomers.

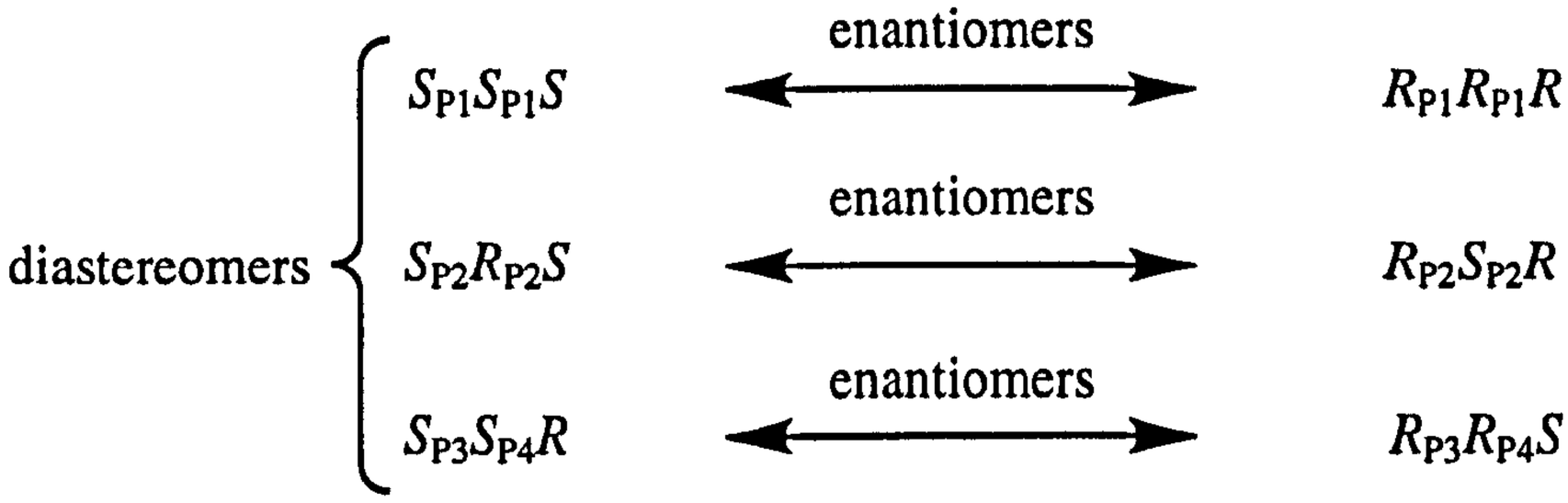

Figure 3.2: The relationship between enantiomers, diastereomers and the number of expected $^{31}P\{^{1}H\}$ NMR resonances for 'biphenanthrite' (**3.4**). The four different types of phosphorus atom are labelled P1-P4

Indeed, these four signals can be identified in Figure 3.1 (species A-C). In the case of the (*R*,*R*,*R*) / (*S*,*S*,*S*)- and the (*R*,*S*,*R*) / (*S*,*R*,*S*)-diastereomers the two phosphorus atoms are equivalent and the singlets in Figure 3.1 are assigned to these symmetrical isomers. These have been assigned as species A and B respectively since optically pure (*R*,*R*,*R*)-(**3.4**) has been obtained as a single diastereomer from optically pure (*R*)-biphenanthrol (see Pages 101-102) and is unambiguously assigned to the signal at 143.3 p.p.m. In the case of the (*R*,*R*,*S*) / (*S*,*S*,*R*)-diastereomer the two phosphorus atoms are inequivalent and the pair of doublets labelled species C is therefore assigned to this isomer. The ^{7}J(PP) value varies from 20-40 Hz depending on the solvent. Seven-bond coupling of this magnitude has precedent in the literature. It was first observed by Pastor and Rodebaugh in 1988 for the biaryl bis(1,3,2-oxazaphospholidine) (**3.6**).[136] The inequivalent phosphorus atoms in the (*R*,*R*,*S*) / (*S*,*S*,*R*)-diastereomer of this compound had a ^{7}J(PP) of 30 Hz.

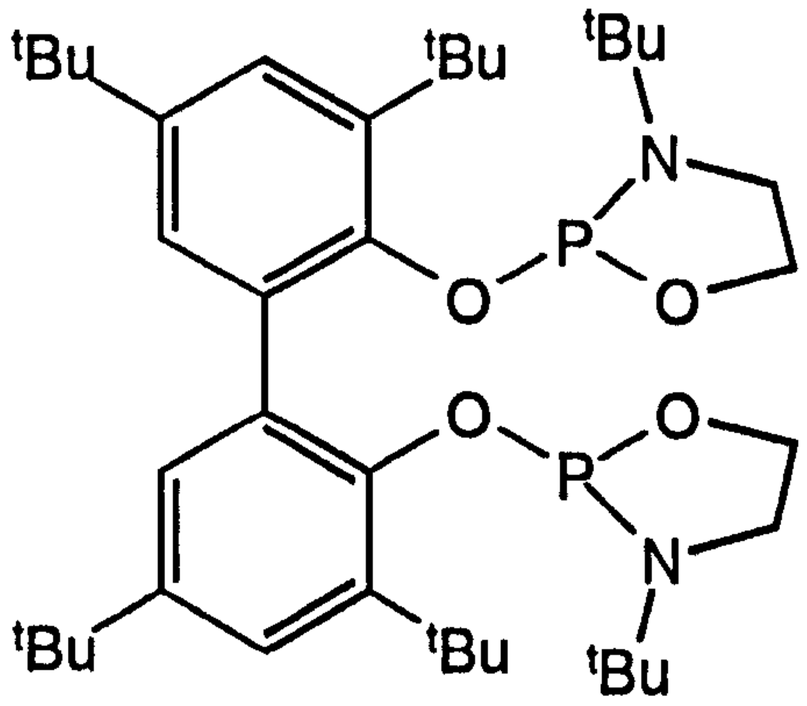

(3.6)

The same workers have also reported ^{8}J(PP) values in the sterically congested diphosphite (**3.7**) and in the phosphorodichloridite intermediate (**3.8**) of 73 Hz and 136 Hz respectively.[137]

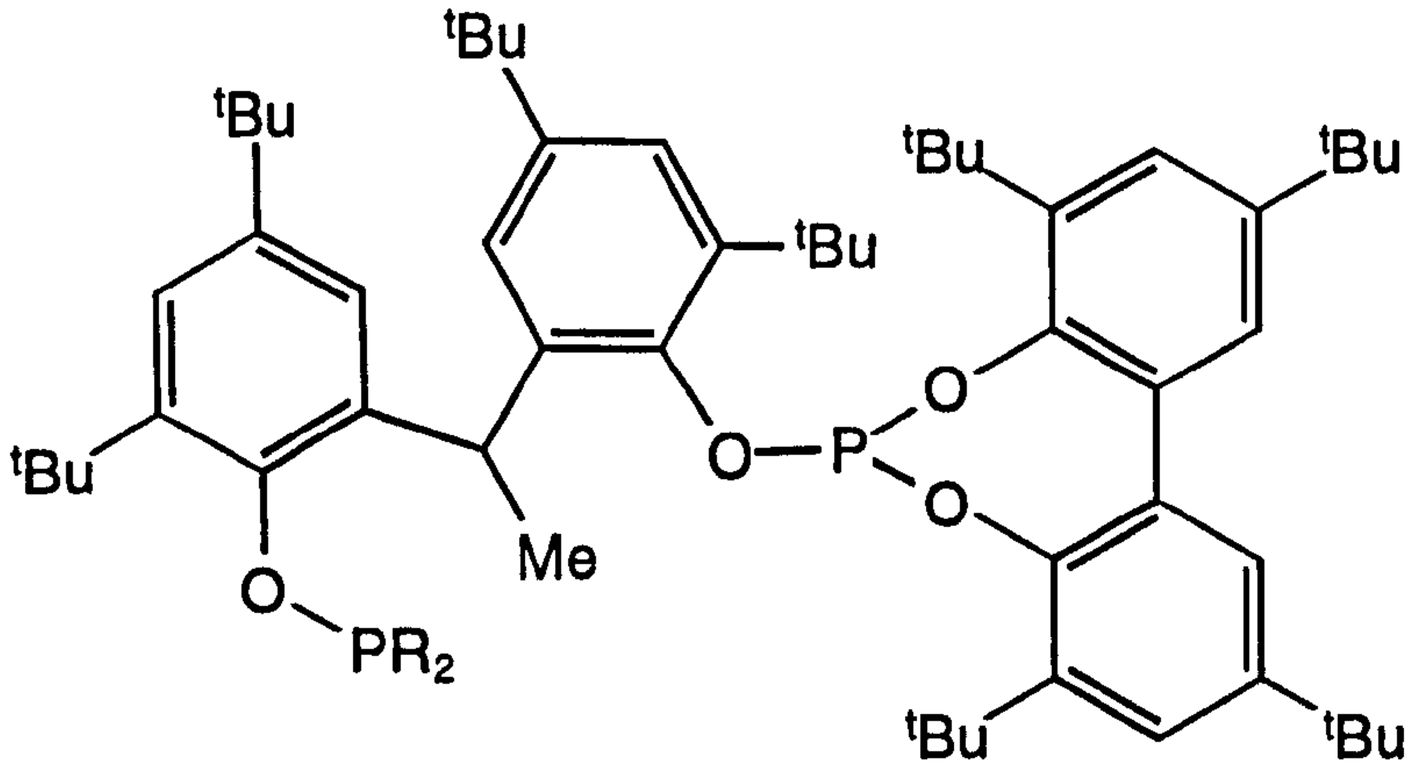

R = PhO, (**3.7**)
R = Cl, (**3.8**)

Although the magnitude of these long-range coupling constants was not explained by these workers, several theories have now emerged to explain this phenomenon. One such theory invokes the through-space mechanism.[138] Szalontai and co-workers[139] have argued that even if crystallographic data shows that in the solid state the interatomic P-P distances are larger than the sum of the van der Waals' radii, a through-space contribution to coupling can still be significant since the translational and vibrational energies in solution may lead to shortened time-averaged P-P interatomic distances.

The restricted geometry possessed by bulky diphosphite (**3.7**) may favour other mechanisms for the long-range transmission of coupling. For example, coupling through the π-system of the aromatic rings[140,141] or through the lone pairs of electrons on the phosphorus atoms[142] is also possible. It is not known at present which one of these mechanisms is operating for (*R,R,S*) / (*S,S,R*)-'biphenanthrite' (**3.4**); indeed the coupling may be the result of several different contributions. The solvent-dependence of the coupling constant suggests that the conformation of the diphosphite is critical to the size of the coupling.

One might expect the (*R,R,R*) / (*S,S,S*)- : (*R,R,S*) / (*S,S,R*)- : (*R,S,R*) / (*S,R,S*)- ratio to be 1:2:1. However, it is clear from Figure 3.1 that the (*R,R,R*) / (*S,S,S*)-diastereomer has been formed in a much lower proportion than the (*R,S,R*) / (*S,R,S*)-diastereomer and therefore some diastereoselectivity is being exhibited.

To elucidate the identity of the remaining species observed in Figure 3.1, it is instructive to consider the mechanism of the 'one-pot' procedure for forming diphosphites from PCl_3 shown in Scheme 3.1.

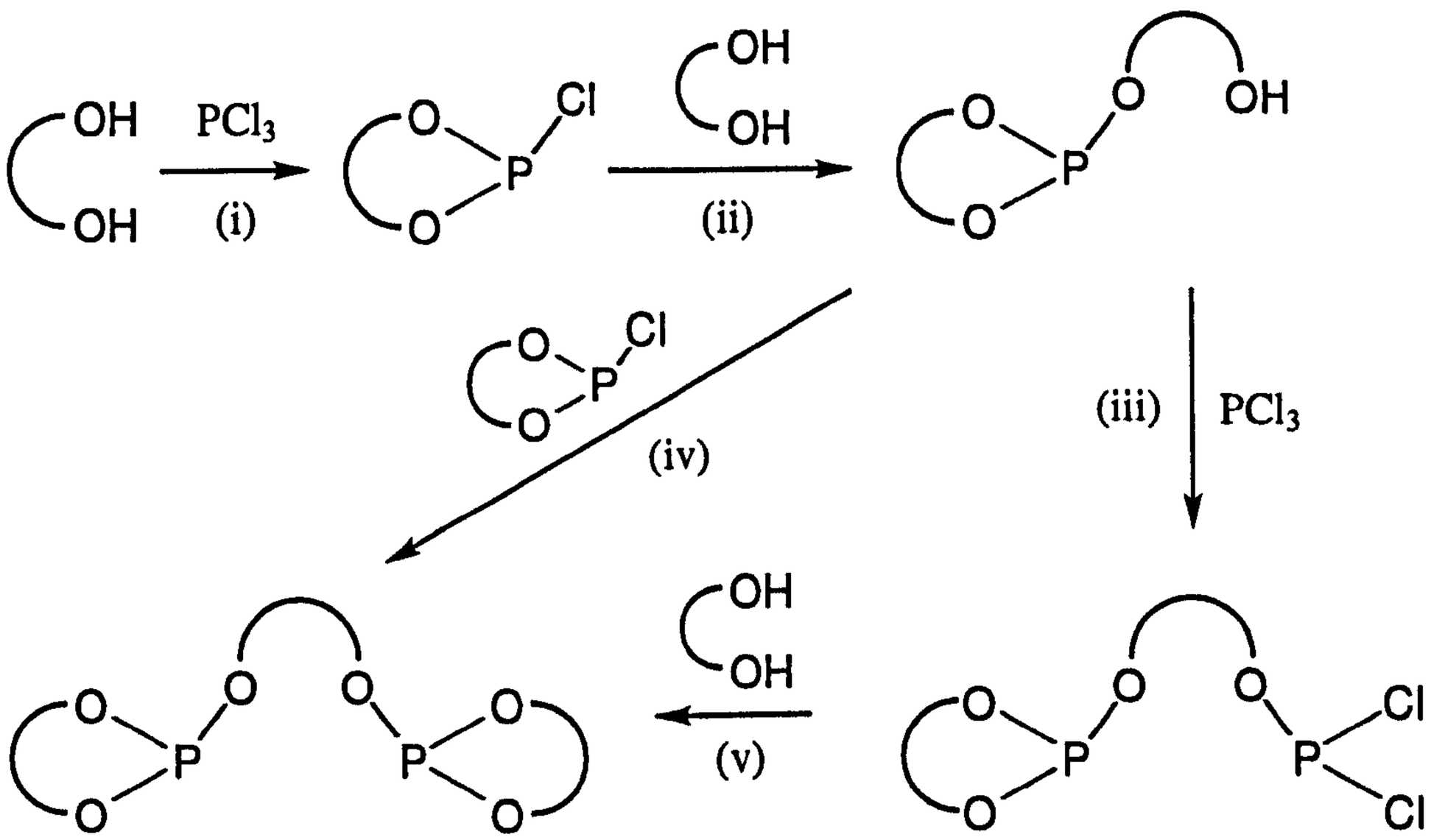

Scheme 3.1: The course of the 'one-pot' diphosphite-forming reaction and the intermediates involved in this process

The first step is the reaction of the diol to form the chlorophosphite {step (i)}. This then reacts with a further equivalent of diol {step (ii)} to produce a hydroxymonophosphite (a phosphite with a pendant hydroxyl group referred to hereafter as a 'dangler' phosphite). Depending upon the rate and order of addition this species will then react either with PCl_3 to form a phosphorodichloridite {step (iii)} or with a molecule of chlorophosphite to form a diphosphite {step (iv)}. The former then reacts with a molecule of diol to produce the diphosphite {step (v)}.

Species D and E (Figure 3.1) have been identified as the two diastereomers of the 'dangler' phosphite (**3.9**). The (*R*,*R*) / (*S*,*S*)-diastereomer has been identified as species D since optically pure (*S*,*S*)-(**3.9**) has been synthesised as a single diastereomer from optically pure (*S*)-biphenanthrol (**3.2**) (see Pages 92-94) and has been unambiguously assigned to the signal at 146.2 p.p.m.

A result of the formation of the 'dangler' side-product (**3.9**) is that there remains some unreacted chlorophosphite (**3.10**) in solution. This will react with an excess of water present to form the phosphonate (**3.11**). However, if only traces of water are present then two equivalents of the chlorophosphite react with one equivalent of water to form the 'POP' pyrophosphite (**3.12**). Two singlets in the $^{31}P\{^{1}H\}$ NMR spectrum at 141.9 p.p.m. and 139.4 p.p.m. have been assigned to the (*R*,*R*) / (*S*,*S*)- and (*R*,*S*) / (*S*,*R*)-diastereomers of this species respectively, since the optically pure diastereomer (*S*,*S*)-(**3.12**) has been synthesised from optically pure (*S*)-biphenanthrol (**3.2**) (see Pages 91-92) and has been unambiguously assigned to the signal at 141.9 p.p.m.

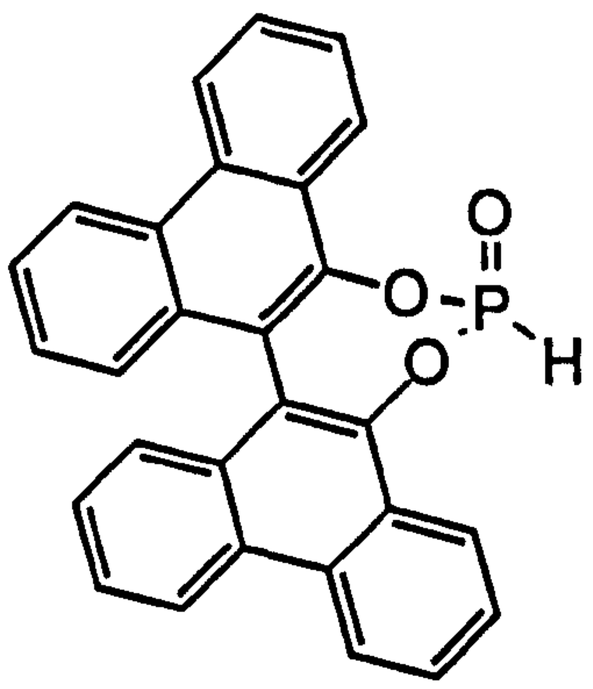

(3.11)

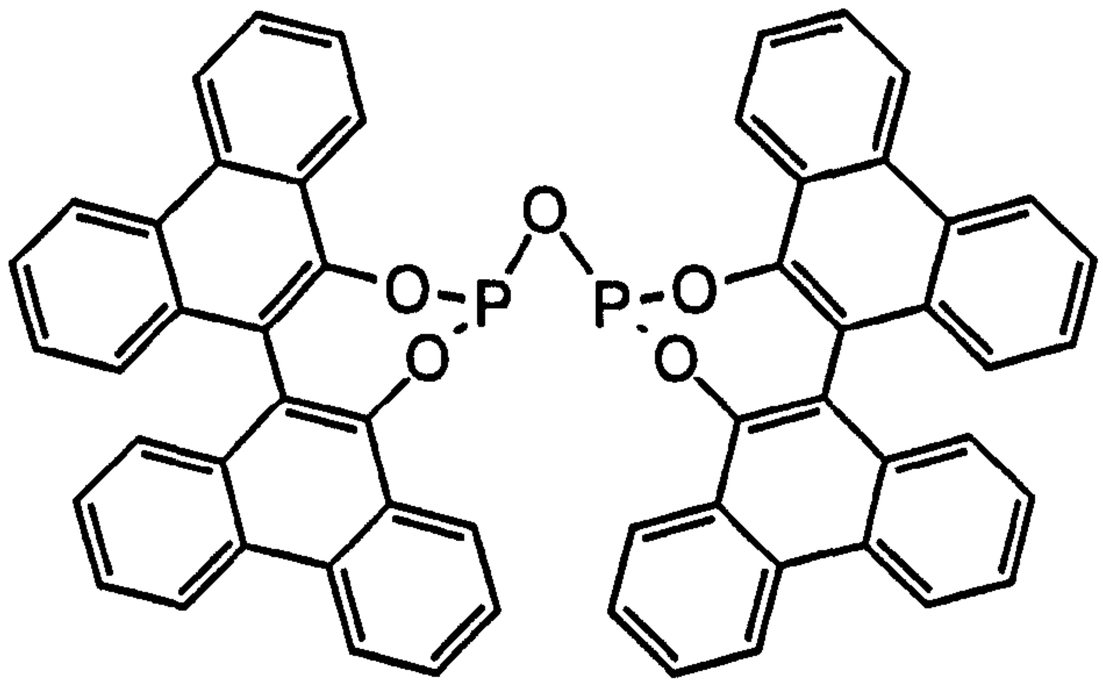

(3.12)

The final side-product of this reaction that has been identified is the furan **(3.13)**, which is formed by dehydration of biphenanthrol **(3.2)**, see Equation 3.2.

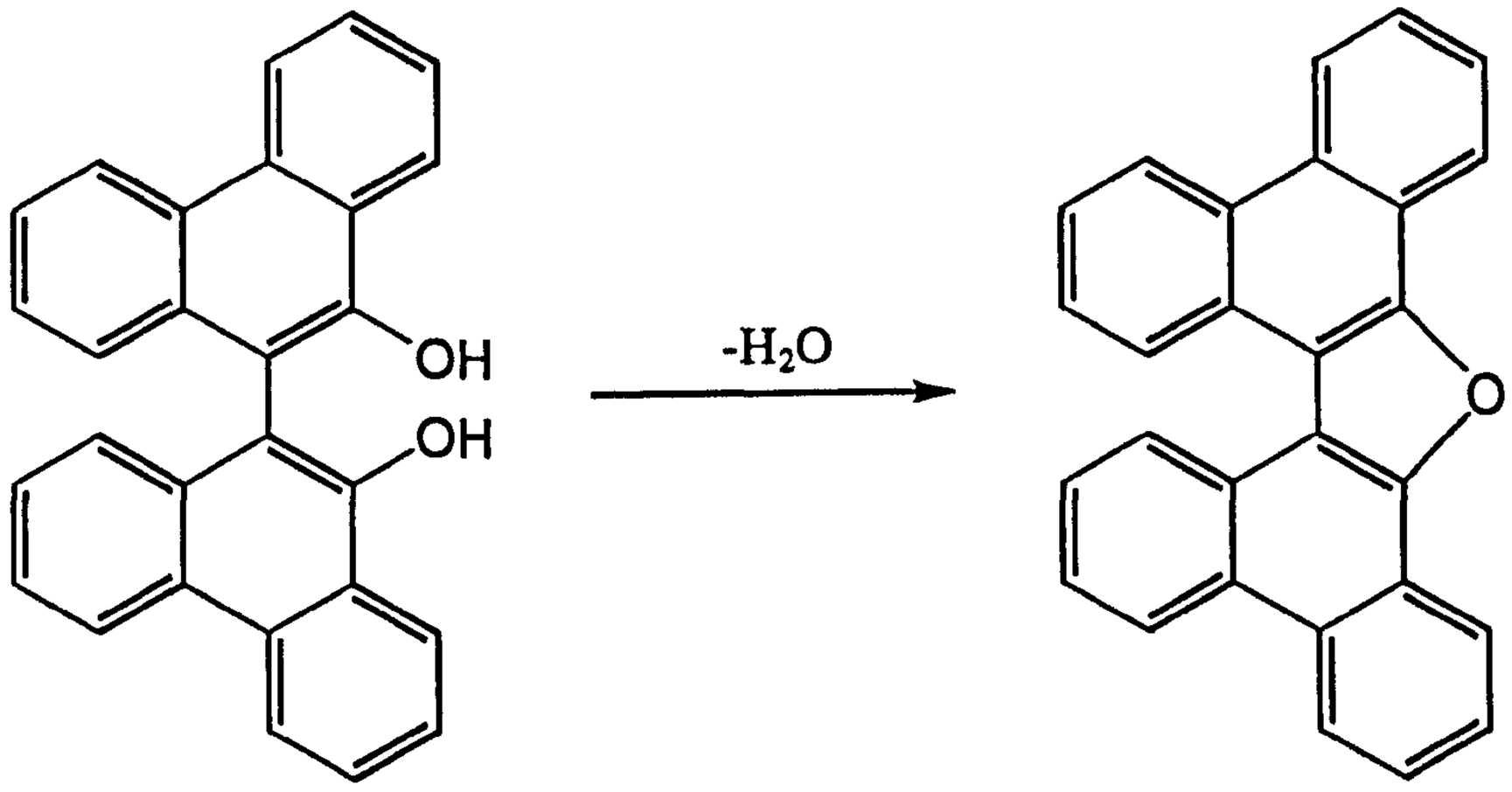

(3.2) **(3.13)**

Equation 3.2

This species has been characterised by X-ray crystallography carried out by Dr D. Ellis in this department, see Figure 3.3. The structure was solved in the space group $P2_1/c$ (No. 14) and shows that the compound is nearly planar, with an angle between the two phenanthryl planes of 14.3°. The bond length and bond angle geometries are all within normal ranges.[143] The minimum and maximum deviations of the carbon atoms from planarity are -0.021 Å / 0.193 Å and 0.006 Å / -0.154 Å for the two phenanthryl rings.

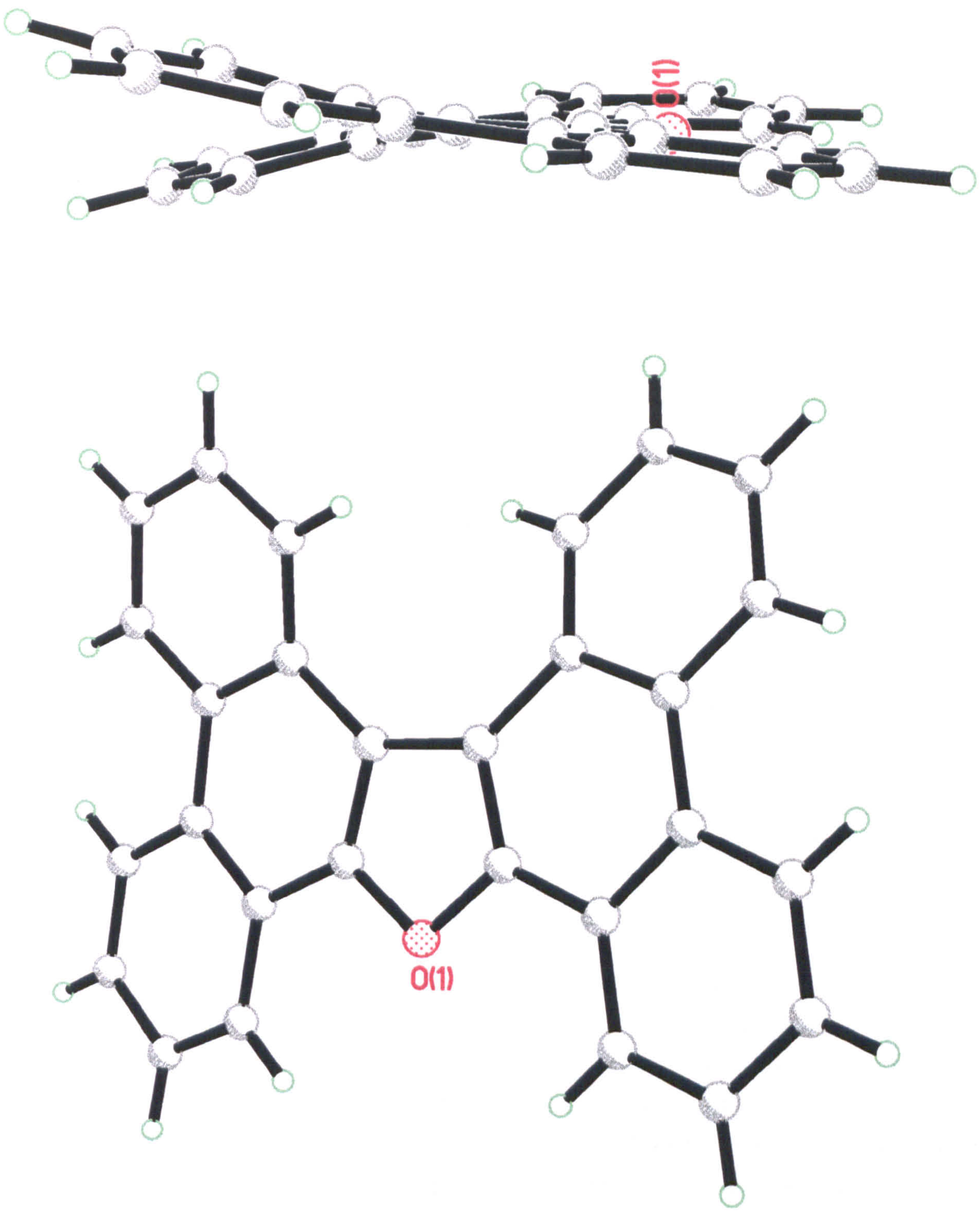

Figure 3.3: Molecular structure of the furan (**3.13**), formed by dehydration of biphenanthrol (**3.2**), showing the skewing of the two phenanthryl moieties

The following Sections will illustrate how the assignment of the signals in Figure 3.1 has been achieved and the syntheses of all the individual species discussed will be reported.

3.2.1.1 Synthesis of chlorophosphite (3.10) from biphenanthrol (3.2)

Chlorophosphites have been prepared by the addition of diols to a large excess of PCl_3 in the presence of a base to remove the HCl produced.[93] These reactions are highly exothermic and are therefore carried out at low temperature. Thus, chlorophosphite (**3.10**) has been prepared both as a racemate and optically pure by reaction of PCl_3 with racemic or optically pure biphenanthrol (**3.2**) respectively in the presence of triethylamine at -40 °C, see Equation 3.3.

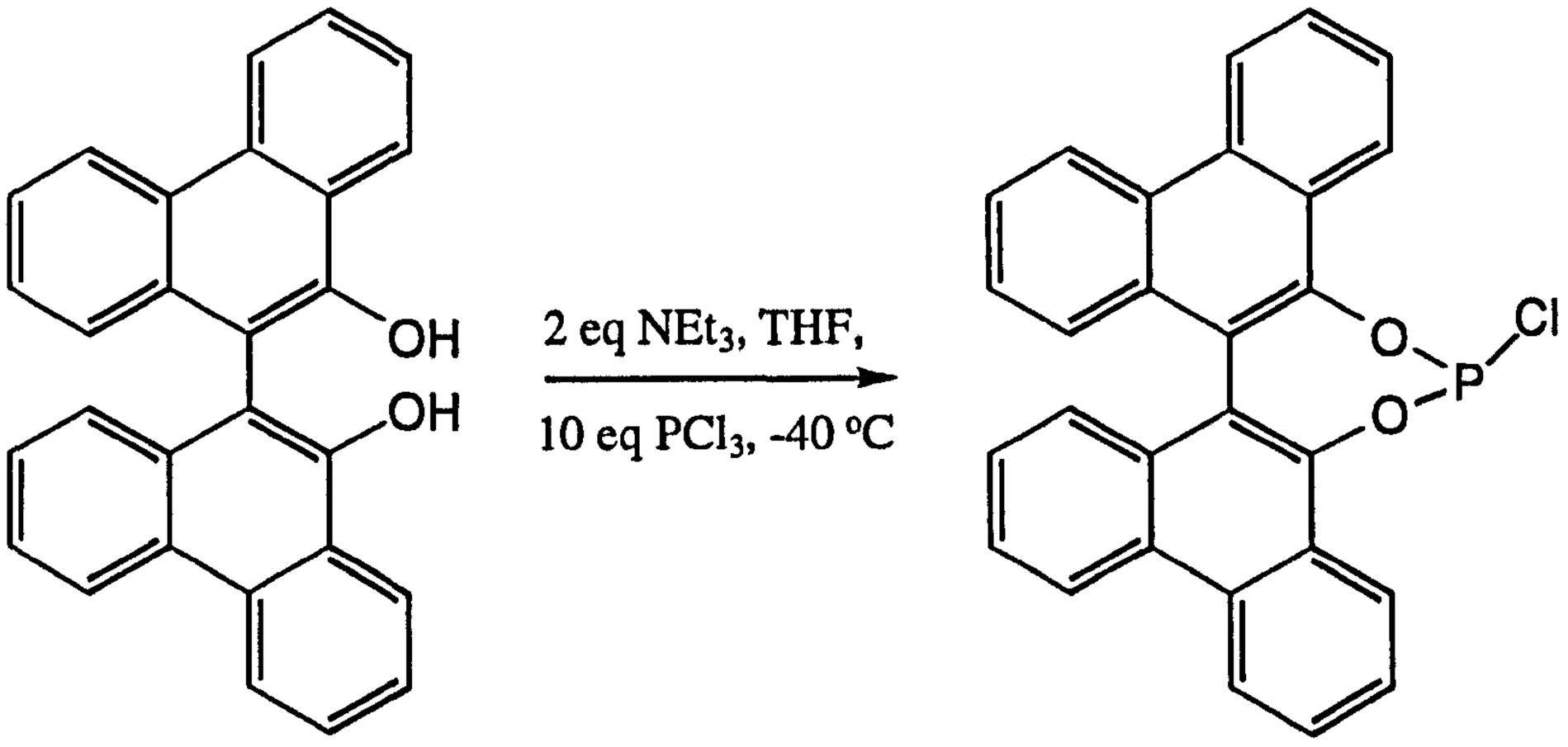

(3.2) **(3.10)** + $2[HNEt_3]Cl$

Equation 3.3

Addition of the NEt_3 to the PCl_3 solution in THF led to the formation of a copious precipitate. At first it was thought that this may be due to the formation of triethylammonium chloride by reaction of the triethylamine with the HCl produced by reaction of the PCl_3 with traces of water in the solvent and / or the triethylamine. However, neither H_3PO_3 (from hydrolysis of the PCl_3) nor H_3PO_4 were observed in the $^{31}P\{^1H\}$ NMR spectrum of the product. We now postulate that the precipitate is the salt (**3.14**). This salt would be a much more reactive electrophile than PCl_3 and would react with the biphenanthrol to give the chlorophosphite; a form of nucleophilic catalysis.

(3.14)

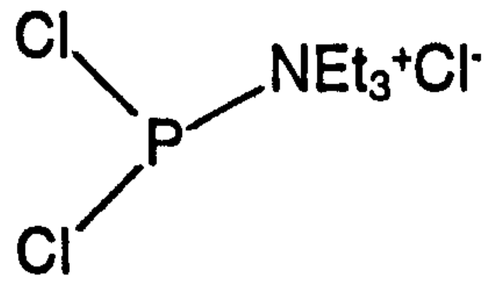

Provided air and moisture were rigorously excluded from the reaction mixture chlorophosphite (**3.10**) could be isolated in pure form in 92% yield and has been characterised by $^{31}P\{^{1}H\}$, $^{13}C\{^{1}H\}$ and ^{1}H NMR spectroscopy, see Table 3.1 and Experimental.

The $^{13}C\{^{1}H\}$ NMR spectrum of (**3.10**) shows twenty-eight carbon signals, not the fourteen that would be expected if the chlorophosphite was C_2-symmetric. The inequivalence is caused by the position of the chlorine atom, which lies closer to one of the phenanthryl moieties than the other rendering the molecule C_1-symmetric. This phenomenon has also been observed for (**3.15**), the analogous chlorophosphite derived from binaphthol,[93] as well as for the monophosphonites (**2.11**) and (**2.12**) described in Section 2.2.1.

(**3.15**)

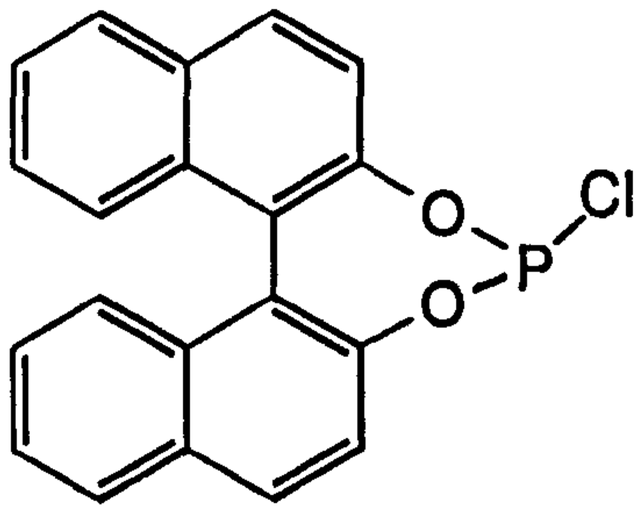

Table 3.1: ^{31}P and ^{1}H NMR data for chlorophosphites (**3.10**) and (**3.15**) and phosphonates (**3.11**) and (**3.16**)

Compound	δ_P ($CDCl_3$)[a]	δ_H ($CDCl_3$)[b]
(**3.10**)	180.9	7.27-7.34 (2H, m)
		7.38 (2H, dd, ^{3}J (HH) 8.4, ^{4}J (HH) 1.1)
		7.57-7.64 (2H, m)
		7.71-7.85 (4H, m)
		8.30 (1H, dd, ^{3}J (HH) 8.1, ^{4}J (HH) 1.1)
		8.42 (1H, dd, ^{3}J (HH) 8.1, ^{4}J(HH) 1.1)
		8.77 (2H, d, ^{3}J(HH) 8.6)
		8.81 (2H, d, ^{3}J(HH) 7.0)
(**3.15**)[c]	178.5[d]	------
(**3.11**)	13.1 (d, ^{1}J(PH) 731)	7.29-7.44 (4H, m)
		7.51 (1H, d, ^{1}J(PH) 732, HP)
		7.60-7.67 (2H, m)
		7.75-7.88 (4H, m)
		8.41-8.47 (2H, m)
		8.75-8.84 (4H, m)

Continued.

Table 3.1 continued:

Compound	δ_P ($CDCl_3$)[a]	δ_H ($CDCl_3$)[b]
(3.16)[c]	13.8 (d, ^1J(PH) 732)[d]	------

a Spectra recorded at 162 MHz at 28 °C. Chemical shifts (δ) in p.p.m. (±0.1) to high frequency of 85% H_3PO_4. Coupling constants (*J*) in Hz (±3).

b Spectra recorded at 400 MHz at 28 °C. Chemical shifts (δ) in p.p.m. (±0.01) to high frequency of tetramethylsilane. Coupling constants (*J*) in Hz (±0.1).

c Ref. 93

d Spectra recorded at 36.2 MHz at 28 °C. Chemical shifts (δ) in p.p.m. (±0.1) to high frequency of 85% H_3PO_4. Coupling constants (*J*) in Hz (±3).

Chlorophosphites are generally very moisture sensitive and this cyclic example is no exception. As a solid it can be briefly handled in air but in the presence of traces of water solutions rapidly show the formation of the phosphonate (**3.11**). This susceptibility to hydrolysis has prevented the attainment of satisfactory elemental analysis and characterisation by mass spectrometry. The phosphonate (**3.11**) has been isolated and characterised by ^{31}P and ^1H NMR spectroscopy as well as by mass spectrometry, see Table 3.1 and Experimental. The proton-coupled ^{31}P NMR spectrum displays a characteristically large ^1J(PH) value associated with phosphorus(V);[144] both the chemical shift and the ^1J(PH) coupling constant are very similar to those observed for the phosphonate derivative of binaphthol (**3.16**),[93] see Table 3.1.

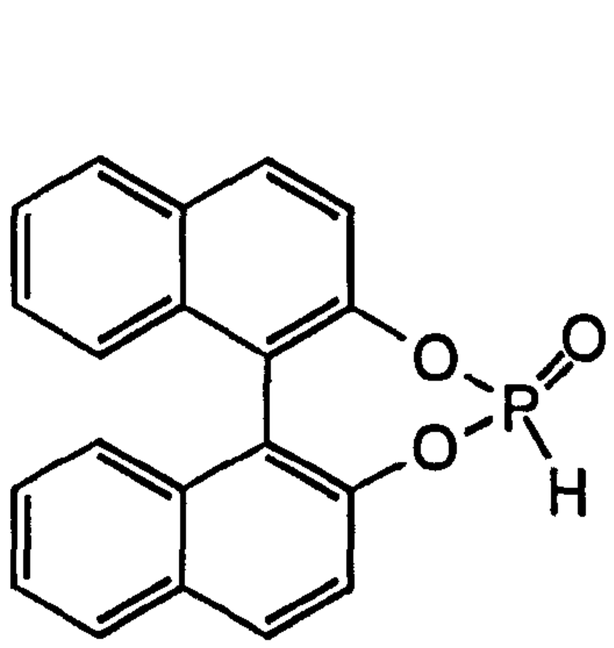

(3.16)

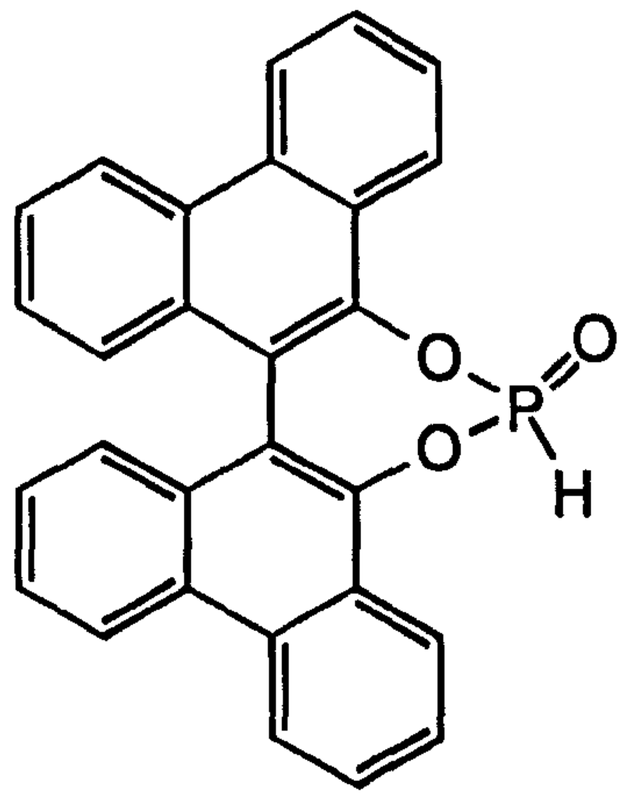

(3.11)

Chlorophosphites such as (**3.10**) are valuable intermediates and can be converted to cyclic aryl phosphites by reaction with anhydrous ROH. The use of optically pure (*R*)- or (*S*)-(**3.10**) allows these new ligands to be synthesised optically pure.

3.2.1.2 Synthesis of 'POP' pyrophosphite (S,S)-(3.12) from optically pure biphenanthrol (S)-(3.2)

The formation of the 'POP' pyrophosphite (**3.12**) as a side-product during efforts to synthesise 'biphenanthrite' (**3.4**) has already been mentioned. 'POP' pyrophosphites have been well documented in the literature[145-147] since the first synthesis of pyrophosphite (**3.17**) in 1931.[148-150]

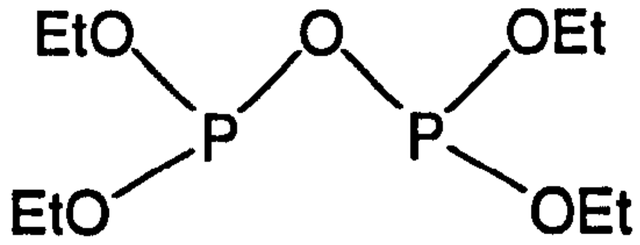

(3.17)

Since (**3.17**) has a rich coordination chemistry, forming binuclear[151-157] and trinuclear[158] complexes, the synthesis of 'POP' pyrophosphite (**3.12**) was attempted.

(*S,S*)-(**3.12**) has been synthesised in quantitative yield from the optically pure chlorophosphite (*S*)-(**3.10**) and water (Equation 3.4) and has been characterised by $^{31}P\{^{1}H\}$ and ^{1}H NMR spectroscopy, see Table 3.2 and Experimental.

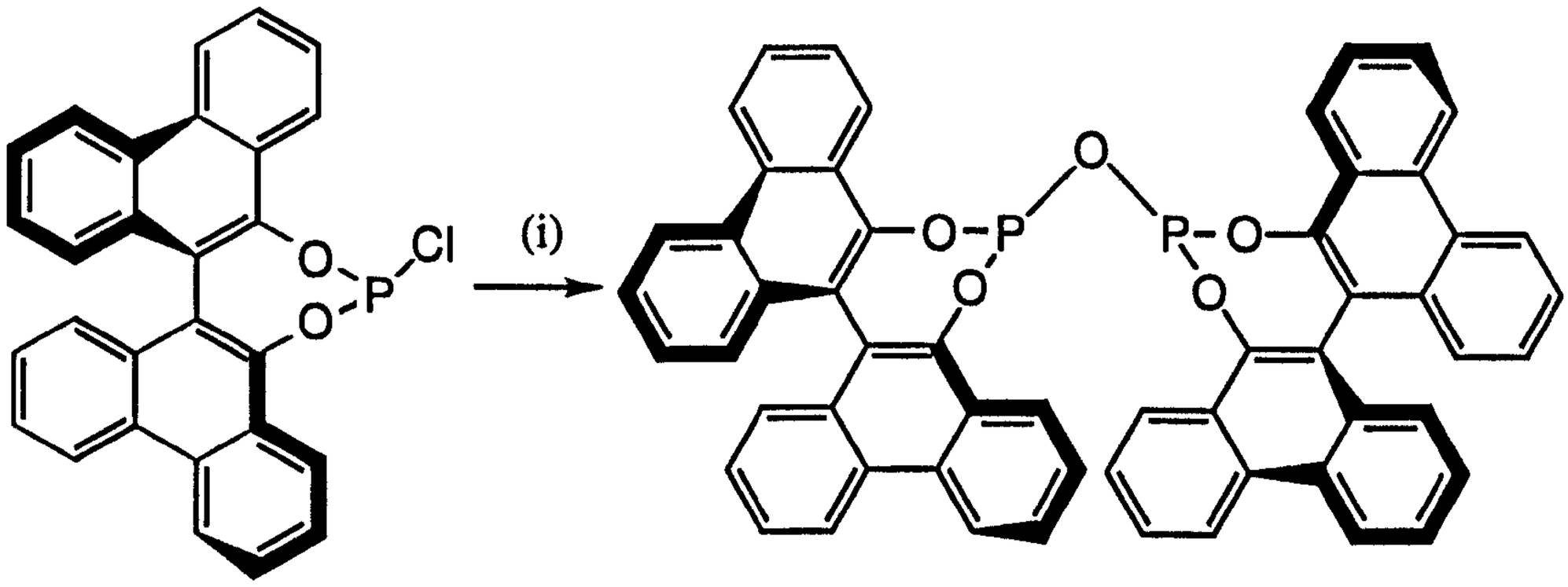

(*S*)-(**3.10**) (*S,S*)-(**3.12**)

(i) 0.5 eq H_2O, 1 eq NEt_3, THF

Equation 3.4

Table 3.2: $^{31}P\{^{1}H\}$ and ^{1}H NMR data for 'POP' pyrophosphites (*R,S*)- and (*S,S*)-(**3.12**)

Compound	δ_P ($CDCl_3$)[a]	δ_H ($CDCl_3$)[b]
(*R,S*)-(**3.12**)	139.4	------
(*S,S*)-(**3.12**)	141.9	7.01 (2H, d, ^{3}J(HH) 8.6)
		7.04-7.09 (2H, m)
		7.14 (2H, d, ^{3}J(HH) 8.2)
		7.17 (2H, d, ^{3}J(HH) 8.5)
		7.30-7.39 (4H, m)
		7.41 (2H, d, ^{3}J(HH) 7.6)
		7.44 (2H, d, ^{3}J(HH) 7.6)
		7.50-7.65 (4H, m)
		8.16 (2H, d, ^{3}J(HH) 8.2)
		8.18 (2H, dd, ^{3}J(HH) 8.1, ^{4}J(HH) 1.1)
		8.37 (2H, d, ^{3}J(HH) 8.2)
		8.43 (2H, d, ^{3}J(HH) 8.2)
		8.50 (2H, d, ^{3}J(HH) 8.2)
		8.53 (2H, d, ^{3}J(HH) 8.9)

a Spectra recorded at 162 MHz at 28 °C. Chemical shifts (δ) in p.p.m. (±0.1) to high frequency of 85% H_3PO_4.

b Spectrum recorded at 400 MHz at 28 °C. Chemical shifts (δ) in p.p.m. (±0.01) to high frequency of tetramethylsilane. Coupling constants (*J*) in Hz (±0.1).

Pyrophosphite (**3.12**) decomposes readily to the phosphonate (**3.11**) in the presence of alumina but can be briefly handled in air as a solid or in solution.

3.2.1.3 Synthesis of 'dangler' monophosphite (S,S)-(3.9) from optically pure (S)-biphenanthrol (3.2)

The 'dangler' monophosphites are interesting ligands in their own right and therefore the synthesis of (*S,S*)-(**3.9**) was undertaken. Dropwise addition of the chlorophosphite (**3.10**) derived from (*S*)-biphenanthrol (**3.2**) to a solution of (*S*)-biphenanthrol (**3.2**) in THF at -40 °C in the presence of one equivalent of triethylamine yielded the desired monophosphite (*S,S*)-(**3.9**). Provided the chlorophosphite was added slowly to the biphenanthrol solution, no diphosphite formation was observed in this reaction but the monophosphite was always formed as a mixture with the 'POP' pyrophosphite (*S,S*)-(**3.12**), see Equation 3.5.

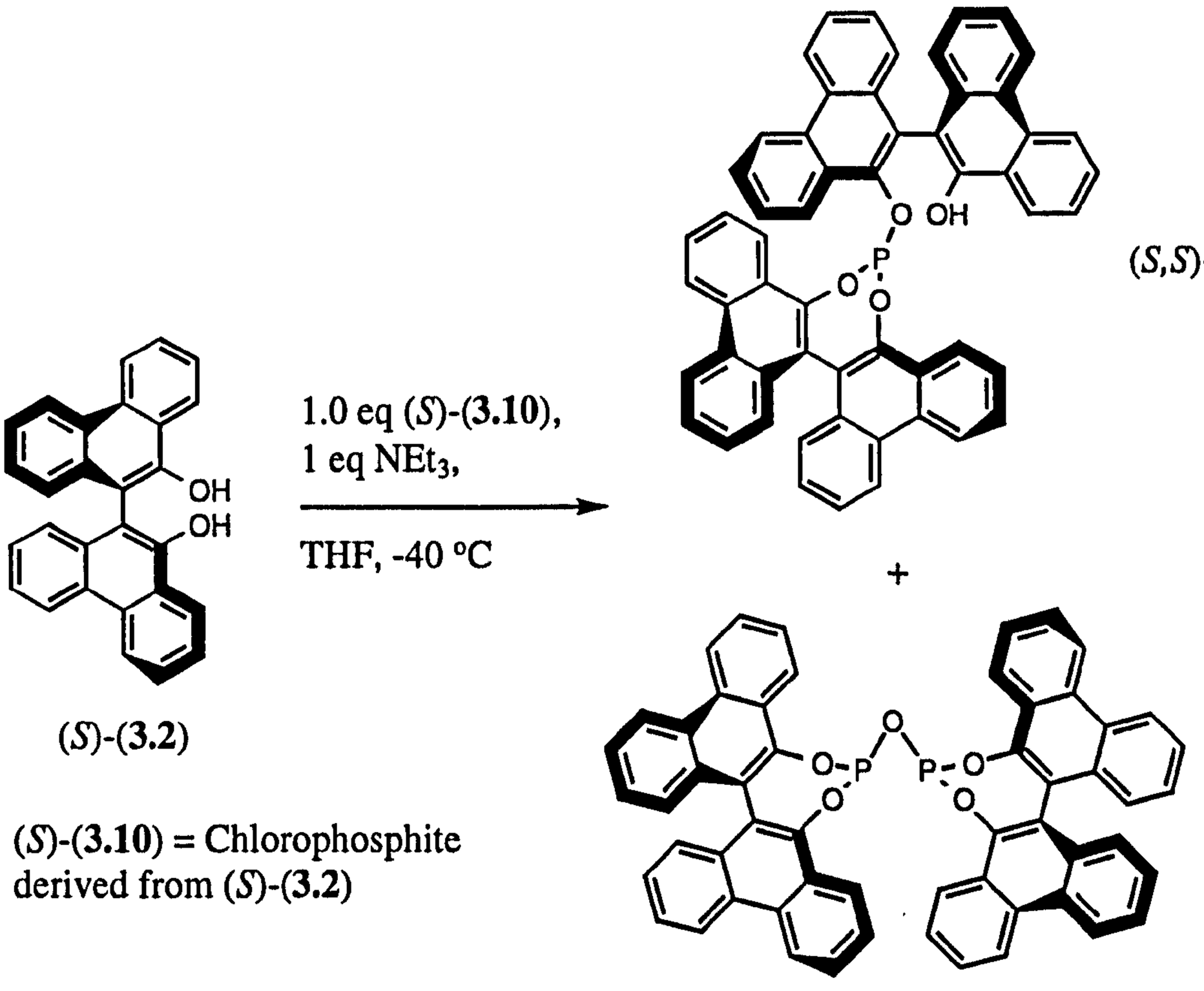

(*S*)-(**3.2**)

(*S*)-(**3.10**) = Chlorophosphite derived from (*S*)-(**3.2**)

(*S*,*S*)-(**3.9**)

(*S*,*S*)-(**3.12**)

Equation 3.5

The 'dangler' phosphite (**3.9**) can be briefly handled in air as a solid and in solution but gradual hydrolysis does occur; for example a solution of (**3.9**) in $CDCl_3$ undergoes *ca.* 60% hydrolysis to the phosphonate (**3.11**) after two days. Furthermore, (**3.9**) is moderately stable to alumina while 'POP' pyrophosphite (**3.12**) is, as mentioned in Section 3.2.1.2, significantly more sensitive. Consequently, stirring a solution of the product mixture over alumina and subsequent filtration through a short alumina plug gave pure (*S*,*S*)-(**3.9**) in 14% yield. This low yield is a consequence of the formation of the side-product (**3.12**) and also the fact that the 'dangler' monophosphite is itself sensitive to hydrolysis and that partial decomposition therefore occurs during the time required for complete hydrolysis of (**3.12**). (*S*,*S*)-(**3.9**) has been characterised by $^{31}P\{^{1}H\}$ and ^{1}H NMR spectroscopy, see Table 3.3 and Experimental.

Table 3.3: $^{31}P\{^{1}H\}$ and ^{1}H NMR data for the 'dangler' monophosphites (**3.9**) and (**3.18**)

Compound	δ_P ($CDCl_3$)	δ_H ($CDCl_3$)
(*R*,*R*)-(**3.18**)[a]	145.0[b]	5.50 (1H, br s, OH)[c] 6.51-7.98 (24H, m, Ph)[d]
(*R*,*S*) / (*S*,*R*)-(**3.18**)[a]	144.7[b]	------
(*S*,*S*)-(**3.9**)	146.2[e]	5.86 (1H, br s, OH) 7.22 (1H, d, ^{3}J(HH) 7.6) 7.25-7.33 (2H, m) 7.27 (1H, d, ^{3}J(HH) 7.0) 7.33-7.40 (4H, m) 7.40-7.47 (3H, m) 7.47-7.57 (3H, m) 7.58-7.67 (3H, m) 7.73 (1H, d, ^{3}J(HH) 7.0) 7.76 (1H, d, ^{3}J(HH) 7.3) 7.80-7.92 (2H, m) 7.93 (1H, d, ^{3}J(HH) 8.2) 8.13 (1H, d, ^{3}J(HH) 8.2) 8.63 (1H, d, ^{3}J(HH) 8.2) 8.65 (1H, d, ^{3}J(HH) 8.2) 8.71 (1H, d, ^{3}J(HH) 7.0) 8.79 (4H, d, ^{3}J(HH) 8.2) 8.81 (1H, d, ^{3}J(HH) 8.2) 8.92 (1H, d, ^{3}J(HH) 7.9)[f]
(*R*,*S*) / (*S*,*R*)-(**3.9**)	146.4[e]	------

a Ref. 93

b Spectra recorded at 36.2 MHz at 28 °C. Chemical shifts (δ) in p.p.m. (±0.1) to high frequency of 85% H_3PO_4.

c On shaking the sample with D_2O, the OH resonance disappeared and a broad signal appeared at δ 4.80 p.p.m. corresponding to DHO.

d Spectrum recorded at 270 MHz at 28 °C. Chemical shifts (δ) in p.p.m. (±0.01) to high frequency of tetramethylsilane.

e Spectra recorded at 162 MHz at 28 °C. Chemical shifts (δ) in p.p.m. (±0.1) to high frequency of 85% H_3PO_4.

f Spectrum recorded at 400 MHz at 28 °C. Chemical shifts (δ) in p.p.m. (±0.01) to high frequency of tetramethylsilane. Coupling constants (*J*) in Hz (±0.1).

The chemical shifts δ_P of the two diastereomers of (**3.9**) are characteristically[93] slightly downfield (by 0.7-4.6 p.p.m.) of those of the diastereomers of 'biphenanthrite' (**3.4**). The ^{1}H NMR spectrum shows that there are thirty-two aromatic signals and a

single OH resonance at δ_H 5.86 p.p.m., similar to δ_H 5.50 p.p.m. for the OH in biphenanthrol (**3.2**).

In contrast to the experience with biphenanthrol, none of the corresponding 'dangler' (**3.18**) was observed in the synthesis of 'binaphthite' (**3.1**) and efforts to synthesise the 'dangler' (**3.18**) by reaction of the chlorophosphite (**3.15**) with one equivalent of binaphthol (Equation 3.6) gave mixtures of (**3.18**) and 'binaphthite' (**3.1**).[93]

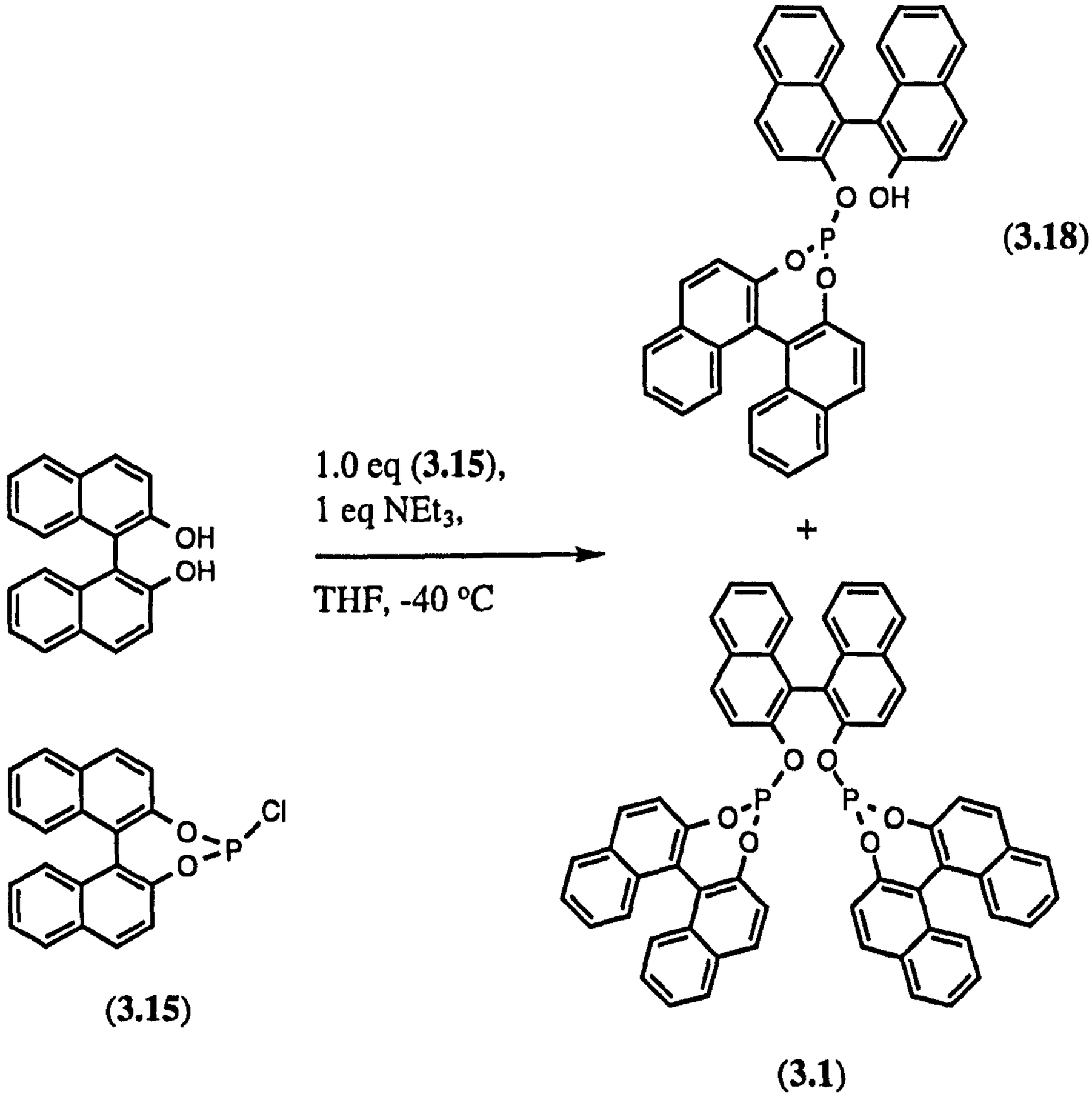

(3.18)

(3.15)

(3.1)

Equation 3.6

The stability of (**3.9**) may be due to the bulky biphenanthryl units providing steric protection and inhibiting reaction with the chlorophosphite (**3.10**). This would also explain why (**3.9**) can be synthesised free of 'biphenanthrite' under the conditions of Equation 3.5, whilst attempts to make the less bulky 'dangler' (**3.18**) always result in the formation of mixtures with 'binaphthite' (Equation 3.6).

As illustrated in Scheme 3.1, the 'dangler' (**3.9**) may react with PCl_3 remaining in solution to form the phosphorodichloridite (**3.19**). Signals consistent with the formation of two diastereomers of (**3.19**) (from the two diastereomers of the 'dangler')

have been observed in the $^{31}P\{^{1}H\}$ NMR spectra of the crude reaction mixtures, see Table 3.4. A similar species (**3.8**) has been observed by Pastor and Rodebaugh[137] and the $^{31}P\{^{1}H\}$ NMR data for this compound are included in Table 3.4 for comparison.

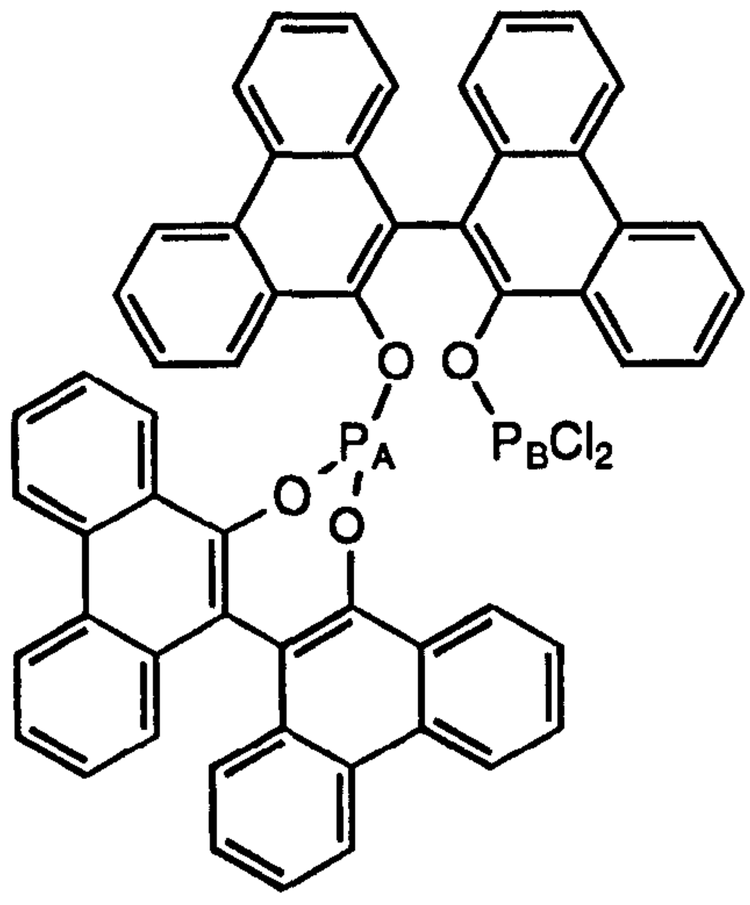

(3.19)

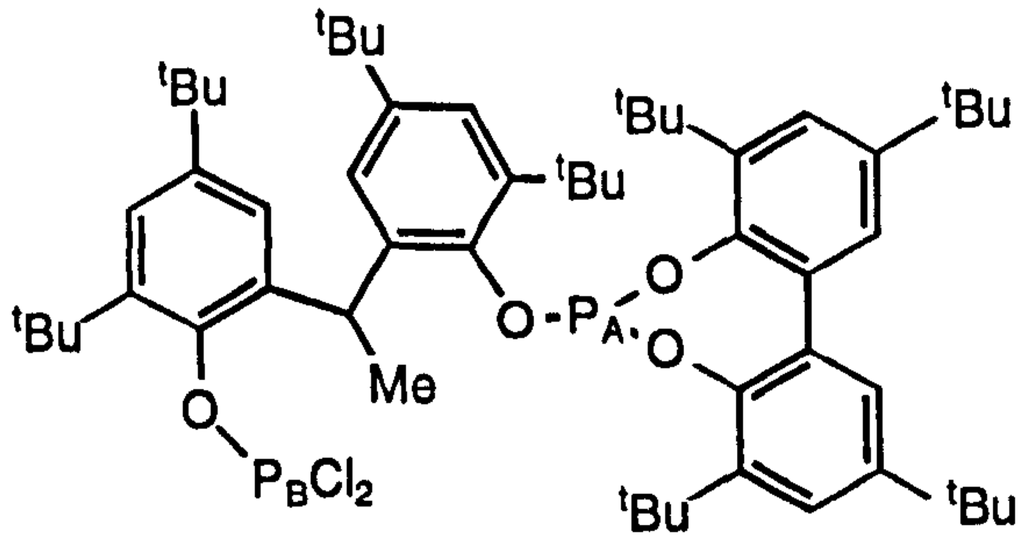

(3.8)

Table 3.4: $^{31}P\{^{1}H\}$ NMR data for the phosphorodichloridites (**3.8**) and (**3.19**)

Compound	δ_P ($CDCl_3$ / THF 1:2)[a]
(**3.8**)[b]	140.4 (d, ^{8}J(PP) 136, P_A)
	202.4 (d, ^{8}J(PP) 136, P_B)
(**3.19**)[c]	143.9 (d, ^{7}J(PP) 28, P_A)
	201.7 (d, ^{7}J(PP) 27, P_B)
(**3.19**)[c]	144.0 (d, ^{7}J(PP) 70, P_A)
	201.0 (d, ^{7}J(PP) 70, P_B)

a Spectra recorded at 162 MHz at 28 °C. Chemical shifts (δ) in p.p.m. (±0.1) to high frequency of 85% H_3PO_4. Coupling constants (*J*) in Hz (±3).

b Spectrum recorded at 202.33 MHz in C_6D_6. Chemical shifts (δ) in p.p.m. (±0.1) to high frequency of 85% H_3PO_4. Coupling constants (*J*) in Hz (±1).[137]

c The assignment of these signals to specific diastereomers of (**3.19**) remains ambiguous.

In the $^{31}P\{^{1}H\}$ NMR spectrum there are two doublets in the cyclic aryl phosphite region and two doublets in the phosphorodichloridite region. The values of the chemical shifts are in close agreement with those obtained for (**3.8**) and the large phosphorus-phosphorus coupling is presumably occurring by a similar mechanism to that observed for (*R,R,S*) / (*S,S,R*)-'biphenanthrite' (**3.4**) which has been discussed previously, see Pages 83-84.

If the phosphorodichloridite (**3.19**) could be prepared by reaction of the 'dangler' (**3.9**) with PCl_3, it might prove to be a very useful synthon since it would be expected to react with alcohols to form a range of unsymmetrical diphosphites, see

Equation 3.7, though we have not attempted such syntheses. Thus, by reaction of optically pure (*S,S*)-(**3.19**) with (*R*)-biphenanthrol it might prove possible to obtain the optically pure (*S,S,R*)-diastereomer of 'biphenanthrite' (**3.4**).

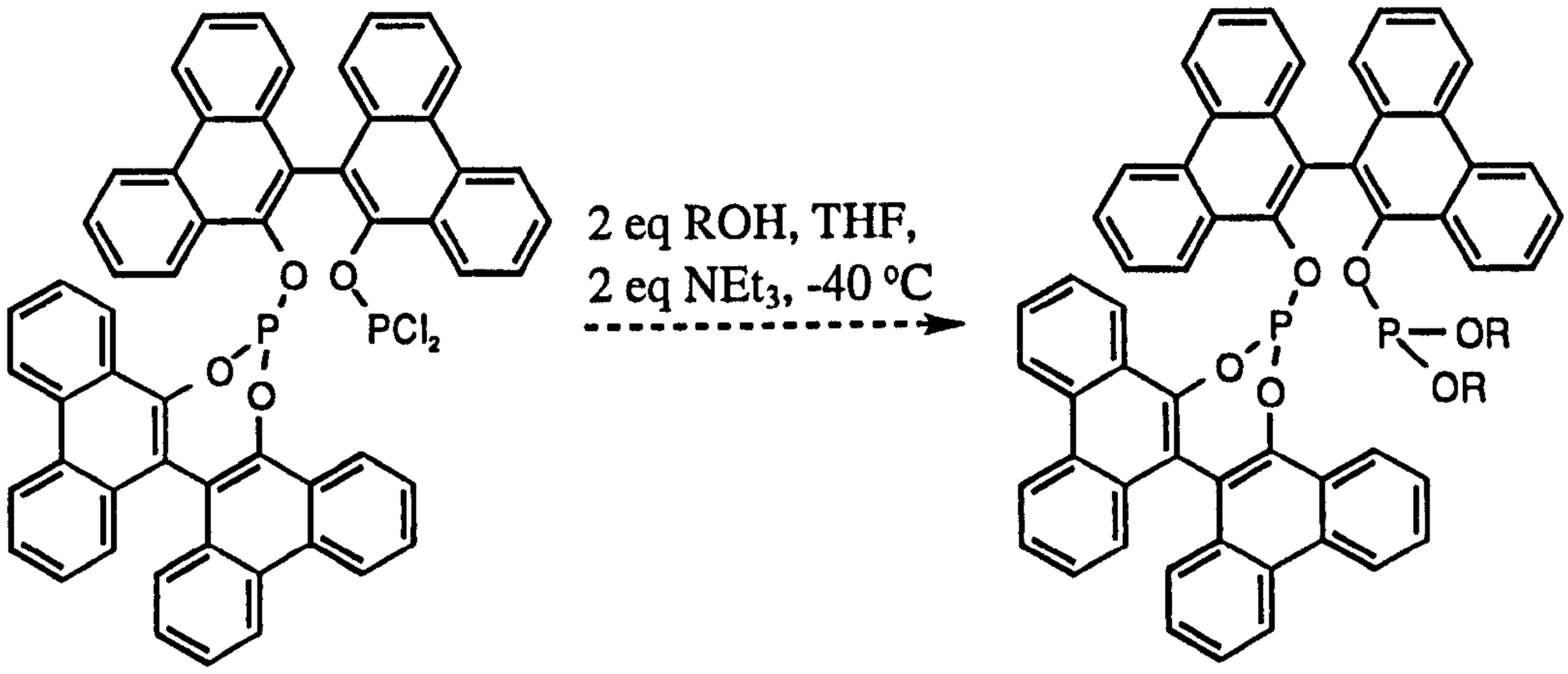

(3.19)

Equation 3.7

3.2.1.4 Synthesis of the (R,S,R)- / (S,R,S)-diastereomer of 'biphenanthrite' (3.4)

The formation of the 'dangling' phosphite and the 'POP' pyrophosphite side-products, (**3.9**) and (**3.12**) respectively, has proved a major obstacle in the synthesis of 'biphenanthrite' (**3.4**). 'Biphenanthrite' is air- and moisture-stable but decomposes to biphenanthrol (**3.2**) on a silica column. It can be filtered through a short alumina plug to remove $[HNEt_3]Cl$, the phosphonate (**3.11**) and the pyrophosphite (**3.12**) but, like the 'dangler' (**3.9**), exposure to alumina for longer periods to carry out column chromatography resulted in decomposition to biphenanthrol (**3.2**). Recrystallisation was unsuccessful and hence the diphosphite (**3.4**) could not easily be obtained pure.

Consequently, efforts focused upon driving the reaction to completion. It was reasoned that more nucleophilic aryloxide species may eliminate the formation of 'dangler' (**3.9**). Several attempts at the synthesis of 'biphenanthrite' (**3.4**) by reaction of (±)-biphenanthrol (**3.2**) with PCl_3 in various solvents using different bases have, unfortunately, shown that this is not the case. However, the reaction of the disodium salt of (±)-biphenanthrol with 0.5 eq (±)-chlorophosphite (**3.10**) in THF at -40 °C (Scheme 3.2) unexpectedly produced a single diastereomer of 'biphenanthrite' (**3.4**), a single diastereomer of 'dangling' phosphite (**3.9**) and a single diastereomer of the 'POP' pyrophosphite (**3.12**).

Throughout the course of these investigations it was discovered that 'biphenanthrite' (**3.4**) is remarkably stable to base and much more stable than either triphenylphosphite, the 'dangling' phosphite (**3.9**) or the 'POP' pyrophosphite (**3.12**). Thus, solutions of (**3.4**) are stable for months in the absence of base and for at least

21 h in the presence of aqueous 1M potassium hydroxide solution. This stability can be attributed to a combination of the stabilisation imparted by the seven-membered rings and the hydrophobic organic backbone. The lower stability of the 'dangler' (**3.9**) can be ascribed to the hydrophilic hydroxyl group in the vicinity of the phosphite functionality which can 'direct' water molecules towards the labile P-O bonds.

This difference in stability to base led to a method for the isolation of pure (*R,S,R*) / (*S,R,S*)-'biphenanthrite' (**3.4**), see Scheme 3.2. The reaction of the disodium salt of (±)-biphenanthrol with 0.5 eq (±)-chlorophosphite (**3.10**) in THF at -40 °C and subsequent purification by stirring a dichloromethane solution of the isolated reaction mixture with potassium hydroxide solution overnight gave pure (*R,S,R*) / (*S,R,S*)-(**3.4**) as a single diastereomer in 46% yield. This compound has been characterised by $^{31}P\{^{1}H\}$ NMR spectroscopy, see Table 3.6 and Experimental.

The formation of a single diastereomer of 'biphenanthrite' (**3.4**) starting from racemic biphenanthrol (**3.2**) is quite remarkable and it was subsequently hypothesised that an excess of sodium hydride catalysed isomerisation reactions to produce the thermodynamically most stable diphosphite (**3.4**) and 'dangler' phosphite (**3.9**). To provide evidence that such an isomerisation reaction was occurring, an NMR sample of the diastereomeric mixture of the 'dangler' phosphite (**3.9**) was prepared and 7.2 mol equiv of sodium hydride were added. The reaction was followed by $^{31}P\{^{1}H\}$ NMR spectroscopy and it was observed that the intensity of the (*R,S*) / (*S,R*)-diastereomer gradually fell relative to that of the (*R,R*) / (*S,S*)-diastereomer (see Table 3.5) whilst no other phosphorus-containing products were observed.

Table 3.5: Sodium hydride-catalysed isomerisation of the diastereomeric mixture of 'dangler' phosphite (**3.9**)

Time (h)	Percentage composition[a]	
	(*R,S*) / (*S,R*)-(**3.9**)	(*R,R*) / (*S,S*)-(**3.9**)
Start	66	34
0[b]	59	41
2	53	47
4	46	54
22	46	54
24[c]	18	82

a Percentage compositions calculated from integration of the two resonances in the $^{31}P\{^{1}H\}$ NMR spectra. Spectra recorded in $CDCl_3$ at 162 MHz at 28 °C.
b Immediately after sodium hydride was added.
c 7.8 mol equiv sodium hydride added immediately prior to this measurement.

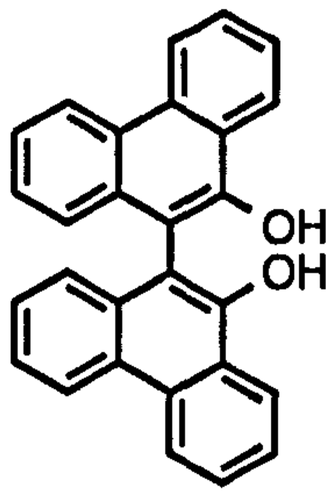

(±)-(**3.2**)

2 eq NaH

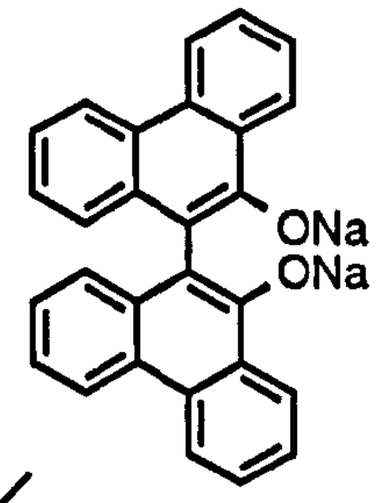

0.5 eq (**3.10**),
THF, -40 °C

(**3.10**) =
Chlorophosphite of
(±)-biphenanthrol

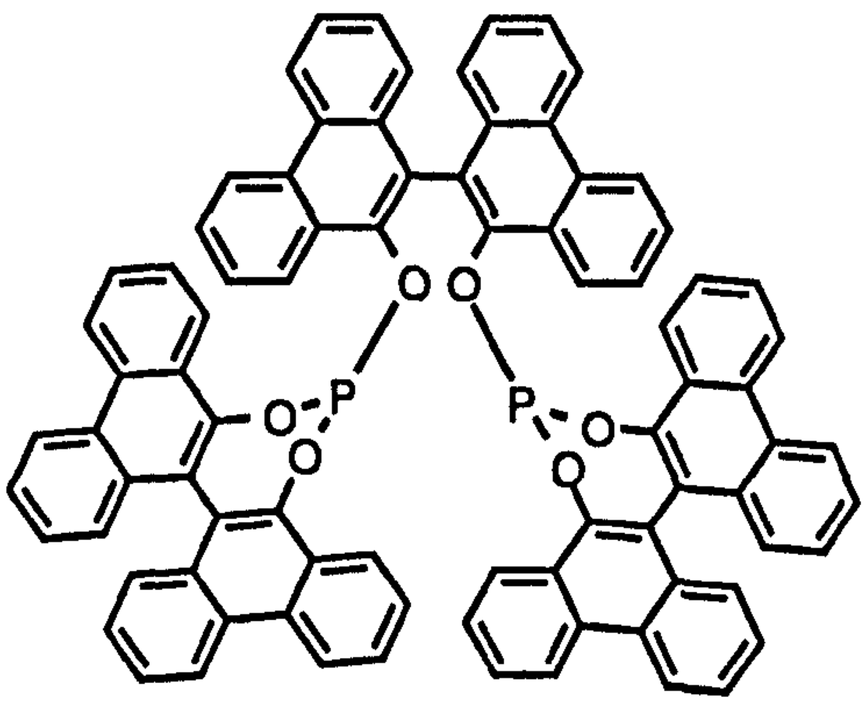

(*R*,*S*,*R*) / (*S*,*R*,*S*)-(**3.4**)

+

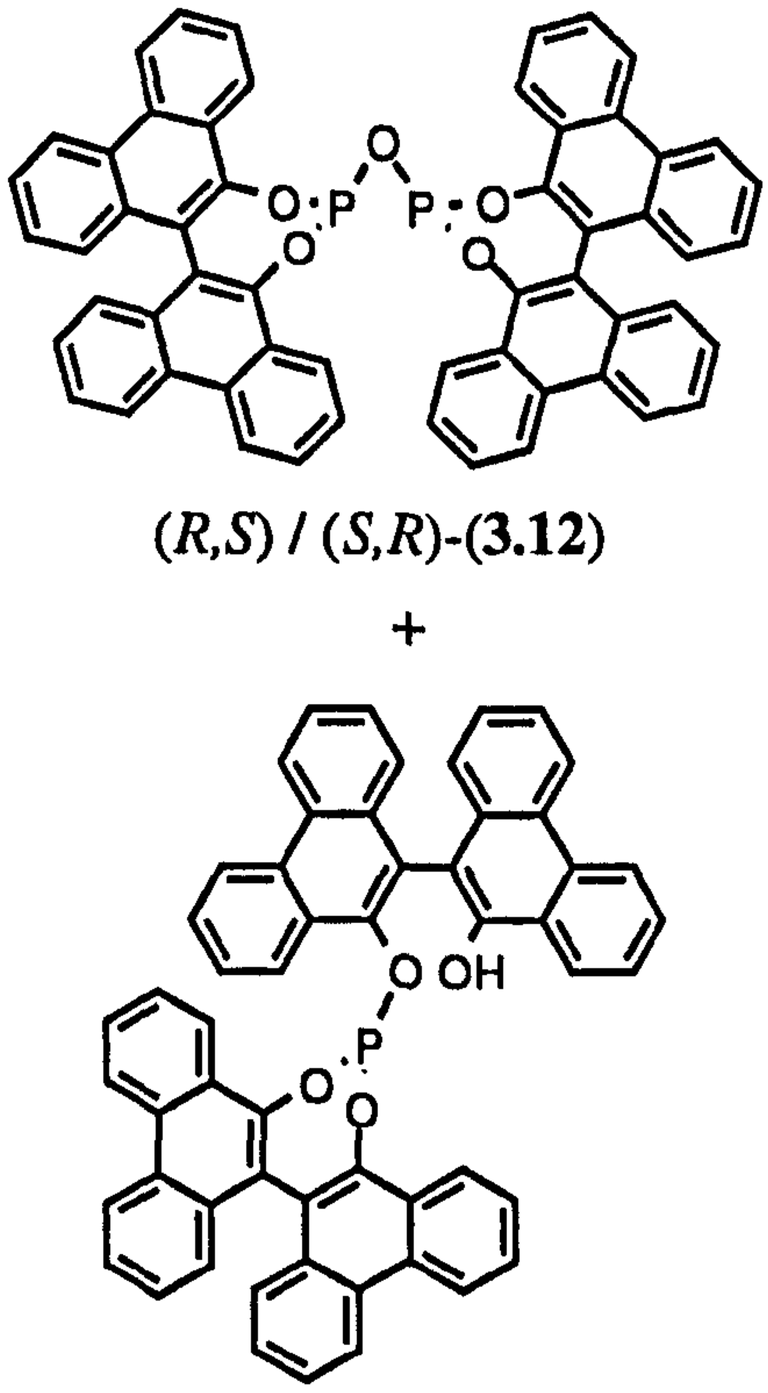

(*R*,*S*) / (*S*,*R*)-(**3.12**)

+

(*R*,*R*) / (*S*,*S*)-(**3.9**)

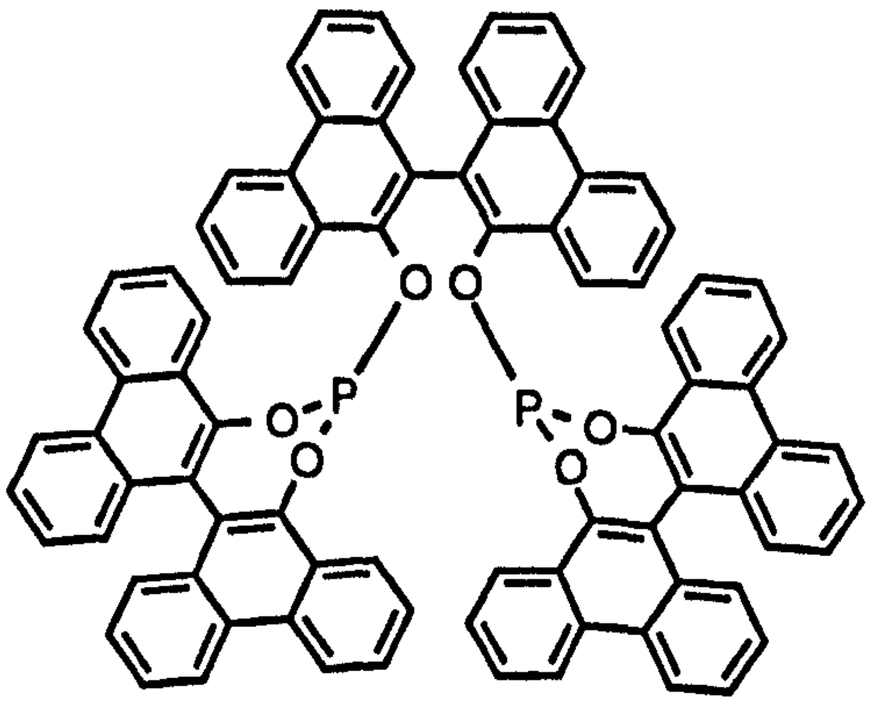

(*R*,*S*,*R*) / (*S*,*R*,*S*)-(**3.4**)

ORGANIC LAYER

CH_2Cl_2,
1M $KOH_{(aq)}$,
overnight

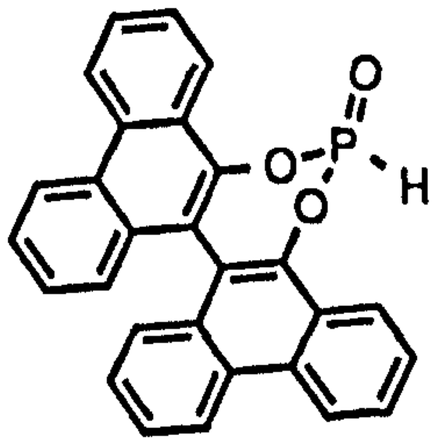

(±)-(**3.11**)

AQUEOUS LAYER

Scheme 3.2: Synthesis of (*R*,*S*,*R*) / (*S*,*R*,*S*)-'biphenanthrite' (**3.4**) as a single diastereomer in 46% overall yield

This result is consistent with the occurrence of the isomerisation reaction shown in Equation 3.8.

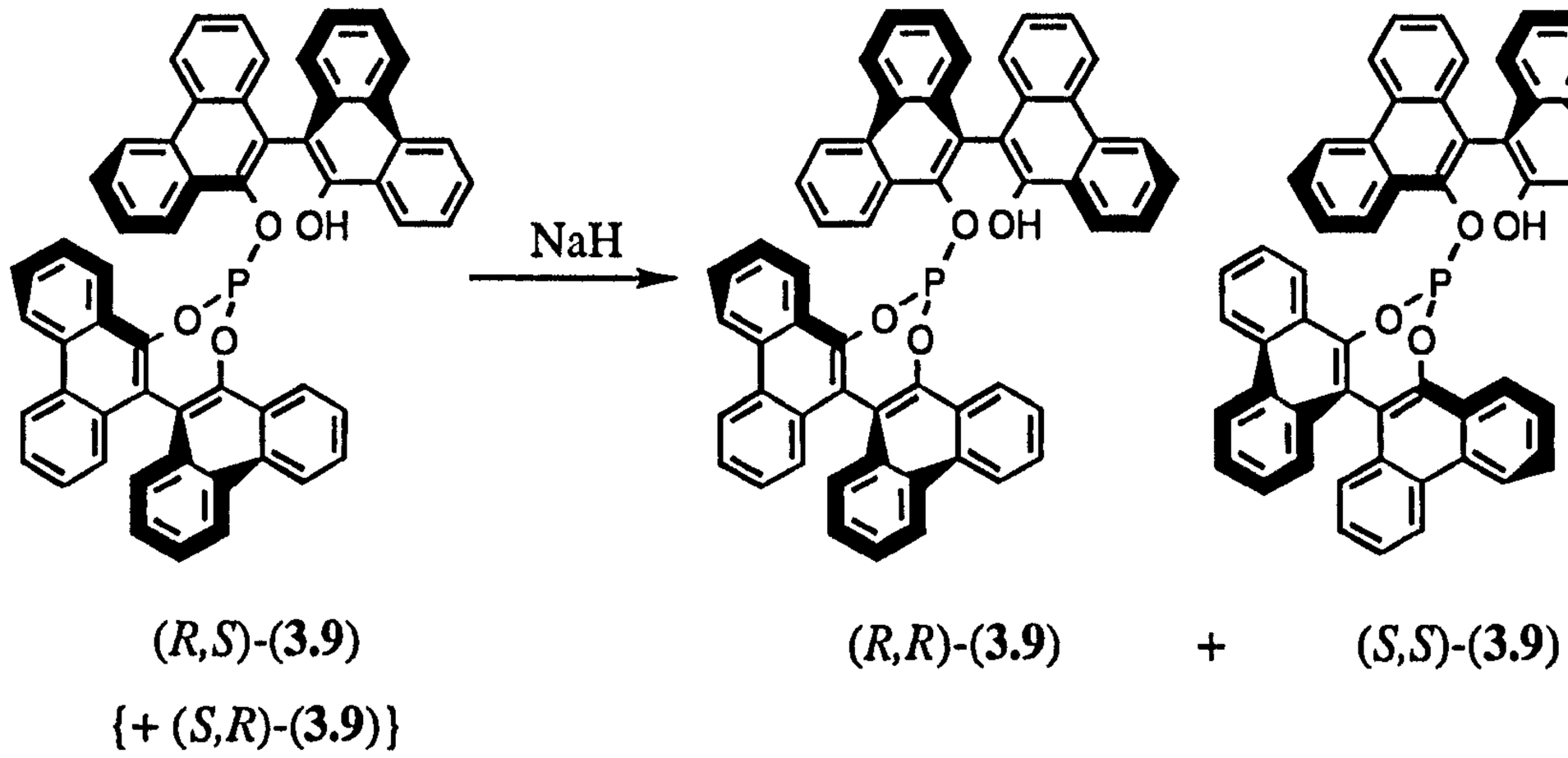

(*R,S*)-(**3.9**)
{+ (*S,R*)-(**3.9**)}

(*R,R*)-(**3.9**) + (*S,S*)-(**3.9**)

Equation 3.8

From these experiments it appears that the (*R,R*) / (*S,S*)-'dangler' (**3.9**) and the (*R,S,R*) / (*S,R,S*)-diphosphite (**3.4**) are the thermodynamic diastereomers. This would explain the significant diastereoselectivity in favour of the (*R,S,R*) / (*S,R,S*)-diastereomer in the original attempted synthesis of 'biphenanthrite' (see Section 3.2.1). No such diastereoselectivity was observed with 'binaphthite' (**3.1**)[93] and, indeed, efforts to form (*R,S,R*)-'binaphthite' (**3.1**) failed due to isomerisation of this diastereomer to a mixture containing predominantly the (*R,R,R*)-diastereomer.[93,159] This suggests that the thermodynamic product for 'binaphthite' (**3.1**) is the (*R,R,R*)-diastereomer.

3.2.1.5 Synthesis of the diastereomeric mixture of 'biphenanthrite' (3.4)

The diastereomeric mixture of 'biphenanthrite' (**3.4**) was synthesised in 66% yield by reaction of (±)-biphenanthrol (**3.2**) with PCl_3 in the presence of triethylamine in THF at -40 °C and subsequent decomposition of the side-products formed (Equation 3.9). It should be noted that the purification procedure in this case employs first an acid and then a base wash since it was found that acid-catalysed hydrolysis was the most effective way to remove the pyrophosphite (**3.12**) and base-catalysed hydrolysis was the most effective way to remove the 'dangler' (**3.9**).

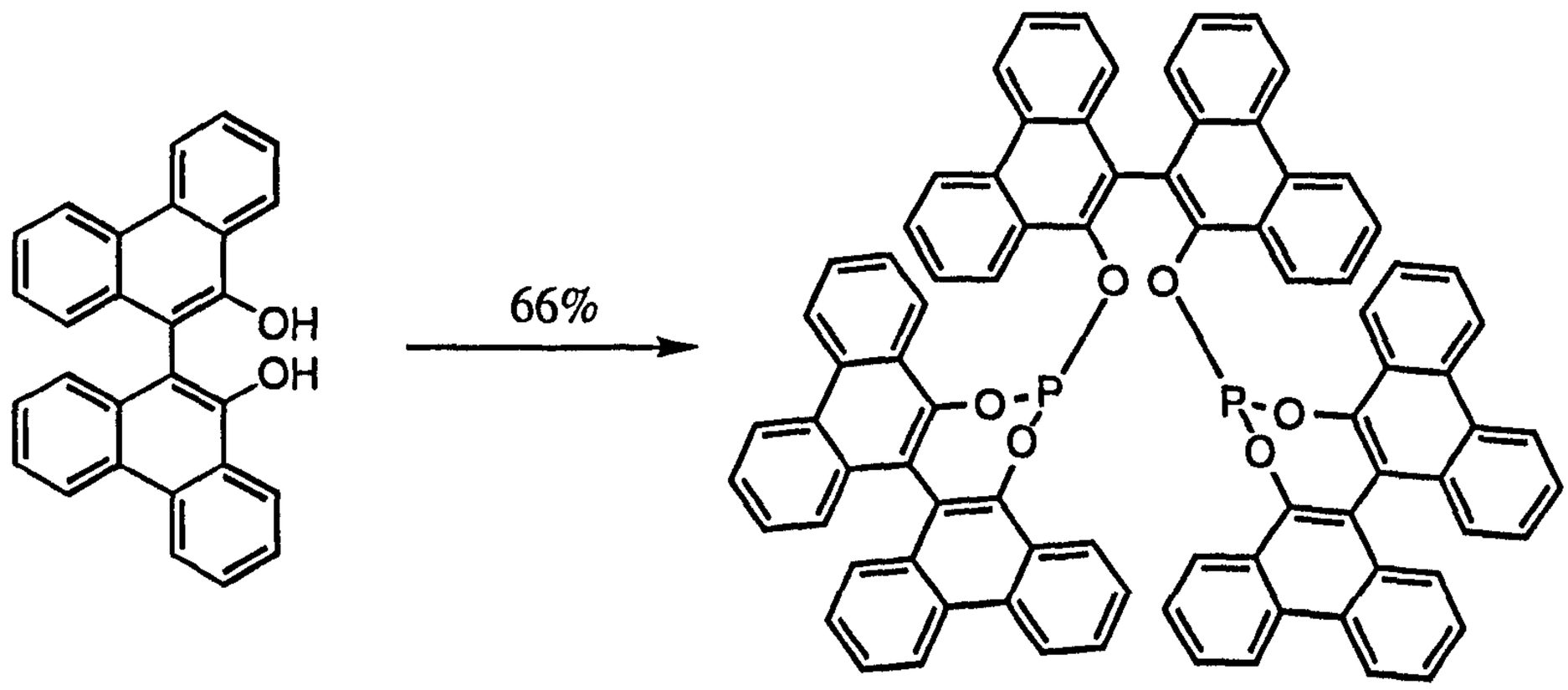

(3.2) **(3.4)**

Reaction conditions:
(i) 0.67 eq PCl_3, 2 eq NEt_3, THF, -40 °C
(ii) 2M $HCl_{(aq)}$
(iii) 2M $KOH_{(aq)}$

Equation 3.9

The diastereomeric mixture has been characterised by $^{31}P\{^1H\}$ NMR spectroscopy, see Table 3.6 and Experimental.

3.2.1.6 Synthesis of optically pure (R,R,R)-'biphenanthrite' (3.4) from (R)-biphenanthrol (3.2)

Optically pure (*R,R,R*)-'biphenanthrite' (**3.4**) was synthesised in 56% yield from (*R*)-biphenanthrol (**3.2**) (Equation 3.10) using a similar procedure to that used for the synthesis of the diastereomeric mixture and has been characterised by $^{31}P\{^1H\}$ and ^1H NMR spectroscopy, see Table 3.6 and Experimental.

Table 3.6: $^{31}P\{^1H\}$ NMR data for the three diastereomers of 'biphenanthrite' **(3.4)**

Compound	δ_P ($CDCl_3$)[a]
(*R,R,S*) / (*S,S,R*)-(**3.4**)	141.8 (d, ^7J(PP 40)
	145.3 (d, ^7J(PP) 40)
(*R,S,R*) / (*S,R,S*)-(**3.4**)	145.5[b]
(*R,R,R*)-(**3.4**)	143.3

a Spectra recorded at 162 MHz at 28 °C. Chemical shifts (δ) in p.p.m. (±0.1) to high frequency of 85% H_3PO_4. Coupling constants (*J*) in Hz (±3).
b Spectrum recorded in CD_2Cl_2.

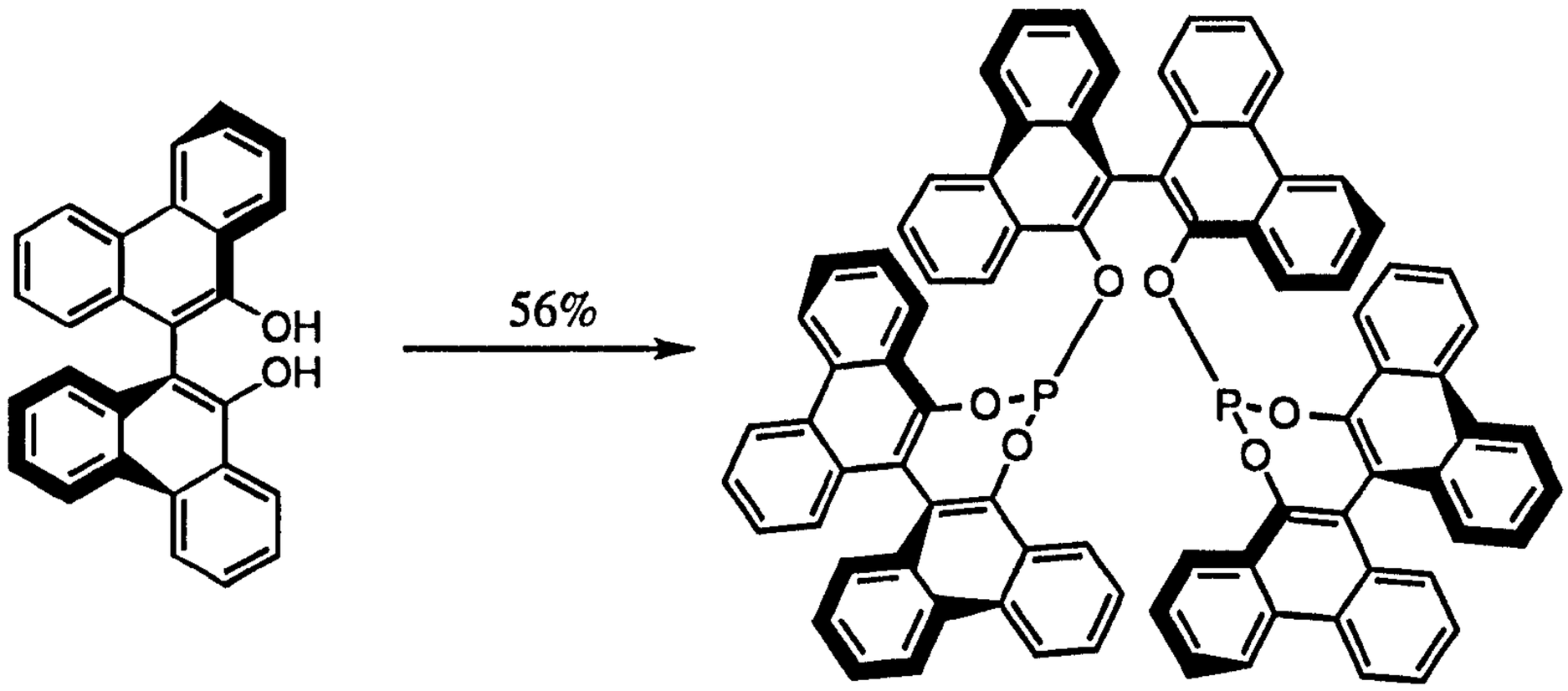

(*R*)-(**3.2**) (*R,R,R*)-(**3.4**)

Reaction conditions:
(i) 0.67 eq PCl_3, 2 eq NEt_3, THF, -40 °C
(ii) 2M $HCl_{(aq)}$
(iii) 2M $KOH_{(aq)}$

Equation 3.10

3.2.2 Synthesis of mixed diphosphites derived from biphenanthrol (3.2) and binaphthol

3.2.2.1 Synthesis of the mixed diphosphite 'pnp' (3.5)

The diastereomeric mixture of the mixed diphosphite 'pnp' (**3.5**) has been synthesised by reaction of (±)-binaphthol with 2.2 equivalents of the chlorophosphite (**3.10**) derived from (±)-biphenanthrol (**3.2**) in the presence of triethylamine. An acid wash was utilised in this synthesis to hydrolyse the pyrophosphite side-product (**3.12**) and the excess of chlorophosphite. The resultant phosphonate (**3.11**) was extracted with a base wash, enabling the isolation of the diastereomeric mixture of 'pnp' (**3.5**) in 53% yield, see Equation 3.11.

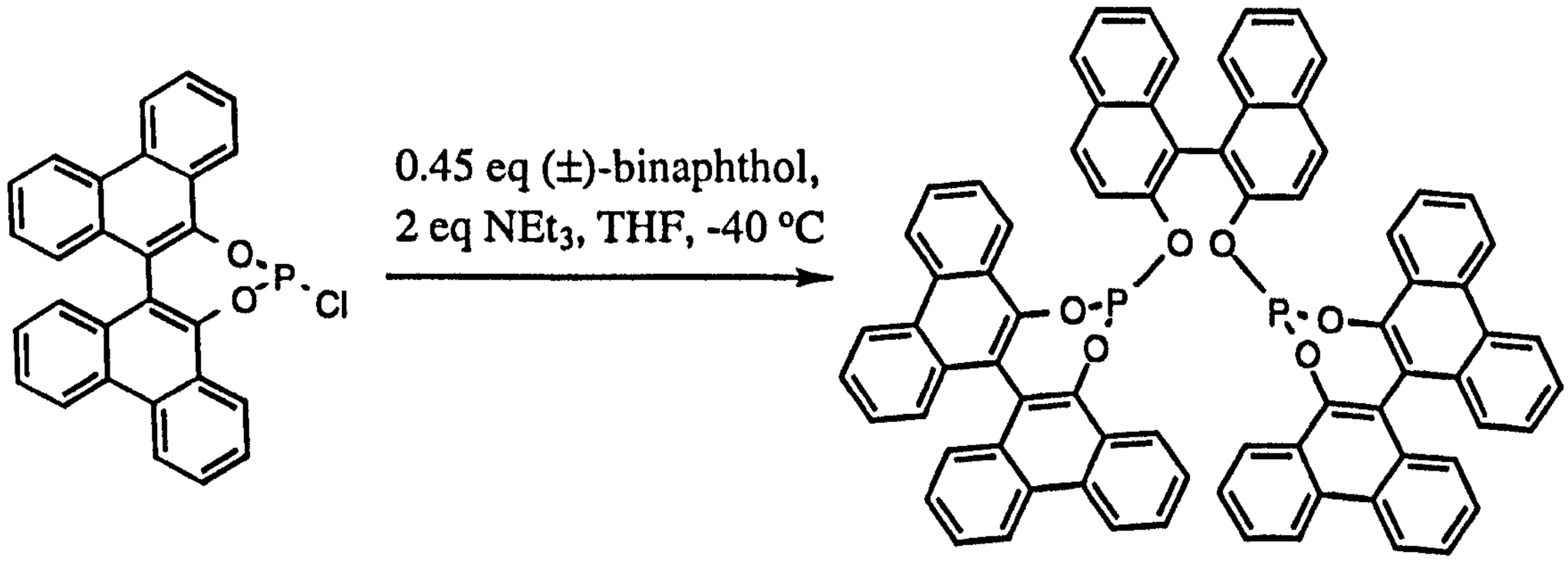

(±)-(**3.10**) (**3.5**), 53% yield

Equation 3.11

Significantly, no 'pn' 'dangler' phosphite side-product (**3.20**) was produced during this reaction.

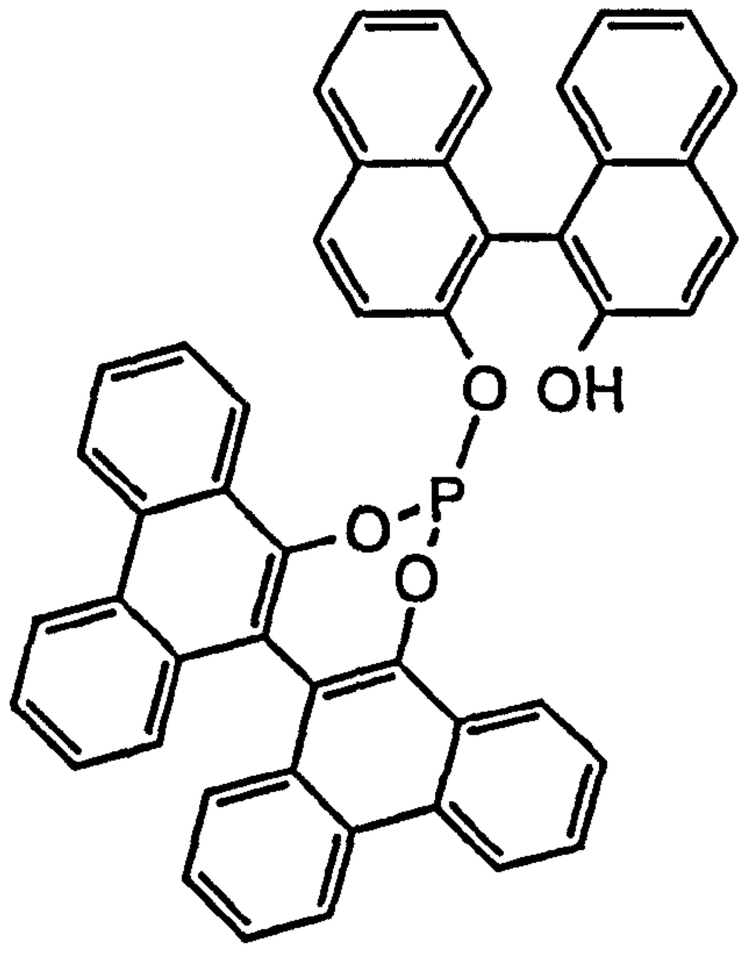

(3.20)

The diastereomeric mixture of 'pnp' (**3.5**) has been characterised by $^{31}P\{^{1}H\}$ NMR spectroscopy and mass spectrometry, see Figure 3.4, Table 3.7 and Experimental.

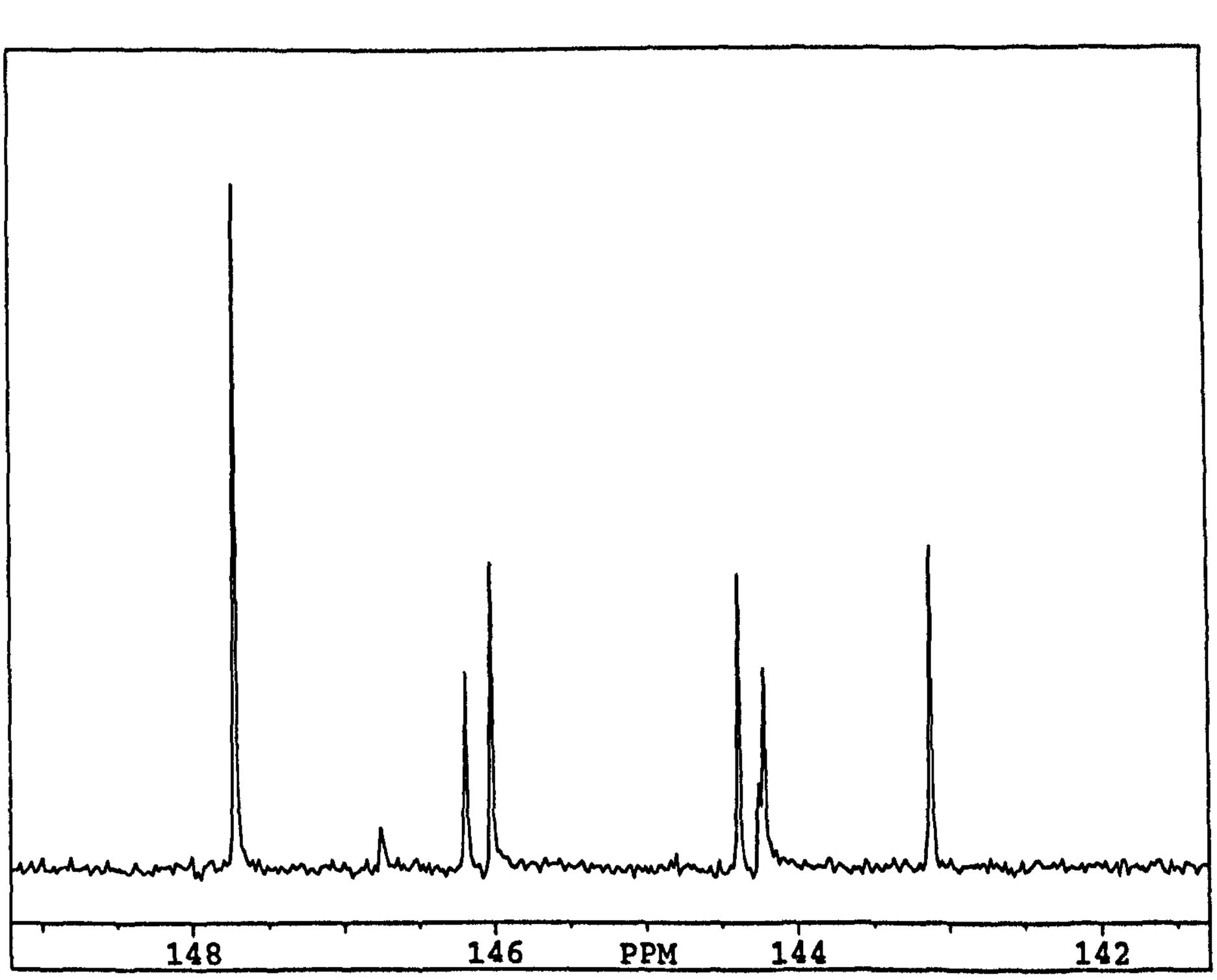

Figure 3.4: $^{31}P\{^{1}H\}$ NMR spectrum of the diastereomeric mixture of mixed diphosphite 'pnp' (**3.5**)

Table 3.7: $^{31}P\{^{1}H\}$ NMR data for the diastereomeric mixture of mixed diphosphite 'pnp' (**3.5**)

Compound	δ_P ($CDCl_3$)[a]
(*R*,*R*,*R*) / (*S*,*S*,*S*)-(**3.5**)	143.1
(*R*,*S*,*R*) / (*S*,*R*,*S*)-(**3.5**)	147.7
(*R*,*R*,*S*) / (*S*,*S*,*R*)-(**3.5**)	144.3 (d, ^{7}J(PP) 28)
	146.1 (d, ^{7}J(PP) 27)

a Spectrum recorded at 162 MHz at 28 °C. Chemical shifts (δ) in p.p.m. (±0.1) to high frequency of 85% H_3PO_4. Coupling constants (*J*) in Hz (±3).

The diphosphite 'pnp' (**3.5**) is also remarkably stable to hydrolysis. It appears to be indefinitely air- and moisture-stable in the solid state, with no hydrolysis products observed after 4 months. It is also air- and moisture-stable in solution and is stable upon exposure to base (2M KOH) for 4 h and to acid (2M HCl) for 10 min (the times are those used in the synthesis to purify the diphosphite).

It is also significant to note that no isomerisation of the diphosphite to 'npp' (**3.21**) was observed under these reaction conditions. Under similar reaction conditions (*R*,*S*,*R*)-'binaphthite' (**3.1**) undergoes an isomerisation to form (*R*,*R*,*R*)- and (*S*,*S*,*S*)-'binaphthite'.[93,159] This suggests that 'pnp' is thermodynamically more stable than the 'npp' isomer.

'npp' (**3.21**)

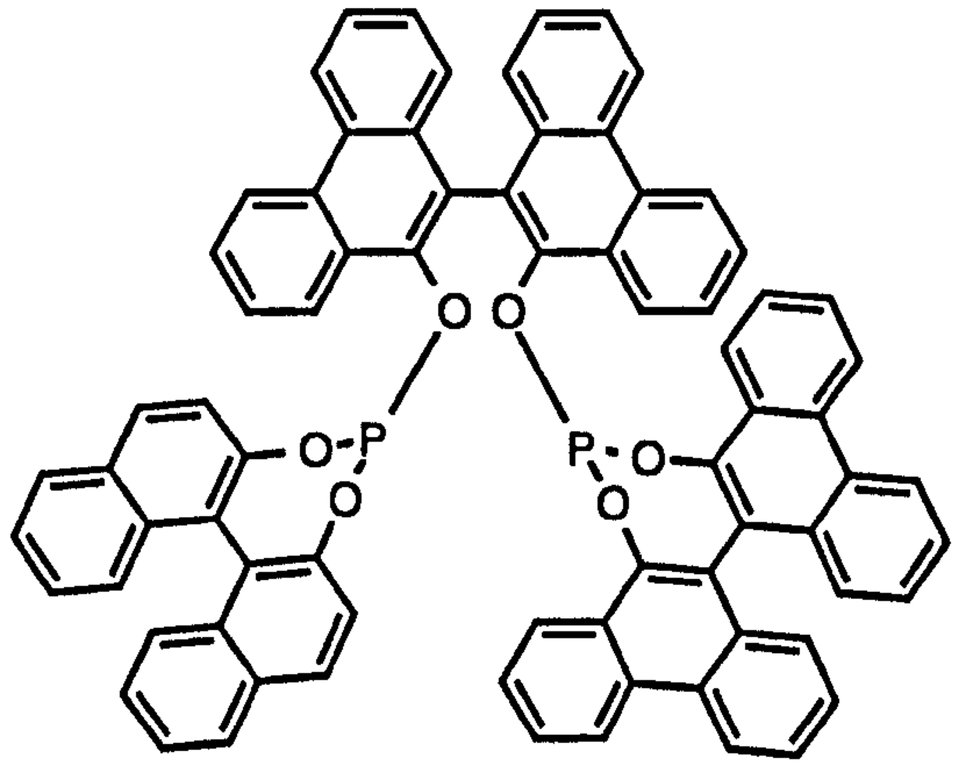

The origin of this greater stability may be in steric interactions between the terminal and bridging groups. The diphosphite with the least bulky bridging group appears to be favoured. This is consistent with the fact that the reaction to form the bulky 'biphenanthrite' (**3.4**) always results in formation of mixtures containing 'dangler' (**3.9**). The (*R*,*S*,*R*) / (*S*,*R*,*S*)-diastereoselectivity in the 'biphenanthrite' may also be a result of bridging-terminal steric clashing being minimised in this isomer.

The optically pure diphosphites (*R*,*S*,*R*)-'pnp' (**3.5**) and (*R*,*R*,*R*)-'pnp' (**3.5**) were synthesised as single diastereomers following similar procedures using optically

pure (*R*)-(9,9'-biphenanthryl-10,10'-diyl)chlorophosphite (**3.10**) and (*S*)- or (*R*)-binaphthol respectively. These species have been characterised by $^{31}P\{^{1}H\}$ NMR spectroscopy and mass spectrometry, see Table 3.7 and Experimental.

3.2.2.2 Attempted synthesis of mixed diphosphite 'npn' (3.22)

It was envisaged that the mixed diphosphite 'npn' (**3.22**) could be synthesised from the disodium salt of biphenanthrol (**3.2**) and two equivalents of the chlorophosphite (**3.15**) derived from binaphthol. However, the reaction was found to be much more complicated, as the $^{31}P\{^{1}H\}$ NMR spectrum of the crude product mixture (Figure 3.5) shows. The three diastereoisomers of the desired product are assigned to singlets A, B and C. The (*R,R,S*) / (*S,S,R*)-diastereoisomer should have inequivalent phosphorus atoms but, in this case, they are coincident. The signals D and E have been tentatively assigned as the two diastereoisomers of the 'np' 'dangler' (**3.23**). The two diastereoisomers of the binaphthol-derived 'POP' pyrophosphite (**3.24**) formed by reaction of chlorophosphite (**3.15**) with 0.5 equivalents of water are not present in Figure 3.5 but have been observed on occasion during such reactions.

'npn'
(3.22)

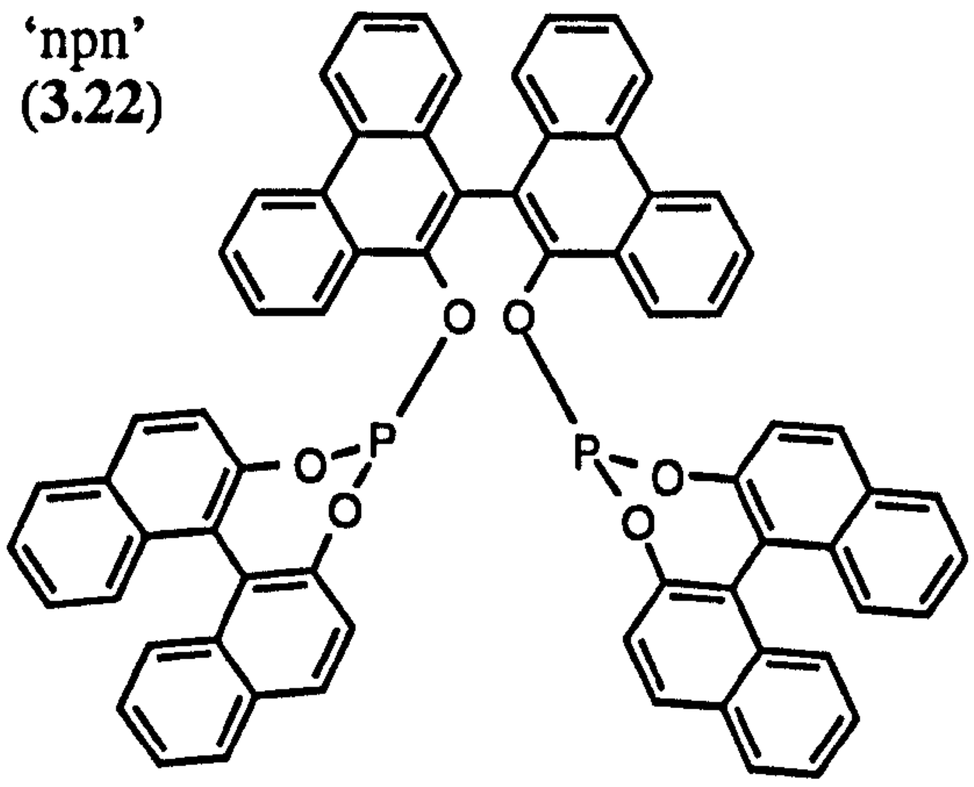

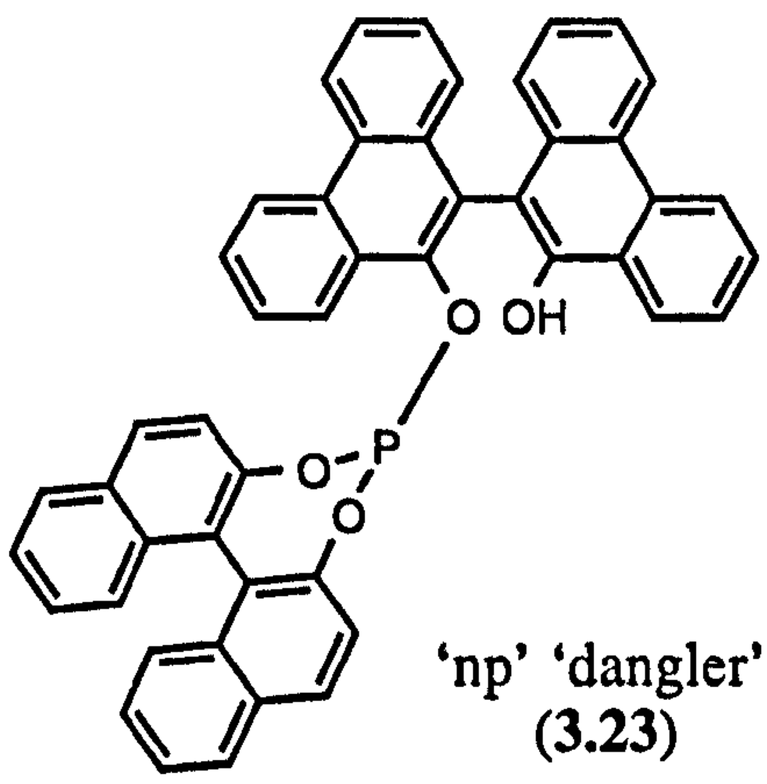

'np' 'dangler'
(3.23)

(3.24)

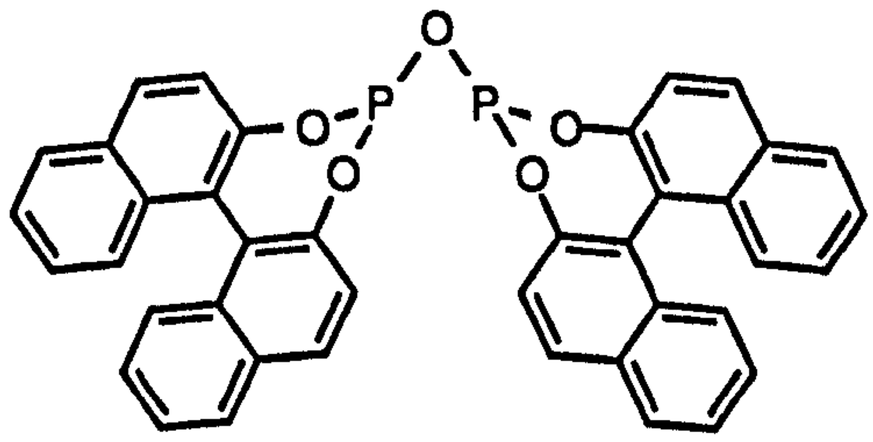

The proportion of F (see Figure 3.5) formed was found to be a function of the exact reaction conditions; it was greatly increased if the chlorophosphite was added slowly to the disodium salt instead of adding the disodium salt slowly to the chlorophosphite. It might be that F is 'nnp' (**3.25**), formed either by isomerisation of 'npn', see Equation 3.12, or by isomerisation of the 'np' 'dangler' (**3.23**) to the 'pn' 'dangler' (**3.20**) and subsequent reaction with the binaphthol-derived chlorophosphite (**3.15**). This deserves further investigation.

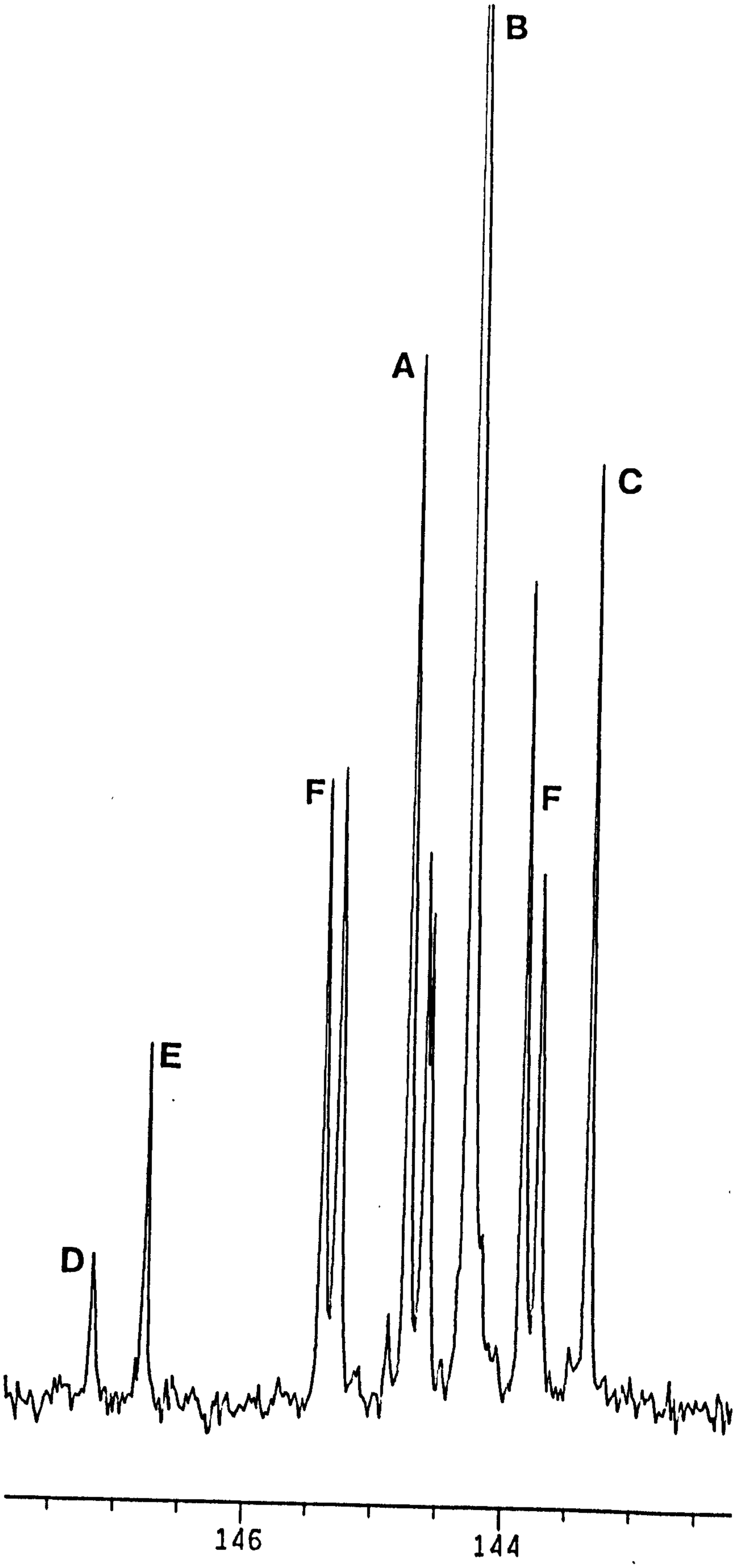

Figure 3.5: $^{31}P\{^{1}H\}$ NMR spectrum of a typical product mixture obtained during the attempted synthesis of diphosphite 'npn' (3.22)

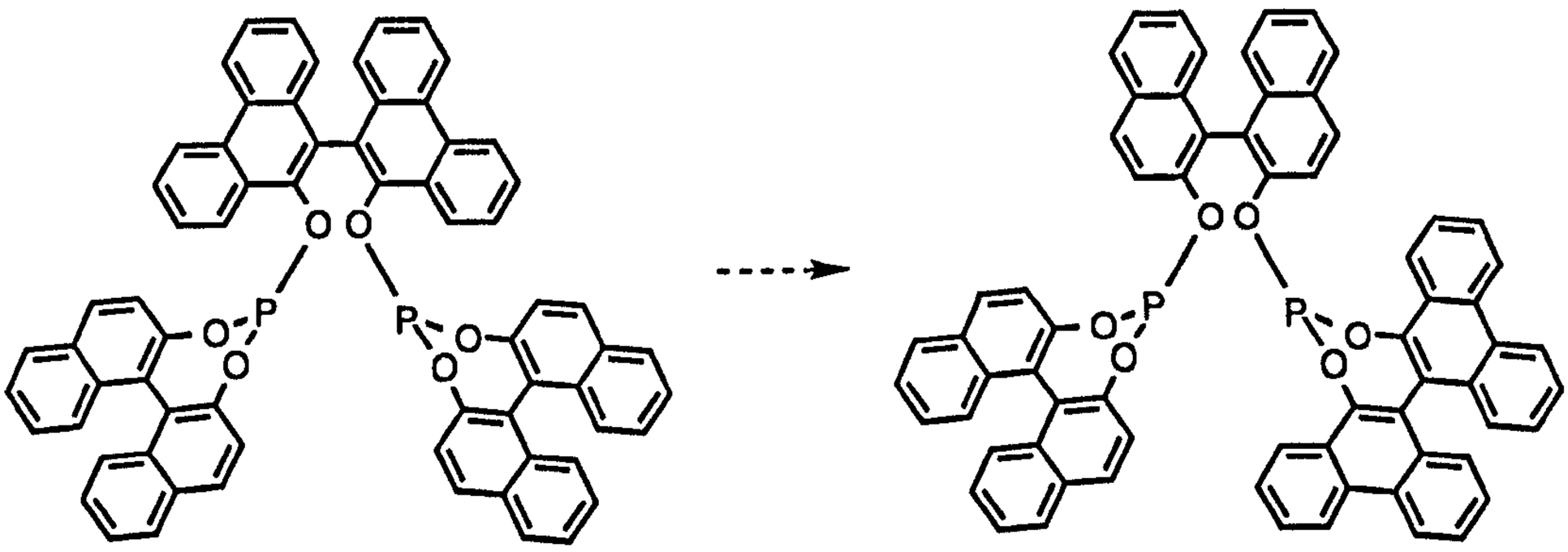

'npn' (**3.22**) 'nnp' (**3.25**)

Equation 3.12

The product mixture has been characterised by $^{31}P\{^{1}H\}$ NMR spectroscopy, see Table 3.8.

Table 3.8: $^{31}P\{^{1}H\}$ NMR data for the product mixture containing 'dangler' phosphite (**3.23**), diphosphite 'npn' (**3.22**), pyrophosphite (**3.24**) and isomerisation product 'nnp' (**3.25**)

Compound	δ_P ($CDCl_3$)[a]
Diastereomeric mixture (**3.23**)	146.7 (s)
	147.1 (s)
Diastereomeric mixture (**3.22**)	143.3 (s)
	144.2 (s)
	144.7 (s)
Diastereomeric mixture (**3.24**)	135.7
	136.6
(**3.25**)	143.8 (d, ^{7}J(PP) 18)
	145.3 (d, ^{7}J(PP) 18)

a Spectra recorded at 162 MHz at 28 °C. Chemical shifts (δ) in p.p.m. (±0.1) to high frequency of 85% H_3PO_4. Coupling constants (*J*) in Hz (±3).

3.3 Synthesis of cyclic aryl phosphites derived from dimethyl-1,1'-binaphthyl-2,2'-dihydroxy-3,3'-dicarboxylate (3.3)

Preliminary studies have been undertaken into the synthesis of cyclic aryl phosphites derived from dimethyl-1,1'-binaphthyl-2,2'-dihydroxy-3,3'-dicarboxylate (**3.3**). Hence, racemic chlorophosphite (**3.26**) was prepared by reaction of PCl_3 with racemic (**3.3**) in the presence of triethylamine at -40 °C, see Equation 3.13.

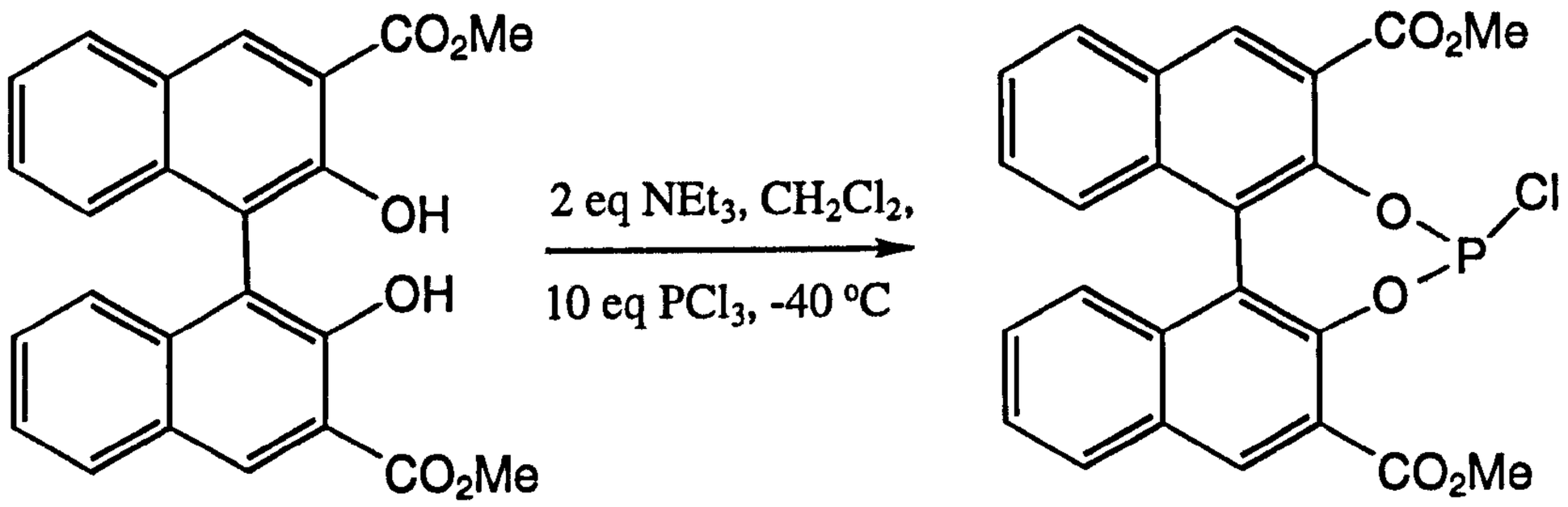

(3.3) **(3.26)**, + 2[$HNEt_3$]Cl

Equation 3.13

The reaction was carried out in dichloromethane because of the insolubility of the diester (**3.3**) in THF. Provided air and moisture were rigorously excluded from the reaction mixture chlorophosphite (**3.26**) could be isolated in pure form in a yield of 88%. This compound has been characterised by $^{31}P\{^1H\}$, $^{13}C\{^1H\}$ and ^1H NMR spectroscopy, see Table 3.9 and Experimental.

As has already been discussed in Section 3.2.1.1, chlorophosphites derived from C_2-symmetric diols are C_1-symmetric and, thus, the $^{13}C\{^1H\}$ NMR spectrum of (**3.26**) shows sixteen aromatic signals (rather than the expected ten) and there are two resonances at 52.78 and 52.92 p.p.m. corresponding to the two inequivalent methoxy carbons of the ester functionalities.

Chlorophosphite (**3.26**) is very moisture sensitive. Whilst it can be briefly handled in air as a solid, solutions show the presence of the phosphonate (**3.27**), see Table 3.9, in the presence of traces of water. This susceptibility to hydrolysis has prevented the attainment of mass spectral data and satisfactory elemental analysis for (**3.26**).

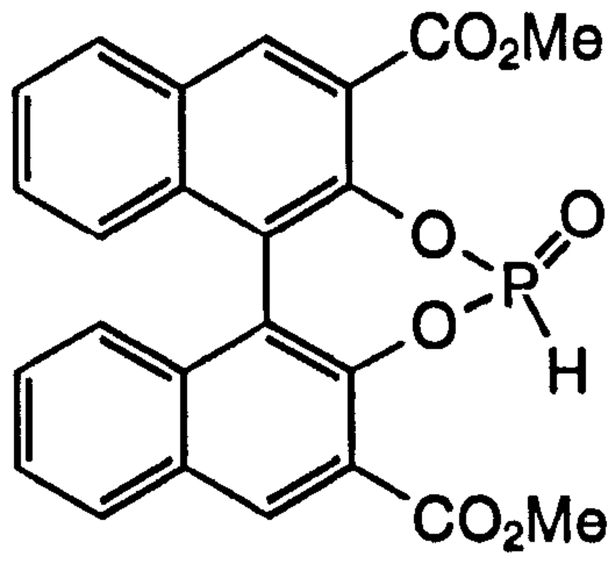

(3.27)

Chlorophosphite (**3.26**) is a valuable precursor to cyclic aryl phosphites by reaction with anhydrous ROH. This is exemplified by the synthesis of the monophosphite (**3.28**) in 91% yield by reaction of (**3.26**) with one equivalent of

phenol in the presence of triethylamine at -40 °C, see Equation 3.14. This monophosphite can be handled in air as a solid and in solution and has been characterised by $^{31}P\{^{1}H\}$ and ^{1}H NMR spectroscopy, see Table 3.9 and Experimental.

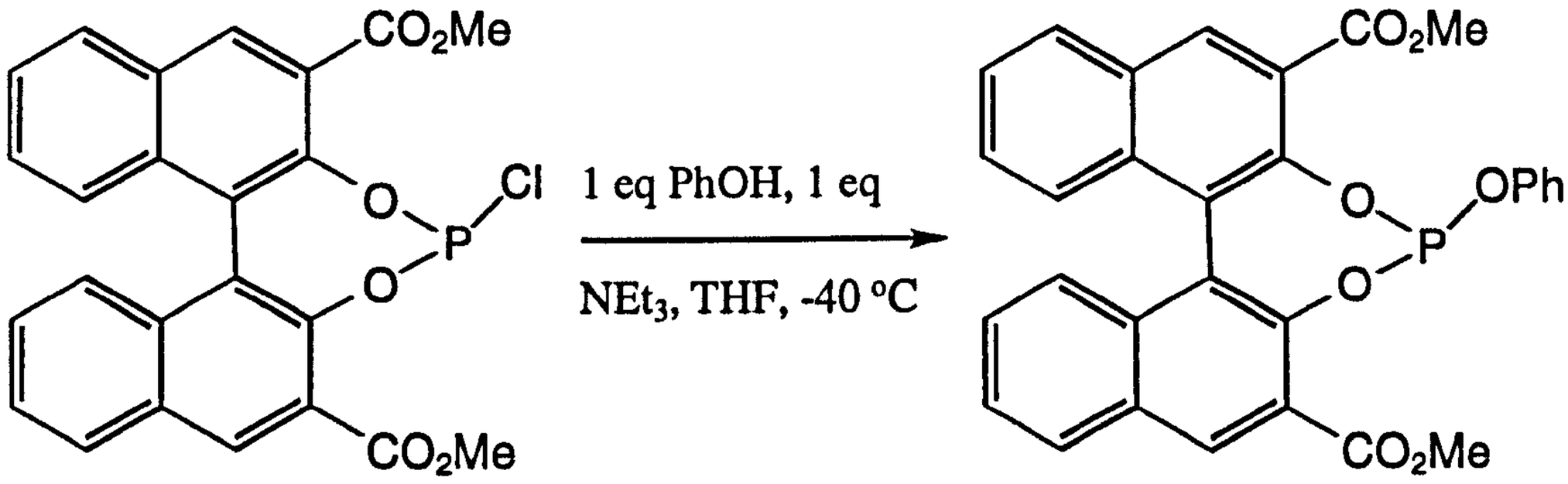

(3.26) **(3.28)**

Equation 3.14

The reaction of two equivalents of a chlorophosphite with one equivalent of water to form 'POP' pyrophosphites and the interest in this class of ligands has already been discussed, see Section 3.2.1.2. Consequently, the diastereomeric mixture of 'POP' pyrophosphite (**3.29**) was synthesised by the reaction shown in Equation 3.15 and characterised by $^{31}P\{^{1}H\}$ NMR spectroscopy, see Table 3.9 and Experimental. Pyrophosphite (**3.29**) is similar in stability to (**3.12**). For example, it can be briefly handled in air as a solid or in solution (although it is hydrolysed if left exposed to air for longer periods) but decomposes readily in the presence of alumina.

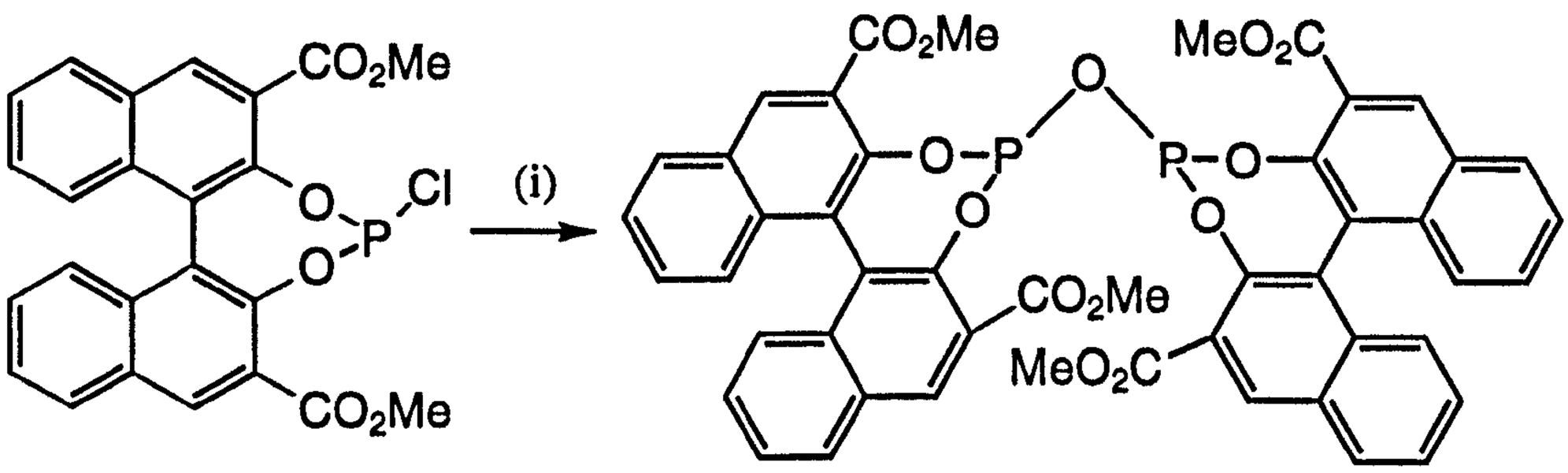

(3.26) **(3.29)**

Reaction conditions:
(i) 0.5 eq H_2O, 1 eq NEt_3, CH_2Cl_2

Equation 3.15

Table 3.9: $^{31}P\{^{1}H\}$ and ^{1}H NMR data for chlorophosphite (**3.26**), phosphonate (**3.27**), monophosphite (**3.28**) and pyrophosphite (**3.29**)

Compound	δ_P (CD_2Cl_2)[a]	δ_H (CD_2Cl_2)[b]
(3.26)	180.7	4.02 (3H, s, CH_3O) 4.04 (3H, s, CH_3O') 7.26 (1H, dd, ^{3}J(HH) 8.6, ^{4}J(HH) 0.9) 7.30 (1H, dd, ^{3}J(HH) 8.6, ^{4}J(HH) 0.6) 7.38-7.45 (2H, m) 7.55-7.61 (2H, m) 8.10 (2H, d, ^{3}J(HH) 8.2) 8.70 (1H, s, H4) 8.73 (1H, s, H4')
(3.27)[c]	14.0	------
(3.28)[c]	145.4	------
Diastereomer 1 of **(3.29)**[c,d]	138.8	------
Diastereomer 2 of **(3.29)**[c,d]	136.6	------

a Spectra recorded at 162 MHz at 28 °C. Chemical shifts (δ) in p.p.m. (±0.1) to high frequency of 85% H_3PO_4.

b Spectrum recorded at 400 MHz at 28 °C. Chemical shifts (δ) in p.p.m. (±0.01) to high frequency of tetramethylsilane. Coupling constants (*J*) in Hz (±0.1).

c Spectra recorded in $CDCl_3$.

d The assignment of these two signals to the specific diastereomers {(*R*,*R*) / (*S*,*S*)- and (*R*,*S*)-} has not been achieved.

3.4 Discussion of ^{31}P NMR chemical shifts

The values of the chemical shifts (δ_P) for the cyclic aryl phosphites and chlorophosphites that have been synthesised are collected in Table 3.10. The chemical shifts of the various diastereomers of diphosphites (**3.4**) and (**3.5**) and that of monophosphite (**3.28**) all lie within the narrow range 141.8-147.7 p.p.m. This range lies downfield from the normal region for triarylphosphites (127-133 p.p.m.).[160] A similar phenomenon was observed for 'binaphthite' (**3.1**) (δ_P 144.7 for the (*R*,*R*,*R*)-diastereomer) and it was proposed[93] that the deshielding of the phosphorus nucleus is due to a twist in the seven-membered P(OCCCCO) ring causing an increase in the O-P-O bond angle. It is well known for phosphines that the larger the C-P-C angle, the greater the *p*-character in the lone pair and hence the greater the deshielding of the phosphorus nucleus.[133,135,144]

Table 3.10: Chemical shift (δ_P) values for cyclic aryl phosphites, pyrophosphites and chlorophosphites

Compound	δ_P ($CDCl_3$)[a]
(3.10)	180.9
(3.26)[b]	180.7
(*S,S*)-(**3.12**)	141.9
(*R,S*)-(**3.12**)	139.4
(*R,S*)-(**3.29**)[c]	136.6
(*R,R*) / (*S,S*)-(**3.29**)[c]	138.8
(*S,S*)-(**3.9**)	146.2
(*S,R*) / (*R,S*)-(**3.9**)	146.4
(3.28)	145.4
(*R,R,R*)-(**3.4**)	143.3
(*R,S,R*) / (*S,R,S*)-(**3.4**)[b]	145.5
(*R,R,S*) / (*S,S,R*)-(**3.4**)	141.8 (d, ^7J(PP 40) 145.3 (d, ^7J(PP) 40)
(*R,R,R*)-(**3.5**)	143.1
(*R,S,R*)-(**3.5**)	147.7
(*R,R,S*) / (*S,S,R*)-(**3.5**)	144.3 (d, ^7J(PP) 28) 146.1 (d, ^7J(PP) 27)

a Spectra recorded at 162 MHz at 28 °C. Chemical shifts (δ) in p.p.m. (±0.1) to high frequency of 85% H_3PO_4. Coupling constants (J) in Hz (±3).
b Spectra recorded in CD_2Cl_2.
c The relative assignment of these two diastereomers to the two resonances is arbitrary.

The chemical shifts of the chlorophosphites (**3.10**) and (**3.26**) are also downfield of the normal range by *ca.* 20 p.p.m. (*cf.* δ_P 160.5 p.p.m. for $PCl(OPh)_2$).[161]

The chemical shifts of the various diastereomers of pyrophosphites (**3.12**) and (**3.29**) all lie within the narrow range 136.6-141.9 p.p.m., upfield from the phosphites, whilst the two diastereomers of the 'dangler' (**3.9**) have chemical shifts that are characteristically[93] slightly downfield (by 0.7-4.6 p.p.m.) of those of the various diastereomers of diphosphite (**3.4**).

3.5 Coordination chemistry of cyclic aryl diphosphites

This Section describes the preliminary complexation studies that have been carried out on the diphosphites (**3.4**) and (**3.5**).

3.5.1 Complexes of tris (9,9'-biphenanthryl-10,10'-diyl) diphosphite 'biphenanthrite' (3.4)

3.5.1.1 Dichloroplatinum(II) complexes

The preparation of platinum(II) complexes of cyclic aryl phosphites serves as a useful initial guide to the reactivity of these ligands. Reaction of one equivalent of the diastereomeric mixture of 'biphenanthrite' (**3.4**) with $[PtCl_2(cod)]$ results in the formation of the three possible diastereomers of the dichloroplatinum(II) complex (**3.30**) and these have been characterised by $^{31}P\{^1H\}$ and $^{195}Pt\{^1H\}$ NMR spectroscopy, see Table 3.11 and Experimental.

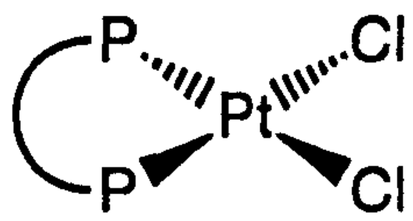

(3.30)

Table 3.11: $^{31}P\{^1H\}$ NMR data for the diastereomeric mixture of the dichloroplatinum(II) complex (**3.30**)

Diastereomer	δ_P[a]	$\Delta\delta$	^1J(PPt)
(*R*,*R*,*R*) / (*S*,*S*,*S*)[b]	88.6 (s)[c]	-54.7	5700
(*R*,*R*,*S*) / (*S*,*S*,*R*)[d]	89.4 (d, ^2J(PP) 24)	------	5716
	90.2 (d, ^2J(PP) 24)		5667
(*R*,*S*,*R*) / (*S*,*R*,*S*)[d]	87.0 (br s)	-58.5	5783

a Spectra recorded at 162 MHz at 28 °C. Chemical shifts (δ) in p.p.m. (±0.1) to high frequency of 85% H_3PO_4. Coupling constants (*J*) measured in Hz (±3).

b δ_{Pt}: 144.6 (t); spectrum recorded in $CDCl_3$ at 85.6 MHz at 28 °C. Chemical shift (δ) in p.p.m. (±0.1) to high frequency of Ξ (^{195}Pt) 21.4 MHz.

c Spectrum recorded in $CDCl_3$.

d Spectra recorded in CH_2Cl_2 / $CDCl_3$ (5:2).

The signals for the three diastereomers are: a sharp singlet, a broad singlet and a pair of doublets. The latter can be unambiguously assigned to the (*R*,*R*,*S*) / (*S*,*S*,*R*)-diastereomer on account of the inequivalence of the two phosphorus atoms in this species. The sharp singlet has been identified as the (*R*,*R*,*R*) / (*S*,*S*,*S*)-diastereomer by synthesis of the optically pure (*R*,*R*,*R*)-complex by reaction of optically pure (*R*,*R*,*R*)-'biphenanthrite' with $[PtCl_2(cod)]$. This enables us to assign the broad singlet as the (*R*,*S*,*R*) / (*S*,*R*,*S*)-diastereomer. The broadness observed for the (*R*,*S*,*R*) / (*S*,*R*,*S*)-

diastereomer is indicative of a fluxional process. Unfortunately, the low solubility of this complex has foiled our efforts at low temperature NMR studies but such studies have been performed on the (*R,R,R*)-diastereomer of the dichloroplatinum(II) complex derived from (*R,R,R*)-'binaphthite'. At room temperature a broad singlet is observed, which becomes a pair of doublets at low temperature.[93,162] It has been proposed that this fluxionality is due to interconversions of different conformations of the nine-membered Pt(POCCCCOP) chelate ring.[93,162]

The $^{31}P\{^{1}H\}$ chemical shifts lie in the range 87-91 p.p.m. This is a similar range to that observed for the three diastereomers of the analogous dichloroplatinum(II) complex of 'binaphthite' (66.6-95.3 p.p.m.)[93] and, in the same way as it affected the chemical shifts of the ligands themselves, the twist in the seven-membered ring causes deshielding. Chemical shifts in *cis*-dichloroplatinum(II) complexes of phosphite ligands which do not contain this seven-membered ring are much lower (*ca.* 30 p.p.m. upfield; *cf.* 59.3 p.p.m. for $[PtCl_2\{P(OPh)_3\}_2]$).[134,163] However, the coordination chemical shifts ($\Delta\delta$) for the diastereomers of complex (**3.30**) are very similar to those of dichloroplatinum(II) complexes for normal aryl phosphite ligands (*cf.* $\Delta\delta$ -68.8 p.p.m. for $[PtCl_2\{P(OPh)_3\}_2]$) and the ^{1}J(PPt) values are typical of *cis*-dichloroplatinum(II) phosphite complexes (*cf.* ^{1}J(PPt) 5793 Hz for *cis*-$[PtCl_2\{P(OPh)_3\}_2]$),[134] indicating that the nine-membered Pt(POCCCCOP) chelate ring has no effect on either the phosphorus chemical shifts or the ^{1}J(PPt) values.

The $^{195}Pt\{^{1}H\}$ NMR spectrum of (*R,R,R*)-(**3.30**) has been recorded. The chemical shift is 144.6 p.p.m., which is *ca.* 80 p.p.m. upfield of those of complexes of phosphites which do not contain the seven-membered ring. (*cf.* 224 p.p.m. for *cis*-$[PtCl_2\{P(OPh)_3\}_2]$).[163,164] However, the analogous dichloroplatinum(II) complex derived from (*R,R,R*)-'binaphthite' possesses a chemical shift of 310.2 p.p.m., downfield of the chemical shift for *cis*-$[PtCl_2\{P(OPh)_3\}_2]$, and the reason for the discrepancy in these values is presently unclear.

Single crystals of the (*S,R,S*) / (*R,S,R*)-diastereomer of (**3.30**) have been grown from a solution of the diastereomeric mixture in CH_2Cl_2 / $CDCl_3$ (5:2) and the structure determined by X-ray crystallography carried out by Dr D. Ellis in this department (see Figure 3.6). The structure was solved in the *P*-1 (No. 2) space group with a single formula unit, two molecules of dichloromethane and four molecules of chloroform in the unit cell. The complex was found to contain the (*S,R,S*)-diastereomer of 'biphenanthrite' (**3.4**). The coordination geometry at platinum is square planar with the diphosphite ligand in a *cis* arrangement. Selected bond lengths and angles are shown in Table 3.12.

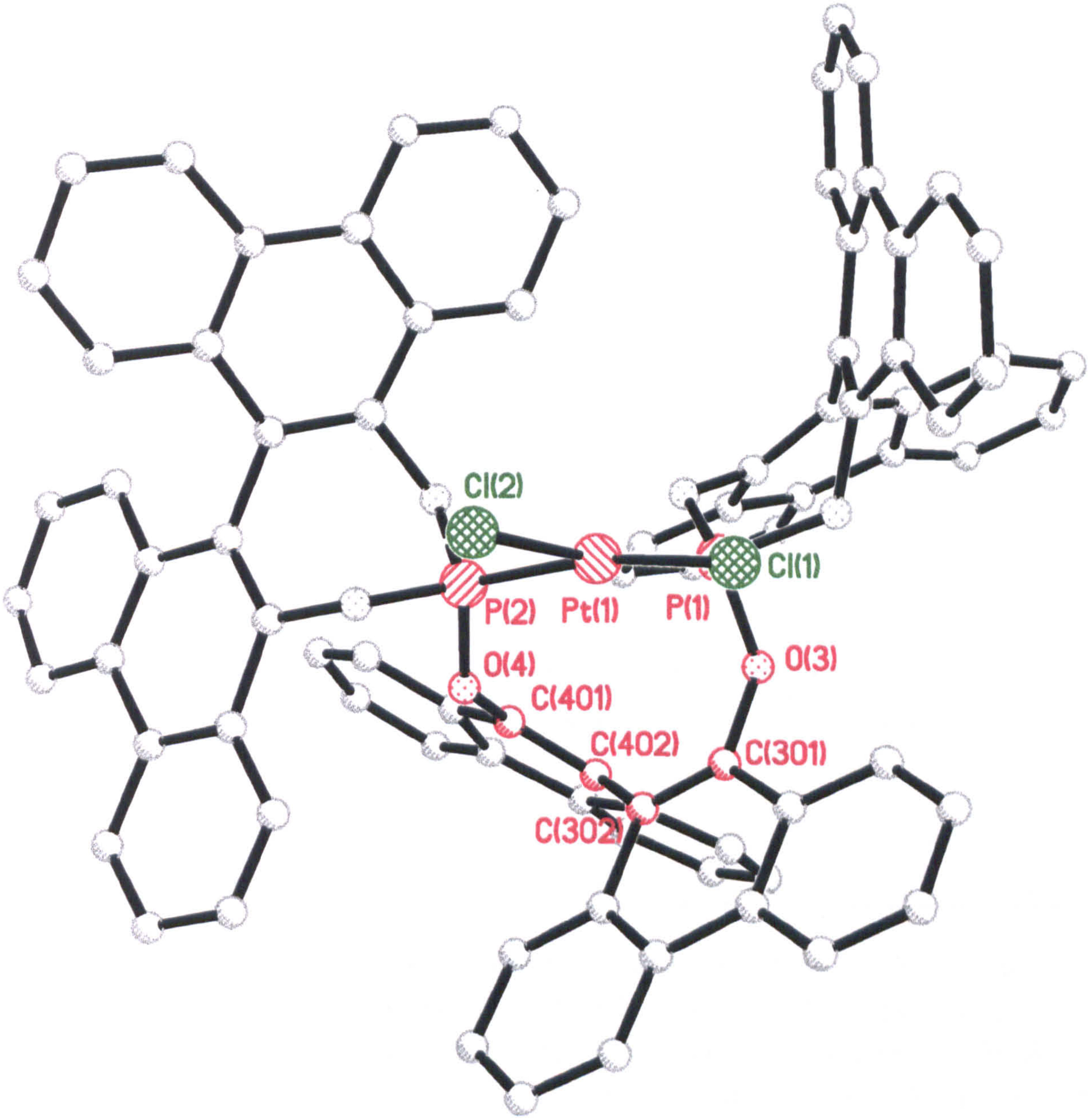

Figure 3.6: Molecular structure of dichloroplatinum(II) complex (*S,R,S*)-(**3.30**). All hydrogen atoms are omitted for clarity. The nine-membered chelate ring is shown in orange

Table 3.12: Selected bond lengths (Å) and bond angles (°) in dichloroplatinum(II) complex (*S,R,S*)-(**3.30**)

Atoms	Bond length (Å)	Atoms	Bond angle (°)
Pt-P(1)	2.224 (4)	P(1)-Pt-P(2)	97.61 (16)
Pt-P(2)	2.212 (4)	Cl(1)-Pt-P(1)	88.44 (16)
Pt-Cl(1)	2.313 (4)	Cl(2)-Pt-P(2)	89.57 (15)
Pt-Cl(2)	2.339 (4)	Cl(1)-Pt-Cl(2)	85.66 (15)

The platinum coordination plane is distorted by 12.3° with a twist between the PtP_2 and $PtCl_2$ planes, which causes the observed deviation of the two chlorine atoms in opposite directions from the PtP_2 plane; Cl(1) = 0.385 Å and Cl(2) = -0.284 Å, see Figure 3.6. It is also apparent from Figure 3.6 that the phenanthryl unit containing C(301) is shielding one of the vacant axial sites at platinum.

Single crystals of the optically pure complex (*R,R,R*)-(**3.30**) have been grown from $CDCl_3$ and the structure determined by X-ray crystallography carried out by Miss A. Gillon in this department (see Figure 3.7). The structure was solved in the $P2_12_12_1$ space group with a single formula unit and six molecules of chloroform in the unit cell. The coordination geometry at platinum is square planar with the diphosphite ligand in a *cis* arrangement. Selected bond lengths and angles are shown in Table 3.13.

Table 3.13: Selected bond lengths (Å) and bond angles (°) in dichloroplatinum(II) complex (*R,R,R*)-(**3.30**)

Atoms	Bond length (Å)	Atoms	Bond angle (°)
Pt-P(1)	2.234 (2)	P(1)-Pt-P(2)	101.00 (7)
Pt-P(2)	2.206 (2)	Cl(1)-Pt-P(1)	82.70 (8)
Pt-Cl(1)	2.330 (2)	Cl(2)-Pt-P(2)	89.29 (8)
Pt-Cl(2)	2.335 (2)	Cl(1)-Pt-Cl(2)	87.47 (9)

Tables 3.12 and 3.13 show that, in both diastereomers, the Pt-Cl bond lengths are similar to those of other *cis* Pt(II)-Cl bonds[129] and the Pt-P bond lengths are similar to the mean value taken from a range of Pt-$P(OPh)_3$ complexes {2.226 Å}.[143] However, the chelate structures are notably different, see Figures 3.6 and 3.7. The nine-membered chelate is completely below the coordination plane in Figure 3.6 but it is both above and below the plane in Figure 3.7. The difference is even more pronounced when the two structures are overlayed with the Pt-Cl(2) bonds overlapping, Figure 3.8. Such differences in ring conformation may explain the different catalytic properties of the rhodium(I) complexes of (*R,S,R*)- and (*R,R,R*)-'pnp' (**3.5**) (see Section 3.6).

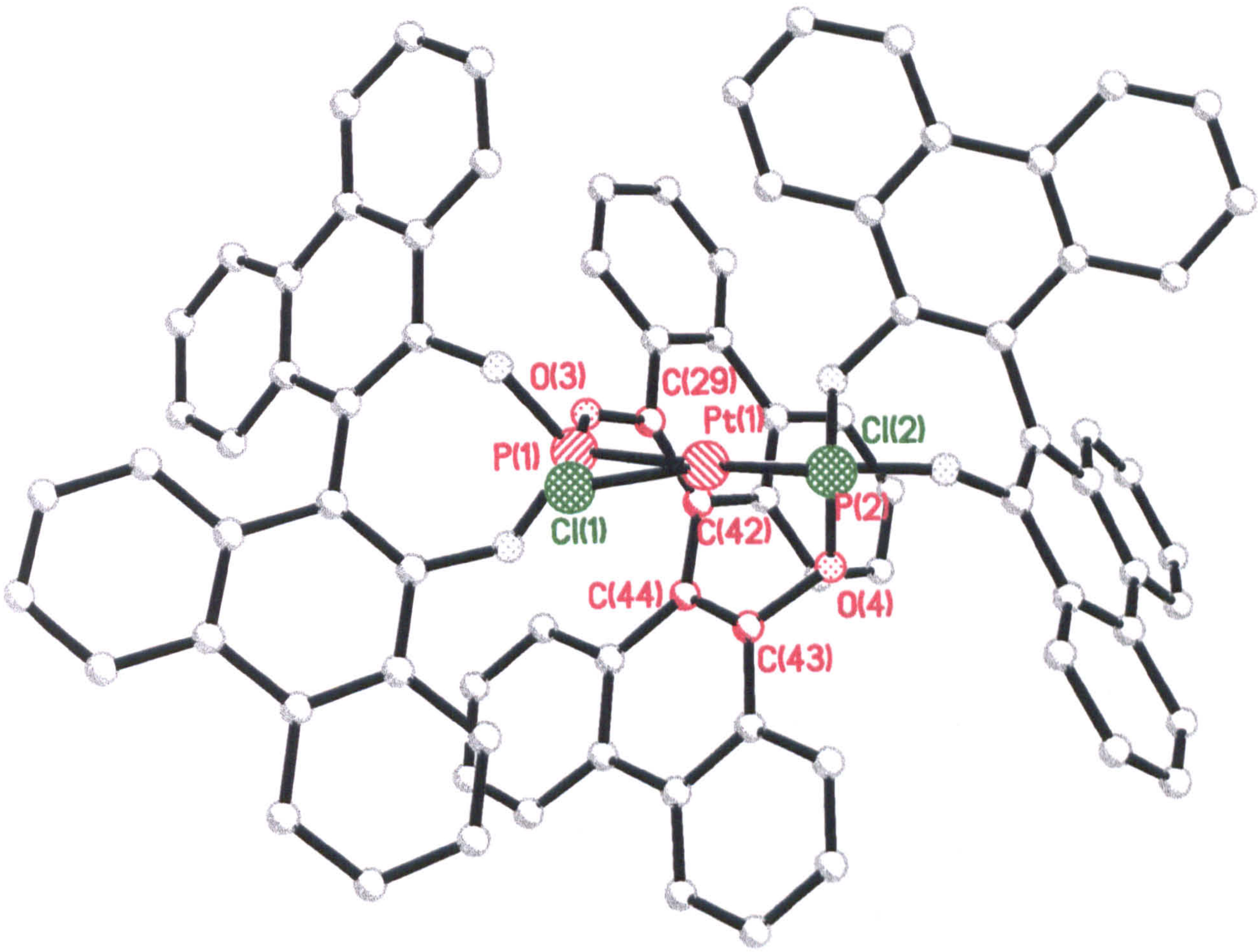

Figure 3.7: Molecular structure of dichloroplatinum(II) complex (*R,R,R*)-(**3.30**). All hydrogen atoms are omitted for clarity. The nine-membered chelate ring is shown in orange

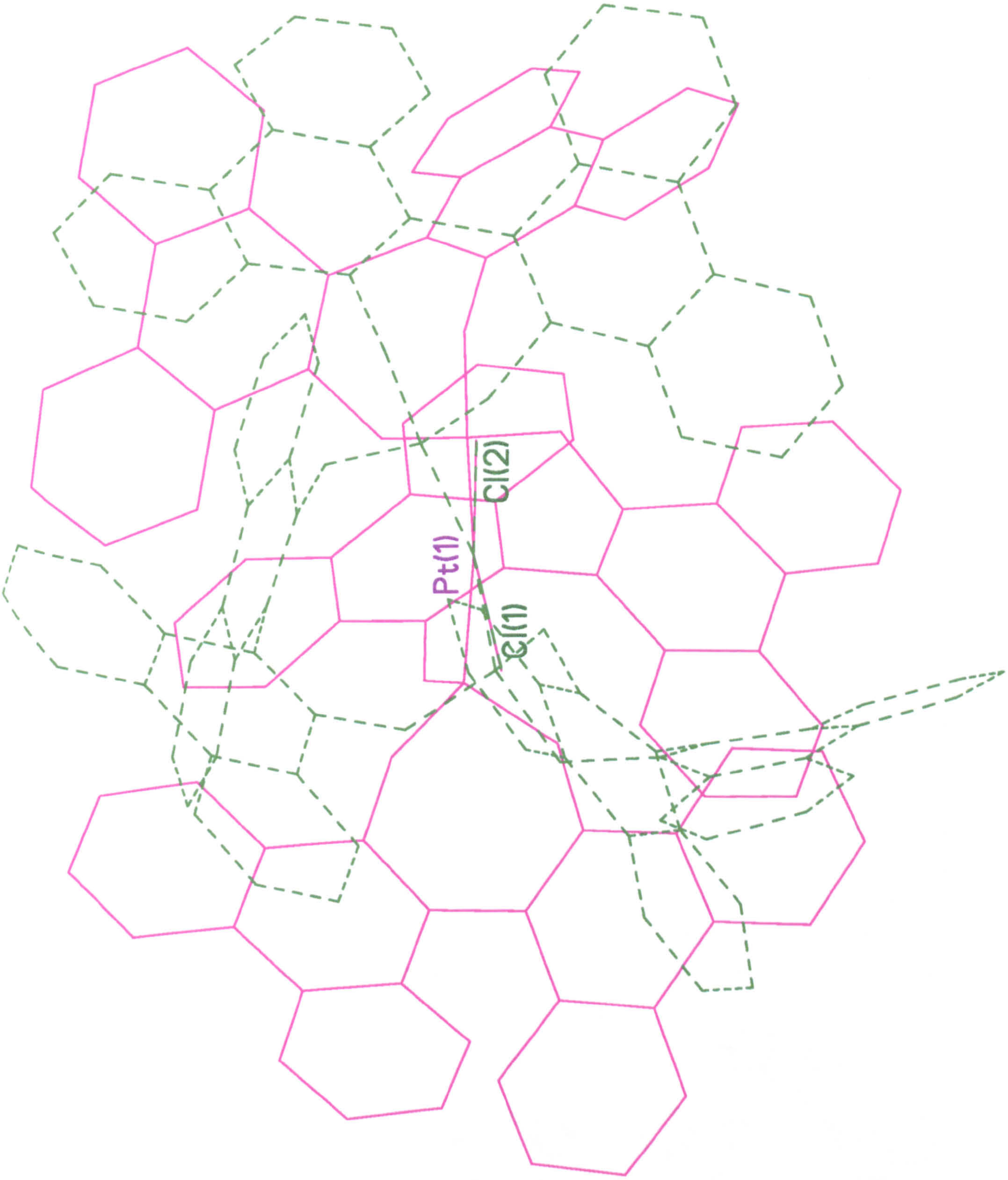

Figure 3.8: Overlay of the (S,R,S)- and (R,R,R)-diastereomers of the dichloroplatinum(II) complex (**3.30**). Hydrogen atoms are omitted for clarity and the two structures are overlayed with the Pt-Cl(2) bonds overlapping

3.5.1.2 Platinum(0) complex of the (R,S,R) / (S,R,S)-diastereomer

Reaction of one equivalent of the (*R*,*S*,*R*) / (*S*,*R*,*S*)-diastereomer of 'biphenanthrite' (**3.4**) with [Pt(nb)$_3$] resulted in the formation of the monochelate complex (**3.31**), as shown by the $^{195}Pt\{^1H\}$ NMR spectrum which shows a doublet of doublets with a δ_{Pt} value of -666.0 p.p.m. This is in the range typical for platinum(0)-alkene complexes of aryl phosphites (-475 to -755 p.p.m.).[165,166] The two ^1J(PPt) values of 5981 and 6232 Hz are also in the range typical for platinum(0)-alkene complexes of aryl phosphites (5135-6270 Hz).[165,166]

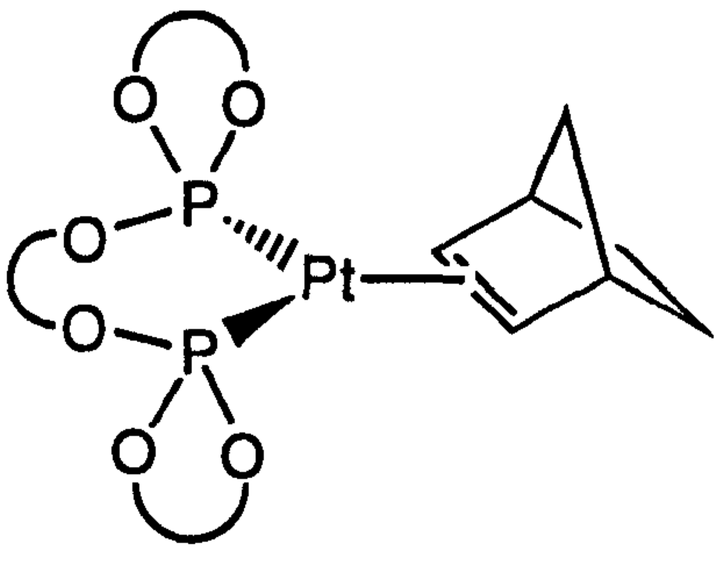

(3.31)

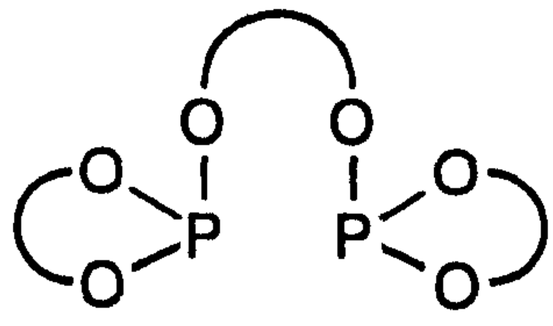

(*R*,*S*,*R*) / (*S*,*R*,*S*)-(**3.4**)

The $^{31}P\{^1H\}$ NMR spectrum of this species comprises a pair of doublets, each with platinum satellites. The inequivalence of the phosphorus atoms may be due to hindered rotation about the Pt-nb bond, which would confer C_1-symmetry upon the complex. The δ_P values of 180.1 and 172.6 p.p.m. are about 30 p.p.m. downfield of those of platinum(0)-alkene complexes of normal aryl phosphites (133.4-149.1 p.p.m.)[165,166] and, as in the dichloroplatinum(II) complexes, this is attributed to deshielding of the phosphorus nucleii by twists in the P(OCCCCO) rings.

The formation of this mono(chelate) is a reflection of the bulk of the organic backbone since the less bulky ligand 'biphenite' (**3.32**) has been shown to form, under similar conditions, the bis(chelate) (**3.33**).[93] The mono(chelate) (**3.34**) was synthesised by an alternative route[93] and the $^{31}P\{^1H\}$ and $^{195}Pt\{^1H\}$ NMR data for this compound are in close agreement with those obtained for (**3.31**), see Table 3.14.

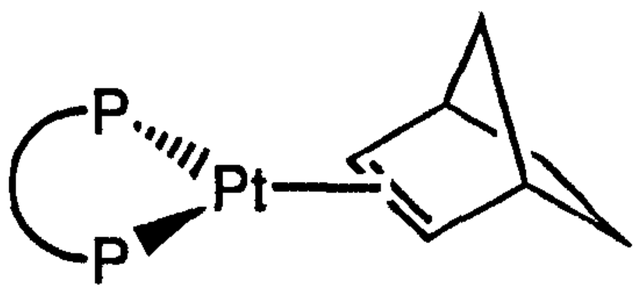

(3.34)

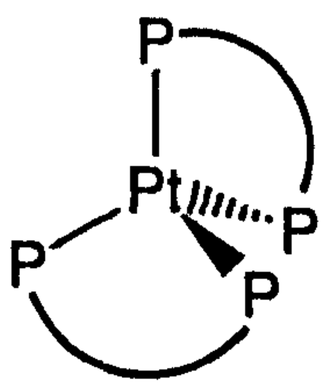

(3.33)

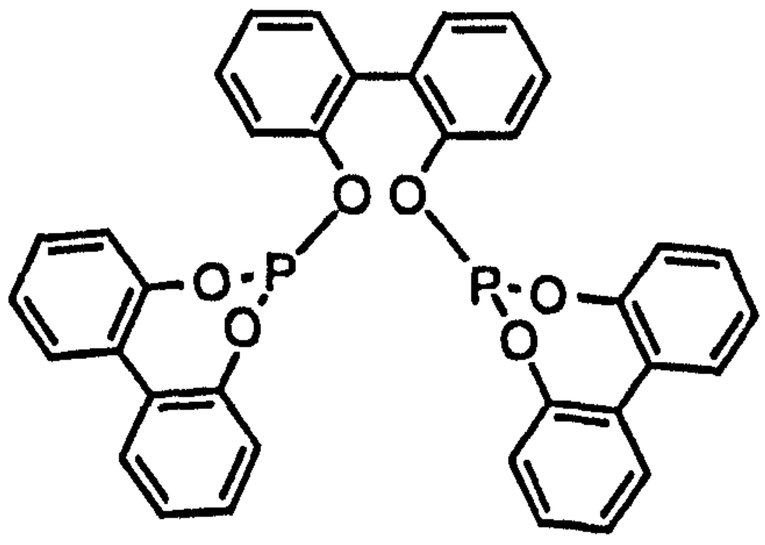

(3.32), 

Table 3.14: $^{31}P\{^{1}H\}$ and $^{195}Pt\{^{1}H\}$ NMR data for the platinum(0) complexes **(3.31)**, **(3.33)** and **(3.34)**

Compound	δ_P	δ_{Pt}[a]	$^{1}J(PPt)$[b]
(*R,S,R*) / (*S,R,S*)-**(3.31)**[c]	172.6 (d, ^{2}J(PP) 156)	-666.0 (dd)	6232
	180.1 (d, ^{2}J(PP) 156)[d]		5981
(3.33)[e]	137.1 (major)	-1149.9 (quin)	5703
	140.4 (minor)[f]	-1135.5 (quin)[g]	5693
(3.34)[e]	177.4[f]	-726.5 (t)[h]	6060

a Spectra recorded at 85.6 MHz at 28 °C. Chemical shifts (δ) in p.p.m. (±0.1) to high frequency of Ξ (^{195}Pt) 21.4 MHz.
b Coupling constants (*J*) measured in Hz (±3).
c Spectra recorded in C_6D_6 / CH_2Cl_2 (1:2).
d Spectrum recorded at 162 MHz at 28 °C. Chemical shifts (δ) in p.p.m. (±0.1) to high frequency of 85% H_3PO_4. Coupling constants (*J*) measured in Hz (±3).
e Ref. 93
f Spectra recorded at 36.2 MHz in $CDCl_3$ at 28 °C. Chemical shifts (δ) in p.p.m. (±0.1) to high frequency of 85% H_3PO_4.
g Spectrum recorded in $CDCl_3$.
h Spectrum recorded at 19.2 MHz in CD_2Cl_2 at 28 °C. Chemical shift (δ) in p.p.m. (±0.5) to high frequency of Ξ (^{195}Pt) 21.4 MHz.

3.5.2 Complexes of bis(9,9' - biphenanthryl - 10,10' - diyl)-μ-(1,1'-binaphthyl-2,2'-diyl)diphosphite 'pnp' (3.5)

3.5.2.1 Dichloroplatinum(II) complexes

Reaction of one equivalent of the diastereomeric mixture of the mixed diphosphite 'pnp' (**3.5**) with [$PtCl_2$(cod)] resulted in the formation of the three possible diastereomers of the dichloroplatinum(II) complex (**3.35**), which have been characterised by $^{31}P\{^{1}H\}$ and $^{195}Pt\{^{1}H\}$ NMR spectroscopy as well as by mass spectrometry, see Table 3.15, Figure 3.9 and Experimental.

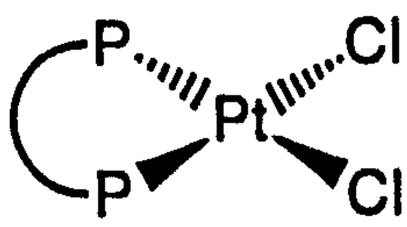

(3.35)

In a similar fashion to the $^{31}P\{^{1}H\}$ NMR spectrum obtained for the diastereomeric mixture of **(3.30)**, three species are observed; a sharp singlet, a broad singlet and a pair of doublets. The latter can be unambiguously assigned to the (*R,R,S*) / (*S,S,R*)-diastereomer. The broad singlet has been identified as the (*R,R,R*) / (*S,S,S*)-diastereomer by synthesis of the optically pure (*R,R,R*)-complex by reaction of optically pure (*R,R,R*)-'pnp' (**3.5**) with [$PtCl_2$(cod)]. This enables us to assign the sharp singlet to the (*R,S,R*) / (*S,R,S*)-diastereomer. The broadness observed for the (*R,R,R*) / (*S,S,S*)-diastereomer is attributed to fluxionality caused by interconversions

Table 3.15: $^{31}P\{^{1}H\}$ and $^{195}Pt\{^{1}H\}$ NMR data for the diastereomeric mixture of the dichloroplatinum(II) complex **(3.35)**

Diastereomer	δ_P ($CDCl_3$)[a]	^2J(PP)[b]	δ_{Pt} ($CDCl_3$)[c]	^1J(PPt)[b]
(*R,R,R*) / (*S,S,S*)	80.1 (br s)	------	323.2 (t)	5916
(*R,R,S*) / (*S,S,R*)	71.7 (d)	15	318.6 (dd)	5905
	90.8 (d)	15		6049
(*R,S,R*) / (*S,R,S*)	77.6 (s)	------	291.1 (t)	5857

a Spectra recorded at 162 MHz at 28 °C. Chemical shifts (δ) in p.p.m. (±0.1) to high frequency of 85% H_3PO_4.

b Coupling constants (*J*) measured in Hz (±3).

c Spectra recorded at 85.6 MHz at 28 °C. Chemical shifts (δ) in p.p.m. (±0.1) to high frequency of Ξ (^{195}Pt) 21.4 MHz.

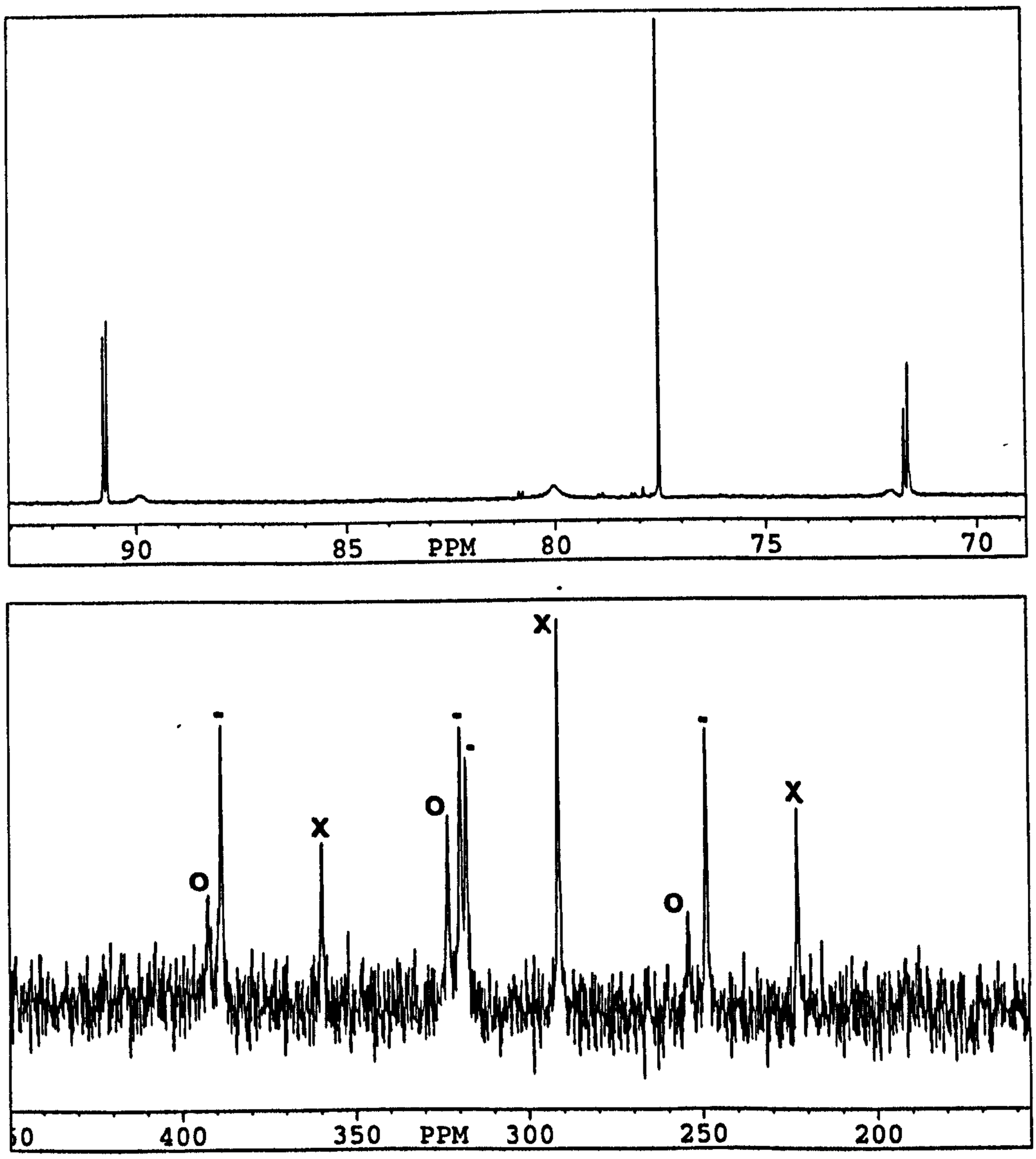

Figure 3.9: $^{31}P\{^{1}H\}$ and $^{195}Pt\{^{1}H\}$ NMR spectra for the diastereomeric mixture of dichloroplatinum(II) complex **(3.35)**

of different conformations of the nine-membered Pt(POCCCCOP) chelate ring. The low solubility of this complex has thwarted our efforts to probe this further *via* low temperature NMR studies.

The δ_P values and δ_{Pt} values, see Table 3.15, are similar to those of the analogous dichloroplatinum(II) complex of (*R,R,R*)-'binaphthite' (δ_P 79.8 p.p.m. and δ_{Pt} 310.2 p.p.m.)[93] and, in the same way as it affected the chemical shifts of the ligands themselves, the twist in the seven-membered ring causes deshielding. Chemical shifts in *cis*-dichloroplatinum(II) complexes of phosphite ligands which do not contain this seven-membered ring are much lower (δ_P *ca.* 30 p.p.m. upfield; *cf.* 59.3 p.p.m. for *cis*-$[PtCl_2\{P(OPh)_3\}_2]$; δ_{Pt} *ca.* 70-100 p.p.m. upfield; *cf.* 224 p.p.m. for *cis*-$[PtCl_2\{P(OPh)_3\}_2]$).[134,163,164]

3.5.2.2 Dichloropalladium(II) complexes

Reaction of one equivalent of the diastereomeric mixture of diphosphite 'pnp' (**3.5**) with $[PdCl_2(NCPh)_2]$ resulted in the formation of the three possible diastereomers of the dichloropalladium(II) complex (**3.36**), which have been characterised by $^{31}P\{^1H\}$ NMR spectroscopy and mass spectrometry, see Table 3.16, Figure 3.10 and Experimental.

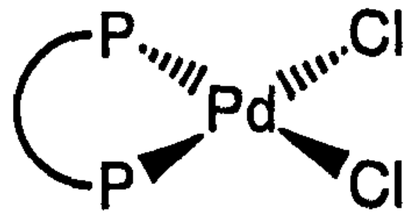

(3.36)

Table 3.16: $^{31}P\{^1H\}$ NMR data for the diastereomeric mixture of dichloropalladium(II) complex (**3.36**)[a]

Diastereomer	δ_P ($CDCl_3$)	^2J(PP)
(*R,R,R*) / (*S,S,S*)	105.6 (br s)	------
(*R,R,S*) / (*S,S,R*)	97.0 (d)	70
	115.9 (d)	73
(*R,S,R*) / (*S,R,S*)	103.4 (s)	------

a Spectra recorded at 162 MHz at 28 °C. Chemical shifts (δ) in p.p.m. (±0.1) to high frequency of 85% H_3PO_4. Coupling constants (*J*) measured in Hz (±3).

The two doublets correspond to the (*R,R,S*) / (*S,S,R*)-diastereomer and the broad singlet has been assigned to the (*R,R,R*) / (*S,S,S*)-diastereomer by synthesis of the optically pure (*R,R,R*)-complex using optically pure (*R,R,R*)-'pnp' (**3.5**). Hence it is apparent that in complexes (**3.35**) and (**3.36**) of the 'pnp' ligand the signal for the (*R,R,R*) / (*S,S,S*)-diastereomer is broad at room temperature whilst in complex (**3.30**) of 'biphenanthrite' it is the (*R,S,R*) / (*S,R,S*)-diastereomer which gives rise to a broad signal at room temperature.

The δ_P values are similar to that of the analogous dichloropalladium(II) complex of (*S,S,S*)-'binaphthite' (δ_P 105.0 p.p.m.).[93] Typical chemical shifts in *cis*-dichloropalladium(II) complexes of phosphite ligands which do not contain a seven-membered ring are *ca.* 20 p.p.m. upfield; *cf.* δ_P 83.4 p.p.m. for *cis*-$[PdCl_2\{P(OPh)_3\}_2]$.[134]

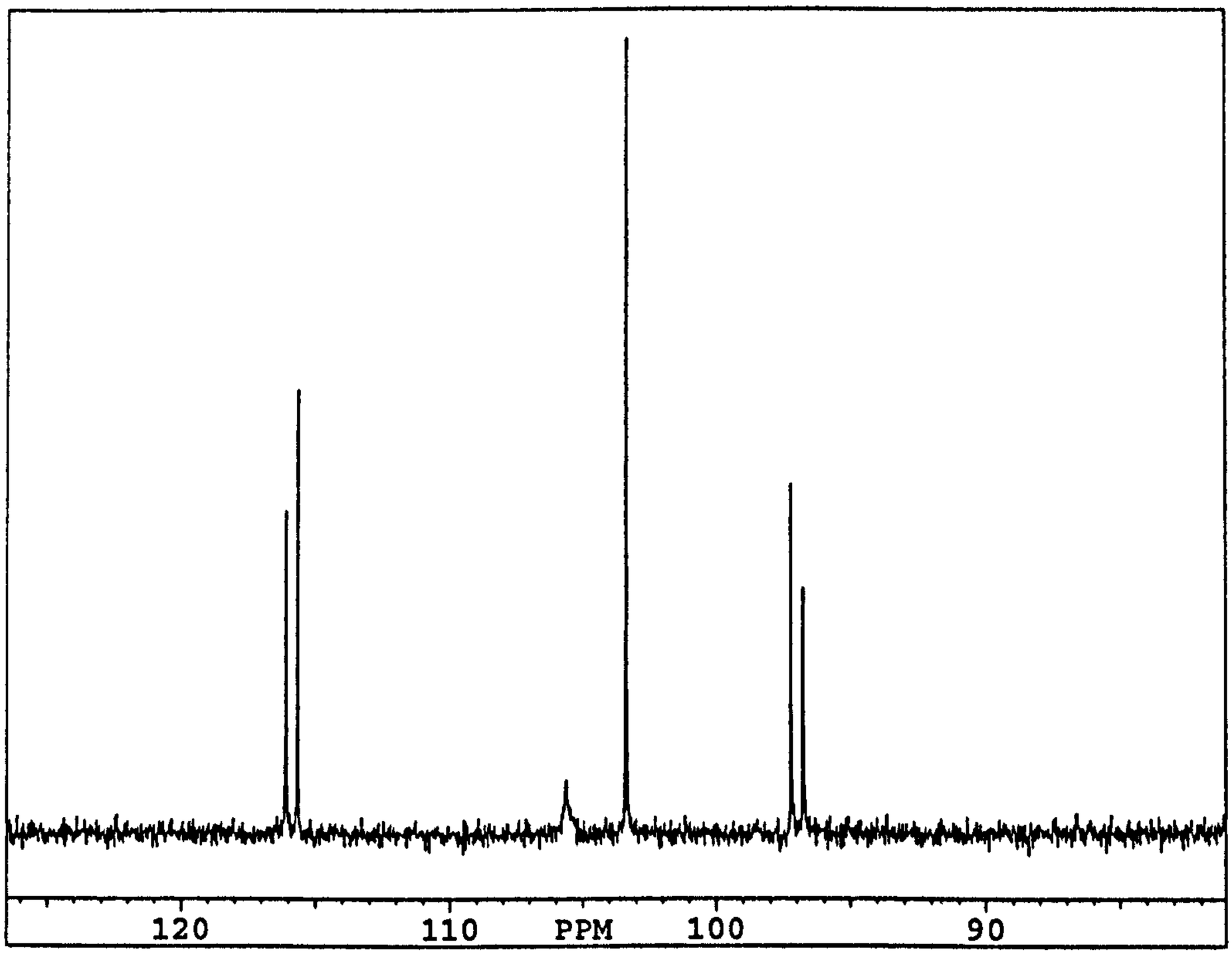

Figure 3.10: $^{31}P\{^1H\}$ NMR spectrum for the diastereomeric mixture of dichloropalladium(II) complex **(3.36)**

3.5.2.3 Rhodium(I) complexes

Reaction of one equivalent of the diastereomeric mixture of 'pnp' **(3.5)** with $[Rh(CO)_2(dpm)]$ gave the rhodium(I)-diphosphite complex **(3.37)**. This complex, which is of particular interest since it is a potential catalyst for asymmetric hydroformylation, has been characterised by $^{31}P\{^1H\}$ NMR spectroscopy, see Table 3.17 and Experimental.

(3.37)

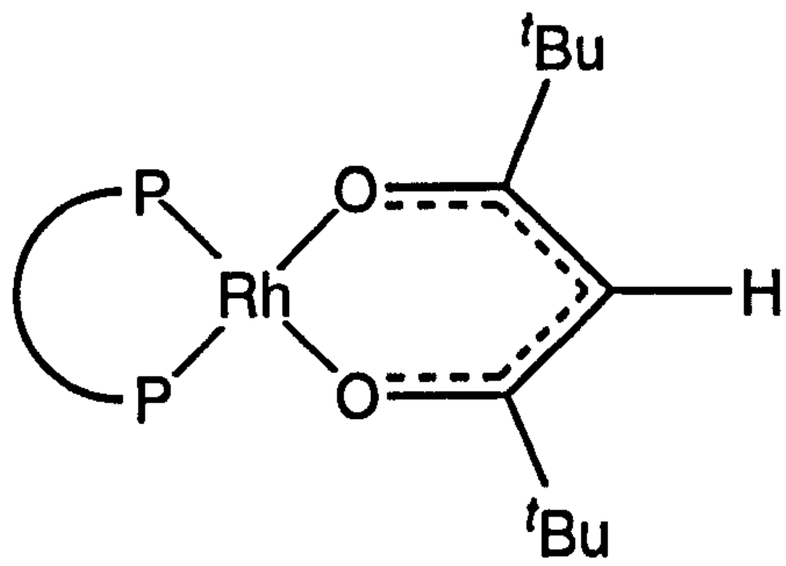

Table 3.17: $^{31}P\{^{1}H\}$ NMR data for the diastereomeric mixture of rhodium(I) complex **(3.37)**

Diastereomer	δ_P ($CDCl_3$)[a]	^{2}J(PP)[b]	^{1}J(PRh)[b]
(*R*,*R*,*R*) / (*S*,*S*,*S*)[c]	142.4 (d)	------	290
(*R*,*R*,*S*) / (*S*,*S*,*R*)	139.5 (dd)	119	299
	150.2 (dd)	117	297
(*R*,*S*,*R*) / (*S*,*R*,*S*)[c]	143.3 (d)	------	299

a Spectra recorded at 162 MHz at 28 °C. Chemical shifts (δ) in p.p.m. (±0.1) to high frequency of 85% H_3PO_4.
b Coupling constants (*J*) measured in Hz (±3).
c The relative assignment of these two diastereomers is ambiguous.

The $^{31}P\{^{1}H\}$ NMR spectrum shows two doublets and a pair of doublet of doublets. The species containing the inequivalent phosphorus atoms is assigned to the (*R*,*R*,*S*) / (*S*,*S*,*R*)-diastereomer whilst the assignment of the two doublets is ambiguous.

3.6 Asymmetric hydroformylation of styrene derivatives catalysed by rhodium(I) complexes of cyclic aryl diphosphites

This Section describes the preliminary results we have obtained in the asymmetric hydroformylation of styrene and *p*-methoxystyrene using rhodium(I) complexes of the optically pure diphosphites (*R*,*R*,*R*)-'biphenanthrite' **(3.4)**, (*R*,*R*,*R*)-'pnp' **(3.5)** and (*R*,*S*,*R*)-'pnp' **(3.5)**, see Scheme 3.3. The results are compared with those obtained using (*R*,*R*,*R*)-'binaphthite' **(3.1)**[94] in order to assess the effect of the bulkier organic substituents upon the catalytic activities, the regioselectivities and the enantioselectivities.

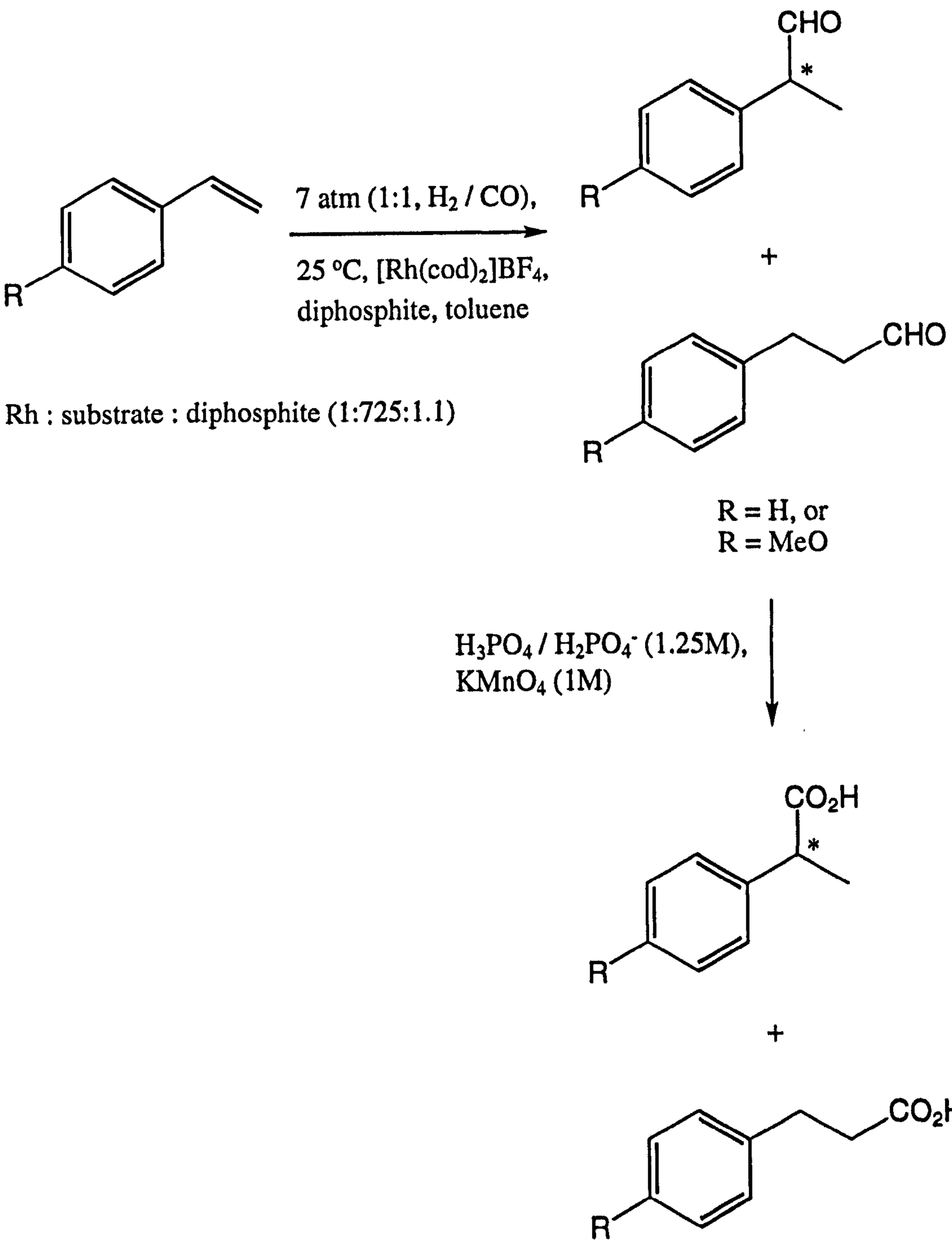

Scheme 3.3: Asymmetric hydroformylation (and subsequent oxidation) of styrene and *p*-methoxystyrene catalysed by rhodium(I)-diphosphite complexes

The aldehyde products are susceptible to racemisation *via* enolisation. Consequently, the reaction mixtures are immediately plunged into a buffer solution upon removal from the autoclave and are subsequently converted to the corresponding carboxylic acids *via* Jones oxidation. The acids do not undergo racemisation, enabling analysis to be performed. The results are shown in Table 3.18. It has already been mentioned in Section 1.5.3 that the catalyst derived from (*R*,*R*,*R*)-'binaphthite' (**3.1**) is highly active and regioselective (towards the branched aldehyde) but effects only

Table 3.18: Catalytic results for the asymmetric hydroformylation of styrene and *p*-methoxystyrene using rhodium(I) complexes of optically pure diphosphites (*R,R,R*)-(**3.1**), (*R,R,R*)-(**3.4**), (*R,S,R*)-(**3.5**) and (*R,R,R*)-(**3.5**)

Entry	Method	Rhodium complex[a]	Ligand	Substrate	% conversion[b]	% branched[b]	% ee[c]
1[d]	A[e]	$[Rh(cod)_2]BF_4$	(*R,R,R*)-(**3.1**)	styrene	86	81	23 (*R*)
2[d]	A[e]	$[Rh(cod)_2]BF_4$	(*R,R,R*)-(**3.1**)	*p*-methoxystyrene	70	69	42 (*R*)
3	B[f]	$[Rh(cod)_2]BF_4$	(*R,R,R*)-(**3.4**)	*p*-methoxystyrene	70	50	< 10
4[g]	B[f]	$[Rh(cod)_2]BF_4$	(*R,R,R*)-(**3.5**)	*p*-methoxystyrene	0	-----	-----
5	B[f]	$[Rh(cod)_2]BF_4$	(*R,S,R*)-(**3.5**)	*p*-methoxystyrene	68	92	71 (*R*)
6	A[e]	$[Rh(cod)_2]BF_4$	(*R,S,R*)-(**3.5**)	*p*-methoxystyrene	83	91	66 (*R*)
7	B[f]	$[Rh(CO)_2(dpm)]$	(*R,S,R*)-(**3.5**)	*p*-methoxystyrene	51	91	70 (*R*)
8	B[f]	$[Rh(cod)_2]BF_4$	(*R,S,R*)-(**3.5**)	styrene	57	96	72 (*R*)

a The catalyst was generated *in situ* by reaction of $[Rh(cod)_2]BF_4$ (3.3 mg, 8.1 μmol) or $[Rh(CO)_2(dpm)]$ (2.8 mg, 8.1 μmol) with the diphosphite (8.9 μmol , 1.1 mol equiv) in deoxygenated toluene (8 cm^3).

b Calculated by GC analysis of a sample of the aldehyde product mixture prior to oxidation.

c Calculated by GC analysis of the carboxylic acid product mixture.

d Ref. 94

e A: The solution of catalyst (8.1 μmol, 0.0014 mol equiv) in toluene (8 cm^3) was placed in the autoclave, which was charged first with CO (3.5 atm) and then with H_2 (3.5 atm). The solution was stirred at 25 °C for 16 h to preactivate the catalyst. Then the substrate (5.873 mmol) and toluene (2 cm^3) were added and the autoclave was again charged with CO (3.5 atm) and H_2 (3.5 atm). The reaction mixture was stirred at 25 °C for 22 h and then work-up was performed.

f B: The solution of catalyst (8.1 μmol, 0.0014 mol equiv) and substrate (5.873 mmol) in toluene (10 cm^3) was placed in the autoclave, which was charged first with CO (3.5 atm) and then with H_2 (3.5 atm) . The reaction mixture was stirred at 25 °C for 22 h and then work-up was performed.

g This appears to be an anomalous result and the experiment should be repeated.

modest enantioselectivities, Entries 1 and 2. The analogous catalyst derived from (*R,R,R*)-'biphenanthrite' (**3.4**) is also an active catalyst (70% conversion) but it is significantly less regioselective (50% of the branched isomer) and effects no observable enantioselectivity, Entry 3. The lower regioselectivity is not surprising since the ligand is bulkier and hence we might expect to form a higher proportion of the linear aldehyde *via* the less sterically demanding linear alkylrhodium species. However, the failure of this ligand to effect asymmetric induction was very surprising and this experiment should be repeated and confirmed.

The rhodium(I) catalyst derived from (*R,R,R*)-(**3.5**) was also tested for the asymmetric hydroformylation of *p*-methoxystyrene but, disappointingly, this complex was found to be inactive under the reaction conditions, Entry 4. This is very surprising in view of the results obtained with (*R,R,R*)-'binaphthite' and (*R,R,R*)-'biphenanthrite' and the experiment should be repeated to check the validity of the result obtained.

Finally, the rhodium(I) complex of (*R,S,R*)-(**3.5**) was tested for the asymmetric hydroformylation of *p*-methoxystyrene and styrene. We were pleased to discover that this is a very efficient catalyst for these reactions, Entries 5 and 8. High activities (68% and 57% conversions respectively), excellent regioselectivities (92% and 96% respectively in favour of the branched aldehyde) and high enantioselectivities (71% ee and 72% ee respectively) were exhibited. Preactivation of the catalyst, by stirring a solution of the complex under CO / H_2 for 16 h prior to introduction of the substrate, led to higher conversions (83%) but a slightly lower enantioselectivity (66%), compare Entries 5 and 6. Use of the [$Rh(CO)_2$(dpm)] starting material had very little effect upon the selectivity of the catalyst although the activity was significantly lower, compare Entries 5 and 7.

The results obtained with (*R,S,R*)-(**3.5**) show that it is a very promising catalyst and further work is required in order to optimise the reaction conditions and realise its full potential. The reason for the success of this ligand is not yet fully understood but it is apparent that the (*R,S,R*)-diastereomer of the 'pnp' diphosphite (**3.5**) is the 'matched' one, whilst the (*R,R,R*)-diastereomer is the 'mismatched' case. It has already been shown in Section 3.5.1.1 that the (*R,R,R*) / (*S,S,S*)- and (*R,S,R*) / (*S,R,S*)-diastereomers of 'biphenanthrite' (**3.4**) adopt very different conformations in the dichloroplatinum(II) complex (**3.30**) and it seems plausible that the various diastereomers of the 'pnp' diphosphite (**3.5**) will exhibit similar differences in conformation upon coordination to a metal. This could well be a contributing factor to the observed difference in catalytic properties.

Chapter 4

Asymmetric Hydrogenation of α-Enamides: Mechanism and Catalytic Results

4.1 Introduction to the transition metal-catalysed hydrogenation of olefins

The addition of hydrogen to olefins occupies an important position amongst transition metal-mediated transformations. For example, the importance of developing catalysts for the asymmetric hydrogenation of α-enamides leading to a diverse array of unnatural α-amino acids has already been discussed in Chapter 1. Consequently, this process has been the most extensively studied asymmetric catalytic reaction yet developed. A wide range of ligands and catalysts has been examined and, currently, the best systems employ cationic rhodium(I) complexes of optically active C_2-symmetric diphosphines. These complexes are of the type [Rh(diene)(diphosphine)]X; where the diene is *cis,cis*-1,5-cyclooctadiene or *cis,cis*-2,5-norbornadiene and X is a non-coordinating anion such as BF_4^-, SbF_6^-, OTf^- *etc.* In this Section the current theories regarding the mode of action of these cationic rhodium(I) complexes will be presented. The mechanism of hydrogenation of a simple olefin such as 1-hexene is discussed first in Section 4.1.1 and the complications that arise for more elaborate substrates such as α-enamides are presented in Section 4.1.2. The mechanism accounts for the asymmetric induction obtained with these prochiral substrates when optically active diphosphines are employed as ligands. Finally, a summary of the state-of-the-art systems that are currently available is given in Section 4.1.3.

4.1.1 General mode of action of cationic rhodium(I) complexes [Rh(diene)L_2]X in the hydrogenation of simple olefins

The cationic rhodium and iridium complexes of the general formula [M(diene)L_a]X (L = monodentate phosphine ligand; a = 2 or 3) were first made by Osborn and Schrock[167-171] and fulfil the basic criteria that a complex requires in order to act as a catalyst; namely that they possess free coordination sites, that different coordination numbers exist for a given oxidation state and that several oxidation states can be easily accessed. They were synthesised from the binuclear complexes [{M(μ-Cl)(diene)}$_2$] in a variety of ways,[172,173] including that shown in Scheme 4.1 which was our chosen route.

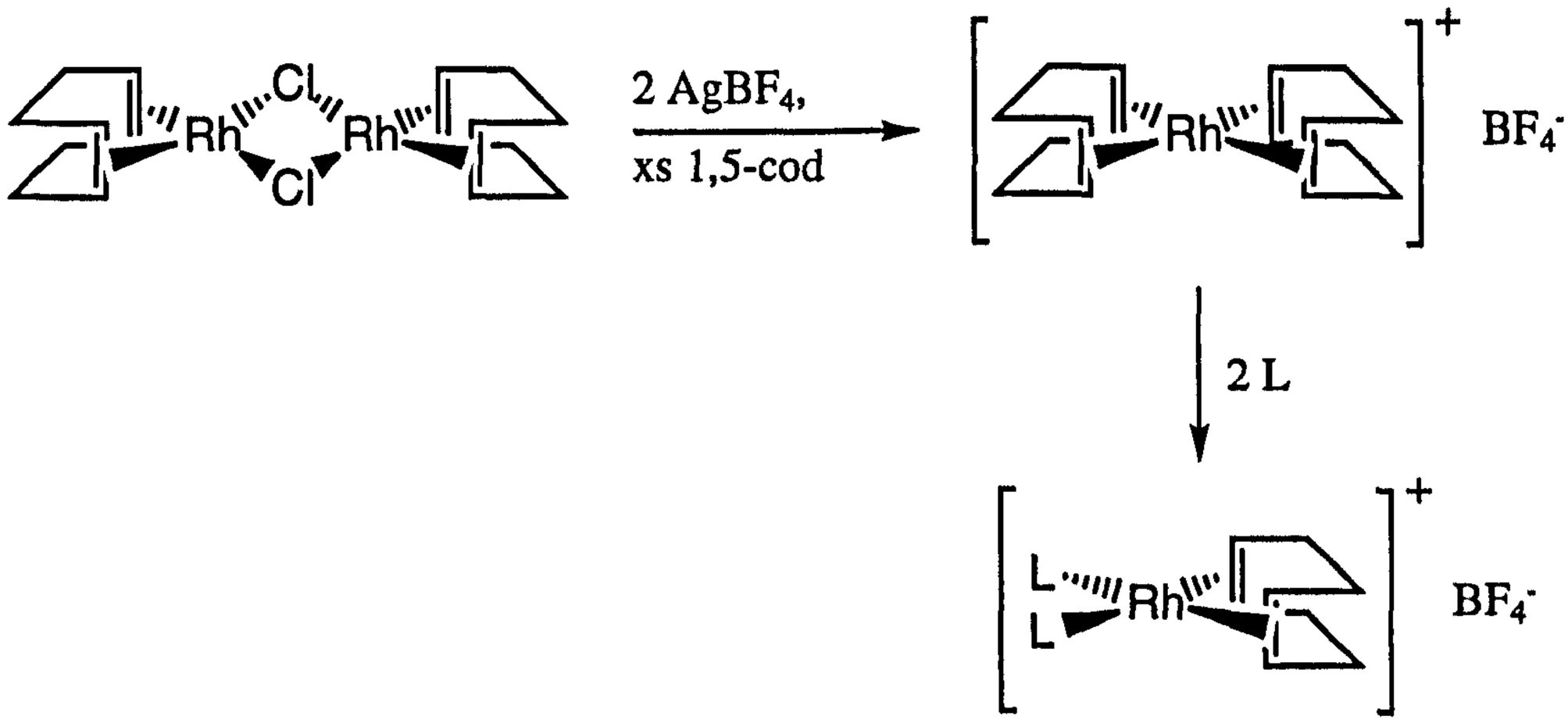

Scheme 4.1: Synthesis of $[Rh(cod)L_2]BF_4$ from $[\{Rh(\mu\text{-}Cl)(cod)\}_2]$

A plausible mechanism for the hydrogenation of a simple monosubstituted olefin such as 1-hexene in a solvent S catalysed by a cationic rhodium(I) complex of a monodentate phosphine ligand L is shown in Scheme 4.2.[174] This shows two major pathways **A** and **B** by which an olefin can be hydrogenated. In Path **A** the cationic dihydride $[RhH_2L_2S_2]^+$ (**4.1**) is the active catalytic species, the generation of which from $[Rh(diene)L_2]X$ (**4.10**) and hydrogen was first investigated by Schrock and Osborn.[167-171] The suggested pathway for the formation of (**4.1**) is shown in Scheme 4.3.

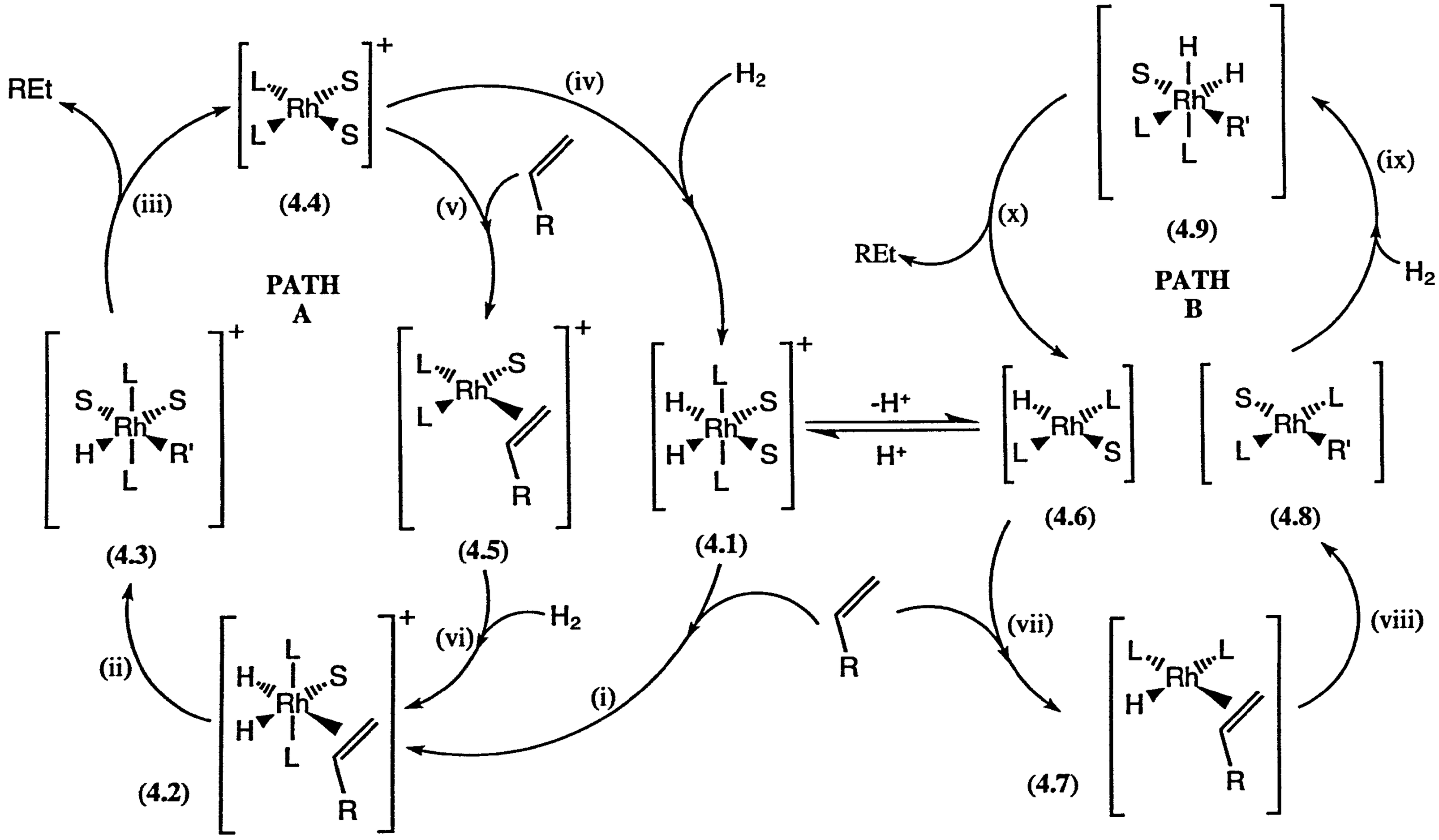

Scheme 4.2: Plausible mechanism for the hydrogenation of a simple monosubstituted olefin in a solvent S catalysed by a cationic rhodium(I) complex of a monodentate phosphine ligand L; R' = RCH_2CH_2

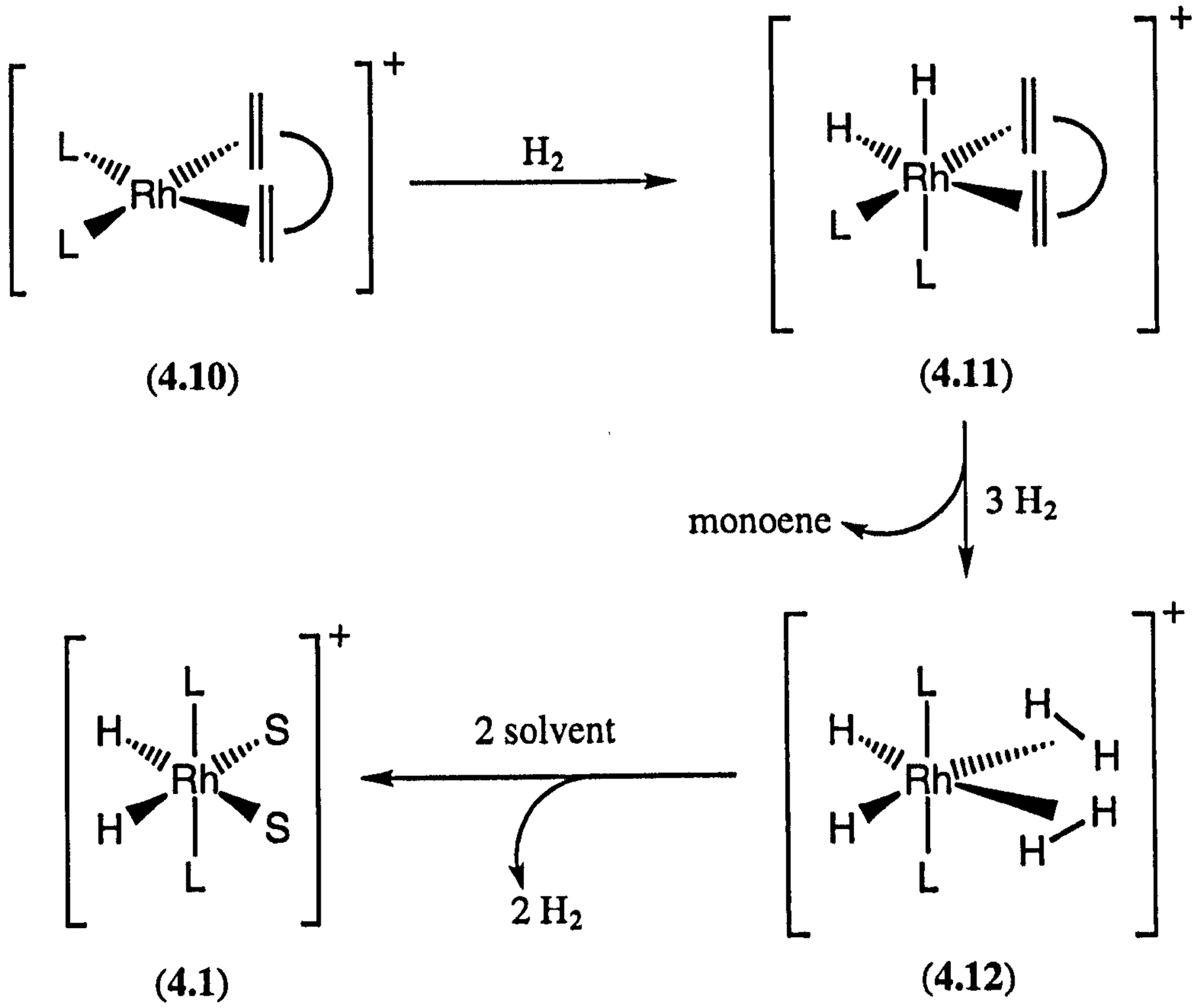

(4.10) **(4.11)** **(4.12)** **(4.1)**

Scheme 4.3: Generation of the catalytic species $[RhH_2L_2S_2]^+$ **(4.1)** *via* hydrogenation of the precursor $[Rh(diene)L_2]^+$ **(4.10)**

The first step is oxidative addition of H_2 to the complex $[Rh(diene)L_2]^+$ **(4.10)**, affording the dihydride species *cis*-$[RhH_2(diene)L_2]^+$ **(4.11)**. This intermediate would be short-lived and partial hydrogenation of the diene subsequently occurs under hydrogen in the presence of a solvent S to yield the species $[RhH_2L_2S_2]^+$ **(4.1)**, possibly *via* the cationic dihydrogen complex $[RhH_2(\eta^2\text{-}H_2)_2L_2]^+$ **(4.12)**.[174]

Simple alkene substrates enter the coordination sphere by displacing a solvent molecule from $[RhH_2L_2S_2]^+$ **(4.1)**, to give $[RhH_2L_2(olefin)S]^+$ **(4.2)** in which the olefin substrate is *cis*- to one hydride and *trans*- to the other {step (i)}.[174] Then β-hydride migration to the olefin (of the *cis*-hydride) occurs {step (ii)}. This would generate a *trans*-alkyl-hydride complex $[RhRHL_2S_2]^+$, from which reductive elimination of the product is not feasible. Hence, either the migration is accompanied by a stereochemical rearrangement or a rapid rearrangement occurs after the migration and the *cis*-alkyl-hydride complex $[RhRHL_2S_2]^+$ **(4.3)** is formed. Reductive elimination of the product {step (iii)} then occurs to yield $[RhL_2S_2]^+$ **(4.4)**, which can then either oxidatively add hydrogen to regenerate $[RhH_2L_2S_2]^+$ **(4.1)** {step (iv)}, thereby completing pathway **A**, or an incoming substrate can displace a solvent molecule

{step (v)} to form $[RhSL_2(olefin)]^+$ (**4.5**) which can then oxidatively add hydrogen {step (vi)} to give $[RhH_2L_2(olefin)S]^+$ (**4.2**) and thence rejoin pathway **A**.

Pathway **B** has the rhodium monohydride complex $[RhHL_2S]$ (**4.6**) as the central catalytic species, which is formed by the deprotonation of the dihydride species $[RhH_2L_2S_2]^+$ (**4.1**), see Equation 4.1.

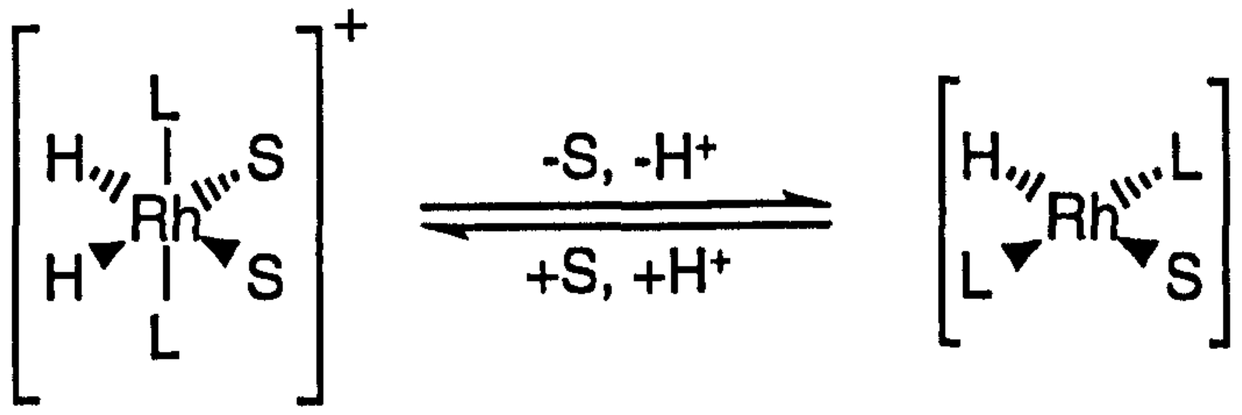

(4.1) **(4.6)**

Equation 4.1

Evidence from deuterium labelling experiments supporting the existence of this species has been obtained by Schrock and Osborn.[171]

Hydrogenation then proceeds *via* olefin displacement of the solvento ligand from (**4.6**) {step (vii)} to form $[RhHL_2(olefin)]$ (**4.7**). Again this process must be accompanied by a simultaneous stereochemical rearrangement or a rapid rearrangement must subsequently occur in order that the olefin is *cis*- to the hydride in species (**4.7**) so that step (viii), β-hydride migration to the olefin to form the metal alkyl complex $[RhRL_2S]$ (**4.8**), can occur easily. After this migration has occurred, oxidative addition of hydrogen {step (ix)} yields the dihydride complex $[RhRH_2L_2S]$ (**4.9**) and the cycle is subsequently completed by the reductive elimination of the product {step (x)}, regenerating the catalytic species $[RhHL_2S]$ (**4.6**).

The monohydride complex (**4.6**) is a much more efficient hydrogenation catalyst than the dihydride complex (**4.1**).[174] It also accounts for the significant amount of isomerisation of olefins such as 1-hexene that occurs during these reactions. Acidic conditions clearly favour pathway **A**, whilst basic conditions and basic phosphine ligands bring pathway **B** into play.

One feature of this system is that the catalytic species, $[RhH_2L_2S_2]^+$ (**4.1**) and $[RhHL_2S]$ (**4.6**), both bind solvent well. Dissociation of solvent from (**4.1**) is necessary before the olefinic substrate can bind to the metal and therefore the rates of reduction are very solvent dependent.[175,176] Further, this system differs from Wilkinson's catalyst $[RhCl(PPh_3)_3]$ in that dissociation of a phosphine ligand is not required for reaction to proceed. Consequently, the steric pressure exerted by the bulky triphenylphosphine ligands that facilitates dissociation ($[RhCl(PEt_3)_3]$ and $[RhCl(PPhEt_2)_3]$ are both catalytically inactive) is unnecessary for these cationic

rhodium complexes and hence a much wider range of ligands can be utilised. This opens up the possibility of employing phosphonites and phosphites for hydrogenation, both of which have smaller cone angles (θ) than the analogous phosphines; *e.g.* $\theta = 145^{o}$ for PPh_3 whilst $\theta = 128^{o}$ for $P(OPh)_3$.[133]

The overall picture is complicated and the rates of hydrogenation and isomerisation will depend strongly on the reaction conditions. Certainly the effect of changing the ligands from phosphines to phosphonites or phosphites can hardly be predicted, although the less basic nature of phosphonites and phosphites makes it likely that the significance of pathway **B** will be diminished.

4.1.2 The mechanism of asymmetric induction in hydrogenation reactions catalysed by cationic rhodium(I) complexes $[Rh(diene)L_2]X$

In Section 4.1.1 the likely course of the hydrogenation of a simple monosubstituted olefin such as 1-hexene was described. The situation becomes much more complicated when prochiral substrates are hydrogenated using complexes of optically active ligands since the issue of enantioselectivity needs to be considered. The hydrogenation of α-enamides will be discussed since this class of substrates has the best understood mechanism. This is largely due to the relentless efforts of the groups of Landis and Halpern,[177,178] Brown[131,179,180] and Bosnich.[181] The accepted mechanism proposed by Landis and Halpern[177,178] for the asymmetric hydrogenation of methyl-(*Z*)-2-acetamidocinnamate (**4.13**) catalysed by a cationic rhodium(I) complex containing an optically pure bidentate diphosphine ligand such as (*R,R*)-Chiraphos (**4.14**) is illustrated in Scheme 4.4.

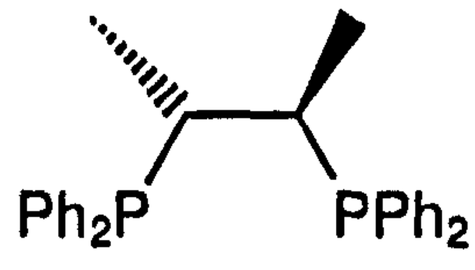

(*R,R*)-Chiraphos (**4.14**)

Throughout this Section we have arbitrarily chosen the (*R,R*)-Chiraphos enantiomer; of course if the (*S,S*)-isomer was used then all the stereochemical arguments in the discussion below would be (literally) inverted.

Several key features of this mechanism and the manner in which it differs to that for simpler substrates, Scheme 4.2, will now be dealt with in turn. The first is that the reaction initially proceeds *via* the coordination of the α-enamide substrate to $[RhP_2^*S_2]^+$ (**4.15**), itself generated by the partial hydrogenation of the diene in the precursor $[Rh(diene)P_2^*]^+$, see Section 4.1.1. It is significant that the substrate chelates

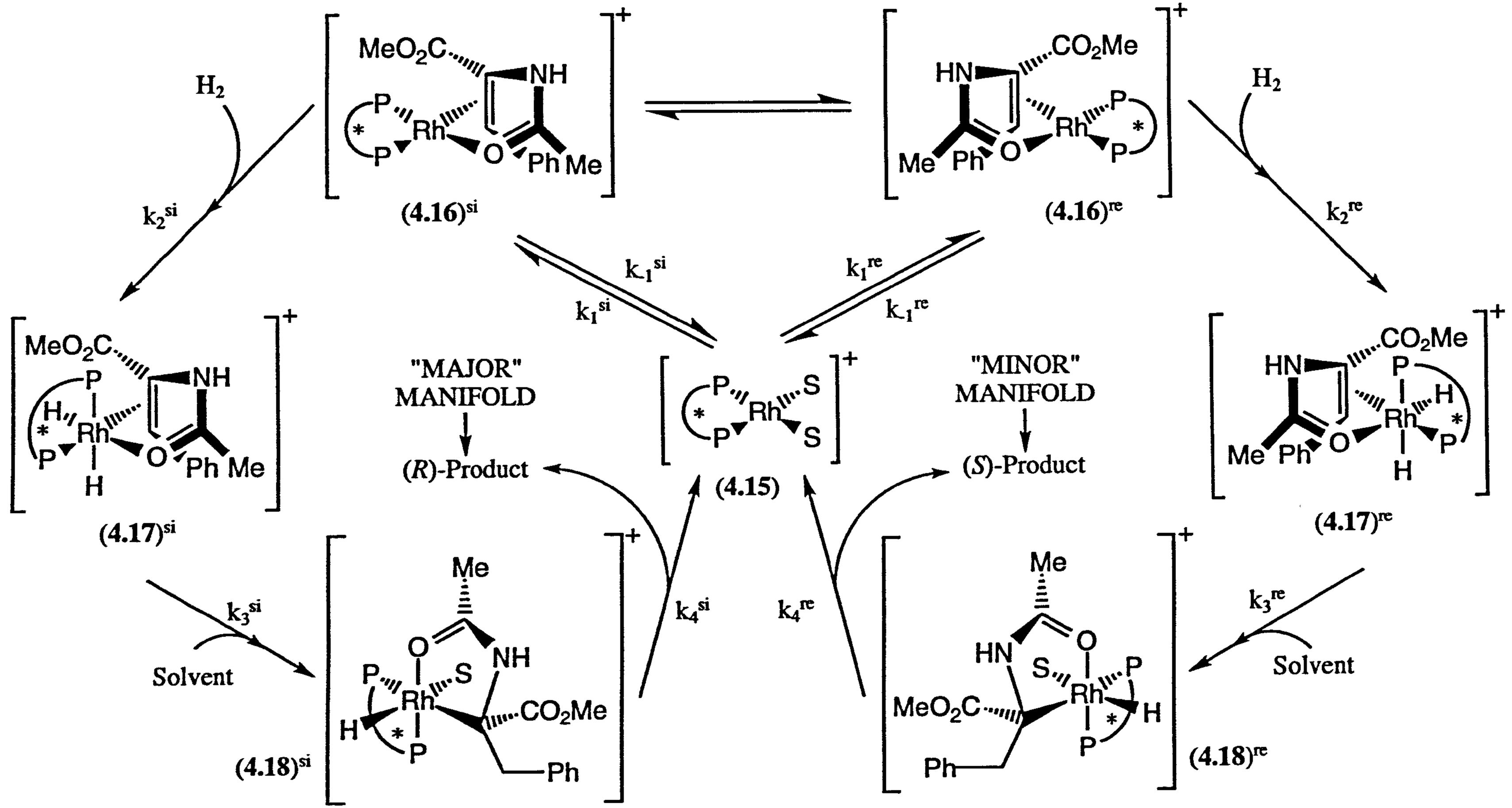

Scheme 4.4: Mechanism of the asymmetric hydrogenation of methyl-(Z)-2-acetamidocinnamate **(4.13)** catalysed by a cationic rhodium{(*R,R*)-Chiraphos} complex in solvent S

to the metal with coordination occurring *via* both the carbon-carbon double bond and a lone pair of electrons on the oxygen of the amide carbonyl.[182-184] This generates a mixture of the two diastereomeric compounds **(4.16)**^{si} and **(4.16)**^{re}, which correspond to *si*- and *re*-face coordination respectively. A vital part of the mechanism that accounts for the asymmetric inductions is that this coordination is reversible and, consequently, a pre-equilibrium is set up between the two diastereomers, strongly favouring formation of **(4.16)**^{si} when (*R,R*)-Chiraphos (**4.14**) is the ancillary ligand. It is due to the predominance of species **(4.16)**^{si} that the left-hand cycle in Scheme 4.4 is labelled as the "Major Manifold".

Recent work by the groups of Brown[179,185] and Bender[186,187] has shown that an intramolecular pathway also exists for the interconversion of the two diastereomers **(4.16)**^{si} and **(4.16)**^{re} *via* an intermediate (**4.19**) in which the α-enamide substrate is bound to the metal solely by the lone pair of electrons on the amide carbonyl, see Scheme 4.5.

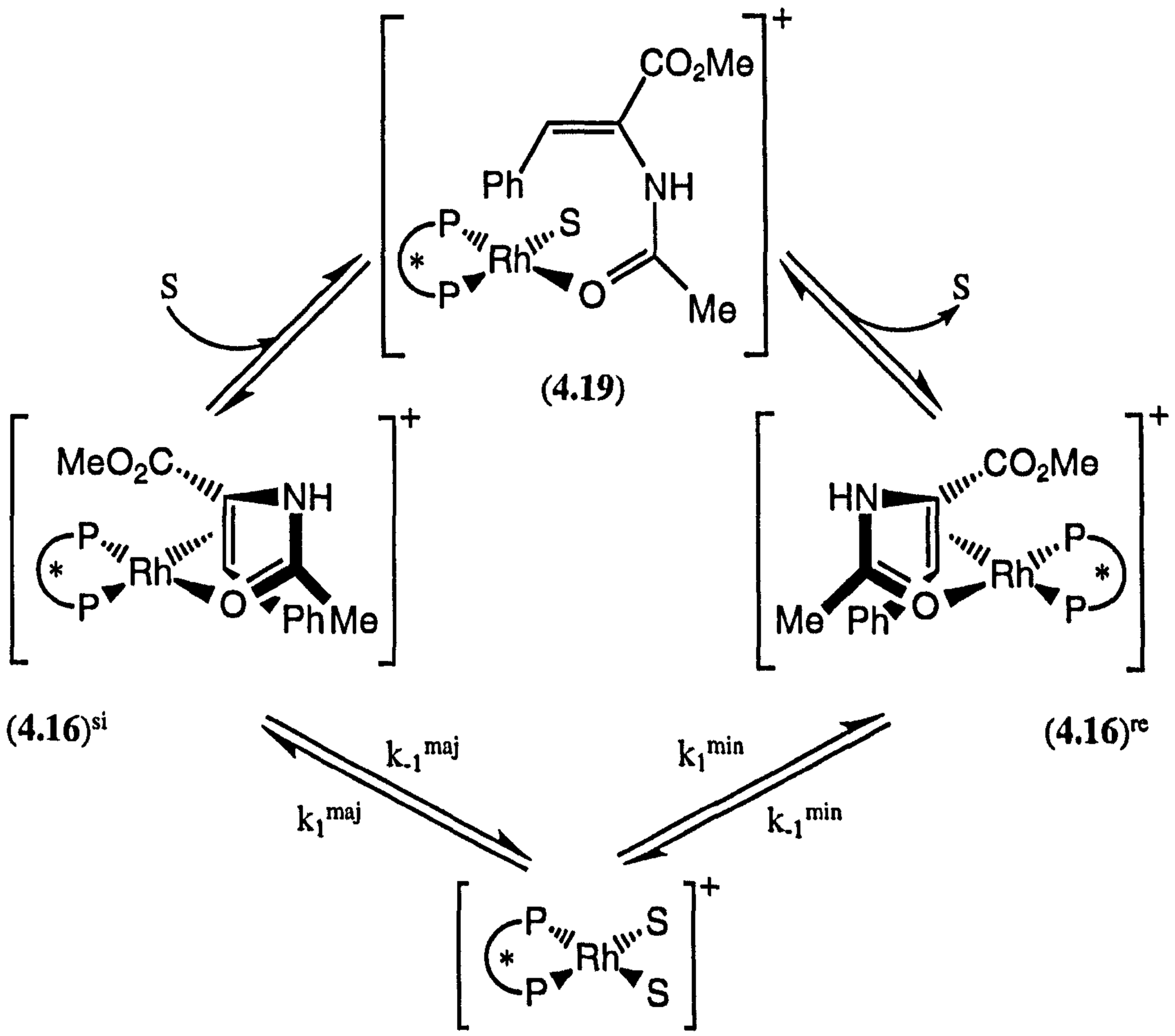

(4.15)

Scheme 4.5: Interconversion of the two diastereomeric rhodium-substrate complexes **(4.16)**^{si} and **(4.16)**^{re}

The next step in the catalytic cycle is oxidative addition of hydrogen to generate the diastereomers **(4.17)**^{si} and **(4.17)**^{re}. The existence of these diastereomeric dihydride intermediates has not been verified by direct observation despite the efforts of the groups of Brown and Halpern but their existence is consistent with the currently available data. This step is irreversible[178] and rate-limiting at ambient temperatures under moderate hydrogen pressures. Furthermore, since this is the first irreversible step in a cycle involving diastereomeric transition states, the structural origins of the enantioselectivity are completely defined by this step. Therefore this crucial step will now be discussed in detail.

Perhaps the most fascinating feature of these reactions is the fact that the major enantiomer of the product that is formed is produced *via* the "Minor Manifold" of Scheme 4.4, which implies that the minor diastereomer present in the pre-equilibrium, **(4.16)**^{re}, is very much more reactive than the major diastereomer **(4.16)**^{si}.[177,182,183,188,189] Further, for this higher reactivity to translate to high enantioselectivity, it is important that the equilibration between **(4.16)**^{si} and **(4.16)**^{re} is much faster than the oxidative addition. Needless to say much work has gone into examining the cause of the higher reactivity of **(4.16)**^{re} and a summary of the conclusions to date will now be presented. This phenomenon has been found to be general irrespective of the ligand structure, though most of the investigations have centred on the Chiraphos ligand (**4.14**). This bidentate diphosphine ligand binds the metal to form a five-membered chelate ring with four pendant phenyl groups. Knowles and co-workers have proposed that the orientation of these aryl rings is imposed by the ligand chirality and that it is their orientation that is responsible for the stereochemical control in asymmetric hydrogenation.[190,191] It is well known that saturated five-membered chelate rings adopt puckered chiral conformations[192] (labelled λ and δ) which rapidly invert in the absence of ring substituents.[193] In the case of (*R,R*)-Chiraphos (**4.14**) the two methyl substituents fix the ring into a λ conformation where the substituents are in equatorial positions, see Figure 4.1.

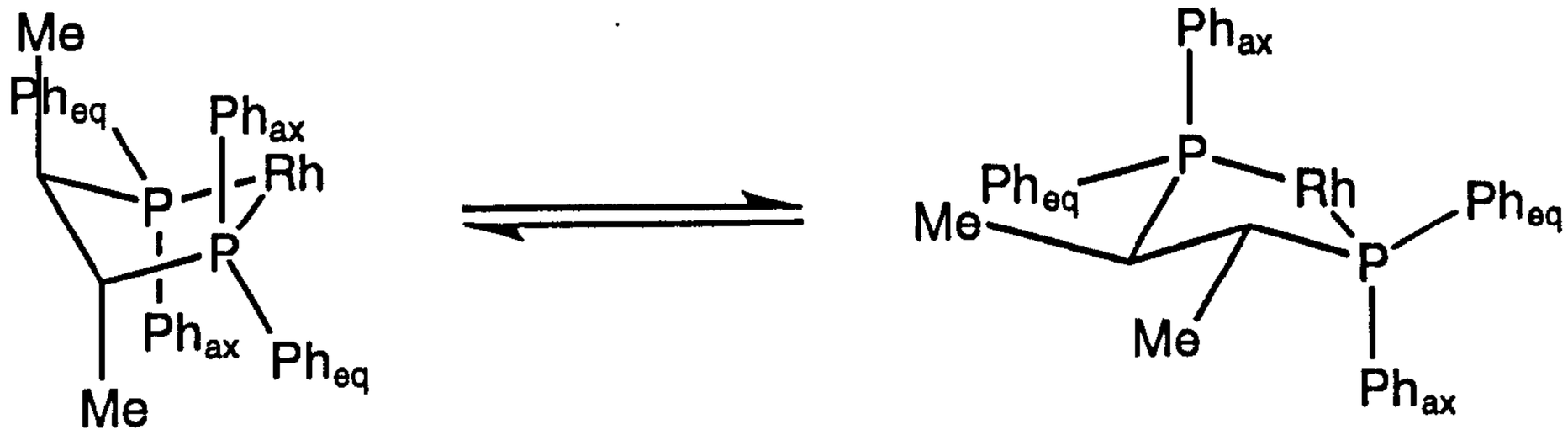

Disfavoured δ conformation - two methyl groups are in axial positions.

Preferred λ conformation - two methyl groups are in equatorial positions.

Figure 4.1: Possible conformations of the five-membered ring formed by chelation of (*R,R*)-Chiraphos (**4.14**) to rhodium

One consequence of the ring being fixed in this single chiral conformation is that there are two different types of phenyl groups: pseudo-axial and pseudo-equatorial. The many X-ray crystal structures of rhodium-diphosphine complexes show that, in general, the pseudo-axial aryl rings are 'edge-on' to the metal, whilst the pseudo-equatorial rings are 'face-on' with an overall C_2-symmetry, see Figure 4.2.

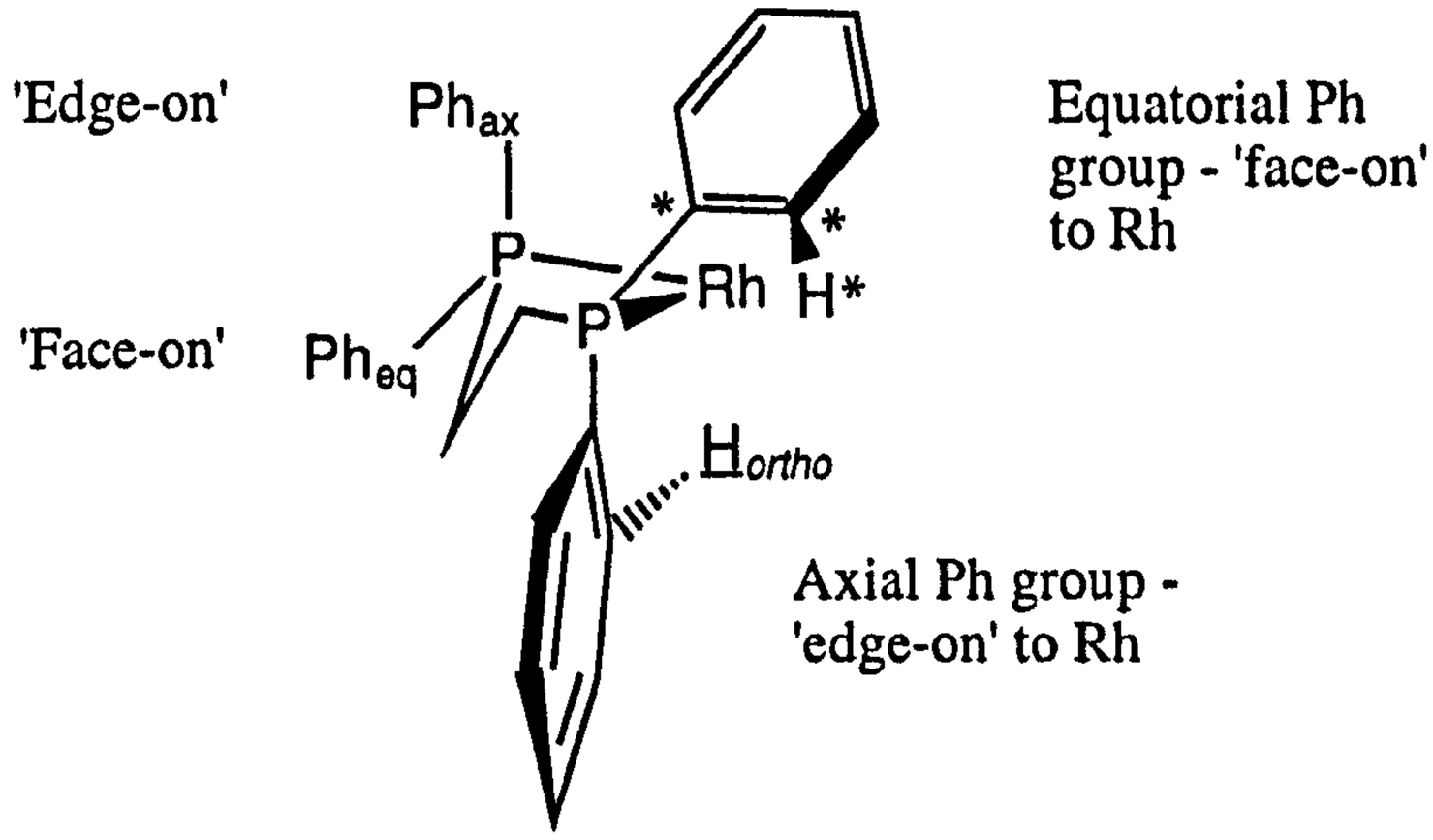

Figure 4.2: 'Edge-face' array of axial and equatorial phenyl substituents on phosphorus in a five-membered rhodium-diphosphine chelate ring

The aryl rings are defined[131] as being pseudo-axial or pseudo-equatorial depending on the value of the torsion angle ϕ about P-Rh-P-C_{aryl}, see Figure 4.3, and are in an 'edge-on' or a 'face-on' conformation depending on the value of the torsion angle θ about Rh-P-C_{aryl}-C_{ortho}, see Figure 4.3. The idealised arrangement is where a pseudo-axial 'edge-on' ring has a value of θ = 0° and ϕ = 100° and a pseudo-equatorial 'face-on' ring has a value of θ = 70° and ϕ = 130°.[131]

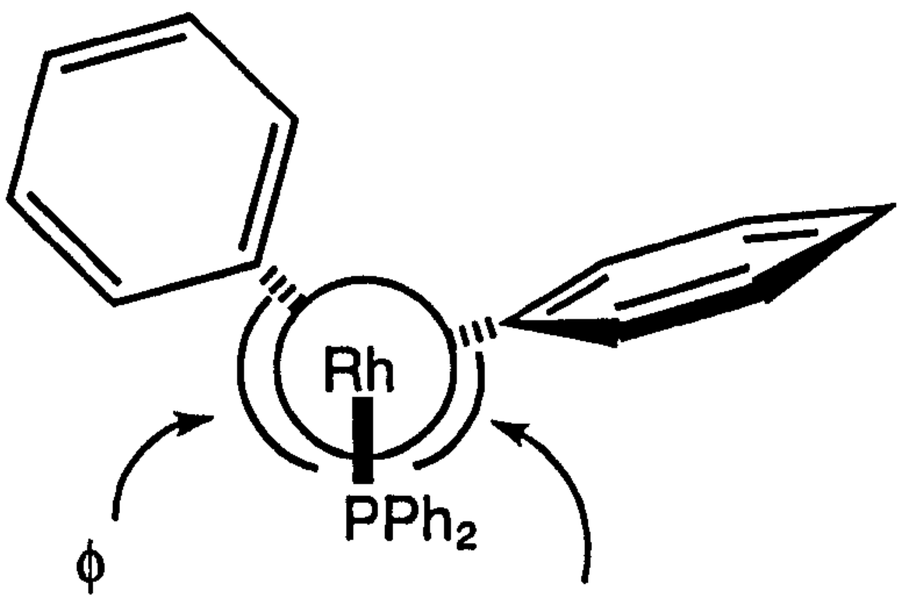

Figure 4.3: Parameters defining the conformation of the pendant aryl rings

This 'edge-face' array seems to be a general feature of these species and it has been proposed that one contributor to this favoured conformation is an agostic interaction[130] between C-H_{ortho} bonds, see Figure 4.2, of pseudo-axial aryl groups and the rhodium.[131]

It was originally suggested[190] that the 'edge-on' pseudo-axial phenyl groups are more sterically demanding than the 'face-on' pseudo-equatorial phenyl groups. However, in subsequent work Brown[131] argued that the C_{ipso}, C_{ortho} and H_{ortho} atoms (starred in Figure 4.2) of the pseudo-equatorial aryl groups present a more sterically demanding environment. Whichever is the case, there is definitely a difference in steric bulk between the two environments and hence the chirality in the backbone of the ligand has generated a chiral array of the donor atom substituents. The faces of a prochiral

olefin will be discriminated largely by this chiral arrangement of the phenyl groups, despite the fact that the actual chiral centers are on distant carbon atoms.[194] Pendant aryl groups are a key feature of many of the successful ligands for asymmetric hydrogenation and this principle is likely to operate in all of those systems where substituents in the backbone make the chelate ring conformationally rigid.

Apparent exceptions to this conformational rigidity are the *o*-anisyl ligands Dipamp (**4.20**) and Camp (**4.21**).

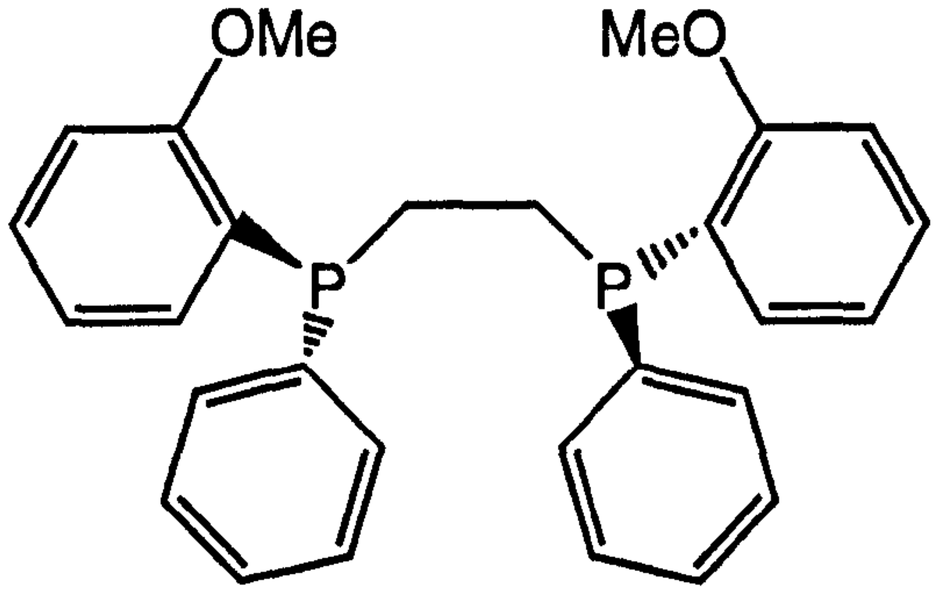

Dipamp (**4.20**)

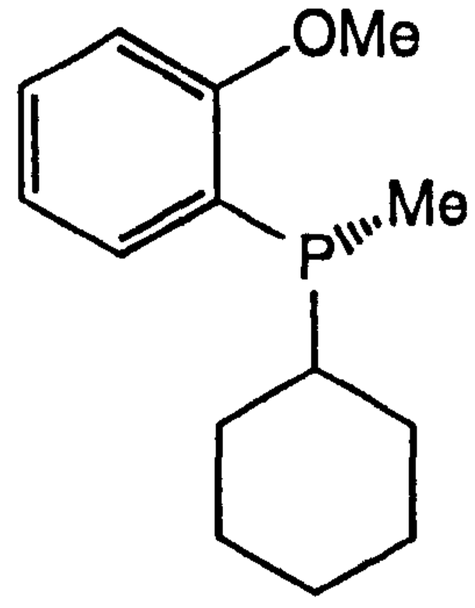

Camp (**4.21**)

These two ligands are chiral at phosphorus but, at first sight, it seems unlikely that Dipamp[195] and Camp should adopt a single rigid chiral conformation. However, it has been proposed that the chelate ring chirality is fixed in the Dipamp system by weak coordination of the oxygen atoms of the methoxy groups of the pseudo-equatorial *o*-anisyl rings to the rhodium in the two apical positions making Dipamp a pseudo-tetradentate ligand,[196,197] see Figure 4.4. A similar argument may explain the effectiveness of the monodentate Camp ligand.[198]

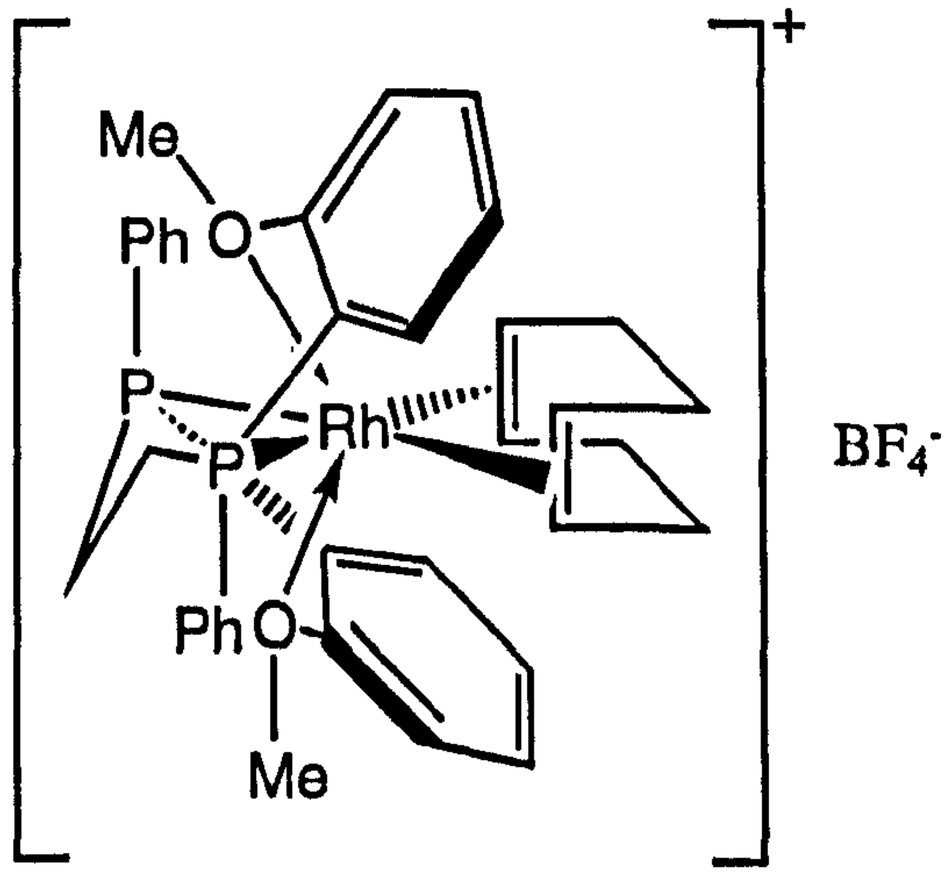

Figure 4.4: Conformational rigidity imposed by the Dipamp ligand (**4.20**)

One other class of ligand deserves mention at this stage on account of its remarkable success[199-201] in the asymmetric hydrogenation of α-enamides.

Et-Duphos (**4.22**)[199,200] is fixed in a rigid five-membered chelate ring, but here the rigidity is imposed by the planarity of the phenylene backbone, see Figure 4.5.

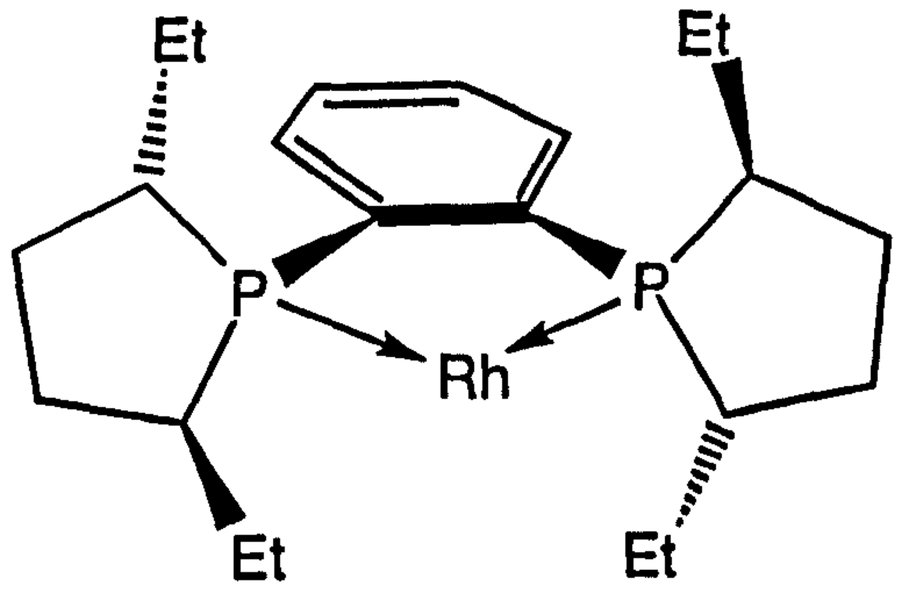

Figure 4.5: The rigid five-membered rhodium-chelate of (*S,S*)-Et-Duphos (**4.22**)

From the pictures presented in Figures 4.1, 4.2, 4.4 and 4.5 for the rhodium-diphosphine chelates, we can account for the observed higher reactivity of the minor diastereomers. For example, molecular graphics have been used to identify the difference in enthalpy between the two diastereomers (**4.16**)^{si} and (**4.16**)^{re} with the main destabilising interactions in (**4.16**)^{re} being between the CO_2Me group of the substrate and the C_{ipso}, C_{ortho} or H_{ortho} of the adjacent 'face-on' pseudo-equatorial aryl group, see Figure 4.2.[131] The CO_2Me group is in an uncongested region of space for (**4.16**)^{si}. Further, on going to the corresponding enamide dihydrides (**4.17**)^{si} and (**4.17**)^{re} it was found that the steric energies are reversed, with (**4.17**)^{si} being much less stable due to van der Waals' repulsions between the P-aryl groups and both the CO_2Me group and the amide methyl group. These repulsions are largely absent for (**4.17**)^{re}.

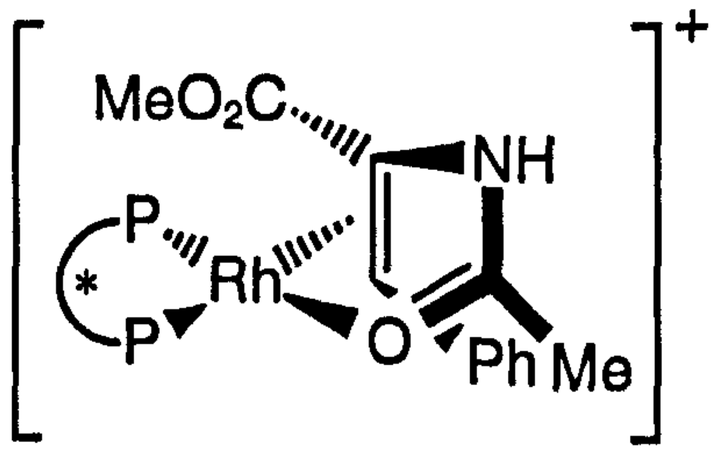

(**4.16**)^{si}

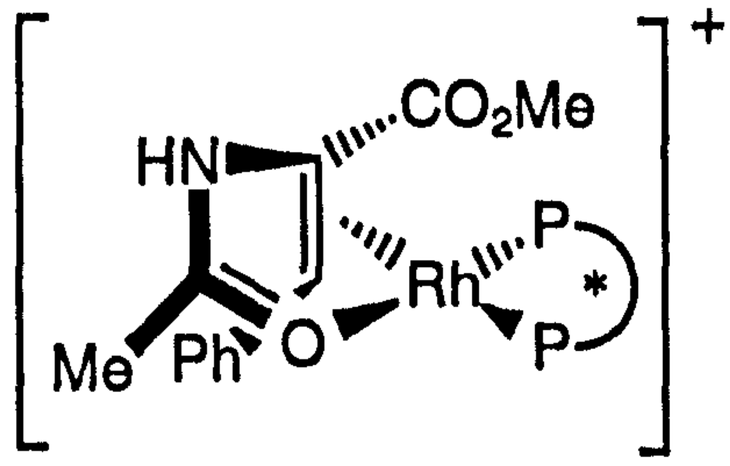

(**4.16**)^{re}

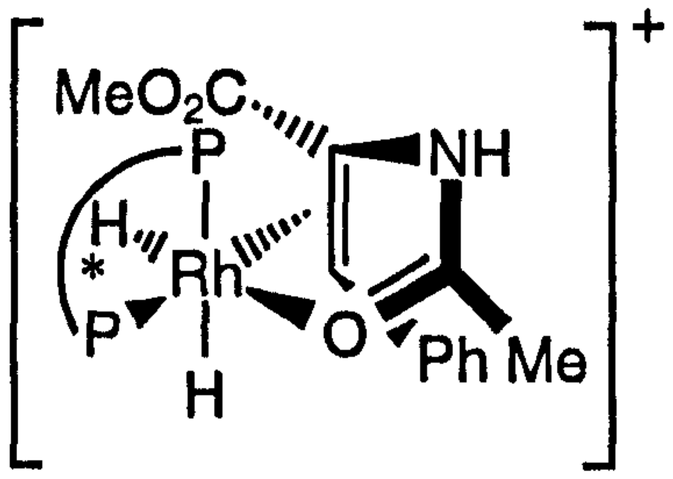

(**4.17**)^{si}

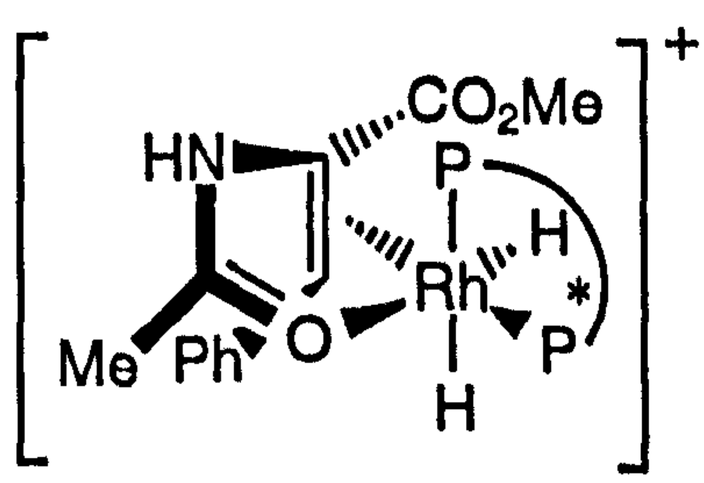

(**4.17**)^{re}

The higher energy of **(4.16)**^{re} compared to **(4.16)**^{si}, the reversal in these relative energies for the enamide dihydrides **(4.17)** and the fact that the oxidative addition reaction has a late transition state account for the fact that the minor diastereomer present in the pre-equilibrium, **(4.16)**^{re}, is much more reactive than the major one, **(4.16)**^{si}, and gives rise to the major product of hydrogenation. Many studies support the idea that the presence of the CO_2Me group is vital for a high optical yield and if it is replaced by H then the enantioselectivity is poor.[202]

It now remains to explain why (*R,R*)-Chiraphos **(4.14)**, (*R,R*)-Dipamp **(4.20)** and (*S,S*)-Et-Duphos **(4.22)** give (*S*)-amino acid derivatives. Kagan has proposed that rhodium-diphosphine chelates of λ configuration (as illustrated in Figure 4.6) give (*S*)-amino acid derivatives during hydrogenation.[203] For these systems *si*-face coordination is preferred but the minor diastereomer present (*re*-face coordination) is much more reactive and thus the (*S*)-product is formed predominantly. By the same arguments the enantiomeric δ configuration would give (*R*)-amino acid derivatives. Whilst Kagan's rule is entirely empirical, there are no exceptions to it. The λ configuration is favoured for (*R,R*)-Dipamp **(4.20)** due to the requirement that the *o*-anisyl rings adopt a pseudo-equatorial conformation.[196,197]

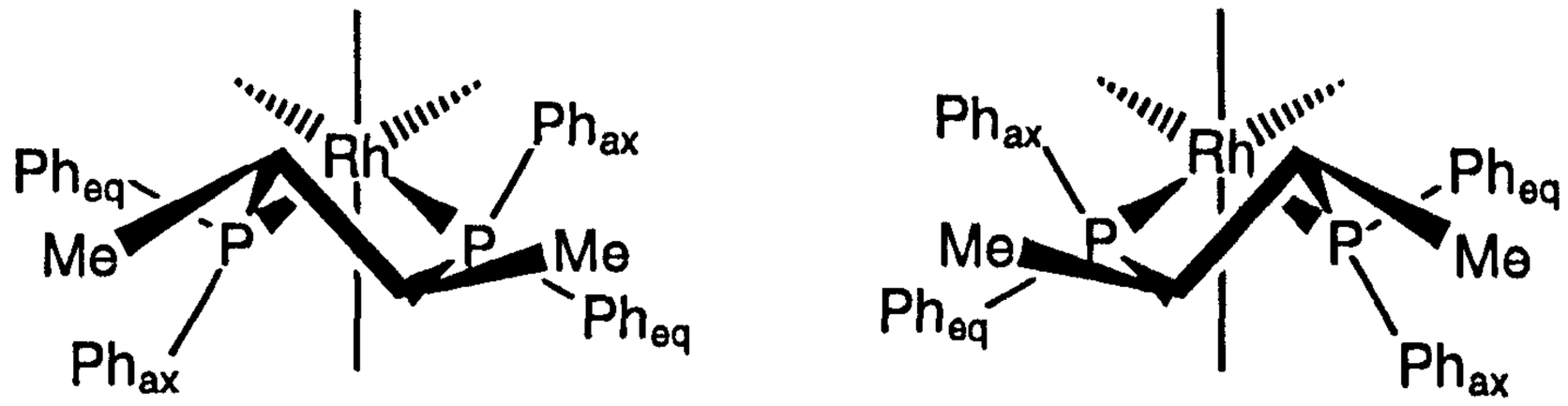

δ - preferred conformation for (*S,S*)-Chiraphos

λ - preferred conformation for (*R,R*)-Chiraphos

Figure 4.6: The chiral δ and λ conformations of the rhodium(Chiraphos) chelate ring

The rule predicts but does not explain the absolute stereochemistries of the products. Moreover, for important ligands like Et-Duphos **(4.22)**, which has a planar backbone, this rule does not apply. Quadrant diagrams[204] can be used to explain the origin of the optical inductions. Considering (*R,R*)-Chiraphos **(4.14)** and (*R,R*)-Dipamp **(4.20)** first and assuming Brown's postulate that a 'face-on' aryl ring is more sterically demanding than an 'edge-on' one,[131] then it is apparent from Figure 4.7 that one 'diagonal' is more sterically congested than the other.

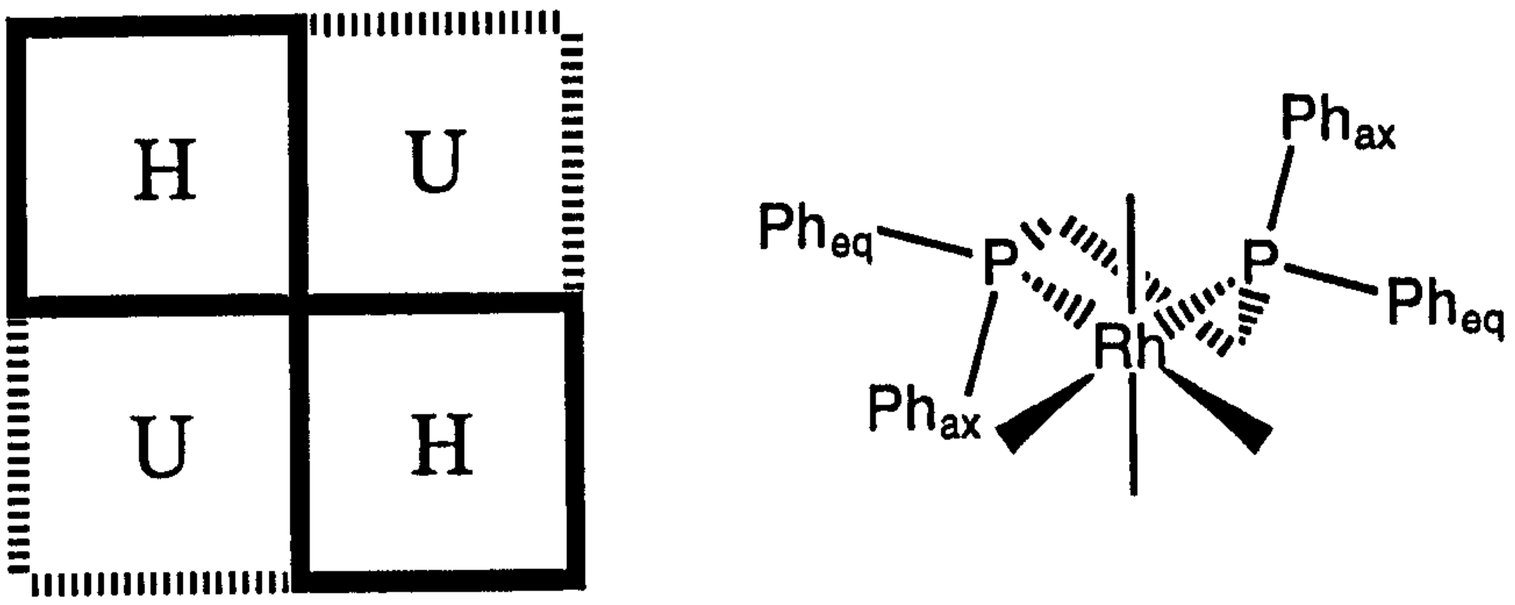

H = Hindered, 'face-on' equatorial Ph groups
U = Less hindered, 'edge-on' axial Ph groups

Figure 4.7: Quadrant blocking in the preferred λ conformation of (*R*,*R*)-Chiraphos (**4.14**) and (*R*,*R*)-Dipamp (**4.20**)

If we now look at the corresponding quadrant diagram for methyl-(*Z*)-2-acetamidocinnamate (**4.13**), then it is apparent that the same diagonal is more hindered for *re*-face coordination and less hindered for *si*-face coordination, see Figure 4.8. Thus, *si*-face coordination is the more energetically favoured.

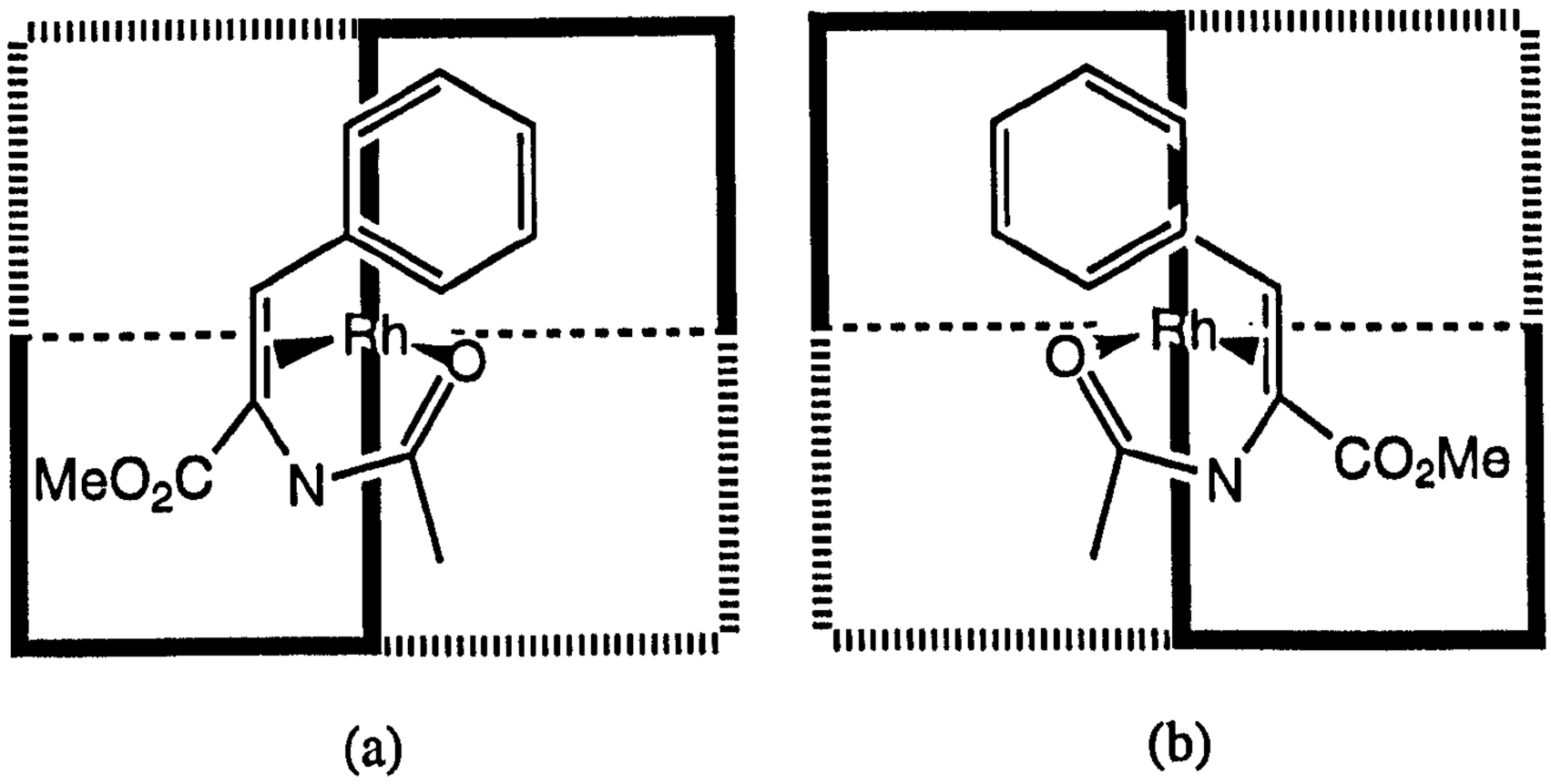

Figure 4.8: Quadrant blocking by the substrate methyl-(*Z*)-2-acetamidocinnamate (**4.13**) for (a) *si*-face and (b) *re*-face coordination

Halpern showed[177,182,189] that the less stable rhodium-substrate complex is the one that reacts to form the major product enantiomer. From the quadrant arguments presented above, this corresponds to *re*-face coordination. Hence the quadrant model correctly predicts that the (*S*)-amino acid derivative will predominate.

If we now consider Burk's proposed quadrant diagram for (*R*,*R*)-Et-Duphos (**4.22**),[199] see Figure 4.9, it is apparent that the diastereomer of the rhodium-substrate complex that is most hindered, and consequently least stable, is the one in which the substrate is bound to the *re*-face, *cf.* Figures 4.8 and 4.9.

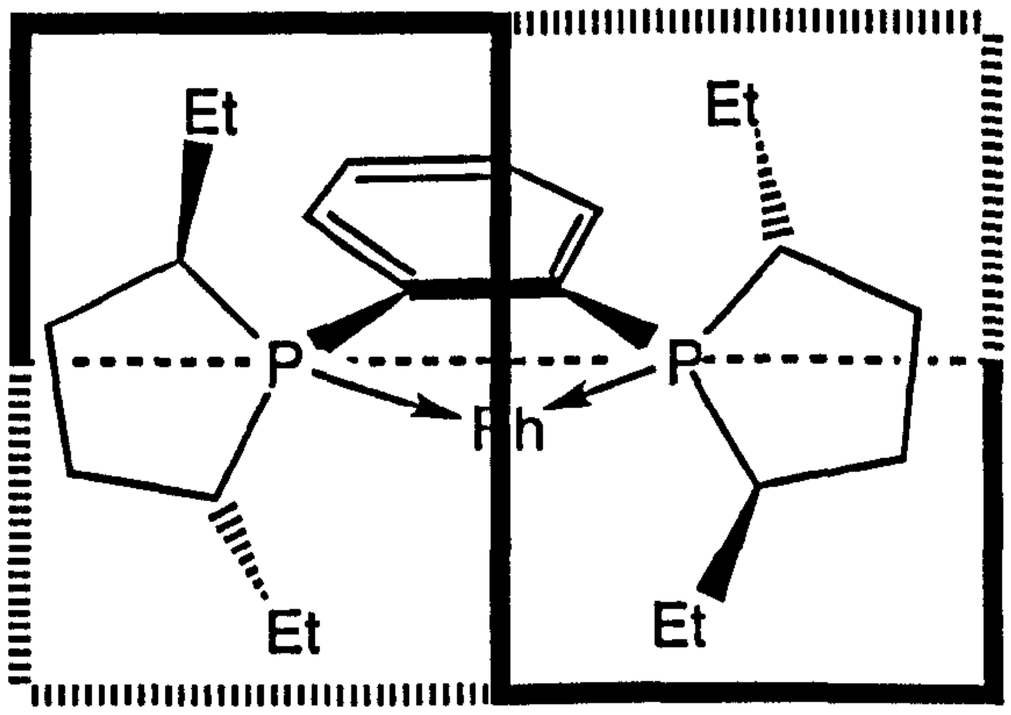

Figure 4.9: Burk's proposed quadrant blocking by (*R*,*R*)-Et-Duphos (**4.22**)

Thus, it might be expected that the (*S*)-amino acid derivative would be produced. The observed production of the (*R*)-enantiomer implies one of two possibilities; either the reaction is proceeding *via* the more stable rhodium-substrate complex for this ligand system or the quadrant diagram proposed does not accurately represent the steric blocking of the Et-Duphos ligand. Preliminary mechanistic work by Burk and Brown[205] has indicated that this system is in fact no different from the other rhodium-diphosphine catalysts and that the minor, less stable rhodium-substrate diastereomer present is the one that gives the major enantiomer of the product. If the quadrant diagram for (*R*,*R*)-Et-Duphos (**4.22**) were as shown in Figure 4.10 then the observed results with this ligand would be explicable.

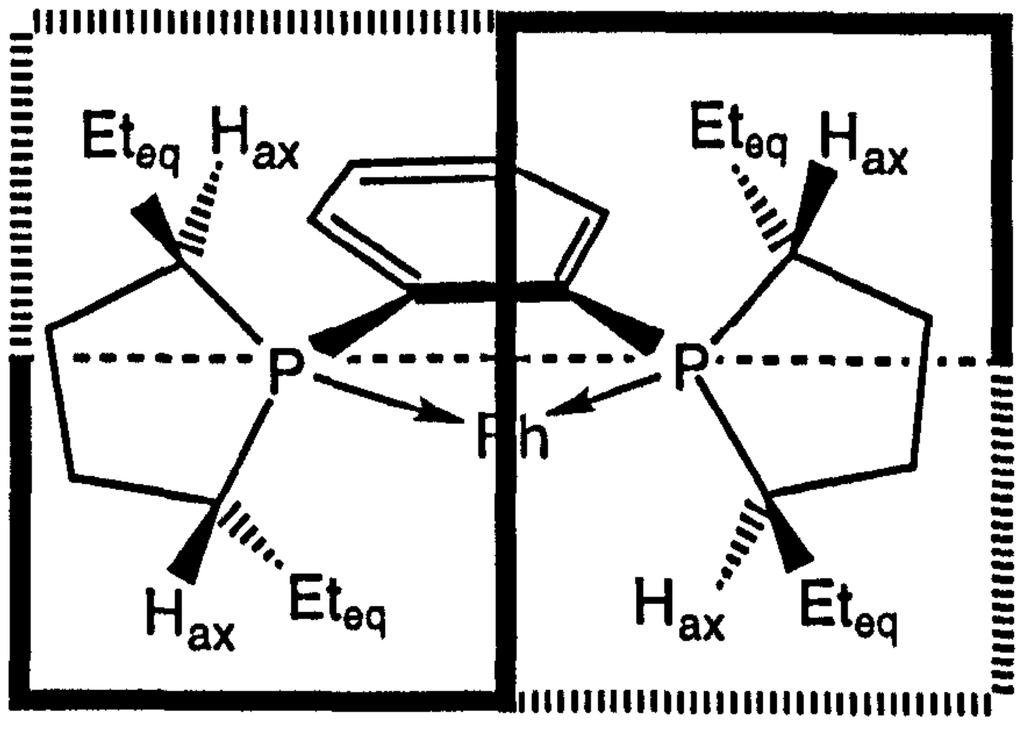

Figure 4.10: Proposed quadrant blocking by (*R*,*R*)-Et-Duphos (**4.22**)

Using the following reasoning this proposal can be justified. The ethyl groups may be fixed in pseudo-equatorial positions in the five-membered rings, which place the *ipso*-hydrogens in pseudo-axial positions, see Figure 4.10. It may be that it is these atoms that are sterically limiting, thereby causing the diastereomer of the rhodium-substrate complex in which the substrate is bound to the *si*-face to be the most hindered and consequently less stable. Hydrogenation of this species would then lead to the observed (*R*)-amino acid derivative.

The crystal structure of [Rh(cod){(*S*,*S*)-Me-Duphos}] is shown in Figure 4.11.[199] Considering the phospholane ring in the foreground, it can be seen that the hydrogen atom H(18A) is in an axial position whilst the methyl group $H_3C(19)$ is in an equatorial position. They appear to be of similar steric bulk and it is clear that detailed molecular modelling is required to study the exact interactions that occur when the substrate binds to the complex. It is suffice to say that at this point a quadrant diagram cannot be predicted with any certainty.

Brown[131] and Bosnich[181] have modelled in detail the side-on (parallel) approach of H-H. The two Rh-H distances are kept equal throughout the addition since the reaction has a late transition state and the work of Dedieu[206] has shown that end-on (perpendicular) H-H approach is only energetically feasible during the early stages of the reaction. The H_2 molecule was positioned such that its midpoint was located on the axis perpendicular to the square plane, with the H-H bond parallel to either the P-Rh-O or the P-Rh-C axes. This leads to four possible trajectories of H_2 approach for each of the diastereomers (**4.16**), two above and two below the square plane,[207] see Figure 4.12.

Both Brown and Bosnich came to the same conclusion utilising different molecular graphics procedures that, of the four possible trajectories per diastereomer, only one route is sterically feasible for each diastereomer: trajectory C in Figure 4.12 where the H_2 molecule approaches from below the square plane along the P-Rh-O axis resulting in formation of the diastereomers $(\mathbf{4.17})^{si}$ and $(\mathbf{4.17})^{re}$ which have one Rh-H bond aligned in such a fashion that transfer to the β-olefinic carbon is stereoelectronically favoured, see Equation 4.2.[208] This β-hydride migration proceeds rapidly and irreversibly[178,209] to form the alkylhydride species $(\mathbf{4.18})^{si}$ and $(\mathbf{4.18})^{re}$ respectively, which have been observed spectroscopically at low temperatures.[210]

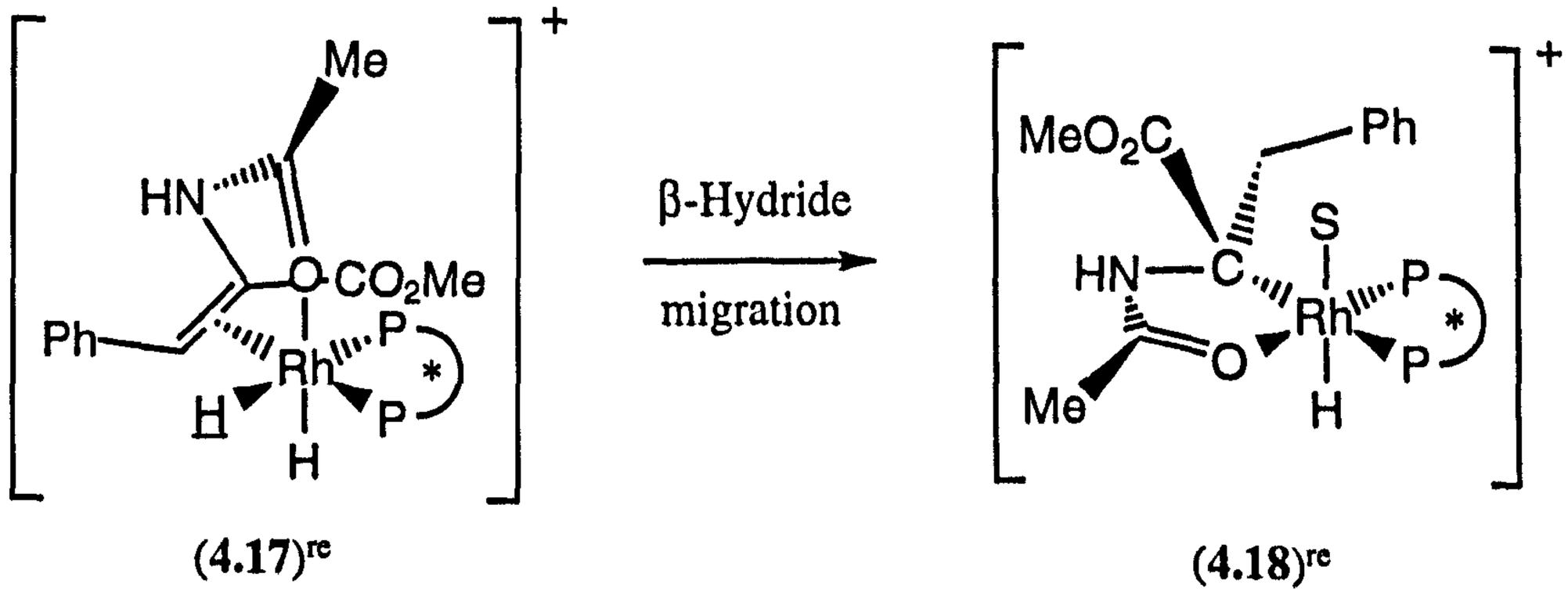

$(\mathbf{4.17})^{re}$ $(\mathbf{4.18})^{re}$

Equation 4.2

The final step in the cycle is reductive elimination[209] of the (*S*)- and the (*R*)-products from $(\mathbf{4.18})^{re}$ and $(\mathbf{4.18})^{si}$ respectively, regenerating the species $[RhP_2^*S_2]^+$ (**4.15**) and completing the catalytic cycle.

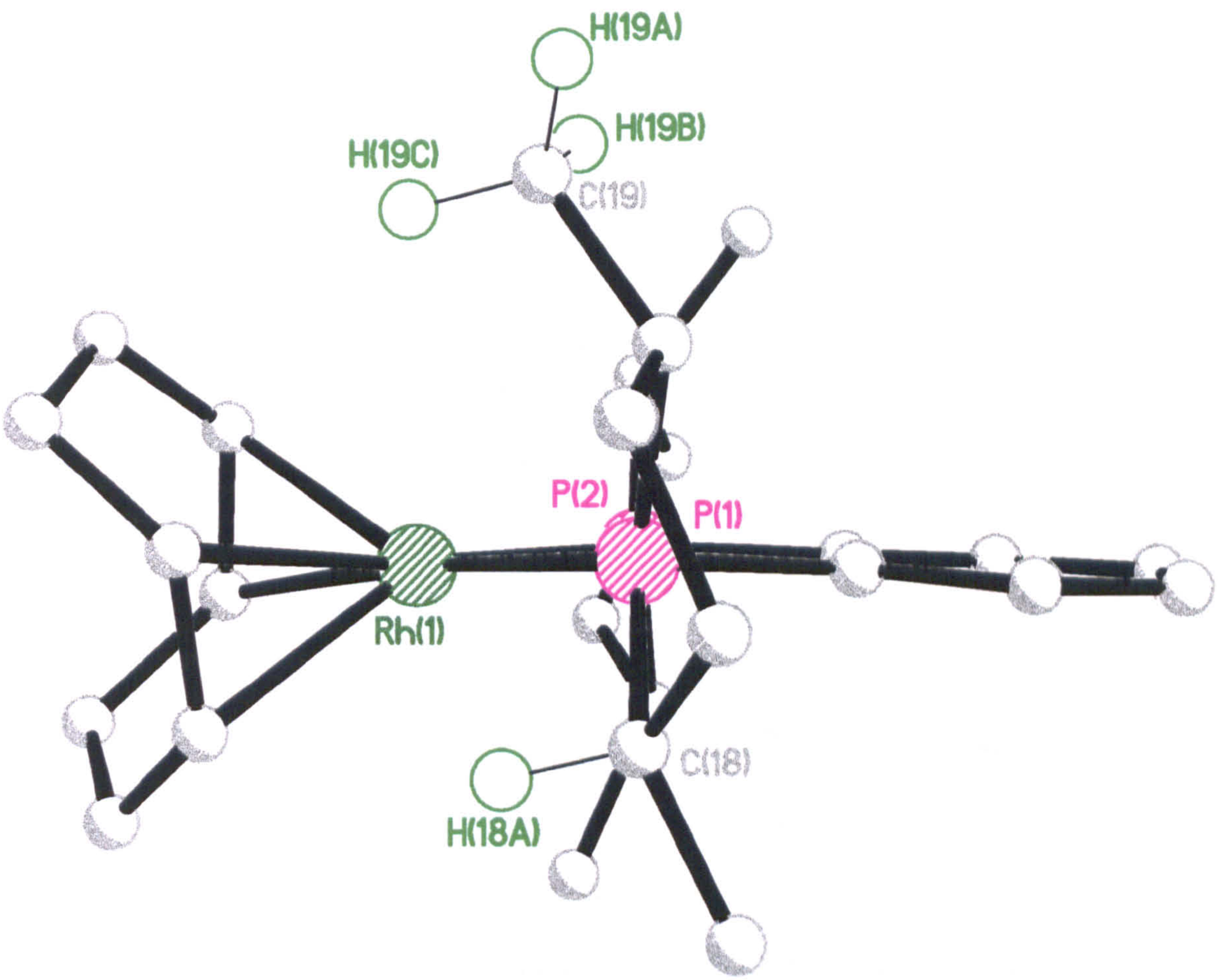

Figure 4.11: Molecular structure of [Rh(cod){(*S*,*S*)-Me-Duphos}]. All hydrogen atoms except H(18) and H(19A-C) are omitted for clarity

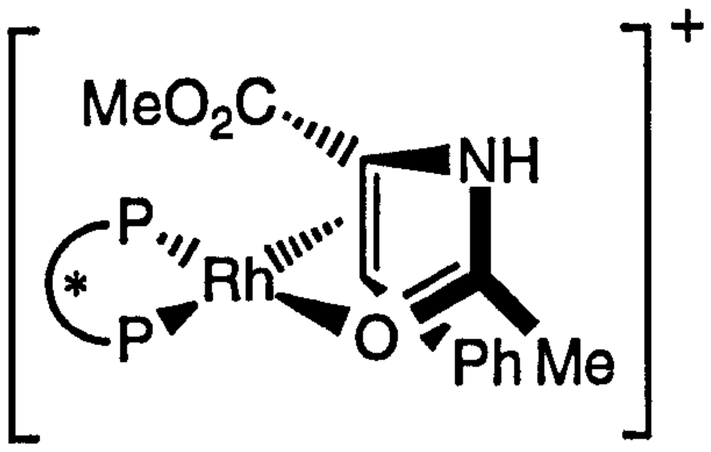

Cooordination
to *si*-face.
(4.16)^{si}

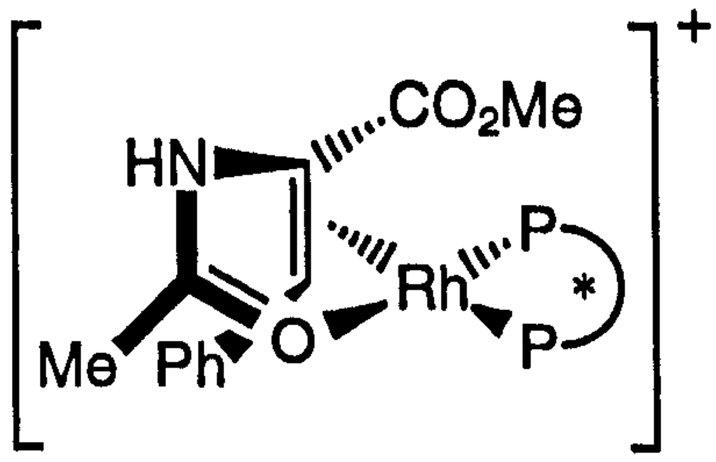

Cooordination
to *re*-face.
(4.16)^{re}

Attack from top face along P-Rh-O axis, trajectory A

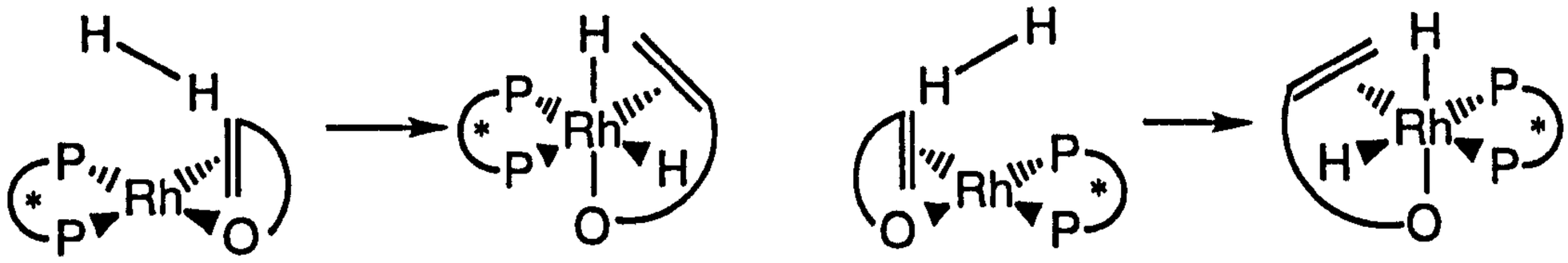

Attack from top face along P-Rh-C_α axis, trajectory B

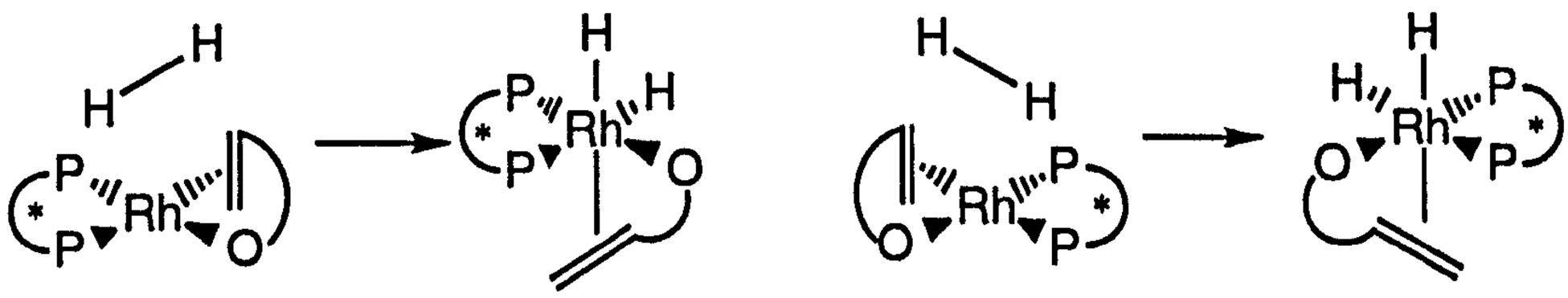

Attack from bottom face along P-Rh-O axis, trajectory C

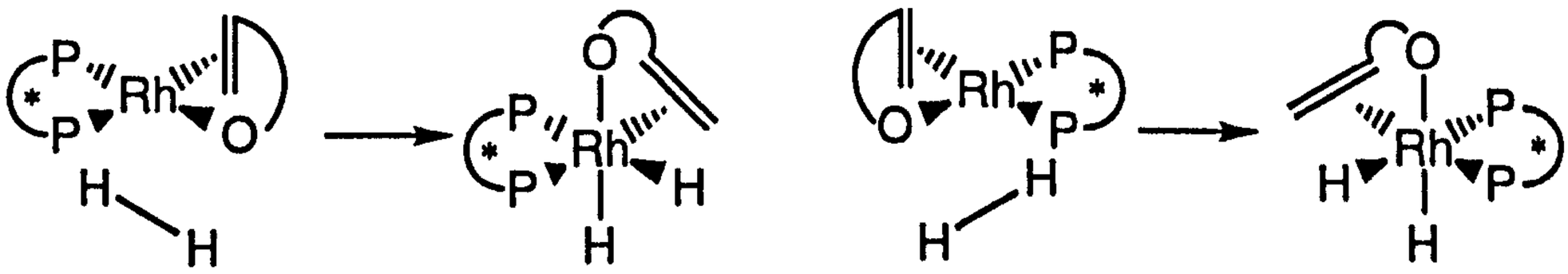

Attack from bottom face along P-Rh-C_α axis, trajectory D

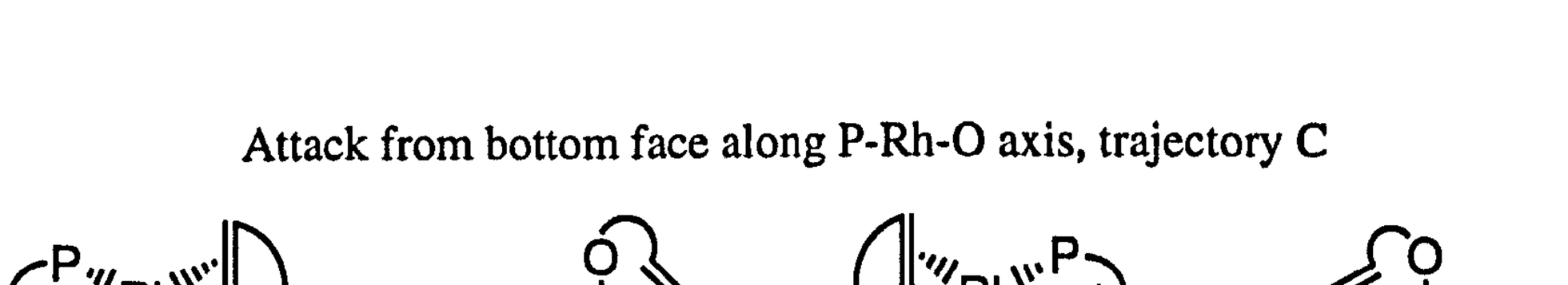

Figure 4.12: The possible trajectories of the H_2 molecule during its oxidative addition to the major and minor diastereomers of complex (*R*,*R*)-(**4.16**)

4.1.3 State-of-the-art asymmetric hydrogenation systems

More than a thousand chiral diphosphines have been synthesised and most of these have been tested for asymmetric α-enamide hydrogenation.[72,211,212] Consequently there have been several surveys of the available ligands and substrates.[213] In this Section diphosphines with the greatest potential for the manufacture of α-amino acids *via* asymmetric hydrogenation are reviewed. These chiral diphosphine ligands are illustrated in Figure 4.13 and the enantioselectivities obtained in the hydrogenation of a set of (*Z*)-α-enamide derivatives using cationic rhodium(I) catalysts derived from these diphosphines are depicted in Table 4.1.

Most of the ligands listed perform well with (*Z*)-2-amidocinnamic acid derived substrates which have a β-phenyl substituent. However, the enantioselectivities usually fall sharply when substituted β-phenyl groups are present[215] or, as can be seen from Table 4.1, if β-alkyl substituted α-enamides are hydrogenated. It can also be seen from Table 4.1 that the hydrogenation of methyl-2-acetamidoacrylate (**4.31**) proceeds with roughly the same or slightly lower enantioselectivity than the hydrogenation of methyl-(*Z*)-2-acetamidocinnamate (**4.13**). The significance of this final observation will be apparent when the results obtained for our ligands are considered in the next Section.

It is evident that the best (and most general) hydrogenation system for this type of substrate is the rhodium(Et-Duphos) complex which also has the ability to hydrogenate a wide variety of α-enamides bearing β-aryl and β-alkyl substituents with high enantioselectivities.[199,200] The cationic rhodium(Et-Duphos) catalyst has many other advantages. It is extremely efficient (substrate to catalyst ratios of 50000:1), robust and tolerates a wide range of solvents and functionality within the substrate. Further, in contrast to virtually all the other systems in Table 4.1, little or no temperature and pressure dependence is shown. Finally, the rhodium(Et-Duphos) and rhodium(BPE) catalysts will hydrogenate β,β-disubstituted α-enamides with high enantioselectivities.[201]

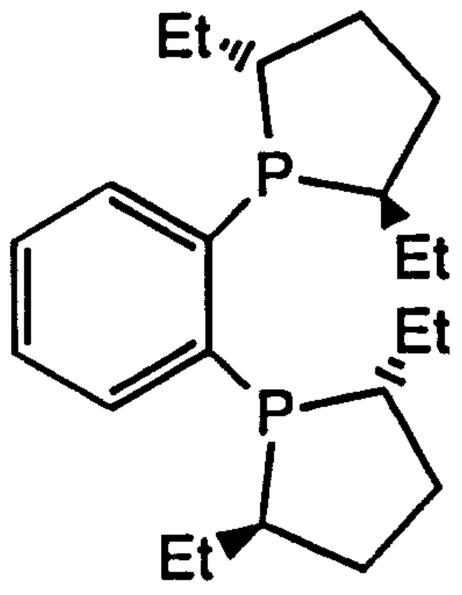

(4.22), Et-Duphos

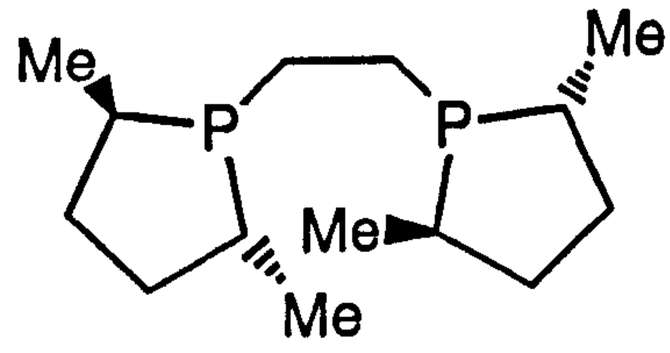

(4.24), Me-BPE

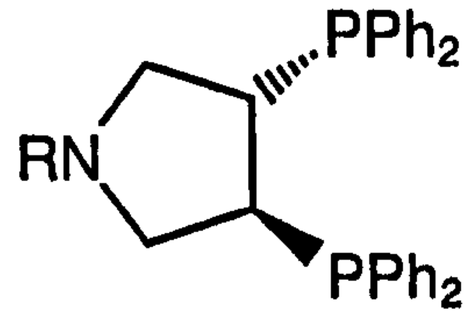

(4.25), Deguphos

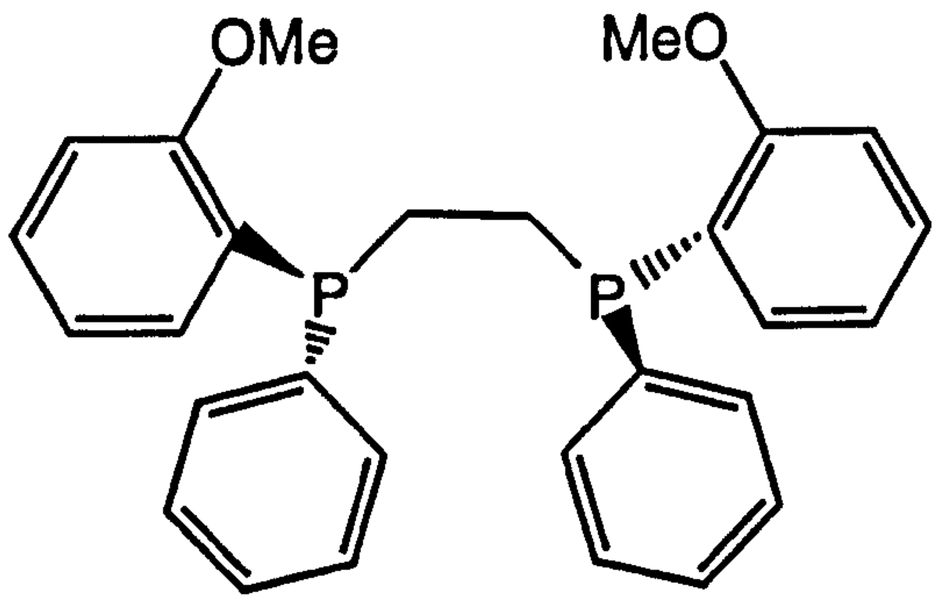

(4.20), Dipamp

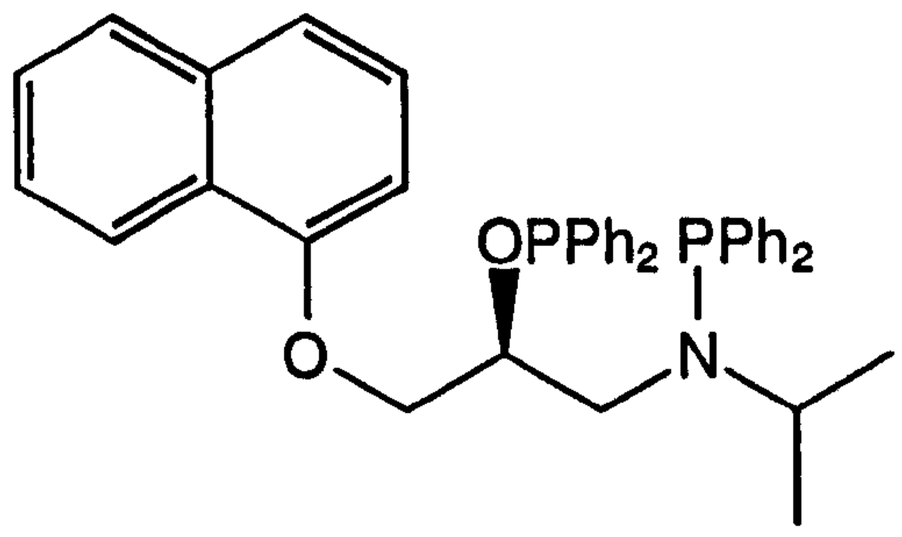

(4.26), Propraphos

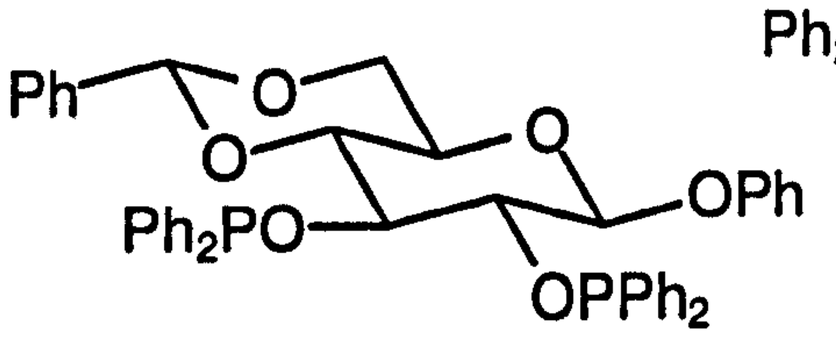

(4.27), 2,3-Carbophos

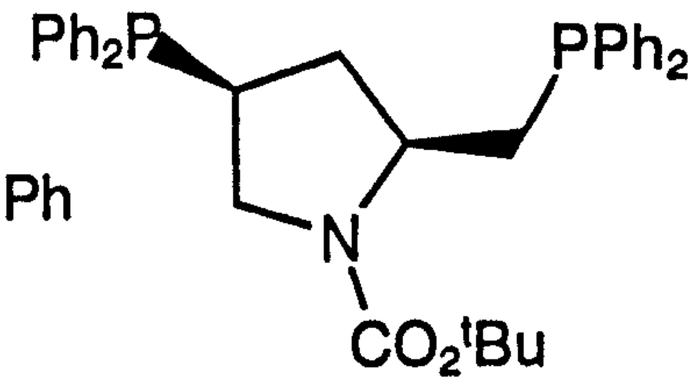

(4.28), BPPM

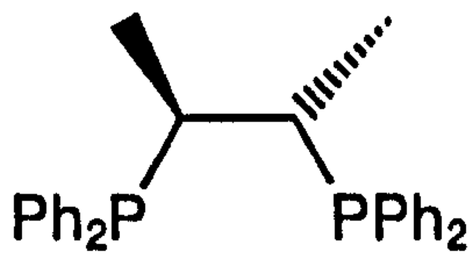

(4.14), Chiraphos

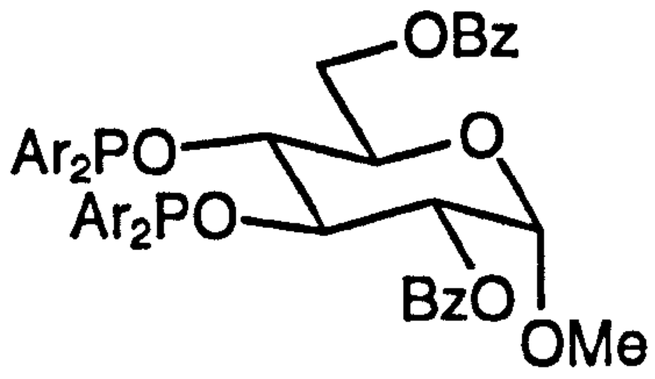

(4.29), 3,4-Carbophos

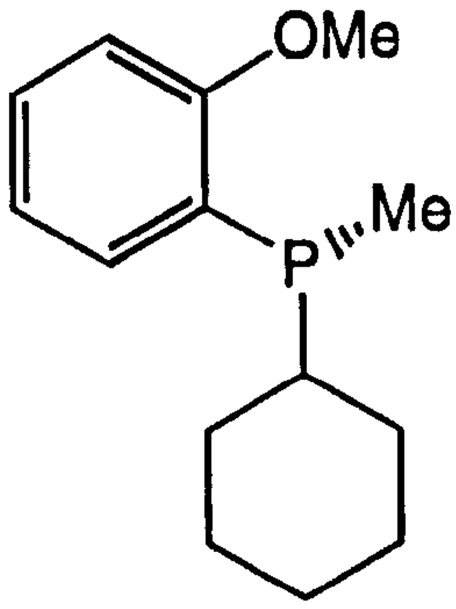

(4.21), Camp

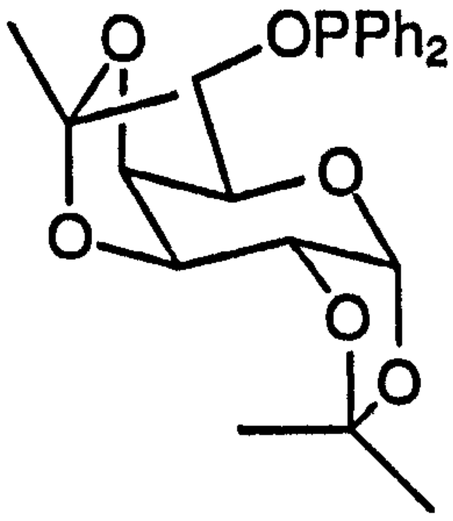

(4.30)

Figure 4.13: The best diphosphine ligands for the asymmetric hydrogenation of α–enamides

Table 4.1: Enantioselectivities obtained[a] in the asymmetric hydrogenation of a range of (Z)-α-enamide derivatives using cationic rhodium(I) complexes of ligands (**4.22**)-(**4.30**)

Substrate	**4.22**[b]	**4.24**[c]	**4.25**[d]	**4.20**[e]	**4.26**[f]	**4.27**/ **4.29**[g]	**4.28**[h]	**4.14**[i]	**4.21**	**4.30**
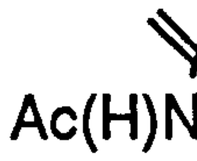	99	86C**H**	---	95	---	91	82	79	---	---
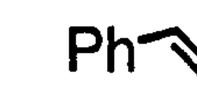	99	85[j]	99	94	88	99	91	89	86	67[k]
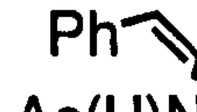	99	---	93	96	86	96	93	85	---	---
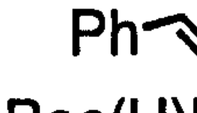	99	---	---	95	93	87	82	---	---	---
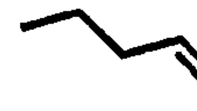	99	---	---	96	---	---	80	82	---	---
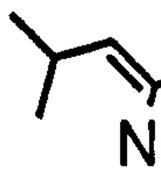	99	---	---	65	---	86	57	71	---	---
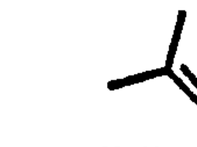	...	98	15	55	---	26	0	---	---	---

a Data from the indicated literature references. Hydrogenations were, unless otherwise noted, carried out using cationic catalyst precursors of the type [Rh(cod)(diphosphine)]X, (X=BF_4^-, PF_6^-, SbF_6^-, OTf^-).

b Ref. 199,200

c Ref. 201

d Ref. 214

e Ref. 190,215,216

f Ref. 217-219

g Ref. 220,221

h Ref. 215,216,222

i Ref. 194,216

j Ref. 223

k Catalyst prepared *in situ* from [{Rh(μ-Cl)(diene)}$_2$].

However, the main drawback of these ligands is the fact that they are synthesised *via* lengthy and challenging procedures. For example, the syntheses of the Duphos and BPE ligands are shown in Scheme 4.6.

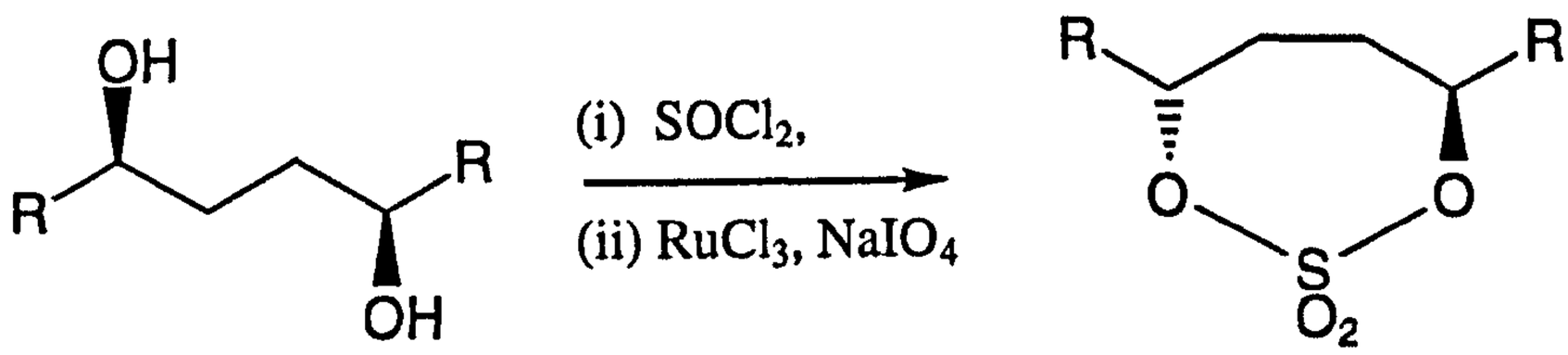

(4.32) **(4.33)**

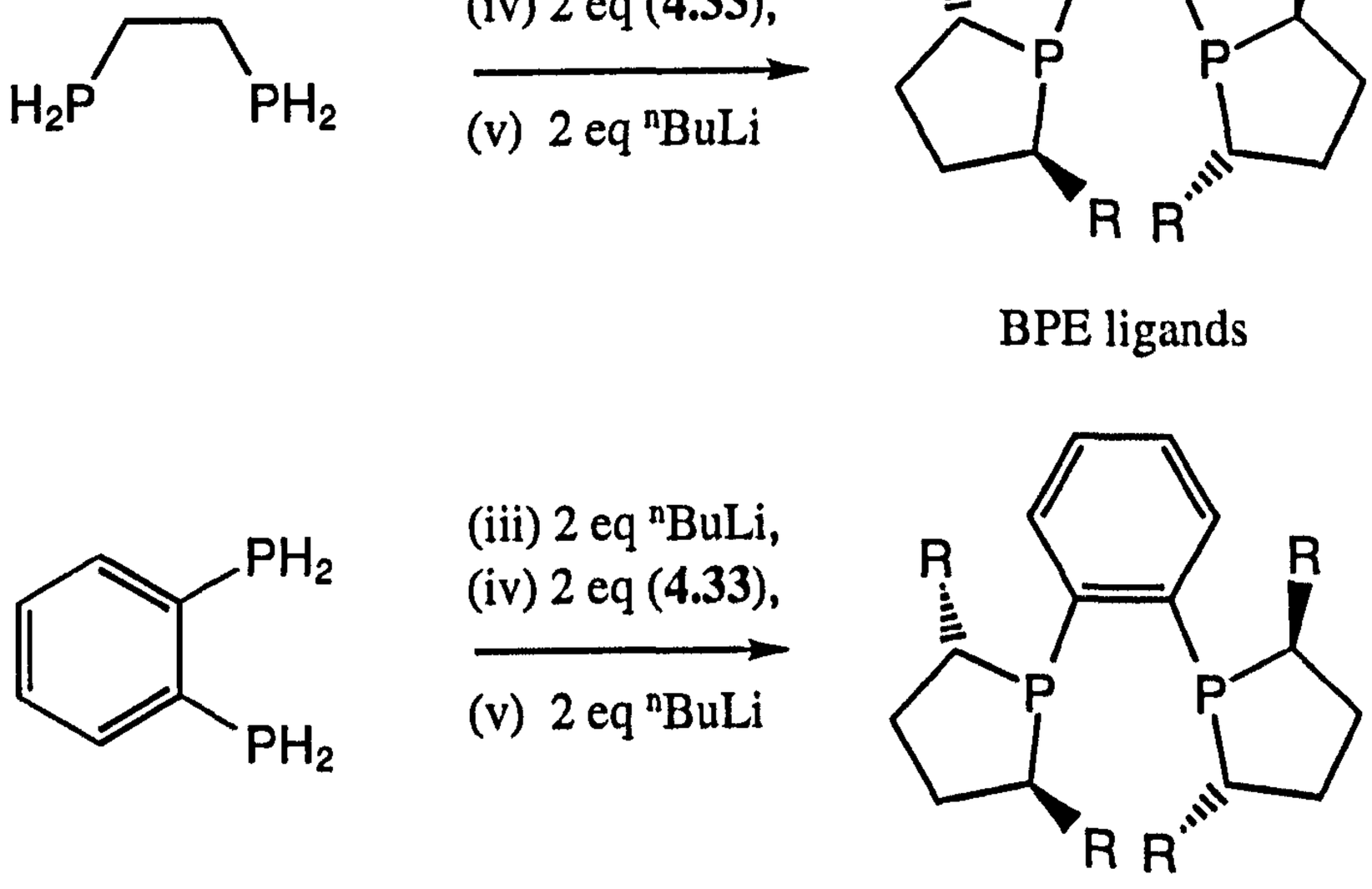

Scheme 4.6: The syntheses of the Duphos and BPE ligands

The two primary diphosphines are exceptionally air sensitive and difficult to handle. Further, the optically active diols (**4.32**) are themselves prepared *via* a three step procedure. Consequently, the price of both these, and other, commercially available ligands is high, even compared to the high costs of the rhodium precursors, see Table 4.2.

Table 4.2: Typical prices[a] for the chiral ligands (**4.22**), (**4.24**) and (**4.14**)

Ligand	Quantity	Price
$RhCl_3$	250 mg	£40
Et-Duphos (**4.22**)	500 mg	£220
Me-BPE (**4.24**)	500 mg	£240
Chiraphos (**4.14**)	1 g	£125

a Prices from the 1998/1999 Strem catalogue.

This highlights one of the key features of phosphite and phosphonite chemistry and one of the advantages of employing these types of ligands where possible, namely that they are comparatively easy to synthesise by reaction of one of a wide range of cheap, readily available optically pure diols with the appropriate phosphorus electrophile. A more detailed discussion of the syntheses of phosphonites and phosphites is presented in Chapter 1.

The phosphine ligand Camp (**4.21**) and the phosphinite (**4.30**) have been included in Table 4.1 since they represent the best enantioselectivities obtained in the asymmetric hydrogenation of α-enamides employing cationic rhodium(I) complexes of monodentate phosphorus(III) ligands. Camp (**4.21**) is chiral at phosphorus but, importantly, contains the *ortho*-anisyl group which, as discussed in the previous Section, has been proposed to be important for asymmetric induction.[196-198] The monophosphinite (**4.30**) on the other hand is a monodentate version of the diphosphinites (**4.27**) and (**4.29**).[220,221] However, the enantioselectivity achieved with (**4.30**) is significantly lower than with the diphosphines above; a demonstration of the observation that enantioselective catalysis is generally much more effective with bidentate, preferably C_2-symmetric, ligands.

4.2 Cationic rhodium(I)-phosphonite complexes as catalysts for asymmetric hydrogenation

This Section will describe the preliminary studies that we have undertaken to investigate the potential of rhodium(I)-phosphonite complexes as catalysts for asymmetric hydrogenation. Due to both time constraints and the preliminary nature of this work we have endeavoured to screen the rhodium(I) complexes of several ligands in the asymmetric hydrogenation of several substrates in order to gain an overview of their potential rather than concentrate on optimising the conditions for one particular ligand with one given substrate.

The results are broken down into two subsections. The first describes the catalysis using the rhodium(I) complex (*S,S*)-(**4.34**) of monophosphonite (*S*)-(**4.35**)

derived from (*S*)-biphenanthrol and includes, for comparison, the unpublished results obtained in our group by Martorell and Pringle using the rhodium(I) complex (*S,S*)-(**4.36**) of monophosphonite ligand (*S*)-(**4.37**) derived from (*S*)-binaphthol.

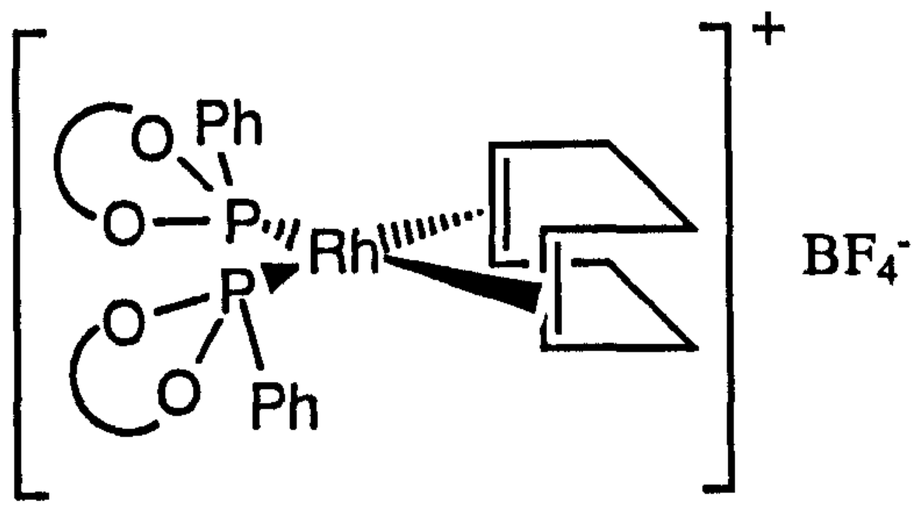

(*S,S*)-(**4.34**) when 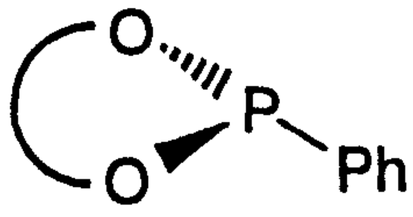 = (*S*)-(**4.35**)
(*S,S*)-(**4.36**) = (*S*)-(**4.37**)

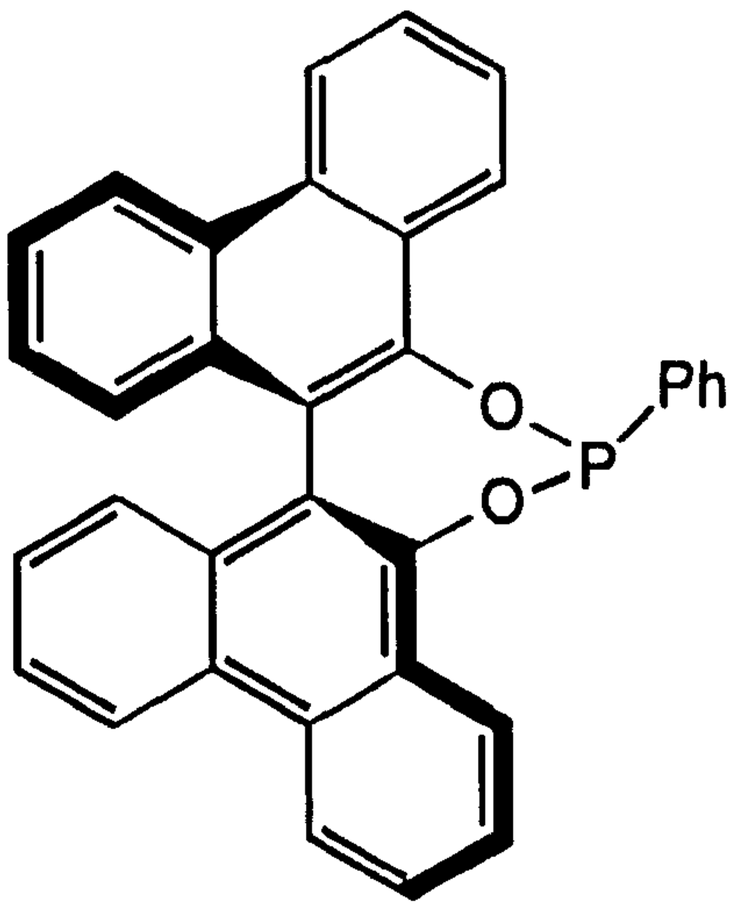

(4.35)

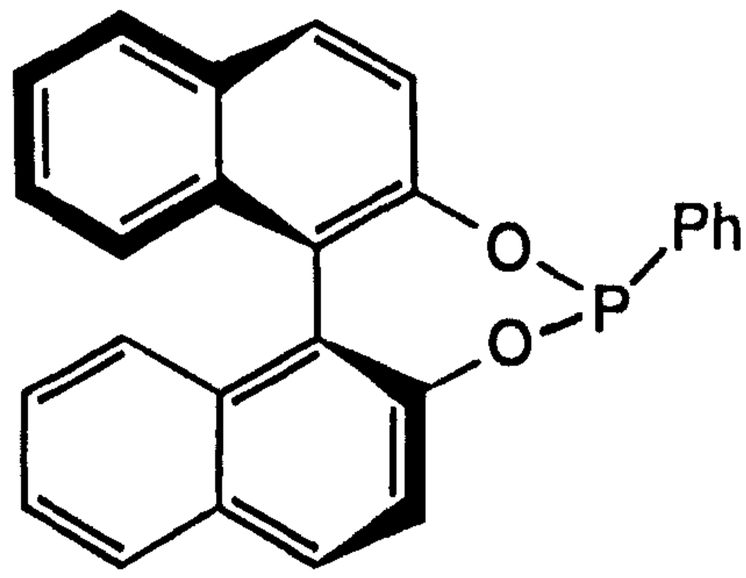

(4.37)

This comparison allows the influence of the more bulky ligand (**4.35**) upon both the catalytic activity and the enantioselectivity to be studied.

The second subsection describes the results obtained using the rhodium(I) complex (*S,S*)-(**4.38**) of diphosphonite ligand (*S,S*)-(**4.39**) derived from (*S*)-biphenanthrol and includes, for comparison, those obtained by Reetz[18] using the rhodium(I) complex (*R,R*)-(**4.40**) of the binaphthol analogue (*R,R*)-(**4.41**).

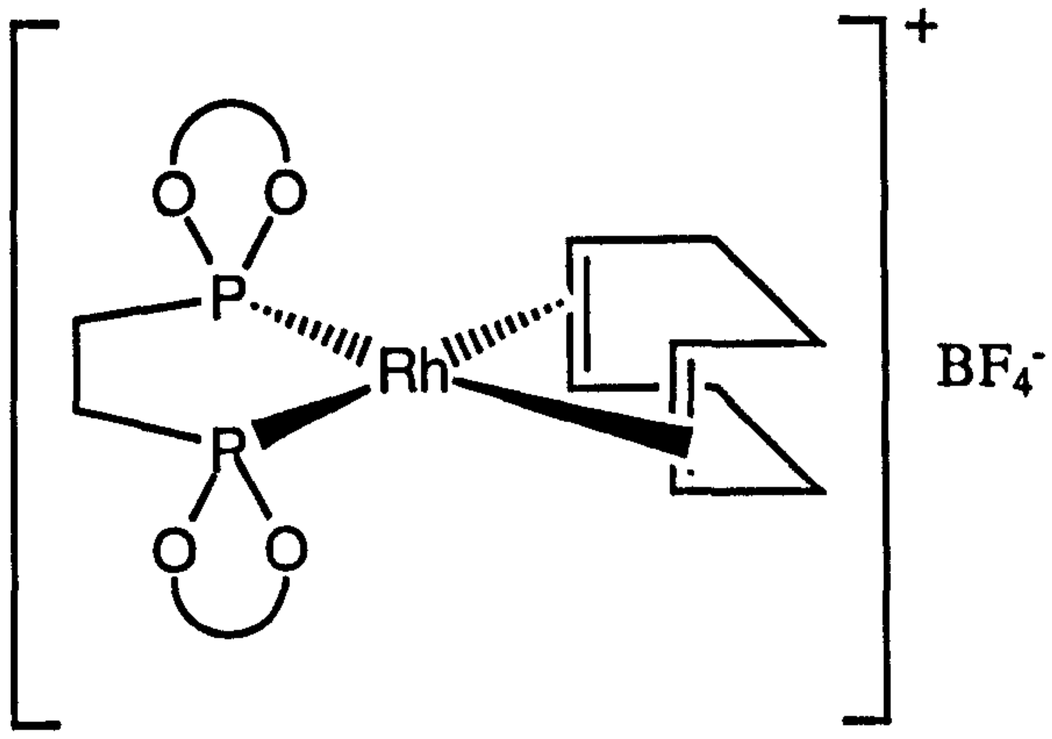

(4.38) when 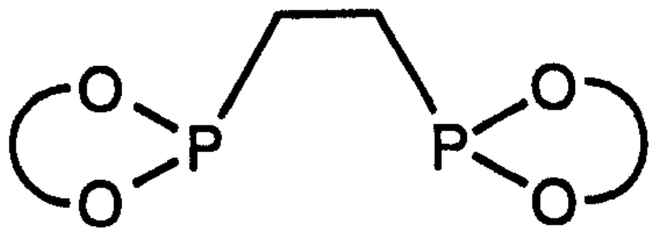 = **(4.39)**
(4.40) **(4.41)**

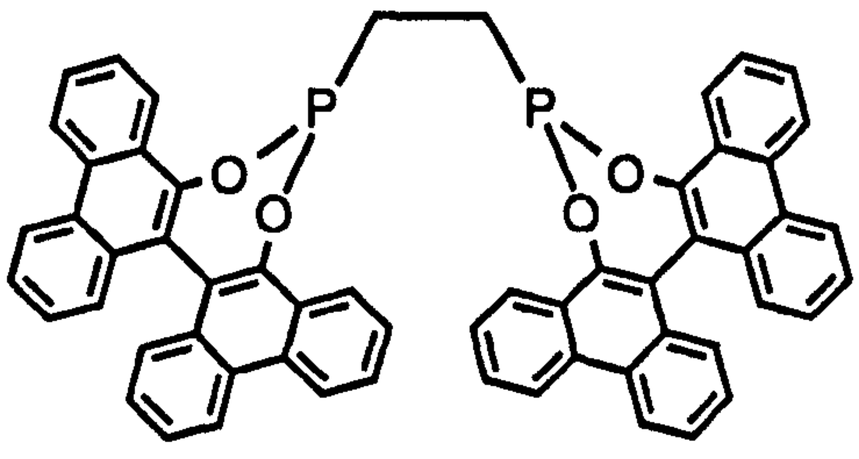

(4.39)

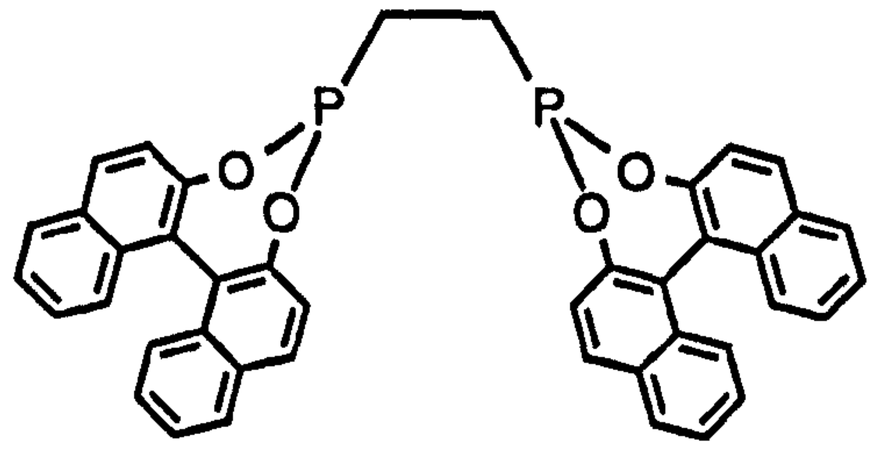

(4.41)

Once again this comparison allows the influence of the increased steric bulk of the biphenanthrol-derived ligand (**4.39**) upon the catalytic activity and the enantioselectivity to be studied.

This subsection also includes the catalytic performance of the rhodium(I) complex (*S*)-(**4.42**) of the mixed, C_1-symmetric phosphinophosphonite ligand (*S*)-(**4.43**) derived from (*S*)-biphenanthrol. The results from this system offer the opportunity to examine the influence upon catalysis of both the mixed electronic properties of the two phosphorus atoms and the C_1-symmetry of the ligand.

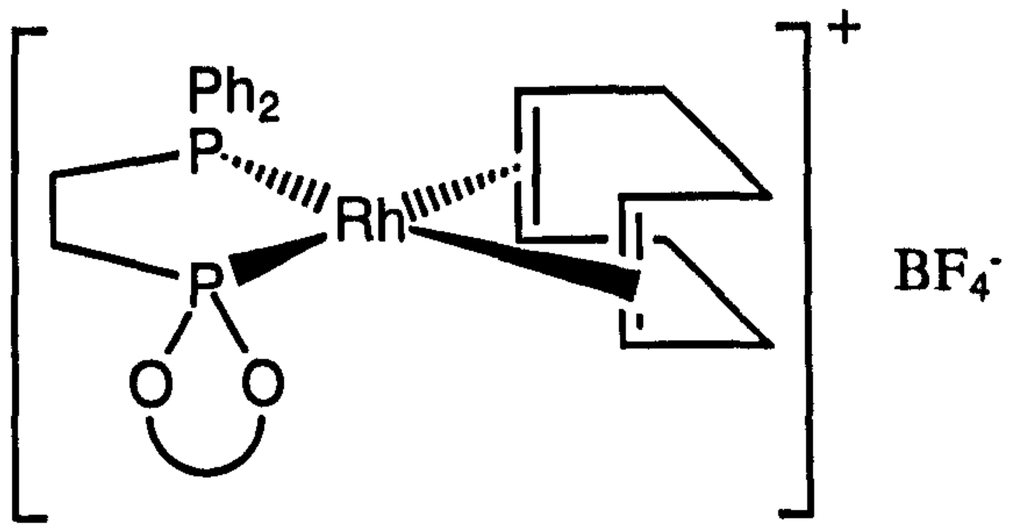

(*S*)-(**4.42**)

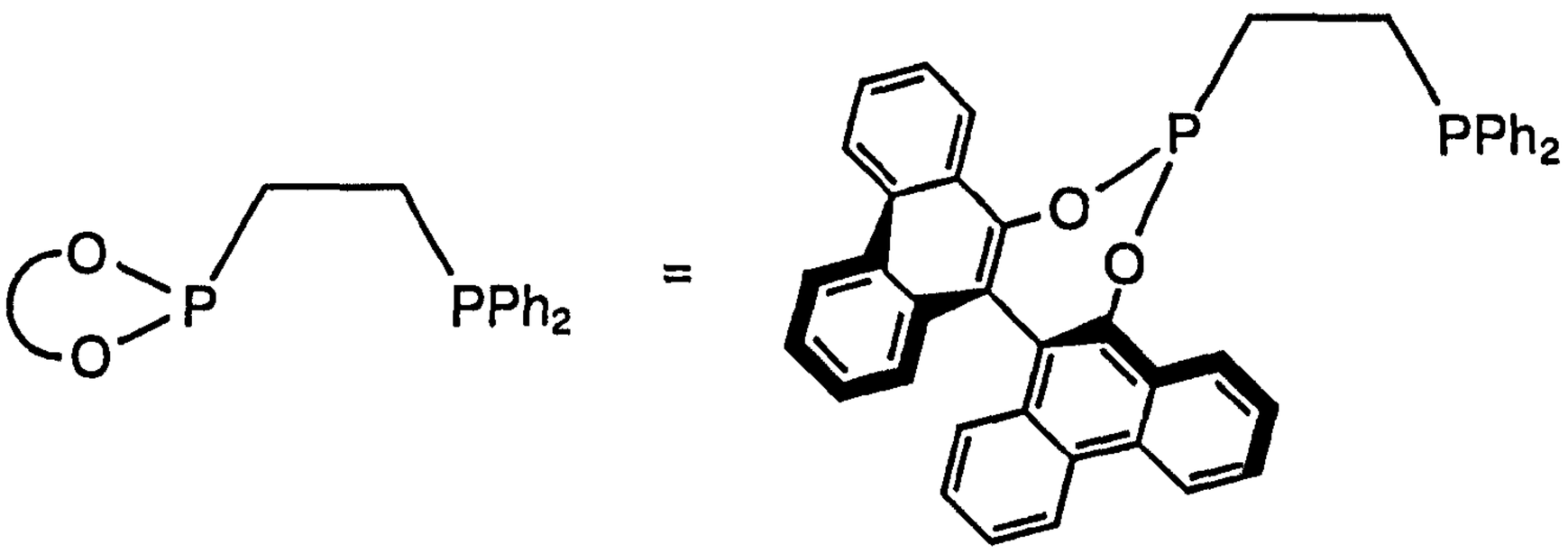

(*S*)-(**4.43**)

4.2.1 Monophosphonites

As discussed in Chapter 1, the asymmetric catalytic hydrogenation of α-enamides has emerged as one of the most practicable and cost effective routes to a diverse array of both (D)- and (L)-α-amino acids. In fact the asymmetric hydrogenation of α-enamides such as methyl-2-acetamidoacrylate (**4.31**) now often serves as a benchmark for assessing the relative effectiveness of new chiral ligands. Hence, the rhodium(I) complex (*S,S*)-(**4.36**) was tested by Martorell and Pringle for the asymmetric hydrogenation of methyl-2-acetamidoacrylate (**4.31**) in order to examine the effectiveness of the monophosphonite ligand (*S*)-(**4.37**),[36] see Equation 4.3.

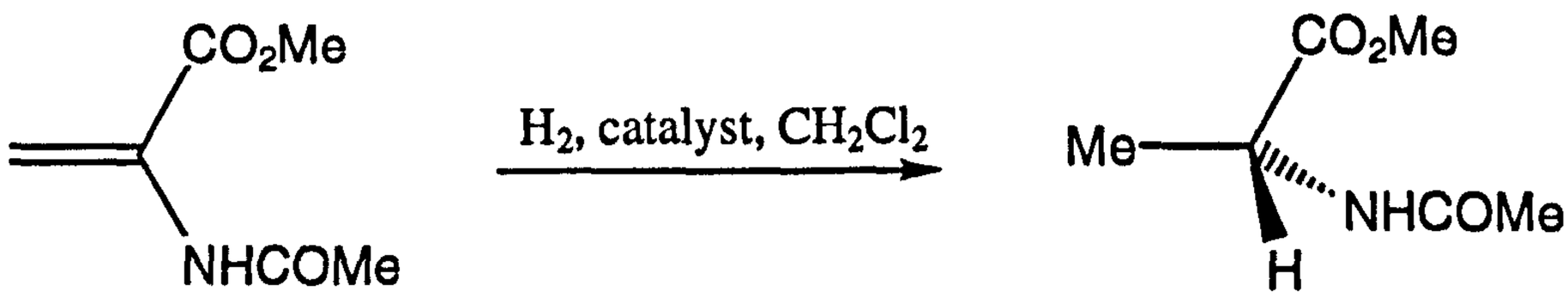

(4.31) **(*R*)-(4.44)**

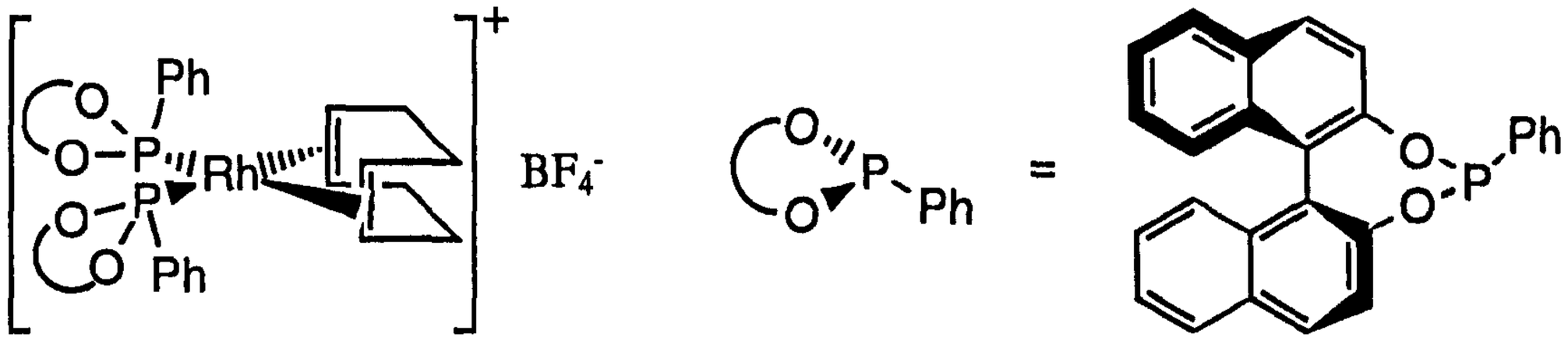

Catalyst: (*S,S*)-(**4.36**) (*S*)-(**4.37**)

Equation 4.3

The optical yield for this reaction is 73% and conversion is quantitative. The high enantioselectivity is significant because enantioselective hydrogenation catalysis is generally only effective with bidentate, preferably C_2-symmetric, ligands where the conformation is fixed by a rigid backbone. To the best of our knowledge this is the highest enantioselectivity for the asymmetric hydrogenation of methyl-2-acetamidoacrylate (**4.31**) obtained using a monodentate phosphorus(III) ligand and the first example of a monophosphonite effecting asymmetric induction in hydrogenation.

Why does the rhodium(I) complex (**4.36**) of monophosphonite (**4.37**) induce such high enantioselectivity? One possibility is that this coordinated ligand adopts a favoured conformation which leads to steric hindrance of one diagonal of the quadrant diagram. This conjecture relies on restricted rotation about the M-P bonds, which is consistent with the broad $^{31}P\{^{1}H\}$ NMR spectrum obtained for complex (*S,S*)-(**4.36**).[36]

Heartened by this result, the rhodium(I) complex (*S,S*)-(**4.34**) was tested for the hydrogenation of both methyl-2-acetamidoacrylate (**4.31**) and methyl-(Z)-2-acetamidocinnamate (**4.13**), see Equation 4.4, so that a comparison between the ligands derived from biphenanthrol and binaphthol could be made.

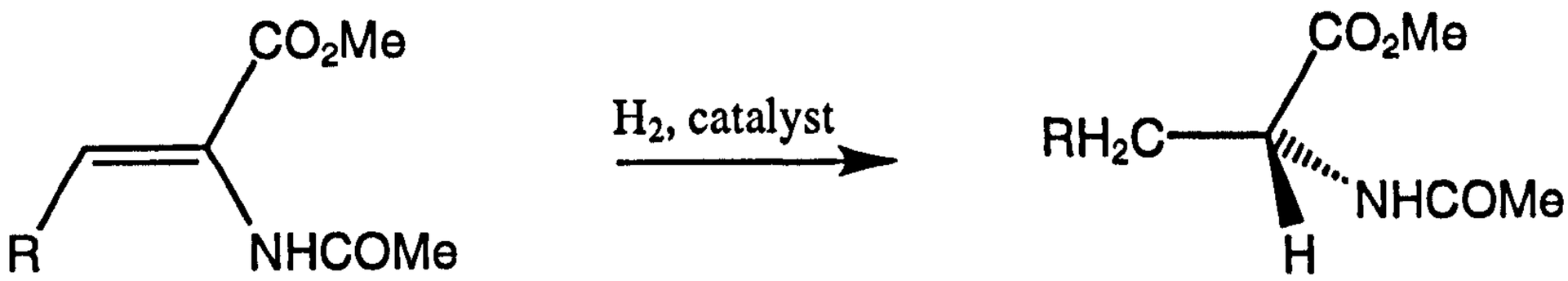

R = H, **(4.31)**
R = Ph, **(4.13)**

R = H, (*R*)-**(4.44)**
R = Ph, (*R*)-**(4.45)**

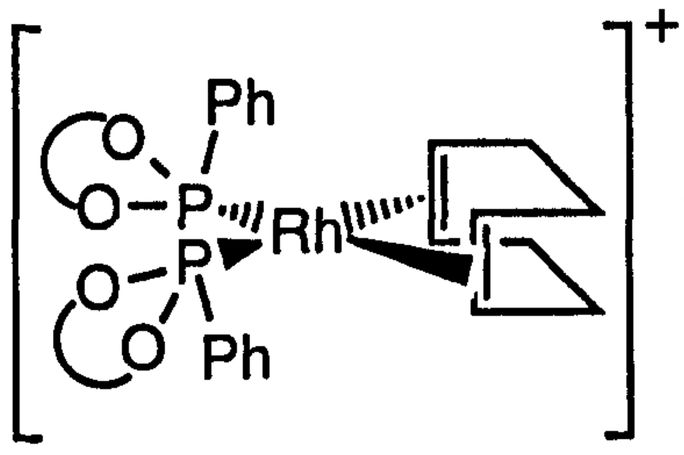

Catalyst: (*S,S*)-**(4.34)**

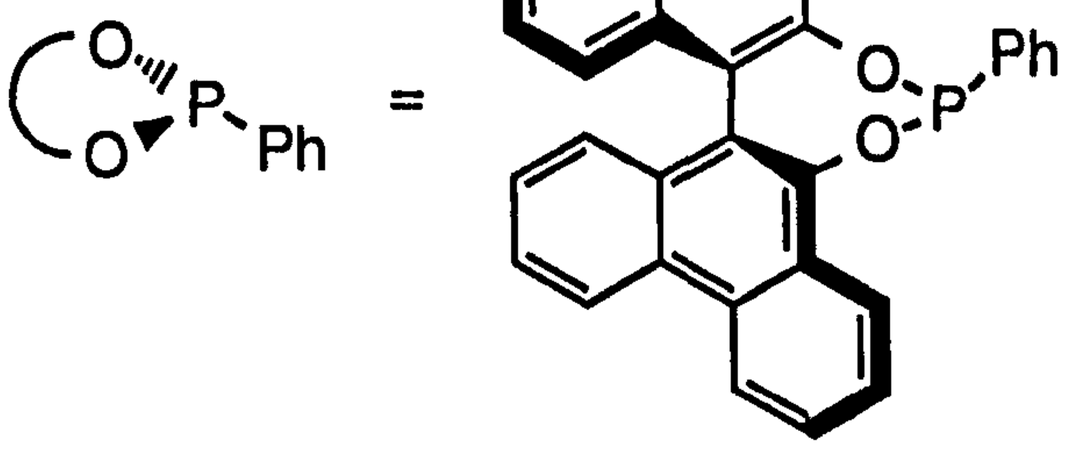

(*S*)-**(4.35)** .

Equation 4.4

The results are presented in Table 4.3. Entries 1-4 are the results obtained by Martorell and Pringle[36] with complex (*S,S*)-**(4.36)** whilst Entries 5-10 are the author's work with complex (*S,S*)-**(4.34)**.

From Table 4.3 it is clear that the increased bulk has a positive effect on the enantioselectivity in the hydrogenation of methyl-2-acetamidoacrylate **(4.31)**, compare Entries 1 and 5. The same enantiomer of the product **(4.44)** is produced by (*S,S*)-**(4.34)** and (*S,S*)-**(4.36)**, which is consistent with the ligands (*S*)-**(4.35)** and (*S*)-**(4.37)** adopting favoured conformations in complexes (*S,S*)-**(4.34)** and (*S,S*)-**(4.36)** respectively in which the same diagonal of the quadrant diagram is sterically hindered. As mentioned above, this conjecture relies on restricted rotation about the M-P bonds and it is interesting to note that a broad signal is also observed in the $^{31}P\{^{1}H\}$ NMR spectrum of complex (*S,S*)-**(4.34)**, see Section 2.3.2.1.

Comparison of Entry 4 with Entry 9 shows that the reaction is significantly slower with the rhodium(I) complex **(4.34)** of the more bulky ligand **(4.35)**. It is likely that the decrease in rate is due to a decrease in stability of the rhodium-substrate complexes $(\mathbf{4.16})^{si}$ and $(\mathbf{4.16})^{re}$ leading to a reduced equilibrium concentration of these species.

Table 4.3: Catalytic results for the asymmetric hydrogenation of methyl-2-acetamidoacrylate (**4.31**) and methyl-(*Z*)-2-acetamidocinnamate (**4.13**) using rhodium(I) complexes (*S,S*)-(**4.36**) and (*S,S*)-(**4.34**)

Entry[a]	Complex[b]	Solvent[c]	% Conversion[d]	% ee[d]
1[e]	(*S,S*)-(**4.36**)	CH_2Cl_2	100	73 (*R*)
2[e]	(*S,S*)-(**4.36**)	1,2-dichlorobenzene	100	78 (*R*)
3[e]	(*S,S*)-(**4.36**)	1,2-dibromoethane	87	80 (*R*)
4[e,f]	(*S,S*)-(**4.36**)	CH_2Cl_2	100	73 (*R*)
5	(*S,S*)-(**4.34**)	CH_2Cl_2	100	78 (*R*)
6	(*S,S*)-(**4.34**)	1,2-dichlorobenzene	90	75 (*R*)
7	(*S,S*)-(**4.34**)	1,2-dibromoethane	62	92 (*R*)
8	(*S,S*)-(**4.34**)	1,2-diiodoethane[g]	0	------
9[h]	(*S,S*)-(**4.34**)	CH_2Cl_2	47	84 (*R*)
10[i]	(*S,S*)-(**4.34**)	CH_2Cl_2	97	59 (*R*)

a Reaction conditions: methyl-2-acetamidoacrylate (**4.31**) (497.4 mg, 3.475 mmol), catalyst (9.4 mg, 0.0073 mmol, 0.0021 mol equiv) and solvent (7.5 cm^3) were placed in a stainless steel autoclave, which was pressurised to 1.5 atm with H_2 and the reaction mixture was stirred for 20 h at 25 °C.

b Complexes were preformed in all cases.

c Solvents were deoxygenated thoroughly before use by bubbling N_2 through them for 10 min.

d Calculated by GC.

e Ref. 36

f Reaction mixture was stirred for 3 h at 25 °C.

g The solution (1.7 M in CH_2Cl_2) was prepared by the addition of 1,2-diiodoethane (3.6 g, 12.8 mmol) to deoxygenated dichloromethane (7.5 cm^3).

h Reaction mixture was stirred for 12 h at 25 °C.

i Reaction conditions: methyl-(Z)-2-acetamidocinnamate (**4.13**) (497.4 mg, 2.271 mmol), catalyst (6.1 mg, 0.0048 mmol, 0.0021 mol equiv) and solvent (4.9 cm^3) were placed in a stainless steel autoclave, which was pressurised to 1.5 atm with H_2 and the reaction mixture was stirred for 20 h at 25 °C.

Solvent effects on the enantioselectivity of hydrogenation reactions have been observed before and have been attributed to changes in the precise conformation adopted by the rhodium-substrate complex caused by the secondary solvation sphere.[194] Table 4.3 shows that the solvent can have a dramatic effect on the enantioselectivities obtained with the monophosphonite complexes (*S,S*)-(**4.34**) and (*S,S*)-(**4.36**). In 1,2-dibromoethane an enantioselectivity of 92% is obtained with complex (*S,S*)-(**4.34**), see Entry 7, which is the highest enantioselectivity obtained in the asymmetric hydrogenation of an α-enamide using a monodentate phosphorus(III) ligand. Further, this is an improvement on the enantioselectivity obtained by Reetz[18] (see Section 1.3.2) using the bidentate diphosphonite (**4.41**). The reason for the acute sensitivity of these systems to solvent effects is not clear but perhaps solvation

influences the rate of M-P bond rotation which earlier we speculated may be the source of the high enantioselectivities.

Entry 10 shows the result obtained in the asymmetric hydrogenation of methyl-(*Z*)-2-acetamidocinnamate (**4.13**). The conversion is excellent (97%) but the enantioselectivity is moderate (57%). The same sense of enantioface discrimination is observed with this substrate {(*S,S*)-(**4.34**) favouring formation of (*R*)-(**4.45**)} as with methyl-2-acetamidoacrylate (**4.31**).

4.2.2 Bidentate phosphonites

The rhodium(I) complex (*S,S*)-(**4.38**) of diphosphonite (*S,S*)-(**4.39**) has been tested as a catalyst for the asymmetric hydrogenation of methyl-2-acetamidoacrylate (**4.31**) in order to compare the results with those obtained by Reetz[18] for the less bulky diphosphonite (**4.41**).

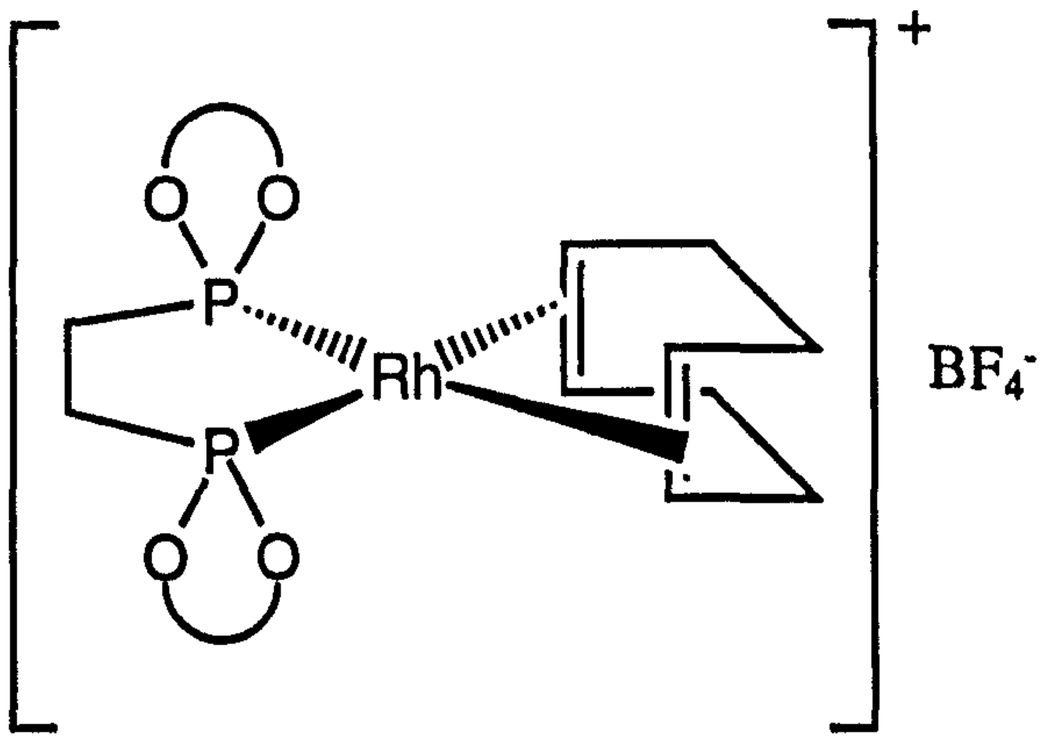

(4.38) when 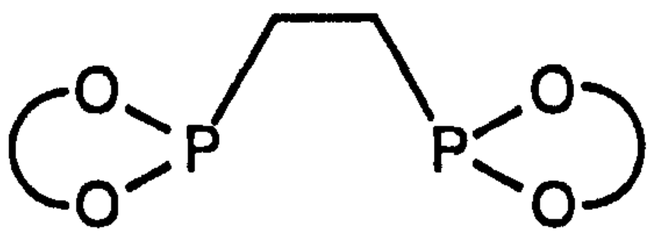 = **(4.39)**
(4.40) **(4.41)**

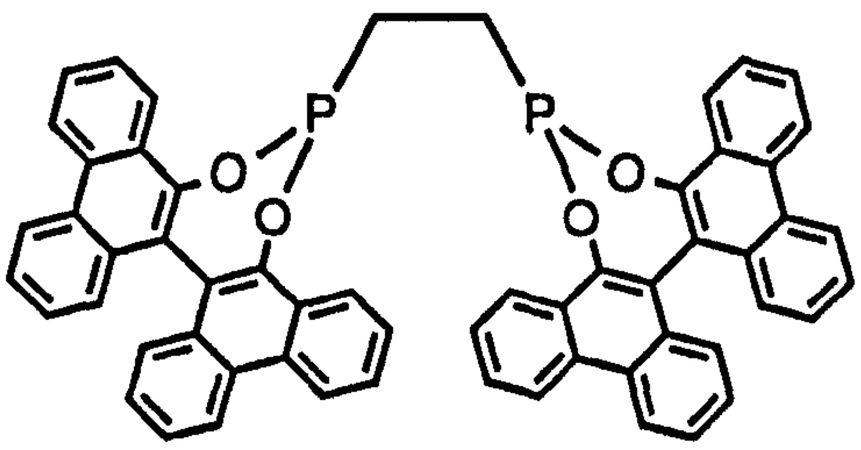

(4.39)

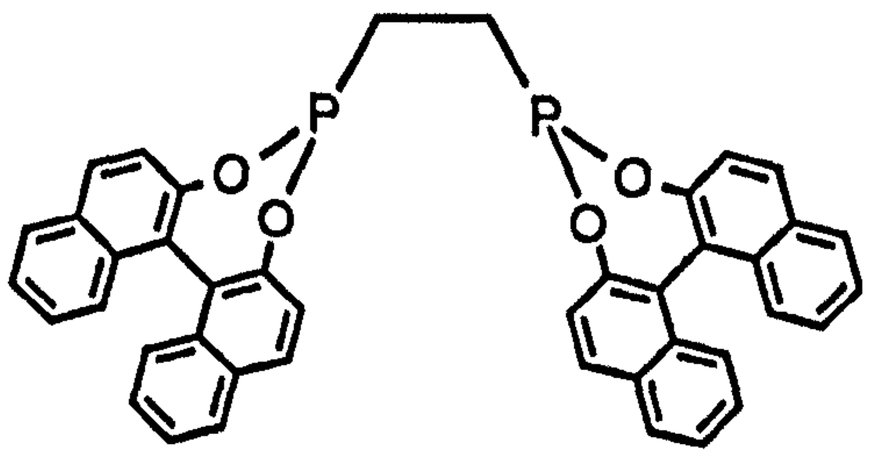

(4.41)

The results are shown in Table 4.4.

Table 4.4: Catalytic results for the asymmetric hydrogenation of methyl-2-acetamidoacrylate (**4.31**) using rhodium(I) complexes (**4.40**) and (*S,S*)-(**4.38**)

Entry[a]	Complex[b]	Solvent[c]	Temperature (°C)	% Conversion[d]	% ee[d]
1[e,f]	(*R,R*)-(**4.40**)[g]	CH_2Cl_2	25	100	90 (*R*)
2	(*S,S*)-(**4.38**)	CH_2Cl_2	25	13	41 (*R*)
3[h]	(*S,S*)-(**4.40**)	CH_2Cl_2	25	100	89 (*R*)

a Reaction conditions: methyl-2-acetamidoacrylate (497.4 mg, 3.475 mmol), catalyst (8.5 mg, 0.0073 mmol, 0.0021 mol equiv) and solvent (7.5 cm^3) were placed in a stainless steel autoclave, which was pressurised to 1.5 atm with H_2 and the reaction mixture was stirred for 20 h at the specified temperature.
b Complexes were preformed unless otherwise indicated.
c Solvents were deoxygenated thoroughly before use by bubbling N_2 through them for 10 min.
d Calculated by GC.
e Ref. 18
f Reaction conditions: methyl-2-acetamidoacrylate (c = 0.1 mol dm^{-3}), catalyst (substrate:catalyst = 1000:1) and solvent were placed in an autoclave, which was pressurised to 1.3 atm with H_2 and the reaction mixture was stirred for 20 h at the specified temperature.
g Catalyst prepared *in situ* with ligand:rhodium = 1:1.
h Ref. 36

Entry 1 shows the result obtained by Reetz[18] for the rhodium(I) complex (**4.40**) of diphosphonite (**4.41**). Complete conversion of substrate to product occurs with excellent enantioselectivity, 90%, with (*R,R*)-(**4.40**) favouring formation of the (*R*)-product. The rhodium(I) complex (**4.38**) of the more bulky diphosphonite (**4.39**) results in a large fall in reaction rate and enantioselectivity, see Entry 2.

Although X-ray crystallographic data is not available for the rhodium(I) complexes (**4.38**) and (**4.40**), a structure has been obtained for the platinum(II) complex (**4.46**) of diphosphonite ligand (*S,S*)-(**4.39**), see Figures 4.14 and 4.15, and we will use this to attempt to explain the poorer selectivity of our new diphosphonite (**4.39**) in terms of quadrant diagram arguments.

It is apparent from Figures 4.14 and 4.15 that there is considerable steric hindrance of all four quadrants by the phenanthryl moieties, which would explain the fall in reaction rate and enantioselectivity. If the binaphthol-derived analogue was to adopt a similar conformation then the quadrant diagram would be as shown in Figure 4.16. The 'extra' phenyl rings of the biphenanthryl system, shaded in purple for the phenanthryl moieties in the foreground in Figures 4.14 and 4.15, occupy the two unhindered quadrants of Figure 4.16.

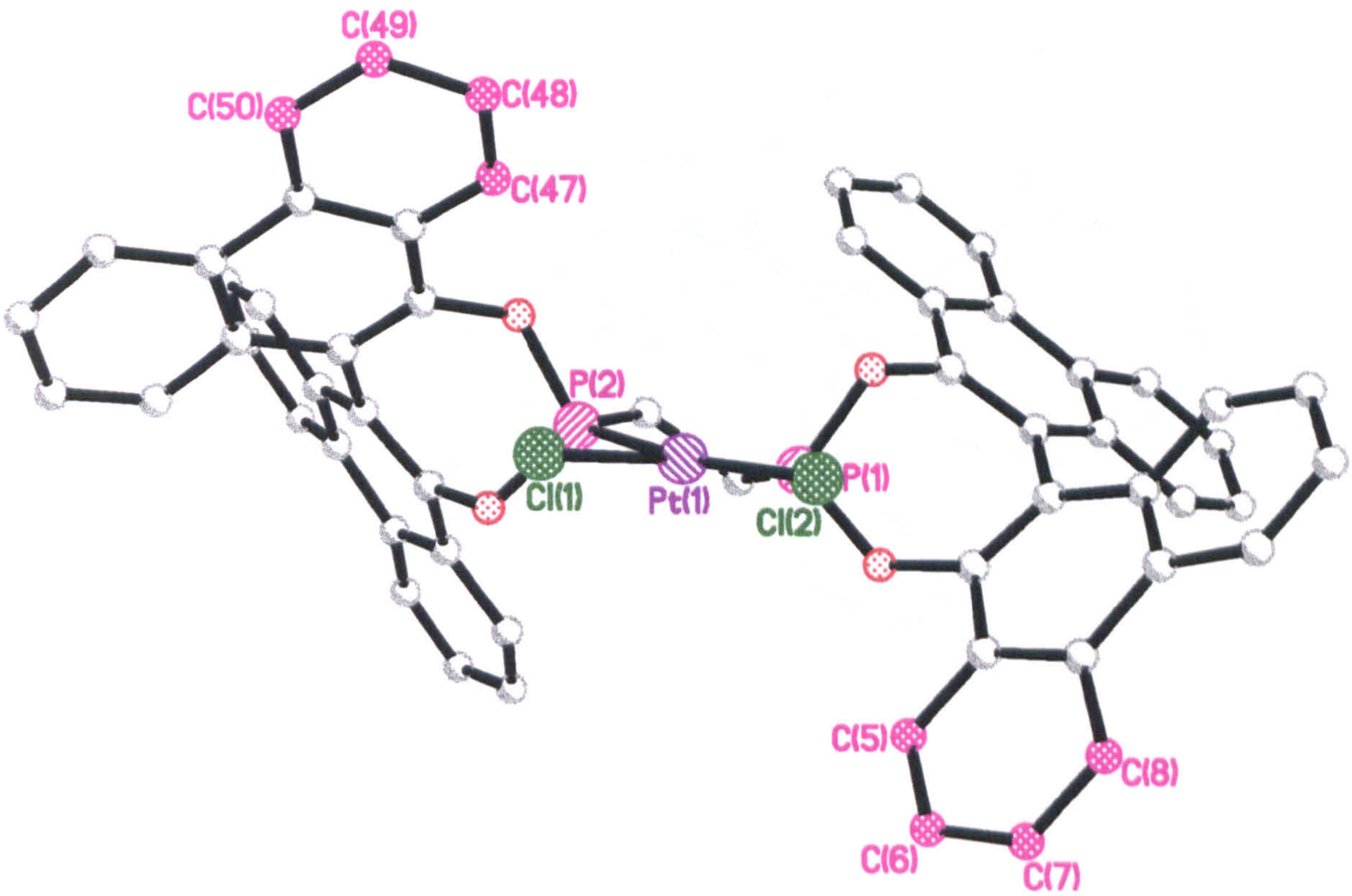

Figure 4.14: Molecular structure of the dichloroplatinum(II) complex (*S*,*S*)-(**4.39**). All hydrogen atoms are omitted for clarity. The 'extra' phenyl rings of the biphenanthryl system are shaded in purple for the phenanthryl moieties in the foreground

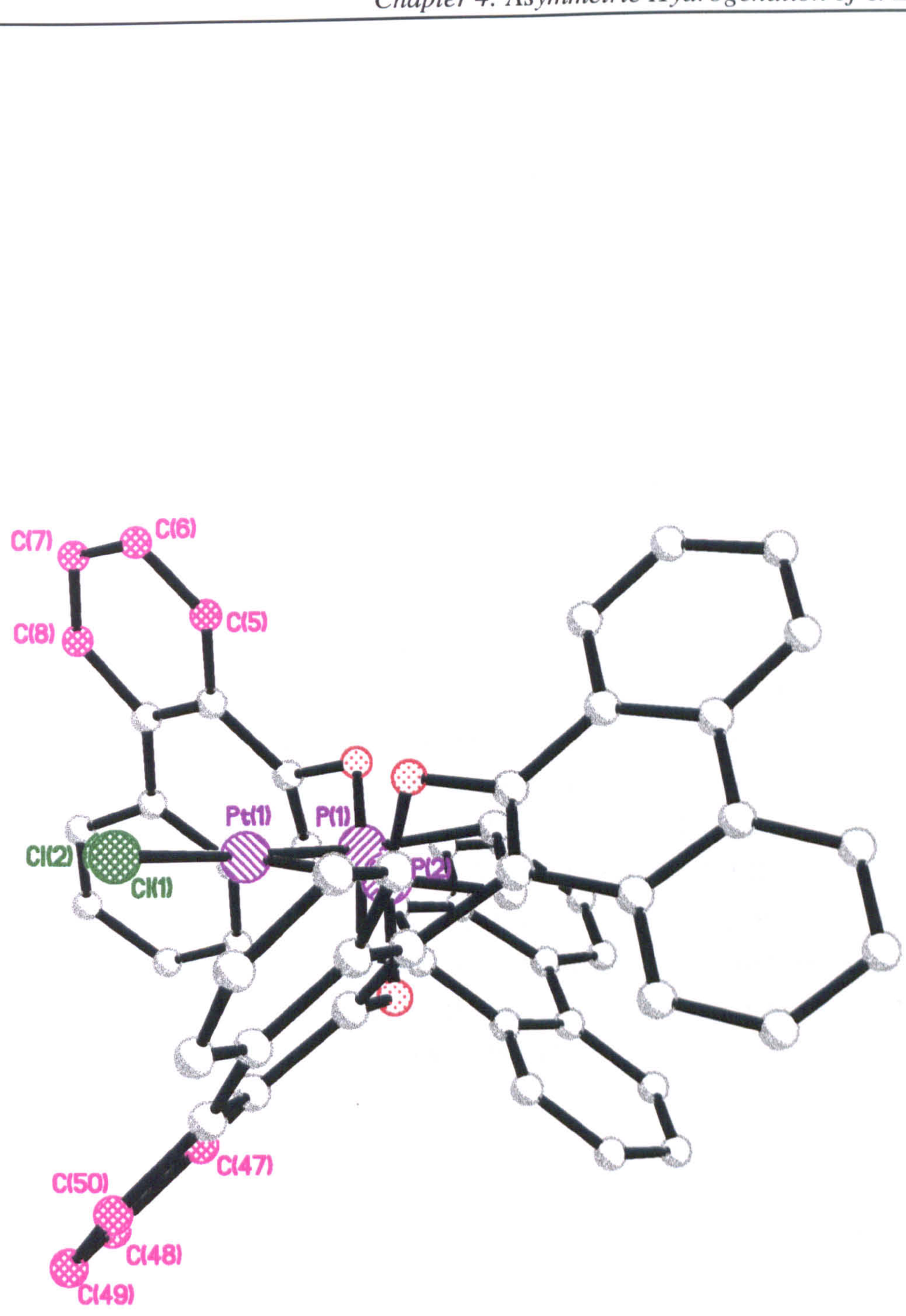

Figure 4.15: Molecular structure of the dichloroplatinum(II) complex (*S,S*)-(**4.39**). All hydrogen atoms are omitted for clarity

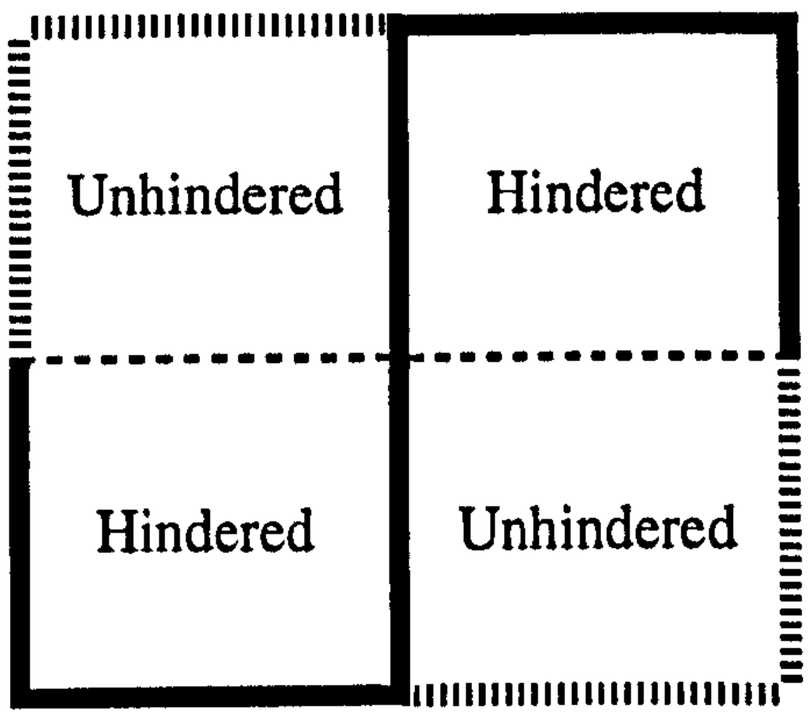

Figure 4.16: Predicted quadrant blocking by diphosphonite ligand (*S,S*)-(**4.41**)

From Figure 4.16 and the arguments presented in Section 4.1.2, we would expect the binaphthol-derived rhodium(I) complex (*S,S*)-(**4.40**) to favour formation of the (*R*)-product. This is indeed the preferred enantiomer obtained using the biphenanthrol-derived rhodium(I) complex (*S,S*)-(**4.38**). However, Reetz reports preferred formation of the (*R*)-enantiomer when (*R,R*)-(**4.40**), not (*S,S*)-(**4.40**), was utilised.[18] This result contradicts our current understanding and so the work carried out on complex (**4.40**) was repeated by Martorell and Pringle,[36] who found that (*S,S*)-(**4.40**) gave (*R*)-(**4.44**), see Entry 3, which suggests that Reetz is in error.

The rhodium(I) complex (*S*)-(**4.42**) derived from phosphinophosphonite ligand (*S*)-(**4.43**) has been tested as a catalyst for the asymmetric hydrogenation of methyl-2-acetamidoacrylate (**4.31**) and methyl-(*Z*)-2-acetamidocinnamate (**4.13**), see Equation 4.5. The results are shown in Table 4.5.

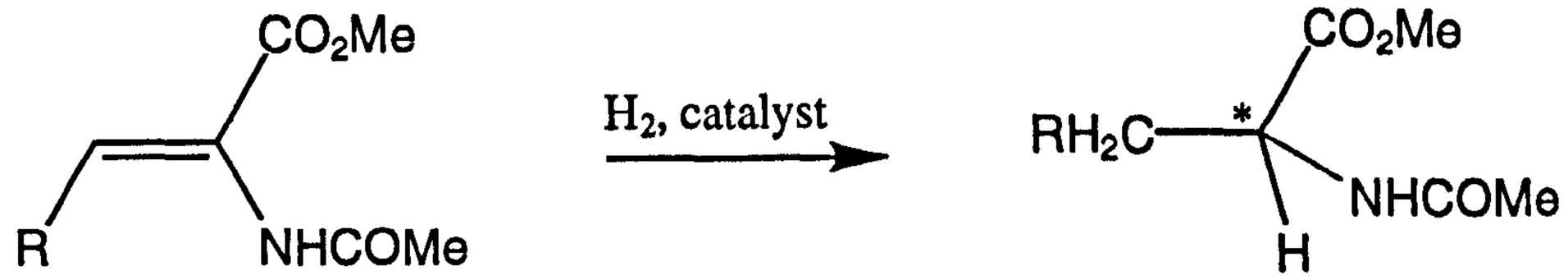

R = H, (**4.31**)
R = Ph, (**4.13**)

R = H, (**4.44**)
R = Ph, (**4.45**)

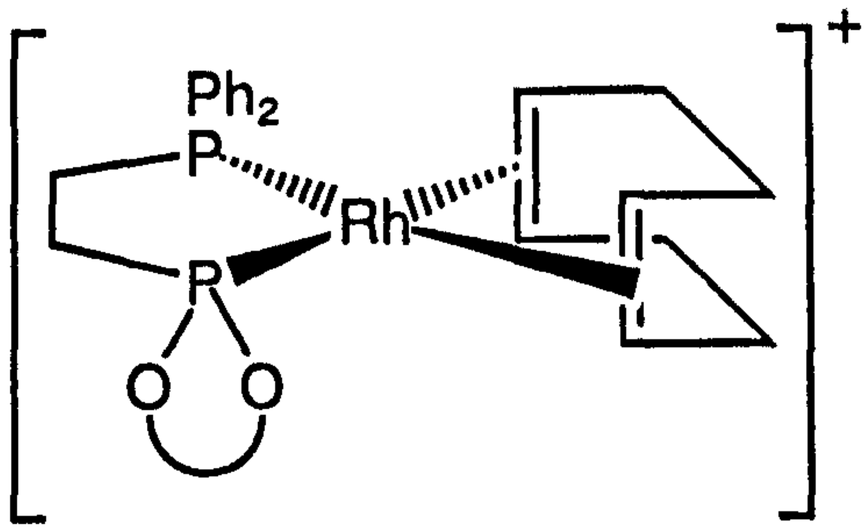

Catalyst: (*S*)-(**4.42**)

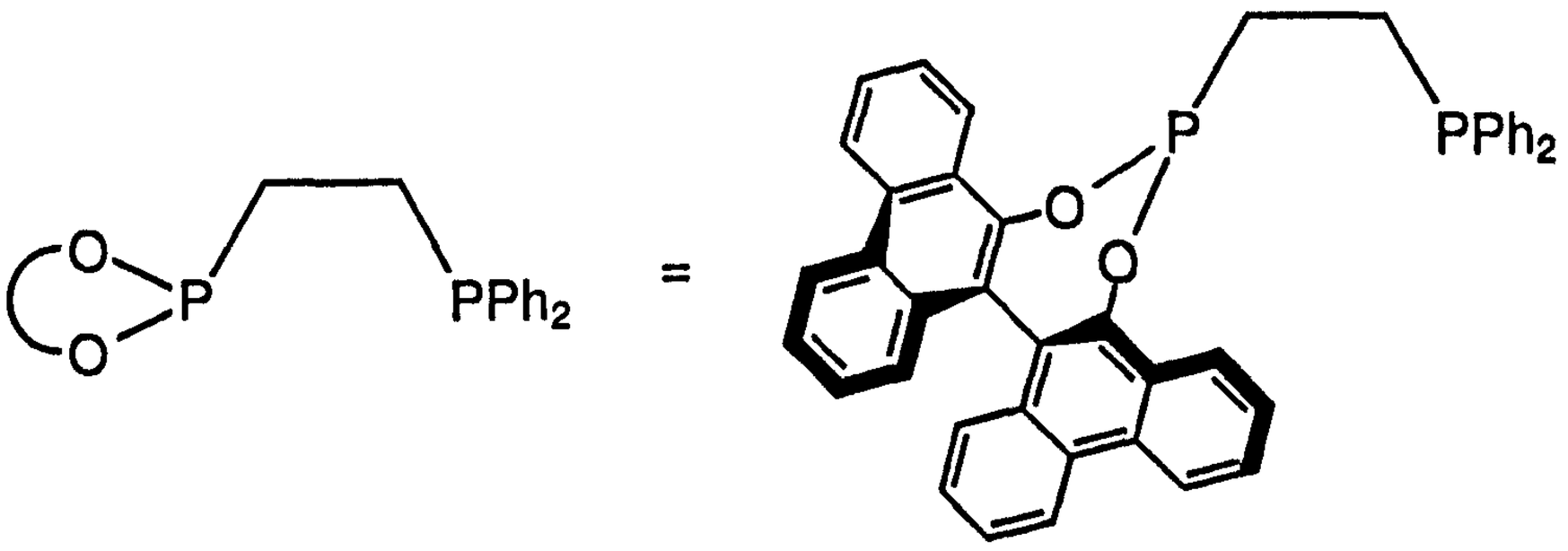

(*S*)-(**4.43**)

Equation 4.5

Table 4.5: Catalytic results for the asymmetric hydrogenation of methyl-2-acetamidoacrylate (**4.31**) and methyl-(*Z*)-2-acetamidocinnamate (**4.13**) using rhodium(I) complex (*S*)-(**4.42**)

Entry[a]	Complex[b]	Solvent[c]	% Conversion[d]	% ee[d]
1[e]	(*S*)-(**4.42**)	CH_2Cl_2	100	84 (*R*)
2[e]	(*S*)-(**4.42**)	1,2-dichlorobenzene	62	82 (*R*)
3[f]	(*S*)-(**4.42**)	1,2-dibromoethane	97	88 (*R*)
4[g]	(*S*)-(**4.42**)[h]	CH_2Cl_2	100	88 (*R*)
5[i]	(*S*)-(**4.42**)[h]	1,2-dibromoethane	100	86 (*R*)

a Reaction conditions: methyl-2-acetamidoacrylate (**4.31**), catalyst (0.0021 mol equiv) and solvent were placed in a stainless steel autoclave, which was pressurised to 1.5 atm with H_2 and the reaction mixture was stirred for 20 h at 25 °C.

b Complexes were formed *in situ* by addition of $[Rh(cod)_2]BF_4$ and phosphinophosphonite (*S*)-(**4.43**) (1.1 mol equiv with respect to the rhodium) to the reaction mixture.

c Solvents were deoxygenated thoroughly before use by bubbling N_2 through them for 10 min.

d Calculated by GC.

e Scale: methyl-2-acetamidoacrylate (**4.31**) (994.8 mg, 6.950 mmol), $[Rh(cod)_2]BF_4$ (6.0 mg, 0.0146 mmol), phosphinophosphonite (*S*)-(**4.43**) (10.0 mg, 0.0161 mmol) and solvent (15 cm^3).

f Scale: methyl-2-acetamidoacrylate (**4.31**) (746.1 mg, 5.213 mmol), $[Rh(cod)_2]BF_4$ (4.5 mg, 0.0110 mmol), phosphinophosphonite (*S*)-(**4.43**) (7.5 mg, 0.0121 mmol) and solvent (11.3 cm^3).

g Reaction conditions: methyl-(*Z*)-2-acetamidocinnamate (**4.13**) (480.0 mg, 2.192 mmol), catalyst (0.0048 mmol, 0.0027 mol equiv) and solvent (5.9 cm^3) were placed in a stainless steel autoclave, which was pressurised to 1.5 atm with H_2 and the reaction mixture was stirred for 20 h at 25 °C.

h Catalyst formed *in situ* from $[Rh(cod)_2]BF_4$ (2.4 mg, 0.0048 mmol, 0.0027 mol equiv) and phosphinophosphonite (*S*)-(**4.43**) (4.0 mg, 0.0053 mmol, 0.0030 mol equiv).

i Reaction conditions: methyl-(*Z*)-2-acetamidocinnamate (**4.13**) (180.0 mg, 0.822 mmol), catalyst (0.0048 mmol, 0.0072 mol equiv) and solvent (5.9 cm^3) were placed in a stainless steel autoclave, which was pressurised to 1.5 atm with H_2 and the reaction mixture was stirred for 20 h at 25 °C.

It can be seen from Table 4.5 that the rhodium(I) complex (*S*)-(**4.42**) is an excellent catalyst for asymmetric hydrogenation, with high activity and high asymmetric inductions (up to 88% ee for both substrates). The rates and enantioselectivities of the hydrogenation reactions with this catalyst are less sensitive to solvation effects than those catalysed by the rhodium(I) complex (*S,S*)-(**4.34**) of monophosphonite (*S*)-(**4.35**). Complex (*S*)-(**4.42**) shows the same sense of enantioface discrimination for both substrates and produces products {(**4.44**) or (**4.45**)} with the (*R*)-configuration. The absence of X-ray crystallographic data or molecular modelling studies precludes further rationalisation.

This is the first example of the use of a phosphinophosphonite ligand in asymmetric catalysis and the promising results that have been obtained bode well for the potential of this class of ligands.

4.3 Cationic rhodium(I)-diphosphite complexes as catalysts for asymmetric hydrogenation

The application of chiral diphosphites in the asymmetric hydrogenation of α-enamides is a largely unexplored area. However in a recent publication, Reetz showed the potential for this class of ligands with the attainment of enantioselectivities up to 89% in the asymmetric hydrogenation of methyl-2-acetamidoacrylate (**4.31**) using a rhodium(I) complex of diphosphite (**4.47**),[20] see Section 1.4.

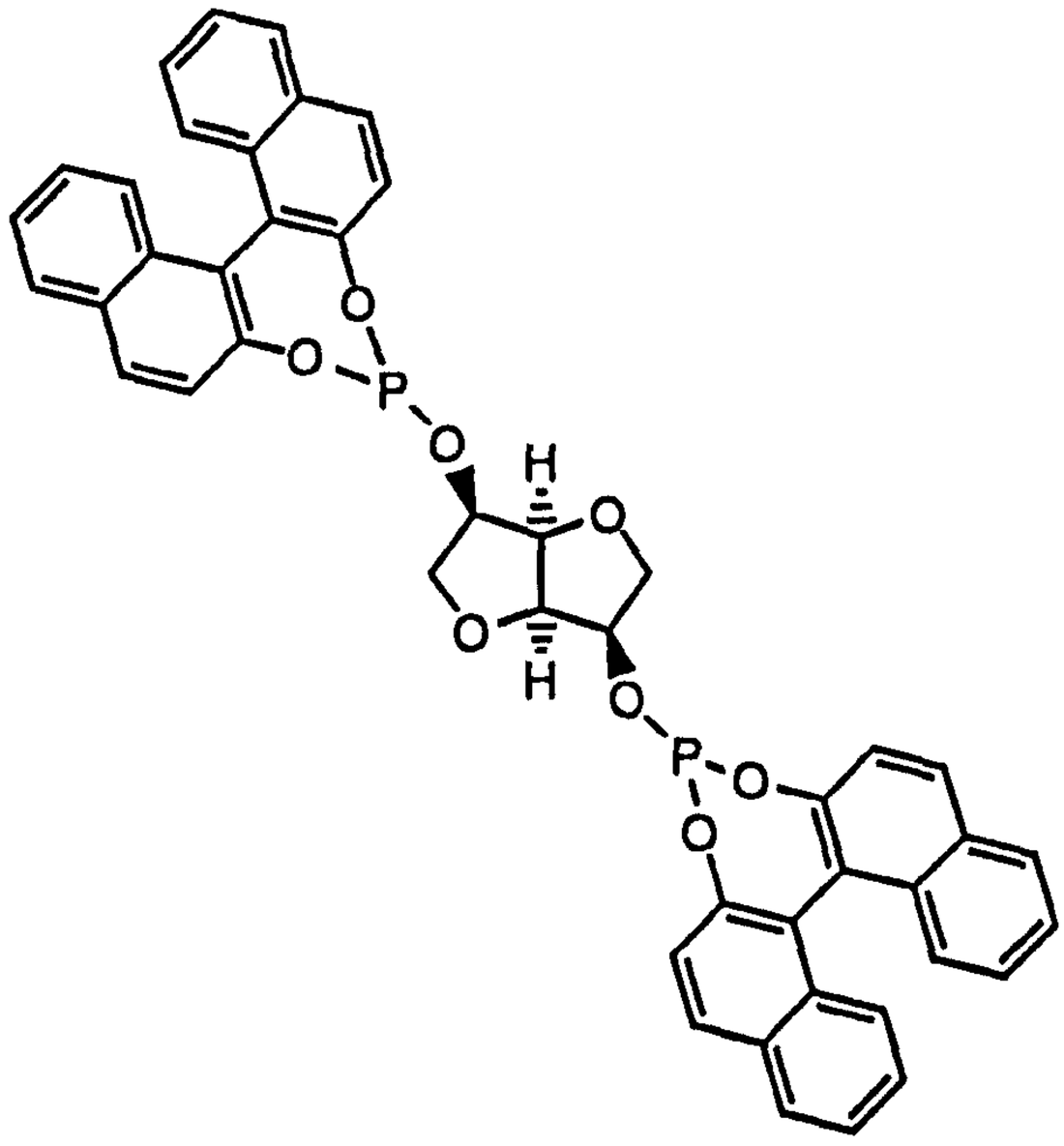

(4.47)

Consequently it was decided to test the rhodium(I) complexes (*R,S,R*)- and (*R,R,R*)-(**4.48**) of the cyclic aryl diphosphite ligands (*R,S,R*)- and (*R,R,R*)-(**4.49**) in the asymmetric hydrogenation of methyl-2-acetamidoacrylate (**4.31**), see Equation 4.6. The results are presented in Table 4.6.

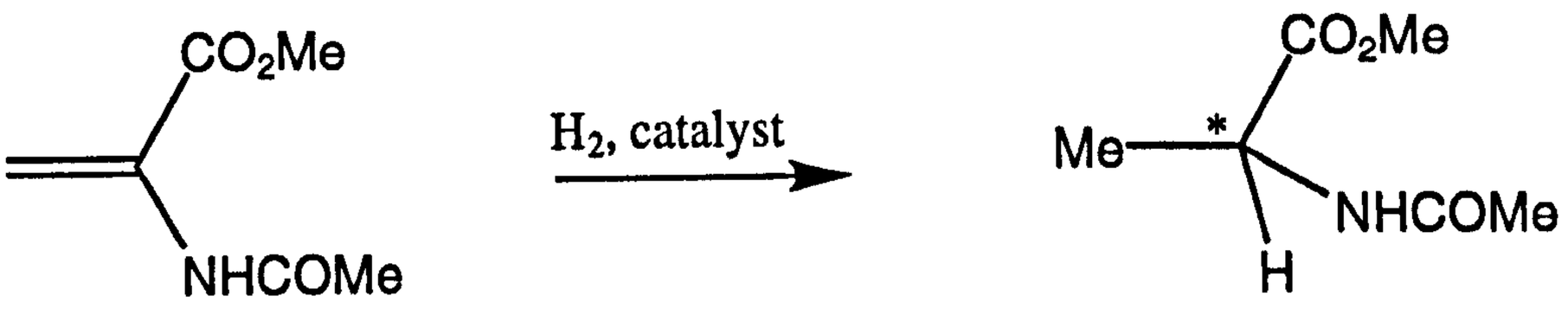

(4.31) **(4.44)**

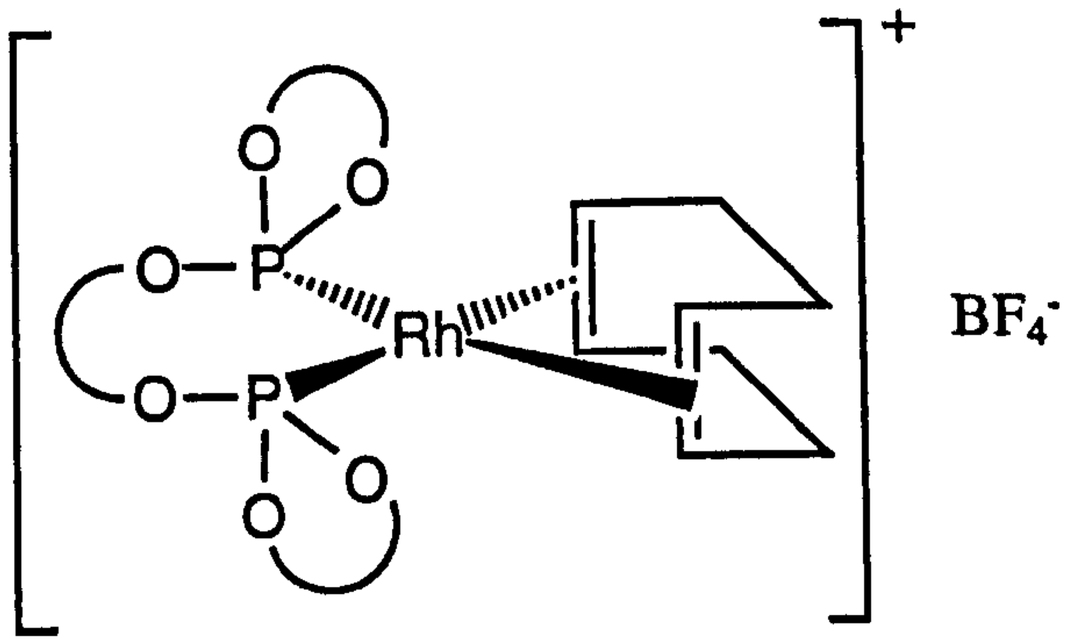

Catalyst: **(4.48)**

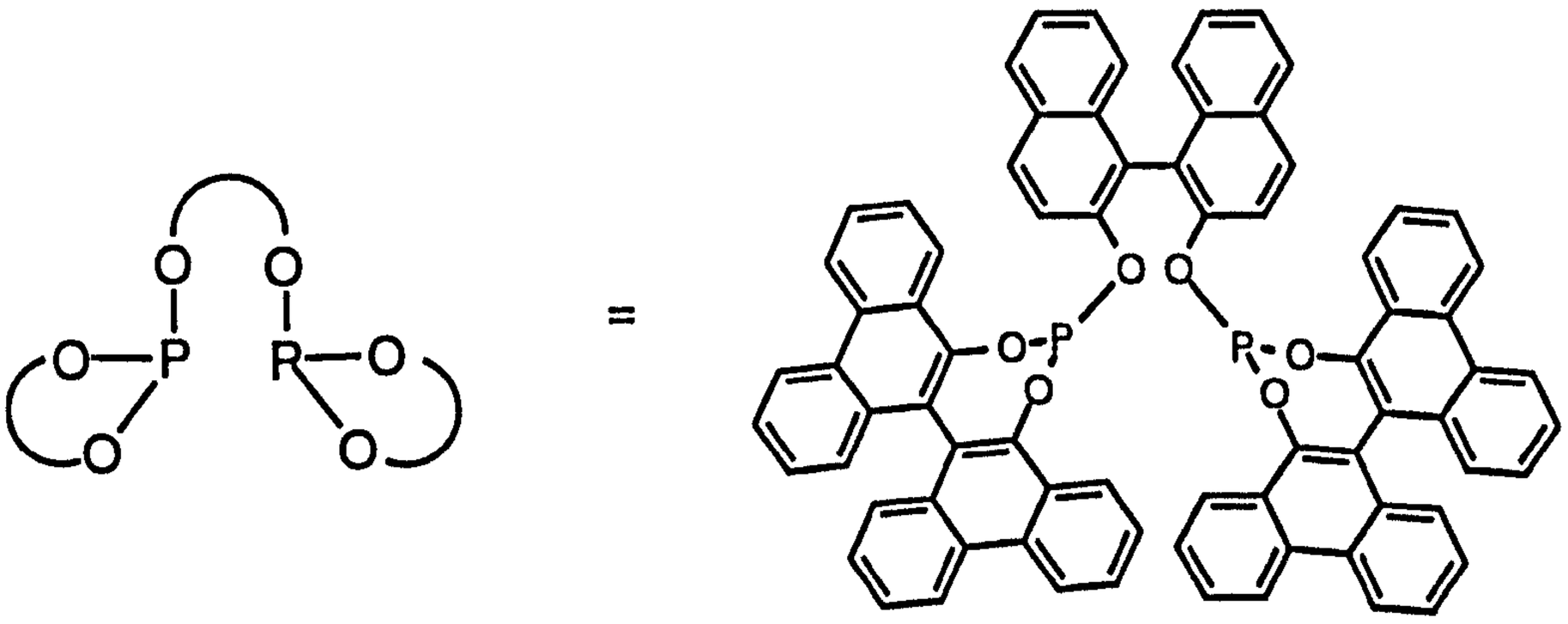

(4.49)

Equation 4.6

Table 4.6: Catalytic results for the asymmetric hydrogenation of methyl-2-acetamidoacrylate (**4.31**) using rhodium(I) complexes (*R,S,R*)- and (*R,R,R*)-(**4.48**)

Entry[a]	Complex[b]	Solvent[c]	% Conversion[d]	% ee[d]
1	(*R,S,R*)-(**4.48**)	CH_2Cl_2	13[e]	68 (*S*)
2	(*R,S,R*)-(**4.48**)	1,2-dichlorobenzene	81	43 (*S*)
3	(*R,S,R*)-(**4.48**)	1,2-dibromoethane	8	26 (*S*)
4	(*R,R,R*)-(**4.48**)	CH_2Cl_2	100	38 (*R*)
5	(*R,R,R*)-(**4.48**)	1,2-dibromoethane	1.5	8 (*R*)

a Reaction conditions: methyl-2-acetamidoacrylate (746.1 mg, 5.217 mmol), catalyst (0.0111 mmol, 0.0021 mol equiv) and solvent (11.3 cm^3) were placed in a stainless steel autoclave, which was pressurised to 1.5 atm with H_2 and the reaction mixture was stirred for 20 h at 25 °C.

b Complexes were formed *in situ* by addition of $[Rh(cod)_2]BF_4$ (4.5 mg, 0.0111 mmol, 0.0021 mol equiv) and diphosphite (**4.49**) (13.5 mg, 0.0121 mmol, 0.0023 mol equiv) to the reaction mixture.

c Solvents were deoxygenated thoroughly before use by bubbling N_2 through them for 10 min.

d Calculated by GC.

e The low conversion in this reaction appears anomalous and the experiment should be repeated.

The low conversion observed in Entry 1 appears anomalous and this reaction should be repeated. The results show that the rates and enantioselectivities are highly sensitive to solvation effects and that, of the solvents studied, the reactions carried out in dichloromethane give the highest enantioselectivities.

Further, it is apparent from Table 4.6 that the stereochemistry of the major enantiomer of the product (**4.44**) is controlled by the absolute configuration of the bridging binaphthyl moiety in diphosphite (**4.49**). This is the opposite situation to that reported by Reetz for diphosphite (**4.47**) where the stereochemistry of the major enantiomer of the product is determined by the absolute configuration of the terminal binaphthyl moieties.[20] It also appears that the (*S*)-selective catalyst, derived from (*R,S,R*)-(**4.49**), is the 'matched' case.

Chapter 5

Experimental

E.1 General experimental details

Unless otherwise stated, all reactions were carried out under a dry nitrogen atmosphere using standard Schlenk line techniques. Glassware was flame-dried and allowed to cool *in vacuo* before use. Syringes and needles were oven-dried overnight and allowed to cool in a desiccator prior to use. Solvents were dried and degassed by refluxing under a nitrogen atmosphere over appropriate drying agents; calcium hydride (for dichloromethane), magnesium (for ethanol and methanol), sodium wire / benzophenone (for THF and 2,2-dimethoxypropane) and sodium (for toluene). Dry pentane and methanol were purchased from Aldrich Chemical Company, stored over 4 Å and 3 Å activated molecular sieves respectively and were degassed by freeze-pump-thaw methods prior to use. Commercial reagents were used as supplied unless otherwise stated. PCl_3 was distilled under a nitrogen atmosphere and NEt_3 was dried by refluxing under a nitrogen atmosphere over potassium hydroxide. Both reagents were degassed by freeze-pump-thaw methods prior to use.

Starting materials prepared by literature methods were $Ph_2PCH_2CH_2P(NMe_2)_2$,[128] $[PtCl_2(cod)]$,[224] $[Pt(nb)_3]$,[225] $[PdCl_2(NCPh)_2]$,[226] $[Rh_2Cl_2(CO)_4]$,[227] $[Rh_2Cl_2(cod)_2]$[228] and $[Rh(cod)_2]BF_4$.[172,173] The rhodium complex $[Rh(CO)_2(dpm)]$ was supplied by Du Pont.

Elemental analyses were carried out by the Microanalytical Laboratory of the School of Chemistry, Bristol University. Electron Impact and Fast Atom Bombardment mass spectra were recorded on an MD800 and an Autospec by the Mass Spectrometry Service, Bristol University. Infrared spectra were recorded on a Perkin Elmer 1600 series by the author. Optical rotations were recorded by the author using a PE 241 MC polarimeter.

$^{31}P\{^1H\}$, $^{13}C\{^1H\}$, $^{195}Pt\{^1H\}$ and ^1H NMR spectra were recorded by the author at the ambient temperature of the probe unless otherwise stated. Deuterated solvents, which were dried over 4 Å molecular sieves and degassed by freeze-pump-thaw methods prior to use, were used to provide the field / frequency lock. An external D_2O source was used in the case of the Jeol EX90 NMR spectrometer.

The following spectrometers were used:

^1H NMR spectra;	Jeol GX270 (270 MHz) or Jeol GX400 (400 MHz) with chemical shifts to high frequency of internal tetramethylsilane.
$^{13}C\{^1H\}$ NMR spectra;	Jeol GX270 (67.9 MHz) or Jeol GX400 (100 MHz) with chemical shifts relative to the solvent used.
$^{31}P\{^1H\}$ and ^{31}P NMR spectra;	Jeol FX90Q (36.2 MHz), Jeol EX90 (36.2 MHz) or Jeol GX400 (162 MHz) with chemical shifts to high frequency of H_3PO_4.

$^{195}Pt\{^{1}H\}$ NMR spectra; Jeol GX400 (85.6 MHz) with chemical shifts to high frequency of Ξ (^{195}Pt) = 21.4 MHz.

E.2 Chapter 2: Phosphonites: Synthesis and Coordination Chemistry

E.2.1 Syntheses of 9,9'-biphenanthryl-10,10'-diol (2.2) and dimethyl-1,1'-binaphthyl-2,2'-dihydroxy-3,3'-dicarboxylate (2.1)

Preparation of 9-bromophenanthrene (2.5)

A stirred suspension of phenanthrene (**2.4**) (99.2 g, 0.557 mol) in dichloromethane (100 cm^3) was heated to reflux in a flask fitted with a condenser which was vented to a 2M solution of sodium hydroxide to quench the HBr produced during the reaction. Once dissolution had been effected, a solution of bromine (29 cm^3, 0.563 mol, 1.01 mol equiv) in dichloromethane (70 cm^3) was added dropwise over 2 h to the refluxing solution, during which time much fuming, due to the evolution of HBr, was observed. The solution was maintained at reflux for a further 4 h, after which the fuming had ceased. The solution was allowed to cool to room temperature and the dichloromethane was removed by distillation under nitrogen. The dark yellow, oily residue was purified by reduced pressure distillation to give a pale yellow liquid (b.p.$_{1.0}$ 169-178 °C {Lit.[121] b.p.$_{2.0}$ 177-190 °C}). Upon cooling the liquid to room temperature, the crude 9-bromophenanthrene (**2.5**) (111.7 g, 78%) was obtained as a yellow solid. Recrystallisation from hot ethanol afforded, after collection of three separate crops, 9-bromophenanthrene (**2.5**) (55.0 g, 38%) as pale yellow needles, m.p. 59-61 °C {Lit.[121] m.p. 65-66 °C}; δ_H ($CDCl_3$): 7.58 (1H, td, ^3J(HH) 7.5 Hz, ^4J(HH) 1.2 Hz), 7.64 (1H, dd, ^3J(HH) 8.2 Hz, ^4J(HH) 1.4 Hz), 7.67-7.71 (2H, m), 7.78 (1H, d, ^3J(HH) 7.8 Hz), 8.09 (1H, s, H10), 8.35-8.37 (1H, m), 8.61-8.67 (2H, m); *m/z* (EI): 258 ($^{81}BrM^{+\cdot}$, 100%), 256 ($^{79}BrM^{+\cdot}$, 100%), 177 ($M\text{-}Br^+$, 35%), 176 ($M\text{-}HBr^{+\cdot}$, 44%).

Preparation of 9-hydroxyphenanthrene (2.3)

Magnesium shavings (4.14 g, 0.171 mol, 1.1 mol equiv) were activated by vigorous stirring overnight under nitrogen to produce a fine black powder. A dropping funnel was charged with a solution of 9-bromophenanthrene (**2.5**) (40.0 g, 0.155 mol) in tetrahydrofuran (130 cm^3). Enough of this green solution was added to cover the magnesium powder and the resulting suspension was stirred vigorously until spontaneous reflux occurred. The remainder of the solution was added dropwise over 50 min at such a rate as to maintain reflux without external heating. After the addition was completed, the reaction mixture was heated to reflux for a further 2 h and the

resulting grey solution of the Grignard reagent was then allowed to cool to room temperature. A separate solution of trimethyl borate (19.3 cm^3, 0.171 mol, 1.1 mol equiv) in tetrahydrofuran (85 cm^3) was cooled to -10 °C and the Grignard solution was added dropwise over 2 h to this solution keeping the temperature at ≤ -5 °C. The thick white suspension produced was stirred at -5 °C for 1 h and was then cooled to -10 °C. Glacial acetic acid (14 cm^3) was added, followed by the dropwise addition over 15 min of a solution of 30% aqueous hydrogen peroxide (17.4 cm^3) in distilled water (15.7 cm^3) whilst keeping the temperature at ≤ 0 °C. The resultant brown solution was allowed to warm to room temperature and stirred for 40 min. Saturated ammonium chloride solution (200 cm^3) was added, followed by tetrahydrofuran (100 cm^3) and the organic layer was separated. The organic layer was washed with saturated sodium bicarbonate solution (200 cm^3), distilled water (200 cm^3) and brine (3 x 200 cm^3), dried ($MgSO_4$), filtered and the solvent was removed under reduced pressure to yield a brown oil. This oil was dissolved in toluene and the solvent was removed under reduced pressure to yield 9-hydroxyphenanthrene (**2.3**) (28.4 g, 94%) as a light brown powder, m.p. 135 °C {Lit. m.p. 139-141 °C}; *m/z* (EI): 194 ($M^{+\cdot}$, 100%), 165 ($M\text{-}29^{+\cdot}$, 69%).

Preparation of 9,9'-biphenanthryl-10,10'-diol (2.2)

To a stirred solution of 9-hydroxyphenanthrene (**2.3**) (14.5 g, 75 mmol) in methanol (300 cm^3) at room temperature was added copper(II) nitrate trihydrate (36.1 g, 0.149 mol, 2 mol equiv). To the resulting deep blue solution was added dropwise benzylamine (49 cm^3, 0.449 mol, 6 mol equiv) to give a thick brown suspension. This reaction mixture was stirred under nitrogen overnight and then quenched with 2M hydrochloric acid (250 cm^3) to afford a thick blue-white suspension. The layers were partitioned by the addition of brine (200 cm^3) and dichloromethane (200 cm^3). The organic layer was separated and washed with 2M ammonium hydroxide solution (3 x 300 cm^3) until the aqueous layer remained colourless, rather than the deep blue colour that formed if copper salts were still present in the organic phase. The organic layer was then washed with brine (2 x 300 cm^3), dried ($MgSO_4$), filtered and the solvent was removed under reduced pressure to yield (±)-9,9'-biphenanthryl-10,10'-diol (**2.2**) (14.4 g, quantitative yield) as a yellow solid, m.p. 232 °C {Lit.[119] m.p. 234-236 °C}; δ_H ($CDCl_3$): 5.50 (2H, s, OH), 7.27 (2H, dd, ^3J(HH) 8.4 Hz, ^4J(HH) 1.2 Hz), 7.35 (2H, ddd, ^3J(HH) 8.2 Hz, $^3J'$(HH) 6.9 Hz, ^4J(HH) 1.2 Hz), 7.54 (2H, ddd, ^3J(HH) 8.3 Hz, $^3J'$(HH) 6.8 Hz, ^4J(HH) 1.5 Hz), 7.72 (2H, ddd, ^3J(HH) 8.2 Hz, $^3J'$(HH) 7.0 Hz, ^4J(HH) 1.2 Hz), 7.82 (2H, ddd, ^3J(HH) 8.3 Hz, $^3J'$(HH) 7.0 Hz, ^4J(HH) 1.4 Hz), 8.46 (2H, dd, ^3J(HH) 8.1 Hz, ^4J(HH) 1.1 Hz), 8.75 (2H, d, ^3J(HH) 8.3 Hz), 8.81 (2H, d, ^3J(HH) 8.3 Hz); *m/z* (EI): 386 ($M^{+\cdot}$, 100%), 368 ($M\text{-}18^{+\cdot}$, 24%), 165 ($M\text{-}221^{+\cdot}$, 55%).

Preparation of (R,R)-(+)-N,N,N',N'-tetramethyltartaric acid diamide (2.9)

Dimethylamine (35 cm^3, 0.544 mol, 4.7 mol equiv) was condensed into a round-bottomed flask at -78 °C that was protected from atmospheric moisture by a silica gel drying tube. Freshly distilled methanol (20 cm^3) was added to afford a pale green solution, which was allowed to warm to room temperature and then (*R,R*)-(+)-diethyl tartrate (**2.8**) (20 cm^3, 0.117 mol) was added. The reaction mixture was swirled to effect complete dissolution and was then allowed to stand for 4 days. Removal of the solvent under reduced pressure yielded an oily white solid, which formed a fine white suspension upon the addition of toluene. The solvent was removed under reduced pressure and the product was dried overnight *in vacuo* to yield (*R,R*)-(+)-*N,N,N',N'*-tetramethyltartaric acid diamide (**2.9**) (22.2 g, 93%) as a white solid, m.p. 191 °C {Lit.[125] m.p. 189-190 °C}; $[\alpha]_D$ +44° (*c*, 2.5 in ethanol) {Lit.[125] $[\alpha]_D$ +43° (*c*, 3.0 in ethanol)}.

(*S,S*)-(-)-*N,N,N',N'*-tetramethyltartaric acid diamide (**2.9**) was also prepared using this procedure starting from (*S,S*)-(-)-diethyl tartrate (**2.8**).

Preparation of (R,R)-(+)-N,N,N',N'-tetramethyl-2,2-dimethyl-1,3-dioxolane-trans-4,5-dicarboxamide (2.7)

(*R,R*)-(+)-*N,N,N',N'*-tetramethyltartaric acid diamide (**2.9**) (10 g, 49 mmol) was suspended under nitrogen in toluene (100 cm^3). The reaction mixture was heated to reflux in order to achieve complete dissolution and distilled 2,2-dimethoxypropane (18 cm^3, 0.146 mol, 3 mol equiv) and *p*-toluenesulphonic acid monohydrate (500 mg, 2.5 mmol, 0.05 mol equiv) were added. The reaction mixture was maintained at reflux for 45 min and was then allowed to cool to room temperature. It was then washed with 2M potassium carbonate solution (100 cm^3), dried ($MgSO_4$), filtered and the solvent was removed under reduced pressure. Co-evaporation with pentane (50 cm^3) to remove the last traces of toluene and drying overnight *in vacuo* yielded (*R,R*)-(+)-*N,N,N',N'*-tetramethyl-2,2-dimethyl-1,3-dioxolane-*trans*-4,5-dicarboxamide (**2.7**) (7.1 g, 59%) as a white solid, m.p. 83 °C {Lit.[118] m.p. 86-88 °C}; $[\alpha]_D$ +2.4° (*c*, 4 in chloroform) {Lit.[118] $[\alpha]_D$ +2.5° (*c*, 1.4 in chloroform)}.

(*S,S*)-(-)-*N,N,N',N'*-tetramethyl - 2,2 - dimethyl - 1,3 - dioxolane - *trans* - 4,5 - dicarboxamide (**2.7**) was also prepared using this procedure starting with (*S,S*)-(-)-*N,N,N',N'*-tetramethyltartaric acid diamide (**2.9**).

Resolution of 9,9'-biphenanthryl-10,10'-diol (2.2)

A suspension of (±)-9,9'-biphenanthryl-10,10'-diol (**2.2**) (0.895 g, 2.3 mmol) in ethanol (40 cm^3) was heated to give a cloudy solution. (*R,R*)-(+)-*N,N,N',N'*-tetramethyl-2,2-dimethyl-1,3-dioxolane-*trans*-4,5-dicarboxamide (**2.7**) (1.128 g, 4.6 mmol, 2 mol equiv) was added and the hot solution was filtered to remove any remaining undissolved (±)-9,9'-biphenanthryl-10,10'-diol (**2.2**). The clear filtrate was left to cool to room temperature and then left undisturbed overnight to allow crystallisation to occur. The mother liquor was decanted off and the colourless prisms that had formed were washed with ethanol (2 x 5 cm^3) and dissolved, with warming, in benzene (5 cm^3). The resulting solution was filtered through a short silica column and the solvent was removed under reduced pressure to yield (*S*)-9,9'-biphenanthryl-10,10'-diol (**2.2**) (224 mg, 0.6 mmol, 25%) as a yellow solid, $[\alpha]_D$ -65.4° (*c*, 0.9 in $CHCl_3$) {Lit.[119] $[\alpha]_D$ -71.0° (*c*, 1.0 in chloroform)}. The mother liquor was combined with the ethanol washings, concentrated to *ca.* 20 cm^3 and left to stand at room temperature for 48 h. The resulting colourless prisms that formed were isolated by filtration, washed with ethanol (2 x 5 cm^3) and dissolved, with warming, in benzene (5 cm^3). The resulting solution was filtered through a short silica column and the solvent was removed under reduced pressure to yield (*R*)-enriched 9,9'-biphenanthryl-10,10'-diol (**2.2**) (440 mg, 1.1 mmol, 49%, 34% ee) as a yellow solid, $[\alpha]_D$ +22.0° (*c*, 1.0 in $CHCl_3$) {Lit.[119] $[\alpha]_D$ +71.0° (*c*, 1.0 in chloroform)}.

Optically pure (*R*)-9,9'-biphenanthryl-10,10'-diol (**2.2**) and (*S*)-enriched 9,9'-biphenanthryl-10,10'-diol (**2.2**) (34% ee) were also obtained following this procedure using (*S,S*)-(-)-*N,N,N',N'* - tetramethyl - 2,2 - dimethyl - 1,3 - dioxolane - *trans* - 4,5 - dicarboxamide (**2.7**).

Preparation of methyl-3-hydroxy-2-naphthoate (2.10)

3-Hydroxy-2-naphthoic acid (94 g, 0.5 mol) was suspended in absolute methanol (1.0 dm^3) with stirring under nitrogen. Sulphuric acid (25 cm^3) was added dropwise over 5 min and the reaction mixture was then heated to reflux for 5 h, when thin layer chromatography indicated the reaction was near completion. The reaction mixture was concentrated to *ca.* 300 cm^3 and then poured into ice-water (600 cm^3). The solid precipitate was isolated by filtration and washed with water (2 x 100 cm^3). This solid was dissolved in dichloromethane (500 cm^3) and washed with aqueous potassium carbonate (2 x 100 cm^3) and water (2 x 100 cm^3). Separation and evaporation of the dichloromethane layer gave methyl-3-hydroxy-2-naphthoate (**2.10**) (95 g, 94%) as an off-white solid, δ_H ($CDCl_3$): 4.03 (3H, s, MeO), 7.30-7.40 (2H, m), 7.53 (1H, t), 7.70 (1H, d), 7.81 (1H, d), 8.50 (1H, s), 10.43 (1H, s).

Preparation of dimethyl-1,1'-binaphthyl-2,2'-dihydroxy-3,3'-dicarboxylate (2.1)

Methyl-3-hydroxy-2-naphthoate (95 g, 0.47 mol) was dissolved under nitrogen in absolute methanol (1.0 dm^3) containing anhydrous copper(II) chloride (135 g, 1.0 mol, 2.1 mol equiv). *tert*-Butylamine (210 cm^3, 2.0 mol, 4.3 mol equiv) was added dropwise over 1 h, keeping the temperature below 30 °C. The resulting solution was heated to 50 °C for 14 h, when thin layer chromatography indicated the reaction was complete. The mixture was cooled to 10 °C and acidified to pH 4 over 1 h by dropwise addition of 6M HCl (335 cm^3, 2.0 mol, 4.3 mol equiv). The resulting yellow precipitate was collected by filtration and washed with water (3 x 100 cm^3) and diethyl ether (3 x 50 cm^3). The crude product was dissolved in dichloromethane and washed with 2M ammonium hydroxide solution (3 x 300 cm^3) until the aqueous layer remained colourless, rather than the deep blue colour that formed if copper salts were still present in the organic phase. The organic layer was then washed with brine (2 x 300 cm^3), dried ($MgSO_4$), filtered and the solvent was removed under reduced pressure to yield dimethyl-1,1'-binaphthyl-2,2'-dihydroxy-3,3'-dicarboxylate (**2.1**) (73.4 g, 78%) as a yellow solid, δ_H ($CDCl_3$): 4.04 (6H, s), 7.10-7.18 (2H, m), 7.28-7.36 (4H, m), 7.88-7.94 (2H, m), 8.67 (2H, s), 10.70 (2H, s).

E.2.2 Synthesis of phosphonites derived from 9,9'-biphenanthryl-10,10'-diol (2.2) and dimethyl-1,1'-binaphthyl-2,2'-dihydroxy-3,3'-dicarboxylate (2.1)

E.2.2.1 Mono- and diphosphonite syntheses from $RPCl_2$ species

Preparation of (±)-(9,9'-biphenanthryl-10,10'-diyl)phenylphosphonite (2.12)

To a stirred solution of dichlorophenylphosphine (70 µl, 0.52 mmol, 1.0 mol equiv) in THF (10 cm^3) at -10 °C was added triethylamine (144 µl, 1.03 mmol, 2.0 mol equiv). To the resulting cloudy white suspension at -10 °C a solution of (±)-9,9'-biphenanthryl-10,10'-diol (**2.2**) (200 mg, 0.52 mmol) in THF (10 cm^3) was added dropwise over 10 min. After stirring the reaction mixture at -10 °C for 1 h, the resulting thick white precipitate of triethylammonium chloride that had formed was removed by filtration through celite to leave a pale green solution. The solvent was removed *in vacuo* to afford a pale green foam which was triturated with pentane (10 cm^3) to yield (±)-(9,9'-biphenanthryl-10,10'-diyl)phenylphosphonite (**2.12**) (207 mg, 81%) as a pale green solid, δ_P ($CDCl_3$): 186.5; δ_H ($CDCl_3$): 7.07-7.13 (2H, m), 7.22-7.30 (2H, m), 7.31-7.37 (2H, m), 7.40 (1H, d, ^3J(HH) 8.2 Hz), 7.47 (1H, d, ^3J(HH) 8.2 Hz), 7.50-7.63 (6H, m), 7.69-7.75 (1H, m), 7.77-7.83 (1H, m), 8.42 (1H, d, ^3J(HH) 8.2 Hz), 8.63 (1H, d, ^3J(HH) 8.2 Hz), 8.73 (1H, d, ^3J(HH) 8.5 Hz), 8.80 (1H, d, ^3J(HH) 8.2 Hz), 8.84 (1H, d, ^3J(HH) 8.5 Hz);

δ_C ($CDCl_3$): 121.19 (s), 121.23 (s), 122.00 (s), 122.05 (s), 122.11 (s), 122.87 (s), 122.91 (s), 122.95 (s), 123.11 (s), 125.53 (s), 125.74 (s), 126.26 (s), 126.33 (s), 126.51 (s), 127.08 (s), 127.17 (s), 127.23 (s), 127.41 (s), 127.74 (s), 127.85 (s), 127.88 (s), 127.92 (s), 128.29 (s), 128.73 (s), 130.15 (s), 130.43 (s), 130.86 (s), 131.38 (s), 131.54 (s), 131.94 (s), 132.14 (s), 138.98 (d, ^1J(CP) 35 Hz, C-P), 145.73 (d, ^2J(CP) 7 Hz, C-O), 146.48 (d, ^2J(CP) 4 Hz, C-O'); *m/z* (NH_3, CI): 493 ($M+H^+$, 100%), 415 ($M-Ph^+$, 22%).

(*S*)-(9,9'-biphenanthryl-10,10'-diyl)phenylphosphonite (**2.12**) was also prepared using this procedure starting with (*S*)-9,9'-biphenanthryl-10,10'-diol (**2.2**).

*Preparation of (±) - (dimethyl - 1,1' - binaphthyl - 3,3' - dicarboxylate - 2,2' - diyl)phenylphosphonite (**2.11**)*

To a stirred solution of dichlorophenylphosphine (169 µl, 1.25 mmol, 1.0 mol equiv) in dichloromethane (5 cm^3) at -20 °C was added triethylamine (347 µl, 2.49 mmol, 2.0 mol equiv). The solution was warmed to -10 °C and a solution of dimethyl - 1,1' - binaphthyl - 2,2' - dihydroxy - 3,3' - dicarboxylate (**2.1**) (500 mg, 1.24 mmol) in dichloromethane (13 cm^3) was added dropwise over 10 min. The reaction mixture was allowed to warm to room temperature and stirred for 1 h. After this time the solvent was removed *in vacuo* to afford an off-white solid residue. THF (25 cm^3) was added and the resulting thick white precipitate of triethylammonium chloride was removed by filtration through celite to leave a yellow solution. The solvent was removed *in vacuo* to afford a yellow foam which was triturated with pentane (10 cm^3) to yield (±)-(dimethyl-1,1'-binaphthyl-3,3'-dicarboxylate-2,2'-diyl)phenylphosphonite (**2.11**) (209 mg, 33%) as a yellow solid, δ_P ($CDCl_3$): 184.4; δ_H ($CDCl_3$): 3.58 (3H, s, MeO), 3.95 (3H, s, MeO'), 7.24 (1H, d, ^3J(HH) 7.6 Hz), 7.27 (1H, d, ^3J(HH) 7.0 Hz), 7.31-7.41 (5H, m), 7.45 (1H, d, ^3J(HH) 8.2 Hz), 7.47 (1H, d, ^3J(HH) 8.8 Hz), 7.49 (1H, d, ^3J(HH) 7.9 Hz), 7.51 (1H, d, ^3J(HH) 8.2 Hz), 7.94 (1H, d, ^3J(HH) 7.6 Hz), 8.03 (1H, d, ^3J(HH) 8.6 Hz), 8.32 (1H, s, H4), 8.69 (1H, s, H4'); δ_C ($CDCl_3$): 52.13 (s, MeO), 52.68 (s, MeO'), 124.19 (s), 124.90 (s), 125.89 (s), 126.12 (s), 126.75 (s), 126.82 (s), 128.14 (s), 128.21 (s), 128.52 (s), 128.72 (s), 129.67 (s), 129.76 (s), 129.80 (s), 129.95 (s), 130.00 (s), 130.60 (s), 130.88 (s), 132.43 (s), 133.11 (s), 133.35 (s), 134.48 (s), 134.95 (s), 137.40 (s), 138.10 (d, ^1J(CP) 37 Hz, C-P), 146.47 (d, ^2J(CP) 6 Hz, C-O), 148.12 (d, ^2J(CP) 4 Hz, C-O'), 166.06 (s, C=O), 170.77 (s, C=O'); *m/z* (NH_3, CI): 509 ($M+H^+$, 100%), 402 ($M-106^+$, 55%), 371 ($M-137^+$, 88%).

*Preparation of the diastereomeric mixture 1,2-bis[(9,9'-biphenanthryl-10,10'-diyl)phosphonito]ethane (**2.16**)*

To a stirred solution of $Cl_2PCH_2CH_2PCl_2$ (**2.17**) (97 µl, 0.64 mmol, 0.5 mol equiv) in THF (15 cm^3) at -15 °C was added triethylamine (361 µl, 2.59 mmol, 2 mol equiv). A solution of (±)-9,9'-biphenanthryl-10,10'-diol (**2.2**) (500 mg, 1.30 mmol) in THF (15 cm^3) was added dropwise over 10 min to the resulting cloudy white suspension at -15 °C. The reaction mixture was allowed to warm to -10 °C and stirred for 1 h. After this time, the thick white precipitate of triethylammonium chloride that had formed was removed by filtration through celite. The solvent was removed *in vacuo* to afford a green foam which was triturated with pentane (10 cm^3) to yield the diastereomeric mixture 1,2-bis{(9,9'-biphenanthryl-10,10'-diyl)phosphonito}ethane (**2.16**) {(*R,R*) / (*S,S*) : (*R,S*) *ca.* 1:3} (550 mg, 99%) as a green solid, δ_P (THF / $CDCl_3$ 4:1): 211.8 {(*R,R*) / (*S,S*)}, 212.6 {(*R,S*)}.

(*S,S*)-1,2-bis{(9,9'-biphenanthryl-10,10'-diyl)phosphonito}ethane (**2.16**) was also prepared using this procedure starting with (*S*)-9,9'-biphenanthryl-10,10'-diol (**2.2**), δ_P ($CDCl_3$): 211.7; δ_H ($CDCl_3$): 1.94-2.08 (2H, m), 2.93-3.06 (2H, m), 7.24-7.36 (8H, m), 7.53-7.76 (12H, m), 8.17 (4H, d, ^3J(HH) 8.2 Hz), 8.69-8.77 (8H, m); δ_C ($CDCl_3$): 27.20 (dd, ^1J(CP) 44 Hz, ^2J(CP) 20 Hz, PCH_2), 121.13 (s), 121.94 (s), 122.83 (s), 122.93 (s), 123.07, 123.13 (s), 125.87 (s), 125.92 (s), 126.73 (s), 127.13 (s), 127.30 (s), 127.42 (s), 127.83 (s), 127.94 (s), 128.10 (s), 128.41 (s), 128.83 (s), 131.39 (s), 131.61 (s), 132.03 (s), 145.80 (s, C-O), 146.93 (s, C-O').

E.2.2.2 Phosphinophosphonite synthesis from $RP(NMe_2)_2$ species

*Preparation of (±) - 1 - {(9,9' - biphenanthryl - 10,10' - diyl)phosphonito} - 2 - diphenylphosphinoethane (**2.21**)*

To a stirred solution of $Ph_2PCH_2CH_2P(NMe_2)_2$ (**2.20**) (315 mg, 0.95 mmol, 1 mol equiv) in toluene (15 cm^3) was added a solution of 9,9'-biphenanthryl-10,10'-diol (**2.2**) (366 mg, 0.95 mmol) in toluene (15 cm^3). The reaction mixture was heated to reflux under nitrogen for 16 h and then allowed to cool to room temperature. The solvent was removed *in vacuo* to afford a pale green foam which was triturated with pentane (10 cm^3) to yield (±)-1-{(9,9'-biphenanthryl-10,10'-diyl)phosphonito}-2-diphenylphosphinoethane (**2.21**) (578 mg, 97%) as a pale green solid, δ_P ($CDCl_3$): -12.8 (d, ^3J(PP) 28 Hz, $\underline{P}Ph_2$), 215.5 (d, ^3J(PP) 31 Hz, $\underline{P}(OAr)_2$); δ_H ($CDCl_3$): 1.67-1.79 (2H, m), 2.06-2.18 (1H, m), 2.30-2.40 (1H, m), 7.14-7.39 (14H, m), 7.53-7.62 (2H, m), 7.66 (1H, td, ^3J(HH) 7.6 Hz, ^4J(HH) 1.0 Hz), 7.73 (1H, td, ^3J(HH) 7.6 Hz, ^4J(HH) 1.0 Hz), 7.75-7.81 (2H, m), 8.19 (1H, dd, ^3J(HH) 8.1 Hz, ^4J(HH) 1.1 Hz), 8.35 (1H, dd, ^3J(HH) 7.8 Hz, ^4J(HH) 1.4 Hz), 8.76 (2H, dd, ^3J(HH) 8.2 Hz,

^4J(HH) 2.5 Hz), 8.79 (2H, d, ^3J(HH) 8.2 Hz); δ_C ($CDCl_3$): 19.56 (t, ^1J(CP), ^2J(CP) 15 Hz, H_2CPPh_2), 31.77 (dd, ^1J(CP) 37 Hz, ^2J(CP) 13 Hz, $H_2CP(OAr)_2$), 121.28 (d, ^2J(CP) 4 Hz, HCCPPh$_2$), 123.10 (s), 125.50 (s), 125.87 (s), 125.90 (s), 126.72 (s), 126.80 (s), 127.29 (s), 127.38 (s), 127.44 (s), 127.89 (s), 127.95 (s), 128.06 (s), 128.13 (s), 128.44 (s), 128.55 (s), 128.61 (s), 128.66 (s), 128.81 (s), 128.85 (s), 128.88 (s), 129.25 (s), 131.50 (s), 131.70 (s), 131.77 (s), 132.12 (s), 132.65 (s), 132.76 (s), 132.83 (s), 132.94 (s), 138.01 (d, ^1J(CP) 15 Hz, C-P), 145.80 (s, C-O), 146.93 (s, C-O').

(*S*)-1-{(9,9'-biphenanthryl-10,10'-diyl)phosphonito}-2-(diphenylphosphino)-ethane (**2.21**) was also prepared using this procedure starting with (*S*)-9,9'-biphenanthryl-10,10'-diol (**2.2**).

E.2.3 Coordination chemistry of phosphonites derived from 9,9'-biphenanthryl-10,10'-diol (2.2) and dimethyl-1,1'-binaphthyl-2,2'-dihydroxy-3,3'-dicarboxylate (2.1)

E.2.3.1 Dichloroplatinum(II) complexes

E.2.3.1.1 Monophosphonites (2.12) and (2.11)

Preparation of the diastereomeric mixture cis-[PtCl$_2$[(9,9'-biphenanthryl-10,10'-diyl)phenylphosphonite}$_2$] (2.23)

To a stirred solution of (±)-(9,9'-biphenanthryl-10,10'-diyl)phenylphosphonite (**2.12**) (124 mg, 0.25 mmol) in THF (5 cm^3) was added [$PtCl_2$(cod)] (47 mg, 0.13 mmol, 0.5 mol equiv). The yellow solution was stirred for 14 h during which time a white precipitate formed. The solvent was removed *in vacuo* to yield the diastereomeric mixture of *cis*-[$PtCl_2$[(9,9'-biphenanthryl-10,10'-diyl) phenylphosphonite}$_2$] (**2.23**) {major : minor *ca.* 10:1} (158 mg, quantitative) as an off-white solid, δ_P ($CDCl_3$): 122.3 (s, ^1J(PPt) 4943 Hz, minor isomer), 122.9 (s, ^1J(PPt) 4908 Hz, major isomer).

Preparation of {(R,R)/(S,S)}-cis-[PtCl$_2$[(dimethyl-1,1'-binaphthyl-3,3'-dicarboxylate-2,2'-diyl)phenylphosphonite}$_2$] (2.22)

To a stirred solution of (±)-(dimethyl-1,1'-binaphthyl-3,3'-dicarboxylate-2,2'-diyl)phenylphosphonite (**2.11**) (125 mg, 0.25 mmol) in THF (5 cm^3) was added [$PtCl_2$(cod)] (40 mg, 0.11 mmol, 0.43 mol equiv). The solution was stirred for 2 h during which time a white precipitate formed. The solvent was removed *in vacuo* to yield {(*R*,*R*) / (*S*,*S*)}-*cis*-[$PtCl_2$[(dimethyl-1,1'-binaphthyl-3,3'-dicarboxylate-2,2'-diyl)phenylphosphonite}$_2$] (**2.22**) (126 mg, 92%) as a yellow solid, δ_P (CD_2Cl_2): 123.1 (s, ^1J(PPt) 4979 Hz); δ_H (CD_2Cl_2): 3.89 (6H, s, MeO), 3.96 (6H, s, MeO'), 6.80-6.87 (4H, m), 6.94 (2H, d, ^3J(HH) 7.0 Hz), 6.97 (2H, d, ^3J(HH) 7.3 Hz),

7.20-7.33 (4H, m), 7.41 (2H, dd, ^3J(HH) 8.2 Hz, ^4J(HH) 0.9 Hz), 7.42 (2H, dd, ^3J(HH) 6.7 Hz, ^4J(HH) 1.2 Hz), 7.52-7.58 (2H, m), 7.79 (2H, d, ^3J(HH) 7.9 Hz), 7.87 (2H, d, ^3J(HH) 9.5 Hz), 7.98 (2H, s), 8.12 (2H, d, ^3J(HH) 8.2 Hz), 8.56 (2H, s, H4), 8.62 (2H, s, H4'); δ_C (CD_2Cl_2): 51.53 (s, MeO), 53.11 (s, MeO'), 123.39 (s), 124.30 (s), 124.83 (s), 126.77 (s), 126.97 (s), 127.41 (s), 127.45 (s), 127.81 (s), 127.96 (s), 128.00 (s), 128.38 (s), 128.98 (s), 129.53 (s), 129.68 (s), 130.12 (s), 130.45 (s), 131.20 (s), 131.58 (s), 131.76 (s), 132.80 (s), 133.08 (s), 133.33 (s), 134.10 (s), 134.18 (s), 137.39 (s), 144.08 (d, ^2J(CP) 9 Hz, C-O), 145.14 (d, ^2J(CP) 17 Hz, C-O'), 166.08 (s, C=O), 170.94 (s, C=O'); δ_{Pt} (CD_2Cl_2): 162.7 (t, ^1J(PtP) 4989 Hz); *m/z* (FAB): 1246 (M-Cl^+, 100%); elemental analysis {calculated for $C_{60}H_{42}O_{12}P_2PtCl_2.0.5(CHCl_3).0.5(C_4H_8O)$}: C, 54.85 {54.45}; H, 3.38 {3.40}.

*E.2.3.1.2 Diphosphonite (S,S)-(**2.16**) and phosphinophosphonite (±)-(**2.21**) Preparation of (S,S)-cis-[$PtCl_2$(1,2-bis{(9,9'-biphenanthryl-10,10'-diyl)phosphonito} ethane)] (**2.24**)*

To a stirred solution of (*S,S*)-1,2-bis{(9,9'-biphenanthryl-10,10'-diyl)phosphonito}ethane (**2.16**) (136 mg, 0.16 mmol) in THF (5 cm^3) was added [$PtCl_2$(cod)] (45 mg, 0.12 mmol, 0.76 mol equiv). The solution was stirred for 30 min, during which time a white precipitate formed. The solvent was removed *in vacuo* to yield (*S,S*)-*cis*-[$PtCl_2$(1,2-bis{(9,9'-biphenanthryl-10,10'-diyl)phosphonito} ethane)] (**2.24**) (128 mg, 94%) as a white solid, δ_P (CD_2Cl_2): 159.4 (s, ^1J(PPt) 4868 Hz); δ_H (CD_2Cl_2): 1.91-2.14 (4H, m), 7.28 (8H, dd, ^3J(HH) 3.7 Hz, ^4J(HH) 1.5 Hz), 7.57-7.64 (4H, m), 7.67-7.80 (10H, m), 8.24 (2H, dd, ^3J(HH) 7.9 Hz, ^4J(HH) 1.2 Hz), 8.52 (2H, d, ^3J(HH) 9.5 Hz), 8.72 (2H, d, ^3J(HH) 8.6 Hz), 8.76 (2H, d, ^3J(HH) 8.9 Hz), 8.78 (2H, dd, ^3J(HH) 7.9 Hz, ^4J(HH) 1.2 Hz); δ_C (CD_2Cl_2): 29.89 (dd, ^1J(CP) 51 Hz, ^2J(CP) 18 Hz, PCH_2), 119.30 (s), 121.65 (s), 121.73 (s), 123.12 (s), 123.50 (s), 123.74 (s), 123.88 (s), 124.16 (s), 126.08 (s), 127.08 (s), 127.47 (s), 127.74 (s), 128.36 (s), 128.64 (s), 128.86 (s), 128.89 (s), 129.13 (s), 129.46 (s), 129.53 (s), 131.03 (d, ^2J(CP) 22 Hz, C-O), 132.16 (d, ^2J(CP) 17 Hz, C-O'); δ_{Pt} (CD_2Cl_2) 186.1 (t, ^1J(PtP) 4877 Hz); elemental analysis {calculated for $C_{58}H_{36}O_4P_2PtCl_2.1.5(CHCl_3).2.5(C_4H_8O)$}: C, 56.31 {56.24}; H, 3.86 {3.90}.

Preparation of (±)-cis-[$PtCl_2$(1-{(9,9'-biphenanthryl-10,10'-diyl)phosphonito}-2-diphenylphosphinoethane)] (2.25)

To a stirred solution of (±)-1-{(9,9'-biphenanthryl-10,10'-diyl)phosphonito}-2-diphenylphosphinoethane (**2.21**) (141 mg, 0.22 mmol) in THF (3 cm^3) was added [$PtCl_2$(cod)] (71 mg, 0.19 mmol, 0.85 mol equiv). The solution was stirred for 1 h during which time a thick white precipitate formed. The solvent was removed *in vacuo* and the residue was digested in dichloromethane (10 cm^3) and isolated by filtration to yield (±)-*cis*-[$PtCl_2$(1-{(9,9'-biphenanthryl-10,10'-diyl)}phosphonito-2-diphenylphosphinoethane)] (**2.25**) (107 mg, 63%) as a white solid, δ_P (d_6-dmso): 44.3 (s, ^1J(PPt) 3465 Hz, $\underline{P}Ph_2$), 160.5 (s, ^1J(PPt) 5066 Hz, $\underline{P}(OAr)_2$); δ_H (d_6-dmso): 2.23-2.41 (2H, m), 2.67-3.09 (2H, m), 7.17 (1H, d, ^3J(HH) 8.6 Hz), 7.25 (1H, d, ^3J(HH) 8.2 Hz), 7.37 (1H, d, ^3J(HH) 7.6 Hz), 7.42 (1H, d, ^3J(HH) 7.9 Hz), 7.61-7.74 (8H, m), 7.80 (1H, d, ^3J(HH) 6.7 Hz), 7.83 (1H, d, ^3J(HH) 6.7 Hz), 7.89 (2H, d, ^3J(HH) 7.6 Hz), 7.92 (2H, d, ^3J(HH) 7.6 Hz), 7.94-8.04 (2H, m), 8.17 (1H, d, ^3J(HH) 7.9 Hz), 8.43 (1H, d, ^3J(HH) 8.2 Hz), 8.97-9.00 (3H, m), 9.06 (1H, d, ^3J(HH) 8.5 Hz); δ_C (d_6-dmso): 119.20 (s), 120.10 (s), 122.33 (s), 123.04 (s), 123.35 (s), 123.70 (s), 123.77 (s), 125.29 (s), 126.31 (s), 126.73 (s), 126.92 (s), 127.06 (s), 127.21 (s), 127.39 (s), 127.52 (s), 128.43 (s), 128.52 (s), 128.63 (s), 128.69 (s), 128.74 (s), 128.87 (s), 129.00 (s), 129.04 (s), 129.15 (s), 130.10 (s), 130.26 (s), 131.38 (s), 131.43 (s), 132.07 (s), 132.53 (s), 133.26 (d, ^1J(CP) 11 Hz, C-P), 133.85 (d, ^1J(CP) 11 Hz, C-P'), 144.04 (d, ^2J(CP) 13 Hz, C-O), 144.76 (d, ^2J(CP) 9 Hz, C-O'); δ_{Pt} (d_6-dmso): 84.3 (dd, ^1J($PtPPh_2$) 3463 Hz, ^1J($PtP(OAr)_2$) 5063 Hz); *m/z* (FAB): 894 (M^+, 6%), 859 ($M-Cl^+$, 55%), 368 ($M-526^+$, 65%), 307 ($M-587^+$, 100%), 289 ($M-605^+$, 50%), 213 ($M-671^+$, 80%).

E.2.3.2 Rhodium(I) complexes

E.2.3.2.1 Monophosphonites (2.12) and (2.11)

Preparation of (S,S) - cis - [Rh (cod) {(9,9' - biphenanthryl - 10,10' - diyl) phenylphosphonite}$_2$]BF_4 (2.27)

To a stirred solution of (*S*)-(9,9'-biphenanthryl-10,10'-diyl)phenylphosphonite (**2.12**) (309 mg, 0.63 mmol, 2 mol equiv) in dichloromethane (10 cm^3) was added [$Rh(cod)_2$]BF_4 (127 mg, 0.31 mmol). The reaction mixture was stirred for 1 h and the solvent was then removed *in vacuo* to yield (*S,S*)-*cis*-[Rh(cod){(9,9'-biphenanthryl-10,10'-diyl)phenylphosphonite}$_2$]BF_4 (**2.27**) (325 mg, 82%) as an orange solid, δ_P {CH_2Cl_2 / C_6D_6 (3:2)}: 173.1 (br d, ^1J(PRh) 214 Hz).

Preparation of (±) - [Rh (CO) (dpm) {(9,9' - biphenanthryl - 10,10' - diyl) phenylphosphonite}] (2.32)

To a stirred yellow solution of (±)-(9,9'-biphenanthryl-10,10'-diyl)phenylphosphonite (**2.12**) (171 mg, 0.35 mmol, 2 mol equiv) in THF (5 cm^3) was added $[Rh(CO)_2(dpm)]$ (59 mg, 0.17 mmol); vigorous bubbling was observed. The resulting dark red solution was stirred overnight and the solvent was then removed *in vacuo*. The dark red solid residue was digested in methanol (5 cm^3) and isolated by filtration to yield (±)-[Rh(CO)(dpm){(9,9'-biphenanthryl-10,10'-diyl)phenylphosphonite}] (**2.32**) (80 mg, 58%) as a cream solid, δ_P (CD_2Cl_2): 189.2 (d, ^1J(PRh) 248 Hz); δ_H (CD_2Cl_2): 0.86 (9H, s, ^{t}Bu), 1.15 (9H, s, ^{t}Bu'), 5.84 (1H, s), 7.16 (2H, td, ^3J(HH) 7.6 Hz, ^4J(HH) 2.4 Hz), 7.29-7.40 (5H, m), 7.45 (1H, d, ^3J(HH) 7.9 Hz), 7.58-7.69 (4H, m), 7.79 (1H, d, ^3J(HH) 8.2 Hz), 7.83 (1H, td, ^3J(HH) 7.8 Hz, ^4J(HH) 1.2 Hz), 7.97 (1H, d, ^3J(HH) 7.3 Hz), 8.00 (1H, d, ^3J(HH) 7.3 Hz), 8.58 (1H, d, ^3J(HH) 7.3 Hz), 8.67 (1H, d, ^3J(HH) 8.6 Hz), 8.75 (1H, d, ^3J(HH) 8.2 Hz), 8.87 (2H, t, ^3J(HH) 9.2 Hz); *m/z* (FAB): 807 ($M+H^+$, 28%), 794 ($M-12^+$, 44%), 778 ($M-CO^+$, 100%), 623 ($M-dpm^+$, 32%), 595 ($M-dpm-CO^+$, 92%), 455 ($M-351^+$, 52%), 368 ($M-438^+$, 40%); IR (CH_2Cl_2): 2005 cm^{-1} {υ_{CO} (Rh-CO)}.

Preparation of (±)-[Rh(CO)(dpm){(dimethyl-1,1'-binaphthyl-3,3'-dicarboxylate-2,2'-diyl)phenylphosphonite}] (2.31)

To a stirred yellow solution of (±)-(dimethyl-1,1'-binaphthyl-3,3'-dicarboxylate-2,2'-diyl)phenylphosphonite (**2.11**) (67 mg, 0.13 mmol, 2 mol equiv) in THF (5 cm^3) was added $[Rh(CO)_2(dpm)]$ (23 mg, 0.067 mmol); vigorous bubbling was observed. The resulting dark red solution was stirred overnight and the solvent was then removed *in vacuo*. The dark red oily residue was dissolved in methanol (2.5 cm^3) and allowed to stand for 5 min, during which time a cream precipitate formed. This product was isolated by filtration to yield (±)-[Rh(CO)(dpm){(dimethyl-1,1'-binaphthyl-3,3'-dicarboxylate-2,2'-diyl)phenylphosphonite}] (**2.31**) (28 mg, 51%) as a cream solid, δ_P (CD_2Cl_2): 187.0 (d, ^1J(PRh) 250 Hz); δ_H ($CDCl_3$): 0.70 (9H, s, ^{t}Bu), 1.18 (9H, s, ^{t}Bu'), 3.70 (3H, s, MeO), 4.04 (3H, s, MeO'), 5.77 (1H, s), 7.24-7.54 (9H, m), 7.78 (1H, d, ^3J(HH) 7.0 Hz), 7.81 (1H, d, ^3J(HH) 7.3 Hz), 7.94 (1H, d, ^3J(HH) 8.2 Hz), 8.05 (1H, d, ^3J(HH) 7.9 Hz), 8.35 (1H, s, H4), 8.69 (1H, s, H4'); *m/z* (FAB): 845 ($M+Na^+$, 8%), 794 ($M-CO^+$, 100%), 639 ($M-dpm^+$, 52%); IR (CH_2Cl_2): 2008 cm^{-1} {υ_{CO} (Rh-CO)}.

E.2.3.2.2 Diphosphonite (S,S)-(2.16)

Preparation of (S,S) - [Rh (cod) (1,2-bis{(9,9' - biphenanthryl - 10,10' - diyl) phosphonito}ethane)] (2.33)

To a stirred red solution of $[Rh(cod)_2]BF_4$ (58 mg, 0.14 mmol) in dichloromethane (5 cm^3) was added dropwise over 5 min a solution of (*S,S*)-1,2-bis{(9,9'-biphenanthryl-10,10'-diyl)phosphonito}ethane (**2.16**) (116 mg, 0.14 mmol, 1 mol equiv) in dichloromethane (10 cm^3). The resulting yellow solution was stirred for a further 30 min and the solvent was then removed *in vacuo* to yield (*S,S*)-[Rh(cod)(1,2-bis{(9,9'-biphenanthryl-10,10'-diyl)phosphonito}ethane)] (**2.33**) (156 mg, quantitative) as a red solid, δ_P ($CDCl_3$): 205.7 (d, ^1J(PRh) 229 Hz); δ_H ($CDCl_3$): 1.47-1.64 (4H, m, CH_2{cod}), 1.91-2.04 (2H, m, PC<u>H</u>H'), 2.20-2.50 (4H, m, CH_2{cod}), 2.53-2.63 (2H, m, PCH<u>H</u>'), 5.30 (2H, br s, CH{cod}), 5.59 (2H, br s, CH{cod}), 7.30-7.44 (8H, m), 7.61-7.70 (4H, m), 7.81-7.96 (6H, m), 8.06 (2H, t, ^3J(HH) 7.5 Hz), 8.72 (2H, d, ^3J(HH) 8.2 Hz), 8.74-8.88 (10H, m).

E.2.3.2.3 Phosphinophosphonite (2.21)

Preparation of (S)-[Rh(cod)(1 - {(9,9' - biphenanthryl - 10,10' - diyl)phosphonito}-2-diphenylphosphinoethane)] (2.35)

To a stirred red solution of $[Rh(cod)_2]BF_4$ (64 mg, 0.16 mmol) in dichloromethane (5 cm^3) was added a solution of (*S*)-1-{(9,9'-biphenanthryl-10,10'-diyl)phosphonito}-2-diphenylphosphinoethane) (**2.21**) (98 mg, 0.16 mmol, 1 mol equiv) in dichloromethane (10 cm^3) dropwise over 5 min. The resulting yellow solution was stirred for a further 30 min and the solvent was then removed *in vacuo* to yield (*S*) - [Rh (cod) (1 - (9,9' - biphenanthryl - 10,10' - diyl)phosphonito-2-diphenylphosphinoethane)] (**2.35**) (145 mg, quantitative) as a red solid, δ_P {CH_2Cl_2 / C_6D_6 (3:2)}: 56.2 (dd, ^1J(PRh) 153 Hz, ^2J(PP) 28 Hz, <u>P</u>Ph_2), 207.3 (dd, ^1J(PRh) 220 Hz, ^2J(PP) 30 Hz, <u>P</u>$(OAr)_2$).

Reaction of two equivalents of (±)-1-{(9,9'-biphenanthryl-10,10'-diyl)phosphonito}-2-diphenylphosphinoethane (2.21) with [{RhCl(CO)$_2$}$_2$]

To a stirred solution of (±)-1-{(9,9'-biphenanthryl-10,10'-diyl)phosphonito}-2-diphenylphosphinoethane (**2.21**) (183 mg, 0.29 mmol, 1.9 mol equiv) in THF (3 cm^3) was added [{RhCl(CO)$_2$}$_2$] (57 mg, 0.15 mmol). Vigorous bubbling was observed and the resulting dark red solution was stirred for 1 h, during which time a red precipitate formed. The solvent was removed *in vacuo*, THF (2 cm^3) was added and the solvent was removed *in vacuo* to afford a red solid. $^{31}P\{^1H\}$ NMR spectroscopy showed this to be a mixture of the two diastereomers {(*R,R*) / (*S,S*) and (*R,S*) *ca.* 2.5:1} of [Rh(1 - {(9,9' - biphenanthryl - 10,10' - diyl)phosphonito} - 2-diphenylphosphinoethane)$_2$]Cl (**2.36**), δ_P (CD_2Cl_2): 53.1 (dd, ^1J(PRh) 126 Hz,

^2J(PP) 305 Hz, $\underline{P}Ph_2$), 222.7 (dd, ^1J(PRh) 190 Hz, ^2J(PP) 307 Hz, $\underline{P}(OAr)_2$) {(*R,R*) / (*S,S*)}; 53.1 (dd, ^1J(PRh) 130 Hz, ^2J(PP) 370 Hz, $\underline{P}Ph_2$), 222.7 (dd, ^1J(PRh) 192 Hz, ^2J(PP) 368 Hz, $\underline{P}(OAr)_2$) {(*R,S*)}, and [RhCl(CO)(1-{(9,9'-biphenanthryl-10,10'-diyl)phosphonito}-2-diphenylphosphinoethane)] (**2.40**), δ_P (CD_2Cl_2): 52.0 (dd, ^1J(PRh) 133 Hz, ^2J(PP) 34 Hz, $\underline{P}Ph_2$), 216.3 (dd, ^1J(PRh) 222 Hz, ^2J(PP) 36 Hz, $\underline{P}(OAr)_2$); {(**2.36**) : (**2.40**) *ca.* 3.5:13}.

E.2.3.3 Platinum(0) complexes - NMR studies

E.2.3.3.1 Monophosphonite (2.12)

Reaction of one equivalent of (±)-(9,9'-biphenanthryl-10,10'-diyl)phenylphosphonite (2.12) with [Pt(nb)$_3$]

To an NMR solution of (±)-(9,9'-biphenanthryl-10,10'-diyl)phenylphosphonite (**2.12**) (15.0 mg, 0.030 mmol) in $CDCl_3$ (0.5 cm^3) was added [Pt(nb)$_3$] (14.5 mg, 0.030 mmol, 1 mol equiv). The reaction was followed by $^{31}P\{^1H\}$ and $^{195}Pt\{^1H\}$ NMR spectroscopy, which showed the formation of the three diastereomers of [Pt(nb){(9,9'-biphenanthryl-10,10'-diyl)phenylphosphonite}$_2$] (**2.42**), δ_P ($CDCl_3$): 196.6 (d, ^1J(PPt) 4920 Hz, ^2J(PP) 76 Hz), 200.6 (d, ^1J(PPt) 4950 Hz, ^2J(PP) 76 Hz) {(*R,R*) / (*S,S*)-}; 198.5 (s, ^1J(PPt) 4976 Hz) {(*S,R*)-}; 198.6 (s, ^1J(PPt) 5045 Hz) {(*R,S*)-}; δ_{Pt} ($CDCl_3$): -556.1 (dd, ^1J(PPt) 4920 Hz, $^1J'$(PPt) 4950 Hz) {(*R,R*)/(*S,S*)-}; -538.5 (t, ^1J(PPt) 4976 Hz) {(*S,R*)-}; -503.1 (t, ^1J(PPt) 5045 Hz) {(*R,S*)-}.

E.2.3.3.2 Phosphinophosphonite (2.21)

Reaction of one equivalent of (±)-1-{(9,9'-biphenanthryl-10,10'-diyl)phosphonito}-2-diphenylphosphinoethane (2.21) with [Pt(nb)$_3$]

To an NMR solution of (±)-1-{(9,9'-biphenanthryl-10,10'-diyl)phosphonito}-2-diphenylphosphinoethane (**2.21**) (22 mg, 0.035 mmol) in $CDCl_3$ (0.5 cm^3) was added [Pt(nb)$_3$] (17 mg, 0.036 mmol, 1 mol equiv). The reaction was followed by $^{31}P\{^1H\}$ NMR spectroscopy, which showed the formation of a complicated mixture of species (see Section 2.3.3.2 for more details).

E.3 Chapter 3: Cyclic Aryl Diphosphites: Synthesis, Coordination Chemistry and Application in Asymmetric Hydroformylation

E.3.2 Synthesis of cyclic aryl phosphites derived from 9,9'-biphenanthryl-10,10'-diol (3.2)

E.3.2.1 Synthesis of the diphosphite 'biphenanthrite' (3.4) from 9,9'-biphenanthryl-10,10'-diol (3.2)

Preparation of (±)-(9,9'-biphenanthryl-10,10'-diyl)chlorophosphite (3.10)

To a solution of PCl_3 (4.5 cm^3, 51.6 mmol, 10 mol equiv) in THF (35 cm^3) at -40 °C was added NEt_3 (1.45 cm^3, 10.4 mmol, 2 mol equiv). A solution of (±)-9,9'-biphenanthryl-10,10'-diol (**3.2**) (2.00 g, 5.2 mmol) in THF (35 cm^3) was then added dropwise over 1 h whilst the temperature was maintained at -40 °C. The thick white suspension that formed was then stirred at -40 °C for 1 h, warmed to room temperature and then stirred for a further 2 h. The precipitate of triethylammonium chloride was removed by filtration under nitrogen through oven-dried celite and the solvent and excess PCl_3 were removed *in vacuo*. The yellow residue was dissolved in toluene (20 cm^3) and the insoluble precipitate of triethylammonium chloride was removed by filtration under nitrogen through oven-dried celite. The solvent was removed *in vacuo* to afford a pale yellow oil which was triturated with pentane (20 cm^3) to yield (±)-(9,9'-biphenanthryl-10,10'-diyl)chlorophosphite (**3.10**) (2.150 g, 92%) as a fine yellow solid, δ_P ($CDCl_3$): 180.9; δ_H ($CDCl_3$): 7.27-7.34 (2H, m), 7.38 (2H, dd, ^3J(HH) 8.4 Hz, ^4J(HH) 1.1 Hz), 7.57-7.64 (2H, m), 7.71-7.85 (4H, m), 8.30 (1H, dd, ^3J(HH) 8.1 Hz, ^4J(HH) 1.1 Hz), 8.42 (1H, dd, ^3J(HH) 8.1 Hz, ^4J(HH) 1.1 Hz), 8.77 (2H, d, ^3J(HH) 8.6 Hz), 8.81 (2H, d, ^3J(HH) 7.0 Hz); δ_C ($CDCl_3$): 121.19 (s), 121.23 (s), 122.58 (s), 122.67 (s), 122.93 (s), 123.02 (s), 123.77 (s), 126.24 (s), 126.46 (s), 126.60 (s), 126.70 (s), 126.75 (s), 126.92 (s), 127.21 (s), 127.63 (s), 128.05 (s), 128.14 (s), 128.18 (s), 128.23 (s), 128.62 (s), 128.69 (s), 129.04 (s), 130.88 (s), 130.97 (s), 131.39 (s), 131.83 (s), 144.74 (d, ^2J(CP) 4 Hz, C-O), 145.08 (d, ^2J(CP) 6 Hz, C-O').

(*S*)- and (*R*)-(9,9'-biphenanthryl-10,10'-diyl)chlorophosphite (**3.10**) were also prepared using this procedure starting with (*S*)- and (*R*)-9,9'-biphenanthryl-10,10'-diol (**3.2**) respectively.

*Formation of (±)-(9,9'-biphenanthryl-10,10'-diyl)phosphonate (**3.11**)*

Exposure of (±)-(9,9'-biphenanthryl-10,10'-diyl)chlorophosphite (**3.10**) to moisture resulted in gradual hydrolysis to form (±)-(9,9'-biphenanthryl-10,10'-diyl)phosphonate (**3.11**) as a yellow solid, δ_P ($CDCl_3$): 13.1 (d, ^1J(PH) 731 Hz); δ_H ($CDCl_3$): 7.29-7.44 (4H, m), 7.51 (1H, d, ^1J(HP) 732 Hz), 7.60-7.67 (2H, m), 7.75-7.88 (4H, m), 8.41-8.47 (2H, m), 8.75-8.84 (4H, m); *m/z* (NH_3, CI): 433 ($M+H^+$, 100%).

*Preparation of (S,S)-bis(9,9'-biphenanthryl-10,10'-diyl)pyrophosphite (**3.12**)*

To a solution of (*S*)-(9,9'-biphenanthryl-10,10'-diyl)chlorophosphite (**3.10**) (202 mg, 0.45 mmol) in THF (15 cm^3) at 0 °C was added NEt_3 (62 µl, 0.45 mmol, 1 mol equiv), affording a cloudy white suspension. A solution of distilled H_2O (4 µl, 0.22 mmol, 0.5 mol equiv) in THF (5 cm^3) was then added dropwise over 10 min whilst the temperature was maintained at 0 °C. The reaction mixture was warmed to room temperature and stirred for 1 h. The thick white precipitate of triethylammonium chloride that formed during the reaction was removed by filtration under nitrogen through oven-dried celite and the solvent was then removed *in vacuo* to yield (*S,S*)-bis(9,9'-biphenanthryl-10,10'-diyl)pyrophosphite (**3.12**) (190 mg, quantitative) as a yellow solid, δ_P ($CDCl_3$): 141.9 (s); δ_H ($CDCl_3$): 7.01 (2H, d, ^3J(HH) 8.6 Hz), 7.04-7.09 (2H, m), 7.14 (2H, d, ^3J(HH) 8.2 Hz), 7.17 (2H, d, ^3J(HH) 8.5 Hz), 7.30-7.39 (4H, m), 7.41 (2H, d, ^3J(HH) 7.6 Hz), 7.44 (2H, d, ^3J(HH) 7.6 Hz), 7.50-7.65 (4H, m), 8.16 (2H, d, ^3J(HH) 8.2 Hz), 8.18 (2H, dd, ^3J(HH) 8.1 Hz, ^4J(HH) 1.1 Hz), 8.37 (2H, d, ^3J(HH) 8.2 Hz), 8.43 (2H, d, ^3J(HH) 8.2 Hz), 8.50 (2H, d, ^3J(HH) 8.2 Hz), 8.53 (2H, d, ^3J(HH) 8.9 Hz).

*Preparation of (S,S)-(9,9'-biphenanthryl-10,10'-diyl)(10'-hydroxy-9,9'-biphenanthryl-10-yl)phosphite (**3.9**)*

To a solution of (*S*)-9,9'-biphenanthryl-10,10'-diol (**3.2**) (257 mg, 0.67 mmol) in THF (10 cm^3) at -40 °C was added NEt_3 (93 µl, 0.67 mmol, 1 mol equiv). A solution of (*S*)-(9,9'-biphenanthryl-10,10'-diyl)chlorophosphite (**3.10**) (300 mg, 0.67 mmol, 1 mol equiv) in THF (15 cm^3) was added dropwise over 5 min and the reaction mixture was then stirred at -40 °C for 1 h. The thick white precipitate of triethylammonium chloride that formed during the reaction was removed by filtration under nitrogen through a plug consisting of oven-dried celite and alumina. The solvent was removed *in vacuo* and the pale yellow solid residue was dissolved in dichloromethane (20 cm^3). Alumina was added and the mixture was stirred for 30 min and then filtered through a short alumina plug. The solvent was removed under reduced pressure and the oily residue was triturated with pentane (10 cm^3) to yield (*S,S*)-(9,9'-biphenanthryl-10,10'-diyl)(10'-hydroxy-9,9'-biphenanthryl-10-yl)phosphite

(**3.9**) (72 mg, 14%) as an off-white solid, δ_P ($CDCl_3$): 146.2 (s); δ_H ($CDCl_3$): 5.86 (1H, br s, OH), 7.22 (1H, d, ^3J(HH) 7.6 Hz), 7.25-7.33 (2H, m), 7.27 (1H, d, ^3J(HH) 7.0 Hz), 7.33-7.40 (4H, m), 7.40-7.47 (3H, m), 7.47-7.57 (3H, m), 7.58-7.67 (3H, m), 7.73 (1H, d, ^3J(HH) 7.0 Hz), 7.76 (1H, d, ^3J(HH) 7.3 Hz), 7.80-7.92 (2H, m), 7.93 (1H, d, ^3J(HH) 8.2 Hz), 8.13 (1H, d, ^3J(HH) 8.2 Hz), 8.63 (1H, d, ^3J(HH) 8.2 Hz), 8.65 (1H, d, ^3J(HH) 8.2 Hz), 8.71 (1H, d, ^3J(HH) 7.0 Hz), 8.79 (4H, d, ^3J(HH) 8.2 Hz), 8.81 (1H, d, ^3J(HH) 8.2 Hz), 8.92 (1H, d, ^3J(HH) 7.9 Hz).

*Preparation of {(R,S,R)/(S,R,S)}-tris(9,9'-biphenanthryl-10,10'-diyl)diphosphite (**3.4**) 'biphenanthrite'*

To a solution of (±)-9,9'-biphenanthryl-10,10'-diol (**3.2**) (300 mg, 0.78 mmol) in THF (40 cm^3) was added a suspension of sodium hydride (42 mg, 1.75 mmol, 2.2 mol equiv) in THF (5 cm^3) and the reaction mixture was stirred under nitrogen for 50 min. The resulting deep yellow solution was added dropwise over 20 min to a solution of (±)-(9,9'-biphenanthryl-10,10'-diyl)chlorophosphite (**3.10**) (870 mg, 1.93 mmol, 2.5 mol equiv) in THF (40 cm^3) at -40 °C. The resulting fine white suspension was allowed to warm to room temperature and stirred for 75 min. The reaction mixture was then plunged into saturated sodium bicarbonate solution (40 cm^3) and distilled water (40 cm^3) was added. The monophasic solution was extracted with diethyl ether (80 cm^3) and the organic extract was separated, dried ($MgSO_4$), filtered and the solvent was removed under reduced pressure to yield a fine yellow solid (955 mg). This crude product mixture was dissolved in dichloromethane (40 cm^3) and 1M potassium hydroxide solution (40 cm^3) was added. The biphasic mixture was stirred vigorously for 17 h and the two layers of the resulting emulsion were allowed to separate. The organic layer was removed, dried ($MgSO_4$), filtered and the solvent was removed under reduced pressure to yield {(*R,S,R*) / (*S,R,S*)}-tris(9,9'-biphenanthryl-10,10'-diyl)diphosphite (**3.4**) (435 mg, 46%) as a fine yellow solid, δ_P (CD_2Cl_2): 145.5 (s).

*Isomerisation of the diastereomeric mixture (9,9'-biphenanthryl-10,10'-diyl)(10'-hydroxy-9,9'-biphenanthryl-10-yl)phosphite (**3.9**)*

To a solution of the diastereomeric mixture of (9,9'-biphenanthryl-10,10'-diyl)(10'-hydroxy-9,9'-biphenanthryl-10-yl)phosphite (**3.9**) (30 mg, 0.04 mmol) in $CDCl_3$ (0.6 cm^3) was added sodium hydride (6.5 mg, 0.27 mmol, 7.2 mol equiv). The resultant grey suspension was monitored by $^{31}P\{^1H\}$ NMR spectroscopy. After 24 h, extra sodium hydride (7 mg, 0.29 mmol, 7.8 mol equiv) was added and the reaction mixture was again monitored by $^{31}P\{^1H\}$ NMR spectroscopy.

Preparation of the diastereomeric mixture tris(9,9'-biphenanthryl-10,10'-diyl)diphosphite (3.4)

To a solution of (±)-9,9'-biphenanthryl-10,10'-diol (**3.2**) (1.155 g, 2.99 mmol) and triethylamine (834 µl, 5.98 mmol, 2 mol equiv) in THF (13 cm^3) at -40 °C was added a solution of PCl_3 (174 µl, 1.99 mmol, 0.67 mol equiv) in THF (5 cm^3) dropwise over 7 min. The resulting thick white suspension was stirred at -40 °C for 10 min, warmed to room temperature and then stirred for a further 50 min. The reaction mixture was poured into 2M hydrochloric acid (20 cm^3) and the organic layer was separated. The organic extract was washed with 2M potassium hydroxide solution (20 cm^3) and distilled water (20 cm^3), dried ($MgSO_4$), filtered and the solvent removed under reduced pressure to yield the diastereomeric mixture tris(9,9'-biphenanthryl-10,10'-diyl)diphosphite (**3.4**) (804 mg, 66%) as a fine yellow solid, δ_P ($CDCl_3$): 141.8 (d, ^7J(PP) 40 Hz), 145.3 (d, ^7J(PP) 40 Hz) {(*R,R,S*) / (*S,S,R*)-}; 143.3 (s) {(*R,R,R*) / (*S,S,S*)-}; 145.3 (s) {(*R,S,R*) / (*S,R,S*)-}.

(*R,R,R*)-tris(9,9'-biphenanthryl-10,10'-diyl)diphosphite (**3.4**) was prepared in 56% yield using this procedure starting with (*R*)-9,9'-biphenanthryl-10,10'-diol (**3.2**), δ_P ($CDCl_3$): 143.3 (s); δ_H ($CDCl_3$): 6.50 (1H, t, ^3J(HH) 7.5 Hz), 7.10 (1H, t, ^3J(HH) 7.5 Hz), 7.14-7.26 (3H, m), 7.29 (4H, dd, ^3J(HH) 8.1 Hz, ^4J(HH) 1.4 Hz), 7.36 (2H, dd, ^3J(HH) 6.9 Hz, ^4J(HH) 1.1 Hz), 7.38 (2H, dd, ^3J(HH) 8.2 Hz, ^4J(HH) 1.2 Hz), 7.45 (1H, d, ^3J(HH) 8.2 Hz), 7.47-7.53 (1H, m), 7.55 (2H, dd, ^3J(HH) 7.0 Hz, ^4J(HH) 1.5 Hz), 7.57 (2H, dd, ^3J(HH) 8.2 Hz, ^4J(HH) 1.5 Hz), 7.59-7.62 (2H, m), 7.69 (1H, t, ^3J(HH) 7.2 Hz), 7.73 (2H, dd, ^3J(HH) 7.0 Hz, ^4J(HH) 0.9 Hz), 7.75 (2H, dd, ^3J(HH) 8.1 Hz, ^4J(HH) 1.1 Hz), 7.83 (2H, dd, ^3J(HH) 7.0 Hz, ^4J(HH) 1.2 Hz), 7.85 (2H, dd, ^3J(HH) 7.0 Hz, ^4J(HH) 1.5 Hz), 8.02 (1H, d, ^3J(HH) 8.5 Hz), 8.48 (4H, dd, ^3J(HH) 8.2 Hz, ^4J(HH) 0.9 Hz), 8.58 (1H, d, ^3J(HH) 8.5 Hz), 8.63 (1H, d, ^3J(HH) 7.6 Hz), 8.65 (1H, d, ^3J(HH) 8.5 Hz), 8.71 (1H, d, ^3J(HH) 7.9 Hz), 8.74 (1H, d, ^3J(HH) 7.3 Hz), 8.77 (4H, d, ^3J(HH) 8.2 Hz), 8.83 (4H, d, ^3J(HH) 8.5 Hz).

E.3.2.2 Synthesis of mixed diphosphites derived from 9,9'-biphenanthryl-10,10'-diol (3.2) and binaphthol

Preparation of the diastereomeric mixture bis(9,9'-biphenanthryl-10,10'-diyl)-µ-(1,1'-binaphthyl-2,2'-diyl)diphosphite 'pnp' (3.5)

To a solution of (±)-(9,9'-biphenanthryl-10,10'-diyl)chlorophosphite (**3.10**) (748 mg, 1.66 mmol, 2.2 mol equiv) in THF (40 cm^3) at -40 °C was added triethylamine (210 µl, 1.51 mmol, 2 mol equiv). A solution of (±)-binaphthol (216 mg, 0.75 mmol) in THF (30 cm^3) was then added dropwise over 30 min whilst the temperature was maintained at -40 °C. The resulting thick white suspension was warmed to room temperature and stirred for 1 h. The precipitate of triethylammonium

chloride was removed by filtration through oven-dried celite and the solvent was removed *in vacuo*. The yellow residue was dissolved in dichloromethane (80 cm^3) and 2M potassium hydroxide solution (80 cm^3) was added. The biphasic mixture was stirred vigorously for 4 h. The resulting emulsion was partitioned and the organic layer was separated and washed with distilled water (80 cm^3). 2M Hydrochloric acid (80 cm^3) was added and the resulting biphasic mixture was stirred vigorously for 10 min. The resulting emulsion was partitioned and the organic layer was separated, washed with distilled water (80 cm^3), 2M potassium hydroxide solution (80 cm^3) and brine (80 cm^3), dried ($MgSO_4$), filtered and the solvent was removed under reduced pressure to yield the diastereomeric mixture of bis(9,9'-biphenanthryl-10,10'-diyl)-μ-(1,1'-binaphthyl-2,2'-diyl)diphosphite 'pnp' (**3.5**) (447 mg, 53%) as a fine yellow solid, δ_P ($CDCl_3$): 143.1 (s) {(*R,R,R*) / (*S,S,S*)-}; 144.3 (d, ^7J(PP) 28 Hz), 146.1 (d, ^7J(PP) 27 Hz) {(*R,R,S*) / (*S,S,R*)-}; 147.7 (s) {(*R,S,R*) / (*S,R,S*)-}; *m/z* (FAB): 1137 ($M+Na^+$, 20%), 1115 ($M+H^+$, 35%), 683 ($M-431^+$, 100%).

Optically pure (*R,S,R*)-bis(9,9'-biphenanthryl-10,10'-diyl)-μ-(1,1'-binaphthyl-2,2'-diyl)diphosphite 'pnp' (**3.5**) has been synthesised using this procedure starting with (*R*)-(9,9'-biphenanthryl-10,10'-diyl)chlorophosphite (**3.10**) and (*S*)-binaphthol, δ_P ($CDCl_3$): 147.7 (s); *m/z* (FAB): 1137 ($M+Na^+$, 20%), 1115 ($M+H^+$, 35%), 683 ($M-431^+$, 100%).

Optically pure (*R,R,R*)-bis(9,9'-biphenanthryl-10,10'-diyl)-μ-(1,1'-binaphthyl-2,2'-diyl)diphosphite 'pnp' (**3.5**) has been synthesised using this procedure starting with (*R*)-(9,9'-biphenanthryl-10,10'-diyl)chlorophosphite (**3.10**) and (*R*)-binaphthol, δ_P ($CDCl_3$): 143.1 (s); *m/z* (FAB): 1137 ($M+Na^+$, 20%), 1115 ($M+H^+$, 35%), 683 ($M-431^+$, 100%).

3.3 Synthesis of cyclic aryl phosphites derived from dimethyl-1,1'-binaphthyl-2,2'-dihydroxy-3,3'-dicarboxylate (3.3)

*Preparation of (±) - (dimethyl - 1,1' - binaphthyl - 3,3' - dicarboxylate - 2,2' - diyl) chlorophosphite (**3.26**)*

To a solution of PCl_3 (3.1 cm^3, 35.5 mmol, 10 mol equiv) in dichloromethane (20 cm^3) at -40 °C was added NEt_3 (1.0 cm^3, 7.2 mmol, 2 mol equiv). A solution of (±)-dimethyl - 1,1' - binaphthyl - 2,2' - dihydroxy - 3,3' - dicarboxylate (**3.3**) (1.411 g, 3.5 mmol) in dichloromethane (40 cm^3) was then added dropwise over 25 min whilst the temperature was maintained at -40 °C. The reaction mixture was warmed to room temperature and stirred for 1 h. The solvent and excess PCl_3 were removed *in vacuo* and the residue was dissolved in toluene. The insoluble precipitate of triethylammonium chloride was removed by filtration under nitrogen through oven-dried celite and the solvent was removed *in vacuo* to afford a pale yellow foam which

was triturated with pentane (20 cm^3) to yield (±)-(dimethyl-1,1'-binaphthyl-3,3'-dicarboxylate-2,2'-diyl)chlorophosphite (**3.26**) (1.440 g, 88%) as a fine yellow solid, δ_P (CD_2Cl_2): 180.7; δ_H (CD_2Cl_2): 4.02 (3H, s, MeO), 4.04 (3H, s, MeO'), 7.26 (1H, dd, ^3J(HH) 8.6 Hz, ^4J(HH) 0.9 Hz), 7.30 (1H, dd, ^3J(HH) 8.6 Hz, ^4J(HH) 0.6 Hz), 7.38-7.45 (2H, m), 7.55-7.61 (2H, m), 8.10 (2H, d, ^3J(HH) 8.2 Hz), 8.70 (1H, s, H4), 8.73 (1H, s, H4'); δ_C (CD_2Cl_2): 52.78 (s, MeO), 52.92 (s, MeO'), 123.32 (s), 124.07 (s), 125.00 (s), 126.19 (s), 126.73 (s), 126.94 (s), 129.06 (s), 129.24 (s), 129.99 (s), 130.65 (s), 131.01 (s), 134.34 (s), 134.60 (s), 134.69 (s), 145.27 (s, C-O), 145.99 (s, C-O'), 165.46 (s, C=O).

*Preparation of (±) - (dimethyl - 1,1' - binaphthyl - 3,3' - dicarboxylate - 2,2' - diyl) phenylphosphite (**3.28**)*

To a solution of (±)-(dimethyl-1,1'-binaphthyl-3,3'-dicarboxylate-2,2'-diyl) chlorophosphite (**3.26**) (400 mg, 0.86 mmol) in THF (10 cm^3) at -40 °C was added triethylamine (120 µl, 0.86 mmol, 1 mol equiv). To the resulting cloudy solution was added a solution of phenol (81 mg, 0.86 mmol, 1 mol equiv) in THF (10 cm^3) dropwise over 10 min whilst the temperature was maintained at -40 °C. The reaction mixture was warmed to room temperature and stirred for 50 min. The thick white precipitate of triethylammonium chloride was removed by filtration under nitrogen through oven-dried celite and the solvent was removed *in vacuo* to afford a pale yellow foam. This foam was triturated with pentane (10 cm^3) to yield (±)-(dimethyl-1,1'-binaphthyl-3,3'-dicarboxylate-2,2'-diyl)phenylphosphite (**3.28**) (411 mg, 91%) as a fine off-white solid, δ_P ($CDCl_3$): 145.4 (s); δ_H ($CDCl_3$): 3.86 (3H, s, MeO), 4.03 (3H, s, MeO'), 7.11-7.20 (3H, m), 7.23 (1H, dd, ^3J(HH) 8.6 Hz, ^4J(HH) 0.6 Hz), 7.29 (1H, d, ^3J(HH) 8.5 Hz), 7.31-7.40 (2H, m), 7.33 (1H, d, ^3J(HH) 8.2 Hz), 7.35 (1H, d, ^3J(HH) 7.9 Hz), 7.46-7.54 (2H, m), 8.02 (2H, t, ^3J(HH) 8.8 Hz), 8.63 (1H, s), 8.68 (1H, s).

*Preparation of the diastereomeric mixture bis(dimethyl-1,1'-binaphthyl-3,3'-dicarboxylate-2,2'-diyl)pyrophosphite (**3.29**)*

To a solution of (±)-(dimethyl-1,1'-binaphthyl-3,3'-dicarboxylate-2,2'-diyl) chlorophosphite (**3.26**) (200 mg, 0.43 mmol) in THF (15 cm^3) at 0 °C was added NEt_3 (60 µl, 0.43 mmol, 1 mol equiv). After addition a cloudy white suspension was formed. A solution of distilled H_2O (4 µl, 0.22 mmol, 0.52 mol equiv) in THF (5 cm^3) was then added dropwise over 10 min whilst the temperature was maintained at 0 °C. The reaction mixture was warmed to room temperature and stirred for 1 h. The thick white precipitate of triethylammonium chloride that formed during the reaction was removed by filtration under nitrogen through oven-dried celite and the solvent was then removed *in vacuo* to yield the diastereomeric mixture bis(dimethyl-1,1'-

binaphthyl-3,3'-dicarboxylate-2,2'-diyl)pyrophosphite (**3.29**) (188 mg, quantitative) as a yellow solid, δ_P ($CDCl_3$): 136.6 (s); 136.8 (s).

E.3.5 Coordination chemistry of cyclic aryl diphosphites

E.3.5.1 Complexes of tris (9,9'-biphenanthryl-10,10'-diyl) diphosphite (3.4)

*Preparation of the diastereomeric mixture cis-[$PtCl_2$(tris(9,9'-biphenanthryl-10,10'-diyl)diphosphite)] (**3.30**)*

To a solution of the diastereomeric mixture of tris(9,9'-biphenanthryl-10,10'-diyl)diphosphite (**3.4**) (87 mg, 0.072 mmol) in dichloromethane (5 cm^3) was added [$PtCl_2$(cod)] (27 mg, 0.072 mmol, 1 mol equiv). The reaction mixture was stirred for 1 h and the solvent was removed *in vacuo* to yield the diastereomeric mixture of *cis* - [$PtCl_2$(tris(9,9' - biphenanthryl - 10,10' - diyl) diphosphite)] (**3.30**) (106 mg, quantitative) as a yellow solid, δ_P (CH_2Cl_2 / $CDCl_3$ 5:2): 87.0 (br s, ^1J(PPt) 5783 Hz) {(*R,S,R*) / (*S,R,S*)}; 88.6 (s, ^1J(PPt) 5700 Hz) {(*R,R,R*) / (*S,S,S*)}; 89.4 (d, ^2J(PP) 24 Hz, ^1J(PPt) 5716 Hz), 90.2 (d, ^2J(PP) 24 Hz, ^1J(PPt) 5667 Hz) {(*R,R,S*) / (*S,S,R*)}.

Optically pure (*R,R,R*) - *cis* - [$PtCl_2$(tris (9,9' - biphenanthryl - 10,10' - diyl) diphosphite)] (**3.30**) was synthesised following the same procedure starting with optically pure (*R,R,R*)-tris(9,9'-biphenanthryl-10,10'-diyl)diphosphite (**3.4**), δ_P ($CDCl_3$): 88.6 (s, ^1J(PPt) 5700 Hz); δ_{Pt} ($CDCl_3$): 144.6 (t, ^1J(PPt) 5700 Hz).

*Preparation of {(R,S,R) / (S,R,S)} - [Pt(nb)(tris(9,9' - biphenanthryl - 10,10' - diyl) diphosphite)] (**3.31**)*

To a solution of (*R,S,R*) / (*S,R,S*) - tris(9,9' - biphenanthryl - 10,10' - diyl) diphosphite (**3.4**) (80 mg, 0.066 mmol) in dichloromethane (5 cm^3) was added [$Pt(nb)_3$] (31 mg, 0.065 mmol, 1 mol equiv) and the reaction mixture was stirred under nitrogen for 80 min. The solvent was removed *in vacuo* to yield {(*R,S,R*) / (*S,R,S*)}-[Pt(nb)(tris(9,9'-biphenanthryl-10,10'-diyl)diphosphite)] (**3.31**) (99 mg, quantitative) as an off-white solid, δ_P (C_6D_6 / CH_2Cl_2 1:2): 172.6 (d, ^2J(PP) 156 Hz, ^1J(PPt) 6232 Hz), 180.1 (d, ^2J(PP) 156 Hz, ^1J(PPt) 5981 Hz); δ_{Pt} (C_6D_6 / CH_2Cl_2 1:2): -666.0 (dd, ^1J(PPt) 5981 Hz, $^1J'$(PPt) 6232 Hz).

E.3.5.2 Complexes of bis(9,9' - biphenanthryl - 10,10' - diyl)-μ-(1,1'-binaphthyl-2,2'-diyl)diphosphite 'pnp' (3.5)

Preparation of the diastereomeric mixture cis-[$PtCl_2$(bis(9,9'-biphenanthryl-10,10'-diyl)-μ-(1,1'-binaphthyl-2,2'-diyl)diphosphite)] (3.35)

To a solution of the diastereomeric mixture of bis(9,9'-biphenanthryl-10,10'-diyl)-μ-(1,1'-binaphthyl-2,2'-diyl)diphosphite (**3.5**) (100 mg, 0.090 mmol) in dichloromethane (10 cm^3) was added [$PtCl_2$(cod)] (31 mg, 0.083 mmol, 0.9 mol equiv) and the reaction mixture was stirred for 6 h. The solvent was removed *in vacuo* to yield the diastereomeric mixture of *cis*-[$PtCl_2$(bis(9,9'-biphenanthryl-10,10'-diyl)-μ-(1,1'-binaphthyl-2,2'-diyl)diphosphite)] (**3.35**) (114 mg, quantitative) as a yellow solid, δ_P ($CDCl_3$): 71.7 (d, ^2J(PP) 15 Hz, ^1J(PPt) 5905 Hz), 90.8 (d, ^2J(PP) 15 Hz, ^1J(PPt) 6049 Hz) {(*R,R,S*) / (*S,S,R*)}; 77.6 (s, ^1J(PPt) 5857 Hz) {(*R,S,R*) / (*S,R,S*)}; 80.1 (br s, ^1J(PPt) 5916 Hz) {(*R,R,R*) / (*S,S,S*)}; δ_{Pt} ($CDCl_3$): 291.1 (t, ^1J(PPt) 5857 Hz) {(*R,S,R*) / (*S,R,S*)}; 318.6 (dd, ^1J(PPt) 5905 Hz, $^1J'$(PPt) 6049 Hz) {(*R,R,S*) / (*S,S,R*)}; 323.2 (t, ^1J(PPt) 5916 Hz) {(*R,R,R*) / (*S,S,S*)}; *m/z* (FAB): 1344 ($M\text{-}Cl^+$, 100%).

Following a similar procedure, optically pure (*R,R,R*)-*cis*-[$PtCl_2$(bis(9,9'-biphenanthryl-10,10'-diyl)-μ-(1,1'-binaphthyl-2,2'-diyl)diphosphite)] (**3.35**) has been synthesised using optically pure (*R,R,R*)-bis(9,9'-biphenanthryl-10,10'-diyl)-μ-(1,1'-binaphthyl-2,2'-diyl)diphosphite (**3.5**), δ_P ($CDCl_3$): 80.1 (br s, ^1J(PPt) 5916 Hz); δ_{Pt} ($CDCl_3$): 323.2 (t, ^1J(PPt) 5916 Hz); *m/z* (FAB): 1344 ($M\text{-}Cl^+$, 100%).

Preparation of the diastereomeric mixture cis-[$PdCl_2$(bis(9,9'-biphenanthryl-10,10'-diyl)-μ-(1,1'-binaphthyl-2,2'-diyl)diphosphite)] (3.36)

To a solution of the diastereomeric mixture of bis(9,9'-biphenanthryl-10,10'-diyl)-μ-(1,1'-binaphthyl-2,2'-diyl)diphosphite (**3.5**) (100 mg, 0.090 mmol) in dichloromethane (10 cm^3) was added [$PdCl_2$(NCPh)$_2$] (33 mg, 0.086 mmol, 1.0 mol equiv) and the reaction mixture was stirred for 6 h. The solvent was removed *in vacuo* to yield the diastereomeric mixture of *cis*-[$PdCl_2$(bis(9,9'-biphenanthryl-10,10'-diyl)-μ-(1,1'-binaphthyl-2,2'-diyl)diphosphite)] (**3.36**) (111 mg, quantitative) as an orange solid, δ_P ($CDCl_3$): 97.0 (d, ^2J(PP) 70 Hz), 115.9 (d, ^2J(PP) 73 Hz) {(*R,R,S*) / (*S,S,R*)}; 103.4 (s) {(*R,S,R*) / (*S,R,S*)}; 105.6 (br s) {(*R,R,R*) / (*S,S,S*)}; *m/z* (FAB): 1256 ($M\text{-}Cl^+$, 84%), 683 ($M\text{-}608^+$, 100%).

Following a similar procedure, optically pure (*R,R,R*)-*cis*-[$PdCl_2$(bis(9,9'-biphenanthryl-10,10'-diyl)-μ-(1,1'-binaphthyl-2,2'-diyl)diphosphite)] (**3.36**) has been synthesised using optically pure (*R,R,R*)-bis(9,9'-biphenanthryl-10,10'-diyl)-μ-(1,1'-binaphthyl-2,2'-diyl)diphosphite (**3.5**), δ_P ($CDCl_3$): 105.6 (br s); *m/z* (FAB): 1256 ($M\text{-}Cl^+$, 84%), 683 ($M\text{-}608^+$, 100%).

Preparation of the diastereomeric mixture [Rh(dpm)(bis(9,9'-biphenanthryl-10,10'-diyl)-μ-(1,1'-binaphthyl-2,2'-diyl)diphosphite)] (3.37)

To a solution of the diastereomeric mixture of bis(9,9'-biphenanthryl-10,10'-diyl)-μ-(1,1'-binaphthyl-2,2'-diyl)diphosphite (**3.5**) (50 mg, 0.045 mmol) in dichloromethane (5 cm^3) was added [$Rh(CO)_2(dpm)$] (16 mg, 0.047 mmol, 1.0 mol equiv) and the reaction mixture was stirred for 6 h. The solvent was removed *in vacuo* to give a red solid. This was dissolved in dichloromethane (5 cm^3) and the solvent again removed *in vacuo* to yield the diastereomeric mixture of [Rh(dpm)(bis(9,9'-biphenanthryl-10,10'-diyl)-μ-(1,1'-binaphthyl-2,2'-diyl)diphosphite)] (**3.37**) (63 mg, quantitative) as a yellow solid, δ_P ($CDCl_3$): 139.5 (dd, ^2J(PP) 119 Hz, ^1J(PRh) 299 Hz), 150.2 (dd, ^2J(PP) 117 Hz, ^1J(PRh) 297 Hz) {(*R,R,S*) / (*S,S,R*)}; 142.4 (d, ^1J(PRh) 290 Hz); 143.3 (d, ^1J(PRh) 299 Hz).

E.3.6 Asymmetric hydroformylation of styrene derivatives catalysed by rhodium(I) complexes of cyclic aryl diphosphites

The asymmetric hydroformylation reactions were carried out at the University of Tarragona under the supervision of Dr. Elena Fernandez.

The rhodium(I) complexes were generated *in situ* by stirring a solution of the diphosphite (1.1 mol equiv with respect to the rhodium) with the appropriate rhodium(I) starting material in toluene. The toluene was deoxygenated thoroughly before use by bubbling nitrogen through it for 10 min. Percentage conversions, regioselectivities and ee's were calculated by GC. A typical experimental procedure is described:

The appropriate rhodium(I) complex (8.1 μmol, 0.00138 mol equiv) was dissolved in toluene (4 cm^3) and a solution of the diphosphite (8.9 μmol, 0.00152 mol equiv) in toluene (4 cm^3) was added. The resulting yellow solution was stirred for 10 min. A solution of the substrate (5.87 mmol) in toluene (2 cm^3) was added and the reaction mixture was placed in an autoclave, which was charged with CO (3.5 atm) and then with H_2 (3.5 atm). The reaction mixture was stirred at 25 °C for 22 h. The reaction mixture was then removed from the autoclave and immediately plunged into a buffer solution of H_3PO_4 / H_2PO_4- (pH = 5.5, 1.25M). This mixture was then stirred for 1 min and added to $KMnO_4$ (10 cm^3, 1M). The reaction mixture was then stirred vigorously for 2 h, after which time a brown suspension was observed if hydroformylation had been successful. Saturated Na_2SO_3 solution was added (5 cm^3) and the reaction mixture was acidified with concentrated hydrochloric acid. The resulting white suspension was extracted with diethyl ether (2 x 10 cm^3) and the solvent was removed under reduced pressure. Sodium hydroxide solution

(10 cm^3, 2M) was added, the aqueous layer was washed with diethyl ether (10 cm^3), acidified with concentrated hydrochloric acid, extracted with diethyl ether (10 cm^3) and the organic extract was washed with distilled water (10 cm^3), dried ($MgSO_4$), filtered and the solvent removed under reduced pressure to afford a white solid. This product mixture was dissolved in toluene (2 cm^3) and then analysed by Gas Chromatography.

E.4 Rhodium(I) complexes of phosphonites and phosphites as catalysts for the asymmetric hydrogenation of α-enamides

The asymmetric hydrogenation reactions were carried out at the University of Tarragona under the supervision of Dr. Elena Fernandez.

The rhodium(I) complexes of the monophosphonite (*S*)-(**4.35**) and the diphosphonite (*S,S*)-(**4.39**) were preformed whilst those of the phosphinophosphonite (*S*)-(**4.43**) and the diphosphites (*R,R,R*)- and (*R,S,R*)-(**4.49**) were generated *in situ* by stirring a solution of the ligand (1.1 mol equiv with respect to the rhodium) with $[Rh(cod)_2]BF_4$ in the appropriate solvent. The solvents were deoxygenated thoroughly before use by bubbling nitrogen through them for 10 min. Percentage conversions and ee's were calculated by Gas Chromatography. See Tables 4.3-4.6 in Sections 4.2 and 4.3 for the exact reaction conditions, but a typical reaction procedure is described:

To a solution of the phosphinophosphonite (*S*)-(**4.43**) (7.5 mg, 12.1 μmol, 0.00232 mol equiv) in dichloromethane (7.5 cm^3) was added $[Rh(cod)_2]BF_4$ (4.5 mg, 11.0 μmol, 0.00211 mol equiv). The resulting yellow solution was stirred for 10 min and then a solution of methyl-2-acetamidoacrylate (746.1 mg, 5.213 mmol) in dichloromethane (3.8 cm^3) was added. The reaction mixture was placed in a stainless steel autoclave, which was pressurised to 1.5 atm with H_2 and the reaction mixture was stirred for 20 h at 25 ^oC. The reaction mixture was removed from the autoclave and then analysed by Gas Chromatography.

References

1 I.W. Wainer and D.E. Drayer, *Drug Stereochemistry*, Marcel Dekker, New York, 1988.
2 A.N. Collins, G.N. Sheldrake and J. Crosby, *Chirality in Industry*, John Wiley, Chichester, 1992.
3 J.S. Millership and A. Fitzpatrick, *Chirality*, 1993, **5**, 573.
4 M. Beller and C. Bolm, *Transition Metals for Organic Synthesis*, Wiley-VCH, Weinheim, 1998.
5 D.C. Roberts and F. Vallaccio, *The Peptides*, eds. E. Gross and J. Meisenhofer, Academic Press, New York, 1983, ch. 6.
6 A.F. Spatola, *The Chemistry and Biochemistry of Amino Acids, Peptides and Proteins*, ed. B. Weinstein, Marcel Dekker, New York, 1983, vol. 7, p. 267.
7 A. Giannis and T. Kolter, *Angew. Chem., Int. Ed. Engl.*, 1994, **32**, 1244.
8 J. Gante, *Angew. Chem., Int. Ed. Engl.*, 1994, **33**, 1699.
9 R.M. Williams, *Synthesis of Optically Active α-Amino Acids*, Pergamon Press, Oxford, 1989.
10 M.T. Reetz, *Angew. Chem., Int. Ed. Engl.*, 1991, **30**, 1531.
11 A. Studer, *Synthesis*, 1996, 793.
12 J.M. Kerr, S.C. Banville and R.N. Zuckermann, *J. Am. Chem. Soc.*, 1993, **115**, 2529.
13 W.S. Knowles and M.J. Sabacky, *J. Chem. Soc., Chem. Commun.*, 1968, 1445.
14 L. Horner, H. Siegel and H. Büthe, *Angew. Chem., Int. Ed. Engl.*, 1968, **7**, 942.
15 W.S. Knowles, *J. Chem. Educ.*, 1986, **63**, 222.
16 J.W. Scott, *Ind. Chem. News*, 1986, **7**, 32.
17 L. Dahlenburg and C. Eckert, *J. Organomet. Chem.*, 1998, **564**, 227.
18 M.T. Reetz, A. Gosberg, R. Goddard and S-H Kyung, *J. Chem. Soc., Chem. Commun.*, 1998, 2077.
19 D.J. Wink, T.J. Kwok and A. Yee, *Inorg. Chem.*, 1990, **29**, 5006.
20 M.T. Reetz and T. Neugebauer, *Angew. Chem., Int. Ed. Engl.*, 1999, **38**, 179.
21 W.J. Richter, *Phosphorus, Sulfur Relat. Elem.*, 1981, **10**, 395.
22 D. Seebach, M. Hayakawa, J. Sakaki and W.B. Schweizer, *Tetrahedron*, 1993, **49**, 1711.
23 J. Sakaki, W.B. Schweizer and D. Seebach, *Helv. Chim. Acta*, 1993, **76**, 2654.
24 D. Haag, J. Runsink and H-D. Scharf, *Organometallics*, 1998, **17**, 398.
25 Y. Uozumi and T. Hayashi, *J. Am. Chem. Soc.*, 1991, **113**, 9887.

26 Y. Uozumi, S-Y. Lee and T. Hayashi, *Tetrahedron Lett.*, 1992, **33**, 7185.
27 Y. Uozumi, A. Tanahashi, S-Y. Lee and T. Hayashi, *J. Org. Chem.*, 1993, **58**, 1945.
28 Y. Uozumi and T. Hayashi, *Tetrahedron Lett.*, 1993, **34**, 2335.
29 I. Ojima and K. Hirai, *Asymmetric Synthesis*, ed. J.D. Morrison, Academic Press, Orlando, 1985, vol. 5, ch. 4 and refs therein.
30 K. Yamamoto and T. Hayashi, M. Kumada, *J. Organomet. Chem.*, 1972, **46**, C65.
31 K. Yamamoto and T. Hayashi, M. Kumada, *J. Organomet. Chem.*, 1973, **54**, C45.
32 N.C. Payne and D.W. Stephan, *Inorg. Chem.*, 1982, **21**, 182.
33 H. Brunner and W. Miehling, *J. Organomet. Chem.*, 1984, 275, C17.
34 A.F.M.M. Rahman and S.B. Wild, *J. Mol. Catal.*, 1987, **39**, 155.
35 K. Achiwa, *Fundamental Research in Homogeneous Catalysis*, ed. M. Tsutsui, Plenum, New York, 1979, vol. 3, 549.
36 A. Martorell and P.G. Pringle, unpublished work.
37 K. Tani, T. Yamagata and K. Nagata, *Acta Crystallogr., Sect. C*, 1994, **50**, 1274.
38 T. Hattori, M. Shijo, S. Kumagai and S. Miyano, *Chem. Express.*, 1991, **6**, 335.
39 Y. Uozumi and T. Hayashi, *J. Am. Chem. Soc.*, 1991, **113**, 9887.
40 H. Tye, D. Smyth, C. Eldred and M. Wills, *J. Chem. Soc., Chem. Commun.*, 1997, 1053.
41 I.E. Nifantev, L.F. Manzhukova, M.Y. Antipin, Y.T. Struchkov and E.E. Nifant'ev, *Russ. J. Gen. Chem.*, 1995, **65**, 682.
42 S.P. Shum and S.D. Pastor, *Abstracts of Papers of the American Chemical Society*, 1999, **217**, 194 (INOR).
43 F. Agbossou, J.-F. Carpentier and A. Morteux, *Chem. Rev.*, 1995, **95**, 2485.
44 N. Sakai, S. Mano, K. Nozaki and H. Takaya, *J. Am. Chem. Soc.*, 1993, **115**, 7033.
45 EP 0 614 901 A1/1984.
46 T. Higashizima, N. Sakai, K. Nozaki and H. Takaya, *Tetrahedron Lett.*, 1994, **35**, 2023.
47 N. Sakai, K. Nozaki and H. Takaya, *J. Chem. Soc., Chem. Commun.*, 1994, 395.
48 Y. Pottier, A. Mortreux and F. Petit, *J. Organomet. Chem.*, 1989, **370**, 333.
49 A.L. Bandini, G. Banditelli, E. Cesarotti, G. Minghetti and B. Bovio, *Inorg. Chem.*, 1992, **31**, 391.

50 G. Harrison, PhD Thesis, University of Bristol, 1998.
51 C. Carraz, PhD Thesis, University of Bristol, 1998.
52 D.A. Knight and T.L. Schull, *Tetrahedron: Asymmetry*, 1999, **10**, 207.
53 P. Stoss and R. Hemmer, *Adv. Carbohydr. Chem. Biochem.*, 1992, **49**, 93.
54 S.D. Pastor, S.P. Shum, R.K. Rodebaugh, A.D. Debellis and F.H. Clarke, *Helv. Chim. Acta*, 1993, **76**, 900.
55 C.A. Tolman and J.W. Faller, *Homogeneous Catalysis with Metal Phosphine Complexes*, ed. L.H. Pignolet, Plenum, New York, 1983, p. 81.
56 C. Masters, *Homogeneous Transition-Metal Catalysis - A Gentle Art*, Chapman and Hall, London, 1981, p. 120.
57 A. Mortreux and F. Petit, *Catalysis by Metal Complexes*, eds. R. Ugo and B.R. James, D. Reidel, Dordrecht, 1988.
58 G.W. Parshall, *Homogeneous Catalysis: The Applications and Chemistry of Catalysis by Soluble Transition Metal Complexes*, Wiley, New York, 1980.
59 I. Thatchenko, *Comprehensive Organometallic Chemistry*, eds. G. Wilkinson, F.G.A. Stone and E.W. Abel, Pergamon, Oxford, 1981, vol. 8, p. 101.
60 K. Weissermel and H.-J. Arpe, *Industrial Organic Chemistry*, VCH, Cambridge, 1993, p. 123.
61 M. Beller, B. Cornils, C.D. Frohning and C.W. Kohlpaintner, *J. Mol. Catal. A*, 1995, **104**, 17.
62 B. Cornils, W.A. Herrmann and M. Rasch, *Angew. Chem., Int. Ed. Engl.*, 1994, **33**, 2144.
63 R. Pruett, *Adv. Organomet. Chem.*, 1979, **17**, 1.
64 B. Cornils, *New Synthesis with Carbon Monoxide*, ed. J. Falbe, Springer-Verlag, Berlin, 1980, p. 133.
65 C. Botteghi, S. Gladiali, V. Bellagamba, R. Ercoli and A. Gamba, *Chim. Ind. (Milan)*, 1981, **63**, 29.
66 H. Siegel and W. Himmele, *Angew. Chem.*, 1980, **92**, 182.
67 C. Botteghi, R. Ganzerla, M. Lenarda and C. Moretti, *J. Mol. Catal.*, 1987, **40**, 129.
68 M. Tanaka, Y. Watanabe, T. Mitsudo, K. Yamamoto and Y. Takegami, *Chem. Lett.*, 1972, 483.
69 G. Consiglio and P. Pino, *Adv. Chem. Ser.*, 1982, **196**, 371.
70 G. Consiglio and P. Pino, *Top. Curr. Chem.*, 1982, **105**, 77.
71 C. Botteghi, S. Paganelli, A. Schionato and M. Marchetti, *Chirality*, 1991, **3**, 355.
72 G. Consiglio, *Catalytic Asymmetric Synthesis*, ed. I. Ojima, VCH, Weinheim, 1993, p. 273.

73 R. Noyori, *Asymmetric Catalysis in Organic Synthesis*, Wiley, New York, 1994, p. 162.
74 S. Gladiali, J.C. Bayón and C. Claver, *Tetrahedron: Asymmetry*, 1995, **6**, 1453.
75 H. Siegel and W. Himmele, *Angew. Chem., Int. Ed. Engl.*, 1980, **19**, 178.
76 J.P. Rieu, A. Boucherle, H. Cousse and G. Mouzin, *Tetrahedron*, 1986, **42**, 4095.
77 J.F. Stille and G. Parrinello, *J. Mol. Catal.*, 1983, **21**, 203.
78 G. Parrinello and J.F. Stille, *J. Am. Chem. Soc.*, 1987, **109**, 7122.
79 F. Spindler, B. Pugin, H.-P. Jalett, H.-P. Buser, W. Pittelkow and H.-U. Blaser, *Catalysis of Organic Reactions*, ed. R.E. Malz, Marcel Dekker, New York, 1996, p. 153.
80 G. Parrinello and J.F. Stille, *J. Am. Chem. Soc.*, 1987, **109**, 7122.
81 J.F. Stille, H. Su, P. Brechot, G. Parrinello and L.S. Hegedus, *Organometallics*, 1991, **10**, 1183.
82 USP 4 769 498/1988.
83 EP 54 986/1982.
84 USP 4 599 206/1986.
85 USP 4 789 753/1988.
86 USP 4 748 261/1988.
87 P.W.N.M. van Leeuwen and C.F. Roobeek, *J. Organomet. Chem.*, 1983, **258**, 343.
88 A. van Rosy, E.N. Orij, P.C.J. Kamer, F. van den Aardweg and P.W.N.M. van Leeuwen, *J. Chem. Soc., Chem. Commun.*, 1991, 1096.
89 T. Jongsma, G. Challa and P.W.N.M. van Leeuwen, *J. Organomet. Chem.*, 1991, **421**, 121.
90 A. van Rosy, J.N.H. de Bruijn, K.F. Roobeek, P.C.J. Kamer and P.W.N.M. van Leeuwen, *J. Organomet. Chem.*, 1996, **507**, 69.
91 A. van Rooy, E.N. Orij, P.C.J. Kamer and P.W.N.M. van Leeuwen, *Organometallics*, 1995, **14**, 34.
92 M.J. Baker, K.N. Harrison, A.G.Orpen, P.G. Pringle and G. Shaw, *J. Chem. Soc., Chem. Commun.*, 1991, 803.
93 M.J. Baker, PhD Thesis, University of Bristol, 1992.
94 P. Uriz, E. Fernandez, C. Claver, P.G. Pringle and M.J. Baker, unpublished work.
95 G.J.H. Buisman, P.C.J. Kamer and P.W.N.M. van Leeuwen, *Tetrahedron: Asymmetry*, 1993, 4, 1625.

96 N. Sakai, K. Nozaki, K. Mashima and H. Takaya, *Tetrahedron: Asymmetry*, 1992, **3**, 583.

97 USP 911 518/1992 (*Chem. Abstr.*, 1994, **119**, 159 872).

98 G.J.H. Buisman, M.E. Martin, E.J. Vos, A. Klootwijik, P.C.J. Kamer and P.W.N.M. van Leeuwen, *Tetrahedron: Asymmetry*, 1995, **6**, 719.

99 G.J.H. Buisman, E.J. Vos, P.C.J. Kamer and P.W.N.M. van Leeuwen, *J. Chem. Soc., Dalton Trans.*, 1995, 409.

100 G.J.H. Buisman, L.A. van der Veen, A. Klootwijk, W.G.J. de Lange, P.C.J. Kamer, P.W.N.M. van Leeuwen and D. Vogt, *Organometallics*, 1997, **16**, 2929.

101 T.V. RajanBabu and T.A. Ayers, *Tetrahedron Lett.*, 1994, **35**, 4295.

102 T.V. RajanBabu and A.L. Casalnuovo, *Pure Appl. Chem.*, 1994, 1535.

103 T. Horiuchi, E. Shirakawa, K. Nozaki and H. Takaya, *Organometallics*, 1997, **16**, 2981.

104 K. Nozaki, N. Sakai, T. Nanno, T. Higashijiamma, S. Mano, T. Horiuchi and H. Takaya, *J. Am. Chem. Soc.*, 1997, **119**, 4413.

105 P.W.N.M. van Leeuwen, G.J.H. Buisman, A. van Rooy and P.C.J. Kamer, *Recl. Trav. Chim. Pays-Bas*, 1994, **113**, 61.

106 G.J.H. Buisman, L.A. van der Veen, P.C.J. Kamer and P.W.N.M. van Leeuwen, *Organometallics*, 1997, **16**, 5681.

107 J.M. Brown and A.G. Kent, *J. Chem. Soc., Perkin Trans. 2*, 1987, 1597.

108 C.P. Casey and G.T. Whiteker, *Isr. J. Chem.*, 1990, **30**, 299.

109 W.A. Herrmann and B. Cornils, *Angew. Chem., Int. Ed. Engl.*, 1997, **36**, 1047.

110 B. Cornils and W.A. Herrmann, *Applied Homogeneous Catalysis with Organometallic Compounds*, VCH-Wiley, Weinheim, 1996, vol. 1, p. 3.

111 C.P. Casey and L.M. Petrovich, *J. Am. Chem. Soc.*, 1995, **117**, 6007.

112 R. Noyori and H. Takaya, *Chem. Scr.*, 1985, **25**, 83.

113 R. Noyori and H. Takaya, *Acc. Chem. Res.*, 1990, **23**, 345.

114 G. Consiglio and P.Pino, *Top. Curr. Chem.*, 1982, **105**, 77.

115 P. Meakin, J.P. Jesson, F.N. Tebbe and E.L. Muetterties, *J. Am. Chem. Soc.*, 1971, **93**, 1797.

116 P. Meakin, E.L. Muetterties and J.P. Jesson, *J. Am. Chem. Soc.*, 1972, **94**, 5271.

117 W. Tam, DuPont Chemical Company, personal communication.

118 F. Toda and K. Tanaka, *J. Org. Chem.*, 1988, **53**, 3607.

119 K. Yamamoto, H. Fukushima and M. Nakazaki, *J. Chem. Soc., Chem. Commun.*, 1984, 1111.

121 C.A. Dornfeld, J.E. Callen and G.H. Coleman, *Org. Synth.*, collective vol. **3**, 134.
125 D. Seebach, H-O. Kalinowski, W. Langer, G. Crass and E-M. Wilka, *Org. Synth.*, collective vol. **7**, 41.
126 M. Hovorka, J. Günterová and J. Závada, *Tetrahedron Lett.*, 1990, **31**, 413.
127 C.J. Cobley, PhD Thesis, University of Bristol, 1997.
128 R.B. King and W.F. Masler, *J. Am. Chem. Soc.*, 1977, **99**, 4001.
129 A. Crispini, K.N. Harrison, A.G. Orpen, P.G. Pringle and J.P. Wheatcroft, *J. Chem. Soc., Dalton Trans.*, 1996, 1069.
130 M.Brookhart and M.L.H. Green, *J. Organomet. Chem.*, 1983, **250**, 395.
131 J.M. Brown and P.L. Evans, *Tetrahedron*, 1988, **44**, 4905.
132 J.A. Davies and F.R. Hartley, *Chem. Rev.*, 1981, **81**, 79.
133 C.A. Tolman, *Chem. Rev.*, 1977, **77**, 313.
134 N. Ahmed, E.W. Ainscough, T.A. James and S.D. Robinson, *J. Chem. Soc., Dalton Trans.*, 1973, 1148.
135 P.S. Pregosin and K.W. Kunz, *^{31}P and ^{13}C NMR of Transition Metal Phosphine Complexes*, eds. P. Diehl, E. Fluck and R. Kosfeld, Springer-Verlag, Berlin, 1979.
136 S.D. Pastor and R.K. Rodebaugh, *J. Am. Chem. Soc.*, 1988, **110**, 6547.
137 S.D. Pastor and R.K. Rodebaugh, *Helv. Chim. Acta*, 1993, **76**, 900.
138 L. Petrakis and C.H. Sederholm, *J. Chem. Phys.*, 1961, **35**, 1243.
139 G. Szalontai, J. Bakos, I. Tõth and B. Heil, *Magn. Reson. Chem.*, 1987, **25**, 761.
140 L. Ernst, *J. Chem. Soc., Chem. Commun.*, 1977, 375.
141 L. Ernst, *Org. Magn. Reson.*, 1977, **9**, 35.
142 R.A. Pascal Jr., A.P. West Jr. and D. Van Engen, *J. Am. Chem. Soc.*, 1990, **112**, 6406.
143 A.G. Orpen, L. Brammer, F.H. Allen, O. Kennard, D.G. Watson and R. Taylor, *J. Chem. Soc., Dalton Trans.*, 1989, S1.
144 R.G. Cavell, *Methods in Stereochemical Analysis 8, Phosphorus-31 NMR Spectroscopy in Stereochemical Analysis: Organic Compounds and Metal Complexes*, eds. J.G. Verkade and L.D. Quin, VCH, Florida, 1987, vol. 8, p. 233.
145 P.C. Crofts, J.H.H. Markes and H.N. Rydon, *J. Chem. Soc.*, 1958, 4250.
146 K.M. Abraham and J.R. van Wazer, *Inorg. Chem.*, 1975, **14**, 1099.
147 A.E. Arbuzov and A.I. Razumov, *Zh. Obshch. Khim.*, 1937, **7**, 1762.
148 A.E. Arbuzov and B.A. Arbuzov, *J. Prakt. Chem.*, 1931, **130**, 103.
149 A.E. Arbuzov and B.A. Arbuzov, *J. Prakt. Chem.*, 1931, **131**, 337.

150 A.E. Arbuzov and B.A. Arbuzov, *Berichte*, 1932, **65**, 195.

151 A.L. du Preez, I.L. Marais, R.J. Haines, A. Pidcock and M. Safari, *J. Organomet. Chem.*, 1977, **141**, C10.

152 J. Gimeno, V. Riera, M.A. Ruiz, A.M.M. Lanfredi and A. Tiripicchio, *J. Organomet. Chem.*, 1984, **268**, C13.

153 V. Riera and M.A. Ruiz, *J. Chem. Soc., Dalton Trans.*, 1987, 1551.

154 D.W. Prest, M.J. Mays, A.G. Orpen and R.K. McMullan, *J. Organomet. Chem.*, 1982, **240**, 395.

155 D.W. Prest, M.J. Mays and P.R. Raithby, *J. Chem. Soc., Dalton Trans.*, 1982, 2021.

156 R.J. Haines, A. Pidcock and M. Safari, *J. Chem. Soc., Dalton Trans.*, 1977, 830.

157 D.E. Berry, K.A. Beveridge, G.W. Bushnell, K.R. Dixon and A. Pidcock, *Can. J. Chem.*, 1986, **64**, 343.

158 D.W. Prest, M.J. Mays, P.R. Raithby and A.G. Orpen, *J. Chem. Soc., Dalton Trans.*, 1982, 737.

159 E. Costa, A. Martorell, P. Uriz and P.G. Pringle, unpublished work.

160 J.G. Verkade and K.J. Coukran, *Organic Phosphorus Compounds*, eds. G.M. Kosalopoff and L. Maier, Wiley-Interscience, New York, 1972, vol. 2, p. 1.

161 J-M. Savariault, M.H. Micoud, P. Cassoux and J-F. Labarre, *Bull. Soc. Chim. Fr.*, 1971, **6**, 2413.

162 M.J. Baker, E. Costa, D. Ellis, N. Fletcher, K.N. Harrison, A.G. Orpen, P.G. Pringle and G. Shaw, unpublished work.

163 P.S. Pregosin and S.N. Sze, *Helv. Chim. Acta*, 1978, **61**, 1848.

164 H.C. Clark and A.M. de P. Nicholas, *Magn. Reson. Chem.*, 1990, **28**, 99.

165 M.J. Baker, K.N. Harrison, A.G. Orpen, P.G. Pringle and G. Shaw, *J. Chem. Soc., Dalton Trans.*, 1992, 2607.

166 K.N. Harrison, PhD Thesis, University of Bristol, 1990.

167 J.R. Shapley, R.R. Schrock and J.A. Osborn, *J. Am. Chem. Soc.*, 1969, **91**, 2816.

168 R.R. Schrock and J.A. Osborn, *J. Chem. Soc., Chem. Commun.*, 1970, 567.

169 R.R. Schrock and J.A. Osborn, *J. Am. Chem. Soc.*, 1971, **93**, 2397.

170 R.R. Schrock and J.A. Osborn, *J. Am. Chem. Soc.*, 1971, **93**, 3089.

171 R.R. Schrock and J.A. Osborn, *J. Am. Chem. Soc.*, 1976, **98**, 2134.

172 M.A. Garralda and L.A. Oro, *Transition Met. Chem.*, 1980, **5**, 65 and refs therein.

173 M.A. Esteruelas, PhD Thesis, University of Zaragoza, 1983 and refs therein.

174 P.A. Chaloner, M.A. Esteruelas, F. Joó and L.A. Oro, *Homogeneous Hydrogenation*, Kluwer Academic Publishers, 1994, ch. 2 and refs therein.
175 R. Uson, L.A. Oro, M.J. Fernández and R. Sariego, *Rev. Acad. Cienc. Zaragoza*, 1980, **35**, 87.
176 R.H. Crabtree, P.C. Demon, D. Eden, J.M. Mihelcic, C.A. Parnell, J.M. Quirk and G.E. Morris, *J. Am. Chem. Soc.*, 1982, **104**, 6994.
177 C. Landis and J. Halpern, *J. Am. Chem. Soc.*, 1987, **109**, 1746.
178 C. Landis and T. Brauch, *Inorg. Chim. Acta*, 1998, **270**, 285.
179 J.M. Brown, P.A. Chaloner and G.A. Morris, *J. Chem. Soc., Perkin Trans. 2*, 1987, 1583.
180 J.M. Brown, *Chem. Soc. Rev.*, 1993, **22**, 25 and refs therein.
181 P.L. Bogdan, J.J. Irwin and B. Bosnich, *Organometallics*, 1989, **8**, 1450.
182 A.S.C. Chan, J.J. Pluth and J. Halpern, *J. Am. Chem. Soc.*, 1980, **102**, 5952.
183 B. McCulloch and J. Halpern, *Organometallics*, 1990, **9**, 1392.
184 N.W. Alcock, J.M. Brown and P.J. Maddox, *J. Chem. Soc., Chem. Commun.*, 1986, 1532 and refs therein.
185 J.M. Brown, J.A. Ramsden and J.M. Claridge, *J. Chem. Soc., Chem. Commun.*, 1995, 2469.
186 H. Bircher, B.R. Bender and W. von Phillipsborn, *Magn. Reson. Chem.*, 1993, **31**, 293.
187 B.R. Bender, M. Koller, D. Nanz and W. von Phillipsborn, *J. Am. Chem. Soc.*, 1993, **115**, 5889.
188 J.M. Brown and P.A. Chaloner, *J. Chem. Soc., Chem. Commun.*, 1980, 344.
189 P.S. Chua, N.K. Roberts, B. Bosnich, S.J. Okrasinski and J. Halpern, *J. Chem. Soc., Chem. Commun.*, 1981, 1278.
190 B.D. Vineyard, W.S. Knowles, M.J. Sabacky, G.L. Bachman and D.J. Weinkauff, *J. Am. Chem. Soc.*, 1977, **99**, 5946.
191 W.S. Knowles, *Acc. Chem. Res.*, 1983, **16**, 106.
192 E.J. Corey and J.C. Bailar, *J. Am. Chem. Soc.*, 1959, **81**, 2620.
193 J.K. Beattie, *Acc. Chem. Res.*, 1971, **4**, 253.
194 M.D. Fryzuk and B. Bosnich, *J. Am. Chem. Soc.*, 1977, **99**, 6262.
195 B. Bosnich and S.B. Wild, *J. Am. Chem. Soc.*, 1970, **92**, 459.
196 B. Bosnich, W.G. Jackson and S.B. Wild, *J. Am. Chem. Soc.*, 1973, **95**, 8269.
197 B. Bosnich, S.T.D. Lo and E.A. Sullivan, *Inorg. Chem.*, 1975, **14**, 2305.
198 W.S. Knowles, M.J. Sabacky and B.D. Vineyard, *J. Chem. Soc., Chem. Commun.*, 1972, 10.

199 M.J. Burk, J.E. Feaster, W.A. Nugent and R.L. Harlow, *J. Am. Chem. Soc.*, 1993, **115**, 10125.

200 M.J. Burk, M.F. Gross, T. Gregory, P. Harper, C.S. Kalberg, J.R. Lee and J.P. Martinez, *Pure Appl. Chem.*, 1996, **68**, 37.

201 M.J. Burk, M.F. Gross and J.P. Martinez, *J. Am. Chem. Soc.*, 1995, **117**, 9375.

202 J.M. Brown and D. Parker, *Organometallics*, 1982, **1**, 1350.

203 H.B. Kagan, *Comprehensive Organometallic Chemistry*, eds. G. Wilkinson, F.G.A. Stone and E.W. Abel, Pergamon Press, 1982, vol. 8, p. 463.

204 K.E. Koenig, M.J. Sabacky, G.L. Bachman, W.C. Christopfel, H.D. Barnstorff, R.B. Friedman, W.S. Knowles, B.R. Stultz, B.D. Vineyard and D.J. Weinkauff, *Ann. N.Y. Acad. Sci.*, 1980, **333**, 16.

205 S.K. Armstrong, J.M. Brown and M.J. Burk, *Tetrahedron Lett.*, 1993, **34**, 879.

206 A. Dedieu, *Topics in Physical Organometallic Chemistry 1*, 1985, 1 and refs therein.

207 P.A. MacNeil, N.K. Roberts and B. Bosnich, *J. Am. Chem. Soc.*, 1981, **103**, 2273.

208 T.W. Dekleva and B.R. James, *J. Chem. Soc., Chem. Commun.*, 1983, 1350.

209 J. Halpern, *Asymmetric Synthesis*, ed. J.D. Morrison, Academic Press, New York, 1985, vol. 5, p. 41 and refs therein.

210 A.S.C. Chan and J. Halpern, *J. Am. Chem. Soc.*, 1980, **102**, 838.

211 R. Noyori, *Asymmetric Catalysis in Organic Synthesis*, Wiley, New York, 1993.

212 H. Brunner and W. Zettlmeier, *Handbook of Enantioselective Catalysis*, VCH, Weinheim, 1993.

213 L. Markó and J. Bakos, *Aspects Homogeneous Catal.*, 1981, **4**, 145.

214 U. Nagel, E. Kinzel, J. Andrade and G. Prescher, *Chem. Ber.*, 1986, **119**, 3326.

215 K.E. Koenig, *Asymmetric Synthesis*, ed. J.D. Morrison, Academic Press, New York, 1985, vol. 5, ch. 3.

216 J.W. Scott, D.D. Keith, G. Nix Jr., D.R. Parrish, S. Remington, G.P. Roth, J.M. Townsend, D. Valentine Jr., R. Yang, *J. Org. Chem.*, 1981, **46**, 5086.

217 H.J. Kreuzfeld, C. Döbler, H.W. Krause and C. Facklam, *Tetrahedron: Asymmetry*, 1993, **4**, 2047.

218 H.W. Krause, H. Foken and H. Pracejus, *New J. Chem.*, 1989, **13**, 615.

219 H.W. Krause, H.J. Kreuzfeld, U. Schmidt, C. Döbler, M. Michalik, S. Taudien and C. Fischer, *Chirality*, 1996, **8**, 173.

220 R. Selke and H. Pracejus, *J. Mol. Catal.*, 1986, **37**, 213.
221 USP 5 510 507/1996.
222 I. Ojima, T. Kogure and N. Yoda, *J. Org. Chem.*, 1980, **45**, 4728.
223 M.J. Burk, J.E. Feaster and R.L. Harlow, *Organometallics*, 1990, **9**, 2653.
224 J.X. McDermott, J.F. White and G.M. Whitesides, *J. Am. Chem. Soc.*, 1976, **98**, 6521.
225 L.E. Crascall and J.L. Spencer, *Inorg. Synth.*, 1990, **28**, 126.
226 M.S. Kharasch, R.C. Seyler and F.R. Mayo, *J. Am. Chem. Soc.*, 1938, **60**, 882.
227 R. Cramer, *Inorg. Synth.*, 1974, **15**, 14.
228 G. Gordano and R.H. Crabtree, *Inorg. Synth.*, 1979, **19**, 218.